# Acute kidney injury: from pathology to phytotherapy

**Edited by**
Ya-long Feng, Wuelton Monteiro, Xuezhong Gong
and Hua Chen

**Published in**
Frontiers in Pharmacology

**Generative AI statement**
Any alternative text (Alt text) provided alongside figures in the articles in this ebook has been generated by Frontiers with the support of artificial intelligence and reasonable efforts have been made to ensure accuracy, including review by the authors wherever possible. If you identify any issues, please contact us.

## About Frontiers

Frontiers is more than just an open access publisher of scholarly articles: it is a pioneering approach to the world of academia, radically improving the way scholarly research is managed. The grand vision of Frontiers is a world where all people have an equal opportunity to seek, share and generate knowledge. Frontiers provides immediate and permanent online open access to all its publications, but this alone is not enough to realize our grand goals.

## Frontiers journal series

The Frontiers journal series is a multi-tier and interdisciplinary set of open-access, online journals, promising a paradigm shift from the current review, selection and dissemination processes in academic publishing. All Frontiers journals are driven by researchers for researchers; therefore, they constitute a service to the scholarly community. At the same time, the *Frontiers journal series* operates on a revolutionary invention, the tiered publishing system, initially addressing specific communities of scholars, and gradually climbing up to broader public understanding, thus serving the interests of the lay society, too.

## Dedication to quality

Each Frontiers article is a landmark of the highest quality, thanks to genuinely collaborative interactions between authors and review editors, who include some of the world's best academicians. Research must be certified by peers before entering a stream of knowledge that may eventually reach the public - and shape society; therefore, Frontiers only applies the most rigorous and unbiased reviews. Frontiers revolutionizes research publishing by freely delivering the most outstanding research, evaluated with no bias from both the academic and social point of view. By applying the most advanced information technologies, Frontiers is catapulting scholarly publishing into a new generation.

## What are Frontiers Research Topics?

Frontiers Research Topics are very popular trademarks of the *Frontiers journals series*: they are collections of at least ten articles, all centered on a particular subject. With their unique mix of varied contributions from Original Research to Review Articles, Frontiers Research Topics unify the most influential researchers, the latest key findings and historical advances in a hot research area.

Find out more on how to host your own Frontiers Research Topic or contribute to one as an author by contacting the Frontiers editorial office: frontiersin.org/about/contact

# Acute kidney injury: from pathology to phytotherapy

**Topic editors**

Ya-long Feng — Xianyang Normal University, China

Wuelton Monteiro — Fundação de Medicina Tropical Doutor Heitor Vieira Dourado (FMT-HVD), Brazil

Xuezhong Gong — Shanghai Municipal Hospital of Traditional Chinese Medicine, China

Hua Chen — Ningxia Medical University, China

# Table of contents

# Editorial: Acute kidney injury: from pathology to phytotherapy

Ya-Long Feng [1]*[‡], Wan-Ying Ma[1‡], Yin-Xuan Jiang[1], Le Shui[1], Hua Chen [2]* and Xue-Zhong Gong [3]*

[1]Department of Life Science, Xianyang Normal University, Xianyang, Shaanxi, China, [2]College of Pharmacy, Ningxia Medical University, Yinchuan, Ningxia, China, [3]Department of Nephrology, Shanghai Municipal Hospital of Traditional Chinese Medicine, Shanghai University of Traditional Chinese Medicine, Shanghai, China

KEYWORDS

acute kidney injury, traditional medical herb, pathology, phytotherapy, natural product

> Editorial on the Research Topic
> Editorial: Acute Kidney Injury: from Pathology to Phytotherapy

## Introduction

Acute kidney injury (AKI), defined by an abrupt rise in serum creatinine and a decrease in urinary output, causes a high morbidity and mortality worldwide (Ronco et al., 2019). Due to the poor understanding of AKI pathophysiology, effective drugs for AKI treatment remain lacking. Therefore, the cellular and molecular mechanisms of AKI should be deeply studied, which will be beneficial for developing therapy drugs against AKI.

Traditional medical herb has been used to treat AKI for many years. A large number of compounds have been isolated and identified from traditional medical herbs. Recent studies reveal that some of these compounds can alleviate AKI by inhibiting inflammation, oxidative stress, and apoptosis. Noteworthily, some compounds exhibited their therapeutic efficacy on AKI in clinics, such as anisodamine, indicating an important source of traditional medical herbs in drug discovery for AKI. However, the active ingredients and mechanisms of traditional medical herbs against AKI are still poorly understood.

The present Research Topic aims at collecting the manuscripts demonstrating the novel findings in the pathological process of AKI and the protective effects of compounds derived from traditional medical herbs against AKI. After rigorous peer reviews, a total of 16 manuscripts were published.

## The biomarker for AKI diagnosis

The early diagnosis and intervention are very important for AKI treatment. Ryu et al. found that the urinary L-liver-type fatty acid-binding protein (L-FABP) level had a close relationship with AKI progression (Yasuda et al.). Further study revealed that the L-FABP level should be measured at 6 and 12 h after kidney injury than only one time at 6 h, suggesting a more precise diagnose method for AKI. In addition, Gong et al. found that the serum levels of human epididymis protein 4 (HE4) and N-terminal pro-B-type natriuretic peptide (NT-proBNP) were increased in patients with chronic kidney diseases (CKD) and patients with AKI on CKD (Song

et al.). The level of HE4 is positively correlated with the disease severity, and patients with higher levels of HE4 and NT-proBNP usually have poorer prognosis. These results suggest that the serum levels of HE4 and NT-proBNP are impactful predictors of AKI on CKD.

## The cellular and molecular mechanisms of AKI

Chen et al. conducted a comprehensive bibliometric analysis of AKI and immune-related studies from the past two decades, identifying COVID-19, immune checkpoint inhibitors, regulated necrosis, cirrhosis-related AKI, and other emerging Research Topic as key research foci in recent years (Chen et al.).

Proprotein convertase subtilisin/kexin type 9 (PCSK9) is mainly expressed in liver and regulates cholesterol metabolism. The PCSK9 inhibitors are lipid-lowering drugs. Liu conducted a disproportionality analysis through the Food and Drug Administration Adverse Event Reporting System database and found that the treatment with PCSK9 inhibitors might induce AKI (Liu). In addition, vancomycin had significant nephrotoxicity. Pan et al. found that the incidence of vancomycin-associated acute kidney injury (VA-AKI) in patients with infective endocarditis (IE) was slightly higher than in general adult patients through conducting a large retrospective cohort study (Kunming et al.). It is worth noting that the combination of vancomycin with contrast agents significantly increased the nephrotoxic in patients with IE. In addition, vancomycin therapy longer than 10.75 days increased the risk of AKI. These results are beneficial for preventing AKI.

The NF-κB signaling pathway plays a key role in inflammation and oxidative stress. Ren et al. reviewed the important role of NF-κB signaling pathway in AKI, which provided a new insight to the treatment of AKI by targeting the NF-κB signaling pathway (Ren et al.). In addition, arachidonic acid (AA) is a main component of cell membrane lipids and is associated with kidney function. Li et al. reviewed the main metabolic pathways of AA in inflammation and oxidative stress during the processes of AKI, diabetic nephropathy and renal cell carcinoma (Li et al.).

Calprotectin (S100A8/A9) is crucial for leukocyte recruitment and inflammatory response. Shi et al. found that the S100A9 expression was increased continuously in AKI mice (Shi et al.). The S100A9 inhibitor, paquinimod, significantly improved renal function by inhibiting renal tubular epithelial cell apoptosis, inflammation, superoxide production, and mitochondrial dynamic imbalance, which suggested that S100A9 was a therapeutic target for treating AKI. In addition, apolipoprotein M (apoM) plays a key role in the reabsorption function of the kidney. Bisgaard et al. found that apoM was detectable in plasma of kidney-specific human transgenic mice and was secreted to both the apical (urine) and basolateral (blood) compartment from proximal tubular epithelial cells in HK-2 cells-overexpressed human apoM, suggesting a crucial role of apoM in sequestering molecules from excretion in urine (Bisgaard et al.). However, the overexpression of apoM did not protect against AKI.

Pyruvate kinase M2 (PKM2) is a rate-limiting enzyme in glycolysis. Chen et al. highlighted its critical roles in of kidney disease progression, including podocyte injury, fibroblast activation and proliferation, macrophage polarization, and T cell regulation (Chen et al.). Notably, both the activators and inhibitors of PKM2 showed a therapeutic effect in kidney diseases, underscoring their potential as AKI treatment strategies.

## Traditional medical herbs against AKI

Huangqi-Danshen decoction (HDD) is a well-known Chinese herbal preparation and shows a reno-protective effect. Liu et al. found that HDD protected against AKI by suppressing apoptosis, inflammation and oxidative stress via modulating the NAD$^+$ biosynthesis (Liu et al.). *Panax notoginseng* is used to treat haemorrhage, blood-stasis, swelling and pain in China. Li et al. found that *Panax notoginseng* rhizomes (PNR) could decrease serum creatinine and urea nitrogen levels, reduce renal infarct areas and renal tubular cell injury areas, and inhibit renal cell apoptosis via the downregulation of MMP9, TP53 and IL-6 in mice with ischemia and reperfusion injury (Li et al.). *Prunella vulgaris* has a long history for treating kidney diseases in China. Yang et al. found that the main bio-active ingredients of *Prunella vulgaris* against COVID-19-associated AKI were quercetin, luteolin and kaempferol through the network pharmacology and molecular docking analysis (Yang et al.). The inhibition of NF-κB signaling pathway might be the key mechanism of *Prunella vulgaris* against AKI. *Rhizoma Chuanxiong* (CX) and *Radix et Rhizoma Rhei* (DH) are well known traditional Chinese medicines. Li et al. found that the core bio-active ingredients of CX and DH included aloe-emodin, (-)-catechin, β-sitosterol and folic acid though network pharmacology method (Li et al.). In contrast media-induced AKI rats, CX and DH alleviated AKI by regulating inflammation, cell death and cell cycle processes via inhibiting the p38-MAPK/p53 signaling pathway. Yue-bi-tang (YBT) is a traditional formula used to treat edema. Li et al. found that YBT alleviated edema by decreasing renal microvascular permeability via suppressing the Cav-1/eNOS signaling pathway in Adriamycin-treated rats (Li et al.).

Myricitrin is a natural flavonoid compound with diverse pharmacological properties, such as anti-oxidant, anti-inflammation and anti-cancer activities. Huang et al. found that the pretreatment of myricitrin significantly rescued HK-2 cells from cell death and reduced iron overload (Lin et al.). The protective effect of myricitrin could be reserved by the inducer of ferritinophagy rapamycin, which might suggest that myricitrin ameliorated kidney injury by attenuating ferritinophagy-mediated ferroptosis.

## Conclusion

The Research Topic "Acute Kidney Injury: From Pathology to Phytotherapy" has collected worthy studies and contributions on the subject of AKI, highlighting the promising therapeutic property of traditional medical herb. We hope that you enjoy and gain from the Research Topic, which will surely promote the drug development for AKI and the further application of traditional medical herb.

## Author contributions

Y-LF: Writing – original draft. W-YM: Writing – review and editing. Y-XJ: Writing – review and editing. LS: Writing – review

and editing. HC: Writing – review and editing. X-ZG: Writing – review and editing.

## Funding

The author(s) declare that no financial support was received for the research and/or publication of this article.

## Conflict of interest

The authors declare that the research was conducted in the absence of any commercial or financial relationships that could be construed as a potential conflict of interest.

## Reference

Ronco, C., Bellomo, R., and Kellum, J. A. (2019). Acute kidney injury. *Lancet* 394, 1949–1964. doi:10.1016/S0140-6736(19)32563-2

## Generative AI statement

The author(s) declare that no Generative AI was used in the creation of this manuscript.

## Publisher's note

All claims expressed in this article are solely those of the authors and do not necessarily represent those of their affiliated organizations, or those of the publisher, the editors and the reviewers. Any product that may be evaluated in this article, or claim that may be made by its manufacturer, is not guaranteed or endorsed by the publisher.

# A molecular network-based pharmacological study on the protective effect of *Panax notoginseng* rhizomes against renal ischemia–reperfusion injury

Dan-Dan Li[1†], Na Li[2†], Chui Cai[1], Chun-Mian Wei[1], Guang-Hua Liu[1], Ting-Hua Wang[2]* and Fu-Rong Xu[1]*

[1]Yunnan Key Laboratory of Dai and Yi Medicine, Yunnan University of Chinese Medicine, Kunming, Yunnan, China, [2]Department of Laboratory Animal Science, Kunming Medical University, Kunming, Yunnan, China

**Objective:** We aimed to explore the protective effect of *Panax notoginseng* rhizomes (PNR) on renal ischemia and reperfusion injury (RIRI) and the underlying molecular network mechanism based on network pharmacology and combined systemic experimental validation.

**Methods:** A bilateral RIRI model was established, and Cr, SCr, and BUN levels were detected. Then, the PNR was pretreated 1 week before the RIRI model was prepared. To determine the effects of the PNR in RIRI, histopathological damage and the effect of PNRs to the kidney was assessed, using TTC, HE, and TUNEL staining. Furthermore, the underlying network pharmacology mechanism was detected by screening drug−disease intersection targets from PPI protein interactions and GO and KEGG analysis, and the hub genes were screened for molecular docking based on the Degree value. Finally, the expression of hub genes in kidney tissues was verified by qPCR, and the protein expression of related genes was further detected by Western blot (WB).

**Results:** PNR pretreatment could effectively increase Cr level, decrease SCr and BUN levels, reduce renal infarct areas and renal tubular cell injury areas, and inhibit renal cell apoptosis. By using network pharmacology combined with bioinformatics, we screened co-targets both *Panax notoginseng* (Sanchi) and RIRI, acquired ten hub genes, and successfully performed molecular docking. Of these, pretreatment with the PNR reduced the mRNA levels of IL6 and MMP9 at postoperative day 1 and TP53 at postoperative day 7, and the protein expression of MMP9 at postoperative day 1 in IRI rats. These results showed that the PNR could decrease kidney pathological injury in IRI rats and inhibit apoptotic reaction and cell inflammation so as to improve renal injury effectively, and the core network mechanism is involved in the inhibition of MMP9, TP53, and IL-6.

**Conclusion:** The PNR has a marked protective effect for RIRI, and the underlying mechanism is involved in inhibiting the expression of MMP9, TP53, and IL-6. This striking discovery not only provides fruitful evidence for the protective effect of the PNR in RIRI rats but also provides a novel mechanic explanation.

# 1 Introduction

Renal ischemia and reperfusion injury is the main clinical cause of acute kidney injury (AKI) in critical illnesses (Vanmassenhove et al., 2017), and is also unavoidable in approximately 80% of patients after renal transplantation (Wang et al., 2020b). It is estimated that the annual morbidity and mortality of AKI is increasing worldwide, and most patients are concentrated in developing countries (Mehta et al., 2015). Among them, China had become the region with the most severe incidence of AKI (Zhao and Yang, 2018). Undoubtedly, AKI leads to an increased risk of chronic kidney disease and end-stage renal disease (Chawla et al., 2014; Sato et al., 2020), which are a burden not only for the individual but also for the society, the nation, and the world. Hence, the treatment of AKI is particularly urgent, but there are no effective therapeutic drugs available, leading to the fact that prevention of RIRI is the key to treating kidney injury (Ding et al., 2021), especially since early prevention can improve its prognosis. Previously, the use of pharmacological interventions to reduce ischemia−reperfusion on kidney injury had great clinical importance. Ischemia−reperfusion injury (IRI) can not only induce a pathological condition that initially restricts blood supply to organs and subsequently restores it but also results in blood perfusion and an accompanying imbalance in local tissue oxygen supply and demand, further damaging tissues and organs. Renal ischemic injury occurs mainly in tubular epithelial cells (TECs) and is characterized by ischemic necrosis of TECs as a central feature. In this process, ischemia and hypoxia usually lead to metabolic dysfunction of tissues and organs, causing organismal damage. The specific mechanism of RIRI is not completely clear, but is closely related to apoptosis (Wu et al., 2018), oxidative stress (Han and Lee, 2019), and inflammatory response (Bonavia and Singbartl, 2018; Singbartl et al., 2019).

According to clinical manifestations, RIRI is caused by deficiency of Qi and blood and blood stasis syndrome according to the traditional Chinese medicine (TCM). Therefore, for treating RIRI, TCM can advantageously focus on activating blood circulation, removing blood stasis, and tonifying Qi (Liu et al., 2021b). Of these, the efficacy of *Panax notoginseng* (Sanchi) is appropriate in dispersing blood stasis and stopping bleeding, invigorating blood, and relieving pain. The dried roots and rhizomes of *Panax notoginseng* (Burk.) F.H. Chen, Sanchi mainly contain *Panax notoginseng* saponins (PNS), flavonoids, amino acids, polysaccharides, and other active ingredients; it could be considered a potential indicator for treating AKI. Additionally, Sanchi has modern pharmacological effects such as immune regulation, anticoagulation, antioxidant, free radical scavenging, estrogen-like, anti-inflammatory, vasodilatory, and protection of ischemic−reperfused tissues (Chan et al., 2002; Liu et al., 2020b; Zhang et al., 2021a). Therefore, clinical applications have expanded from traditional cardiovascular and cerebrovascular diseases to also have good therapeutic effects on the kidney, lung, liver, and other parts affected the disease (Zhang et al., 2018; Xie et al., 2020; Liu et al., 2021c; Huang et al., 2022).

Currently, experimental studies have shown that PNS has protective effects on cerebral and myocardial ischemia−reperfusion organs (Wang et al., 2020a; Zhang et al., 2021a), and the effect of Notoginsenoside $R_1$ reducing IRI in the kidney is markedly observed (Fan et al., 2020). However, the content of PNS in different parts is different, with the highest content in its rhizomes and the second highest in its roots (Wang et al., 2014). Moreover, as Chinese herbal medicine has multi-component, multi-target, and multi-pathway characteristics, it needs a systematical method to analyze the protective effect of Sanchi on RIRI. Here, by using network pharmacology combined with biological information, we detect the effect of PNR for treating AKI and explore the involved network mechanism. Finally, experimental animal models were designed to demonstrate the protective effect of PNR pretreatment on RIRI. Our data provide a basic theoretical basis for application of Sanchi to improve the treatment of AKI in future clinical practice.

# 2 Materials and methods

## 2.1 Drugs and animals

Drugs: Sanchi (rhizomes, Yunnan Wenshan Kunqi Pharmaceutical Co., Ltd., production batch number: 20211001).

Animals: SPF male Sprague–Dawley rats (weight 200–240 g) provided by the Department of Laboratory Animal Science, Kunming Medical University. No. SCXK (Yunnan) K2020-0004, Animal Ethics Code: kmmu20221856.

## 2.2 Pharmacological experimental design

The bilateral renal ischemia–reperfusion injury model is considered to better simulate the pathological process of AKI in humans and more closely resembles bilateral kidney injury in clinical patients (Wei and Dong, 2012), so the bilateral RIRI model was chosen for this experiment.

SD rats were randomly divided into the sham group (sham, N = 15), model group (IRI, N = 30), and PNR group (PNR, N = 30). According to the clinical dose–effect relationship (equivalent dose ratio of 200-g rats to 70-kg humans converted by body surface area 0.018), the PNR group was administered 270 mg/kg PNR by gavage once daily for 7 days. An equal volume of saline was given to the sham group and the IRI group.

The injury peaked after 24 h of reperfusion and reached a plateau after 7 days, so the mold was taken at days 1 and 7 after successful modeling, and blood, 24 h urine, and both kidneys were collected before the end of the experiment.

## 2.3 Animal models

According to the methods of Yin et al. (2017), the rats were anesthetized with sodium pentobarbital (40 mg/kg) by

intraperitoneal injection, 1 h after the last dose, (fasting 12 h before surgery and normal supply of drinking water) and fixed prone on a surgical plate (placed on a heating pad at 37°C–38°C to maintain a constant body temperature). The skin on the back was used, disinfected with iodine, and a longitudinal incision of approximately 2-cm in length was made by cutting the skin layer at the midline of two points under the bilateral rib arches on the back. Then, the incision was pulled above the positions of the left and right kidneys. Afterward, the muscle layer was cut, the bilateral kidneys were bluntly separated and exposed, the bilateral renal arteries were separated, and the bilateral renal arteries were ligated in all the groups of rats, except for the sham group. The kidneys were infiltrated with saline drip at 37°C inside the incision and then covered with sterile gauze to maintain moisture. After ligating the bilateral renal arteries for 40 min and releasing them, the color of the kidney gradually changed from purple-black to bright red, indicating that the kidney was well-perfused again. The heating pad was removed after the rats were awake.

The success of the model was judged by observing the color of the kidney, which changed from red to purple-black in ischemia and from purple-black to red in reperfusion, combined with the analyses of urine and blood biochemistry.

## 2.4 Testing methods

### 2.4.1 Urine and blood biochemical analysis

The urine at postoperative days 1 and 7 was collected using a metabolic cage and sent to Chenggong Hospital of Kunming Medical University for testing the levels of urinary creatinine (Cr).

At the end of the experiment, blood was collected from the heart, and non-anticoagulated blood samples were prepared and stored at 4°C. The non-anticoagulated blood samples were centrifuged at 4°C and 3 000 r/min for 15 min, and the supernatant (serum) was extracted, and serum creatinine (SCr) and blood urea nitrogen (BUN) levels were measured using an automatic biochemical analyzer (Beckman Coulter K.K.).

### 2.4.2 Histopathology
#### 2.4.2.1 2, 3, 5-Triphenyl tetrazolium chloride (TTC) staining

After the SD rats were anesthetized, both the kidneys were removed *in vivo*, the blood was quickly dried on the surface and placed in a refrigerator at −80°C for about 20 min, and then removed to cut coronally (thickness about 2 mm) at −20°C. The TTC staining solution was quickly added and placed in a thermostat at 37°C for 30 min to avoid light staining, and then the TTC staining solution was carefully aspirated and added to an appropriate amount of 4% paraformaldehyde, stored at 4°C, and fixed overnight. Then, the sections were taken out and observed and photographed.

#### 2.4.2.2 Hematoxylin and eosin (HE) staining

The kidney tissues were fixed by soaking in 4% paraformaldehyde and coronally cut into two longitudinal flaps to make paraffin sections (thickness about 5 μm), and after dewaxing and hydration, the sections were stained with hematoxylin–eosin

stain and sealed, and photographed using a full section scanner (3DHISTECH Ltd.).

#### 2.4.2.3 TdT-mediated dUTP-FITC nick end-labeling (TUNEL) staining

After dewaxing, hydration, and antigen repair, the paraffin sections of kidney tissues at postoperative day 7 were rinsed with 0.01 mol/L PBS (pH = 7.6) thrice, 5 min each time and sealed at room temperature for 3 h by adding an appropriate amount of 0.3% Triton X-100 solution (5% sheep serum preparation). According to the TUNEL kit's (Roche) instructions, the TUNEL reaction mixture (TdT: fluorescein labeled dUTP = 1 : 9) was added to the cartridge and incubated at 37°C for 1 h, then stained with DAPI staining solution (DAPI: anti-fluorescence quencher = 1:3000) at room temperature for 5 min, and sealed. The sections was observed and photographed for analysis using a Leica fluorescence microscope (Leica Microsystems Ltd.).

## 2.5 Network pharmacology

### 2.5.1 Screening of drug ingredients and targets

The constituents and related targets of Sanchi were searched by using the TCMSP database (https://old.tcmsp-e.com/index.php). First, we selected "Herb name" in the search box; entered the drug name; clicked "Search"; set "OB" ≥ 30%, "DL" ≥ 0.18, and other parameters as default values as the screening conditions; and obtained the relevant active ingredients of the drug (Zhao et al., 2021). Then, according to the Molecular ID of the active ingredient, the target protein name corresponding to the active ingredient was queried in Related Targets, the clinically validated targets of the species "*Homo sapiens*" were screened by the UniProt platform (https://www.uniprot.org/), the obtained target names were standardized and corrected by comparing the protein names, the target gene names and corresponding numbers were summarized, and the duplicate and mismatched targets were removed to summarize the potential targets.

### 2.5.2 Disease gene collection

We searched the GeneCards database (https://www.genecards.org/) and entered the keyword "Renal ischemia–reperfusion injury" to download the gene for RIRI.

### 2.5.3 Venn intersection diagram

Using the Venny 2.1.0 online platform (https://bioinfogp.cnb.csic.es/tools/venny/), we entered "Drug" in List 1 and "Disease" in List 2, then pasted the corresponding genes to screen 106 "drug–disease intersection targets," and made the Venn intersection diagram.

### 2.5.4 GO enrichment and KEGG pathway analysis

Through the Metascape platform (https://metascape.org/gp/index.html#/main/step1), we first pasted "Drug–disease intersection target" from Venny to or paste a gene list box, followed by selecting *Homo sapiens* as the species of input, then clicked "Custom analysis," and finally analyzed BP, CC, MF, and KEGG under "Enrichment" and downloaded the compressed package under "Analysis report page."

### 2.5.5 Construction of the protein–protein interaction (PPI) network

According to the drug–disease intersection target in Venny, we opened the STRING network database platform (https://cn.string-db.org/), selected Multiple proteins, then pasted the intersection target in List of name, and selected *Homo sapiens* in Organisms to construct the PPI network map.

### 2.5.6 Hub gene screening

Hub genes were screened with Cytoscape 3.8.0 software, and the protein interaction table obtained in PPI was imported into Cytoscape. Furthermore, ten hub genes were screened by using the cytoHubba plug-in and Degree value, and histograms were made with the magnitude of the Degree value.

### 2.5.7 Network relationship diagram of "disease–active drug ingredient–key target–KEGG signaling pathway"

Tables with disease genes, drug active ingredient Mol numbers and their genes, and KEGG signaling pathways were imported into the Cytoscape software to create their network relationship diagram.

### 2.5.8 Molecular docking analysis

The PDB database was used to download the hub gene protein structure, and the PubChem database was used to download the 2D structure of the drug component. The Open Babel software was used to convert the sdf format of the drug component structure to mol2 format and then to dehydrate and de-ligand it with the PyMOL software. With the gene target protein as the receptor and drug as the ligand, molecular docking analysis was performed with AutoDock Vina software. Finally, PyMOL software was used to embellish it and calculate the hydrogen bond length, label the residue name, and export the ligand, overall picture.

## 2.6 Quantitative real-time (qPCR)

We explored the molecular mechanism of PNR pretreatment on RIRI based on the Hub gene screened by network pharmacology and molecular docking results. An appropriate amount of rat kidney tissues on postoperative days 1 and 7 was selected, homogenized with 1 ml TRIzol (Takara), and 200 μl chloroform was added to extract the upper aqueous phase. Then, isopropyl alcohol was added for centrifugation, and the RNA was precipitated at the bottom of the tube. The RNA precipitates were washed with 80% ice-cold ethanol treated with DEPC water (Biosharp), and the RNA purity and concentration were measured using enzyme marker (Thermo). The reverse transcription reaction system was prepared according to the reverse transcription kit's (DBI Bioscience) instructions, and the cDNA was placed at −20℃ after synthesis and centrifugation. The qPCR reaction system was prepared and gradually added to the 96-well plate. After the sample addition was completed, the reaction was amplified in a PCR instrument (BIO-RAD). The reaction conditions were as follows: 95℃ for 5 min, 95℃ for 10 s, 55℃–60℃ for 20 s, and 72℃ for 20 s for a total of 40 cycles. Relative expression was calculated by the $2^{-\Delta\Delta Ct}$ method. The specific primer sequence is shown in Table 1.

## 2.7 Western blot

Proteins were extracted from kidney tissues using RIPA lysis buffer and centrifuged at 4℃ and 12,000 rpm for 15 min, and the supernatant was extracted for use. The protein concentration was determined by a BCA kit (Beyotime). After separation using 12.5% SDS-PAGE gels (EpiZyme), proteins were transferred to PVDF membranes and the membranes were sealed in 5% skim milk for 1 h. Then, the membranes were incubated with primary antibody 3²-actin (1:5000, mouse antibody, 43 KD, Affinity), MMP9 (1:1000, rabbit antibody, 78 KD, Affinity) in a vertical shaker at 4℃ for 16 h. After rinsing, sheep anti-rabbit IgG or sheep anti-mouse IgG (1: 5,000, Abbkine) was added and incubated for 1 h at room temperature. Finally, an ECL chemiluminescence substrate kit (Biosharp) was used for development, image information was acquired in the gel imager, and the data were processed using ImageJ software.

## 2.8 Statistical analysis

One-way ANOVA and statistical comparison among groups were performed using SPSS 26.0 software, the LSD test was applied when variance was homogeneous, Dunnett's T3 test was applied when the variance of data in qPCR was uneven, and the Tamheri test was applied when the variance of other experimental data was uneven. $P < 0.05$ was considered significant, and GraphPad Prism 8.0 was used to indicate significance between the two groups.

# 3 Results

## 3.1 PNR improves renal injury after IRI

Creatinine and blood urea nitrogen were used as common biomarkers for early kidney injury. Compared with the sham group, the IRI group showed significant decrease in the Cr content and increase in the SCr and BUN content at postoperative days 1 and 7, confirming a decrease in glomerular filtration rate and renal dysfunction, and the changes in each index at postoperative day 1 were higher than those at day 7, indicating greater renal damage at postoperative day 1. Moreover, compared with the IRI group, the Cr level was significantly higher and the SCr and BUN levels were significantly lower in the PNR group, both on postoperative days and 7, and the results of each index showed that the effect of pharmacological intervention was better for postoperative day 1 than for day 7, which significantly improved the renal injury after RIRI. (Figures 1A–C).

## 3.2 PNR reduced the pathological damage of kidney tissue

The area of tissue infarction was observed by TTC staining of kidney sections, and the sham group was red and had no infarcted

**TABLE 1 Primer sequences.**

| Gene | Forward | Reverse |
|------|---------|---------|
| AKT1 | CATGAACGAGTTTGAGTACCT | CTCCTTCTTGAGGATCTTCAT |
| TNF-α | CCACCACGCTCTTCTGTC | GCTACGGGCTTGTCACTC |
| IL6 | GCCTTCCCTACTTCACAAGT | GCCATTGCACAACTCTTTTCT |
| IL1B | GAGCTGAAAGCTCTCCACCT | TTCCATCTTCTTCTTTGGGT |
| TP53 | CCTTACCATCATCACGCTGGAAGAC | AGGACAGGCACAAACACGAACC |
| VEGFA | CTTCAAGCCGTCCTGTGTG | GCTCATCTCTCCTATGTGCT |
| CASP3 | CGGGTCATGGTTCATCCAGT | CTCAAATTCCGTGGCCACCT |
| PTGS2 | ACTCTATCACTGGCATCCG | GAGCAAGTCCGTGTTCAAG |
| MMP9 | CCTCAAGTGGCACCATCAT | GCGACACCAAACTGGATGA |
| HIF1A | TCCCATACAAGGCAGCA | GAAACCCCACAGACAACAA |
| GAPDH | GACATGCCGCCTGGAGAAAC | AGCCCAGGATGCCCTTTAGT |

**TABLE 2 Molecular docking results of Sanchi with hub genes.**

| Gene | PDB ID | Binding energy (kJ/mol) |
|------|--------|--------------------------|
| AKT1 | 7NH4 | −15.857 |
| TNF | 7MLR | −13.012 |
| IL6 | 5ZO6 | −13.012 |
| IL1B | 6Y8I | −13.347 |
| TP53 | 7L1N | −7.740 |
| VEGFA | 6ZBR | −6.987 |
| CASP3 | 7RN9 | −14.937 |
| PTGS2 | 5F19 | −1.255 |
| MMP9 | 4XCT | −17.405 |
| HIF1A | 7LVS | −14.477 |

area as observed by the staining results. Compared with the sham group, the IRI group clearly showed non-red areas, indicating tissue infarction and an increase in the area of tissue damage resulting from postoperative day 1 compared with day 7. In contrast, compared with the IRI group, the PNR group had significantly fewer non-red areas, less infarct area, and significantly less damage at postoperative day 7 compared with day 1. (Figures 2A, B).

HE staining was used to observe the TEC morphology and score pathological damage such as swelling, vacuolization, and tubular formation of TECs with reference to LIU et al. (Liu et al., 2020a). A total of ten fields of view were randomly selected and scored 0–5 for TEC pathological injury. The details are as follows: 0: normal; 1: histological changes <10% of the damaged area; 2: similar changes >10% but <25% of the damaged area; 3: similar changes involving >25% but <50% of the damaged area; 4: similar changes involving >50% but <75% of the damaged area; 5: similar changes involving >75% of the damaged area. The results showed that the renal tubular cells in the sham group had normal morphology and

tight arrangement. Compared with the sham group, the IRI group had a severe absence of cell morphology at postoperative day 1 and showed tubular formation and protein accumulation in the tubular lumen ($p < 0.001$), and a more slight absence of cell morphology at postoperative day 7, but showed tubular interstitial inflammatory factor infiltration and tubular dilatation ($p < 0.001$). While compared with the IRI group, cell morphology recovered in the PNR group at postoperative day 1, which significantly reduced tubular formation and protein accumulation in the lumen ($p < 0.001$). Cell morphology recovered significantly at day 7 postoperatively, which improved interstitial inflammatory factor infiltration and expansion ($p < 0.001$). Also, it can be seen that the IRI and PNR groups were more severely injured at postoperative day 1 than at day 7 (Figures 2C, D).

TUNEL staining was used to assess the consequence of RIRI and the protective influence of the PNR, and the number of positive cells and apoptosis rate from three random fields were calculated (apoptosis rate = number of positive cells/total number of cells × 100%). The results showed that the sham group had a higher number of DAPI-stained cells, normal cell morphology with sub-circular shape, and almost no apoptosis. Compared with the sham group, the IRI group at postoperative day 7 showed a significant decrease in the number of cells and an increase in the number of positive cells, observed with an irregular change in cell morphology ($p < 0.001$). Compared with the IRI group, the number of cells in the PNR group increased, the cell morphology tended to be normal, and the number of positive cells was significantly reduced ($p < 0.01$) (Figures 2E, F).

## 3.3 Network relationship between Sanchi and RIRI

The results showed that 181 active ingredient targets of Sanchi were found in TCMSP, and 1,238 disease genes of RIRI were obtained in the GeneCards database. The relationship of gene targets between drug and disease was analyzed through the Venny 2.1.0 online platform, and 106 intersection genes (key targets) were obtained
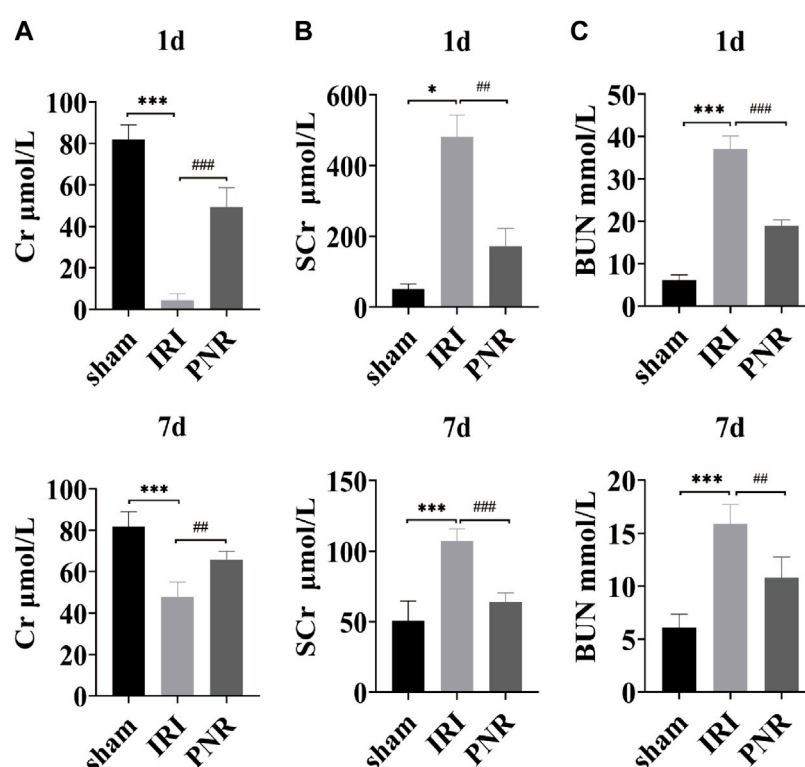
**FIGURE 1**
Results of the effect of PNR pretreatment on urine and blood biochemical indexes at days 1 and 7 postoperatively. **(A)** Cr content in each group (N = 4−6); **(B)** SCr content in each group (N = 3−7); **(C)** BUN content in each group (N = 4−7). Compared with the sham group, ***$p < 0.001$, *$p < 0.05$; compared with the IRI group, ###$p < 0.001$, ##$p < 0.01$.

(Figure 3A). GO enrichment results of key targets were analyzed in the Metascape platform to - LogP values to screen the top 10 biological processes (BP), cellular components (CC), and molecular functions (MF). Among them, responding to inorganic substance is the most important BP, membrane raft is the most important CC, and cytokine receptor binding is the most important MF (Figure 3B). Meanwhile, KEGG signaling pathway analysis was performed for key targets, the top 20 signaling pathways were screened by - LogP values, and interleukin-4 and interleukin-13 signaling were the most important signaling pathways (Figure 3D).

The PPI network map was produced in the STRING network database platform using key targets (Figure 3E). The PPI relationship table was imported using the Cytoscape software, and the hub genes were screened from the largest to the smallest according to the Degree value: AKT1, TNF, IL-6, IL-1B, TP53, VEGFA, CASP3, PTGS2, MMP9, and HIF1A. Meanwhile, we constructed the hub gene network diagram and histogram (Figure 3C). Finally, a network relationship diagram of the disease, drug active ingredients, and key targets and KEGG signaling pathways was constructed (Figure 3F).

## 3.4 Molecular docking results

When the binding energy is less than 0 kJ/mol, the drug ligand can spontaneously bind to the receptor protein, where less than -5 kJ/mol

indicates good binding ability, and the lower the binding energy, the better the docking result (Gao et al., 2022). All hub genes were successfully molecularly docked according to the results, and the docking results were visualized using PyMOL software (Figure 4). Among them, MMP9 has the lowest binding energy to ligand molecules (-17.405 kJ/mol) and the strongest binding capacity (Table 2).

## 3.5 qPCR results

The mRNA expression of ten hub genes (AKT1, TNF, IL-6, IL-1B, TP53, VEGFA, CASP3, PTGS2, MMP9, and HIF1A) was measured by qPCR in renal tissues at postoperative days 1 and 7, and the results showed that the $p$ values of IL-6, MMP9, and TP53 genes were less than 0.05, with statistical significance. Compared with the sham group, the IRI group showed significantly elevated mRNA expression of IL-6 and MMP9 at day 1 postoperatively and TP53 at day 7 postoperatively. In contrast, the PNR group showed decreased mRNA expression of IL-6 and MMP9 at 24 h of reperfusion and TP53 at day 7 of reperfusion in IRI rats (Figure 5).

## 3.6 WB results

According to the qPCR results, MMP9 expression at postoperative day 1 showed the most significant difference
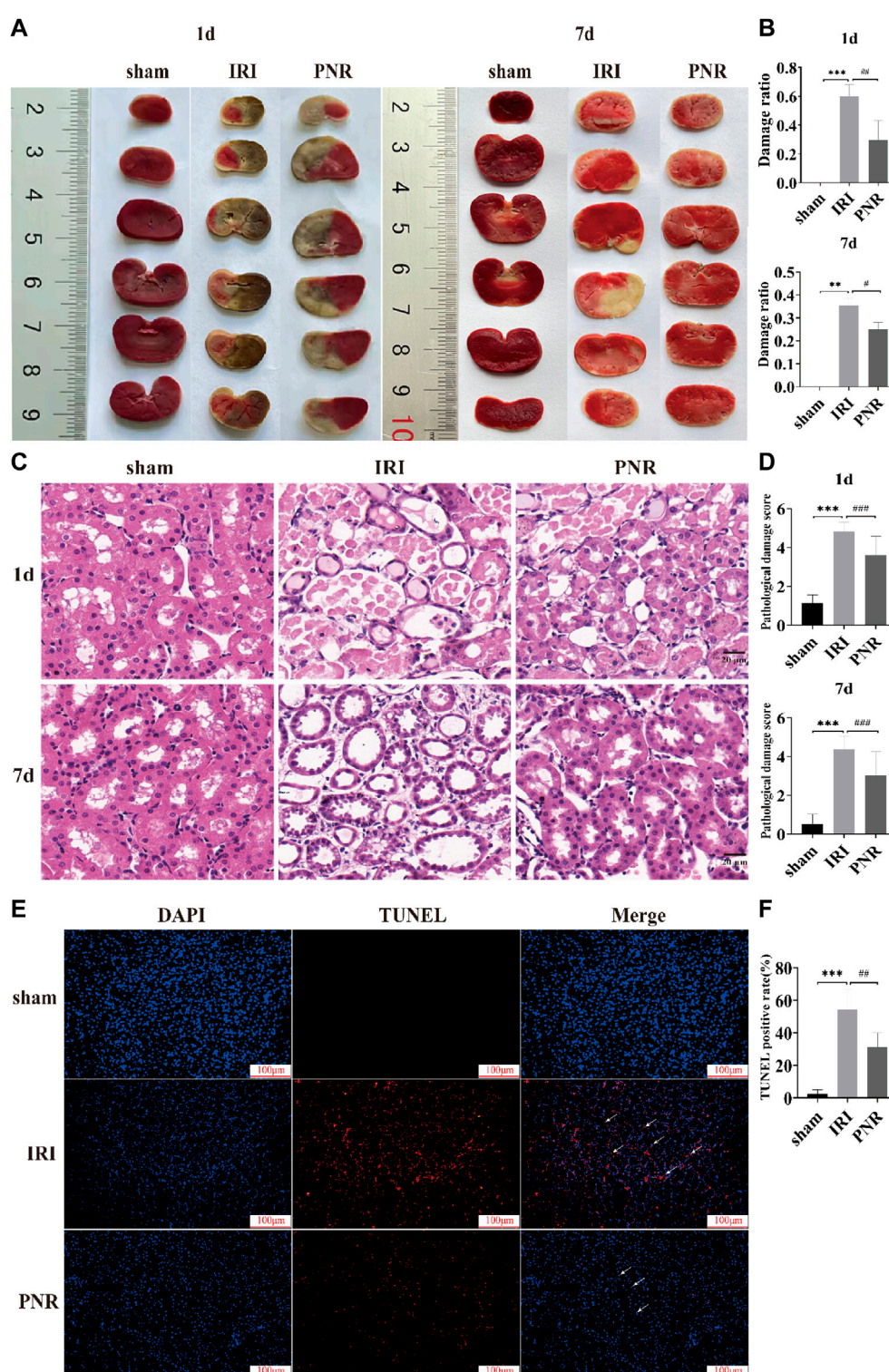
**FIGURE 2**
Results of histopathological damage to RIRI kidneys by **pretreatment** with the PNR. **(A)** TTC staining results of PNR pretreatment on each group at postoperative days 1 and 7; **(B)** statistical results of the ratio of TTC staining damage (N = 3–4); **(C)** HE staining results of PNR pretreatment on each group at postoperative days and 7 (×400 magnification, scale bar = 20 μm); **(D)** statistical results of HE staining pathological damage score (N = 3); **(E)** TUNEL staining results of PNR pretreatment on each group at postoperative day 7 (×200 magnification, scale bar = 100 μm); **(F)** statistical results of TUNEL staining-positive cells (N = 3). Compared with the sham group, ***$p < 0.001$, **$p < 0.01$; compared with the IRI group, ###$p < 0.001$, ##$p < 0.01$, and #$p < 0.05$.
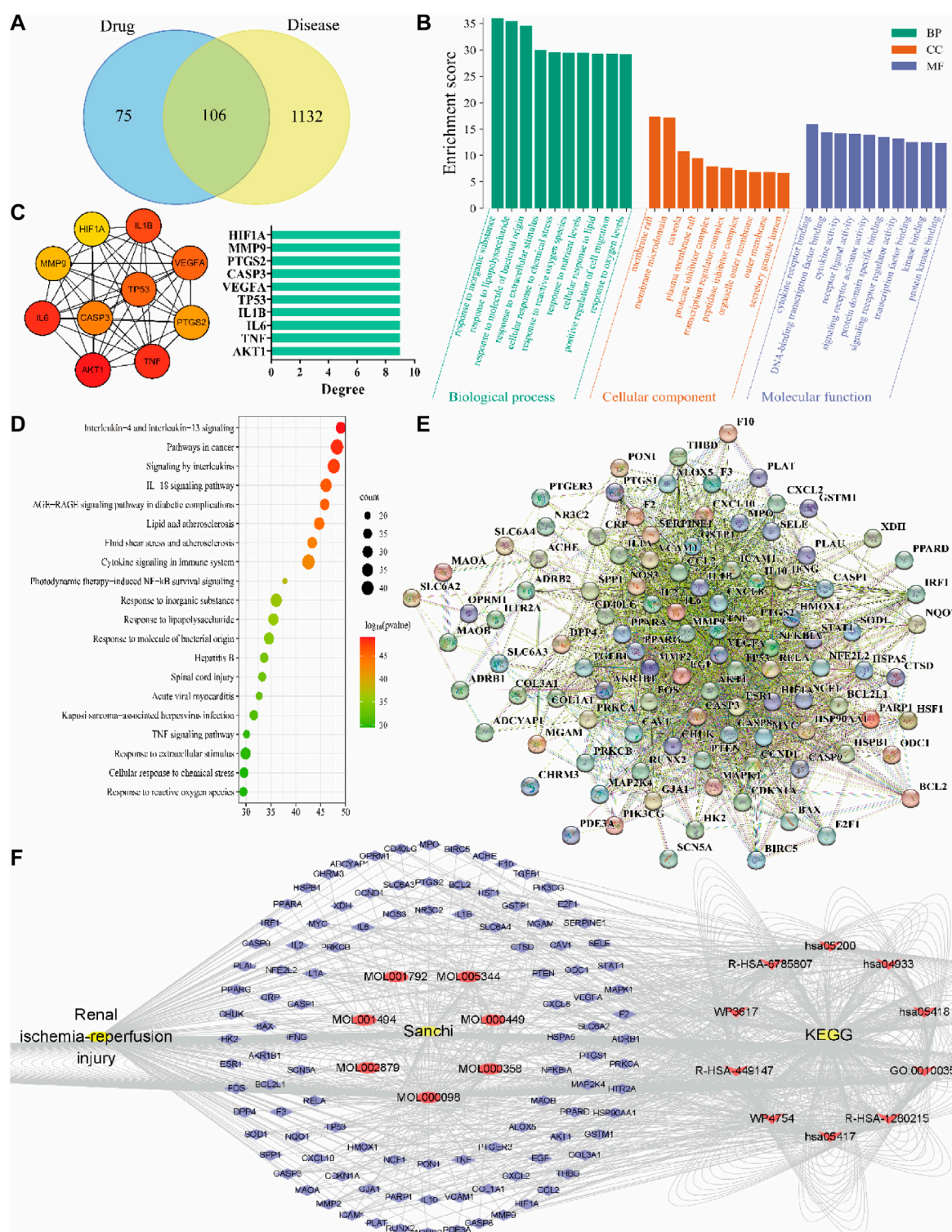
**FIGURE 3**
Results of drug-disease network relationship analysis using network pharmacology methods. **(A)** Drug-disease Venny intersection diagram, with the drug (Sanchi) targets on the left, the disease (RIRI) targets on the right, and the two intersection targets in the middle; **(B)** GO enrichment analysis of drug-disease; **(C)** Hub genes screened according to the PPI network relationships and rounded from the largest to smallest with the Degree value changes, and Degree—hub genes histogram with the Degree values as horizontal coordinates and genes as vertical coordinates; **(D)** KEGG signaling pathway analysis of drug-disease; **(E)** PPI network relationship diagram; **(F)** The network of "disease-drug active ingredient-key target-KEGG signaling pathway", from left to right, is the disease (RIRI), drug (Sanchi) and its seven active ingredients Mol numbers, key targets (blue outer circle), and the first ten pathways of KEGG.
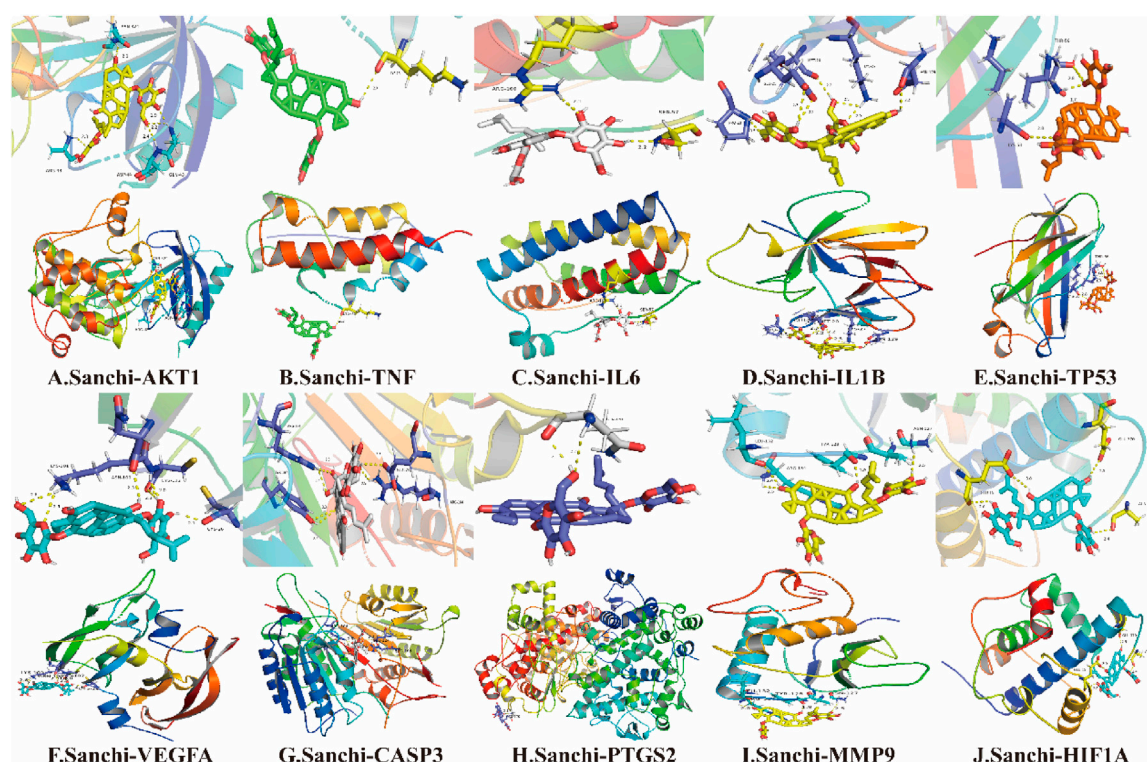
**FIGURE 4**
Molecular docking results of Sanchi and hub gene-related proteins.

among the groups, and MMP9 was selected as a target for further validation of PNR action on RIRI. WB assay results showed increased MMP9 protein levels in the IRI and PNR groups compared to the sham group, but the PNR group had lower protein levels than the IRI group (Figure 6).

# 4 Discussion

In this study, data from the measurement of urine and blood biochemical indexes and observation of kidney morphology showed that the pretreatment with the PNR could reduce renal injury after IRI, improve TEC morphology, and inhibit apoptosis. Furthermore, the network pharmacological approach was used to elucidate the network relationship between Sanchi and RIRI. Then, we analyzed the results of GO enrichment and KEGG signaling pathways and used molecular docking to validate ten hub genes and analyze them by qPCR assay. These results indicated that PNR pretreatment could reduce the kidney injury caused by IRI in rats by inhibiting the expression of IL-6, MMP9, and TP53 in kidney tissues. In particular, MMP9 was further validated by WB assay for its important role in the pathological process of RIRI. Among them, the modulation of MMP9 and TP53 by the PNR in RIRI has not been reported, which provides a new research direction for the in-depth study of the mechanism of action of Sanchi on RIRI. In addition, these findings suggest that the PNR is an effective potential medicine for preventing RIRI.

## 4.1 PNR pretreatment has a protective effect against RIRI

By detecting the content of renal injury markers—creatinine and blood urea nitrogen, we found that PNR pretreatment significantly improved the abnormal Cr, SCr, and BUN content in the IRI group, reduced IRI-induced kidney damage in TTC staining, improved renal tubular cell morphology in HE staining, and reduced the number of positive cells in TUNEL staining. These results indicated that the PNR can improve renal injury and abnormal changes in TEC morphology caused by IRI and suggested that the PNR could play an important role in protecting the kidney of IRI rats.

The urine and blood biochemical index test is a common method for clinical examination of RIRI (Zhu et al., 2019). The results showed that IRI rats had elevated SCr and BUN levels in the blood and decreased Cr levels in the urine, suggesting kidney damage. Increased SCr and BUN content and impaired renal function after IRI were also observed in the study by Sun et al. (2020). In the observation of renal cell morphology, we could see that IRI rats pretreated with the PNR significantly reduced the expansion of TECs, infiltration of inflammatory factors in the interstitium, and tubular formation, and TEC injury is a key feature of the initial phase of RIRI (Basile et al., 2012). The study had shown that pectin-like polysaccharides extracted from Sanchi can improve TEC morphology and have an anti-fibrotic effect on the kidneys (Huang et al., 2022). In addition, PNR pretreatment reduced renal apoptosis in IRI rats, consistent with the findings that reduced apoptosis protected
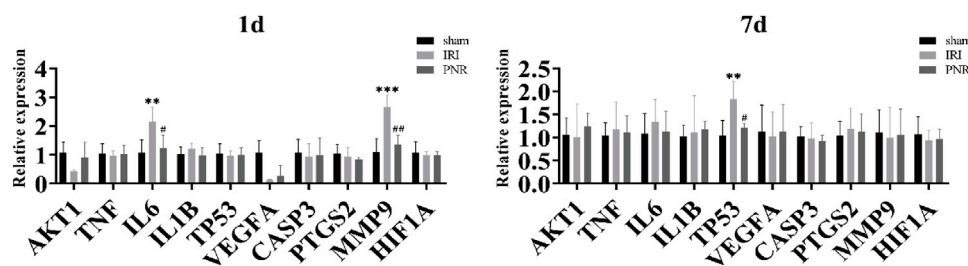
FIGURE 5
qPCR measurement of mRNA expression of ten hub genes in kidney tissues at days 1 and 7 postoperatively. Compared with the sham group, ***$p <$ 0.001, **$p <$ 0.01; compared with the IRI group, ##$p <$ 0.01, #$p <$ 0.05.

against renal injury (Shao et al., 2021), suggesting that apoptosis could be central in RIRI. In conclusion, the PNR can protect the kidney by affecting Cr, SCr, and BUN contents, improving renal cell morphology and reducing apoptosis, and can be used as a potential medicine to prevent the occurrence of RIRI.

## 4.2 Sanchi and RIRI network relationship

### 4.2.1 Molecular mechanism of Sanchi and RIRI

In this experiment, through in-depth analyses of the network relationship between Sanchi and RIRI and its molecular mechanism, we identified the most important BP, CC, MF, and signaling pathways of Sanchi for treating RIRI, indicating that Sanchi can exert anti-inflammatory, antioxidant, immune regulatory, and other pharmacological effects on RIRI by using multiple targets and pathways, suggesting that Sanchi can be used to treat RIRI through multiple pathways, providing a certain research basis for the research of Sanchi in treating RIRI.

GO enrichment analysis revealed that the most important BP is response to inorganic substances, which is involved in apoptosis and mitochondrial dysfunction during RIRI (Hou et al., 2021). The most important CC is the membrane raft, which is involved in intracellular cholesterol transport, and during the renal injury phase, cholesterol transfer to the endoplasmic reticulum is increased and cholesterol ester production is increased. Cholesterol enrichment in the plasma membrane was shown to be protective against ischemic injury in the proximal tubule, as well as a manifestation of the response to injury (Zager et al., 2002). The most important MF is cytokine receptor binding, where cytokines bind to their receptors and play a gene-regulatory role in treating RIRI by mediating related signaling pathways (Ge et al., 2017).

The analysis of the first ten KEGG signaling pathways revealed that the first pathway was interleukin-4 and interleukin-13 signaling, and that the cytokines IL-4 and IL-13 mediated the polarization of renal macrophages or dendritic cells to the M2a (associated with wound healing and tissue repair) phenotype, thereby reversing recovery from RIRI (Zhang et al., 2017). The second pathway is pathways in cancer, signal transducer and activator of transcription 3 (STAT3) mediates many cancer-related signaling pathways and has an important role in immunomodulation against cancer and

tumors (Zou et al., 2020), while it is also involved in promoting M2 polarization in renal macrophages, suppressing inflammatory responses, regulating immunity, and reducing RIRI (Chen et al., 2021; Liu et al., 2021d). The third pathway is signaling by interleukins; a variety of interleukins have been shown to regulate related genes with positive or negative effects on RIRI (Liang et al., 2017; Ding et al., 2019; Aiello et al., 2020). The fourth pathway is the IL-18 signaling pathway, showing that RIRI is associated with IL-18-induced pro-inflammatory factor production, and inhibition of IL-18 expression can effectively reduce renal injury and fibrosis (Yang et al., 2015; Liang et al., 2018). The fifth pathway is the AGE-RAGE signaling pathway in diabetic complications, and diabetic nephropathy is a diabetic microvascular complication and one of the causes of kidney injury. Activation of the AGE-RAGE signaling pathway will aggravate kidney injury through a series of pathways such as apoptosis, inflammatory response, oxidative stress, and mitochondrial dysfunction (Chen et al., 2020; Bhattamisra et al., 2021). The sixth pathway is lipid and atherosclerosis; lipid peroxidation occurs during RIRI, which is one of the important pathological processes of atherosclerosis, and anti-lipid peroxidation can reduce atherosclerosis (Erpicum et al., 2018; Bai et al., 2020). The seventh pathway is fluid shear stress and atherosclerosis, a chronic inflammatory disease of the vasculature driven by lipids and characterized by plaque formation at the site of pathogenesis (Schaftenaar et al., 2016); fluid shear stress can modulate vascular function to affect atherosclerosis formation (Cunningham and Gotlieb, 2005) and also reduce IRI by inhibiting apoptotic proteins (Zhang et al., 2021b). The eighth pathway is cytokine signaling in the immune system, where macrophages play an important role in the control of inflammation or repair after RIRI through T cells that contribute to the shift to an anti-inflammatory phenotype (Hasegawa et al., 2021). The ninth pathway is photodynamic therapy-induced NF-κB survival signaling, and inhibition of NF-κB signaling pathway-mediated inflammatory response and apoptosis protects against RIRI (Younis and Ghanim, 2022). The tenth pathway is response to inorganic substances; calcium overload is a key factor causing apoptosis of renal tubular cells after IRI (Hou et al., 2021), whereas $H_2O_2$ production increases during ischemia–reperfusion, and $H_2O_2$ affects renal mitochondrial function (Kamarauskaite et al., 2020).
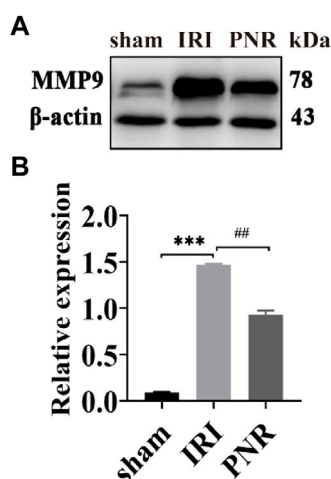
**FIGURE 6**
Results of MMP9 protein expression in kidney tissues at day 1 postoperatively (N = 3). **(A)** Protein bands for each group of MMP9 and $\beta$-actin detected by WB. **(B)** MMP9 protein expression in the kidneys of each group. Compared with the sham group, ***$p < 0.001$; compared with the IRI group, ##$p < 0.01$.

In conclusion, Sanchi could reduce the damage of IRI to the kidneys by affecting response to inorganic substances, membrane raft, cytokine receptor binding, and the most important signaling pathways of interleukin-4 and interleukin-13 signaling.

### 4.2.2 Validation of Sanchi and RIRI core genes

We established a PPI network relationship between Sanchi and RIRI intersection targets and screened ten hub genes for molecular docking and qPCR validation. It was found that the PNR could inhibit the expression of IL-6, MMP9, and TP53, and the WB assay further showed that the PNR could inhibit MMP9 protein expression. These results suggested that the PNR could regulate the related genes to reduce the kidney damage by RIRI and prompted us to pay attention to the changes in these related genes in the development of RIRI disease.

The PPI network relationship map was produced in the STRING network database platform, and the hub genes screened with the Degree value using the cytoHubba plug-in in Cytoscape software are AKT1, TNF, IL6, IL1B, TP53, VEGFA, CASP3, PTGS2, MMP9, and HIF1A, which may be involved in the molecular mechanism of Sanchi in treating RIRI (Chin et al., 2014; Zeng et al., 2021). Among them, the ten most closely related pairs of genes were obtained as AKT1–NOS3, AKT1–HSP90AA1, BCL2L1–TP53, CASP1–IL1B, CAV1–NOS3, CCND1–CDKN1A, CCND1–ESR1, CDKN1A–TP53, CHUK–NFKBIA, and ESR1–HSP90AA1. Analysis of these ten gene pairs showed that AKT1, CCND1, CDKN1A, ESR1, NOS3, HSP90AA1, and TP53 recurrently appear to be linked to other targets, which may play an important role in the treatment of RIRI by Sanchi (Murakami et al., 2017).

Using the screened hub genes and the drug ligand for molecular docking validation, the binding energy showed that both Sanchi and Hub genes were bound. Through qPCR detection of ten hub genes, we found that pretreatment of the PNR could regulate IL-6 and MMP9 at

postoperative day 1 and TP53 at postoperative day 7 to protect the kidneys of IRI rats, which indicates IL-6, MMP9, and TP53 could be considered crucial molecular targets of the PNR in RIRI treatment. Furthermore, detection of MMP9 protein expression in renal tissues at postoperative day 1 by WB revealed that the PNR could effectively inhibit its expression, suggesting that we could pay attention to the effect of early RIRI on MMP9 and could prevent further attack of RIRI on the organism by inhibiting its expression.

IL-6 is a 26-kD secreted protein that stimulates antibody production by B cells and plays a role in physiological activities such as growth and development and regulation of immunity and metabolism and is also an important cytokine involved in inflammatory diseases of the body. Targeting the anti-IL-6 cascade may serve as an effective approach to treat inflammatory diseases (Kang et al., 2020). As a pro-inflammatory factor, IL-6 is an inflammatory marker of RIRI (Tian et al., 2020). Studies by Im, (2020) showed that ginsenosides $Rb_1$, $Rg_1$, and $Rg_3$ can inhibit the expression of the inflammatory marker IL-6 and promote the regression of the inflammatory response. The application of notoginsenoside $R_1$ pretreatment by Fan et al., (2020) reduced IL-6 levels in RIRI. It showed that the improvement of reperfusion 24-h kidney injury in this experiment was related to the anti-inflammatory effect of the pretreatment of the PNR, which reduced the expression of IL-6.

Matrix metalloproteinase 9 (MMP9) is a gelatinase of the zinc atom-dependent endopeptidase family of matrix metalloproteinases (MMPs) (Xin et al., 2015). MMP9 can disrupt the vascular basement membrane to reduce the renal vascular density and digest the extracellular matrix (ECM) to facilitate the spread of monocyte infiltration, and indirectly activate neutrophils and promote inflammatory responses (Kwiatkowska et al., 2016). The upregulation of MMP9 expression is associated with many kidney diseases (Ersan et al., 2017), and the degree and duration of its expression could affect the extent of kidney injury (Novak et al., 2010). Notoginsenoside $R_1$ could improve ischemic injury by downregulating the MMP9 expression through the Caveolin1/MMP2/9 pathway (Liu et al., 2021a). PNGL (notoginseng leaf triterpene) reduced the pro-inflammatory mediator MMP9 and inhibited MAPK and NF-$\kappa$B signaling pathways, which had a protective effect against IRI (Xie et al., 2019). In our observation, the expression of MMP9 increased in RIRI but decreased in the PNR group, which indicated that the inhibition of MMP9 expression at 24 h of reperfusion by pretreatment of the PNR prevented further damage to the kidney tissue by ischemia–reperfusion.

The tumor suppressor gene TP53 can encode p53 protein. As the main transcription factor of the organism, p53 protein is involved in the transcription of a large number of protein-coding genes, which can mediate transcriptional regulation of biological life activity processes and play a key role in regulating cell cycle, apoptosis, cell autophagy, DNA repair, cellular senescence, and other cellular metabolism processes (Aubrey et al., 2016; Hu et al., 2019). p53 is involved in renal tubular cell senescence and accelerates renal fibrosis (Luo et al., 2018). Knockout of p53 can reduce kidney cell apoptosis, cell necrosis, oxidative stress, inflammatory response, fibrosis, and other factors to improve RIRI (Ying et al., 2014). Thus, pretreatment of the PNR inhibited TP53 gene expression to reduce renal injury at day 7 of reperfusion.

In summary, using network pharmacology methods, molecular docking techniques, qPCR, and WB, we investigated the molecular mechanism of the PNR to improve RIRI, indicating that IL-6, MMP9, and TP53 have important roles in inflammatory responses, and also affect pathophysiological activities such as apoptosis, cell necrosis, and oxidative stress in the organism. Moreover, this experiment found for the first time that the PNR could inhibit MMP9 and TP53 expression to prevent further kidney damage after IRI, which provided some theoretical basis for the subsequent clinical application of the PNR.

## 5 Conclusion

The present results showed that pretreatment with the PNR improved effectively renal injury, reduced apoptosis in RIRI rats, and protected ischemic–reperfused kidneys. The main mechanism may be related to the regulation of IL-6, MMP9, and TP53 genes. Therefore, PNR pretreatment may be a potential strategy for treating RIRI.

## Data availability statement

The original contributions presented in the study are included in the article/Supplementary Material, further inquiries can be directed to the corresponding authors.

## Ethics statement

The animal study was reviewed and approved by Animal Experimentation Ethics Review Committee of Kunming Medical University.

## Author contributions

D-DL, T-HW, and F-RX conceived and designed this experiment. NL and C-MW completed the network pharmacology section. D-DL, CC, and G-HL completed the pharmacological experiments and analyzed the data, and D-DL wrote the manuscript. All authors read and approve the manuscript.

## Conflict of interest

The authors declare that the research was conducted in the absence of any commercial or financial relationships that could be construed as a potential conflict of interest.

## Publisher's note

All claims expressed in this article are solely those of the authors and do not necessarily represent those of their affiliated organizations, or those of the publisher, the editors, and the reviewers. Any product that may be evaluated in this article, or claim that may be made by its manufacturer, is not guaranteed or endorsed by the publisher.

## Supplementary material

The Supplementary Material for this article can be found online at: https://www.frontiersin.org/articles/10.3389/fphar.2023.1134408/full#supplementary-material

## References

Aiello, S., Podestà, M. A., Rodriguez-Ordonez, P. Y., Pezzuto, F., Azzollini, N., Solini, S., et al. (2020). Transplantation-induced ischemia-reperfusion injury modulates antigen presentation by donor renal CD11c(+)F4/80(+) macrophages through IL-1R8 regulation. *J. Am. Soc. Nephrol. JASN* 31, 517–531. doi:10.1681/ASN.2019080778

Aubrey, B. J., Strasser, A., and Kelly, G. L. (2016). Tumor-suppressor functions of the TP53 pathway. *Cold Spring Harb. Perspect. Med.* 6, a026062. doi:10.1101/cshperspect.a026062

Bai, T., Li, M., Liu, Y., Qiao, Z., and Wang, Z. (2020). Inhibition of ferroptosis alleviates atherosclerosis through attenuating lipid peroxidation and endothelial dysfunction in mouse aortic endothelial cell. *Free Radic. Biol. Med.* 160, 92–102. doi:10.1016/j.freeradbiomed.2020.07.026

Basile, D. P., Anderson, M. D., and Sutton, T. A. (2012). Pathophysiology of acute kidney injury. *Compr. Physiol.* 2, 1303–1353. doi:10.1002/cphy.c110041

Bhattamisra, S. K., Koh, H. M., Lim, S. Y., Choudhury, H., and Pandey, M. (2021). Molecular and biochemical pathways of catalpol in alleviating diabetes mellitus and its complications. *Biomolecules* 11, 323. doi:10.3390/biom11020323

Bonavia, A., and Singbartl, K. (2018). A review of the role of immune cells in acute kidney injury. *Pediatr. Nephrol.* 33, 1629–1639. doi:10.1007/s00467-017-3774-5

Chan, R. Y., Chen, W. F., Dong, A., Guo, D., and Wong, M. S. (2002). Estrogen-like activity of ginsenoside Rg1 derived from Panax notoginseng. *J. Clin. Endocrinol. Metab.* 87, 3691–3695. doi:10.1210/jcem.87.8.8717

Chawla, L. S., Eggers, P. W., Star, R. A., and Kimmel, P. L. (2014). Acute kidney injury and chronic kidney disease as interconnected syndromes. *N. Engl. J. Med.* 371, 58–66. doi:10.1056/NEJMra1214243

Chen, J., Chen, Y., Shu, A., Lu, J., Du, Q., Yang, Y., et al. (2020). Radix rehmanniae and corni fructus against diabetic nephropathy via AGE-RAGE signaling pathway. *J. diabetes Res.* 2020, 8358102. doi:10.1155/2020/8358102

Chen, Z., Wang, M., Yang, S., Shi, J., Ji, T., Ding, W., et al. (2021). Butyric acid protects against renal ischemia-reperfusion injury by adjusting the treg/Th17 balance via HO-1/p-STAT3 signaling. *Front. Cell Dev. Biol.* 9, 733308. doi:10.3389/fcell.2021.733308

Chin, C. H., Chen, S. H., Wu, H. H., Ho, C. W., Ko, M. T., and Lin, C. Y. (2014). cytoHubba: identifying hub objects and sub-networks from complex interactome. *BMC Syst. Biol.* 8 (4), S11. doi:10.1186/1752-0509-8-S4-S11

Cunningham, K. S., and Gotlieb, A. I. (2005). The role of shear stress in the pathogenesis of atherosclerosis. *Lab. Invest.* 85, 9–23. doi:10.1038/labinvest.3700215

Ding, C., Han, F., Xiang, H., Wang, Y., Li, Y., Zheng, J., et al. (2019). Probiotics ameliorate renal ischemia-reperfusion injury by modulating the phenotype of macrophages through the IL-10/GSK-3β/PTEN signaling pathway. *Pflugers Arch.* 471, 573–581. doi:10.1007/s00424-018-2213-1

Ding, M., Tolbert, E., Birkenbach, M., Akhlaghi, F., Gohh, R., and Ghonem, N. S. (2021). Treprostinil, a prostacyclin analog, ameliorates renal ischemia-reperfusion injury: Preclinical studies in a rat model of acute kidney injury. *Nephrol. Dial. Transpl.* 36, 257–266. doi:10.1093/ndt/gfaa236

Erpicum, P., Rowart, P., Defraigne, J. O., Krzesinski, J. M., and Jouret, F. (2018). What we need to know about lipid-associated injury in case of renal ischemia-reperfusion. *Am. J. Physiol. Ren. Physiol.* 315, F1714–f1719. doi:10.1152/ajprenal.00322.2018

Ersan, S., TanrıSEV, M., Cavdar, Z., CelıK, A., Unlu, M., Kocak, A., et al. (2017). Pretreatment with nebivolol attenuates level and expression of matrix metalloproteinases in a rat model of renal ischaemia-reperfusion injury. *Nephrol. Carlt.* 22, 1023–1029. doi:10.1111/nep.13007

Fan, C., Chen, Q., Ren, J., Yang, X., Ru, J., Zhang, H., et al. (2020). Notoginsenoside R1 suppresses inflammatory signaling and rescues renal ischemia-reperfusion injury in experimental rats. *Med. Sci. Monit.* 26, e920442. doi:10.12659/MSM.920442

Gao, Y., Guo, Z., and Liu, Y. (2022). Analysis of the potential molecular biology of triptolide in the treatment of diabetic nephropathy: A narrative review. *Med. Baltim.* 101, e31941. doi:10.1097/MD.0000000000031941

Ge, G., Zhang, H., Li, R., and Liu, H. (2017). The function of SDF-1-CXCR4 Axis in SP cells-mediated protective role for renal ischemia/reperfusion injury by SHH/GLI1-ABCG2 pathway. *Shock* 47, 251–259. doi:10.1097/SHK.0000000000000694

Han, S. J., and Lee, H. T. (2019). Mechanisms and therapeutic targets of ischemic acute kidney injury. *Kidney Res. Clin. Pract.* 38, 427–440. doi:10.23876/j.krcp.19.062

Hasegawa, S., Inoue, T., Nakamura, Y., Fukaya, D., Uni, R., Wu, C. H., et al. (2021). Activation of sympathetic signaling in macrophages blocks systemic inflammation and protects against renal ischemia-reperfusion injury. *J. Am. Soc. Nephrol.* 32, 1599–1615. doi:10.1681/ASN.2020121723

Hou, X., Huang, M., Zeng, X., Zhang, Y., Sun, A., Wu, Q., et al. (2021). The role of TRPC6 in renal ischemia/reperfusion and cellular hypoxia/reoxygenation injuries. *Front. Mol. Biosci.* 8, 698975. doi:10.3389/fmolb.2021.698975

Hu, W., Chen, S., Thorne, R. F., and Wu, M. (2019). TP53, TP53 target genes (DRAM, TIGAR), and autophagy. *Adv. Exp. Med. Biol.* 1206, 127–149. doi:10.1007/978-981-15-0602-4_6

Huang, C., Jing, X., Wu, Q., and Ding, K. (2022). Novel pectin-like polysaccharide from Panax notoginseng attenuates renal tubular cells fibrogenesis induced by TGF-β. *Carbohydr. Polym.* 276, 118772. doi:10.1016/j.carbpol.2021.118772

Im, D. S. (2020). Pro-resolving effect of ginsenosides as an anti-inflammatory mechanism of panax ginseng. *Biomolecules* 10, 444. doi:10.3390/biom10030444

Kamarauskaite, J., Baniene, R., Trumbeckas, D., Strazdauskas, A., and Trumbeckaite, S. (2020). Increased succinate accumulation induces ROS generation in *in vivo* ischemia/reperfusion-affected rat kidney mitochondria. *Biomed. Res. Int.* 2020, 8855585. doi:10.1155/2020/8855585

Kang, S., Narazaki, M., Metwally, H., and Kishimoto, T. (2020). Historical overview of the interleukin-6 family cytokine. *J. Exp. Med.* 217, e20190347. doi:10.1084/jem.20190347

Kwiatkowska, E., Domanski, L., Bober, J., Safranow, K., Romanowski, M., Pawlik, A., et al. (2016). Urinary metalloproteinases-9 and -2 and their inhibitors TIMP-1 and TIMP-2 are markers of early and long-term graft function after renal transplantation. *Kidney Blood Press Res.* 41, 288–297. doi:10.1159/000443431

Liang, H., Xu, F., Wen, X. J., Liu, H. Z., Wang, H. B., Zhong, J. Y., et al. (2017). Interleukin-33 signaling contributes to renal fibrosis following ischemia reperfusion. *Eur. J. Pharmacol.* 812, 18–27. doi:10.1016/j.ejphar.2017.06.031

Liang, H., Xu, F., Zhang, T., Huang, J., Guan, Q., Wang, H., et al. (2018). Inhibition of IL-18 reduces renal fibrosis after ischemia-reperfusion. *Biomed. Pharmacother.* 106, 879–889. doi:10.1016/j.biopha.2018.07.031

Liu, B., Li, Y., Han, Y., Wang, S., Yang, H., Zhao, Y., et al. (2021a). Notoginsenoside R1 intervenes degradation and redistribution of tight junctions to ameliorate blood-brain barrier permeability by Caveolin-1/MMP2/9 pathway after acute ischemic stroke. *Phytomedicine* 90, 153660. doi:10.1016/j.phymed.2021.153660

Liu, C., Chen, K., Wang, H., Zhang, Y., Duan, X., Xue, Y., et al. (2020a). Gastrin attenuates renal ischemia/reperfusion injury by a PI3K/Akt/Bad-Mediated anti-apoptosis signaling. *Front. Pharmacol.* 11, 540479. doi:10.3389/fphar.2020.540479

Liu, D., Tang, S., Gan, L., and Cui, W. (2021b). Renal-protective effects and potential mechanisms of traditional Chinese medicine after ischemia-reperfusion injury. *Evid. Based Complement. Altern. Med.* 2021, 5579327. doi:10.1155/2021/5579327

Liu, H., Lu, X., Hu, Y., and Fan, X. (2020b). Chemical constituents of Panax ginseng and Panax notoginseng explain why they differ in therapeutic efficacy. *Pharmacol. Res.* 161, 105263. doi:10.1016/j.phrs.2020.105263

Liu, Y. H., Qin, H. Y., Zhong, Y. Y., Li, S., Wang, H. J., Wang, H., et al. (2021c). Neutral polysaccharide from Panax notoginseng enhanced cyclophosphamide antitumor

efficacy in hepatoma H22-bearing mice. *BMC Cancer* 21, 37. doi:10.1186/s12885-020-07742-z

Liu, Z., Meng, Y., Miao, Y., Yu, L., Wei, Q., Li, Y., et al. (2021d). Propofol ameliorates renal ischemia/reperfusion injury by enhancing macrophage M2 polarization through PPARγ/STAT3 signaling. *Aging (Albany NY)* 13, 15511–15522. doi:10.18632/aging.203107

Luo, C., Zhou, S., Zhou, Z., Liu, Y., Yang, L., Liu, J., et al. (2018). Wnt9a promotes renal fibrosis by accelerating cellular senescence in tubular epithelial cells. *J. Am. Soc. Nephrol.* 29, 1238–1256. doi:10.1681/ASN.2017050574

Mehta, R. L., Cerdá, J., Burdmann, E. A., Tonelli, M., GarcíA-GarcíA, G., Jha, V., et al. (2015). International society of nephrology's 0by25 initiative for acute kidney injury (zero preventable deaths by 2025): A human rights case for nephrology. *Lancet* 385, 2616–2643. doi:10.1016/S0140-6736(15)60126-X

Murakami, Y., Tripathi, L. P., Prathipati, P., and Mizuguchi, K. (2017). Network analysis and *in silico* prediction of protein-protein interactions with applications in drug discovery. *Curr. Opin. Struct. Biol.* 44, 134–142. doi:10.1016/j.sbi.2017.02.005

Novak, K. B., Le, H. D., Christison-Lagay, E. R., Nose, V., Doiron, R. J., Moses, M. A., et al. (2010). Effects of metalloproteinase inhibition in a murine model of renal ischemia-reperfusion injury. *Pediatr. Res.* 67, 257–262. doi:10.1203/PDR.0b013e3181ca0aa2

Sato, Y., Takahashi, M., and Yanagita, M. (2020). Pathophysiology of AKI to CKD progression. *Semin. Nephrol.* 40, 206–215. doi:10.1016/j.semnephrol.2020.01.011

Schaftenaar, F., Frodermann, V., Kuiper, J., and Lutgens, E. (2016). Atherosclerosis: The interplay between lipids and immune cells. *Curr. Opin. Lipidol.* 27, 209–215. doi:10.1097/MOL.0000000000000302

Shao, G., He, J., Meng, J., Ma, A., Geng, X., Zhang, S., et al. (2021). Ganoderic acids prevent renal ischemia reperfusion injury by inhibiting inflammation and apoptosis. *Int. J. Mol. Sci.* 22, 10229. doi:10.3390/ijms221910229

Singbartl, K., Formeck, C. L., and Kellum, J. A. (2019). Kidney-immune system crosstalk in AKI. *Semin. Nephrol.* 39, 96–106. doi:10.1016/j.semnephrol.2018.10.007

Sun, W., Li, A., Wang, Z., Sun, X., Dong, M., Qi, F., et al. (2020). Tetramethylpyrazine alleviates acute kidney injury by inhibiting NLRP3/HIF-1α and apoptosis. *Mol. Med. Rep.* 22, 2655–2664. doi:10.3892/mmr.2020.11378

Tian, Y., Shu, J., Huang, R., Chu, X., and Mei, X. (2020). Protective effect of renal ischemic postconditioning in renal ischemic-reperfusion injury. *Transl. Androl. Urol.* 9, 1356–1365. doi:10.21037/tau-20-859

Vanmassenhove, J., Kielstein, J., JöRRES, A., and Biesen, W. V. (2017). Management of patients at risk of acute kidney injury. *Lancet* 389, 2139–2151. doi:10.1016/S0140-6736(17)31329-6

Wang, J. R., Yau, L. F., Gao, W. N., Liu, Y., Yick, P. W., Liu, L., et al. (2014). Quantitative comparison and metabolite profiling of saponins in different parts of the root of Panax notoginseng. *J. Agric. Food Chem.* 62, 9024–9034. doi:10.1021/jf502214x

Wang, L., Chen, X., Wang, Y., Zhao, L., Zhao, X., and Wang, Y. (2020a). MiR-30c-5p mediates the effects of panax notoginseng saponins in myocardial ischemia reperfusion injury by inhibiting oxidative stress-induced cell damage. *Biomed. Pharmacother.* 125, 109963. doi:10.1016/j.biopha.2020.109963

Wang, Z. H., Deng, L. H., Chi, C. W., Wang, H., Huang, Y. Y., and Zheng, Q. (2020b). A preclinical systematic review of curcumin for protecting the kidney with ischemia reperfusion injury. *Oxid. Med. Cell Longev.* 2020, 4546851. doi:10.1155/2020/4546851

Wei, Q., and Dong, Z. (2012). Mouse model of ischemic acute kidney injury: Technical notes and tricks. *Am. J. Physiol. Ren. Physiol.* 303, F1487–F1494. doi:10.1152/ajprenal.00352.2012

Wu, M. Y., Yiang, G. T., Liao, W. T., Tsai, A. P., Cheng, Y. L., Cheng, P. W., et al. (2018). Current mechanistic concepts in ischemia and reperfusion injury. *Cell Physiol. Biochem.* 46, 1650–1667. doi:10.1159/000489241

Xie, L., Zhai, R., Chen, T., Gao, C., Xue, R., Wang, N., et al. (2020). Panax notoginseng ameliorates podocyte EMT by targeting the wnt/β-catenin signaling pathway in STZ-induced diabetic rats. *Drug Des. Devel Ther.* 14, 527–538. doi:10.2147/DDDT.S235491

Xie, W., Zhu, T., Dong, X., Nan, F., Meng, X., Zhou, P., et al. (2019). HMGB1-triggered inflammation inhibition of notoginseng leaf triterpenes against cerebral ischemia and reperfusion injury via MAPK and NF-κB signaling pathways. *Biomolecules* 9, 512. doi:10.3390/biom9100512

Xin, L., Hou, Q., Xiong, Q. I., and Ding, X. (2015). Association between matrix metalloproteinase-2 and matrix metalloproteinase-9 polymorphisms and endometriosis: A systematic review and meta-analysis. *Biomed. Rep.* 3, 559–565. doi:10.3892/br.2015.447

Yang, Y., Zhang, Z. X., Lian, D., Haig, A., Bhattacharjee, R. N., and Jevnikar, A. M. (2015). IL-37 inhibits IL-18-induced tubular epithelial cell expression of pro-inflammatory cytokines and renal ischemia-reperfusion injury. *Kidney Int.* 87, 396–408. doi:10.1038/ki.2014.295

Yin, J., Wang, F., Kong, Y., Wu, R., Zhang, G., Wang, N., et al. (2017). Antithrombin III prevents progression of chronic kidney disease following experimental ischaemic-reperfusion injury. *J. Cell Mol. Med.* 21, 3506–3514. doi:10.1111/jcmm.13261

Ying, Y., Kim, J., Westphal, S. N., Long, K. E., and Padanilam, B. J. (2014). Targeted deletion of p53 in the proximal tubule prevents ischemic renal injury. *J. Am. Soc. Nephrol.* 25, 2707–2716. doi:10.1681/ASN.2013121270

Younis, N. S., and Ghanim, A. M. H. (2022). The protective role of celastrol in renal ischemia-reperfusion injury by activating Nrf2/HO-1, PI3K/AKT signaling pathways, modulating NF-κb signaling pathways, and inhibiting ERK phosphorylation. *Cell Biochem. Biophys.* 80, 191–202. doi:10.1007/s12013-022-01064-6

Zager, R. A., Johnson, A., Hanson, S., and Dela Rosa, V. (2002). Altered cholesterol localization and caveolin expression during the evolution of acute renal failure. *Kidney Int.* 61, 1674–1683. doi:10.1046/j.1523-1755.2002.00316.x

Zeng, Y., Li, N., Zheng, Z., Chen, R., Peng, M., Liu, W., et al. (2021). Screening of hub genes associated with pulmonary arterial hypertension by integrated bioinformatic analysis. *Biomed. Res. Int.* 2021, 6626094. doi:10.1155/2021/6626094

Zhang, J., Guo, F., Zhou, R., Xiang, C., Zhang, Y., Gao, J., et al. (2021a). Proteomics and transcriptome reveal the key transcription factors mediating the protection of Panax notoginseng saponins (PNS) against cerebral ischemia/reperfusion injury. *Phytomedicine* 92, 153613. doi:10.1016/j.phymed.2021.153613

Zhang, J., Li, Q., Shao, Q., Song, J., Zhou, B., and Shu, P. (2018). Effects of panax notoginseng saponin on the pathological ultrastructure and serum IL-6 and IL-8 in pulmonary fibrosis in rabbits. *J. Cell Biochem.* 119, 8410–8418. doi:10.1002/jcb.27045

Zhang, M. Z., Wang, X., Wang, Y., Niu, A., Wang, S., Zou, C., et al. (2017). IL-4/IL-13-mediated polarization of renal macrophages/dendritic cells to an M2a phenotype is essential for recovery from acute kidney injury. *Kidney Int.* 91, 375–386. doi:10.1016/j.kint.2016.08.020

Zhang, Q., Cao, Y., Liu, Y., Huang, W., Ren, J., Wang, P., et al. (2021b). Shear stress inhibits cardiac microvascular endothelial cells apoptosis to protect against myocardial ischemia reperfusion injury via YAP/miR-206/PDCD4 signaling pathway. *Biochem. Pharmacol.* 186, 114466. doi:10.1016/j.bcp.2021.114466

Zhao, J., Mo, C., Shi, W., Meng, L., and Ai, J. (2021). Network pharmacology combined with bioinformatics to investigate the mechanisms and molecular targets of Astragalus radix-panax notoginseng herb pair on treating diabetic nephropathy. *Evid. Based Complement. Altern. Med.* 2021, 9980981. doi:10.1155/2021/9980981

Zhao, Y., and Yang, L. (2018). Perspectives on acute kidney injury strategy in China. *Nephrol. Carlt.* 23 (4), 100–103. doi:10.1111/nep.13458

Zhu, Y., Yin, X., Li, J., and Zhang, L. (2019). Overexpression of microRNA-204-5p alleviates renal ischemia-reperfusion injury in mice through blockage of Fas/FasL pathway. *Exp. Cell Res.* 381, 208–214. doi:10.1016/j.yexcr.2019.04.023

Zou, S., Tong, Q., Liu, B., Huang, W., Tian, Y., and Fu, X. (2020). Targeting STAT3 in cancer immunotherapy. *Mol. Cancer* 19, 145. doi:10.1186/s12943-020-01258-7

# Nephroprotective mechanisms of Rhizoma Chuanxiong and Radix et Rhizoma Rhei against acute renal injury and renal fibrosis based on network pharmacology and experimental validation

Jun Li, Tonglu Li, Zongping Li, Zhiyong Song and Xuezhong Gong*

Department of Nephrology, Shanghai Municipal Hospital of Traditional Chinese Medicine, Shanghai
University of Traditional Chinese Medicine, Shanghai, China

The molecular mechanisms of Rhizoma Chuanxiong (Chuanxiong, CX) and Rhei Radix et Rhizoma (Dahuang, DH) in treating acute kidney injury (AKI) and subsequent renal fibrosis (RF) were investigated in this study by applying network pharmacology and experimental validation. The results showed that aloe-emodin, (–)-catechin, beta-sitosterol, and folic acid were the core active ingredients, and *TP53*, *AKT1*, *CSF1R*, and *TGFBR1* were the core target genes. Enrichment analyses showed that the key signaling pathways were the MAPK and IL-17 signaling pathways. *In vivo* experiments confirmed that Chuanxiong and Dahuang pretreatments significantly inhibited the levels of SCr, BUN, UNAG, and UGGT in contrast media-induced acute kidney injury (CIAKI) rats ($p < 0.001$). The results of Western blotting showed that compared with the control group, the protein levels of p-p38/p38 MAPK, p53, and Bax in the contrast media-induced acute kidney injury group were significantly increased, and the levels of Bcl-2 were significantly reduced ($p < 0.001$). Chuanxiong and Dahuang interventions significantly reversed the expression levels of these proteins ($p < 0.01$). The localization and quantification of p-p53 expression in immunohistochemistry technology also support the aforementioned results. In conclusion, our data also suggest that Chuanxiong and Dahuang may inhibit tubular epithelial cell apoptosis and improve acute kidney injury and renal fibrosis by inhibiting p38 MAPK/p53 signaling.

## 1 Introduction

Acute kidney injury (AKI) is characterized by an abrupt loss of renal function, which mainly manifests as increased serum creatinine levels and decreased urine output (Khwaja, 2012). A meta-analysis showed that total morbidity and mortality rates of adult AKI were 21.6% and 23.9%, respectively (Susantitaphong et al., 2013). There remains no effective treatment for AKI, and prevention is currently the primary focus. While chemical and biological agents with beneficial effects on AKI have been reported, these are still in the

preclinical research stage (Yang et al., 2016; Ronco et al., 2019). Regarding the pathological mechanism of AKI, due to pathological factors, various stress processes in the kidney affect renal tubular epithelial cells by causing oxidative stress damage, inflammation, necrosis, mitochondrial dysfunction, apoptosis, and autophagy (Sureshbabu et al., 2015; Cybulsky, 2017; Kimura et al., 2017). Although the causes of AKI include renal insufficiency, nephrotoxic drugs, and sepsis, their pathological mechanisms are related to hemodynamic changes, oxidative stress, and inflammation injury. In addition to an increased near-term risk of mortality, AKI patients also have a long-term risk of CKD (See et al., 2019). After the occurrence of AKI, if the kidney tissue is repaired excessively or incompletely or if the damage persists, renal dysfunction and renal fibrosis (RF) may occur (He et al., 2017). RF is a common pathway for all kidney injuries, leading to end-stage nephropathy, characterized by tubular atrophy, epithelial cell apoptosis, massive inflammatory cell infiltration, myofibroblast activation, and over-accumulation of the extracellular matrix (Dong et al., 2019; Livingston et al., 2022). Therefore, during the treatment of AKI and subsequent CKD, we have to consider the risk of the occurrence of RF and effective prevention methods. Rhizoma Chuanxiong (Chuanxiong, CX) is derived from the dried rhizome of *Conioselinum anthriscoides* "Chuanxiong" (Apiaceae). Rhei Radix et Rhizoma (Dahuang, DH) is mainly derived from the dried roots and rhizomes of *Rheum officinale* Baill. (Polygonaceae) and *Rheum palmatum* L. (Polygonaceae). Studies have shown that the chemical components in CX mainly include volatile oils, phenolic acids, alkaloids, and polysaccharides, which have good pharmacological activities on cardiovascular and cerebrovascular diseases and the nervous system, liver, and kidneys (Chen et al., 2018). The main chemical components of DH include anthraquinones, flavonoids, and ellagitannins, which have good value in anti-myocardial ischemia and have anti-tumor, anti-inflammatory, and antioxidant effects. In addition, the bound anthraquinone components in DH have laxative effects (Zhang et al., 2021). In terms of traditional Chinese medicine (TCM) theory, *C. anthriscoides* "Chuanxiong" (Apiaceae) (Chuanxiong, CX) and *R. officinale* Baill. (Polygonaceae) (Dahuang, DH) are frequently used to dissipate stasis, activate blood, and remove toxicity (Zheng et al., 2021; Zhou L. et al., 2022). A retrospective study from Taiwan, China, involving 14,718 patients with chronic kidney disease (CKD) showed that TCM, including DH, improved long-term survival in patients with CKD (Huang et al., 2018). CX and DH reportedly reduce the AKI caused by contrast media by inhibiting oxidative stress and regulating apoptosis (Gong et al., 2013). An herbal formula mainly composed of CX and DH also improved AKI in patients with CKD (Gong, 2018). In addition, our study confirmed that tetramethylpyrazine (a characteristic alkaloid of CX) improved AKI caused by arsenic toxicity and contrast media (Gong et al., 2016; Gong et al., 2019). In multiple clinical studies, a CX- and DH-based herbal formula was shown to affect the expression of a variety of RF-associated cytokines as well as improving AKI. This raised the question of whether CX and DH further intervene in the occurrence of RF after AKI. Thus, CX and DH are natural herbs with the potential to treat AKI and RF, and their mechanisms need to be investigated. In this study, we explored the molecular mechanisms of CX and DH intervention in AKI and RF by network pharmacology and experimentally verified in an *in vivo* model.

# 2 Materials and methods

## 2.1 Establishment of CX and DH active ingredients and targets

The relevant chemical components of CX and DH were retrieved from the Traditional Chinese Medicine Systems Pharmacology Database and Analysis Platform (TCMSP) and screened according to their pharmacokinetic characteristics (Ru et al., 2014). Target active ingredients with oral bioavailability (OB) ≥30% and drug-likeness (DL) ≥ 0.18 were identified (Dong et al., 2021). In addition, active ingredients that are used as quality control indicators for CX and DH medicinal materials in the Chinese Pharmacopoeia were also included. Simultaneously, the targets of related components were obtained from TCMSP, and the target proteins were converted into standard genes using the UniProt database (Consortium, 2021). For active ingredients without targets, we predicted the target genes of these small drug molecules through PharmMapper (Liu et al., 2010). Among the predicted target genes, the 10 genes with the highest fit scores were selected for subsequent analysis.

## 2.2 Establishment of AKI- and RF-related targets

Target genes of AKI and RF were obtained from the GeneCards database, DisGeNET database (Piñero et al., 2020), Online Mendelian Inheritance in Man (OMIM) database (Amberger et al., 2015), and Therapeutic Target Database (TTD) (Zhou Y. et al., 2022). The keywords used in the search included "acute kidney injury" and "renal fibrosis." The targets identified in the four databases were combined to remove duplicates and standardize the final target names. The targets of CX and DH were crossed with the disease targets to obtain the core target of drug intervention in disease.

## 2.3 Establishment of a protein−protein interaction network

The protein−protein interaction (PPI) network comprises individual proteins that interact to participate in all aspects of life processes, including biological signal transmission, gene expression regulation, energy and material metabolism, and cell cycle regulation (Snider et al., 2015). After importing potential key target genes into the Search Tool for the Retrieval of Interacting Genes/Proteins (STRING) database (Szklarczyk et al., 2021), we constructed a PPI network to analyze the relationship between key target proteins. Each node represented a protein in the PPI network, and each edge represented a potential functional association between two target genes.

## 2.4 Construction of an "herb–component–target" network

Cytoscape version 3.7.1 was used to construct an "herb–component–disease–target" network to reflect the complex relationship between CX and DH, and the potential target genes of AKI and RF (Shannon et al., 2003). In the visual network, each node represented a compound and target genes, with the lines representing the intermolecular interactions between the compound and target genes. We analyzed the network topology parameters to identify the key compounds and target genes.

## 2.5 GO biological function annotation and KEGG pathway analyses

The potential targets were imported into the Database for Annotation, Visualization, and Integrated Discovery (DAVID) for GO biological process and KEGG pathway enrichment analyses (Huang da et al., 2009a). A threshold of $p$-value <0.05 was used to screen the top biological processes or signaling pathways and visualize the results in the R language.

## 2.6 Screening of core target genes and annotation of GEO expression profiles

Based on the "herb–component–target" network, PPI network, and KEGG analysis, key active ingredients and core target genes were selected. To further confirm the more specific core genes, we verified the expression of the genes in the Gene Expression Omnibus (GEO) database. First, we downloaded the gene set associated with AKI from the GEO database. After sample quality assessment, data standardization, batch effect removal, probe annotation, etc., differentially expressed gene analysis was performed using the limma package in R software (Ritchie et al., 2015). Finally, volcano plot and heatmap were drawn using the ggplot2 and pheatmap packages (Ito and Murphy, 2013).

## 2.7 Molecular docking verification of active ingredients and core target proteins

Based on the "herb–component–target" network, PPI network, and KEGG analysis, key active ingredients and core target proteins were selected. The structural files of the active ingredients and target proteins were downloaded from the PubChem and Protein Data Bank (PDB) databases, respectively (Goodsell et al., 2020; Kim et al., 2021). Discovery Studio v16 was used to process the active ingredient and target protein before docking and perform molecular docking. Finally, the binding activity of the active ingredient to the target protein was evaluated based on the docking score and energy.

## 2.8 Reagents and experimental animals

All chemicals were purchased from Sigma-Aldrich (St. Louis, MO, United States) unless otherwise stated. The contrast media iohexol (Omnipaque) was purchased from Amersham Health (Princeton, NJ, United States). A total of 32 adult 8-0-week-old male Sprague–Dawley rats weighing 200–250 g were purchased from the Shanghai Laboratory Animal Research Center. Rats were housed in an air-conditioned room at 23°C with a 12 h/12 h light/dark cycle. CX and DH were purchased from Shanghai Municipal Hospital of Traditional Chinese Medicine, Shanghai University of Traditional Chinese Medicine. The CX and DH herbal pair (CX 9 g and DH 18 g) was placed in a round-bottomed flask, and eight times the volume of pure water was added and steeped at room temperature for 60 min and boiled for 30 min. Then, the filtrate was filtered through gauze, and six times the volume of pure water was added to the residue and boiled for 30 min and filtered. The two aforementioned filtrates were then combined and placed in a rotary evaporator. After they were rotated, the filtrate was concentrated at 60°C until it contained 2.25 g of raw drug per mL and then set aside. Food and water were provided *ad libitum*, except for the day of dehydration. The animal study was reviewed and approved by the Medicine Animal Ethics Committee of Shanghai University of Traditional Chinese Medicine (Approval No. 2020025).

## 2.9 Induction of CIAKI and drug administration

A well-established rat model of CIAKI was used (Gong et al., 2013). A total of 32 rats were randomly divided into four groups of eight in each group: controls (CON), rats injected with CM (CIAKI), rats treated with CX and DH herbal pair (CXDH) and injected with CM (CIAKI + CXDH), and rats treated with 150 mg/kg/d N-acetylcysteine (NAC) and injected with CM(CIAKI + NAC). The CIAKI + CXDH group was filled with CXDH decoction every day for 7 days before molding, and the gavage amount was converted according to 50 times the normal amount of adult standard body weight (60 kg). The CIAKI + NAC group was given a daily dose of NAC (150 μg/g) intraperitoneally 3 days before molding. The CON and CIAKI groups were given daily gastric lavage with an equal volume of phosphate buffer 7 days before molding. The specific preparation method of the CIAKI model is as follows: SD rats were injected with a nitric oxide synthase inhibitor (NG-nitro-L-arginine methyl ester, L-NAME, 10 mg/kg, i.p.), followed after 15 and 30 min, respectively, by injection of an inhibitor of prostaglandin synthesis (indomethacin, 10 mg/kg, i.p.) and iohexol (1.5–2 g iodine/kg, i.p.). The CON group received injections of an equivalent volume of saline. Animals were euthanized 24 h after modeling, serum was obtained by blood collection from the tail vein, and kidneys were collected for biochemical and morphological examination. The study of urinary N-acetyl-β-glucosaminidase (UNAG) and urinary γ-glutamyl transpeptidase (UGGT) in 24-h urine samples was conducted on the same day.

**TABLE 1 Active ingredients of CX and DH.**

| Herb | Mol. ID | Molecule name | OB (%) | DL | MW | HL |
|---|---|---|---|---|---|---|
| Dahuang (Radix et Rhizoma Rhei) | MOL002293 | Sennoside D_qt | 61.05 | 0.61 | 524.50 | 33.92 |
| | MOL002276 | Sennoside E_qt | 50.69 | 0.61 | 524.50 | 33.59 |
| | MOL002303 | Palmidin A | 32.45 | 0.65 | 510.52 | 32.14 |
| | MOL002268 | Rhein | 47.07 | 0.28 | 284.23 | 32.12 |
| | MOL000471 | Aloe-emodin | 83.38 | 0.24 | 270.25 | 31.49 |
| | MOL002288 | Emodin-1-O-beta-D-glucopyranoside | 44.81 | 0.79 | 432.41 | 29.79 |
| | MOL002259 | Physciondiglucoside | 41.65 | 0.63 | 608.60 | 27.61 |
| | MOL002280 | Torachrysone-8-O-beta-D-(6′-oxayl)-glucoside | 43.02 | 0.74 | 480.46 | 16.29 |
| | MOL002251 | Mutatochrome | 48.64 | 0.61 | 552.96 | 15.73 |
| | MOL002235 | Eupatin | 50.80 | 0.41 | 360.34 | 13.94 |
| | MOL002297 | Daucosterol_qt | 35.89 | 0.70 | 386.73 | 6.12 |
| | MOL002260 | Procyanidin B-5,3′-O-gallate | 31.99 | 0.32 | 730.67 | 5.98 |
| | MOL000358 | Beta-sitosterol | 36.91 | 0.75 | 414.79 | 5.36 |
| | MOL002281 | Toralactone | 46.46 | 0.24 | 272.27 | 3.55 |
| | MOL000554 | Gallic acid-3-O-(6′-O-galloyl)-glucoside | 30.25 | 0.67 | 484.40 | 2.48 |
| | MOL000096 | (−)-Catechin | 49.68 | 0.24 | 290.29 | 0.38 |
| | MOL000472 | Emodin | 24.40 | 0.24 | 270.25 | 0 |
| | MOL001729 | Chrysophanol | 18.64 | 0.21 | 254.25 | 0 |
| | MOL000476 | Physcion | 22.29 | 0.27 | 284.28 | 0 |
| Chuanxiong (Rhizoma Chuanxiong) | MOL000433 | Folic acid | 68.96 | 0.71 | 441.45 | 24.81 |
| | MOL002140 | Perlolyrine | 65.95 | 0.27 | 264.30 | 12.62 |
| | MOL002157 | Wallichilide | 42.31 | 0.71 | 412.57 | 6.848 |
| | MOL001494 | Mandenol | 41.99 | 0.19 | 308.56 | 5.39 |
| | MOL000359 | Sitosterol | 36.91 | 0.75 | 414.79 | 5.37 |
| | MOL002135 | Myricanone | 40.59 | 0.51 | 356.45 | 4.39 |
| | MOL002151 | Senkyunone | 47.66 | 0.24 | 326.52 | 2.42 |
| | MOL000360 | Ferulic acid | 39.56 | 0.06 | 194.2 | 2.38 |
| | MOL002202 | Tetramethylpyrazine | 20.01 | 0.03 | 136.22 | 0 |

## 2.10 Western blot analysis

Western blotting was performed as previously described (Gong et al., 2013). The primary antibodies used were as follows: anti-p38 MAPK (Cell Signaling Technology, 1:1000); anti-phospho-p38 MAPK (Cell Signaling Technology, 1:1000); anti-GAPDH (Cell Signaling Technology, 1: 1000); anti-Bcl-2 (Affinity Biosciences, 1: 1000); anti-Bax (Cell Signaling Technology, 1: 1000); anti-β-actin (Cell Signaling Technology, 1: 1000); anti-p53 (Cell Signaling Technology, 1: 1000); anti-phosphor-p53 (Affinity Biosciences, 1: 1000); HRP-labeled goat anti-rabbit IgG (Beyotime Biotechnology, 1: 1000), and HRP-labeled goat anti-mouse IgG (Beyotime Biotechnology, 1: 1000). All

experiments were performed at least three times (i.e., three separate protein preparations) under the same conditions.

## 2.11 Statistical analysis

Results are expressed as mean ± SD. One-way analysis of variance (ANOVA) with Tukey's *post hoc* multiple-comparison test was used to determine the significance of differences in multiple comparisons. Differences were considered significant if $p < 0.05$, highly significant if $p < 0.01$, and very highly significant if $p < 0.001$.
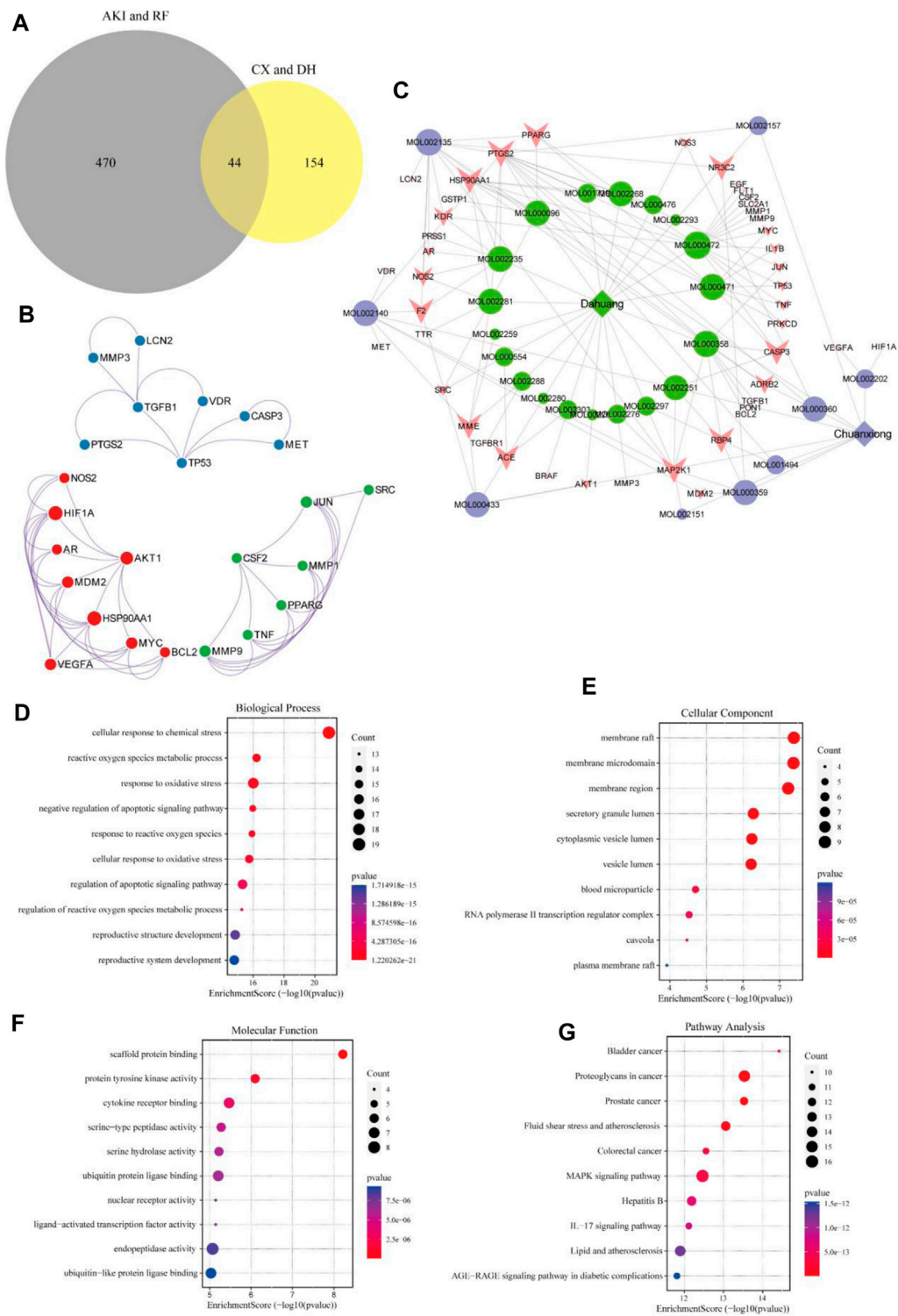
**FIGURE 1**
Target gene network construction and enrichment analysis. Venn diagram of drugs and disease genes **(A)**. PPI network of target genes **(B)**.
"Herb−component−target" network **(C)**. GO and KEGG pathway enrichment analyses **(D−G)**.

**TABLE 2 Target genes in the network.**

| Gene | Name | Gene | Name |
|------|------|------|------|
| TP53 | Tumor protein P53 | FLT1 | Fms-related receptor tyrosine kinase 1 |
| TNF | Tumor necrosis factor | MDM2 | MDM2 proto-oncogene |
| ACE | Angiotensin I-converting enzyme | PTGS2 | Prostaglandin-endoperoxide synthase 2 |
| LCN2 | Lipocalin 2 | PPARG | Peroxisome proliferator-activated receptor gamma |
| IL1B | Interleukin 1 beta | MET | MET proto-oncogene, receptor tyrosine kinase |
| F2 | Coagulation factor II | VDR | Vitamin D receptor |
| MYC | MYC proto-oncogene, bHLH transcription factor | SRC | SRC proto-oncogene, non-receptor tyrosine kinase |
| VEGFA | Vascular endothelial growth factor A | GSTP1 | Glutathione S-transferase pi 1 |
| TGFB1 | Transforming growth factor beta 1 | KDR | Kinase insert domain receptor |
| CASP3 | Caspase 3 | RBP4 | Retinol-binding protein 4 |
| NOS3 | Nitric oxide synthase 3 | PRKCD | Protein kinase C delta |
| MMP9 | Matrix metallopeptidase 9 | ADRB2 | Adrenoceptor beta 2 |
| AKT1 | AKT serine/threonine kinase 1 | NR3C2 | Nuclear receptor subfamily 3 group C member 2 |
| TTR | Transthyretin | MMP1 | Matrix metallopeptidase 1 |
| EGF | Epidermal growth factor | PON1 | Paraoxonase 1 |
| BRAF | B-Raf proto-oncogene, serine/threonine kinase | MMP3 | Matrix metallopeptidase 3 |
| NOS2 | Nitric oxide synthase 2 | HSP90AA1 | Heat shock protein 90 alpha family class A member 1 |
| MME | Membrane metalloendopeptidase | MAP2K1 | Mitogen-activated protein kinase 1 |
| BCL2 | BCL2 apoptosis regulator | SLC2A1 | Solute carrier family 2 member 1 |
| CSF2 | Colony-stimulating factor 2 | PRSS1 | Serine protease 1 |
| HIF1A | Hypoxia-inducible factor 1 subunit alpha | TGFBR1 | Transforming growth factor beta receptor 1 |
| JUN | Jun proto-oncogene, AP-1 transcription factor subunit | AR | Androgen receptor |

# 3 Results

## 3.1 Active ingredients and targets of CX and DH

Among 281 chemical components of CX and DH retrieved from the TCMSP database and screened based on pharmacokinetic characteristics (OB ≥ 30% and DL ≥ 0.18), 23 chemical components were included in the analyses. After including five characteristic compounds (emodin, chrysophanol, physcion, ferulic acid, and tetramethylpyrazine), we ended up with 28 active ingredients. In addition to OB and DL, the molecular name, molecular ID, molecular weight (MW), and half-life (HL) are shown in Table 1. Through combination and deduplication, we obtained 198 active ingredient targets of the 28 active ingredients. Information on the active ingredients and targets of CX and DH is shown in the Supplementary Material.

## 3.2 AKI- and RF-associated target genes

A total of 7,453 AKI-related target genes and 6,581 RF-related target genes were retrieved in GeneCards, of which 1,258 and 668 target genes, respectively, met the screening criteria (relevance score ≥10). A total of 185 AKI-related target genes and 570 RF-related target genes were retrieved in DisGeNET, while nine AKI-related target genes and 14 RF-related target genes were retrieved in OMIM, and three AKI-related target genes and three RF-related target genes were retrieved in TTD. The target genes retrieved from the four databases were intersected and de-duplicated to obtain a total of 514 target genes. Specific target gene information for AKI and RF retrieved from the database is available in the Supplementary Material.

## 3.3 PPI network

A total of 44 potential targets were obtained after the intersection of disease and drug target genes (Figure 1A). The 44 target genes and their full names are shown in Table 2. These 44 target genes were sequentially imported into the STRING database to obtain a PPI network diagram (Figure 1B). Simultaneously, we used CytoHubba plugins to get the top 10 hub genes in terms of connectivity. The top 10 hub genes in the PPI network are tumor necrosis factor (TNF), vascular endothelial growth factor a (VEGFA), cellular tumor antigen p53 (TP53), transcription

factor AP-1 (*JUN*), caspase-3 (*CASP3*), prostaglandin G/H synthase 2 (*PTGS2*), hypoxia-inducible factor 1 subunit alpha (*HIF1A*), epidermal growth factor (*EGF*), interleukin 1 beta (*IL1B*), and matrix metallopeptidase 9 (*MMP9*).

## 3.4 "Herb–component–target" network

To deeply explore the relationship between the active ingredients, core targets, and disease targets of CX and DH, we used Cytoscape to build an "herb–component–target" network (Figure 1C). The network contained 72 nodes, of which 28 represented active ingredients, 44 represented target genes, and 140 represented internode interaction relationships. The larger the area of the node, the more critical the position of the target or compound represented by this node in the network. The degree value was set as the screening condition. The active ingredients with a high core degree in CX are MOL002135, MOL000359, MOL002140, and MOL000433. The active ingredients with a high core degree in DH are MOL000472, MOL000358, MOL002235, MOL000471, and MOL000096. Genes with high connectivity in the network are *PTGS2*, *MAP2K1*, *HSP90AA1*, *RBP4*, *PPARG*, *MME*, *CASP3*, *NR3C2*, etc.

## 3.5 GO biological function annotation and KEGG pathway analyses

To further explore the mechanism of CX and DH in the treatment of AKI and RF, we performed GO biological function annotation and KEGG signaling pathway analyses of the 44 target genes (Huang da et al., 2009b). GO enrichment analysis was divided into biological process (BP), cellular component (CC), and molecular function (MF). The top 10 significantly enriched gene biological function catalogs for each part were used to generate histograms (Figures 1D–F). The BPs involved in these genes mainly included regulation of the apoptotic signaling pathway, negative regulation of the apoptotic signaling pathway, and response to oxidative stress. The CCs mainly included membrane raft, membrane microdomain, and secretory granule lumen. The MFs mainly included scaffold protein binding, protein tyrosine kinase activity, and cytokine receptor binding. In total, 135 signaling pathways were obtained through KEGG pathway enrichment analysis, of which the first 10 are shown in bubble diagrams (Figure 1G). As shown in Figure 1G, multiple signaling pathways were involved in the CX and DH intervention in AKI and RF, including the mitogen-activated protein kinase (MAPK) and interleukin 17 (IL-17) signaling pathways. Compared with the adjusted *p*-value and the number of enriched genes, the MAPK signaling pathway is undoubtedly the most important of these pathways.

## 3.6 Target protein screening and molecular docking

To further screen for more specific target genes, we downloaded the AKI-related GSE30718 dataset from the GEO

database that contains expression profiling data from 28 AKI patients and 11 control patients (Famulski et al., 2012). Concurrently, we visualized the differential expression of genes in the GSE30718 gene set by heatmap and volcano plot (Figures 2A, B). Finally, the expression of key target genes in the MAPK signaling pathway was visualized in the dataset (Figure 2C). Figure 2C shows that the expression of the *TP53*, *AKT1*, *CSF1R*, and *TGFBR1* genes in the AKI group was significantly different from that in the control group ($p <$ 0.05). Since *TP53* is one of the most connected genes in the top 10 hub genes, we selected p53 encoded by *TP53* as the target protein for subsequent molecular docking. The PDB ID of p53 is 6SL6 (Langenberg et al., 2020). We also chose the nine most important active ingredients in the "herb–component–target" network as small-molecule objects for docking. The structures of these small drug molecules were obtained—aloe-emodin, (−)-catechin, beta-sitosterol, eupatin, toralactone, perlolyrine, myricanone, and folic acid (three from CX and five from DH). The receptor target protein and small drug molecules were processed using Discovery Studio v16 software for docking, and a three-dimensional map of the docking results is shown in Figure 3. The docking score and absolute energy of the docking results are shown in Table 3. The results showed that folic acid, beta-sitosterol, and (−)-catechin had better docking effects and may have a potential intervention effect on p53.

## 3.7 CX and DH improved kidney injury in CIAKI rat models

As shown in Figures 4A–D, after 24 h of molding, compared with the CON group, the SCr, BUN, and UNAG levels were markedly elevated ($p <$ 0.001). Both CXDH and NAC pretreatments significantly inhibited SCr, BUN, UNAG, and UGGT in CIAKI rats, and the effects are similar ($p <$ 0.001). Histological analysis (Figure 4E) showed that compared with the CON group, the CIAKI group had severe tubulointerstitial damage, including significant tubular epithelial cell swelling and pronounced vacuolar change, and the glomeruli were basically normal. After treatment with CXDH and NAC, these signs of tissue damage were significantly alleviated.

## 3.8 CX and DH inhibit the p38 MAPK/p53-mediated apoptosis cascade in CIAKI rats

To further verify the effect of CXDH on p38 MAPK/p53 signaling, the expression levels of p38 MAPK, phospho-p38 MAPK (p-p38), p53, Bax, and Bcl-2 were determined by enzyme-linked immunosorbent assay. As shown in Figures 5A–E, the protein levels of p-p38/p38 MAPK, p53, and Bax in the CIAKI group were significantly increased, and the levels of Bcl-2 were significantly decreased ($p <$ 0.001). After CXDH intervention, the expression levels of all these proteins were reversed. The results of immunohistochemistry (IHC) techniques in Figure 5F showed that the positive expression range of p-p53 in the kidney tissue of CIAKI rats was large and the color was brown compared to the CON group. Conversely, after CXDH intervention, the staining
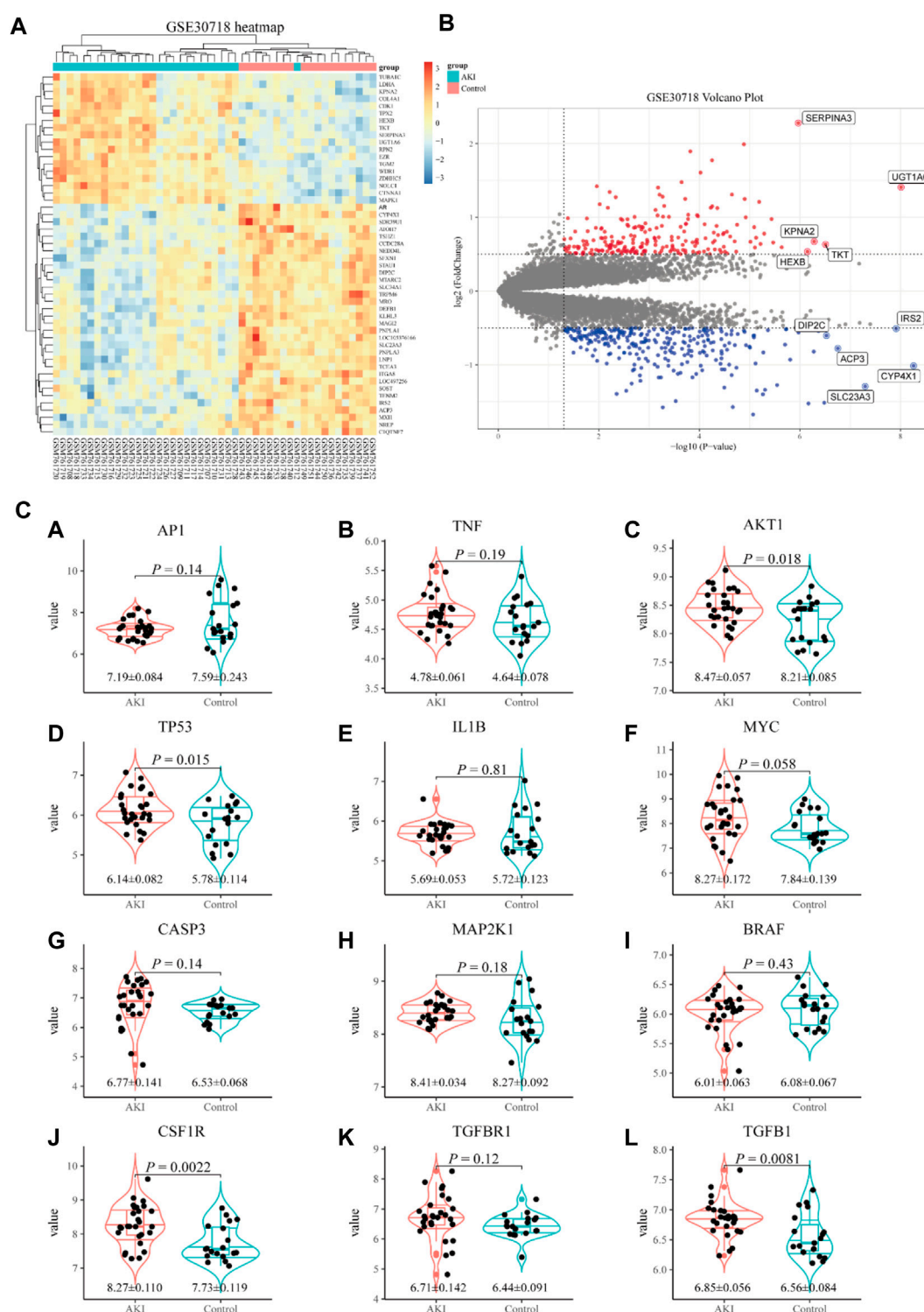
**FIGURE 2**
Screening of key target genes based on the AKI gene expression dataset GSE30718. Heatmap and volcano plot of GSE30718 **(A,B)**. Expression of the hub gene in the MAPK signaling pathway **(C)**. Compared with the control group, the expression of *AP1* **(A)**, *TNF* **(B)**, *AKT1* **(C)**, *TP53* **(D)**, *IL1B* **(E)**, *MYC* **(F)**, *CASP3* **(G)**, *MAP2K1* **(H)**, *BRAF* **(I)**, *CSF1R* **(J)**, *TGFBR1* **(K)**, and *TGFB1* **(L)** in the AKI group.

range and depth of positive expression of p-p53 protein were reduced. The results of IOD/area analysis (Figure 5G) showed that the expression of p-p53 protein in the CIAKI group was significantly increased compared to that in the CON group, and

this trend was significantly reversed after CXDH administration ($p < 0.001$). Taken together, all these findings suggest that CXDH inhibits the expression of p38 MAPK/p53-mediated apoptosis cascade in CIAKI rats and attenuates acute injury to renal tissue.
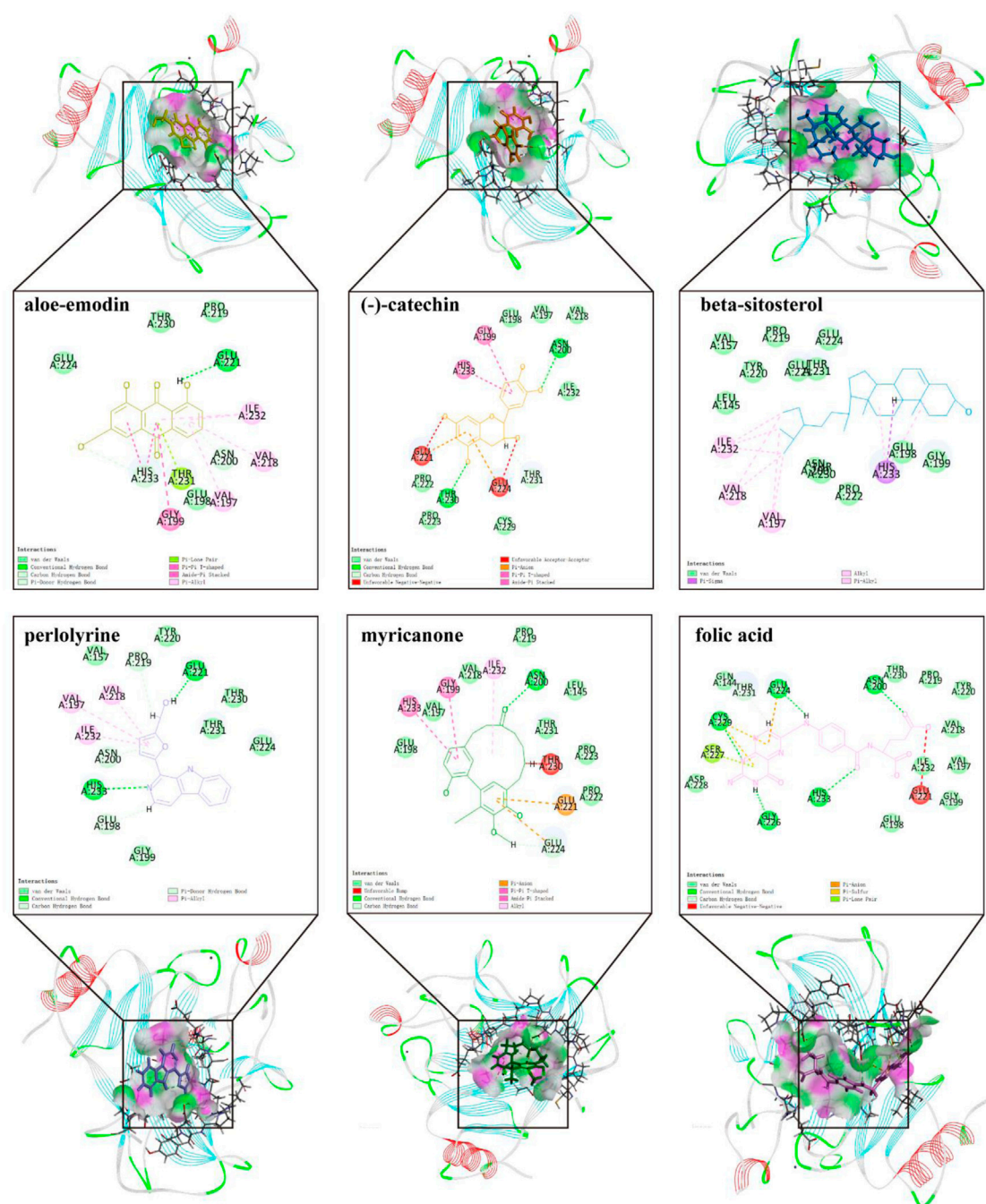
**FIGURE 3**
Results and details of molecular docking.

# 4 Discussion

AKI is an acute kidney disease characterized by acute changes in renal function (Ferenbach and Bonventre, 2015). So far, the incidence and disease burden of AKI are still increasing (Xu et al., 2015; Sawhney and Fraser, 2017). Therefore, there is an urgent need to develop effective treatment methods for AKI. AKI pathogenesis is closely related to oxidative stress, inflammatory injury, apoptosis, and activation of autophagy pathways (Kimura

et al., 2011; Linkermann et al., 2013; Rabb et al., 2016; Kusirisin et al., 2020). The results of the present study revealed that the 28 active ingredients of CX and DH play an important role in AKI treatment and are related to a variety of proteins and signaling pathways, suggesting their potential research value. The "herb–component–target" network showed that many target genes in AKI and RF are regulated by a variety of compounds. These genes included, but were not limited to, *AKT1*, *BCL2*, *CASP3*, *IL1B*, *JUN*, *MAP2K1*, *MDM2*, *MMP3*, *MYC*, *PPARG*, *PTGS2*,

TABLE 3 Docking results of molecules and p53.

| Herb | Mol. ID | Molecule name | Absolute energy | Relative energy | LibDockScore |
|------|---------|---------------|-----------------|-----------------|--------------|
| DH | MOL000472 | Emodin | 0 | 0 | 0 |
| DH | MOL000358 | Beta-sitosterol | 47.7335 | 12.0619 | 91.4289 |
| DH | MOL000471 | Aloe-emodin | 37.18 | 0 | 74.4522 |
| DH | MOL002235 | Eupatin | 0 | 0 | 0 |
| DH | MOL002281 | Toralactone | 0 | 0 | 0 |
| DH | MOL000096 | (−)-Catechin | 32.0703 | 3.2717 | 88.5165 |
| CX | MOL002135 | Myricanone | 86.067 | 10.2008 | 65.5274 |
| CX | MOL002140 | Perlolyrine | 142.725 | 0.00876478 | 84.1469 |
| CX | MOL000433 | Folic acid | 47.6251 | 4.42251 | 104.357 |

*TGFBR1*, *TNF*, and *TP53*. Enrichment analysis showed that the regulation of apoptotic signaling pathway, epithelial cell migration, response to oxidative stress, and MAPK and IL-17 signaling pathways are key parts of the mechanism.

The progression of AKI to CKD is a complex process involving the regulation of multiple cellular and signaling pathways, including inflammatory injury, cell cycle arrest, and cell death regulation, which can ultimately lead to or aggravate RF (Figure 6) (He et al., 2017; Sato et al., 2020). During the acute phase of AKI, the secretion of cytokines and chemokines by the renal tubular epithelial cells (RTECs) increases, leading to interstitial inflammatory cell infiltration. Furthermore, damaged proximal tubules can stimulate the proliferation of macrophages and alter the infiltration of inflammatory cells in the renal interstitium, including driving the transformation of M1 to M2 macrophages (Meng et al., 2014). Chronic hypoxia and inflammatory responses are closely related, and long-term sustained activation of HIF may play a key role in initiating and promoting RF by regulating multiple signaling pathways in CKD (Ullah and Basile, 2019). After renal tubular injury, cell cycle arrest in a certain phase can disrupt the normal injury repair processes. The proportion of RTECs in G2/M arrest is closely related to the degree of fibrosis (Canaud and Bonventre, 2015). The internal regulation of cell death is also involved in the development of RF. When AKI injury persists, endothelial cell apoptosis reduces the peritubular microvessel density of the renal interstitium, resulting in chronic ischemia, hypoxia, and a persistent inflammatory response in the renal interstitium, ultimately leading to RF. Autophagy also plays a bidirectional regulatory role in the conversion of AKI to CKD. Moderate autophagy may protect cells by removing damaged protein aggregates and organelles, whereas excessive autophagy could damage the kidney and promote the occurrence of RF (Shi et al., 2016; Wang et al., 2020). Additionally, the activation of the renin–angiotensin system and mitochondrial damage are both involved in RF.

According to the aforementioned results, CX and DH may improve AKI and subsequent RF by regulating downstream apoptosis through the p38 MAPK/p53 pathway. The MAPK signaling pathway can transduce related extracellular stimulus signals into the cell and nucleus through the three-level kinase cascade pathway and participate in cell proliferation, growth, apoptosis, and other processes (Zhang and Liu, 2002). This pathway is highly evolutionarily conserved and can be divided into four subfamilies: ERK, p38 MAPK, c-Jun amino-terminal kinase (JNK), and ERK5, to form a parallel MAPK signaling pathway. Among these, p38 MAPKs and JNK are involved in the treatment of AKI (Kanellis et al., 2010; Cuarental et al., 2019). p38 MAPKs and JNK have similar functions, participate in various inflammation and stress signal transduction pathways, and regulate cell apoptosis and growth. CIAKI has become a major cause of hospital-acquired AKI (Keaney et al., 2013). Studies conducted by our team and other laboratories have confirmed that apoptosis induced by contrast agents through the p38 MAPK pathway is an important pathogenic mechanism in CIAKI (Gong et al., 2010; Quintavalle et al., 2011). Therefore, p38 MAPK is a promising therapeutic target for CIAKI, and we sought to explore its associated upstream and downstream reaction elements. Apoptosis is one of the downstream effects of p38 MAPK, which is a biochemical cellular breakdown process mediated by a specific set of proteins that interact with and programmed death-induced signals (König et al., 2019). When a cell receives an apoptosis signal, it activates the initial cascade through different signaling pathways and degrades related substrates, leading to apoptosis. Due to the presence of multiple apoptosis signaling pathways, the Bcl-2 family mainly regulates cell apoptosis through the mitochondrial pathway (Chota et al., 2021). Intrarenal stress and ischemia both increase the Bax/Bcl2 ratio, which is the main determinant of cell death (Liu and Baliga, 2005). p53 is one of the elements of the downstream reaction of p38 MAPK and JNK and is also a target of interest in this study. p53 represents a family of tumor suppressors and is a key component of the cell's response to stress (Kruiswijk et al., 2015; Ong and Ramasamy, 2018). Recent experimental studies have provided evidence to support the involvement of p53 in the development of AKI and subsequent renal repair primarily by modulating apoptosis, cell cycle arrest, and so on. Inhibition of the p53-signal-mediated apoptosis process may be an effective strategy to improve tubular injury in AKI (Liu et al., 2016; Ding et al., 2021). Consistent with the findings of previous studies, we observed an increase in p38 MAPK and p53 in the kidney tissue of rats in the model group. The results showed that CX and DH
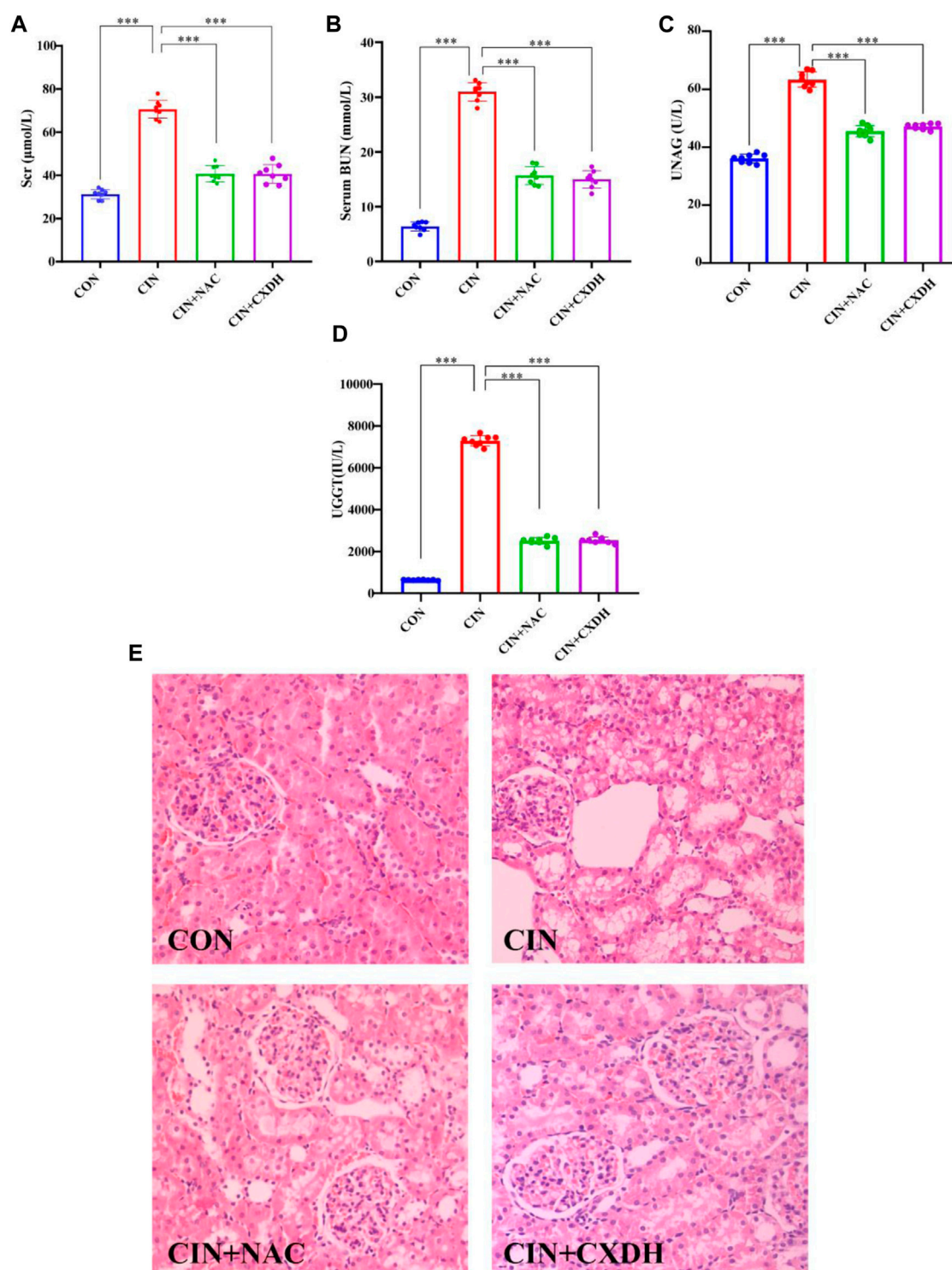
**FIGURE 4**
CX and DH protected the kidney from damage in CIAKI rats. The serum levels of creatinine **(A)**, blood urea nitrogen **(B)**, urinary N-acetyl-β-glucosaminidase **(C)**, and urinary γ-glutamyl transpeptidase **(D)** were examined using automated biochemistry assays. Photomicrographs (original magnification, ×400) illustrate hematoxylin and eosin staining of the kidney tissues from rats in the following groups **(E)**: CON, CIAKI, CIAKI + NAC, and CIAKI + CXDH. Figures are representative of 5−8 rats from each group. Data are represented as means $\pm$ standard deviation (SD; $n$ = 5). *$p$ < 0.05, **$p$ < 0.01, ***$p$ < 0.001.

reduced the expression levels of p-p38/p38 MAPK and p53 in rats with CIAKI and regulated Bcl-2 and Bax to inhibit RTEC apoptosis. In addition to apoptosis, p53 activation leads to cell cycle block that

may also promote RF after AKI. The expression of p21 is upregulated after p53 activation, and high levels of p21 lead to the downregulation of a large number of cell cycle genes, which, in
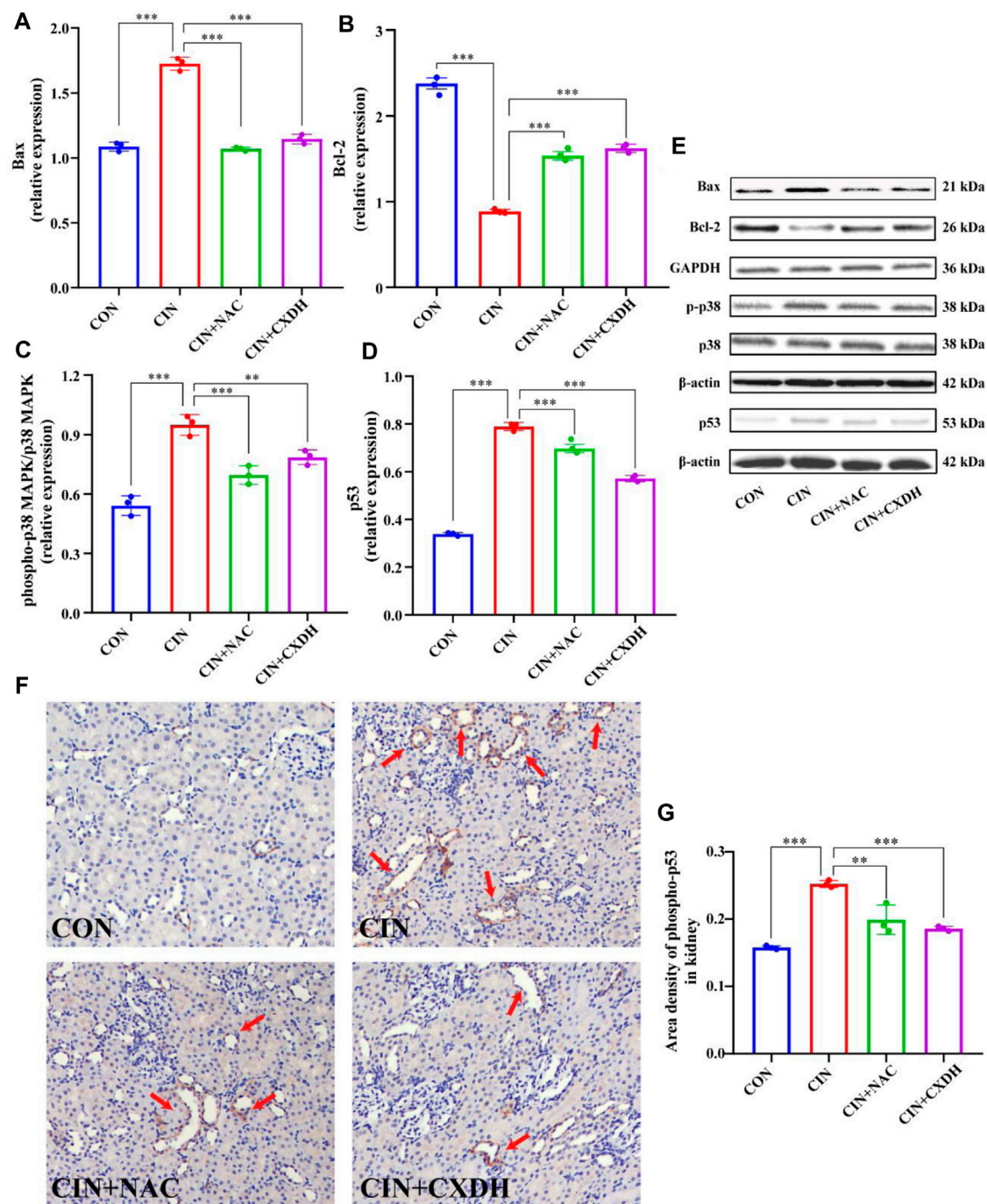
**FIGURE 5**
CX and DH inhibit the p38 MAPK/p53-mediated apoptosis cascade in CIAKI rats. The abundance of Bcl-2 **(A)** and Bax **(B)** was quantified by densitometry and normalized to that of GAPDH. Phospho-p38 MAPK and total-p38 MAPK expression levels by Western blotting (*n* = 3 each) **(C)**. Total-p53 expression by Western blotting (*n* = 3 each) **(D)**. Bcl-2, Bax, phospho-p38 MAPK, total-p38 MAPK, and p53 expression levels by Western blotting (*n* = 3 each) **(E)**. IHC staining of phospho-p53 in CON, CIAKI, CIAKI + NAC, and CIAKI + CXDH groups, respectively **(F)**. Note the positive-stained area (yellow; color refers to the online version only) of IHC staining (arrow). Semiquantitative analysis of phospho-p53 expression in kidneys with IHC **(G)**. Data are shown as means ± SD (*n* = 3 each). **p* < 0.05, ***p* < 0.01, ****p* < 0.001.

turn, leads to cell cycle arrest (Engeland, 2022). Studies have shown that hypoxia-induced upregulation of p53 inhibits the expression of cyclin-dependent kinase 1 (CDK1), cyclin B1 (CyclinB1), and cyclin D1 (CyclinD1), resulting in accumulation of cells at the G2/M phase and activation of profibrotic TGF-β-mediated signaling pathways (Liu et al., 2019). In the ischemic, toxic, and obstructive models of
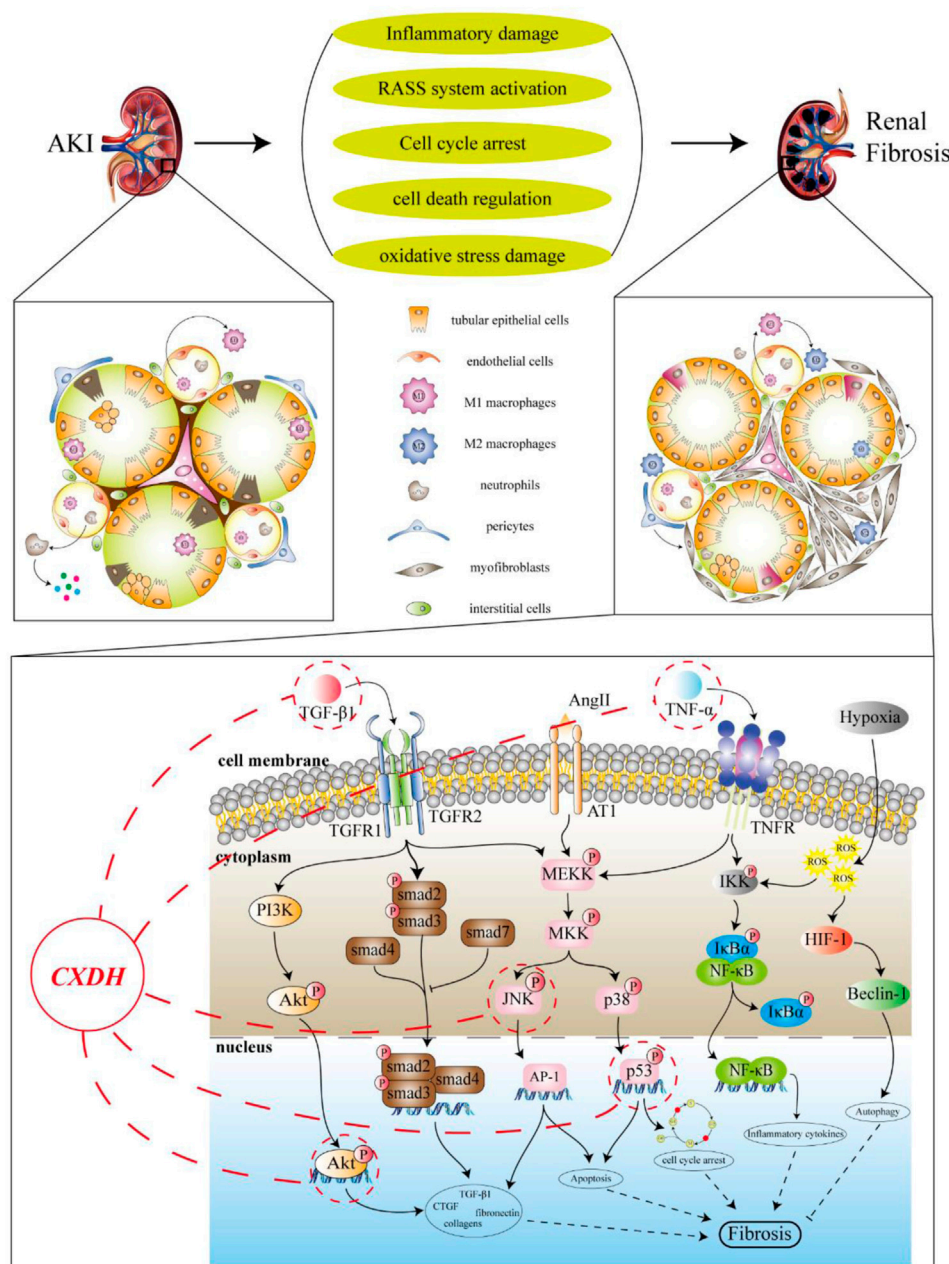
**FIGURE 6**
Target prediction of CX and DH intervention in RF. The progression of AKI to CKD is a complex process involving a variety of pathological processes including inflammatory injury, RASS system activation, cell cycle arrest, cell death, and oxidative stress injury, which can eventually lead to or worsen RF. Behind the fibrosis process, a variety of pathways and signaling molecules are activated, such as TGF-β/smad, MAPK, NF-κB, and PI3K/Akt signaling pathways. According to the target prediction results, it is speculated that CX and DH may reduce RF after AKI by regulating molecules such as p53 and Akt.

AKI, p53 inhibitors can alleviate G2/M arrest and delay the development of RF (Yang et al., 2010). Nonetheless, the role of p53 in contrast or sepsis-induced AKI, two common forms of AKI in hospitalized patients, remains poorly understood (Tang et al., 2019). Therefore, exploring the role of p53 is of practical significance in CIAKI. In summary, CX and DH may inhibit RTEC apoptosis and improve AKI and subsequent RF by inhibiting p38 MAPK/p53 signaling. Meanwhile, based on the "herb–component–target" network, MOL000471 (aloe-emodin) and MOL000472 (emodin)

can be found to have better targeting on p38 MAPK/p53 signaling. Therefore, they can provide a material basis for further mining of efficient herbal metabolites.

# 5 Conclusion

The MAPK signaling pathway plays an important role in acute kidney injury and subsequent RF. The present study emphasizes that

inhibition of renal tubular epithelial cell apoptosis via p38 MAPK/p53 signaling may be an important renoprotective mechanism of CX and DH. Nevertheless, the present study is still incomplete, and the mechanisms of intervention for renal fibrosis require further evaluation in future studies.

## Data availability statement

The datasets presented in this study can be found in online repositories. The names of the repository/repositories and accession number(s) can be found in the article/Supplementary Material.

## Ethics statement

The animal study was reviewed and approved by the Medicine Animal Ethics Committee of Shanghai University of Traditional Chinese Medicine.

## Author contributions

JL and XG designed the work of the article. JL, TL, and XG reviewed the literature available on this topic and wrote the paper. JL, TL, ZL, and ZS ensured the development of experiments and data statistics. All authors approved the paper for publication. As the leader of the project team, XG won the research fundings supporting this manuscript.

## Conflict of interest

The authors declare that the research was conducted in the absence of any commercial or financial relationships that could be construed as a potential conflict of interest.

## Publisher's note

All claims expressed in this article are solely those of the authors and do not necessarily represent those of their affiliated organizations, or those of the publisher, the editors, and the reviewers. Any product that may be evaluated in this article, or claim that may be made by its manufacturer, is not guaranteed or endorsed by the publisher.

## Supplementary material

The Supplementary Material for this article can be found online at: https://www.frontiersin.org/articles/10.3389/fphar.2023.1154743/full#supplementary-material

## References

Amberger, J. S., Bocchini, C. A., Schiettecatte, F., Scott, A. F., and Hamosh, A. (2015). OMIM.org: Online Mendelian Inheritance in Man (OMIM®), an online catalog of human genes and genetic disorders. *Nucleic Acids Res.* 43, D789–D798. doi:10.1093/nar/gku1205

Canaud, G., and Bonventre, J. V. (2015). Cell cycle arrest and the evolution of chronic kidney disease from acute kidney injury. *Nephrol. Dial. Transpl.* 30 (4), 575–583. doi:10.1093/ndt/gfu230

Chen, Z., Zhang, C., Gao, F., Fu, Q., Fu, C., He, Y., et al. (2018). A systematic review on the rhizome of Ligusticum chuanxiong Hort. (Chuanxiong). *Food Chem. Toxicol.* 119, 309–325. doi:10.1016/j.fct.2018.02.050

Chota, A., George, B. P., and Abrahamse, H. (2021). Interactions of multidomain pro-apoptotic and anti-apoptotic proteins in cancer cell death. *Oncotarget* 12 (16), 1615–1626. doi:10.18632/oncotarget.28031

Consortium, U. (2021). UniProt: The universal protein knowledgebase in 2021. *Nucleic Acids Res.* 49 (D1), D480–d489. doi:10.1093/nar/gkaa1100

Cuarental, L., Sucunza-Sáenz, D., Valiño-Rivas, L., Fernandez-Fernandez, B., Sanz, A. B., Ortiz, A., et al. (2019). MAP3K kinases and kidney injury. *Nefrol. Engl. Ed.* 39 (6), 568–580. doi:10.1016/j.nefro.2019.03.004

Cybulsky, A. V. (2017). Endoplasmic reticulum stress, the unfolded protein response and autophagy in kidney diseases. *Nat. Rev. Nephrol.* 13 (11), 681–696. doi:10.1038/nrneph.2017.129

Ding, Y., Zhou, D. Y., Yu, H., Zhu, T., Guo, F., He, Y., et al. (2021). Upregulation of lncRNA NONRATG019935.2 suppresses the p53-mediated apoptosis of renal tubular epithelial cells in septic acute kidney injury. *Cell Death Dis.* 12 (8), 771. doi:10.1038/s41419-021-03953-9

Dong, Y., Zhang, Q., Wen, J., Chen, T., He, L., Wang, Y., et al. (2019). Ischemic duration and frequency determines AKI-to-CKD progression monitored by dynamic changes of tubular biomarkers in IRI mice. *Front. Physiol.* 10, 153. doi:10.3389/fphys.2019.00153

Dong, Y., Zhao, Q., and Wang, Y. (2021). Network pharmacology-based investigation of potential targets of astragalus membranaceous-angelica sinensis compound acting on diabetic nephropathy. *Sci. Rep.* 11 (1), 19496. doi:10.1038/s41598-021-98925-6

Engeland, K. (2022). Cell cycle regulation: p53-p21-RB signaling. *Cell Death Differ.* 29 (5), 946–960. doi:10.1038/s41418-022-00988-z

Famulski, K. S., de Freitas, D. G., Kreepala, C., Chang, J., Sellares, J., Sis, B., et al. (2012). Molecular phenotypes of acute kidney injury in kidney transplants. *J. Am. Soc. Nephrol.* 23 (5), 948–958. doi:10.1681/asn.2011090887

Ferenbach, D. A., and Bonventre, J. V. (2015). Mechanisms of maladaptive repair after AKI leading to accelerated kidney ageing and CKD. *Nat. Rev. Nephrol.* 11 (5), 264–276. doi:10.1038/nrneph.2015.3

Gong, X., Celsi, G., Carlsson, K., Norgren, S., and Chen, M. (2010). N-acetylcysteine amide protects renal proximal tubular epithelial cells against iohexol-induced apoptosis by blocking p38 MAPK and iNOS signaling. *Am. J. Nephrol.* 31 (2), 178–188. doi:10.1159/000268161

Gong, X., Duan, Y., Zheng, J., Ye, Z., and Hei, T. K. (2019). Tetramethylpyrazine prevents contrast-induced nephropathy via modulating tubular cell mitophagy and suppressing mitochondrial fragmentation, CCL2/CCR2-mediated inflammation, and intestinal injury. *Oxid. Med. Cell Longev.* 2019, 7096912. doi:10.1155/2019/7096912

Gong, X., Ivanov, V. N., and Hei, T. K. (2016). 2,3,5,6-Tetramethylpyrazine (TMP) down-regulated arsenic-induced heme oxygenase-1 and ARS2 expression by inhibiting Nrf2, NF-κB, AP-1 and MAPK pathways in human proximal tubular cells. *Arch. Toxicol.* 90 (9), 2187–2200. doi:10.1007/s00204-015-1600-z

Gong, X., Wang, Q., Tang, X., Wang, Y., Fu, D., Lu, H., et al. (2013). Tetramethylpyrazine prevents contrast-induced nephropathy by inhibiting p38 MAPK and FoxO1 signaling pathways. *Am. J. Nephrol.* 37 (3), 199–207. doi:10.1159/000347033

Gong, X. Z. (2018). Recent advances in Chinese medicine for contrast-induced nephropathy. *Chin. J. Integr. Med.* 24 (1), 6–9. doi:10.1007/s11655-017-2906-x

Goodsell, D. S., Zardecki, C., Di Costanzo, L., Duarte, J. M., Hudson, B. P., Persikova, I., et al. (2020). RCSB Protein Data Bank: Enabling biomedical research and drug discovery. *Protein Sci.* 29 (1), 52–65. doi:10.1002/pro.3730

He, L., Wei, Q., Liu, J., Yi, M., Liu, Y., Liu, H., et al. (2017). AKI on CKD: Heightened injury, suppressed repair, and the underlying mechanisms. *Kidney Int.* 92 (5), 1071–1083. doi:10.1016/j.kint.2017.06.030

Huang da, W., Sherman, B. T., and Lempicki, R. A. (2009a). Bioinformatics enrichment tools: Paths toward the comprehensive functional analysis of large gene lists. *Nucleic Acids Res.* 37 (1), 1–13. doi:10.1093/nar/gkn923

Huang da, W., Sherman, B. T., and Lempicki, R. A. (2009b). Systematic and integrative analysis of large gene lists using DAVID bioinformatics resources. *Nat. Protoc.* 4 (1), 44–57. doi:10.1038/nprot.2008.211

Huang, K. C., Su, Y. C., Sun, M. F., and Huang, S. T. (2018). Chinese herbal medicine improves the long-term survival rate of patients with chronic kidney disease in taiwan: A nationwide retrospective population-based cohort study. *Front. Pharmacol.* 9, 1117. doi:10.3389/fphar.2018.01117

Ito, K., and Murphy, D. (2013). Application of ggplot2 to pharmacometric graphics. *CPT Pharmacometrics Syst. Pharmacol.* 2 (10), e79. doi:10.1038/psp.2013.56

Kanellis, J., Ma, F. Y., Kandane-Rathnayake, R., Dowling, J. P., Polkinghorne, K. R., Bennett, B. L., et al. (2010). JNK signalling in human and experimental renal ischaemia/reperfusion injury. *Nephrol. Dial. Transpl.* 25 (9), 2898–2908. doi:10.1093/ndt/gfq147

Keaney, J. J., Hannon, C. M., and Murray, P. T. (2013). Contrast-induced acute kidney injury: How much contrast is safe? *Nephrol. Dial. Transpl.* 28 (6), 1376–1383. doi:10.1093/ndt/gfs602

Khwaja, A. (2012). KDIGO clinical practice guidelines for acute kidney injury. *Nephron Clin. Pract.* 120 (4), c179–c184. doi:10.1159/000339789

Kim, S., Chen, J., Cheng, T., Gindulyte, A., He, J., He, S., et al. (2021). PubChem in 2021: New data content and improved web interfaces. *Nucleic Acids Res.* 49 (D1), D1388–d1395. doi:10.1093/nar/gkaa971

Kimura, T., Isaka, Y., and Yoshimori, T. (2017). Autophagy and kidney inflammation. *Autophagy* 13 (6), 997–1003. doi:10.1080/15548627.2017.1309485

Kimura, T., Takabatake, Y., Takahashi, A., Kaimori, J. Y., Matsui, I., Namba, T., et al. (2011). Autophagy protects the proximal tubule from degeneration and acute ischemic injury. *J. Am. Soc. Nephrol.* 22 (5), 902–913. doi:10.1681/asn.2010070705

Kønig, S. M., Rissler, V., Terkelsen, T., Lambrughi, M., and Papaleo, E. (2019). Alterations of the interactome of Bcl-2 proteins in breast cancer at the transcriptional, mutational and structural level. *PLoS Comput. Biol.* 15 (12), e1007485. doi:10.1371/journal.pcbi.1007485

Kruiswijk, F., Labuschagne, C. F., and Vousden, K. H. (2015). p53 in survival, death and metabolic health: a lifeguard with a licence to kill. *Nat. Rev. Mol. Cell Biol.* 16 (7), 393–405. doi:10.1038/nrm4007

Kusirisin, P., Chattipakorn, S. C., and Chattipakorn, N. (2020). Contrast-induced nephropathy and oxidative stress: Mechanistic insights for better interventional approaches. *J. Transl. Med.* 18 (1), 400. doi:10.1186/s12967-020-02574-8

Langenberg, T., Gallardo, R., van der Kant, R., Louros, N., Michiels, E., Duran-Romaña, R., et al. (2020). Thermodynamic and evolutionary coupling between the native and amyloid state of globular proteins. *Cell Rep.* 31 (2), 107512. doi:10.1016/j.celrep.2020.03.076

Linkermann, A., Bräsen, J. H., Darding, M., Jin, M. K., Sanz, A. B., Heller, J. O., et al. (2013). Two independent pathways of regulated necrosis mediate ischemia-reperfusion injury. *Proc. Natl. Acad. Sci. U. S. A.* 110 (29), 12024–12029. doi:10.1073/pnas.1305538110

Liu, H., and Baliga, R. (2005). Endoplasmic reticulum stress-associated caspase 12 mediates cisplatin-induced LLC-PK1 cell apoptosis. *J. Am. Soc. Nephrol.* 16 (7), 1985–1992. doi:10.1681/asn.2004090768

Liu, L., Zhang, P., Bai, M., He, L., Zhang, L., Liu, T., et al. (2019). p53 upregulated by HIF-1α promotes hypoxia-induced G2/M arrest and renal fibrosis *in vitro* and *in vivo*. *J. Mol. Cell Biol.* 11 (5), 371–382. doi:10.1093/jmcb/mjy042

Liu, M., Huang, G., Wang, T. T., Sun, X., and Yu, L. L. (2016). 3-MCPD 1-palmitate induced tubular cell apoptosis *in vivo* via JNK/p53 pathways. *Toxicol. Sci.* 151 (1), 181–192. doi:10.1093/toxsci/kfw033

Liu, X., Ouyang, S., Yu, B., Liu, Y., Huang, K., Gong, J., et al. (2010). PharmMapper server: A web server for potential drug target identification using pharmacophore mapping approach. *Nucleic Acids Res.* 38, W609–W614. doi:10.1093/nar/gkq300

Livingston, M. J., Shu, S., Fan, Y., Li, Z., Jiao, Q., Yin, X. M., et al. (2022). Tubular cells produce FGF2 via autophagy after acute kidney injury leading to fibroblast activation and renal fibrosis. *Autophagy* 19, 256–277. doi:10.1080/15548627.2022.2072054

Meng, X., Nikolic-Paterson, D., and Lan, H. (2014). Inflammatory processes in renal fibrosis. *Nat. Rev. Nephrol.* 10 (9), 493–503. doi:10.1038/nrneph.2014.114

Ong, A. L. C., and Ramasamy, T. S. (2018). Role of Sirtuin1-p53 regulatory axis in aging, cancer and cellular reprogramming. *Ageing Res. Rev.* 43, 64–80. doi:10.1016/j.arr.2018.02.004

Piñero, J., Ramírez-Anguita, J. M., Saüch-Pitarch, J., Ronzano, F., Centeno, E., Sanz, F., et al. (2020). The DisGeNET knowledge platform for disease genomics: 2019 update. *Nucleic Acids Res.* 48 (D1), D845–D855. doi:10.1093/nar/gkz1021

Quintavalle, C., Brenca, M., De Micco, F., Fiore, D., Romano, S., Romano, M. F., et al. (2011). *In vivo* and *in vitro* assessment of pathways involved in contrast media-induced renal cells apoptosis. *Cell Death Dis.* 2 (5), e155. doi:10.1038/cddis.2011.38

Rabb, H., Griffin, M. D., McKay, D. B., Swaminathan, S., Pickkers, P., Rosner, M. H., et al. (2016). Inflammation in AKI: Current understanding, key questions, and knowledge gaps. *J. Am. Soc. Nephrol.* 27 (2), 371–379. doi:10.1681/asn.2015030261

Ritchie, M. E., Phipson, B., Wu, D., Hu, Y., Law, C. W., Shi, W., et al. (2015). Limma powers differential expression analyses for RNA-sequencing and microarray studies. *Nucleic Acids Res.* 43 (7), e47. doi:10.1093/nar/gkv007

Ronco, C., Bellomo, R., and Kellum, J. A. (2019). Acute kidney injury. *Lancet* 394 (10212), 1949–1964. doi:10.1016/s0140-6736(19)32563-2

Ru, J., Li, P., Wang, J., Zhou, W., Li, B., Huang, C., et al. (2014). Tcmsp: A database of systems pharmacology for drug discovery from herbal medicines. *J. Cheminform* 6, 13. doi:10.1186/1758-2946-6-13

Sato, Y., Takahashi, M., and Yanagita, M. (2020). Pathophysiology of AKI to CKD progression. *Seminars Nephrol.* 40 (2), 206–215. doi:10.1016/j.semnephrol.2020.01.011

Sawhney, S., and Fraser, S. D. (2017). Epidemiology of AKI: Utilizing large databases to determine the burden of AKI. *Adv. Chronic Kidney Dis.* 24 (4), 194–204. doi:10.1053/j.ackd.2017.05.001

See, E. J., Jayasinghe, K., Glassford, N., Bailey, M., Johnson, D. W., Polkinghorne, K. R., et al. (2019). Long-term risk of adverse outcomes after acute kidney injury: A systematic review and meta-analysis of cohort studies using consensus definitions of exposure. *Kidney Int.* 95 (1), 160–172. doi:10.1016/j.kint.2018.08.036

Shannon, P., Markiel, A., Ozier, O., Baliga, N. S., Wang, J. T., Ramage, D., et al. (2003). Cytoscape: A software environment for integrated models of biomolecular interaction networks. *Genome Res.* 13 (11), 2498–2504. doi:10.1101/gr.1239303

Shi, M., Flores, B., Gillings, N., Bian, A., Cho, H. J., Yan, S., et al. (2016). αKlotho mitigates progression of AKI to CKD through activation of autophagy. *J. Am. Soc. Nephrol.* 27 (8), 2331–2345. doi:10.1681/asn.2015060613

Snider, J., Kotlyar, M., Saraon, P., Yao, Z., Jurisica, I., and Stagljar, I. (2015). Fundamentals of protein interaction network mapping. *Mol. Syst. Biol.* 11 (12), 848. doi:10.15252/msb.20156351

Sureshbabu, A., Ryter, S. W., and Choi, M. E. (2015). Oxidative stress and autophagy: Crucial modulators of kidney injury. *Redox Biol.* 4, 208–214. doi:10.1016/j.redox.2015.01.001

Susantitaphong, P., Cruz, D. N., Cerda, J., Abulfaraj, M., Alqahtani, F., Koulouridis, I., et al. (2013). World incidence of AKI: A meta-analysis. *Clin. J. Am. Soc. Nephrol.* 8 (9), 1482–1493. doi:10.2215/cjn.00710113

Szklarczyk, D., Gable, A. L., Nastou, K. C., Lyon, D., Kirsch, R., Pyysalo, S., et al. (2021). The STRING database in 2021: Customizable protein-protein networks, and functional characterization of user-uploaded gene/measurement sets. *Nucleic Acids Res.* 49, D605–d612. doi:10.1093/nar/gkaa1074

Tang, C., Ma, Z., Zhu, J., Liu, Z., Liu, Y., Liu, Y., et al. (2019). P53 in kidney injury and repair: Mechanism and therapeutic potentials. *Pharmacol. Ther.* 195, 5–12. doi:10.1016/j.pharmthera.2018.10.013

Ullah, M. M., and Basile, D. P. (2019). Role of renal hypoxia in the progression from acute kidney injury to chronic kidney disease. *Semin. Nephrol.* 39 (6), 567–580. doi:10.1016/j.semnephrol.2019.10.006

Wang, Y., Cai, J., Tang, C., and Dong, Z. (2020). Mitophagy in acute kidney injury and kidney repair. *Cells* 9 (2), 338. doi:10.3390/cells9020338

Xu, X., Nie, S., Liu, Z., Chen, C., Xu, G., Zha, Y., et al. (2015). Epidemiology and clinical correlates of AKI in Chinese hospitalized adults. *Clin. J. Am. Soc. Nephrol.* 10 (9), 1510–1518. doi:10.2215/cjn.02140215

Yang, L., Besschetnova, T. Y., Brooks, C. R., Shah, J. V., and Bonventre, J. V. (2010). Epithelial cell cycle arrest in G2/M mediates kidney fibrosis after injury. *Nat. Med.* 16 (5), 535–543. doi:10.1038/nm.2144

Yang, Y., Song, M., Liu, Y., Liu, H., Sun, L., Peng, Y., et al. (2016). Renoprotective approaches and strategies in acute kidney injury. *Pharmacol. Ther.* 163, 58–73. doi:10.1016/j.pharmthera.2016.03.015

Zhang, Q., Chen, Y. Y., Yue, S. J., Wang, W. X., Zhang, L., and Tang, Y. P. (2021). Research progress on processing history evolution as well as effect on chemical compositions and traditional pharmacological effects of Rhei Radix et Rhizoma. *Zhongguo Zhong Yao Za Zhi* 46 (3), 539–551. doi:10.19540/j.cnki.cjcmm.20201105.601

Zhang, W., and Liu, H. T. (2002). MAPK signal pathways in the regulation of cell proliferation in mammalian cells. *Cell Res.* 12 (1), 9–18. doi:10.1038/sj.cr.7290105

Zheng, Y. Q., Zeng, J. X., Lin, J. X., Xia, Y. F., and He, G. H. (2021). Herbal textual research on Chuanxiong Rhizoma in Chinese classical prescriptions. *Zhongguo Zhong Yao Za Zhi* 46 (16), 4293–4299. doi:10.19540/j.cnki.cjcmm.20210523.104

Zhou, L., Sun, J., Zhang, T., Tang, Y., Liu, J., Gao, C., et al. (2022a). Comparative transcriptome analyses of different Rheum officinale tissues reveal differentially expressed genes associated with anthraquinone, catechin, and gallic acid biosynthesis. *Genes (Basel)* 13 (9), 1592. doi:10.3390/genes13091592

Zhou, Y., Zhang, Y., Lian, X., Li, F., Wang, C., Zhu, F., et al. (2022b). Therapeutic target database update 2022: Facilitating drug discovery with enriched comparative data of targeted agents. *Nucleic Acids Res.* 50 (D1), D1398–d1407. doi:10.1093/nar/gkab953

# Yue-bi-tang attenuates adriamycin-induced nephropathy edema through decreasing renal microvascular permeability via inhibition of the Cav-1/ eNOS pathway

Tingting Li[1,2,3,4†], Su Cheng[1,2,3,4†], Lin Xu[1,2,3,4], Pinglan Lin[1,2,3,4] and Minghai Shao[1,2,3,4]*

[1]Department of Nephrology, Shuguang Hospital Affiliated to Shanghai University of Traditional Chinese Medicine, Shanghai, China, [2]Key Laboratory of Liver and Kidney Diseases, Ministry of Education, Shanghai University of Traditional Chinese Medicine, Shanghai, China, [3]TCM Institute of Kidney Disease, Shanghai University of Traditional Chinese Medicine, Shanghai, China, [4]Shanghai Key Laboratory of Traditional Chinese Clinical Medicine, Shanghai University of Traditional Chinese Medicine, Shanghai, China

Edema is one of the most typical symptoms of nephrotic syndrome. Increased vascular permeability makes a significant contribution to the progression of edema. Yue-bi-tang (YBT) is a traditional formula with excellent clinical efficacy in the treatment of edema. This study investigated the effect of YBT on renal microvascular hyperpermeability-induced edema in nephrotic syndrome and its mechanism. In our study, the content of target chemical components of YBT was identified using UHPLC-Q-Orbitrap HRMS analysis. A nephrotic syndrome model was replicated based on male Sprague-Dawley rats with Adriamycin (6.5 mg/kg) by tail vein injection. The rats were randomly divided into control, model, prednisone, and YBT (22.2 g/kg, 11.1 g/kg, and 6.6 g/kg) groups. After 14 d of treatment, the severity of renal microvascular permeability, edema, the degree of renal injury, and changes in the Cav-1/ eNOS pathway were assessed. We found that YBT could regulate renal microvascular permeability, alleviate edema, and reduce renal function impairment. In the model group, the protein expression of Cav-1 was upregulated, whereas VE-cadherin was downregulated, accompanied by the suppression of p-eNOS expression and activation of the PI3K pathway. Meanwhile, an increased NO level in both serum and kidney tissues was observed, and the above situations were improved with YBT intervention. It thus indicates YBT exerts therapeutic effects on the edema of nephrotic syndrome, as it improves the hyperpermeability of renal microvasculature, and that YBT is engaged in the regulation of Cav-1/eNOS pathway-mediated endothelial function.

KEYWORDS

Yue-Bi-tang, microvascular permeability, nephrotic syndrome, Cav-1/eNOS, edema

## Introduction

Nephrotic syndrome (NS), one cause of end-stage kidney disease, is characterized by massive proteinuria with peripheral edema, hypoalbuminemia, and hypercholesterolemia as its main clinical features (Hull and Goldsmith, 2008). Although edema is the cardinal manifestation of NS at the onset of illness, its mechanisms and therapeutic strategies of edema have long been studied and have sparked heated debates (Siddall and Radhakrishnan, 2012; Meena and Bagga, 2020). Microvascular hyperpermeability is critical in the pathophysiology of nephrotic edema associated with NS (Rostoker et al., 2000; Siddall et al., 2017). As a consequence, attenuating renal microvascular hyperpermeability might be a key element in preventing edema in the progression of NS.

In addition to the transcellular and paracellular routes, vascular permeability could also occur via caveolae-mediated transcellular pathways (Bauer et al., 2005). Caveolae, 50–100 nm flask-shaped invaginations of the plasma membrane, are abundant in endothelial cells with approximately 73 caveolae per $\mu m^2$ of the endothelium (Xu et al., 2018). Caveolin-1 (Cav-1), the main component of caveolae on the plasma membrane, is a 21–22 KD protein with multiple functions, including plasma protein transport and sorting of signaling molecules such as endothelial nitric oxide synthase (eNOS) and nonreceptor tyrosine kinases (Zhang et al., 2020; Guerit et al., 2021; Luo et al., 2021). Cav-1 inactivates nitric oxide (NO) signaling by binding and inhibiting eNOS, thus regulating vascular permeability and angiogenesis (Frank et al., 2003). Garrean et al. confirmed that the knockout of Cav-1 and the activation of eNOS could attenuate lung microvascular hyperpermeability and edema formation in mice (Garrean et al., 2006). However, the change of the expression in Cav-1 and the activation of eNOS in NS could be attractive targets to ameliorate edema.

Yue-bi-tang (YBT), a popular traditional Chinese herbal medicine, has been widely used clinically to treat edema in NS. It consists of five Chinese herbs: *Ephedra sinica Stapf* (Ma Huang), *Zingiber officinale Roscoe* (Sheng Jiang), *Gypsum Fibrosum* (Shi Gao), *Ziziphus zizyphus* (Da Zao), and *Glycyrrhizae Radix et Rhizoma* (Gan Cao), aiming to "dispel the wind and disperse lung-qi for diuresis." YBT can effectively relieve edema from kidney injuries such as acute glomerulonephritis (Hu et al., 2020). However, the specific molecular mechanisms by which YBT alleviates Adriamycin-induced nephropathy edema remain unknown, which has been limiting its wider use.

The goal of this study is to investigate whether YBT could alleviate Adriamycin-induced nephropathy edema and reduce renal microvascular permeability by inactivating the Cav-1/eNOS pathway.

## Materials and methods

### Animals and drugs

Male Sprague–Dawley (SD) rats (weighing 220 ± 20g) were purchased from Shanghai Bikai Laboratory Animal Technology Co., Ltd. [number: SCXK (Hu) 2018-0006]. All the rats used in the experiments were housed under standard temperature (23°C ± 3°C) and humidity (55% ± 15%) with a 12 h light/12 h dark cycle in SPF condition while being fed with water and food as standard in the Experimental Animal Center of Shanghai University of TCM. The

animal study was reviewed and approved by the Animal Ethics Committee of Shanghai University of Traditional Chinese Medicine (PZSHUTCM220725025).

YBT consists of *Ephedra* 18 g, *Ginger* 9 g, *Gypsum* 24 g, *Fructus Ziziphi Jujubae* 9 g, and *Liquorice* 6 g. The raw herbs for the preparation of YBT were obtained from Shanghai Kangqiao Chinese Medicine Tablet Co., Ltd. (Shanghai, China). All materials were soaked with distilled water 1 time for 30 min and then boiled for 2 h. The medicinal residue from the first extraction was filtered for the second extraction with the same extracting condition. After repeating three times, the mixture of the filtrates was enriched to a concentration of 2.1 g of raw materials per milliliter (w/v). Prednisone was purchased from Guangdong Huanan Pharmaceutical (Guangdong, China). Prednisone was dissolved and diluted in a saline solution with a concentration of 2.5 mg/mL.

### UHPLC-Q-orbitrap HRMS analysis of YBT

The aqueous extract of YBT was treated with a 0.22 μm filter membrane for UHPLC-Q-Orbitrap HRMS analysis. The fingerprints of YBT extracts were obtained by ultra-high-performance liquid chromatography (UHPLC-Q-Orbitrap HRMS, Thermo Fisher Scientific Inc., Grand Island, NY, United States) which was Thermo Fisher Dionex Ultimate 3000 using Chromeleon 7.2 software for operation. UHPLC conditions: The sample chamber was protected from light, the temperature was set at 10°C, and the column temperature was set at 40°C. The separation was performed through an ACQUITY UPLC BEH C18 column (2.1 × 100 mm, 1.7 μm) using a mobile phase of methanol and 0.1% formic acid delivered in gradient elution at a flow rate of 0.3 mL/min: 0-2 min, 4% methanol; 2-6 min, 4%-12% methanol; 6-38 min, 12%-70% methanol; 38-38.5 min, 70% methanol; 38.5-39 min, 70%-95% methanol; 39-43 min, 95% methanol; 43-45 min, 4% methanol. The injection volume was 2 μL. Q-Orbitrap HRMS conditions: The UHPLC tandem quadrupole/ electrostatic field orbital trap mass spectrometry was equipped with an electrospray ion source, and data were analyzed and acquired through Xcalibur 4.1. The ion source was used in positive and negative ion modes, and the optimized mass spectrometry parameters included: capillary temperature of 325°C; sheath gas ($N_2$) flow rate of 45 arb; auxiliary gas ($N_2$) flow rate of 8 arb; sweep gas flow rate of 0 arb; spray voltage of 2.5 kV (negative ions) and 3.2 kV (positive ions); transmission voltage of 50 V; and auxiliary gas heater temperature of 300°C. Full scan mode was used: scan range 80-1200 m/z. Full scan mode was adopted: scan range 80-1200 m/z. Quantitative and qualitative analysis were conducted on ephedrine [(M + H)+, *m/z* 166.12262)], pseudoephedrine [(M + H)+, *m/z* 166.12262], 6-gingerol [(M + Na)+, *m/z* 317.17206], and 8-gingerol [(M + Na)+, *m/z* 345.20343], 10-gingerol [(M + Na)+, *m/z* 373.23483], glycyrrhizin [(M-H)-, *m/z* 417.11877], and glycyrrhetinic acid [(M-H)-, *m/z* 821.396,427]. Maximum injection time (IT): 200 m; scan resolution 70,000 FWHM (m/z/s); automatic gain control (AGC) target: $1.0e^6$.

### Groups and drug administration

After 1 week of acclimatization, apart from the 10 rats randomized into the control group with saline (1.0 mL/100 g), we intravenously administered the rest with Adriamycin (ADR, 6.5 mg/kg dissolved in

saline, Shenzhen Main Luck Pharmaceuticals Inc.) to establish a NS rat model (Teng et al., 2017). In other words, a nephritis model was established by injecting Adriamycin in the caudal vein only once. Two weeks after injection, the successful modeling rats with higher 24 h proteinurias were randomly divided into five groups (10 animals in each group): model group, prednisone (5.0 mg/kg, Guangdong Huanan Pharmaceutical, China) group, and YBT group (YBT 22.2 g/kg, 11.1 g/kg and 6.6 g/kg). The dosage of YBT was calculated according to the equivalent dosage formula of rats and the adult weight of 65 kg. The gavage dosages of YBT and prednisone were also chosen based on the clinical dosage and the result of our preliminary experiment. All the rats were administered distilled water (control group and model group), prednisone, or YBT by means of oral gavage oral gavage once a day for 2 weeks.

## Blood and uric indexes analysis

To assess urinary protein levels, the 24 h urine was acquired on days 0, 14, 21, and 28 with a metabolic cage, respectively. At the end of interventions, blood, and renal tissues were collected. The levels of 24 h urine protein (24 h UTP), albumin (ALB), total cholesterol (TC), serum creatinine (Scr), urea nitrogen (BUN), and hemoglobin (HB) were detected by the automatic biochemical analyzer (AU680, Beckman Coulter, United States) in Clinical Laboratory of Shuguang hospital.

## Kidney and skin wet-to-dry (W/D) weight ratio

The skin and kidneys were removed, washed with physiological saline, and the surface liquid was blotted out with filter paper, weighed wet, and recorded. After putting them into a constant temperature incubator at 50°C for drying, the dry weights were weighed after 72 h. Based on the wet-to-dry weight (W/D) ratio, the degree of kidney and skin edema was evaluated.

## Evans blue staining

Referring to related studies (Aman et al., 2012; Koning et al., 2018), renal microvascular permeability can be evaluated using the Evans Blue dye extravasation method. The 2% Evans Blue (EB) (Sigma-Aldrich, F9037, United States) was injected into the tail vein at 1 mL/kg, circulated *in vivo* for 1 h and perfused with PBS to remove the intravascular Evans Blue dye. Kidney tissues with 100 mg of Evans blue dye were extracted by putting the tissues in formamide (Sigma-Aldrich, F9037, United States) at 1 g/mL. After incubating at 60°C for 24 h, we detected the OD value at the wavelength of 620 nm using the microplate reader (Cytation 3, Biotek, United States)

## Western blot analysis

The total proteins of kidney tissues were extracted with a RIPA lysis buffer including protein hydrolase and phosphatase inhibitors. Protein concentration was calculated using a BCA protein analysis kit (Beyotime Biotech, P0010, China) following the instructions of the manufacturer.

Protein samples were separated by 8% or 1% SDS-PAGE electrophoresis for 90 min, transferred to polyvinylidene difluoride membranes (Millipore, United States) (100 V, 1-2 h), and blocked in 5% non-fat milk in a shaker for 2 h at the room temperature. Afterwards, the membranes were incubated overnight at 4°C with corresponding primary antibodies as follows: anti-Cav-1 (CST, 3267, United States), anti-VE-cadherin (Santa, sc-9989, United States), anti-p-eNOS (Affinity, AF3247, China), anti-p-AKT (CST, 4060, United States), anti-AKT (CST, 4691, United States), anti-PI3K (CST, 4292, United States) and anti-Gapdh (Proteintech, 60004-1-Ig, United States). The binding of the primary antibody was detected by the ECL method (180-501 ECL, Tanon, China) using horseradish peroxidase-conjugated secondary antibodies (goat anti-rabbit IgG, A0208 or goat anti-mouse IgG, A0216, Beyotime Biotech, China). Quantitative analysis was performed using ImageJ software (NIH, Bethesda, MD, United States).

## Histological staining of renal tissue

Kidney tissues were fixed in a 4% paraformaldehyde solution, dehydrated in graded alcohol, embedded in paraffin, and cut into 3 μm slices. After that, hematoxylin-eosin (H&E) staining, Masson's trichrome, and periodic acid-Schiff (PAS) staining were performed according to the standard method. The pathological changes in the glomerulus were observed under light microscopy (Nikon Eclipse 80i, Japan).

## Immunofluorescence (IF) and immunohistochemistry (IHC) analysis

After dewaxing the kidney samples with xylene, the antigen was repaired and closed with 3% BSA at room temperature for 30 min, and the primary antibody Cav-1 (1:100, CST), VE-cadherin (1:50, Santa) were incubated overnight at 4°C, protected from light. Then the sections were washed twice with PBS, incubated in fluorescent secondary antibody for 1 h at 37°C, protected from light, washed with PBS, and stained with DAPI for 5 min. The positive expressions were observed with a fluorescence microscope (Nikon Eclipse80i, Japan) at ×400 magnification. For immunohistochemistry staining, kidney tissues were paraffin sections dewaxed to water, and antigens were repaired. After blocking endogenous peroxidase, anti-p-eNOS (1:50, Affinity, AF3247, China) was added and then incubated overnight at 4°C. Sections were rinsed 3 times in PBS. Then secondary antibodies were incubated at room temperature for 50 min. DAB staining kit (Suokeer, biotech, Nanjing, China) was used for color enhancement and observed under bright field microscopy (Nikon Eclipse 80i, Japan) at ×400 magnification, with positive expression as brownish-yellow particles. Four areas randomly selected in each section were photographed and analyzed by Image-Pro plus version 6.0.

## Evaluation of NO levels

We quantified the NO level in rats' serum and kidney tissues according to the kit specifications (Nanjing Jiancheng Bioengineering Institute, A013-2-1, China), and measured the absorbance of each sample at 550 nm on an enzyme calibrator.
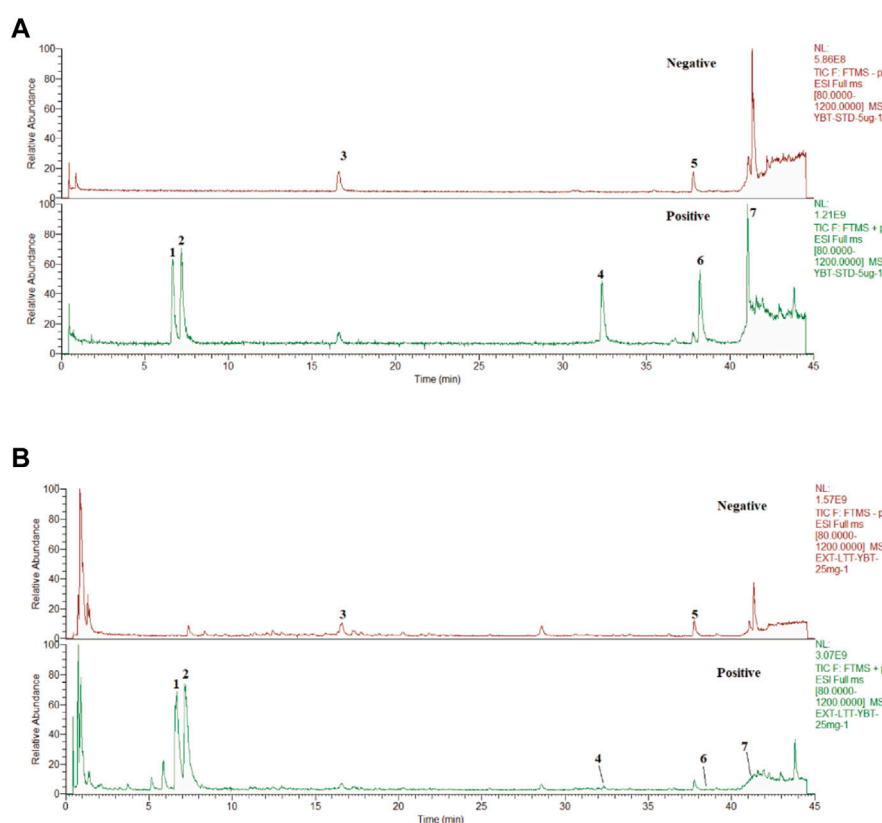
**FIGURE 1**
YBT quality control by UHPLC-Q-Orbitrap HRMS analysis. **(A)** The fingerprint chromatograms of the extract of mixture reference standards in positive and negative ion mode by UHPLC-Q-Orbitrap HRMS.1 = Ephedrine, 2 = pseudoephedrine, 3 = liquidity, 4 = 6-gingerol,5 = glycyrrhizic acid,6 = 8-gingerol,7 = 10-gingerol. **(B)** The fingerprint chromatograms of the extract of YBT in positive and negative ion mode by UHPLC-Q-Orbitrap HRMS. 1 = Ephedrine, 2 = pseudoephedrine, 3 = liquiritin, 4 = 6-gingerol, 5 = glycyrrhizic acid, 6 = 8-gingerol, 7 = 10-gingerol.

## Statistical analysis

All data were expressed as mean ± standard deviation (SD) and analyzed by one-way analysis of variance with LSD-t multiple comparisons using SPSS software (version 26.0, SPSS Inc., Chicago, United States). $p < 0.05$ was considered statistically significant.

## Results

### UHPLC-Q-orbitrap HRMS analysis of YBT

After assessing the quality of YBT by UHPLC-Q-Orbitrap HRMS, the content of target chemical components of YBT was identified. The total ion flow diagrams of YBT extract and mixed control in positive and negative ion modes were shown in Figure 1. And the contents of ephedrine, pseudoephedrine, glycyrrhizin, 6-gingerol, glycyrrhetinic acid, 8-gingerol, and 10-gingerol as the target compounds in YBT extract were measured as 22.66 µg/mL, 18.14 µg/mL, 7.04 µg/mL, 0.50 µg/mL, 11.90 µg/mL, 0.0029 µg/mL and 0.0015 µg/mL, respectively (Table 1).

**TABLE 1 The content of target chemical components of YBT.**

| Peak serial number | Name | Molecular formula | Content (µg/mL) |
|---|---|---|---|
| 1 | Ephedrine | $C_{10}H_{15}NO$ | 22.66 |
| 2 | Pseudoephedrine | $C_{10}H_{15}NO$ | 18.14 |
| 3 | Liquiritin | $C_{21}H_{22}O_9$ | 7.04 |
| 4 | 6-gingerol | $C_{17}H_{26}O_4$ | 0.50 |
| 5 | Glycyrrhizic acid | $C_{42}H_{62}O_{16}$ | 11.90 |
| 6 | 8-gingerol | $C_{43}H_{32}O_{20}$ | 0.0029 |
| 7 | 10-gingerol | $C_{21}H_{34}O_4$ | 0.0015 |

## YBT treatment improved edema and microvascular permeability in rats with the NS model

The occurrence of edema was associated closely with vascular leakage (Fantin et al., 2017). In this study, we used the ADR-induced NS (ADR-NS) model to investigate the effect of YBT on the alleviation of edema and microvascular
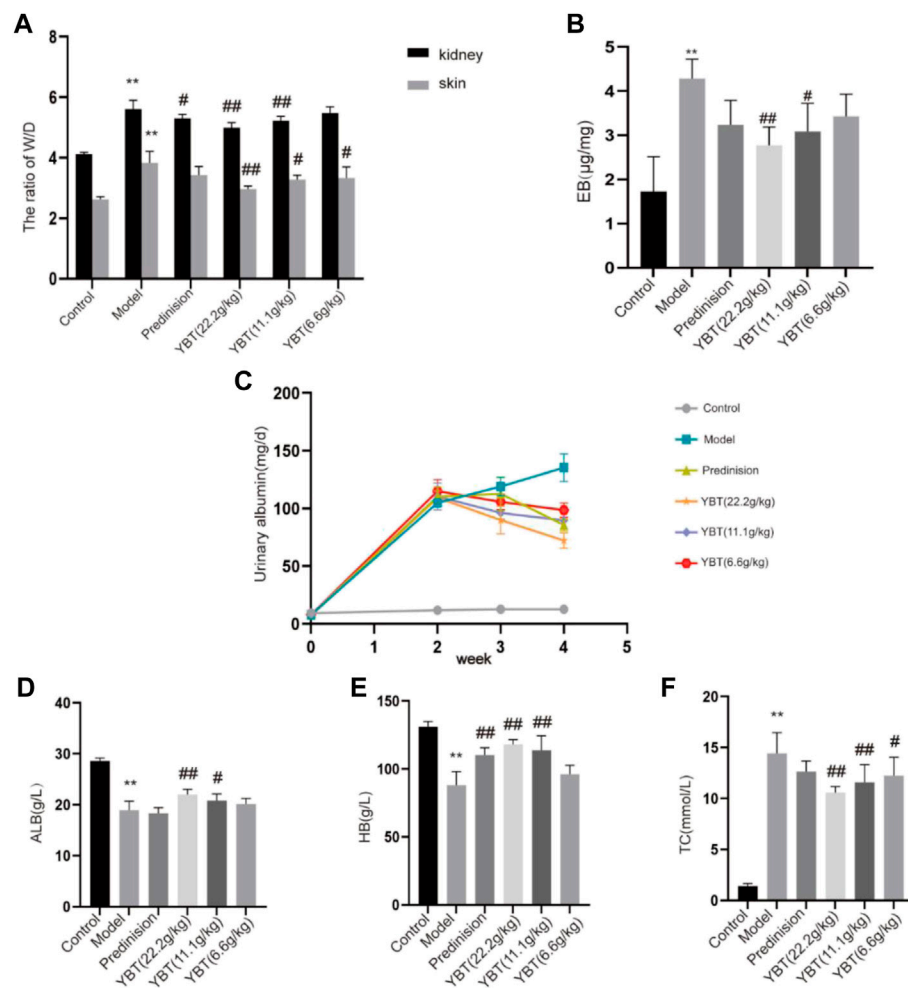
**FIGURE 2**
Effect of YBT on symptoms and renal vascular function in nephrotic syndrome. **(A)** The skin and kidney W/D weight ratio in each group ($n = 6$). **(B)** Evans Blue dye extravasation ($n = 4$). **(C)** 24 h urine protein (24 h UTP): Pre-modeling, 14 days post-modeling, 7 days on medication, 14 days on medication ($n = 6$). **(D–F)**: The level of albumin (ALB), hemoglobin (HB), and total cholesterol (TC) in each group ($n = 6$). Data present means $\pm$ SD, compared with control, $*p < 0.05$, $**p < 0.01$, compared with model, $\#p < 0.05$, $\#\#p < 0.01$.

hyperpermeability. As shown in Figure 2, compared with the control group, the W/D weight ratio of skin and kidney and the content of Evans Blue dye of tissues in the model group was significantly increased (Figures 2A,B); compared with the model group, YBT, and prednisone decreased the W/D weight ratio of skin and kidney and the content of Evans Blue dye of tissues. Meanwhile, compared with the control group, 24 h UTP was raised in the model group. However, YBT and prednisone gradually reduced 24 h UTP after 7 d and 14 d of treatment (Figure 2C). In addition, HB and ALB decreased accompanied by TC increased in rats with an ADR-induced NS model compared with the control group, which were reversed by the YBT therapy and were improved with the high dose of YBT (Figures 2D–F). In conclusion, these findings provided strong evidence that YBT could treat not only edema in nephrotic syndrome by altering microvascular permeability but also other symptoms of nephrotic syndrome.

## YBT reduced renal injury in the NS rat model

To explore the effect of YBT on kidney injury, serum biochemical analysis, HE staining, Masson staining, and PAS staining of kidney tissues were performed on rats. We first tested the levels of serum creatinine and blood urea nitrogen. It was found that the levels of both serum creatinine and blood urea nitrogen in the model group rose compared with the control group. Meanwhile, they could be downregulated via YBT treatment, and the higher the dose the better (Figures 3D,E). Histological analysis of the kidneys showed that the glomeruli of the control group were intact. In contrast, the glomeruli of the model group demonstrated glomeruli adhesion, thickened basement membrane, vacuolation of endothelial cells, collagen deposition by Masson staining, and glycogen deposition by PAS staining. It was observed that the epithelial cells of the renal tubules were vacuolated and deformed, the lumen was enlarged, and the renal interstitium was edematous and infiltrated with inflammatory cells.
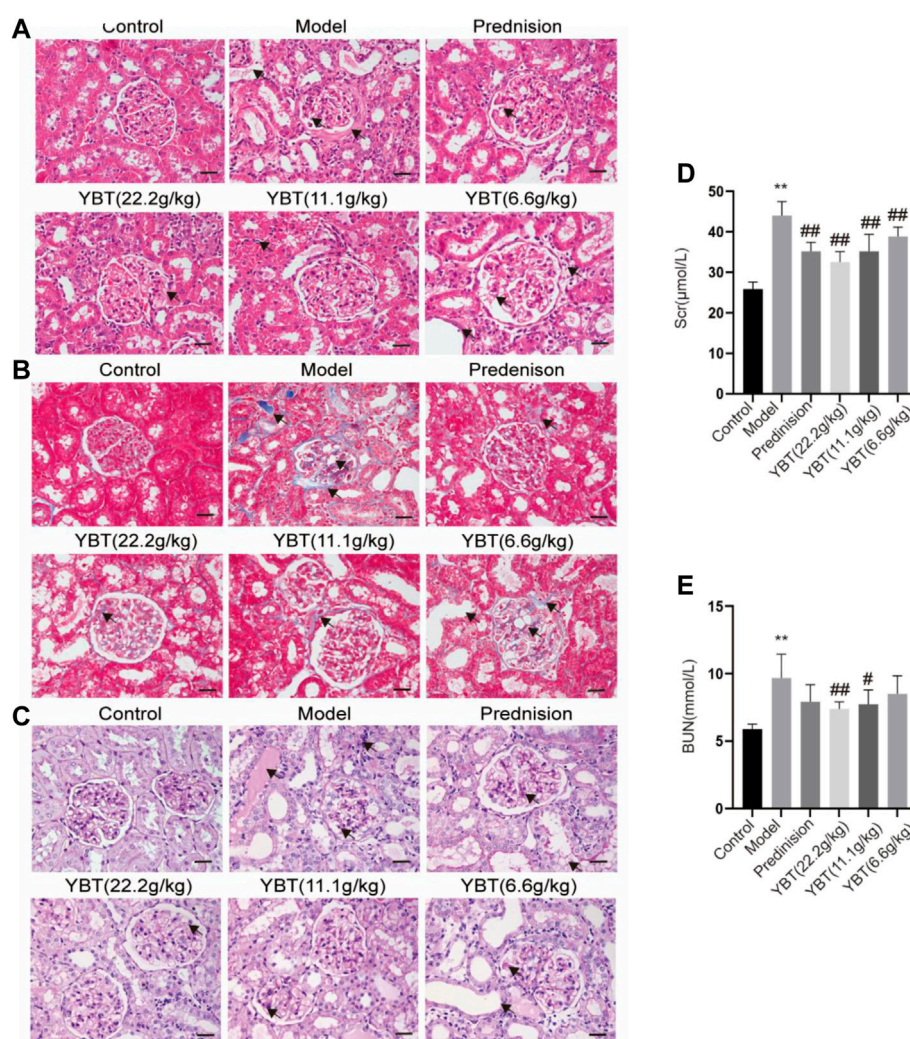
**FIGURE 3**
Effects of YBT on renal function and renal pathology in ADR-NS rats model. **(A)** HE staining of rat kidney tissues. Magnification, ×400. Scale bar, 25 μm. **(B)** Masson's trichrome staining of rat kidney tissues. Magnification, ×400. Scale bar, 25 μm. **(C)** PAS staining of rat kidney tissues. Magnification, ×400. Scale bar, 25 μm. **(D)** and **(E)** The level of serum creatinine (Scr) and urea nitrogen (BUN) ($n = 6$). Values represent mean $\pm$ SD, compared with control, *$p < 0.05$, **$p < 0.01$, compared with model, #$p < 0.05$, ##$p < 0.01$.

Significant improvements were observed in renal pathology after YBT treatment (Figures 3A–C).

YBT improved the vascular filtration barrier possibly by inhibiting Cav-1 expression in the ADR-NS model.

Inhibition of Cav-1 expression could be an effective means of limiting vascular injury by preventing increased transcellular albumin permeability and stabilizing the endothelial junction barrier (Sun et al., 2009; Smit et al., 2018). As shown in the immunohistochemical fluorescence analysis of the kidney tissues, there was an increased Cav-1 expression and a declined VE-cadherin expression in glomerular micro-vessels compared with the control group, indicating that the Cav-1 expression was associated with the vascular barrier. YBT treatment could suppress Cav-1 expression and activate VE-cadherin expression in a dose-dependent manner (Figure 4A). Moreover, the immunoblotting examination demonstrated that the expression of Cav-1 protein elevated, and the VE-cadherin protein expression dropped in the ADR-NS model

group compared with those of the control group (Figures 4B–D). Meanwhile, compared with the model group, YBT suppressed the protein expression of Cav-1 and stimulated the VE-cadherin. Taken together, these experimental results suggested that the YBT treatment for edema in nephrotic syndrome achieved the potential effect in part by modulating the Cav-1 expression to regulate albumin transport across membranes and intercellular adhesion junctions, thereby maintaining the normal barrier function of vascular endothelial cells.

## YBT treatment regulated the expression of Cav-1 associated with altered PI3K/AKT and eNOS signaling

Cav-1 is critical for NO production via inactivating eNOS. Both Cav-1 and eNOS are modulated by PI3K/AKT signaling (Chen et al.,
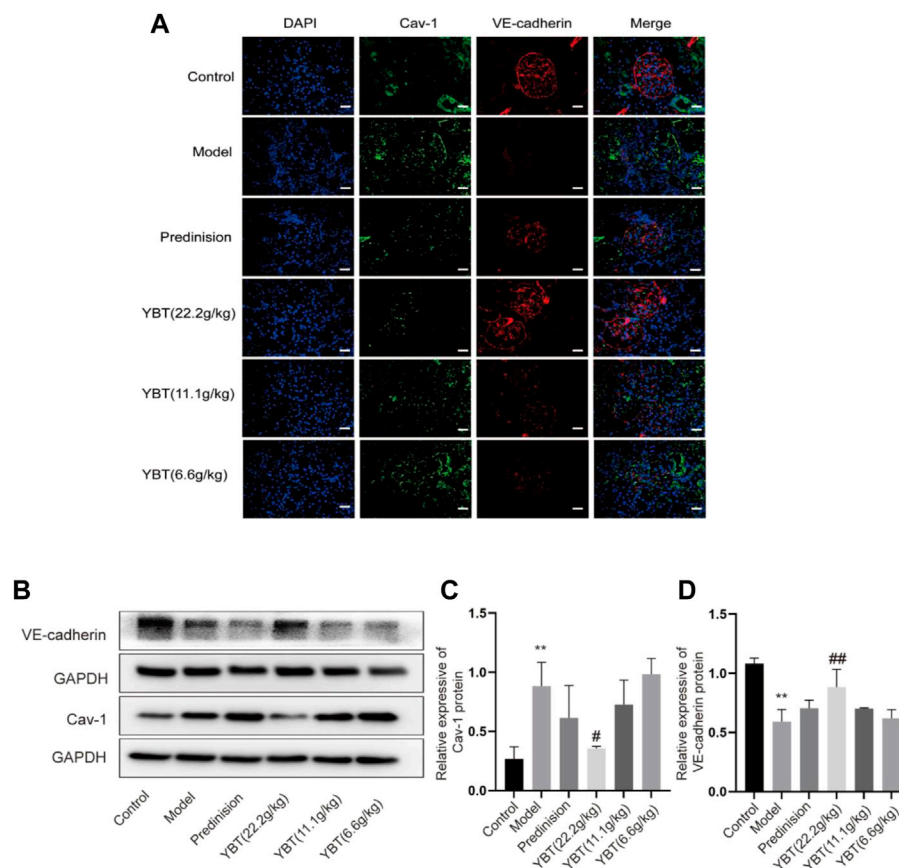
**FIGURE 4**
Effects of YBT on Cav-1-mediated endothelial barrier function in ADR-NS rat model. **(A)** Representative images of immunofluorescence staining of Caveolin-1(Cav-1, green), VE-cadherin (red), and DAPI (blue). Magnification, ×400. Scale bar, 25 μm. **(B)** Western blot analysis of Cav-1 and VE-cadherin expression ($n$ = 3). **(C)** and **(D)** Quantitation of Cav-1 and VE-cadherin expression in each group ($n$ = 3). Date represent mean $\pm$ SD, compared with control, *$p$ < 0.05, **$p$ < 0.01, compared with model, #$p$ < 0.05, ##$p$ < 0.01.

2021; Chen J. et al., 2022). To further understand the effector molecules of YBT-induced Cav-1 regulation, we performed immunoblotting and immunohistochemical experiments on PI3K/AKT and eNOS signaling, respectively. As shown in Figures 5A,B, immunoblotting experiments revealed that AKT phosphorylation levels were elevated, and eNOS phosphorylation was inhibited in the model group. After YBT treatment, AKT phosphorylation levels fell, and eNOS phosphorylation levels grew, preferably at the high dose of YBT. Besides, there was no significant difference in the change of PI3K expression among the groups. As for immunohistochemistry, the results agreed with Western blot that YBT treatment could upregulate the protein expression of p-eNOS with a high dose of YBT being preferred (Figures 5C,D).

To further determine whether YBT treatment affects microvascular permeability by influencing the level of NO which is a product of eNOS, we measured the NO levels in serum as well as kidney tissues. As shown in Figures 5E,F, compared with the control group, NO levels in both serum and renal tissues were reduced in the model group, which were notably elevated by prednisone and YBT treatment, particularly in the YBT high-dose group. In summary, YBT could regulate the Cav-1/eNOS signaling in the NS rat model.

## Discussion

YBT was first described in "Jin-Gui-Yao-Lue," a classical Chinese medicine work. According to the theory of traditional Chinese medicine, YBT is widely used in modern medicine for edema-like diseases due to its excellent effectiveness in improving proteinuria (Hu et al., 2020). Studies have shown that YBT can reduce proteinuria, modulate renal tissue aquaporins, regulate transient receptor potential ion channels, relieve renal damage and protect renal function in rats with adriamycin nephropathy (Song et al., 2020; Liu et al., 2022). YBT consists of *Ephedra sinica Stapf* (Ma Huang), *Zingiber officinale Roscoe* (Sheng Jiang), *Gypsum Fibrosum* (Shi Gao), *Ziziphus zizyphus* (Da Zao), and *Glycyrrhizae Radix et Rhizoma* (Gan Cao). Studies have shown that *E. sinica Stapf* can exert anti-inflammatory, antioxidant, antiviral, and diuretic effects (Zhang et al., 2018; Chen Y. Q. et al., 2022). Quercetin, an extract of *E. sinica Stapf*, can improve vascular leakage and has a protective effect on vascular endothelial cell damage (Tripathi et al., 2019; Kondo-Kawai et al., 2021). *Zingiber officinale Roscoe* has the effect of regulating apoptosis, immunity and inflammation, and cytoskeletal adhesion (Kiyama, 2020). Its main components have potential benefits in the treatment of diabetic nephropathy,
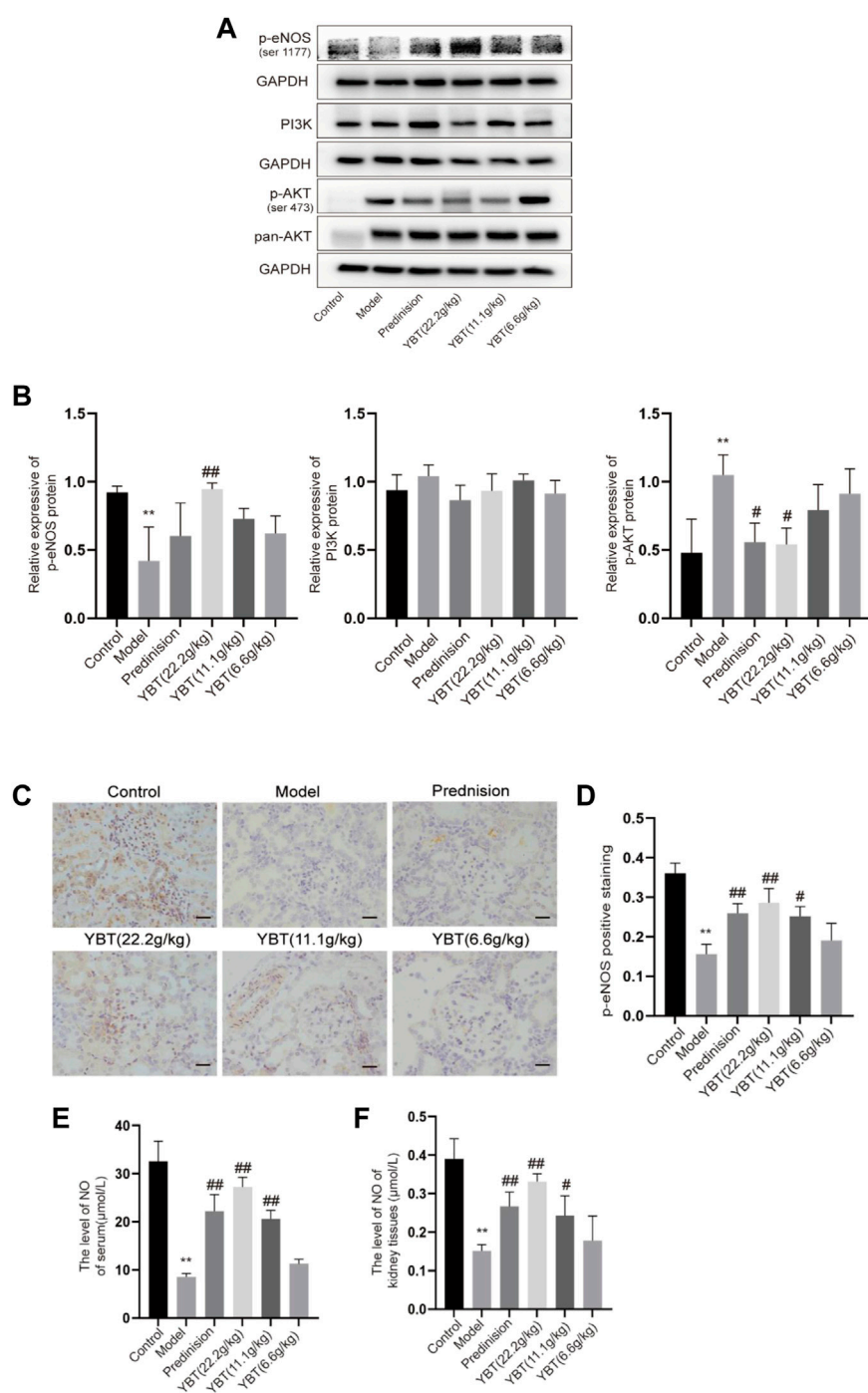
**FIGURE 5**
Effects of YBT on other mechanisms associated with Cav-1 in ADR-NS rat model. **(A)** Western blot analysis of p-eNOS, PI3K, and p-AKT expression ($n = 3$). **(B)** Quantitation of p-eNOS, PI3K, and p-AKT expression in each group ($n = 3$). **(C)** Immunohistochemistry of p-eNOS, Magnification, ×400. Scale bar: 25 μm ($n = 3$). **(D)** Semiquantitative analysis of p-eNOS positive staining ($n = 3$). **(E)** The level of NO of serum per group ($n = 4$). **(F)** The level of NO of kidney tissues per group ($n = 4$). Results represent mean $\pm$ SD, compared with control, $*p < 0.05$, $**p < 0.01$, compared with model, $\#p < 0.05$, $\#\#p < 0.01$.

hypertension, metabolic syndrome, and other diseases (Alsherbiny et al., 2019; Tan et al., 2022). 6-Gingerol increases the integrity of the endothelial cell (EC) barrier and the tight junctions between the periphery and periphery of the EC to maintain normal microvascular function (Zhong et al., 2019). In addition, its

active ingredients can also promote cholesterol efflux from macrophages, reduce oxidative stress, improve inflammation, and induce autophagy, thus exerting vascular protective effects (Li et al., 2021). *Glycyrrhizae Radix et Rhizoma* can inhibit thrombosis, regulate lipid metabolism, antioxidant, and so on, commonly

**FIGURE 6**
Diagram of the mechanisms involved in the study.
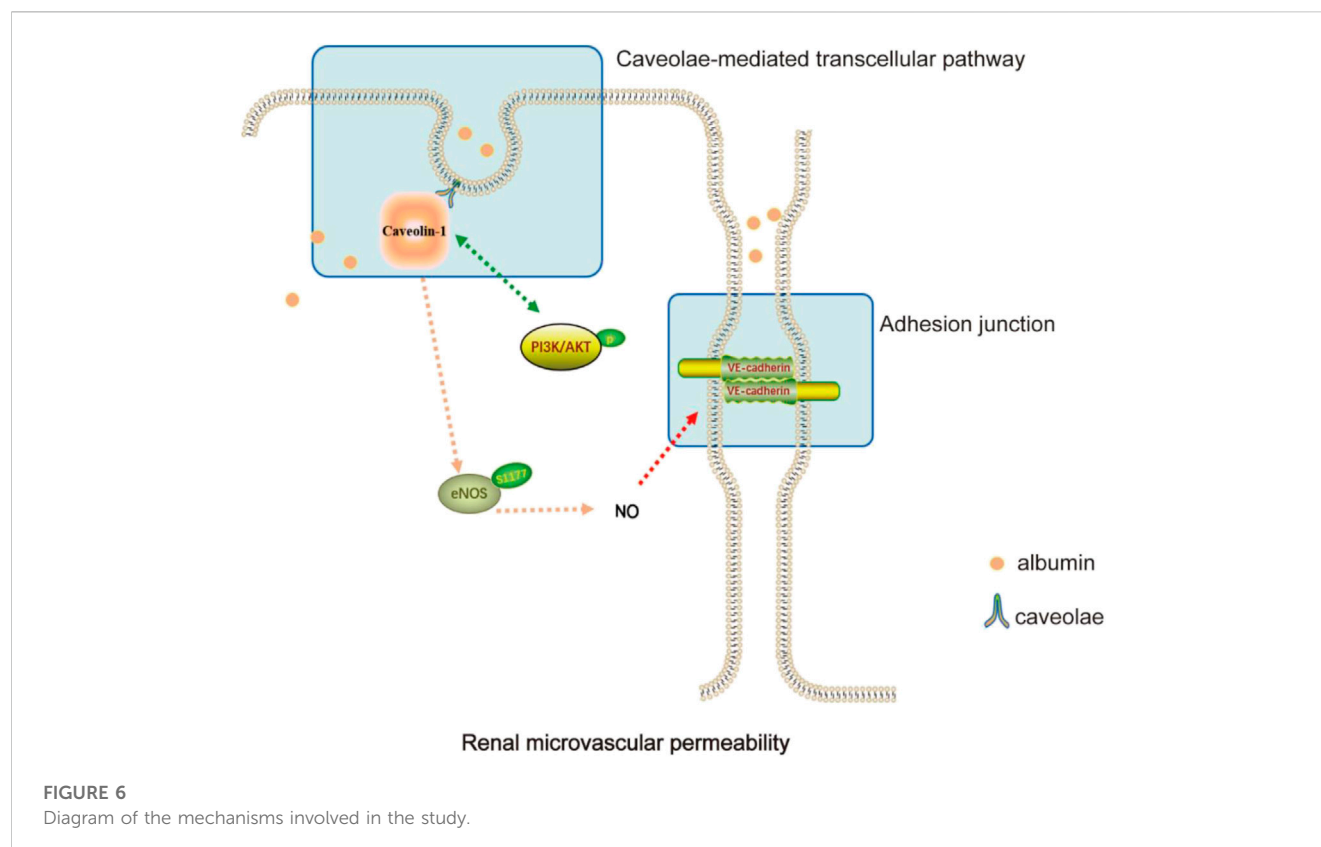
treated for diabetic nephropathy, liver damage, gastrointestinal ulcer, asthma, and other diseases (Sharifi-Rad et al., 2021). Licorice flavonoids, the main active components of *Glycyrrhizae Radix et Rhizoma*, can inhibit NLRP3-mediated vascular endothelial cell scorching by regulating SIRT6 to enable the normal function of blood vessels (He et al., 2023). In this study, we investigated the ameliorative effect of YBT on edema in nephrotic syndrome and its potential regulatory mechanisms. It was demonstrated that YBT significantly reduced the permeability of renal microvasculature in the ADR-induced NS rat model, thereby alleviating edema in the skin and kidneys. Meanwhile, it was also found that YBT significantly mitigated renal dysfunction, hyperlipidemia, and renal histological damage in the NS rats model. It was worth noting that the above mechanism of YBT action was possibly relevant to the regulation of the Cav-1/eNOS signaling pathway (Figure 6).

Regulating microvascular permeability has a crucial role in promoting the treatment of edema in nephrotic syndrome (Gupta et al., 2018). Udwan et al. reported that capillary permeability was altered, and that water filtration coefficients of paracellular and transcellular pathways were increased, while reflex coefficients to proteins were decreased in the NS rat model (Udwan et al., 2016). Some research findings emphasized that inhibiting capillary leakage improved microcirculatory perfusion and consequently reduced organ edema (Dekker et al., 2018; Koning et al., 2018). Based on these discoveries, modulating capillary permeability is a potential approach to ameliorate edema. In addition, YBT has been proven to be clinically effective in treating NS, especially in improving edema. Hu et al.

demonstrated that YBT might reduce pulmonary and renal edema in rats with severe acute pancreatitis via the regulation of water metabolism (Hu et al., 2020). Our data showed skin and kidney edema and increased renal microvascular permeability in rats with adriamycin nephropathy. Figures showed that after 14 days of YBT treatment, the rats' microvascular permeability decreased, and edema was reduced. Meanwhile, the rat NS model was observed to have 24 h massive proteinuria, hypoalbuminemia, hyperlipidemia, and other typical symptoms of nephrotic syndrome, accompanied by elevated serum creatinine and blood urea nitrogen, while YBT treatment significantly improved such symptoms. Our results evidenced that YBT could ameliorate edema by adjusting microvascular permeability, consequently affecting renal function and reducing renal injury. However, the molecular mechanisms of how regulating microvascular permeability is regulated need to be further defined.

Recent studies have shown that Cav-1 is one of the crucial modulators of vascular permeability (Choi et al., 2016; Parton et al., 2020; Ren et al., 2021). Y. Komarova et al. reported that the transport of albumin across the endothelium involved two alternative routes: a transcellular pathway via caveolae-mediated vesicular transport, or a paracellular pathway via junctions between endothelial cells (Komarova and Malik, 2010). Caveolae-mediated transendothelial albumin transport plays are closely connected with the effects of microvascular hyperpermeability (Chen et al., 2012). One study indicated that Cav-1 potentially played a role in cell-cell adhesion, thereby assisting the regulation of paracellular permeability (Drab et al., 2001). VE-cadherin is a significant component of vascular adhesion junctions and is expressed only in endothelial cells

(Vestweber, 2008). In a model where rats had adriamycin nephropathy with elevated endothelial permeability, we observed upregulation of Cav-1 expression and downregulation of VE-cadherin through immunofluorescence and immunoblotting experiments. YBT, especially in high doses, was able to inhibit the expression of Cav-1 and stimulate the expression of VE-cadherin. Consistent with these observations, Zhang et al. reported that in experiments with rats, minor intestinal edema was attenuated because Cav-1 expression was inhibited and VE-cadherin expression was activated in LPS-induced leakage of albumin from small mesenteric veins (Zhang et al., 2014). In summary, YBT could regulate the transcellular and paracellular pathways by affecting Cav-1, thus resulting in reduced renal microvascular leakage of albumin.

In addition to the mechanism we identified above, eNOS is also shown to be involved in the Cav-1-mediated regulation of endothelial cell permeability (Ren et al., 2021). Some studies demonstrated that in cardiovascular and pulmonary diseases, Cav-1 could inhibit eNOS activity, thereby affecting normal angiogenesis and barrier function (Schubert et al., 2002; Sonveaux et al., 2004; Oliveira and Minshall, 2018). NO, derived from eNOS, maintains vascular tone and is essential for normal vascular homeostasis (Bernatchez et al., 2011). Deficient NO production and decreased NO sensitivity would lead to endothelial dysfunction and, ultimately, an imbalance in intravascular homeostasis (Chen et al., 2018). However, the connection between Cav-1 and eNOS has rarely been discussed in studies about glomerular diseases. Meanwhile, it is essential in many fundamental cellular processes to activate PI3K/AKT signaling (Ku et al., 2017; Shu et al., 2022), as it is, simultaneously, a signaling molecule that forms a complex with Cav-1 and is involved in regulating vascular function (Nag et al., 2017; Yang et al., 2017). Given these facts, Cav-1/eNOS and PI3K/AKT pathways may play an important role in regulating glomerular hyperpermeability. To further confirm the ties between Cav-1 and eNOS in glomerular hyperpermeability, we examined the expression of eNOS phosphorylation and NO content. As the data demonstrated, in a state of renal microvascular hyperpermeability, p-eNOS expression was suppressed both in serum and in the kidney, where the production of NO was inhibited, whereas PI3K/AKT signaling was activated. Fortunately, YBT could improve microvascular permeability by stimulating the expression of eNOS phosphorylation, restricting the activation of AKT, enhancing the production of NO, maintaining vascular tone, and improving microvascular permeability.

Our study emphasized is the first exploration in the untouched field of how YBT reduces edema in nephrotic syndrome by modulating vascular permeability. This study focuses on the effects that YBT brings to the regulation of caveolae-mediated transcellular pathways and intercellular adhesion links in endothelial cells. Regretfully, however, assays that we conducted revealed that microvascular skin permeability also varied with the situation. For operational reasons, we failed to obtain valid data support. In the next step, we will continue this experiment to demonstrate our hypothesis that YBT can improve edema in nephrotic syndrome by regulating systemic microvascular permeability.

In conclusion, we believe that YBT can lessen the leakage of albumin through vesicular transport via the Cav-1/eNOS signaling pathway, increase intercellular adhesion junctions, and maintain the permeability of renal microvessels, thus proposing a promising option for treating nephrotic edema and relieving renal damage.

## Data availability statement

The original contributions presented in the study are included in the article/supplementary material, further inquiries can be directed to the corresponding author.

## Ethics statement

The animal study was reviewed and approved by the Animal Ethics Committee of Shanghai University of Traditional Chinese Medicine (PZSHUTCM220725025).

## Author contributions

MS conceived and designed the study; TL and SC completed the experiments and collected the data; LX and PL compiled the figures and revised the initial manuscript. All authors have read and approved the published version of the manuscript.

## Funding

## Conflict of interest

The authors declare that the research was conducted in the absence of any commercial or financial relationships that could be construed as a potential conflict of interest.

The handling editor XG declared a shared parent affiliation with the authors at the time of review.

## Publisher's note

# References

Alsherbiny, M. A., Abd-Elsalam, W. H., El Badawy, S. A., Taher, E., Fares, M., Torres, A., et al. (2019). Ameliorative and protective effects of ginger and its main constituents against natural, chemical and radiation-induced toxicities: A comprehensive review. *Food Chem. Toxicol.* 123, 72–97. doi:10.1016/j.fct.2018.10.048

Aman, J., van Bezu, J., Damanafshan, A., Huveneers, S., Eringa, E. C., Vogel, S. M., et al. (2012). Effective treatment of edema and endothelial barrier dysfunction with imatinib. *Circulation* 126 (23), 2728–2738. doi:10.1161/CIRCULATIONAHA.112.134304

Bauer, P. M., Yu, J., Chen, Y., Hickey, R., Bernatchez, P. N., Looft-Wilson, R., et al. (2005). Endothelial-specific expression of caveolin-1 impairs microvascular permeability and angiogenesis. *Proc. Natl. Acad. Sci. U. S. A.* 102 (1), 204–209. doi:10.1073/pnas.0406092102

Bernatchez, P., Sharma, A., Bauer, P. M., Marin, E., and Sessa, W. C. (2011). A noninhibitory mutant of the caveolin-1 scaffolding domain enhances eNOS-derived NO synthesis and vasodilation in mice. *J. Clin. Invest.* 121 (9), 3747–3755. doi:10.1172/JCI44778

Chen, J., Huang, Y., Hu, X., Bian, X., and Nian, S. (2021). Gastrodin prevents homocysteine-induced human umbilical vein endothelial cells injury via PI3K/Akt/eNOS and Nrf2/ARE pathway. *J. Cell Mol. Med.* 25 (1), 345–357. doi:10.1111/jcmm.16073

Chen, J., Zhang, H., Yang, Y., and Chen, B. (2022a). Quercetin regulates vascular endothelium function in chronic renal failure via modulation of Eph/Cav-1 signaling. *Drug Dev. Res.* 83 (5), 1167–1175. doi:10.1002/ddr.21940

Chen, W., Gassner, B., Borner, S., Nikolaev, V. O., Schlegel, N., Waschke, J., et al. (2012). Atrial natriuretic peptide enhances microvascular albumin permeability by the caveolae-mediated transcellular pathway. *Cardiovasc Res.* 93 (1), 141–151. doi:10.1093/cvr/cvr279

Chen, Y. Q., Chen, H. Y., Tang, Q. Q., Li, Y. F., Liu, X. S., Lu, F. H., et al. (2022b). Protective effect of quercetin on kidney diseases: From chemistry to herbal medicines. *Front. Pharmacol.* 13, 968226. doi:10.3389/fphar.2022.968226

Chen, Z., Olieveira, S. D. S., Zimnicka, A. M., Jiang, Y., Sharma, T., Chen, S., et al. (2018). Reciprocal regulation of eNOS and caveolin-1 functions in endothelial cells. *Mol. Biol. Cell* 29 (10), 1190–1202. doi:10.1091/mbc.E17-01-0049

Choi, K. H., Kim, H. S., Park, M. S., Kim, J. T., Kim, J. H., Cho, K. A., et al. (2016). Regulation of caveolin-1 expression determines early brain edema after experimental focal cerebral ischemia. *Stroke* 47 (5), 1336–1343. doi:10.1161/STROKEAHA.116.013205

Dekker, N. A. M., van Meurs, M., van Leeuwen, A. L. I., Hofland, H. M., van Slyke, P., Vonk, A. B. A., et al. (2018). Vasculotide, an angiopoietin-1 mimetic, reduces pulmonary vascular leakage and preserves microcirculatory perfusion during cardiopulmonary bypass in rats. *Br. J. Anaesth.* 121 (5), 1041–1051. doi:10.1016/j.bja.2018.05.049

Drab, M., Verkade, P., Elger, M., Kasper, M., Lohn, M., Lauterbach, B., et al. (2001). Loss of caveolae, vascular dysfunction, and pulmonary defects in caveolin-1 gene-disrupted mice. *Science* 293 (5539), 2449–2452. doi:10.1126/science.1062688

Fantin, A., Lampropoulou, A., Senatore, V., Brash, J. T., Prahst, C., Lange, C. A., et al. (2017). VEGF165-induced vascular permeability requires NRP1 for ABL-mediated SRC family kinase activation. *J. Exp. Med.* 214 (4), 1049–1064. doi:10.1084/jem.20160311

Frank, P. G., Woodman, S. E., Park, D. S., and Lisanti, M. P. (2003). Caveolin, caveolae, and endothelial cell function. *Arterioscler. Thromb. Vasc. Biol.* 23 (7), 1161–1168. doi:10.1161/01.ATV.0000070546.16946.3A

Garrean, S., Gao, X. P., Brovkovych, V., Shimizu, J., Zhao, Y. Y., Vogel, S. M., et al. (2006). Caveolin-1 regulates NF-kappaB activation and lung inflammatory response to sepsis induced by lipopolysaccharide. *J. Immunol.* 177 (7), 4853–4860. doi:10.4049/jimmunol.177.7.4853

Guerit, S., Fidan, E., Macas, J., Czupalla, C. J., Figueiredo, R., Vijikumar, A., et al. (2021). Astrocyte-derived Wnt growth factors are required for endothelial blood-brain barrier maintenance. *Prog. Neurobiol.* 199, 101937. doi:10.1016/j.pneurobio.2020.101937

Gupta, S., Pepper, R. J., Ashman, N., and Walsh, S. B. (2018). Nephrotic syndrome: Oedema formation and its reatment with diuretics. *Front. Physiol.* 9, 1868. doi:10.3389/fphys.2018.01868

He, J., Deng, Y., Ren, L., Jin, Z., Yang, J., Yao, F., et al. (2023). Isoliquiritigenin from licorice flavonoids attenuates NLRP3-mediated pyroptosis by SIRT6 in vascular endothelial cells. *J. Ethnopharmacol.* 303, 115952. doi:10.1016/j.jep.2022.115952

Hu, J., Zhang, Y. M., Miao, Y. F., Zhu, L., Yi, X. L., Chen, H., et al. (2020). Effects of Yue-Bi-Tang on water metabolism in severe acute pancreatitis rats with acute lung-kidney injury. *World J. Gastroenterol.* 26 (43), 6810–6821. doi:10.3748/wjg.v26.i43.6810

Hull, R. P., and Goldsmith, D. J. (2008). Nephrotic syndrome in adults. *BMJ* 336 (7654), 1185–1189. doi:10.1136/bmj.39576.709711.80

Kiyama, R. (2020). Nutritional implications of ginger: Chemistry, biological activities and signaling pathways. *J. Nutr. Biochem.* 86, 108486. doi:10.1016/j.jnutbio.2020.108486

Komarova, Y., and Malik, A. B. (2010). Regulation of endothelial permeability via paracellular and transcellular transport pathways. *Annu. Rev. Physiol.* 72, 463–493. doi:10.1146/annurev-physiol-021909-135833

Kondo-Kawai, A., Sakai, T., Terao, J., and Mukai, R. (2021). Suppressive effects of quercetin on hydrogen peroxide-induced caveolin-1 phosphorylation in endothelial cells. *J. Clin. Biochem. Nutr.* 69 (1), 28–36. doi:10.3164/jcbn.20-190

Koning, N. J., de Lange, F., van Meurs, M., Jongman, R. M., Ahmed, Y., Schwarte, L. A., et al. (2018). Reduction of vascular leakage by imatinib is associated with preserved microcirculatory perfusion and reduced renal injury markers in a rat model of cardiopulmonary bypass. *Br. J. Anaesth.* 120 (6), 1165–1175. doi:10.1016/j.bja.2017.11.095

Ku, Y. H., Cho, B. J., Kim, M. J., Lim, S., Park, Y. J., Jang, H. C., et al. (2017). Rosiglitazone increases endothelial cell migration and vascular permeability through Akt phosphorylation. *BMC Pharmacol. Toxicol.* 18 (1), 62. doi:10.1186/s40360-017-0169-y

Li, C., Li, J., Jiang, F., Tzvetkov, N. T., Horbanczuk, J. O., Li, Y., et al. (2021). Vasculoprotective effects of ginger (Zingiber officinale Roscoe) and underlying molecular mechanisms. *Food Funct.* 12 (5), 1897–1913. doi:10.1039/d0fo02210a

Liu, H. D., Song, C. D., Song, D., Chen, Y., Ding, Y., Jia, P. P., et al. (2022). Exploration on effects of yuebi decoction and zhenwu decoction on adriamycin nephropathy in rats based on NLRP3/caspase-1/IL-1 β inflammatory pathway. *J. Basic Chin. Med.* 28 (3), 357–361+421. doi:10.19945/j.cnki.issn.1006-3250.2022.03.037

Luo, S., Yang, M., Zhao, H., Han, Y., Jiang, N., Yang, J., et al. (2021). Caveolin-1 regulates cellular metabolism: A potential therapeutic target in kidney disease. *Front. Pharmacol.* 12, 768100. doi:10.3389/fphar.2021.768100

Meena, J., and Bagga, A. (2020). Current perspectives in management of edema in nephrotic syndrome. *Indian J. Pediatr.* 87 (8), 633–640. doi:10.1007/s12098-020-03252-9

Nag, S., Manias, J. L., Kapadia, A., and Stewart, D. J. (2017). Molecular changes associated with the protective effects of angiopoietin-1 during blood-brain barrier breakdown post-injury. *Mol. Neurobiol.* 54 (6), 4232–4242. doi:10.1007/s12035-016-9973-4

Oliveira, S. D. S., and Minshall, R. D. (2018). Caveolin and endothelial NO signaling. *Curr. Top. Membr.* 82, 257–279. doi:10.1016/bs.ctm.2018.09.004

Parton, R. G., Kozlov, M. M., and Ariotti, N. (2020). Caveolae and lipid sorting: Shaping the cellular response to stress. *J. Cell Biol.* 219 (4), e201905071. doi:10.1083/jcb.201905071

Ren, Y., Li, L., Wang, M. M., Cao, L. P., Sun, Z. R., Yang, Z. Z., et al. (2021). Pravastatin attenuates sepsis-induced acute lung injury through decreasing pulmonary microvascular permeability via inhibition of Cav-1/eNOS pathway. *Int. Immunopharmacol.* 100, 108077. doi:10.1016/j.intimp.2021.108077

Rostoker, G., Behar, A., and Lagrue, G. (2000). Vascular hyperpermeability in nephrotic edema. *Nephron* 85 (3), 194–200. doi:10.1159/000045661

Schubert, W., Frank, P. G., Woodman, S. E., Hyogo, H., Cohen, D. E., Chow, C. W., et al. (2002). Microvascular hyperpermeability in caveolin-1 (-/-) knock-out mice. Treatment with a specific nitric-oxide synthase inhibitor, L-NAME, restores normal microvascular permeability in Cav-1 null mice. *J. Biol. Chem.* 277 (42), 40091–40098. doi:10.1074/jbc.M205948200

Sharifi-Rad, J., Quispe, C., Herrera-Bravo, J., Belen, L. H., Kaur, R., Kregiel, D., et al. (2021). Glycyrrhiza genus: Enlightening phytochemical components for pharmacological and health-promoting abilities. *Oxid. Med. Cell Longev.* 2021, 7571132. doi:10.1155/2021/7571132

Shu, Z., Chen, S., Xiang, H., Wu, R., Wang, X., Ouyang, J., et al. (2022). AKT/PACS2 participates in renal vascular hyperpermeability by regulating endothelial fatty acid oxidation in diabetic mice. *Front. Pharmacol.* 13, 876937. doi:10.3389/fphar.2022.876937

Siddall, E. C., and Radhakrishnan, J. (2012). The pathophysiology of edema formation in the nephrotic syndrome. *Kidney Int.* 82 (6), 635–642. doi:10.1038/ki.2012.180

Siddall, E., Khatri, M., and Radhakrishnan, J. (2017). Capillary leak syndrome: Etiologies, pathophysiology, and management. *Kidney Int.* 92 (1), 37–46. doi:10.1016/j.kint.2016.11.029

Smit, K. F., Konkel, M., Kerindongo, R., Landau, M. A., Zuurbier, C. J., Hollmann, M. W., et al. (2018). Helium alters the cytoskeleton and decreases permeability in endothelial cells cultured *in vitro* through a pathway involving Caveolin-1. *Sci. Rep.* 8 (1), 4768. doi:10.1038/s41598-018-23030-0

Song, C. D., Song, D., Jia, P. P., Chen, Y., Hua, S. T., Ma, Y. R., et al. (2020). Effects of zhenwu decoction and yuebi decoction on AQP1/AQP2 in adriamycin nephropathy rats. *J. Basic Chin. Med.* 26 (03), 334–337. doi:10.13193/j.issn.1673-7717.2023.01.002

Sonveaux, P., Martinive, P., DeWever, J., Batova, Z., Daneau, G., Pelat, M., et al. (2004). Caveolin-1 expression is critical for vascular endothelial growth factor-induced ischemic hindlimb collateralization and nitric oxide-mediated angiogenesis. *Circ. Res.* 95 (2), 154–161. doi:10.1161/01.RES.0000136344.27825.72

Sun, Y., Hu, G., Zhang, X., and Minshall, R. D. (2009). Phosphorylation of caveolin-1 regulates oxidant-induced pulmonary vascular permeability via paracellular and transcellular pathways, 615 p following 685. *Circ. Res.* 105 (7), 676–685. doi:10.1161/CIRCRESAHA.109.201673

Tan, H., Chen, J., Li, Y., Li, Y., Zhong, Y., Li, G., et al. (2022). Glabridin, a bioactive component of licorice, ameliorates diabetic nephropathy by regulating ferroptosis and the VEGF/Akt/ERK pathways. *Mol. Med.* 28 (1), 58. doi:10.1186/s10020-022-00481-w

Teng, J., Zang, L., Li, L., Qiu, X., Liu, Y., and Sun, F. (2017). Overall condition improvement in a rat model of nephrotic syndrome treated with CellCept nanoliposomes. *Artif. Cells Nanomed Biotechnol.* 45 (1), 128–134. doi:10.3109/21691401.2016.1138484

Tripathi, A., Kumar, B., and Sagi, S. S. K. (2019). Prophylactic efficacy of Quercetin in ameliorating the hypoxia induced vascular leakage in lungs of rats. *PLoS One* 14 (6), e0219075. doi:10.1371/journal.pone.0219075

Udwan, K., Brideau, G., Fila, M., Edwards, A., Vogt, B., and Doucet, A. (2016). Oxidative stress and nuclear factor κB (NF-κB) increase peritoneal filtration and contribute to ascites formation in nephrotic syndrome. *J. Biol. Chem.* 291 (21), 11105–11113. doi:10.1074/jbc.M116.724690

Vestweber, D. (2008). VE-Cadherin: The major endothelial adhesion molecule controlling cellular junctions and blood vessel formation. *Arterioscler. Thromb. Vasc. Biol.* 28 (2), 223–232. doi:10.1161/ATVBAHA.107.158014

Xu, Q., Du, F., Zhang, Y., Teng, Y., Tao, M., Chen, A. F., et al. (2018). Preeclampsia serum induces human glomerular vascular endothelial cell hyperpermeability via the HMGB1-Caveolin-1 pathway. *J. Reprod. Immunol.* 129, 1–8. doi:10.1016/j.jri.2018.07.001

Yang, H., Chen, Q., Sun, F., Zhao, N., Wen, L., Li, L., et al. (2017). Down-regulation of the klf5-c-Myc interaction due to klf5 phosphorylation mediates resveratrol repressing the caveolin-1 transcription through the PI3K/PKD1/Akt pathway. *PLoS One* 12 (12), e0189156. doi:10.1371/journal.pone.0189156

Zhang, B. M., Wang, Z. B., Xin, P., Wang, Q. H., Bu, H., and Kuang, H. X. (2018). Phytochemistry and pharmacology of genus Ephedra. *Chin. J. Nat. Med.* 16 (11), 811–828. doi:10.1016/S1875-5364(18)30123-7

Zhang, X., Ramirez, C. M., Aryal, B., Madrigal-Matute, J., Liu, X., Diaz, A., et al. (2020). Cav-1 (Caveolin-1) deficiency increases autophagy in the endothelium and attenuates vascular inflammation and atherosclerosis. *Arterioscler. Thromb. Vasc. Biol.* 40 (6), 1510–1522. doi:10.1161/ATVBAHA.120.314291

Zhang, Y., Sun, K., Liu, Y. Y., Zhang, Y. P., Hu, B. H., Chang, X., et al. (2014). Ginsenoside Rb1 ameliorates lipopolysaccharide-induced albumin leakage from rat mesenteric venules by intervening in both trans- and paracellular pathway. *Am. J. Physiol. Gastrointest. Liver Physiol.* 306 (4), G289–G300. doi:10.1152/ajpgi.00168.2013

Zhong, W., Yang, W., Qin, Y., Gu, W., Xue, Y., Tang, Y., et al. (2019). 6-Gingerol stabilized the p-VEGFR2/VE-cadherin/β-catenin/actin complex promotes microvessel normalization and suppresses tumor progression. *J. Exp. Clin. Cancer Res.* 38 (1), 285. doi:10.1186/s13046-019-1291-z

frontiers | Frontiers in Pharmacology

# In *silico* evidence implicating novel mechanisms of *Prunella vulgaris* L. as a potential botanical drug against COVID-19-associated acute kidney injury

Xue-Ling Yang[1†], Chun-Xuan Wang[1†], Jia-Xing Wang[2], Shi-Min Wu[3], Qing Yong[2], Ke Li[2*‡] and Ju-Rong Yang[1*‡]

[1]Department of Nephrology, The Third Affiliated Hospital of Chongqing Medical University, Chongqing, China, [2]Core Research Laboratory, The Second Affiliated Hospital, Xi'an Jiaotong University, Xi'an, China, [3]Beijing Key Laboratory of Bioprocess, College of Life Science and Technology, Beijing University of Chemical Technology, Beijing, China

COVID-19-associated acute kidney injury (COVID-19 AKI) is an independent risk factor for in-hospital mortality and has the potential to progress to chronic kidney disease. *Prunella vulgaris* L., a traditional Chinese herb that has been used for the treatment of a variety of kidney diseases for centuries, could have the potential to treat this complication. In this study, we studied the potential protective role of *Prunella vulgaris* in COVID-19 AKI and explored its specific mechanisms applied by network pharmacology and bioinformatics methods. The combination of the protein-protein interaction network and Gene Ontology and Kyoto Encyclopedia of Genes and Genomes enrichment -target gene network revealed eight key target genes (VEGFA, ICAM1, IL6, CXCL8, IL1B, CCL2, IL10 and RELA). Molecular docking showed that all these eight gene-encoded proteins could be effectively bound to three major active compounds (quercetin, luteolin and kaempferol), thus becoming potential therapeutic targets. Molecular dynamics simulation also supports the binding stability of RELA-encoded protein with quercetin and luteolin. Together, our data suggest that IL6, VEGFA, and RELA could be the potential drug targets by inhibiting the NF-κB signaling pathway. Our *in silico* studies shed new insights into *P. vulgaris* and its ingredients, e.g., quercetin, as potential botanical drugs against COVID-19 AKI, and warrant further studies on efficacy and mechanisms.

KEYWORDS

COVID-19, acute kidney injury, cytokine storm, network pharmacology, molecular docking

## 1 Introduction

Coronavirus disease 2019 (COVID-19) is an extremely contagious disease caused by the severe acute respiratory syndrome coronavirus 2 (SARS-CoV-2) that emerged suddenly in 2019 (Hu et al., 2021a). The World Health Organization (WHO) has reported 632 million confirmed cases and 6.5 million deaths as of 13 November 2022 (Dong et al., 2020). The continuous outbreak of COVID-19 poses a great threat not only

to human health but also to the global economy, society and human life (Daniels and Morton, 2023). Although a large number of studies have been conducted focusing on the prevention and treatment of the disease, the mechanism behind treatment efficacy is not fully understood.

The main symptoms of COVID-19 are fever, cough and dyspnoea, and some patients in the acute phase may experience acute respiratory distress syndrome, sepsis, acute cardiac injury and secondary infection. Moreover, patients may develop multiple organ failure and shock in severe cases (Huang et al., 2020a). For instance, studies have reported a relatively high incidence rate of acute kidney injury (AKI, up to 77%) in patients with COVID-19, especially among those in the ICU (Huang et al., 2020b; Chen et al., 2020; Cheng et al., 2020; Guan et al., 2020; Yang et al., 2020; Matsumoto and Prowle, 2022). The chief pathologic change of AKI is renal tubular damage, with major physical signs of hematuria and proteinuria (Kudose et al., 2020; Han and Ye, 2021; Lin et al., 2022). Studies have reported that COVID-19-associated AKI (COVID-19 AKI) (Nadim et al., 2020) is not only linked to high in-hospital mortality rates but also accompanied by long-term complications, such as persistent AKI, end-stage renal disease and chronic renal insufficiency (Lin et al., 2020; Matsumoto and Prowle, 2022). Therefore, attention must be paid to the occurrence of AKI in patients with COVID-19, and early prevention, timely diagnosis and monitoring are important.

There is limited knowledge about the pathogenesis of AKI related to SARS-CoV-2; however, the current mainstream views are as follows. First, SARS-CoV-2 binds to ACE2 receptors on the surface of resident renal cells, including podocytes and tubular cells, to enter the cells and thus exert a direct damaging effect. Second, SARS-CoV-2 N protein can interact with Smad3 to form a complex to promote Smad3 signaling in response to TGF-β1and activate Smad3 to induce kidney cell death and cause acute kidney injury (AKI) (Wang et al., 2022). Third, the virus-induced cytokine storm and inflammation cause damage to the kidney (Ahmadian et al., 2021). Fourth, vascular endothelial dysfunction, coagulation dysfunction and complement activation may also be important mechanisms for the development of AKI in a subset of patients with COVID-19 (Nadim et al., 2020; Ahmadian et al., 2021; Han and Ye, 2021).

The efficacy of traditional Chinese medicine (TCM) in prevention and control of COVID-19, with medications having antiviral, anti-inflammatory and immune regulatory properties, can significantly reduce the hospitalisation rate and shorten the symptom recovery time (Runfeng et al., 2020; Hu et al., 2021b; Gajewski et al., 2021). *Prunella vulgaris* L. is a Chinese herbal medicine effective against a variety of diseases and has significant antiviral, anti-inflammatory, anti-oxidative and immunomodulatory effects (Bai et al., 2016). Early studies have reported inhibition of *Prunella vulgaris* on HIV, HSV and Ebola infection (Tabba et al., 1989; Yao et al., 1992; Xu et al., 1999; Zhang et al., 2016). In addition, APV can exert a significant antiviral effect by blocking the entry of SARS-CoV-2 into cells (Ao et al., 2021). What is more, *P. vulgaris* is the principal ingredient of Xia Sang Ju formula, a 3-herb traditional herbal remedy recommended for COVID-19 treatment by the Chinese

government, and it alone can also be used as an herbal tea. APV can also protect the kidney through its anti-inflammatory and anti-oxidative effects, which are accomplished by effectively inhibiting the activation, translocation of nuclear factor kappa-B (NF-kB), and generation of ROS, thereby inhibiting the expression of inflammatory factors, such as intracellular cell adhesion molecule-1 (ICAM-1) and monocyte chemoattractant protein-1 (MCP-1) (Namgung et al., 2017). These findings suggest a potential therapeutic role for *P. vulgaris* in COVID-19 AKI; however, the exact mechanism has not been fully investigated.

Network pharmacology is a method for the systematic construction of the ingredients-target-disease network. It reveals the potential pathogenetic molecular mechanisms in a high-throughput manner and provides a new scientific paradigm for the study of Chinese medicine (Nogales et al., 2022). In this study, we aim to gain novel mechanistic insights into *P. vulgaris* and its ingredients, as potential botanical drugs against COVID-19 AKI and to guide further translational research and development. Our research provides new therapeutic ideas and targets for COVID-19 AKI.

# 2 Materials and methods

## 2.1 Obtaining active pharmaceutical ingredients and protein targets

The Traditional Chinese Medicine Systems Pharmacology Database (TCMSP, http://tcmspw.com) was used to search for the main ingredients of *P. vulgaris*, following which the active molecules were filtered by setting a pharmacokinetic index, which considers oral bioavailability (OB) greater than 30% and drug-like (DL) index >0.18 (Ru et al., 2014; Zheng and Wang, 2014). The targets of all active ingredients were downloaded, and protein IDs, gene symbols, as well as annotations were obtained using the Uniprot protein database (https://www.uniprot.org) and STRING database (https://string-db.org) (Consortium, 2015).

## 2.2 Prediction of disease targets

The COVID-19-related target genes were downloaded from the GeneCards database (http://www.genecards.org), Treatment Target Database (TTD, https://db.idrblab.org/ttd) and Human Online Mendelian Inheritance database (OMIM, https://OMIM.org) (Rebhan et al., 1997; Chen et al., 2002; Amberger et al., 2015). The AKI-related target genes were then downloaded from the DisGeNET database (http://www.disgenet.org) and the GeneCards database (Piñero et al., 2017). The intersection target of COVID-19 and AKI was obtained with the Wayne analysis tool, and these target genes were considered the relevant genes for COVID-19-induced AKI. The disease target genes were then intersected with the drug target genes to obtain the drug-disease intersection genes and were considered the possible target genes for *P. vulgaris* against COVID-19 AKI. The Venn diagram was drawn using the online Venny platform (https://bioinfogp.cnb.csic.es/tools/Venny/index.html).

## 2.3 Construction of the compound-target gene network

We used Cytoscape 3.9.1 (http://www.Cytoscape.org) to construct a network of compound-target interactions between the aforementioned drug-disease intersection targets and active compounds of the drug (Shannon et al., 2003). In the network, nodes represent the selected active compounds and targets, while the edges between the nodes represent the interactions between these molecules and genes. The connectivity between molecules and targets in the core structure of the network was determined by means of betweenness (implemented by the plug-in CytoNCA), and the molecule with a larger value was more likely to become a critical compound of COVID-19 AKI (Xia et al., 2020).

## 2.4 Construction of the protein-protein interaction network

The aforementioned disease-drug intersection gene targets were imported into the STRING database (https://string-db.org) to construct the protein-protein interaction (PPI) network (Szklarczyk et al., 2019). Species were selected as *Homo sapiens*, the meaning of network interaction was set as evidence, active sources involved Textmining, Experiments, Databases, Co-expression, Neighborhood, Gene Fusion and Co-occurrence and the minimum interaction score was set as medium confidence (0.4). Following this, the PPI network results of STRING were imported into Cytoscape 3.9.1, and the CytoNCA plugin was used to analyse network topology characteristics, with betweenness as an index to select key target genes by which *P. vulgaris* treat COVID-19 AKI.

## 2.5 GO functional enrichment and KEGG pathway analysis

Gene ontology (GO) functional annotation and Kyoto Encyclopedia of Genes and Genomes (KEGG) pathway enrichment analyses were performed for the aforementioned disease-drug intersection gene targets to reveal potential mechanisms based on biological processes (BP), cellular compounds (CC), molecular functions (MF), and critical signaling pathways. These were implemented using the ClusterProfiler package in R (version 4.1.2) (Li et al., 2021). *p*-values <0.05 and q-value (an adjusted *p*-value, taking in to account the false discovery rate) < 0.05 were considered statistically significant. In addition, visual analysis was performed using the ggplot package and pathview package in R. Cytoscape was used to network all the top 15 enriched BP, CC, MF and the top 20 KEGG pathways that intersected with the aforementioned disease-drug gene targets to identify the genes that appeared most in these enriched results.

## 2.6 Molecular docking technology

First, we downloaded and processed the protein structures for molecular docking. The three-dimensional structures of the proteins were downloaded from the RCSB Protein Data Bank (http://www.rcsb.org) (Berman et al., 2000). Crystal structures of proteins of human origin with a resolution greater than 2 Å were selected, and pdb files with high resolution and single proteins were downloaded. The proteins were processed using AutoDock Tools (version 1.5.6) (Morris et al., 2009), including water removal, hydrogenation, charge calculation and addition of atom type. Finally, the processed proteins were saved as PDBQT files. We then downloaded and processed the ligands for molecular docking. The 3D structure of the molecule was downloaded from PubChem (https://pubchem.ncbi.nlm.nih.gov/) and processed using AutoDock Tools (version 1.5.6) (Wang et al., 2017), involving adjusting charge, detecting and selecting rotatable keys of ligands. Molecular docking was performed using AutoDock Vina 1.12 with the setting of exhaustiveness = 10 and num_modes = 10. Each docking calculation generates ten structures that construct the least energetic ligand-protein complexes. Finally, 3D structure visualisation and 2D interaction mapping of proteins and ligands were performed using Discovery Studio Visualizer 2019, and the docking results were visualised using PyMol 2.5.2.

## 2.7 Molecular dynamics (MD)simulation

MD simulation were performed using Amber 22 (San Francisco, CA, United States of America) (Case et al., 2022). The ff19SB force field (Tian et al., 2019) was used to calculate the system force field parameters. Solvation was performed using the TIP3P water model, and $Na^+$ and $Cl^-$ were added to neutralize the system. Once the system energy was minimised, the system was heated from 0 K to 300 K within 500 ps. System confinement was performed in a canonical ensemble system synthesis, followed by system pre-equilibration at 300 K. Finally, 200 ns MD simulations were carried out in an isothermal isobaric system synthesis, maintaining periodic boundary conditions. All covalent bonds involving hydrogen were constrained by the SHAKE method. The root mean square deviation (RMSD), the root mean square value of atomic fluctuations (RMSF), Solvent accessible surface area (SASA) (Weiser et al., 1999), the free energy of the binding reaction and hydrogen binding were analysed. RMSD and RMSF were defined as 1) and 2), respectively.

$$RMSD = \sqrt{\frac{\sum_{n=1}^{N}\left[m_i * (X_i - Y_i)^2\right]}{M}} \qquad (1)$$

$$RMSF = \sqrt{\frac{\sum_{tj=1}^{T}\left|X_i(t_j) - Y_i\right|^2}{M}} \qquad (2)$$

# 3 Results

## 3.1 Acquisition of the P. vulgaris-target and COVID-19 AKI-associated genes

We obtained 11 active compounds of *P. vulgaris* from the TCMSP database (Table 1), and a total of 197 drug target genes were obtained after de-duplication. In addition, we obtained 372, 52 and three genes related to COVID-19 from the GeneCards,

TABLE 1 Active ingredients of *Prunella vulgaris*.

| Mol ID[a] | Molecule name | OB[b] (%) | DL[c] |
|---|---|---|---|
| MOL000006 | luteolin | 36.16 | 0.25 |
| MOL000098 | quercetin | 46.43 | 0.28 |
| MOL000358 | beta-sitosterol | 36.91 | 0.75 |
| MOL000422 | kaempferol | 41.88 | 0.24 |
| MOL000449 | stigmasterol | 43.83 | 0.76 |
| MOL000737 | morin | 46.23 | 0.27 |
| MOL004355 | spinasterol | 42.98 | 0.76 |
| MOL004798 | delphinidin | 40.63 | 0.28 |
| MOL006767 | vulgaxanthin-I | 56.14 | 0.26 |
| MOL006772 | poriferasterol monoglucoside_qt | 43.83 | 0.76 |
| MOL006774 | stigmast-7-enol | 37.42 | 0.75 |

[a]Mol ID, indicates the ID, of the drug compound defined in the TCMSP.
[b]OB (Oral Bioavailability) is defined as "the rate and extent to which the active ingredient or active moiety is absorbed from a drug product and becomes available at the site of action".
[c]DL (Drug-likeness) index represents the similarity between the composition and known chemical medicine.



FIGURE 1
Venn diagram identifies intersection targets of drug and disease. (A). The intersection genes of AKI with COVID-19 are potential targets for COVID-19 induced AKI. (B). The intersection targets of *Prunella vulgaris* with COVID-19 AKI are possible target genes for *Prunella vulgaris* against COVID-19 AKI.
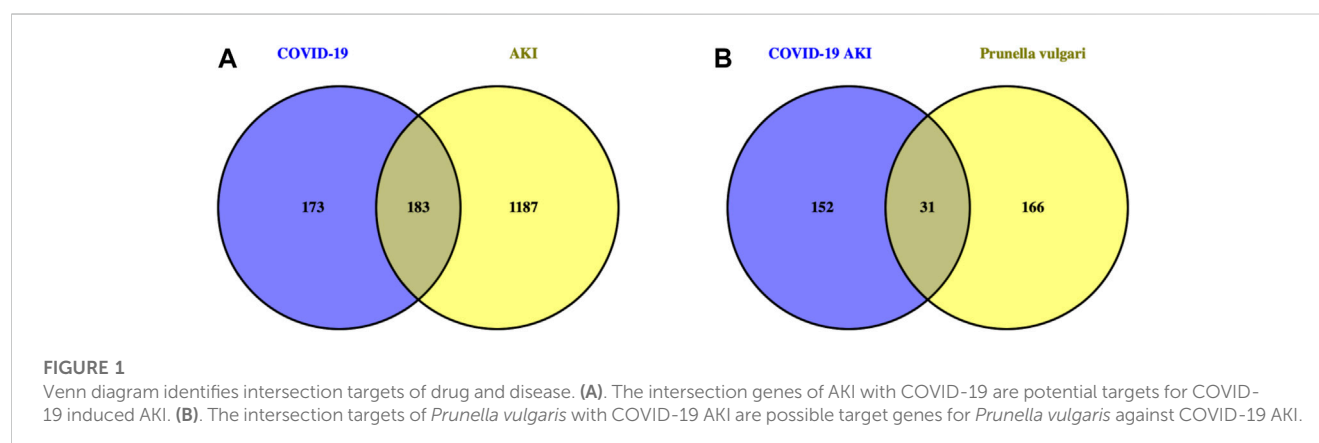
OMIM and TTD databases, respectively, and finally acquired 356 targets after de-duplication. Following this, 163 and 1,315 AKI-related target genes were obtained from the DisGeNET and GeneCards databases, respectively, and finally 1,370 genes were obtained after de-duplication. The intersection of the target genes of AKI and COVID-19 yielded 183 genes that can be considered potential target genes for COVID-19 AKI (Figure 1A).

## 3.2 Construction of the active compound-target network

By intersecting drug target genes and disease-related genes, we finally obtained a relevant gene set, comprising 31 genes, for *P. vulgaris* treating COVID-19 AKI (Figure 1B). Based on the targets of the active ingredient, we found that this intersection gene set was associated with only seven active ingredients (quercetin, luteolin, morin, kaempferol, delphinidin, vulgaxanthin-I and beta-sitosterol). A composite active compounds-target interaction network with 38 nodes (31 genes and seven compounds) and 59 edges (Figure 2A) was visualised using Cytoscape 3.8.0, and node size indicated the importance of the node. We plotted the histogram of the seven chemical compounds based on the results of betweenness (indicates the proportion of the shortest paths through node to all the shortest paths) (Figure 2B) and found that five compounds, including quercetin, luteolin, morin, kaempferol and delphinidin, were more important.

## 3.3 Construction of the PPI network

The PPI (Figure 3A) network of the 31 drug-disease intersection genes was exported from the STRING database, and the result showed that the proteins encoded by these target genes had complex interactions. We imported the PPI network into Cytoscape for further analysis. The CytoNca plugin was used to rank the strength of action of these proteins

**FIGURE 2**
Constructing a drug-ingredients-target network to identify the crucial compounds. **(A)**. A network diagram of *Prunella vulgaris* compound-target interactions was constructed by Cytoscape 3.9.1, and node size indicated the value of betweenness. **(B)**. Histograms show betweenness for the ingredients, and the molecule with a larger value was more likely to become a critical compound of COVID-19 AKI.



**FIGURE 3**
Constructing a PPI network to find essential target genes. **(A)**. PPI network map of targets was downloaded from the STRING database. **(B)**. PPI network map was further visualized with Cytoscape software. **(C)**. Target genes representing the top 20 of betweenness were visualised with histograms.

according to the betweenness, and each node showed different circle sizes, with larger circles having higher values (Figure 3B). The top 20 ranked genes were visualised on a histogram

(Figure 3C). The top 10 genes with the strongest protein interactions were IL6, VEGFA, CXCL8, IL1B, ICAM1, CCL2, IL10, HMOX1, EGFR and HIF1A.

**FIGURE 4**
Enrichment analysis was performed for intersecting genes. **(A)**. A total of top 15 BP, CC and MF terms are visualised with bar chat. **(B)**. Top 20 enriched KEGG terms are visualised with bubble chart. (*$p$-value<0.05, *$q$-value<0.05).
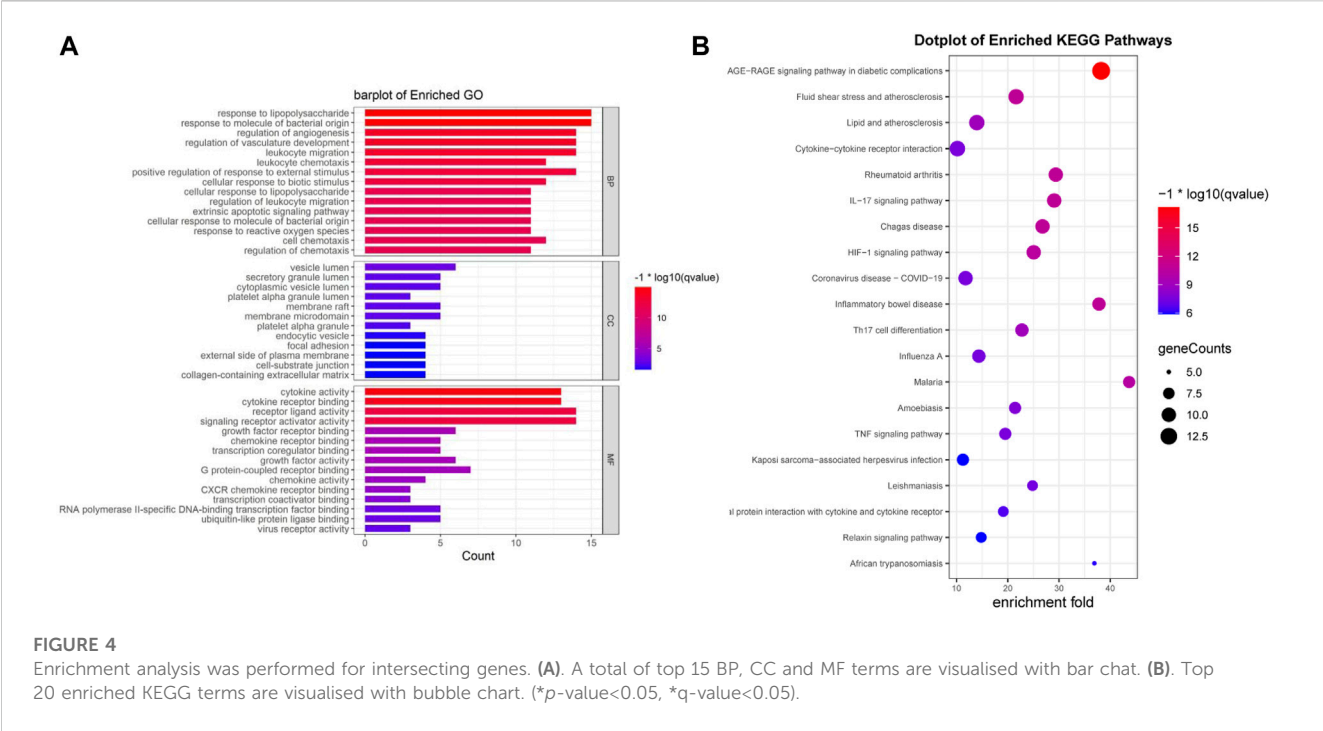
**TABLE 2 Thirteen virus-related GO enrichment terms.**

| Ontology | ID | Description | Enrichment fold[a] | q-value[b] | Count |
|---|---|---|---|---|---|
| BP | GO:0009615 | response to virus | 11.52 | 5.69E-06 | 7 |
| BP | GO:0016032 | viral process | 10.19 | 1.11E-05 | 7 |
| BP | GO:0051607 | defense response to virus | 13.67 | 1.11E-05 | 6 |
| BP | GO:0019058 | viral life cycle | 9.53 | 0.00023579 | 5 |
| BP | GO:0098586 | cellular response to virus | 21.57 | 0.00045209 | 3 |
| BP | GO:0046718 | viral entry into host cell | 12.58 | 0.00156,767 | 3 |
| BP | GO:0050688 | regulation of defense response to virus | 17.51 | 0.00434,012 | 2 |
| BP | GO:0019079 | viral genome replication | 9.22 | 0.01,163,095 | 2 |
| BP | GO:0044793 | negative regulation by host of viral process | 40.26 | 0.01,342,401 | 1 |
| BP | GO:0140374 | antiviral innate immune response | 40.26 | 0.01,342,401 | 1 |
| MF | GO:0001618 | virus receptor activity | 23.39 | 0.00142,444 | 3 |
| BP | GO:0002230 | positive regulation of defense response to virus by host | 38.97 | 0.0011587 | 2 |
| BP | GO:0050691 | regulation of defense response to virus by host | 29.46 | 0.001846 | 2 |

[a]Enrichment fold means a value of the percentage of genes in list belonging to the pathway, divided by the corresponding percentage in the background.
[b]q-value represents an adjusted $p$-value, taking in to account the false discovery rate.

## 3.4 GO enrichment analysis

We performed an enrichment analysis of GO functional annotation to understand the function of intersecting genes. A total of 1,560 GO terms, including 1,510, 12 and 38 biological processes (BP), cellular compounds (CC), molecular functions (MF), respectively, and the top 15 terms were identified (Figure 4A). BP are mainly enriched in cells and the body in response to external stimuli and bacteria, inflammatory responses (leukocyte migration and chemotaxis), regulation of reactive oxygen species (ROS) and apoptosis, in addition to the regulation of angiogenesis and vascular development. CC are mainly concentrated in cell membranes, vesicles, secretory granules and the extracellular matrix. MF is mainly manifested in cytokines, receptor ligands, chemokines, growth factor activity and viral receptor activity. We have presented the results of all 10 GO
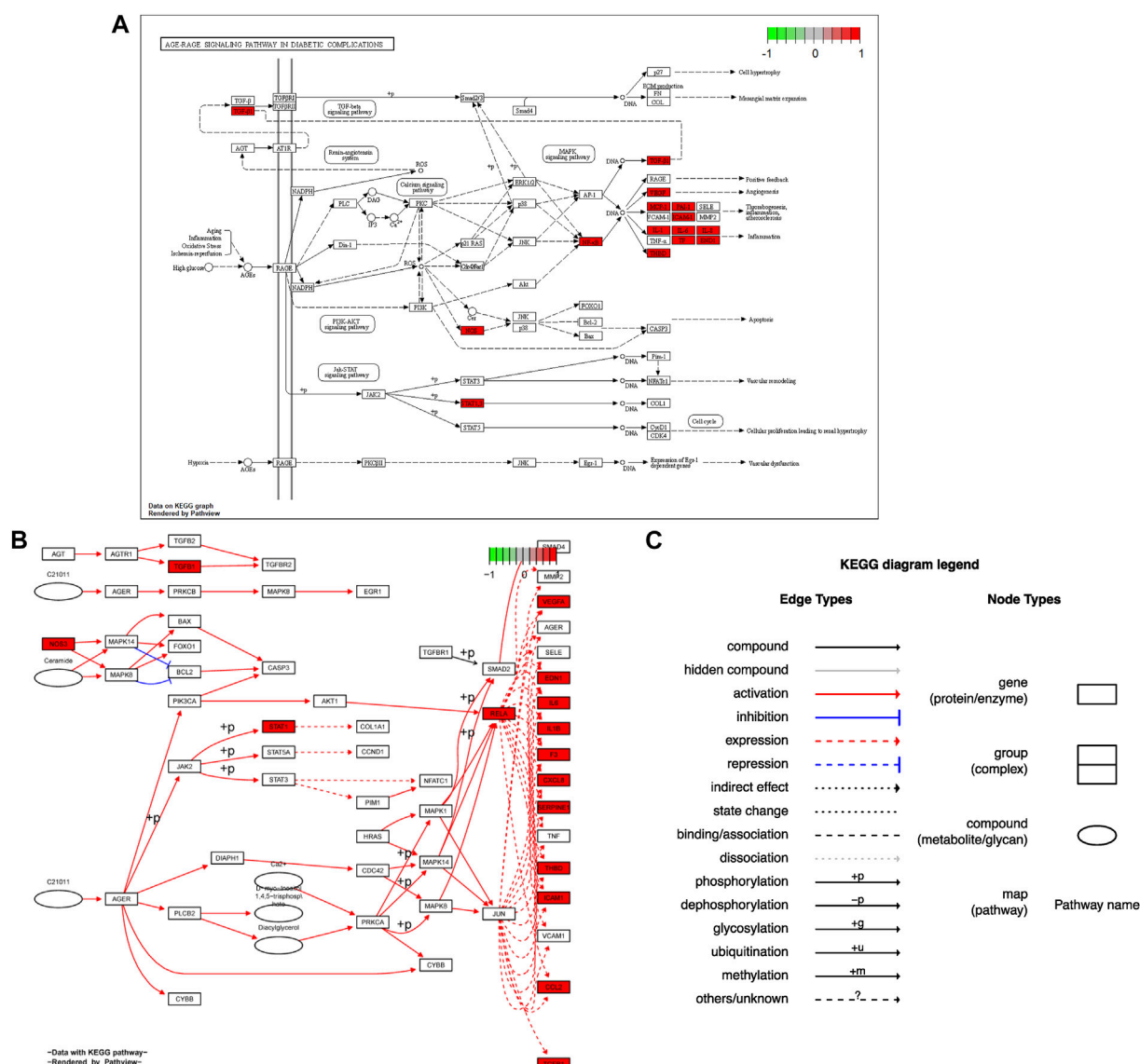
**FIGURE 5**
Hsa 04933 KEGG pathway map were acquired from pathview package in R. **(A)**. Protein KEGG pathway map was present. **(B)**. Gene KEGG pathway map was shown. **(C)**. Annotation of gene KEGG pathway map was obtained.

terms associated with viral invasion after analysis (Table 2), which showed mechanisms that could inhibit SARS-CoV-2 mainly as follows: response to virus, defense response to virus, viral life cycle, cellular response to virus, viral entry into host cell.

## 3.5 KEGG pathway analysis

Seventy-six terms were enriched through the KEGG pathway enrichment analysis, ranked by q-value, and the top 20 KEGG terms were identified (Figure 4B). The KEGG suggests that these target genes are associated with a series of important pathological processes, such as the route of infection by external microorganisms (bacteria, viruses and protozoa), the differentiation of immune cells, and inflammation-related

pathways (signal transduction pathways). We have presented the top enriched pathway map, the advanced glycation end products (AGEs)- regulation of the receptor for AGEs (RAGE) signaling pathway in diabetic complications, which shows that *P. vulgaris* may regulate VEGFA, IL6, IL-8 and ICAM1 expression through RELA (Figure 5A), thereby alleviating angiogenesis, thrombosis and the inflammatory response (Figures 5B,C). All top 20 KEGG pathway maps have been provided (Supplementary File S1). In addition, we have presented 13 terms associated with viral invasion based on the results of the KEGG analysis (Table 3), which suggests that these target genes play an essential role in viral infection. The top 15 BP, 12 CC, 15 MF, and the top 20 KEGG pathways and their associated genes were visualised using Cytoscape (Figure 6). The top nine genes enriched were RELA, ICAM1, IL6, TGFB1, CXCL8, VEGFA,

TABLE 3 Ten virus-associated KEGG pathways.

| ID | Description | Enrichment fold[a] | q-value[b] | Count |
|---|---|---|---|---|
| hsa05171 | Coronavirus disease - COVID-19 | 11.77 | 2.90E-08 | 10 |
| hsa05164 | Influenza A | 14.37 | 3.24E-08 | 9 |
| hsa04061 | Viral protein interaction with cytokine and cytokine receptor | 19.11 | 2.52E-07 | 7 |
| hsa05167 | Kaposi sarcoma-associated herpesvirus infection | 11.26 | 1.30E-06 | 8 |
| hsa05163 | Human cytomegalovirus infection | 8.49 | 3.14E-05 | 7 |
| hsa05162 | Measles | 9.82 | 0.00023886 | 5 |
| hsa05160 | Hepatitis C | 8.7 | 0.00037313 | 5 |
| hsa05161 | Hepatitis B | 8.43 | 0.00042346 | 5 |
| hsa05169 | Epstein-Barr virus infection | 6.76 | 0.00112,339 | 5 |
| hsa05166 | Human T-cell leukemia virus 1 infection | 6.15 | 0.00165,752 | 5 |

[a]Enrichment fold means a value of the percentage of genes in list belonging to the pathway, divided by the corresponding percentage in the background.
[b]q-value represents an adjusted $p$-value, taking in to account the false discovery rate.



FIGURE 6
Constructing a GO and KEGG-target interaction network to find essential target genes.
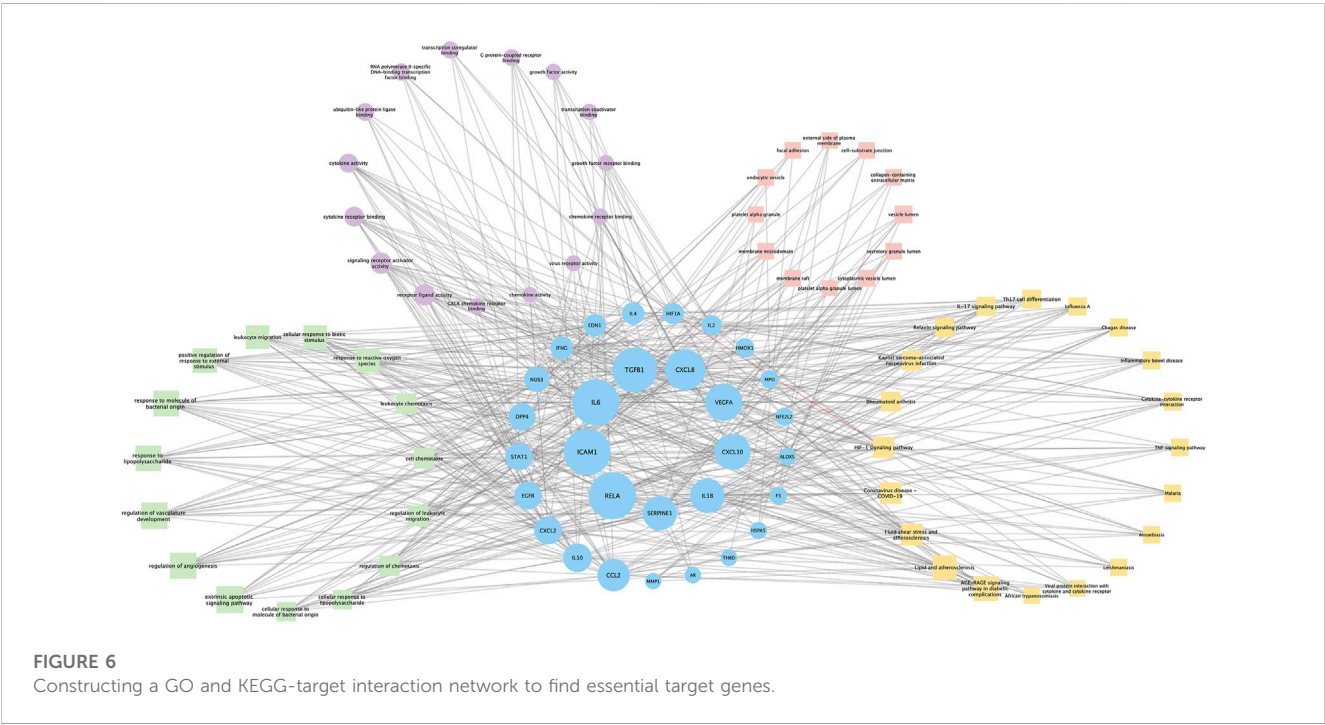
CXCL10, IL1B and SERPINE1. Furthermore, in combination with the results of the PPI network analysis, we identified eight key target genes of *P. vulgaris* associated with COVID-19 AKI, including IL6, VEGFA, CXCL8, IL1B, ICAM1, CCL2, IL10 and RELA.
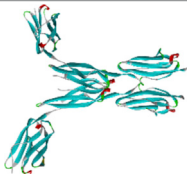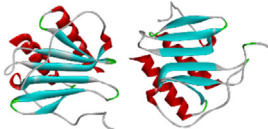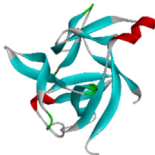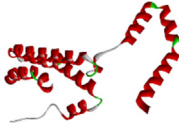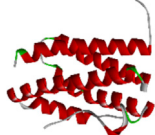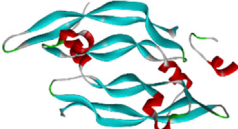
## 3.6 Molecular docking of active compounds and eight key proteins

Based on the previous results, we identified eight key proteins that play critical roles in the effects of *P. vulgaris* on COVID-19 AKI

and obtained their 3D structures from the RCSB Protein Data Bank (Table 4). Based on the identified drug compound targets, we found that only three drug molecules (quercetin, luteolin and kaempferol) acted on the aforementioned eight proteins. Table 5 lists these three compounds and their corresponding predicted targets. Quercetin, luteolin and kaempferol were selected for molecular docking, and their 3D structures were downloaded from PubChem (Table 6). As previously described, binding affinity less than −5.0 and −7.0 kcal/mol suggests good and strong binding activities, respectively (Liu et al., 2022). The molecular docking results (Figure 7) revealed that the three predicted ingredients demonstrated a good docking effect with their corresponding targets, and the interactions were relatively

**TABLE 4 Eight candidate protein structures.**

| Protein | PDB index | Structure without water and ligand |
|---------|-----------|-----------------------------------|
| ICAM1 | 1P53 | |
| IL8 | 1QE6 | |
| IL1B | 1TWM | |
| IL10 | 2H24 | |
| IL6 | 4NI7 | |
| CCL2 | 4ZK9 | |
| RELA | 6GGR | |
| VEGFA | 6ZBR | |

Note: ICAM1, Intercellular Adhesion Molecule 1; IL8, Interleukin 8; IL1B, Interleukin 1 Beta; IL10, Interleukin 10; IL6, Interleukin 6; CCL2, C-C Motif Chemokine Ligand 2; RELA, RELA proto-oncogene (NF-κB subunit); VEGFA, Vascular Endothelial Growth Factor A.

strong. Quercetin had a good affinity for all eight key proteins, luteolin had a good binding ability for RELA, ICAM1, VEGFA, IL6 and CXCL8, and kaempferol could effectively bind to ICAM1.

Thus, the results suggested that these three active compounds, especially quercetin, exerted protective effects against COVID-19 AKI by regulating the aforementioned key target genes.

**TABLE 5 Fourteen kinds of molecular docking results.**

| Molecule | Protein | Affinity (kcal/mol) |
|----------|---------|---------------------|
| luteolin | RELA | −8.7 |
| quercetin | IL8 | −8.4 |
| quercetin | RELA | −7.9 |
| quercetin | ICAM1 | −7.3 |
| quercetin | CCL2 | −7.3 |
| luteolin | ICAM1 | −7.2 |
| quercetin | VEGFA | −7.1 |
| kaempferol | ICAM1 | −7 |
| luteolin | VEGFA | −7 |
| quercetin | IL1B | −6.9 |
| quercetin | IL6 | −6.9 |
| luteolin | IL6 | −6.8 |
| luteolin | IL10 | −6.6 |
| quercetin | IL10 | −6.5 |

## 3.7 MD simulation

Considering that RELA-encoded protein (NF-κB) presents the highest docking scores with molecules, it was chosen for MD simulations. After 200 ns of long-scale MD simulations, the RMSD trend of protein α-carbon atoms (protein backbone) and ligands in the simulated trajectories of the two systems over time showed that the RMSD was small for both RELA-luteolin and RELA-quercetin systems, with the RELA-luteolin system undergoing conformational transitions in a small conformational space and RELA-quercetin system fluctuating in a relatively constant conformational space (Figures 8A,B). The RMSF represents the flexibility changes of the protein during the simulation. The protein in RELA-luteolin and RELA-quercetin shows similar flexibility changes, with larger fluctuations in the loop conformation around residues 150 and 280, consistent with the high flexibility of the loops (Figures 8C,D). The Solvent accessible surface area (SASA) reflects the relative surface area contribution of the ligand exposed to the solvent and the SASA value fluctuated within a relatively constant range for both RELA-luteolin and RELA-quercetin systems (Figure 8E), which is consistent with the stability of the RMSD analysis. Free energy calculations using the Molecular Mechanics-Poisson Bolzmann Surface Area (MM/PBSA) method showed that the free energies of both RELA-luteolin and RELA-quercetin systems were relatively stable (Table 7; Table 8). Additionally, the hydrogen bond analysis indicates strong hydrogen bond interactions in both systems (Figure 8F; Figure 8G; Table 9; Table 10).
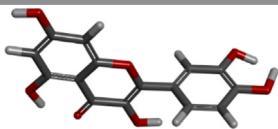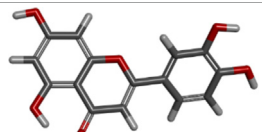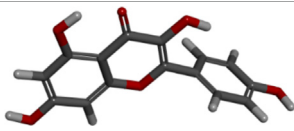
Overall, both RELA-luteolin and RELA-quercetin show good kinetic properties, indicating the correct docking pose. Both luteolin and quercetin fall in small conformational space domains with stable kinetic characteristics of the systems. In addition, they both have strong binding energies and stable hydrogen bond interactions. The results showed that both components luteolin and quercetin of P. vulgaris could stably bind NF-κB, which suggested that P. vulgaris could ameliorate COVID-19 AKI through NF-κB.

## Discussion

The incidence of COVID-19-associated acute kidney injury (AKI) has received increasing attention, particularly in severe cases. Traditional Chinese Medicine (TCM) has made significant contributions to the medical field, with reported preventative and therapeutic effects against COVID-19 and AKI (Li et al., 2019;

**TABLE 6 Molecular information of three candidate ligands.**

| Molecule name | Compound CID[a] | MF[b] | MW[c] | 3D structure |
|---------------|----------------|-------|-------|--------------|
| quercetin | 5280343 | $C_{15}H_{10}O_7$ | 302.23 g/mol | |
| luteolin | 5280445 | $C_{15}H_{10}O_6$ | 286.24 g/mol | |
| kaempferol | 5280863 | $C_{15}H_{10}O_6$ | 286.24 g/mol | |

[a]CID, PubChem Compound Identification.
[b]MF, molecular formula.
[c]MW, molecular weight.
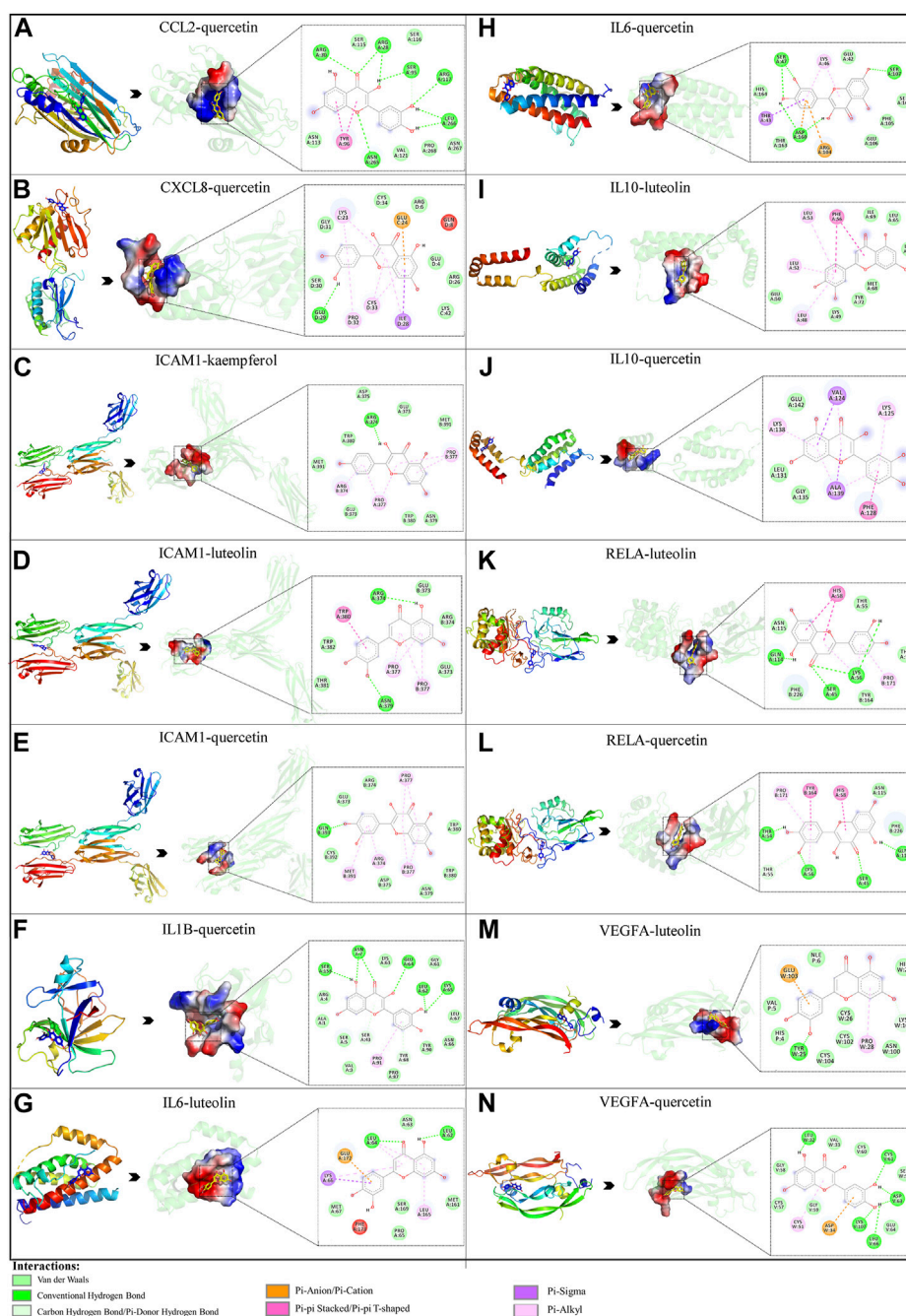
**FIGURE 7**
Molecular docking of three active compounds and eight proteins were performed. **(A–N)** A total of 14 docking results were obtained. On the left of each docking result, 3D structures of ligands and receptors are shown, with active pockets of proteins highlighted in the middle and 2D interaction maps on the right.

Huang Y. F. et al., 2020; Gajewski et al., 2021). In this study, we developed a *P. vulgaris* target COVID-19–related gene set comprising of 31 genes. Analysis using GO and KEGG revealed that *P. vulgaris* can regulate the inflammatory response process and virus defence mechanism. Furthermore, we identified eight key target genes from the total of 31 genes via PPI network and GO and KEGG network analyses. Amongst all the molecules, RELA-encoded protein (NF-κB) showed the highest docking scores;

therefore, it was chosen for MD simulations. These results can potentially promote basic research on SARS-CoV-2 infection and help with target drug design.

*P. vulgaris* is a traditional Chinese herb used in the treatment of various kidney diseases, including diabetic nephropathy and AKI (Bai et al., 2016; Peng et al., 2016; Namgung et al., 2017; Wu et al., 2020). Studies have shown that *P. vulgaris* can inhibit SARS-CoV-2, preventing it from entering cells by blocking the binding of the
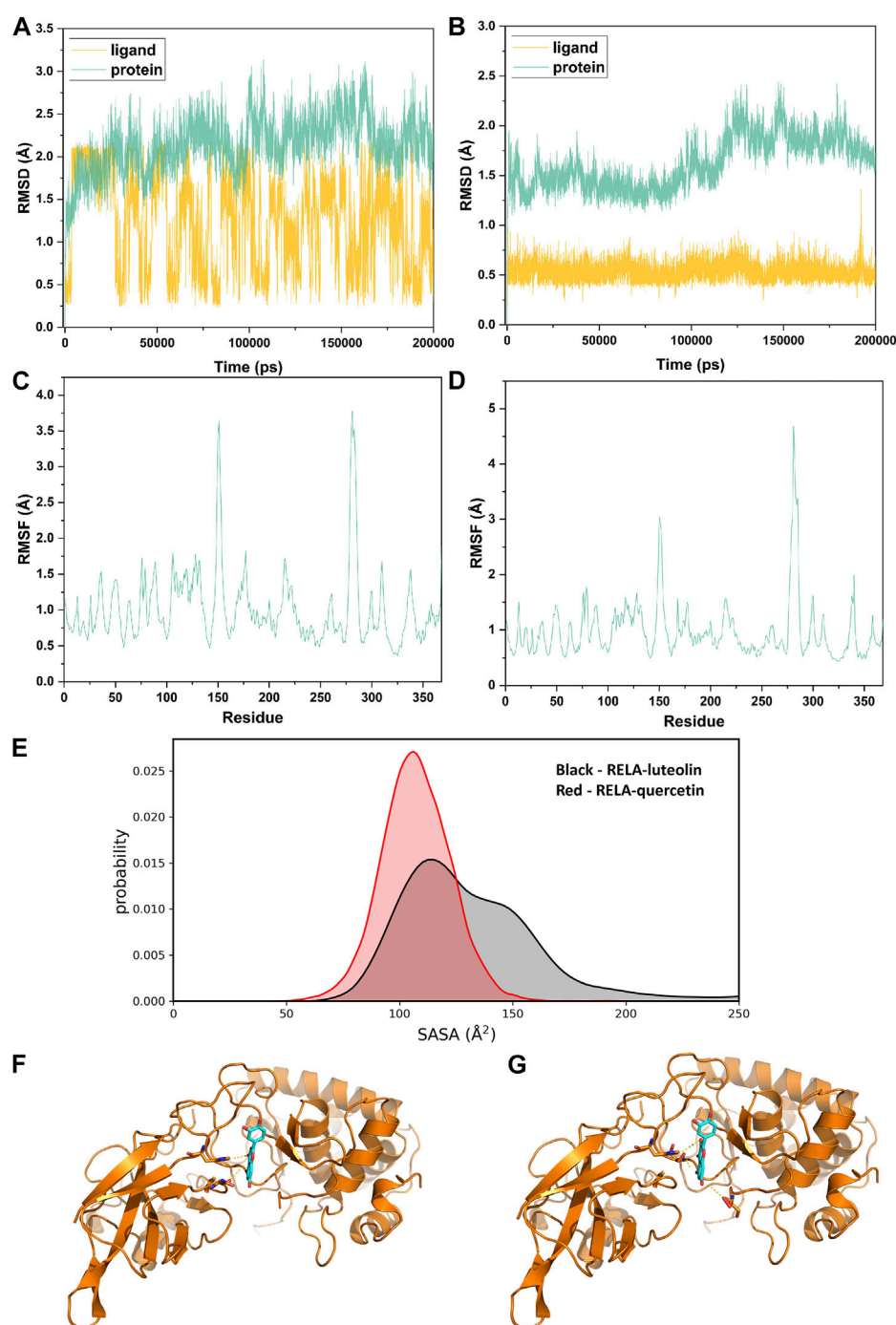
**FIGURE 8**
MD simulation analysis. **(A)** and **(B)**. The RMSD value of RELA-luteolin and RELA-quercetin, respectively. **(C)** and **(D)**. Changes in protein flexibility during simulation of luteolin and quercetin, respectively. **(E)**. Relative surface area contribution of the ligand exposed to the solvent of luteolin and quercetin. **(F)** and **(G)**. Kinetic conformation of the RELA-luteolin and RELA-quercetin systems, respectively.

virus to the ACE2 receptor using its aqueous extract (APV) (Ao et al., 2021). Therefore, we hypothesize that *P. vulgaris* may be pharmacologically effective in treating COVID-19 AKI due to its inhibitory effects on SARS-CoV-2 and protective effects on the kidney. According to the principles of network pharmacology, we first identified effective active compounds of *P. vulgaris* that may ameliorate COVID-19 AKI. Initially, 11 active molecules of

*P. vulgaris* were selected from the TCM database based on OB and DL, followed by the construction of an ingredients-targets network map and molecular docking, three ingredients including quercetin, luteolin and kaempferol were found most significant, as they showed revealed strong interactions with the previously mentioned eight key target proteins. The three identified molecules belong to the group of flavonoid steroids (Kang et al., 2011; Yu et al., 2020; Derosa et al.,

**TABLE 7 MM/PBSA energy analysis of RELA-luteolin.**

| Energy component | Average | Std. Dev. | Std. Err. Of mean |
|---|---|---|---|
| VDWAALS | −28.039 | 3.5066 | 0.4959 |
| EEL | −17.0597 | 11.6462 | 1.647 |
| EPB | 35.5132 | 9.9989 | 1.4141 |
| ENPOLAR | −2.8371 | 0.1992 | 0.0282 |
| ΔG | −12.4226 | 5.6026 | 0.7923 |

Note: VDWAALS, van der Waals energy; EEL; electrostatic energy; EPB; energy calculated by Poisson Boltzmann (PB) equation; ENPOLAR; nonpolar energy; ΔG, binding free energy.

**TABLE 8 MM/PBSA energy analysis of RELA-quercetin.**

| Energy component | Average | Std. Dev. | Std. Err. Of mean |
|---|---|---|---|
| VDWAALS | −31.235 | 2.8066 | 0.3969 |
| EEL | −26.8982 | 11.6517 | 1.6478 |
| EPB | 46.3668 | 9.0074 | 1.2738 |
| ENPOLAR | −3.0681 | 0.1471 | 0.0208 |
| ΔG | −14.8345 | 4.1159 | 0.5821 |

Note: VDWAALS, van der Waals energy; EEL, electrostatic energy; EPB, energy calculated by Poisson Boltzmann (PB) equation; ENPOLAR, nonpolar energy; ΔG, binding free energy.

**TABLE 9 Hydrogen binding during the simulation of the RELA-luteolin system.**

| Acceptor[a] | DonorH[b] | Donor[c] | Frac[d] | AvgDist[e] | AvgAng[f] |
|---|---|---|---|---|---|
| Ligand@O3 | HIE_40@HE2 | HIE_40@NE2 | 0.3152 | 3.0903 | 148.5026 |
| GLN_96@O | Ligand@H9 | Ligand@O2 | 0.2636 | 2.6842 | 162.5045 |
| Ligand@O5 | LYS_38@H | LYS_38@N | 0.227 | 3.1853 | 158.6617 |
| ASN_97@OD1 | Ligand@H10 | Ligand@O4 | 0.1923 | 2.7355 | 164.0721 |

[a]Acceptor, hydrogen bond acceptors.
[b]Acceptor hydrogen donor.
[c]Donor, hydrogen bond donor.
[d]Frac, frequency of occurrence in the simulation.
[e]AvgDist, average distance of hydrogen bonds.
[f]AvgAng, average bond angle of hydrogen bonds.

**TABLE 10 Hydrogen binding during the simulation of the RELA-quercetin system.**

| Acceptor | DonorH | Donor | Frac | AvgDist | AvgAng |
|---|---|---|---|---|---|
| Ligand@O2 | HIE_40@HE2 | HIE_40@NE2 | 0.6069 | 3.0949 | 153.2802 |
| SER_368@OXT | Ligand@H9 | Ligand@O5 | 0.4302 | 2.6539 | 164.0381 |
| SER_27@OG | Ligand@H8 | Ligand@O2 | 0.4083 | 2.868 | 147.5835 |
| SER_368@O | Ligand@H9 | Ligand@O5 | 0.3361 | 2.6502 | 163.8601 |
| Ligand @O7 | LYS_38@H | LYS_38@N | 0.2677 | 3.2296 | 155.2125 |

[a]Acceptor, hydrogen bond acceptors.
[b]Acceptor hydrogen donor.
[c]Donor, hydrogen bond donor.
[d]Frac, frequency of occurrence in the simulation.
[e]AvgDist, average distance of hydrogen bonds.
[f]AvgAng, average bond angle of hydrogen bonds.

2021) and are potential compounds for the treatment of COVID-19 (Luo et al., 2020; Yu et al., 2020; Derosa et al., 2021). Quercetin, luteolin and kaempferol play important roles in the activity of several TCMs against COVID-19. A clinical trial found that quercetin is safe and effective in lowering the serum levels of ALP, q-CRP, and LDH as critical markers involved in COVID-19 severity (Shohan et al., 2022). In addition, their renal protective effects have also been verified in several studies, wherein quercetin has been shown to ameliorate renal injury by inhibiting iron death as well as downregulating the phosphorylation of NF-κB (Tan et al., 2020; Wang et al., 2021), luteolin by regulating P53-dependent tubular apoptosis (Kang et al., 2011), and kaempferol by improving cell injury, oxidative stress and inflammation (Yuan et al., 2021).

Combined with the PPI network and the GO and KEGG-target network, eight key target genes of *P. vulgaris* against COVID-19 AKI were identified, including IL6, VEGFA, CXCL8, IL1B, ICAM1, CCL2, IL10 and RELA. The expression level of these eight genes was strongly associated with COVID-19 AKI. The secretion of cytokines and chemokines, including IL6, CXCL8, IL1B, IL10 and CCL2, is significantly increased in COVID-19 AKI. These inflammatory factors participate in the cytokine storm and act as the important agents causing renal injury (Ahmadian et al., 2021). Studies have shown that IL6 is the most critical mediator in COVID-19 and is closely associated with poor prognosis and mortality (Coomes and Haghbayan, 2020). Excessive IL6 signaling causes several biological effects, such as induction of vascular endothelial growth factor (VEGF) expression, thereby increasing vascular permeability, hyperactivation of T-helper 17 (Th17) cells, and induction of effector T-cell death, resulting in kidney injury (Nechemia-Arbely et al., 2008; Liu et al., 2020). The expression levels of CXCL8, IL1B, CCL-2 and IL10 are also significantly upregulated after SARS-CoV-2 infection and are related to the severity of the disease. CXCL8 control the chemotactic activity of neutrophils and monocytes, IL1B increase the production of IL6 and participate in the differentiation of Th17 cells, CCL-2/MCP-1 can chemoattract monocytes, and the expression of IL10, an anti-inflammatory factor, are feedback increased. These cytokines can result in AKI by causing excessive inflammatory responses (Coperchini et al., 2020; Ahmadian et al., 2021). ICAM1 promotes leukocyte migration through the endothelium, which leads to the infiltration of inflammatory cells and aggravates tissue damage (Ahmadian et al., 2021). VEGFA, a marker of vascular endothelial cell damage, is regulated by hypoxia-inducible factor (HIF). VEGFA is primarily involved in angiogenesis and vascular permeability and is significantly increased in patients with COVID-19, wherein it correlates with the disease severity (Rovas et al., 2021). In addition, TGFB1 is also a related target in the 31genes obtained by intersecting drug target genes and disease-related genes, which may regulate the smad3 activation. As SARS-CoV-2 N protein can enhance TGF-β/Smad3 signaling to cause tubular epithelial cell death and AKI via the G1 cell cycle arrest mechanism, the regulation of TGFB1 might be significant in COVID-19 AKI (Wang et al., 2022).

Molecular docking results revealed that quercetin could bind to all eight key target proteins; luteolin could bind to RELA, ICAM1, VEGFA, IL6 and CXCL8, and kaempferol could bind to ICAM1. Quercetin, luteolin and kaempferol have been reported to have anti-inflammatory and anti-oxidative properties. They can downregulate the production of ICAM1 and MCP-1 to reduce the infiltration of mononuclear cells and inhibit the expression of inflammatory

cytokines IL6, TNF-α, IL8 and IL1B through the NF-κB signaling pathway (Li et al., 2016; Hu et al., 2019). In addition, these compounds can reduce ROS production and VEGF protein concentrations through the Nrf2/HO-1 signaling pathway to alleviate oxidative stress and improve vascular function (Jia et al., 2015; Boeing et al., 2020; Yao et al., 2020; Ozyel et al., 2021). Therefore, it is reasonable to say that *P. vulgaris* can modulate the cytokine storm and improve inflammation, oxidative stress and vascular endothelial function in patients with COVID-19 by targeting the eight core proteins, thereby reducing renal injury.

GO and KEGG pathway analysis revealed that drug-disease intersection genes were substantially enriched in virus-related functions and pathways, which verified the ability of *P. vulgaris* against viruses. GO enrichment mainly focused on inflammation, cytokines, oxidative stress and angiogenesis, among other factors, which coincided with the biological effects of the eight key target genes described earlier. Analysis of the top 20 KEGG signaling pathways revealed that these target genes were mainly enriched in HIF-1, VEGF, NF-κB, JAK/STAT, Th17 cell differentiation, TNF-α and Nrf2 signaling pathways. NF-κB signaling pathway was enriched to the most number of key target genes, and based on its significant effect on COVID-19 (Hariharan et al., 2021), it can be inferred that it is the most important signaling pathway of *P. vulgaris* in antagonising COVID-19 AKI. The effects are accomplished by anti-oxidative and anti-inflammatory actions, improvement in the function of blood vessels, and by reducing inflammatory factors. Th17 cells also play an important role in the pathogenesis of COVID-19. These cells can promote neutrophil migration and reduce Treg responses by releasing cytokines, such as IL-17 and GM-CSF and thus exacerbate inflammation. This is also a key mechanism causing kidney injury (Martonik et al., 2021).

Because of the highest docking score of RELA-encoded protein (NF-κB) with luteolin and quercetin, NF-κB was selected to perform the MD simulation to further examine the binding effect of NF-κB with luteolin and quercetin, respectively, which verified the result of molecular docking. And the MD simulation results suggested good binding stability. In most cells, NF-κB complexes remain inactive and are mainly located in the cytoplasm where they interact with inhibitory IκB proteins. However, when signaling pathways become activated, the IκB protein is degraded, allowing NF-κB dimers to translocate into the nucleus and regulate the expression of target genes (Hayden and Ghosh, 2011). RELA encodes NF-κB, which can be activated by SARS-CoV-2 Viral DNA and RNA, ROS and cytokines, such as TNF-α, IL1B and IL6, can cause nuclear translocation of NF-κB. (Hariharan et al., 2021). NF-κB can participate in host immunity, inflammation, and regulation of proliferation, differentiation, and apoptosis of B cell and T lymphocytes (Hayden and Ghosh, 2011). Activated NF-κB promotes the expression of multiple cytokines (IL1, IL2, IL6, IL12, TNF-α, LT-α, LT-1β and GM-CSF), chemokines (IL8, MIP-1 and MCP-1), adhesion molecules (ICAM, VCAM and E-selectin), and induces effector enzymes (inducible nitric oxide synthase [iNOS]) (Hariharan et al., 2021), which can aggravate the cytokine storm and oxidative stress on the kidney. As mentioned in the manuscript, NF-κB pathway is a major pathway in this study, which can regulate the expression of other core protein, such as IL6. And the inhibition of NF-κB pathway has the potential to reduce the effect of cytokine storm and improve oxidative stress and vascular function. In summary, NF-κB may be the most potential target for the therapy of *P. vulgaris* on COVID-19 AKI.

In the present study, we investigated the potential therapeutic mechanism of the Chinese medicine *P. vulgaris* in COVID-19 AKI based on network pharmacology and molecular docking approaches. Our findings indicated that NF-κB might be the potent pharmacological target of *P. vulgaris* against COVID-19 induced AKI. In addition, we provided several potential targets for COVID-19 AKI treatment, mainly IL6, VEGFA and RELA, which may help to develop new therapeutic strategies. However, as an *in silico* study, our results have not been experimentally verified. But it is still valuable which can and can provide guidance for drug design and further investigations warranted by the study, such as biological studies on binding affinity and activities of target proteins; preclinical and clinical efficacy and toxicity, *etc.*

## Data availability statement

The original contributions presented in the study are included in the article/Supplementary Materials, further inquiries can be directed to the corresponding authors.

## Author contributions

J-RY and KL designed the study; X-LY, C-XW, J-XW, S-MW, QY performed the experiments and collected and analyzed the data; J-RY, KL and X-LY wrote and revised the manuscript. All authors listed have made a substantial, direct, and intellectual contribution to the work and approved it for publication.

## Funding

## Conflict of interest

The authors declare that the research was conducted in the absence of any commercial or financial relationships that could be construed as a potential conflict of interest.

## Publisher's note

All claims expressed in this article are solely those of the authors and do not necessarily represent those of their affiliated organizations, or those of the publisher, the editors and the reviewers. Any product that may be evaluated in this article, or claim that may be made by its manufacturer, is not guaranteed or endorsed by the publisher.

## Supplementary material

The Supplementary Material for this article can be found online at: https://www.frontiersin.org/articles/10.3389/fphar.2023.1188086/full#supplementary-material

## References

Ahmadian, E., Hosseiniyan Khatibi, S. M., Razi Soofiyani, S., Abediazar, S., Shoja, M. M., Ardalan, M., et al. (2021). Covid-19 and kidney injury: Pathophysiology and molecular mechanisms. *Rev. Med. Virol.* 31 (3), e2176. doi:10.1002/rmv.2176

Amberger, J. S., Bocchini, C. A., Schiettecatte, F., Scott, A. F., and Hamosh, A. (2015). OMIM.org: Online Mendelian Inheritance in Man (OMIM®), an online catalog of human genes and genetic disorders. *Nucleic Acids Res.* 43, D789–D798. Database issue). doi:10.1093/nar/gku1205

Ao, Z., Chan, M., Ouyang, M. J., Olukitibi, T. A., Mahmoudi, M., Kobasa, D., et al. (2021). Identification and evaluation of the inhibitory effect of *Prunella vulgaris* extract on SARS-coronavirus 2 virus entry. *PLoS One* 16 (6), e0251649. doi:10.1371/journal.pone.0251649

Bai, Y., Xia, B., Xie, W., Zhou, Y., Xie, J., Li, H., et al. (2016). Phytochemistry and pharmacological activities of the genus Prunella. *Food Chem.* 204, 483–496. doi:10.1016/j.foodchem.2016.02.047

Berman, H. M., Westbrook, J., Feng, Z., Gilliland, G., Bhat, T. N., Weissig, H., et al. (2000). The protein data bank. *Nucleic Acids Res.* 28 (1), 235–242. doi:10.1093/nar/28.1.235

Boeing, T., De Souza, P., Speca, S., Somensi, L. B., Mariano, L. N. B., Cury, B. J., et al. (2020). Luteolin prevents irinotecan-induced intestinal mucositis in mice through antioxidant and anti-inflammatory properties. *Br. J. Pharmacol.* 177 (10), 2393–2408. doi:10.1111/bph.14987

Case, D. A., Duke, R. E., Walker, R. C., Skrynnikov, N. R., Cheatham Iii, T. E., Mikhailovskii, O., et al. (2022). *AMBER 22 reference manual*. San Francisco: University of California.

Chen, N., Zhou, M., Dong, X., Qu, J., Gong, F., Han, Y., et al. (2020). Epidemiological and clinical characteristics of 99 cases of 2019 novel coronavirus pneumonia in wuhan, China: A descriptive study. *Lancet* 395 (10223), 507–513. doi:10.1016/s0140-6736(20)30211-7

Chen, X., Ji, Z. L., and Chen, Y. Z. (2002). Ttd: Therapeutic target database. *Nucleic Acids Res.* 30 (1), 412–415. doi:10.1093/nar/30.1.412

Cheng, Y., Luo, R., Wang, K., Zhang, M., Wang, Z., Dong, L., et al. (2020). Kidney disease is associated with in-hospital death of patients with COVID-19. *Kidney Int.* 97 (5), 829–838. doi:10.1016/j.kint.2020.03.005

Consortium, U. (2015). UniProt: A hub for protein information. *Nucleic Acids Res.* 43, D204–D212. Database issue. doi:10.1093/nar/gku989

Coomes, E. A., and Haghbayan, H. (2020). Interleukin-6 in covid-19: A systematic review and meta-analysis. *Rev. Med. Virol.* 30 (6), 1–9. doi:10.1002/rmv.2141

Coperchini, F., Chiovato, L., Croce, L., Magri, F., and Rotondi, M. (2020). The cytokine storm in COVID-19: An overview of the involvement of the chemokine/chemokine-receptor system. *Cytokine Growth Factor Rev.* 53, 25–32. doi:10.1016/j.cytogfr.2020.05.003

Daniels, G. E., Jr., and Morton, M. H. (2023). COVID-19 recession: Young adult food insecurity, racial disparities, and correlates. *J. Adolesc. Health* 72 (2), 237–245. doi:10.1016/j.jadohealth.2022.09.008

Derosa, G., Maffioli, P., D'angelo, A., and Di Pierro, F. (2021). A role for quercetin in coronavirus disease 2019 (COVID-19). *Phytother. Res.* 35 (3), 1230–1236. doi:10.1002/ptr.6887

Dong, E., Du, H., and Gardner, L. (2020). An interactive web-based dashboard to track COVID-19 in real time. *Lancet Infect. Dis.* 20 (5), 533–534. doi:10.1016/s1473-3099(20)30120-1

Gajewski, A., Kośmider, A., Nowacka, A., Puk, O., and Wiciński, M. (2021). Potential of herbal products in prevention and treatment of COVID-19. Literature review. *Biomed. Pharmacother.* 143, 112150. doi:10.1016/j.biopha.2021.112150

Guan, W. J., Ni, Z. Y., Hu, Y., Liang, W. H., Ou, C. Q., He, J. X., et al. (2020). Clinical characteristics of coronavirus disease 2019 in China. *N. Engl. J. Med.* 382 (18), 1708–1720. doi:10.1056/NEJMoa2002032

Han, X., and Ye, Q. (2021). Kidney involvement in COVID-19 and its treatments. *J. Med. Virol.* 93 (3), 1387–1395. doi:10.1002/jmv.26653

Hariharan, A., Hakeem, A. R., Radhakrishnan, S., Reddy, M. S., and Rela, M. (2021). The role and therapeutic potential of NF-kappa-B pathway in severe COVID-19 patients. *Inflammopharmacology* 29 (1), 91–100. doi:10.1007/s10787-020-00773-9

Hayden, M. S., and Ghosh, S. (2011). NF-κB in immunobiology. *Cell Res.* 21 (2), 223–244. doi:10.1038/cr.2011.13

Hu, B., Guo, H., Zhou, P., and Shi, Z. L. (2021a). Characteristics of SARS-CoV-2 and COVID-19. *Nat. Rev. Microbiol.* 19 (3), 141–154. doi:10.1038/s41579-020-00459-7

Hu, K., Guan, W. J., Bi, Y., Zhang, W., Li, L., Zhang, B., et al. (2021b). Efficacy and safety of lianhuaqingwen capsules, a repurposed Chinese herb, in patients with coronavirus disease 2019: A multicenter, prospective, randomized controlled trial. *Phytomedicine* 85, 153242. doi:10.1016/j.phymed.2020.153242

Hu, Y., Gui, Z., Zhou, Y., Xia, L., Lin, K., and Xu, Y. (2019). Quercetin alleviates rat osteoarthritis by inhibiting inflammation and apoptosis of chondrocytes, modulating synovial macrophages polarization to M2 macrophages. *Free Radic. Biol. Med.* 145, 146–160. doi:10.1016/j.freeradbiomed.2019.09.024

Huang, C., Wang, Y., Li, X., Ren, L., Zhao, J., Hu, Y., et al. (2020a). Clinical features of patients infected with 2019 novel coronavirus in Wuhan, China. *Lancet* 395 (10223), 497–506. doi:10.1016/s0140-6736(20)30183-5

Huang, Y. F., Bai, C., He, F., Xie, Y., and Zhou, H. (2020b). Review on the potential action mechanisms of Chinese medicines in treating Coronavirus Disease 2019 (COVID-19). *Pharmacol. Res.* 158, 104939. doi:10.1016/j.phrs.2020.104939

Jia, Z., Nallasamy, P., Liu, D., Shah, H., Li, J. Z., Chitrakar, R., et al. (2015). Luteolin protects against vascular inflammation in mice and TNF-alpha-induced monocyte adhesion to endothelial cells via suppressing IKBα/NF-κB signaling pathway. *J. Nutr. Biochem.* 26 (3), 293–302. doi:10.1016/j.jnutbio.2014.11.008

Kang, K. P., Park, S. K., Kim, D. H., Sung, M. J., Jung, Y. J., Lee, A. S., et al. (2011). Luteolin ameliorates cisplatin-induced acute kidney injury in mice by regulation of p53-dependent renal tubular apoptosis. *Nephrol. Dial. Transpl.* 26 (3), 814–822. doi:10.1093/ndt/gfq528

Kudose, S., Batal, I., Santoriello, D., Xu, K., Barasch, J., Peleg, Y., et al. (2020). Kidney biopsy findings in patients with COVID-19. *J. Am. Soc. Nephrol.* 31 (9), 1959–1968. doi:10.1681/asn.2020060802

Li, H. D., Meng, X. M., Huang, C., Zhang, L., Lv, X. W., and Li, J. (2019). Application of herbal traditional Chinese medicine in the treatment of acute kidney injury. *Front. Pharmacol.* 10, 376. doi:10.3389/fphar.2019.00376

Li, R., Li, Y., Liang, X., Yang, L., Su, M., and Lai, K. P. (2021). Network Pharmacology and bioinformatics analyses identify intersection genes of niacin and COVID-19 as potential therapeutic targets. *Brief. Bioinform* 22 (2), 1279–1290. doi:10.1093/bib/bbaa300

Li, Y., Yao, J., Han, C., Yang, J., Chaudhry, M. T., Wang, S., et al. (2016). Quercetin, inflammation and immunity. *Nutrients* 8 (3), 167. doi:10.3390/nu8030167

Lin, L., Deng, J., Li, J., Zheng, L., Wu, Z., Tan, W., et al. (2022). Pathogenesis and histological changes of nephropathy associated with COVID-19. *J. Med. Virol.* 95, e28311. doi:10.1002/jmv.28311

Lin, L., Wang, X., Ren, J., Sun, Y., Yu, R., Li, K., et al. (2020). Risk factors and prognosis for COVID-19-induced acute kidney injury: A meta-analysis. *BMJ Open* 10 (11), e042573. doi:10.1136/bmjopen-2020-042573

Liu, B., Li, M., Zhou, Z., Guan, X., and Xiang, Y. (2020). Can we use interleukin-6 (IL-6) blockade for coronavirus disease 2019 (COVID-19)-induced cytokine release syndrome (CRS)? *J. Autoimmun.* 111, 102452. doi:10.1016/j.jaut.2020.102452

Liu, J., Sun, T., Liu, S., Liu, J., Fang, S., Tan, S., et al. (2022). Dissecting the molecular mechanism of cepharanthine against COVID-19, based on a network pharmacology strategy combined with RNA-sequencing analysis, molecular docking, and molecular dynamics simulation. *Comput. Biol. Med.* 151, 106298. doi:10.1016/j.compbiomed.2022.106298

Luo, L., Jiang, J., Wang, C., Fitzgerald, M., Hu, W., Zhou, Y., et al. (2020). Analysis on herbal medicines utilized for treatment of COVID-19. *Acta Pharm. Sin. B* 10 (7), 1192–1204. doi:10.1016/j.apsb.2020.05.007

Martonik, D., Parfieniuk-Kowerda, A., Rogalska, M., and Flisiak, R. (2021). The role of Th17 response in COVID-19. *Cells* 10 (6), 1550. doi:10.3390/cells10061550

Matsumoto, K., and Prowle, J. R. (2022). COVID-19-associated AKI. *Curr. Opin. Crit. Care* 28 (6), 630–637. doi:10.1097/mcc.0000000000000988

Morris, G. M., Huey, R., Lindstrom, W., Sanner, M. F., Belew, R. K., Goodsell, D. S., et al. (2009). AutoDock4 and AutoDockTools4: Automated docking with selective receptor flexibility. *J. Comput. Chem.* 30 (16), 2785–2791. doi:10.1002/jcc.21256

Nadim, M. K., Forni, L. G., Mehta, R. L., Connor, M. J., Jr, Liu, K. D., Ostermann, M., et al. (2020). COVID-19-associated acute kidney injury: Consensus report of the 25th acute disease quality initiative (ADQI) workgroup. *Nat. Rev. Nephrol.* 16 (12), 747–764. doi:10.1038/s41581-020-00356-5

Namgung, S., Yoon, J. J., Yoon, C. S., Han, B. H., Choi, E. S., Oh, H., et al. (2017). *Prunella vulgaris* attenuates diabetic renal injury by suppressing glomerular fibrosis and inflammation. *Am. J. Chin. Med.* 45 (3), 475–495. doi:10.1142/s0192415x1750029x

Nechemia-Arbely, Y., Barkan, D., Pizov, G., Shriki, A., Rose-John, S., Galun, E., et al. (2008). IL-6/IL-6R axis plays a critical role in acute kidney injury. *J. Am. Soc. Nephrol.* 19 (6), 1106–1115. doi:10.1681/asn.2007070744

Nogales, C., Mamdouh, Z. M., List, M., Kiel, C., Casas, A. I., and Schmidt, H. (2022). Network pharmacology: Curing causal mechanisms instead of treating symptoms. *Trends Pharmacol. Sci.* 43 (2), 136–150. doi:10.1016/j.tips.2021.11.004

Ozyel, B., Le Gall, G., Needs, P. W., and Kroon, P. A. (2021). Anti-inflammatory effects of quercetin on high-glucose and pro-inflammatory cytokine challenged vascular endothelial cell metabolism. *Mol. Nutr. Food Res.* 65 (6), e2000777. doi:10.1002/mnfr.202000777

Peng, J., Ren, X., Lan, T., Chen, Y., Shao, Z., and Yang, C. (2016). Renoprotective effects of ursolic acid on ischemia/reperfusion-induced acute kidney injury through oxidative stress, inflammation and the inhibition of STAT3 and NF-κB activities. *Mol. Med. Rep.* 14 (4), 3397–3402. doi:10.3892/mmr.2016.5654

Piñero, J., Bravo, À., Queralt-Rosinach, N., Gutiérrez-Sacristán, A., Deu-Pons, J., Centeno, E., et al. (2017). DisGeNET: A comprehensive platform integrating information on human disease-associated genes and variants. *Nucleic Acids Res.* 45 (D1), D833–D839. doi:10.1093/nar/gkw943

Rebhan, M., Chalifa-Caspi, V., Prilusky, J., and Lancet, D. (1997). GeneCards: Integrating information about genes, proteins and diseases. *Trends Genet.* 13 (4), 163. doi:10.1016/s0168-9525(97)01103-7

Rovas, A., Osiaevi, I., Buscher, K., Sackarnd, J., Tepasse, P. R., Fobker, M., et al. (2021). Microvascular dysfunction in COVID-19: The MYSTIC study. *Angiogenesis* 24 (1), 145–157. doi:10.1007/s10456-020-09753-7

Ru, J., Li, P., Wang, J., Zhou, W., Li, B., Huang, C., et al. (2014). Tcmsp: A database of systems pharmacology for drug discovery from herbal medicines. *J. Cheminform* 6, 13. doi:10.1186/1758-2946-6-13

Runfeng, L., Yunlong, H., Jicheng, H., Weiqi, P., Qinhai, M., Yongxia, S., et al. (2020). Lianhuaqingwen exerts anti-viral and anti-inflammatory activity against novel coronavirus (SARS-CoV-2). *Pharmacol. Res.* 156, 104761. doi:10.1016/j.phrs.2020.104761

Shannon, P., Markiel, A., Ozier, O., Baliga, N. S., Wang, J. T., Ramage, D., et al. (2003). Cytoscape: A software environment for integrated models of biomolecular interaction networks. *Genome Res.* 13 (11), 2498–2504. doi:10.1101/gr.1239303

Shohan, M., Nashibi, R., Mahmoudian-Sani, M. R., Abolnezhadian, F., Ghafourian, M., Alavi, S. M., et al. (2022). The therapeutic efficacy of quercetin in combination with antiviral drugs in hospitalized COVID-19 patients: A randomized controlled trial. *Eur. J. Pharmacol.* 914, 174615. doi:10.1016/j.ejphar.2021.174615

Szklarczyk, D., Gable, A. L., Lyon, D., Junge, A., Wyder, S., Huerta-Cepas, J., et al. (2019). STRING v11: Protein-protein association networks with increased coverage, supporting functional discovery in genome-wide experimental datasets. *Nucleic Acids Res.* 47 (1), D607–D613. doi:10.1093/nar/gky1131

Tabba, H. D., Chang, R. S., and Smith, K. M. (1989). Isolation, purification, and partial characterization of prunellin, an anti-HIV component from aqueous extracts of *Prunella vulgaris*. *Antivir. Res.* 11 (5-6), 263–273. doi:10.1016/0166-3542(89)90036-3

Tan, R. Z., Wang, C., Deng, C., Zhong, X., Yan, Y., Luo, Y., et al. (2020). Quercetin protects against cisplatin-induced acute kidney injury by inhibiting Mincle/Syk/NF-κB signaling maintained macrophage inflammation. *Phytother. Res.* 34 (1), 139–152. doi:10.1002/ptr.6507

Tian, C., Kasavajhala, K., Belfon, K. A., Raguette, L., Huang, H., Migues, A. N., et al. (2019). ff19SB: Amino-acid-specific protein backbone parameters trained against quantum mechanics energy surfaces in solution. *J. Chem. theory Comput.* 16 (1), 528–552. doi:10.1021/acs.jctc.9b00591

Wang, W., Chen, J., Hu, D., Pan, P., Liang, L., Wu, W., et al. (2022). SARS-CoV-2 N protein induces acute kidney injury via smad3-dependent G1 cell cycle arrest mechanism. *Adv. Sci. (Weinh)* 9 (3), e2103248. doi:10.1002/advs.202103248

Wang, Y., Bryant, S. H., Cheng, T., Wang, J., Gindulyte, A., Shoemaker, B. A., et al. (2017). PubChem BioAssay: 2017 update. *Nucleic Acids Res.* 45 (D1), D955–D963. doi:10.1093/nar/gkw1118

Wang, Y., Quan, F., Cao, Q., Lin, Y., Yue, C., Bi, R., et al. (2021). Quercetin alleviates acute kidney injury by inhibiting ferroptosis. *J. Adv. Res.* 28, 231–243. doi:10.1016/j.jare.2020.07.007

Weiser, J., Shenkin, P. S., and Still, W. C. (1999). Approximate atomic surfaces from linear combinations of pairwise overlaps (LCPO). *J. Comput. Chem.* 20 (2), 217–230. doi:10.1002/(sici)1096-987x(19990130)20:2<217::aid-jcc4>3.0.co;2-a

Wu, W. F., Wang, J. N., Li, Z., Wei, B., Jin, J., Gao, L., et al. (2020). 7-Hydroxycoumarin protects against cisplatin-induced acute kidney injury by inhibiting necroptosis and promoting Sox9-mediated tubular epithelial cell proliferation. *Phytomedicine* 69, 153202. doi:10.1016/j.phymed.2020.153202

Xia, Q. D., Xun, Y., Lu, J. L., Lu, Y. C., Yang, Y. Y., Zhou, P., et al. (2020). Network pharmacology and molecular docking analyses on Lianhua Qingwen capsule indicate Akt1 is a potential target to treat and prevent COVID-19. *Cell Prolif.* 53 (12), e12949. doi:10.1111/cpr.12949

Xu, H. X., Lee, S. H., Lee, S. F., White, R. L., and Blay, J. (1999). Isolation and characterization of an anti-HSV polysaccharide from *Prunella vulgaris*. *Antivir. Res.* 44 (1), 43–54. doi:10.1016/s0166-3542(99)00053-4

Yang, X., Yu, Y., Xu, J., Shu, H., Xia, J., Liu, H., et al. (2020). Clinical course and outcomes of critically ill patients with SARS-CoV-2 pneumonia in wuhan, China: A single-centered, retrospective, observational study. *Lancet Respir. Med.* 8 (5), 475–481. doi:10.1016/s2213-2600(20)30079-5

Yao, H., Sun, J., Wei, J., Zhang, X., Chen, B., and Lin, Y. (2020). Kaempferol protects blood vessels from damage induced by oxidative stress and inflammation in association with the Nrf2/HO-1 signaling pathway. *Front. Pharmacol.* 11, 1118. doi:10.3389/fphar.2020.01118

Yao, X. J., Wainberg, M. A., and Parniak, M. A. (1992). Mechanism of inhibition of HIV-1 infection *in vitro* by purified extract of *Prunella vulgaris*. *Virology* 187 (1), 56–62. doi:10.1016/0042-6822(92)90294-y

Yu, R., Chen, L., Lan, R., Shen, R., and Li, P. (2020). Computational screening of antagonists against the SARS-CoV-2 (COVID-19) coronavirus by molecular docking. *Int. J. Antimicrob. Agents* 56 (2), 106012. doi:10.1016/j.ijantimicag.2020.106012

Yuan, P., Sun, X., Liu, X., Hutterer, G., Pummer, K., Hager, B., et al. (2021). Kaempferol alleviates calcium oxalate crystal-induced renal injury and crystal deposition via regulation of the AR/NOX2 signaling pathway. *Phytomedicine* 86, 153555. doi:10.1016/j.phymed.2021.153555

Zhang, X., Ao, Z., Bello, A., Ran, X., Liu, S., Wigle, J., et al. (2016). Characterization of the inhibitory effect of an extract of *Prunella vulgaris* on Ebola virus glycoprotein (GP)-mediated virus entry and infection. *Antivir. Res.* 127, 20–31. doi:10.1016/j.antiviral.2016.01.001

Zheng, C., and Wang, Y. (2014). Prediction of oral bioavailability: Challenges and strategies. *J. Bioequivalence Bioavailab.* 6 (1), 1. doi:10.4172/jbb.10000e47

**Frontiers** | Frontiers in Pharmacology

Check for updates

*CORRESPONDENCE
Shu-Bin Guo,
✉ shubinguo@126.com
Hui-Hua Li,
✉ hhli1935@aliyun.com

# Blockage of S100A8/A9 ameliorates septic nephropathy in mice

Wei Shi, Tian-Tian Wan, Hui-Hua Li* and Shu-Bin Guo*

Beijing Key Laboratory of Cardiopulmonary Cerebral Resuscitation, Department of Emergency Medicine, Beijing Chaoyang Hospital, Capital Medical University, Beijing, China

Septic acute kidney injury (AKI) is the commonest cause of complication of sepsis in intensive care units, but its pathophysiology remains unclear. Calprotectin (S100A8/A9), which is a damage-associated molecular patterns (DAMPs) molecule, exerts a critical role in modulating leukocyte recruitment and inflammatory response during various diseases. However, role of S100A8/A9 in septic AKI is largely unknown. In this research, Septic AKI was triggered by cecal ligation and puncture (CLP) operation in wild-type mice, which treated with or without an S100A9 inhibitor, Paquinimod (Paq, 10 mg/kg) that prevents S100A8/A9 to bind to Toll-like receptor 4 (TLR4). Renal function, pathological changes, cell death, and oxidative stress were evaluated. Our research indicated that the mRNA and protein expression of S100A9 are time-dependently elevated in the kidney following CLP. Moreover, the administration of Paq for 24 h significantly improved CLP-induced renal dysfunction and pathological alterations compared with vehicle treatment in mice. These beneficial effects were associated with the inhibition of CLP-triggered renal tubular epithelial cell apoptosis, inflammation, superoxide production, and mitochondrial dynamic imbalance. What's more, we further confirmed the above findings by cell co-culture experiments. Our study demonstrates that S100A9 is a prominent protein to lead to septic AKI, and the selective inhibition of S100A9 could represent a new therapeutic approach which can treat septic AKI.

KEYWORDS

acute kidney injury, Paquinimod, mitochondrial dynamics, S100A8/A9, sepsis

## 1 Introduction

Sepsis is a systemic inflammatory response in which the host is deregulated by infection. Sepsis is a common disease with a high mortality rate, and acute kidney injury (AKI) is the leading complication in intensive care units, accounting for 45%–70% of all AKIs (Sun et al., 2019). Increasing evidence suggests that multiple pathophysiological processes are involved in the development of septic AKI, including hypoperfusion-induced ischemic injury, microvascular dysfunction, intrarenal redistribution of renal blood flow in the kidney, infiltration, and activation of immune cells, massive release of inflammatory cytokines, and endocrine dysregulation (Quaglia et al., 2022). Although the molecular mechanism of septic AKI is complex, microvascular impairment can alter the function and density of capillaries, leading to intrarenal shunts and renal ischemia. Moreover, inflammation takes a vital part in producing excessive oxidative stress, apoptosis, as well as mitochondrial dysfunction in renal tubular epithelial cells (So et al., 2022). Therefore, it is crucial to identify the key signaling pathways involved in inflammation and mitochondrial dysfunction during septic AKI.

The S100 protein family is an effective amplifying factor for inflammatory responses. S100A8 and S100A9, which belong to the S100 family, are cytoplasmic EF-hand $Ca^{2+}$-binding proteins. They form a heterodimer that is highly expressed in activated neutrophils and monocytes/macrophages. S100A8/A9 protein is widely distributed in human cells, tissues, and body fluids and can be detected in serum, urine, and cerebrospinal fluid (Tammaro et al., 2018; Wang et al., 2018). S100A9 consists of 110 amino acids with a molecular weight of ~13 KDa (Wang et al., 2018). S100A8/A9 is the most abundant damage-associated molecular patterns (DAMPs) molecule [14]. It can tie to toll-like receptor 4 (TLR4) or the receptor for advanced glycation end products (RAGE) to activate JAK/STAT, PI3K/AKT, MAPK/NF-κB, and NLRP3 inflammasome pathways, thereby enhancing proinflammatory response and development of various inflammatory diseases, including autoimmune disease, chronic obstructive pulmonary disease, and cardiovascular disease (Wang et al., 2018). Moreover, studies have reported that S100A8/A9 is related to the great variety of kidney diseases, including ischemia/reperfusion (I/R)-induced AKI, contrast-induced AKI, obstructive and diabetic renal fibrosis, acute urinary tract infection, and glomerulonephritis in different animal models (Dessing et al., 2010; Pepper et al., 2015; Tan et al., 2017; Tammaro et al., 2018; Du et al., 2022; Yao et al., 2022). Further, emerging bioinformatics studies point that S100A9 may act as a potential biomarker and therapeutic aim for septic shock-related renal injury (Tang et al., 2021). While, the role and mechanism of S100A8/A9 in the genesis of AKI in sepsis is poorly understood.

In this research, using Paquinimod (Talley et al., 2021; Zhao et al., 2021; Su et al., 2022) (Paq, also known as ABR25757), an S100A8/A9 specific inhibitor which prevents S100A8/A9 to bind to TLR4, we explored the role of S100A9 in the development of septic AKI in a murine model of cecal ligation and puncture (CLP)-induced sepsis. We found that S100A9 level was notably regulated upwards in the kidney of CLP-treated mice during 24–72 h. CLP-induced renal dysfunction and pathological alterations, including tubular epithelial cell apoptosis, inflammation, and oxidative stress, was ameliorated by using Paq to inhibition of S100A9 in mice. These preventive effects were associated with the inhibition of mitochondrial fission-fusion imbalance by the reduction of dynamin-related protein 1 (Drp1) and an increase in mitofusin-1/2 (Mfn1/2). In addition, we further confirmed the above findings by cell co-culture experiments. Therefore, our results suggest that S100A8/A9 likely has an effect on CLP-induced AKI by impairing Drp1/Mfn1/2-mediated mitochondrial balance, and reducing and suppressing S100A9 may represent a new therapeutic method for septic AKI.

# 2 Methods and materials

## 2.1 Animals

C57BL/6J wild-type (WT) mice were bought from Charles River (China). All mice were cultured in Medical Research Center at the Beijing Chaoyang Hospital (China). They are fed in specific pathogen-free facility at temperature about 25°C–26°C with the condition of 12-hour light-dark cycle. Only male mice were recruited in this paper. All animal experimental procedures are endorsed by the Animal Care and Use Committee of Chao-Yang

Hospital (2021-Animal-35) and complied with regulations for the Care and Use of Laboratory Animals prepared by the U.S. *NIH*.

## 2.2 Cecal ligation and puncture (CLP) operation

Male mice (8 weeks, 22–24 g) were fed for 1 week to facilitate adaptation to their surroundings, and a murine model of sepsis was made by CLP operation as described [20]. Then, the mice ($n = 6$ per group) were treated with 2.5% tribromoethanol (0.01 mL/g; Sigma) via intraperitoneal injection. Further, mid-abdominal laparotomy was performed to expose the abdominal organs, and the cecum was ligated at 1/2 and punctured with a 21-gauge needle. Control-group animals did not undergo ligation and puncture.

## 2.3 Paquinimod treatment

Paquinimod (Paq, HY-100442, MCE, NJ), an S100A9-specific small molecule inhibitor that prevents S100A8/A9 to bind to TLR4, was dissolved directly in castor oil (vehicle) and administered to the mice at dosages of 10 mg/kg by intraperitoneal injection 1 day before and after CLP surgery. The optimal dose of Paq (10 mg/kg) was determined based on a literature review as described (Talley et al., 2021) and our preliminary data. To measure the content of S100A9 mRNA and proteins in the kidney, mice were randomly assigned into four groups and was performed with CLP surgery for 24–72 h (sham, CLP-24 h, CLP-48 h, CLP-72 h, $n = 6$ per group). To examine the role of Paq in our experiment, the mice were subjected to CLP surgery for 48 h (sham + vehicle, sham + Paq(10 mg/kg),CLP + vehicle, CLP + Paq (10 mg/kg), $n = 6$ per group). The sham mice were given an injection intraperitoneally with the same volume of castor oil (vehicle) alone ($n = 6$ per group). The kidney and blood samples were collected to examine their histology, the markers for renal function, and the gene mRNA and protein levels.

## 2.4 Cell co-culture *in vitro*

The cell lines of mouse monocyte/macrophage cell line (RAW264.7; BNCC354753) and mouse renal tubular epithelial cells (mRTECs; BNCC3660478) were purchase from BeNa Culture Collection (BNCC, Beijing). They were cultured in cell incubators at 37°C, 5% $CO_2$, and 95% air. RAW264.7 cells were inoculated in the upper chamber and mRTEC cells were seed in lower chamber of 24-well transwell cell culture (cell number about $1\times10^6$). After cell adherence, RAW264.7 were pretreated with LPS (50 μg/mL) for 24 h. The lower chamber containing mRTEC were pretreated with Paq (150 μM) for 2 h before co-culture of the 2 cells.

For the examination of S100A9 from RAW264.7 cells on mitochondrial fusion and fission related proteins in mRTECs ($n = 3$), 2 cell lines were co-cultureed for 24 and the mRTEC cells were examined using double immunostaining with anti-Drp1 (CST, China, 1:50), anti-Mfn-1 (Proteintech, United States, 1:100), anti-Mfn-2 (Proteintech, 1:100), and anti-ATP5A (Proteintech, United States, 1:300). All images were randomly selected from 5 visual fields for each slice and photographed with a Nikon microscope (Nikon, Tokyo).

For the examination of S100A9 from RAW264.7 cells on oxidative stress and apoptosis, the mRTEC cells ($n$ = 3) were stained with dihydroethidine (DHE, Sigma), anti-cleaved caspase-3 (CST, China, 1:400), respectively. Meanwhile, the RAW264.7 cells were treated with LPS in different concentrations (0,1, 10, 50 μg/mL) for 24 h, and supernatants were absorbed (1,000 rpm, 20 min) to analyze the contents of S100A9, IL-6 or TNF-α with ELISA kits.

## 2.5 Immunofluorescence double staining analysis

For the double immunostaining of kidney tissue, anti-S100A9 (Abcam, United States, 1:1000) and anti-F4/80 (Abacam, 1:400) were used to stain kidney tissue section at 48 h of CLP surgery.

## 2.6 Renal function measurement

Blood samples ($n$ = 6 per group) were obtained from the eyeballs of the mice in each group, stratified, and centrifuged (3,000 rpm, 15 min). Aspirate the upper supernatant and save in a centrifuge tube. The levels of renal function markers were determined using BUN and Cr assay kits (Nanjing Jian cheng) [20].

## 2.7 Histology analysis

Kidney tissues ($n$ = 6 per group) were infiltrated in 4% paraformaldehyde, fixed for 24 h, inserted in paraffin, cut into 5 μm thick slices, and placed on glass slides for hematoxylin and eosin (H&E) and periodic acid-Schiff (PAS) staining as described previously (Wei et al., 2019). All images were randomly selected from 15 visual fields for each slice and photographed. The slices for acute tubular necrosis (ATN) were blindly scored to evaluate the pathological changes, which accounted for the total number of renal tubules.

## 2.8 Immunohistochemistry analysis

The expression levels of S100A9,F4/80, ki67 on the renal sections were determined using immunohistochemistry as previously described (Chen et al., 2022). These expression levels were determined with anti-S100A9 (Abcam, United Kingdom, 1:500), anti-F4/80 antibody (Abcam, United Kingdom, 1:100) or anti-ki67 (Abcam, United Kingdom, 1:300). After the slices were dewaxed, they were incubated with anti-S100A9, anti-F4/80 antibody or anti-ki67 overnight at 4°C. Then, the color reaction was performed using a diaminobenzidine (DAB) coloring kit (Gene Tech, Shanghai, China). All images were randomly selected from 5 visual fields for each slice and photographed with a Nikon microscope (Nikon, Tokyo).

## 2.9 Analysis of apoptosis and oxidative stress

For detection of cell apoptosis, the frozen kidney sections ($n$ = 6 per group) were processed with situ Cell Death Detection Kit (Roche Group) and diamidino-2-phenylindole (DAPI, Sigma) according to the

**TABLE 1 Primer sequences for q PCR analysis.**

| Gene | Gene ID | Sequences |
|---|---|---|
| S100A9 | 20,202 | 5′-ATACTCTAGGAAGGAAGGACACC-3′ |
| | | 5′-TCCATGATGTCATTTATGAGGGC-3′ |
| IL-6 | 16,193 | 5′-GCTACCAAACTGGATATAATCAGGA-3′ |
| | | 5′-CCAGGTAGCTATGGTACTCCAGAA-3′ |
| INF-α | 21,926 | 5′-ATGGCCTCCCTCTCATCAGT-3′ |
| | | 5′-CTTGGTGGTTTGCTACGACG-3′ |
| NOX-1 | 237,038 | 5′-AGCCATTGGATCACAACCTC-3′ |
| | | 5′-AGAAGCGAGAGATCCATCCA-3′ |
| NOX-2 | 13,058 | 5′-TGCACCATGATGAGGAGAAA-3′ |
| | | 5′-CCACACAGGAAAACGCCTAT-3′ |
| GAPDH | 14,433 | 5′--CATCACTGCCACCCAGAAGACTG-3′ |
| | | 5′-ATGCCAGTGAGCTTCCCGTTCAG-3′ |

protocols from manufacturer. For superoxide examination, the frozen kidney sections ($n$ = 5 per group) were processed with 1 μmol/L dihydroethidine (DHE, Sigma) in phosphate-buffer saline buffer for 30 min based on the protocols from producer. $H_2DCFDA$ is also an indicator of oxidative stress. Ice slices were made from fresh kidney tissue without settling sugar and stained with $H_2DCFDA$ for 5 min ($n$ = 5 per group), washes three times in PBS. Fluorescence images were randomly selected from 5 visual fields and photographed. The percentage of TUNEL+ nuclei (red) to DAPI-stained nuclei (blue) was calculated.

## 2.10 Quantitative real-time PCR analysis

Total RNA was acquired from the fresh kidney of sham- or CLP-operated mice with chloroform, isopropyl alcohol, and TRIzol reagent (Takara, Japan) based on the protocols from the manufacturer. A reverse transcription kit (Takara) was applied to compound cDNA. Remove genome reaction and reverse transcription reaction conditions were set at 42°C for 2 min and 37°C for 15 min, respectively. The relative mRNA content of IL-6, TNF-α, NOX1, NOX2, and GAPDH were detected. The mRNA levels were standardized to the GAPDH level and statistically analyzed using the $2^{-\Delta\Delta CT}$. All the primer sequences were acquired from Sheng gong Biotech Co., Ltd. (Shanghai, China) and are presented in Table 1.

## 2.11 Western blot analysis

One-fifth of the kidney tissues were placed in a mixture of 200 μL RIPA (Beyotime, Shanghai) and 2 μL cocktail (Thermo Fisher), minced, and homogenized on ice. Lysates were then centrifuged at 13,300 g for 15 min at 4°C. The clarified supernatant was saved and subsequently analysed for content by using a Bicinchoninic Acid (BCA) assay kit (Thermo Fisher, United States). Equal amounts (40–50 μg) of the supernatants were split in 10% and 15% SDS-PAGE, transferred to membranes, and incubated with primary antibodies overnight at 4°C.
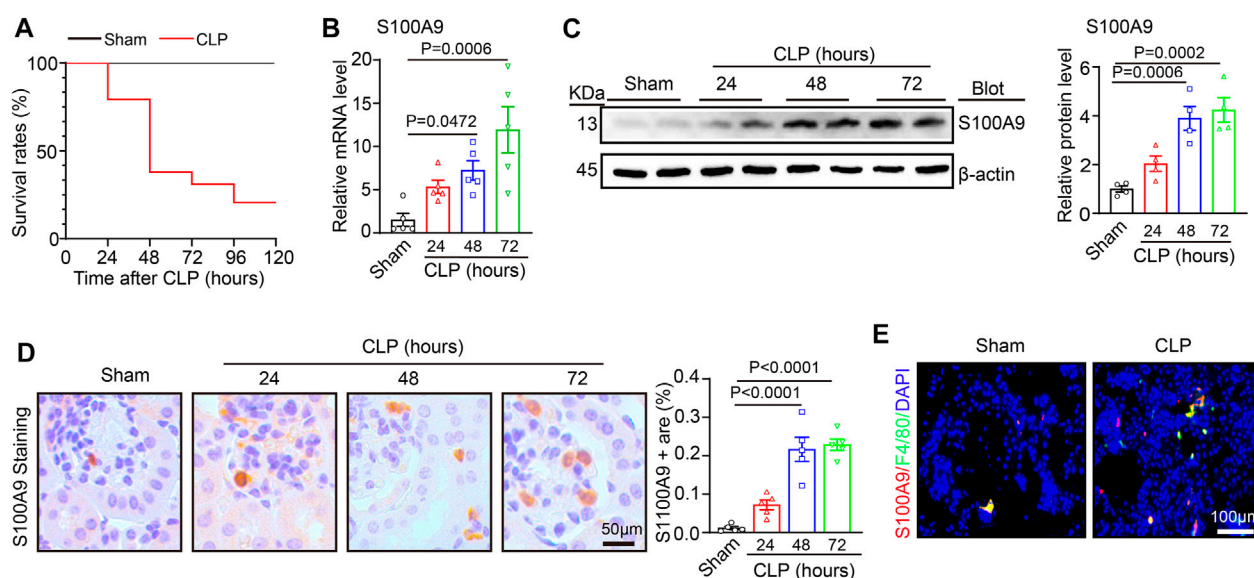
**FIGURE 1**
S100A9 expression level in the kidneys of the mice after cecal ligation and puncture (CLP) surgery: **(A)** male wild-type (WT) mice were applied to sham or CLP operation for 24–120 h. The survival rates of each group at different time points are shown (Sham, $n$ = 5; CLP, $n$ = 29). **(B)** Quantitative polymerase chain reaction analysis of S100A9 mRNA content in the kidneys of the mice at different time points ($n$ = 5). **(C)** Immunoblotting analysis of S100A9 in the kidneys of the mice at different time points (left) and quantifying the protein level ($n$ = 4). **(D)** Immunohistochemical staining of S100A9 in the kidneys of the mice at different time points ($n$ = 5). **(E)** Immunofluorescence double staining of kidney tissue with S100A9 and F4/ 80 antibodies at 48 h of CLP surgery. Scale bar: 50–100 μm.
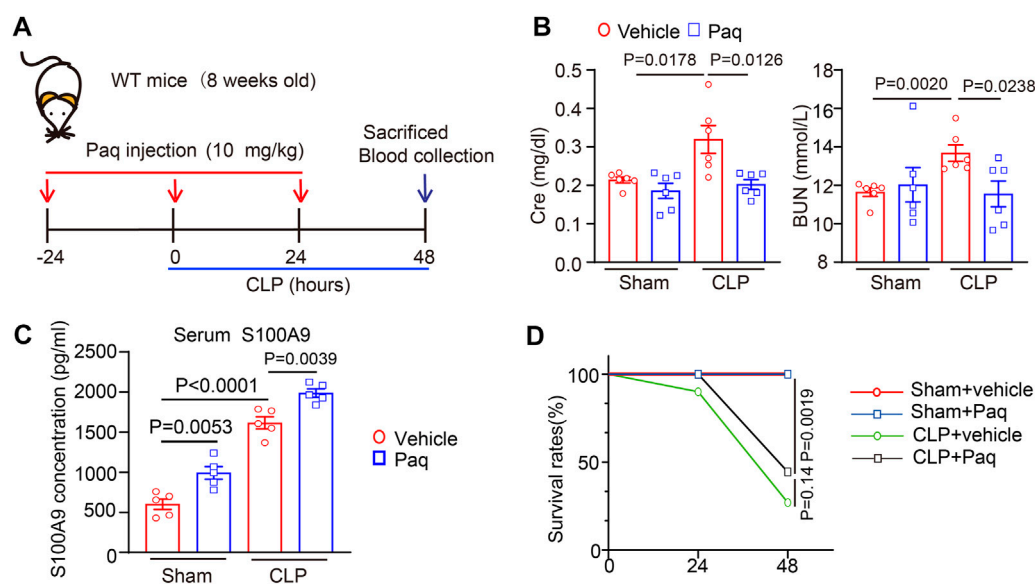


**FIGURE 2**
Administration of Paq to mice improves CLP-induced renal dysfunction. **(A)** Schematic representation for the administration of Paq and CLP surgery.
**(B)** The WT mice were pretreated with Paq at dosages of 10 mg/kg at 24 h before CLP surgery and after 48 h. The content of serum urea nitrogen (BUN) and creatinine (Cr) were tested by using the ELISA kit ($n$ = 6 per group) **(C)** The level of serum S100A9 were tested by using the ELISA kit ($n$ = 5 per group).
**(D)** Survival rates of vehicle- or Paq- ($n$ = 10, 10 mg/kg) treated mice after sham and CLP surgery ($n$ = 9–10 per group).

The optical density was detected with enhanced chemiluminescence (ECL) reagents (Bio-Rad Laboratories) using a Fluorchem R device, and the protein content were standardised to the GAPDH level. The primary antibodies used for Western blotting were as follows: S100A9

(Abcam, United Kingdom, 1:500), Drp1 (CST, American, 1:2000), Mfn1 (CST, American, 1:2000), Mfn2 (CST, American, 1:2000), Bax (Proteintech, American, 1:5000), Bcl-2(Proteintech, American, 1:1000) and β-actin (CST, American, 1:1000).

## 2.12 Measurement of caspase-3 activity

Total 50 mg of kidney from sham-or CLP-operated mice were placed in the liquid provided with the kit and homogenized on ice. The protein content was measure with Bradford method (Beyotime Biotechnology, Shanghai, China). Caspase-3 activity levels were acquired by caspase-3 assay kit (Solarbio, Beijing, China) based on the formation of the chromophore p-nitroaniline (p-NA) by cleavage from the labeled substrate DEVD-pNA following the protocols from the manufacturer. This analysis was used to further confirm the data of immunostaining with cleaved caspase-3 antibody, and TUNEL kit.

## 2.13 Measurement of S100A9,IL-6,TNF-α and malondialdehyde with ELISA kits

Total 50 mg of kidney from sham- or CLP-operated mice ($n$ = 5 per group) were placed in normal saline and homogenized on ice. The homogenate was absorbed (3,000 rpm, 10 min, 4°C) to further analyze. The clarified supernatants were dilute 50 times. Content of protein was measure using a Bicinchoninic Acid (Thermo Fisher, United States). The levels of malondialdehyde (MDA) were determined with MDA assay kits (Nanjing Jiancheng). Total 40 mg of kidney tissue from sham- or CLP-operated mice ($n$ = 5 per group) were placed in fresh lysis buffer, homogenized on ice and then were centrifuged at 10,000 rpm for 5 min to detect the content of IL-6 and TNF-α(Cloud-Clone Crop, Wuhan, China). Blood samples ($n$ = 5 per group) were obtained from the eyeballs of the mice in each group, stratified, and centrifuged (3,000 rpm, 15 min). Supernatant were aspirated and saved in a centrifuge tube to measure the level of S100A9 (Cloud-Clone Crop, Wuhan, China).

## 2.14 Statistical analysis

Statistical analysis was processed by using the SPSS 20 software, and the results are presented as the mean ± SEM. Statistical differences between the two groups were analysed by using an unpaired two-tailed Student's t-test. Comparisons between multiple groups were analysed by using a one-way ANOVA and subsequently a *post hoc* test. Survival rates in each group were analyzed with the Gehan-Breslow and log-rank tests ($n$ = 39–59 animals per group). *p*-value of <0.05 is considered with significant.

# 3 Results

## 3.1 S100A9 is regulated upwards in the kidneys of the CLP-operated mice

To investigate the effect of S100A9 in septic AKI, we generated a sepsis-associated AKI model by CLP surgery. Then, we evaluated the survival condition of the mice at 24, 48, 72, 96, and 120 h after the surgery. Compared with sham controls, the survival rates of the CLP-treated mice were 100%, 80%, 38%, 31%, and 21%, respectively (Figure 1A). Then, the kidney specimens were collected at 24, 48, and 72 h after the surgery, and S100A9 expression was assessed. qPCR and immunoblotting analysis indicated that S100A9 content

at both mRNA and protein was time-dependently regulated upwards in the kidneys of CLP-treated mice after 24, 48, and 72 h (Figures 1B, C). The increased expression of S100A9 proteins in the kidneys of CLP-treated mice was further demonstrated via immunohistochemical staining with an anti-S100A9 antibody. Most S100A9 proteins were distributed in the glomerulus and tubulointerstitium (Figure 1D). Moreover, previous studies suggest that S100A8/A9 was colocalized with Ly6G-positive granulocytes in ischemia/reperfusion (I/R) kidney and obstructive nephropathy (Dessing et al., 2015; Tammaro et al., 2018). Our immunostaining further demonstrated that S100A9 was also colocalized with F4/80-positive macrophages in CLP-treated renal tissue (Figure 1E). Thus, these findings suggest that the upregulation of S100A9 may exert a role in septic AKI.

## 3.2 Administration of Paquinimod improves CLP renal dysfunction in mice

To determine the role of S100A9 on sepsis-induced abnormal kidney function, the WT mice were preinjected with an S100A8/A9 specific inhibitor (Paq, 10 mg/kg) prior to CLP surgery. This dosage of Paq at 10 mg/kg was selected based on our recent studies (Wu et al., 2023; Zhang et al., 2023). After 48 h, the blood samples were collected to evaluate the markers for renal function (Figure 2A). Compared to the vehicle + sham group, CLP surgery significantly increased serum urea nitrogen (BUN) and creatinine (Cr) levels. Notably, Paq at 10 mg/kg markedly attenuated this effect (Figure 2B). Thus, reviewing relevant literature and setting a concentration gradient, we observed that the optimal drug concentration of Paq was 10 mg/kg. Moreover, we detected the level of serum S100A9, and found that serum S100A9 in mice was significantly increased after Paq treatment and CLP surgery (Figure 2C). Finally, we observed that Paq administration slightly improved the survival rate of CLP-treated mice at 48 h compared with CLP group in data (Figure 2D). In all, these data point that Paq can ameliorate sepsis-induced kidney dysfunction.

## 3.3 Administration of Paquinimod attenuates renal pathological changes and apoptosis

Then, we tested whether the inhibition of S100A9 improves pathological changes in the kidney. H&E and PAS staining revealed that CLP surgery significantly augmented renal tubular injury scores, as reflected by increased swelling, vacuolation, necrosis, irregular brush border, and ectasia of the proximal tubular epithelial cells. However, these deleterious effects were markedly reduced in the kidneys of Paq-treated mice (Figures 3A, B). Moreover, we proved that inhibition of S100A9 could decrease the apoptosis of cells in kidney. TUNEL exhibited that the number of apoptotic cells, as indicated by TUNEL-positive in the kidneys of the Paq-treated group was lower than that in the vehicle-treated group after CLP surgery (Figure 3C). What's more, we detected the content of the apoptotic related proteins (Bax and Bcl-2) and Caspase-3 activity with immunoblotting and ELISA kit, respectively. These data proved that Paq treatment substantially
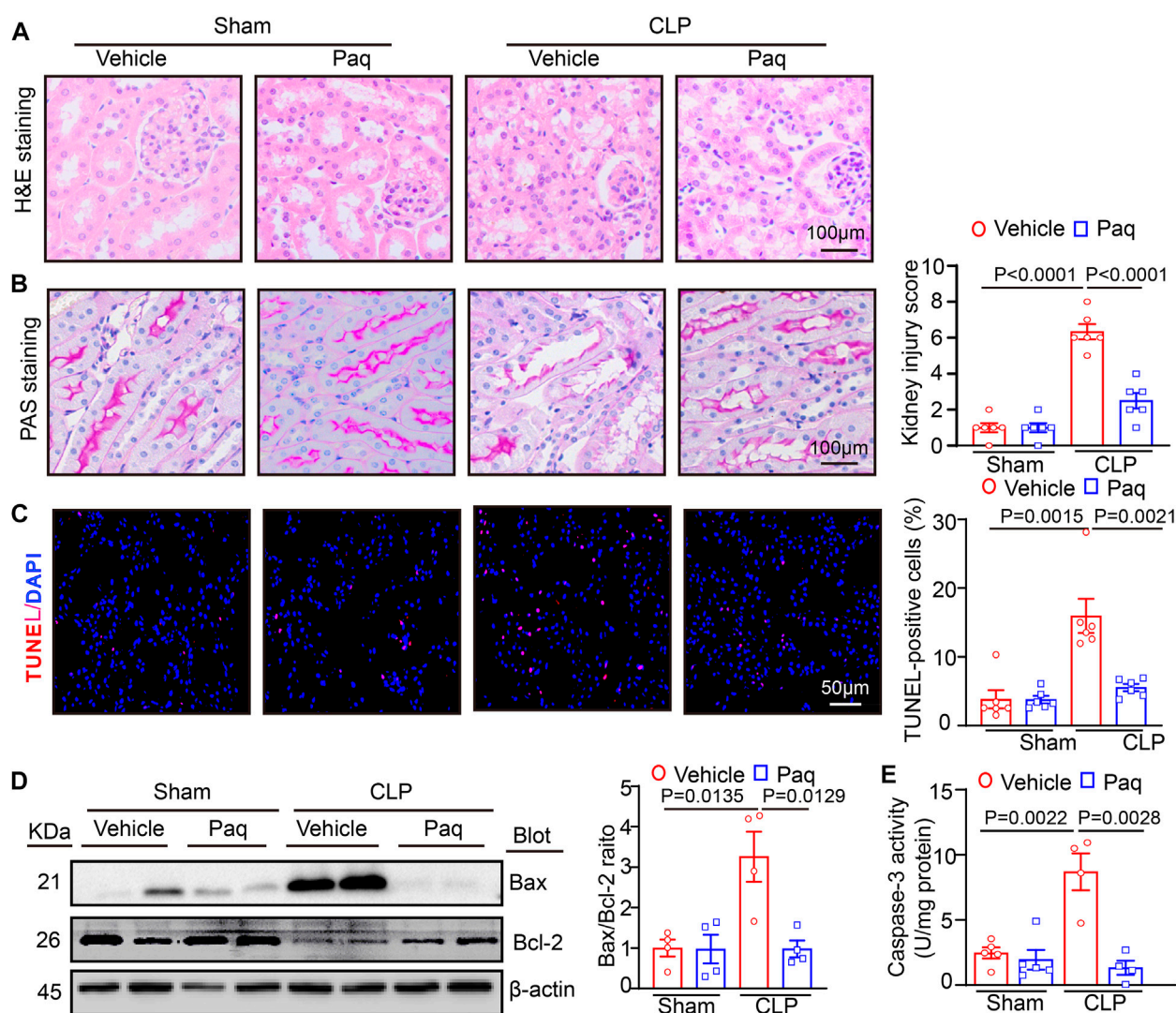
**FIGURE 3**
Blocking S100A9 with Paq suppresses CLP-induced pathological changes and cell apoptosis in the kidneys. The WT mice were pretreated with Paq (10 mg/kg) before CLP surgery and after 48 h. **(A)** Haematoxylin and eosin (H&E) staining of the kidney sections (left). Scale bars: 100 μm. **(B)** Periodic acid-Schiff (PAS) staining of the kidney sections (left) (Scale bars: 100 μm) and quantifying the tubular damage score based on PAS staining (right, $n = 6$ per group). **(C)** TUNEL (red) and DAPI (blue) staining of the kidney sections (left) and quantifying TUNEL-positive apoptotic cells ($n = 6$ per group). Scale bars: 50 μm. **(D)** Immunoblotting analysis of Bax and Bcl-2 protein levels in the kidneys (left) and quantifying the relative Bax/Bcl-2 ratio level ($n = 4$ per group). **(E)** ELISA analysis of caspase-3 activity in the kidney tissues ($n = 4$ or 5 per group).

reduced the CLP-mediated increase of Bax/Bcl-2 ratio levels and Caspase-3 activity in the kidneys compared with vehicle treatment after CLP (Figures 3D, E). Altogether, these findings proved that the inhibition of S100A9 exerts a protective role in septic kidney injury.

## 3.4 Administration of Paquinimod inhibits renal macrophage infiltration and oxidative stress and increases cell proliferation in renal tissue

Since S100A8/A9 can activate different receptors, such as TLR4, to promote leukocyte recruitment and secretion of proinflammatory cytokines, such as IL-6 and TNF-α, leading to kidney injury (Jung

et al., 2019). Paq is a specific inhibitor that prevents the binding of S100A8/A9 to TLR4 (Jha et al., 2021; Wu et al., 2023). Therefore, we tested whether Paq can reduce renal inflammation. Immunohistochemical staining indicated that Paq administration for 48 h substantially inhibited CLP-induced infiltration of F4/80-positive macrophage and increased ki67-positive cell proliferation in the kidneys compared with vehicle treatment (Figures 4A, B). Moreover, oxidative stress is an important pathological occurrence in septic AKI (Carlsson et al., 2005). Next, we determined whether S100A8/A9 inhibition improved oxidative stress in the kidney. We performed DHE and $H_2DCFDA$ (a cell-permeable probe used to detect intracellular ROS level) staining in renal tissues. Our results showed that the relative fluorescence intensities of DHE and $H_2DCFDA$ staining were stronger in the
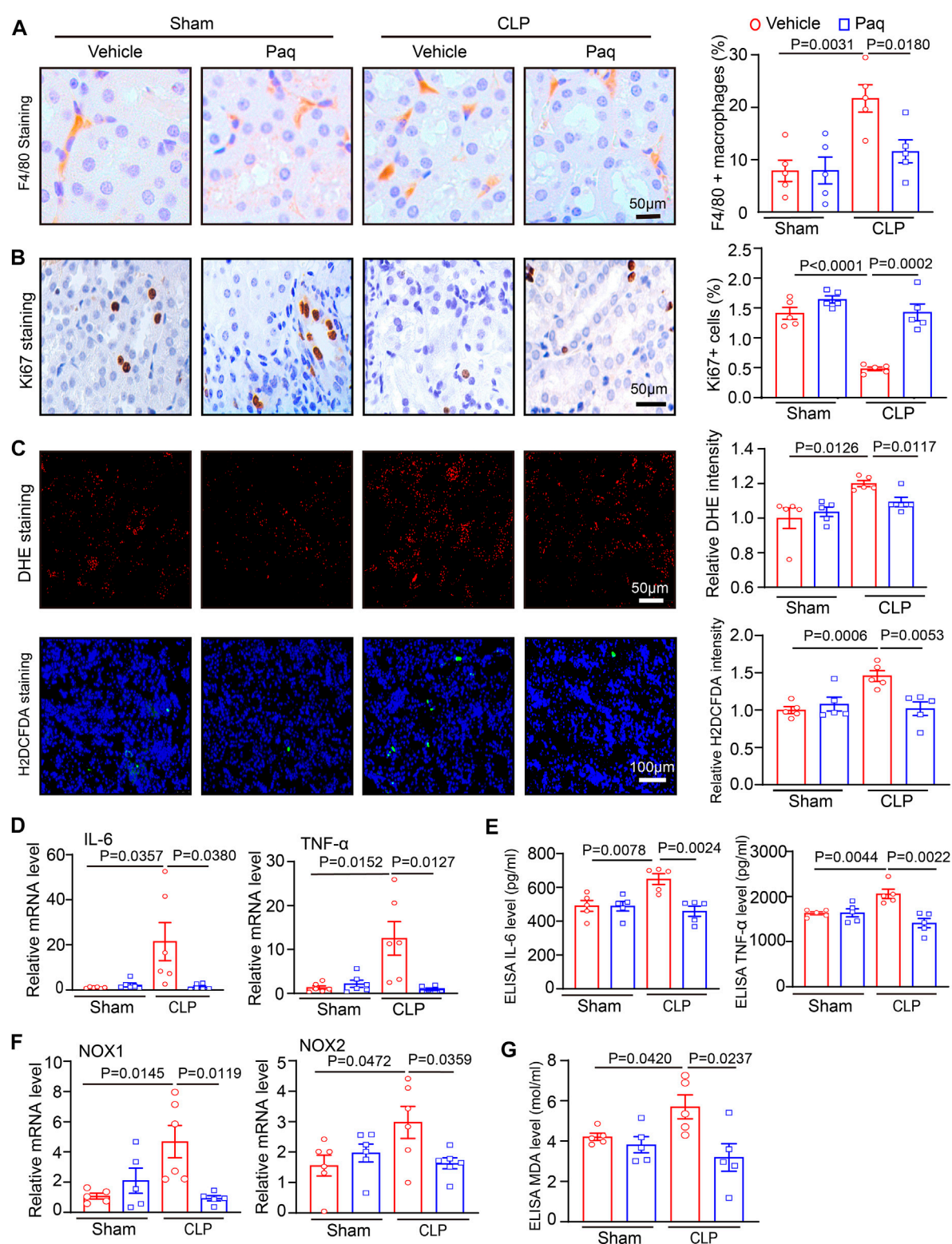
**FIGURE 4**
Blockage of S100A9 with Paq reduces CLP-induced macrophage infiltration and oxidative stress in the kidneys. WT mice were pretreated with Paq (10 mg/kg) and then applied to CLP surgery for 48 h **(A,B)** Immunohistochemical staining of kidney slices with anti-F4/80 antibody and anti-ki67 (left) and quantifying F4/80-positive macrophages (right, $n$ = 5 per group) and ki67-positive cells (right, $n$ = 5 per group). Scale bars: 50 μm. **(C)** DHE and $H_2$DCFDA staining of kidney sections (left) and quantifying relative DHE and $H_2$DCFDA fluorescence intensities ($n$ = 5 per group). Scale bars: 50–100 μm. **(D,F)** qPCR analysis of IL-6, TNF-α, NOX1, and NOX2 mRNA levels in the kidney tissues ($n$ = 5 or 6 per group). **(E,G)** ELISA analysis of IL-6, TNF-α and MDA levels in the kidney tissues ($n$ = 5 per group,IL-6,TNF-α).
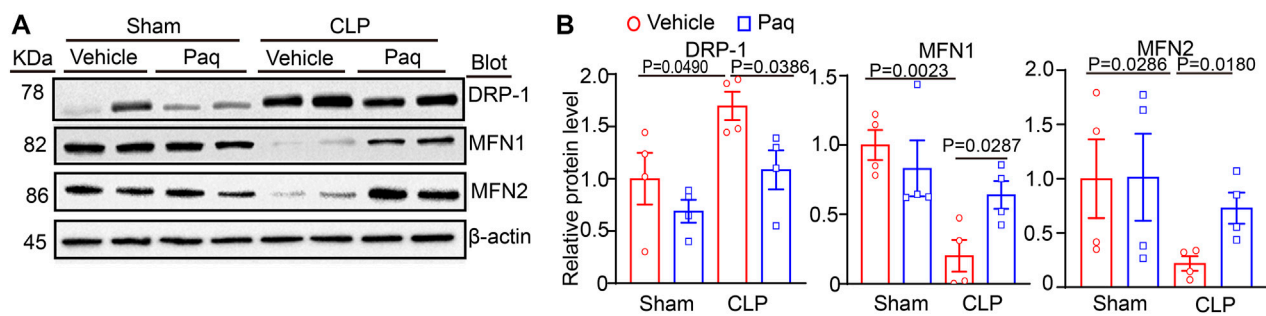
**FIGURE 5**
Inhibition of S100A9 with Paq reverses CLP-induced imbalance of mitochondrial fission and fusion in the kidneys. The WT mice were pretreated with Paq (10 mg/kg) before CLP surgery and after 48 h **(A,B)** Immunoblotting analysis of Drp1, Mfn1, and Mfn2 protein levels in the kidneys (left) and quantifying the relative protein level (*n* = 4 per group).

kidneys of CLP-treated mice, and this enhancement was markedly blocked in the kidneys of Paq-treated mice (Figure 4C). Furthermore, qPCR results showed that the mRNA levels of proinflammatory cytokines (IL-6 and TNF-α) and NADPH oxidase isoforms (NOX1 and NOX2) were also lower in the kidneys of Paq-treated mice than those in the kidneys of CLP-treated mice (Figures 4D, F). Accordingly ELISA results proved that CLP-induced upregulation of IL-6, TNF-α and MDA levels were remarkable reversed in the kidneys of Paq-treated mice (Figures 4E, G). Thus, these data imply that the inhibition of S100A8/A9 binding to TLR4 reduces inflammation, oxidative stress, and increases cell proliferation in the kidneys during sepsis.

## 3.5 Administration of Paquinimod improves the balance of mitochondrial fission and fusion

Studies have pointed that mitochondrial impairment is a key mechanism leading to cell apoptosis and oxidative stress, the hallmarks of AKI(21). To determine the possible molecular mechanism of S100A8/A9 in septic kidney injury, we examined the mitochondrial pro-fission protein Drp1, and pro-fusion proteins Mfn1 and Mfn2, which are important regulators of mitochondrial dynamic balance. Immunoblotting analysis indicated that after 48 h, CLP surgery resulted in a remarkable increase of Drp1 and reduction of Mfn1/2 in the kidneys compared with the sham operation. Still, this change was reversed in the Paq-treated kidneys (Figures 5A, B). This suggested that the inhibition of S100A9 may improve mitochondrial fission-fusion balance and dysfunction, leading to the inhibition of AKI after sepsis.

## 3.6 Paquinimod improves oxidative stress, apoptosis and the balance of mitochondrial fission and fusion in mouse renal tubular epithelial cells (mRTECs)

To further verify the role of Paq in septic nephropathy, we used cell co-culture to confirm relevant experimental results. We

selected RAW264.7 macrophages and mRTEC cells for co-culture to simulate the mode of action of macrophages on renal tubular epithelial cells *in vivo*. Before co-culture, the RAW264.7 macrophages were pretreated with different dosages of LPS (1, 10 and 50 μg/mL) for 24 h and mRTEC cells were pretreated with Paq (150 μM) for 2 h (Figure 6A). ELISA assay indicated that LPS treatment at 50 μg/mL significantly increased levels of S100A9, IL-6, and TNF-α in the culture medium of RAW264.7 cells when compared with vehicle control (Figure 6C). Next, we co-cultured RAW 264.7 and mRTEC cells, and detected the oxidative stress and apoptosis level of mRTEC cells with DHE and cleaved caspase-3 staining, respectively. We found that the relative DHE fluorescence intensity and caspase-3-positive apoptosis were higher in the mRTEC cells of LPS-treated group, and this enhancement was remarkable blocked in the Paq-treated group (Figures 6D, E). Finally, we used double immunostaining to verify the mitochondrial fission and fusion. Drp1/ATP5A double staining show that Drp1-positive content in mitochondrion was remarkably increased in LPS-treated mRTECs, and this effect was markedly attenuated in Paq-treated mRTECs. Conversely. Mfn1/ATP5A and Mfn2/ATP5A staining show that Mfn1 and Mfn2 content in mitochondrion is downregulation in LPS-treated mRTECs, and this reduction was greatly reversed in Paq-treated cells (Figure 6F). Collectively, these results demonstrate that inhibition of S100A9 can ameliorate the imbalance of mitochondrial fission and fusion in mRTECs induced by LPS.

## 4 Discussion

In this paper, we identified a novel role of S100A9 on macrophages in facilitating sepsis-induced AKI and abnormal kidney function. Our results proved that S100A9 expression was highly regulated upwards in the kidneys and macrophages of CLP-treated mice. Blockage of S100A9 with Paq substantially ameliorated CLP-induced abnormal renal function, apoptosis, inflammation, and oxidative stress in tubular epithelial cells likely associated with improving the balance of Drp1/Mfn1/2-mediated mitochondrial dynamics. The results are summarized in Figure 7.
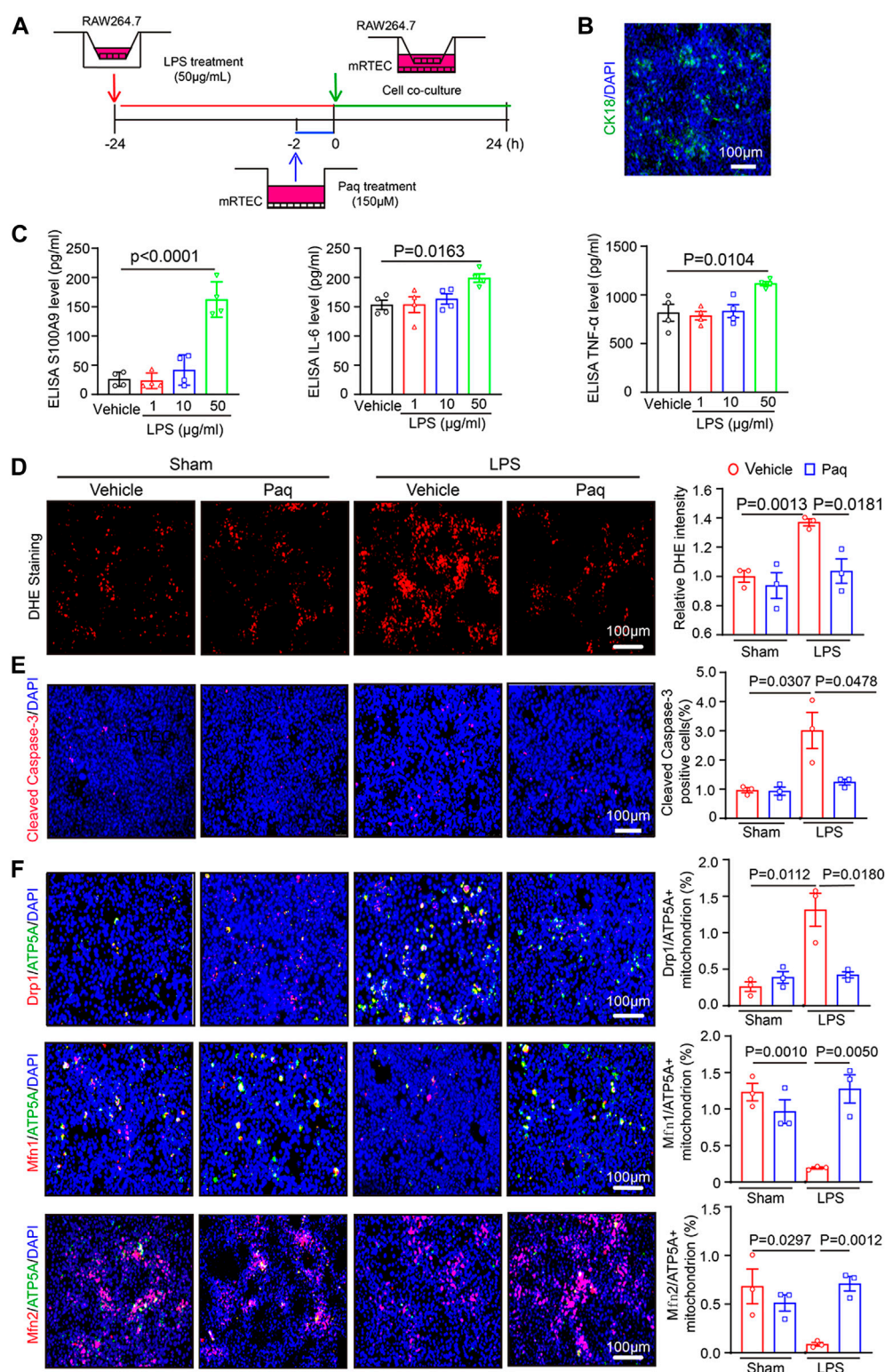
**FIGURE 6**
Blockage of S100A8/A9 with Paq reduces LPS-induced inflammation, oxidative stress, apoptosis, and mitochondrial fission and fusion-related proteins in the mRTEC cells. **(A)** RAW264.7 cells were pretreated with LPS (50 μg/mL) and then co-cultured with the mRTEC cells for 24 h, which were preinjected with Paq (150 μM) for 2 h. **(B)** Immunofluorescence staining of mRETC cells with CK18 antibody. **(C)** ELISA analysis of S100A9, IL-6 and TNF-α levels in the supernatants of cultured RAW264,7 cells ($n$ = 4 per group). **(D)** DHE staining of mRTEC cells (left) and quantifying relative DHE fluorescence intensity ($n$ = 3 per group). Scale bars: 100 μm. **(E)** Immunofluorescence staining of mRETC cells with cleaved caspase-3 antobody. (left) and quantifying apoptosis cells ($n$ = 3 per group). Scale bars: 100 μm. **(F)** Immunofluorescence double staining of mRTEC cells with Drp1/ATP5A, Mfn1/ATP5A, Mfn2/ATP5A antibodies (left) and quantifying relative positive mitochondrion.
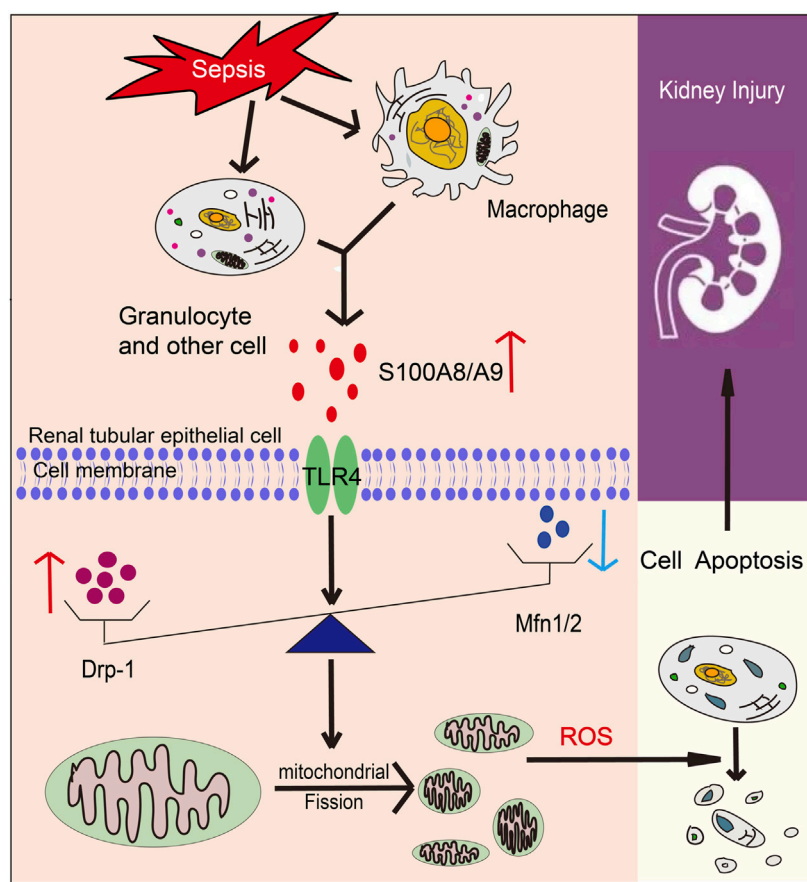
**FIGURE 7**
A working model for S100A8/A9 in regulating sepsis-induced acute kidney injury (AKI). Upon sepsis, S100A9 expression is upregulated and released by macrophages promoting activation of TLR4, which increases Drp1 level and reduces Mfn1/2 level that cause mitochondrial fission-fusion imbalance, excessive oxidative stress and inflammation, leading to epithelial apoptosis and AKI.

Therefore, this study demonstrates that S100A9 has an impact on sepsis-induced AKI, and emphasizes targeting S100A9 as a potential therapeutic option for this disease.

Kidney is may the most common organ which is affected during sepsis. More and more evidence has illuminated that AKI is the leading contributor to sepsis-related morbidity and mortality, and up to 50%–60% of patients with sepsis have AKI (Peerapornratana et al., 2019). In septic AKI, the kidney undergoes pathological changes, including infiltration of inflammatory cells, renal tubular dilation, vacuolisation, swelling and necrosis of epithelial cells, obstruction and distortion of renal tubules, and disappearance of the tubular brush border (Peerapornratana et al., 2019; Wei et al., 2019). In this study, these pathological changes were observed in both H&E and PAS staining, and were improved by use of S100A8/A9 inhibitor Paq. Several studies have demonstrated that proinflammatory cascades are key mediator of septic AKI. As an important inflammatory mediator, S100A8/A9 is highly expressed in stimulated and activated monocytes/macrophages and Ly6G-positive granulocytes in ischemia/reperfusion (I/R) kidney and obstructive nephropathy (Dessing et al., 2015; Tammaro et al., 2018; Wu et al., 2023; Zhang et al.,

2023) and can be released during inflammation and cell necrosis (Carlsson et al., 2005; Wang et al., 2018). Here, our data further confirmed that the S100A9 was expressed in macrophages after CLP and LPS stimulation (Figure 1). Moreover, increased S100A8/A9 expression is associated with inflammation and cell death (Alaedini et al., 2008), and promotes proliferation, differentiation, and apoptosis of tumor cells, epithelial cells, monocyte, and smooth muscle cells (Jukic et al., 2021) Importantly, S100A8/A9 (as an important DAMPs) are involved in various diseases, such as I/R- and contrast-induced AKI, renal fibrosis, and glomerulonephritis in different animal models, via TLR4-or RAGE-mediated activation of multiple signals, and proinflammatory cytokines production (Pepper et al., 2015; Tan et al., 2017; Austermann et al., 2018; Du et al., 2022; Yao et al., 2022). However, there are few studies on the role of S100A8/A9 in septic AKI. In this study, we found that Paq treatment highly enhanced serum levels of S100A9 in mice (Figure 2C). This result may be due to the competitive binding of Paq to TLR4 receptors in tissues, which reduces the binding of S100A8/A9 to TLR4 receptors, finally leads to the increase of free S100A9. Moreover, we discovered for the first time that administration

of S100A9 inhibitor Paq remarkable hinders the binding of S100A9 to TLR4. These results buttressed previous findings and confirmed that S100A9 exerts a protective role in septic AKI, as indicated by the reduction of animal mortality and improvement of renal dysfunction and pathological changes including cell apoptosis, oxidative stress, and inflammatory response in CLP-treated mice (Figures 2–4), confirming that S100A9 critically contributes to CLP-induced AKI and abnormal kidney function.

Recent advances in sepsis-related organ injury in different animal models have increased our knowledge of the pathogenesis of AKI. More and more evidences point that mitochondrial dysfunction may act as a pivotal cause to sepsis-induced organ failure, including renal injury and abnormal kidney function (Sun et al., 2019). Mitochondrial dynamic balance is a pivotal process in normal mitochondrial morphology and function. Several Key dynamin-related GTPases are involved in regulating mitochondrial fusion and fission balance, including Drp1, and optic atrophy1 (OPA1) (Kulek et al., 2020). Among these proteins, Drp1 forms a multimeric complex that wraps the mitochondria to induce mitochondrial fission, whereas Mfn1/2 and OPA1 can fuse the outer and inner mitochondrial membranes to drive mitochondrial fusion (Kulek et al., 2020; Monteith et al., 2022). In response to injuries such as sepsis, the balance of mitochondrial fission and fusion is disrupted, and mitochondria tend to divide [34]. Mitochondrial dynamics are characterized by aberrant cycle of fission/fusion, however, they were more inclined to fission. During AKI in sepsis, mitochondrial fission-associated oxidative stress, apoptosis and pyroptosis were elevated (Liu et al., 2019; Li et al., 2020). Inhibition of Drp1 with its inhibitor Mdivi-1 improve mitochondrial fission and limits the activation of NLRP3-mediated pyroptosis, confirming the role of Drp1 in septic AKI (Liu et al., 2020). SENP3-mediated Drp1 deSUMOylation aggravates LPS-mediated tubular epithelial cell apoptosis during AKI. In contrast, SENP3 knockdown markedly ameliorates LPS-induced effects (Wang et al., 2022). Studies have shown that intracellular accumulation of S100A9 is associated with impaired mitochondrial homeostasis (Monteith et al., 2022). Our results confirmed that S100A9 enhanced sepsis-mediated mitochondrial fission-fusion imbalance, ultimately resulting in excessive oxidative stress and epithelial cell apoptosis of kidney. Conversely, the inhibition of S100A9 can improve these deleterious effects by reducing Drp1 and increasing Mfn1/2 protein levels (Figures 3–5). Here, the protein levels of Drp1 and Mfn1/2 were measured using total proteins from the kidneys tissues at a lower cost with simplicity and ease. However, this approach does not exactly reflect the change of mitochondrial mitochondrial fission and fusion proteins. Thus, we added the mitochondrial markers ATP5A and the mitochondrial fission proteins Drp1, mitochondrial fusion proteins MFN1, MFN2 immunofluorescence double staining to further prove the situation of mitochondrial division and fusion in cell experiment (Figure 6).

Currently, because the underlying pathophysiological processes of AKI in sepsis are not fully understood, this inevitably hinders the effective therapeutic interventions developing. The use of diuretics has not been demonstrated to inhibit or attenuate septic AKI (Peerapornratana et al., 2019). Thus, the routine administration of diuretics for the prevention or treatment of AKI cannot be recommended. Numerous drugs for AKI have been explored. To date, several molecules such as AC607, AB103, ABT-719AB103 (AtoxBio), ciclosporin A, and levosimendan have been examined to prevent or treat AKI in septic animal models and clinical trials. These agents can improve inflammatory response, oxidative stress, and mitochondrial impairment in the kidney during sepsis and other high-stress settings (Gallagher et al., 2017). Moreover, systemic use of alkaline phosphatase can protect against sepsis-induced AKI. This effect is associated with the direct dephosphorylation of endotoxin, which leads to improves survival rates and inhibits of inflammation and organ damage (Pickkers et al., 2018; Singh and Lin, 2021). Moreover, some caspase and interleukin inhibitors have not translated into human investigations of septic AKI (Takeyoshi et al., 2005; Yang et al., 2021). In this study, we used a variety of methods to verify the important role of S100A8/A9 in septic nephropathy *in vivo* and *in vitro*. We used the S100A8/A9 specific inhibitor Paquinimod to demonstrate for the first time that selective inhibition of S100A8/A9 reduces inflammatory responses, oxidative stress, and tubular epithelial apoptosis in septic nephropathy. Immunofluorescence double staining experiment *in vitro* confirmed that S100A8/A9 can increase the mitotic protein and decrease the fusion protein. The mechanism of S100A8/A9 was discussed for the first time. Our paper suggest that S100A8/A9 may be an important new point for the treatment of septic AKI, and provides a theoretical basis for the subsequent drugs development and clinical treatment of septic nephropathy.

This study has several limitations. First, the effect of S100A8/A9 on septic AKI needs to be clarified in S100A9 knockout mice and other animal models of sepsis. Secondly, the precise mechanism for S100A8/A9 to regulate mitochondrial dynamic balance is required to elucidated in further studies.

## 5 Conclusion

Our study demonstrates the damaging role of S100A8/A9 in macrophages in sepsis-induced AKI in mice. Inhibition of S100A9 ameliorated renal inflammation, oxidative stress, and epithelial cell apoptosis associated with mitochondrial Drp1/Mfn1/2 imbalance. Our study also emphasizes that S100A8/A9 may be a potential treated aspect for septic AKI.

## Data availability statement

The raw data supporting the conclusion of this article will be made available by the authors, without undue reservation.

## Ethics statement

The animal study was reviewed and approved by Chao-Yang Hospital of the Capital Medical University (2021-Animal-35).

## Author contributions

WS performed the acquisition and analysis of the data. WS participated in the statistical analysis of the primary data. S-BG provided funding to support the study. S-BG and H-HL supervised the study. H-HL wrote the paper. All authors contributed to the article and approved the submitted version.

## Funding

## Conflict of interest

The authors declare that the research was conducted in the absence of any commercial or financial relationships that could be construed as a potential conflict of interest.

## Publisher's note

All claims expressed in this article are solely those of the authors and do not necessarily represent those of their affiliated organizations, or those of the publisher, the editors and the reviewers. Any product that may be evaluated in this article, or claim that may be made by its manufacturer, is not guaranteed or endorsed by the publisher.

## References

Alaedini, A., Xiang, Z., Kim, H., Sung, Y. J., and Latov, N. (2008). Up-regulation of apoptosis and regeneration genes in the dorsal root ganglia during cisplatin treatment. *Exp. Neurol.* 210 (2), 368–374. doi:10.1016/j.expneurol.2007.11.018

Austermann, J., Spiekermann, C., and Roth, J. (2018). S100 proteins in rheumatic diseases. *Nat. Rev. Rheumatol.* 14 (9), 528–541. doi:10.1038/s41584-018-0058-9

Carlsson, H., Yhr, M., Petersson, S., Collins, N., Polyak, K., and Enerbäck, C. (2005). Psoriasin (S100A7) and calgranulin-B (S100A9) induction is dependent on reactive oxygen species and is downregulated by Bcl-2 and antioxidants. *Cancer Biol. Ther.* 4 (9), 998–1005. doi:10.4161/cbt.4.9.1969

Chen, Y., Zhou, X., and Wu, Y. (2022). The miR-26a-5p/IL-6 axis alleviates sepsis-induced acute kidney injury by inhibiting renal inflammation. *Ren. Fail* 44 (1), 551–561. doi:10.1080/0886022x.2022.2056486

Dessing, M. C., Butter, L. M., Teske, G. J., Claessen, N., van der Loos, C. M., Vogl, T., et al. (2010). S100A8/A9 is not involved in host defense against murine urinary tract infection. *PLoS One* 5 (10), e13394. doi:10.1371/journal.pone.0013394

Dessing, M. C., Tammaro, A., Pulskens, W. P., Teske, G. J., Butter, L. M., Claessen, N., et al. (2015). The calcium-binding protein complex S100A8/A9 has a crucial role in controlling macrophage-mediated renal repair following ischemia/reperfusion. *Kidney Int.* 87 (1), 85–94. doi:10.1038/ki.2014.216

Du, L., Chen, Y., Shi, J., Yu, X., Zhou, J., Wang, X., et al. (2022). Inhibition of S100A8/A9 ameliorates renal interstitial fibrosis in diabetic nephropathy. *Metabolism* 144, 155376. doi:10.1016/j.metabol.2022.155376

Gallagher, K. M., O'Neill, S., Harrison, E. M., Ross, J. A., Wigmore, S. J., and Hughes, J. (2017). Recent early clinical drug development for acute kidney injury. *Expert Opin. Investig. Drugs* 26 (2), 141–154. doi:10.1080/13543784.2017.1274730

Jha, A. K., Gairola, S., Kundu, S., Doye, P., Syed, A. M., Ram, C., et al. (2021). Toll-like receptor 4: An attractive therapeutic target for acute kidney injury. *Life Sci.* 271, 119155. doi:10.1016/j.lfs.2021.119155

Jukic, A., Bakiri, L., Wagner, E. F., Tilg, H., and Adolph, T. E. (2021). Calprotectin: From biomarker to biological function. *Gut* 70 (10), 1978–1988. doi:10.1136/gutjnl-2021-324855

Jung, N., Schenten, V., Bueb, J. L., Tolle, F., and Bréchard, S. (2019). miRNAs regulate cytokine secretion induced by phosphorylated S100a8/A9 in neutrophils. *Int. J. Mol. Sci.* 20 (22), 5699. doi:10.3390/ijms20225699

Kulek, A. R., Anzell, A., Wider, J. M., Sanderson, T. H., and Przyklenk, K. (2020). Mitochondrial quality control: Role in cardiac models of lethal ischemia-reperfusion injury. *Cells* 9 (1), 214. doi:10.3390/cells9010214

Li, H. B., Zhang, X. Z., Sun, Y., Zhou, Q., Song, J. N., Hu, Z. F., et al. (2020). HO-1/PINK1 regulated mitochondrial fusion/fission to inhibit pyroptosis and attenuate septic acute kidney injury. *Biomed. Res. Int.* 2020, 2148706. doi:10.1155/2020/2148706

Liu, J. X., Yang, C., Zhang, W. H., Su, H. Y., Liu, Z. J., Pan, Q., et al. (2019). Disturbance of mitochondrial dynamics and mitophagy in sepsis-induced acute kidney injury. *Life Sci.* 235, 116828. doi:10.1016/j.lfs.2019.116828

Liu, R., Wang, S. C., Li, M., Ma, X. H., Jia, X. N., Bu, Y., et al. (2020). An inhibitor of DRP1 (Mdivi-1) alleviates LPS-induced septic AKI by inhibiting NLRP3 inflammasome activation. *Biomed. Res. Int.* 2020, 2398420. doi:10.1155/2020/2398420

Monteith, A. J., Miller, J. M., Williams, J. M., Voss, K., Rathmell, J. C., Crofford, L. J., et al. (2022). Altered mitochondrial homeostasis during systemic lupus erythematosus impairs neutrophil extracellular trap formation rendering neutrophils ineffective at combating *Staphylococcus aureus*. *J. Immunol.* 208 (2), 454–463. doi:10.4049/jimmunol.2100752

Peerapornratana, S., Manrique-Caballero, C. L., Gómez, H., and Kellum, J. A. (2019). Acute kidney injury from sepsis: Current concepts, epidemiology, pathophysiology, prevention and treatment. *Kidney Int.* 96 (5), 1083–1099. doi:10.1016/j.kint.2019.05.026

Pepper, R. J., Wang, H. H., Rajakaruna, G. K., Papakrivopoulou, E., Vogl, T., Pusey, C. D., et al. (2015). S100A8/A9 (calprotectin) is critical for development of glomerulonephritis and promotes inflammatory leukocyte-renal cell interactions. *Am. J. Pathol.* 185 (5), 1264–1274. doi:10.1016/j.ajpath.2015.01.015

Pickkers, P., Mehta, R. L., Murray, P. T., Joannidis, M., Molitoris, B. A., Kellum, J. A., et al. (2018). Effect of human recombinant alkaline phosphatase on 7-day creatinine clearance in patients with sepsis-associated acute kidney injury: A randomized clinical trial. *Jama* 320 (19), 1998–2009. doi:10.1001/jama.2018.14283

Quaglia, M., Merlotti, G., Colombatto, A., Bruno, S., Stasi, A., Franzin, R., et al. (2022). Stem cell-derived extracellular vesicles as potential therapeutic approach for acute kidney injury. *Front. Immunol.* 13, 849891. doi:10.3389/fimmu.2022.849891

Singh, S. B., and Lin, H. C. (2021). Role of intestinal alkaline phosphatase in innate immunity. *Biomolecules* 11 (12), 1784. doi:10.3390/biom11121784

So, B. Y. F., Yap, D. Y. H., and Chan, T. M. (2022). Circular RNAs in acute kidney injury: Roles in pathophysiology and implications for clinical management. *Int. J. Mol. Sci.* 23 (15), 8509. doi:10.3390/ijms23158509

Su, M., Chen, C., Li, S., Li, M., Zeng, Z., Zhang, Y., et al. (2022). Gasdermin D-dependent platelet pyroptosis exacerbates NET formation and inflammation in severe sepsis. *Nat. Cardiovasc Res.* 1 (8), 732–747. doi:10.1038/s44161-022-00108-7

Sun, J., Zhang, J., Tian, J., Virzi, G. M., Digvijay, K., Cueto, L., et al. (2019). Mitochondria in sepsis-induced AKI. *J. Am. Soc. Nephrol.* 30 (7), 1151–1161. doi:10.1681/ASN.2018111126

Takeyoshi, I., Yoshinari, D., Kobayashi, M., Kurabayashi, M., and Morishita, Y. (2005). A dual inhibitor of TNF-alpha and IL-1 mitigates liver and kidney dysfunction and improves survival in rat endotoxemia. *Hepatogastroenterology* 52 (65), 1507–1510.

Talley, S., Valiauga, R., Anderson, L., Cannon, A. R., Choudhry, M. A., and Campbell, E. M. (2021). DSS-induced inflammation in the colon drives a proinflammatory signature in the brain that is ameliorated by prophylactic treatment with the S100A9 inhibitor paquinimod. *J. Neuroinflammation* 18 (1), 263. doi:10.1186/s12974-021-02317-6

Tammaro, A., Florquin, S., Brok, M., Claessen, N., Butter, L. M., Teske, G. J. D., et al. (2018). S100A8/A9 promotes parenchymal damage and renal fibrosis in obstructive nephropathy. *Clin. Exp. Immunol.* 193 (3), 361–375. doi:10.1111/cei.13154

Tan, X., Zheng, X., Huang, Z., Lin, J., Xie, C., and Lin, Y. (2017). Involvement of S100a8/A9-TLR4-NLRP3 inflammasome pathway in contrast-induced acute kidney injury. *Cell Physiol. Biochem.* 43 (1), 209–222. doi:10.1159/000480340

Tang, Y., Yang, X., Shu, H., Yu, Y., Pan, S., Xu, J., et al. (2021). Bioinformatic analysis identifies potential biomarkers and therapeutic targets of septic-shock-associated acute kidney injury. *Hereditas* 158 (1), 13. doi:10.1186/s41065-021-00176-y

Wang, L., Li, J., and Yu, C. (2022). SENP3 aggravates renal tubular epithelial cell apoptosis in lipopolysaccharide-induced acute kidney injury via deSUMOylation of Drp1. *Kidney Dis. (Basel).* 8 (5), 424–435. doi:10.1159/000525308

Wang, S., Song, R., Wang, Z., Jing, Z., Wang, S., and Ma, J. (2018). S100A8/A9 in inflammation. *Front. Immunol.* 9, 1298. doi:10.3389/fimmu.2018.01298

Wei, S., Gao, Y., Dai, X., Fu, W., Cai, S., Fang, H., et al. (2019). SIRT1-mediated HMGB1 deacetylation suppresses sepsis-associated acute kidney injury. *Am. J. Physiol. Ren. Physiol.* 316 (1), F20–F31. doi:10.1152/ajprenal.00119.2018

Wu, F., Zhang, Y. T., Teng, F., Li, H. H., and Guo, S. B. (2023). S100a8/a9 contributes to sepsis-induced cardiomyopathy by activating ERK1/2-Drp1-mediated mitochondrial fission and respiratory dysfunction. *Int. Immunopharmacol.* 115, 109716. doi:10.1016/j.intimp.2023.109716

Yang, M., Fang, J. T., Zhang, N. S., Qin, L. J., Zhuang, Y. Y., Wang, W. W., et al. (2021). Caspase-1-Inhibitor AC-YVAD-CMK inhibits pyroptosis and ameliorates acute kidney injury in a model of sepsis. *Biomed. Res. Int.* 2021, 6636621. doi:10.1155/2021/6636621

Yao, W., Chen, Y., Li, Z., Ji, J., You, A., Jin, S., et al. (2022). Single cell RNA sequencing identifies a unique inflammatory macrophage subset as a druggable target for alleviating acute kidney injury. *Adv. Sci. (Weinh).* 9 (12), e2103675. doi:10.1002/advs.202103675

Zhang, Y., Wu, F., Teng, F., Guo, S., and Li, H. (2023). Deficiency of S100A9 alleviates sepsis-induced acute liver injury through regulating AKT-AMPK-dependent mitochondrial energy metabolism. *Int. J. Mol. Sci.* 24 (3), 2112. doi:10.3390/ijms24032112

Zhao, B. A., Li, J, Xue, C., Li, J., Ge, H. A., Cheng, B., et al. (2021). Role of the Alarmin S100A9 protein in inducing Achilles tendinopathy in rats. *Ann. Transl. Med.* 9 (22), 1698. doi:10.21037/atm-21-5945

# Elevation of serum human epididymis protein 4 (HE4) and N-terminal pro-B-type natriuretic peptide (NT-proBNP) as predicting factors for the occurrence of acute kidney injury on chronic kidney disease: a single-center retrospective self-control study

Jinye Song†, Ling Chen†, Zheping Yuan† and Xuezhong Gong*

Department of Nephrology, Shanghai Municipal Hospital of Traditional Chinese Medicine, Shanghai
University of Traditional Chinese Medicine, Shanghai, China

**Objectives:** To evaluate whether novel biomarkers of renal injury, serum HE4 and NT-proBNP could predict acute kidney injury (AKI) on chronic kidney disease (CKD) (A on C) and assess the specificity and efficiency of serum creatinine (SCr), HE4 and NT-proBNP in identifying potential AKI. Meanwhile, the potential early-warning value of HE4 and NT-proBNP in CKD patients was explored.

**Methods:** We performed a single-center, retrospective cohort study of 187 adult CKD patients. 32 AKI (grades 1–2) patients with pre-existing CKD (stages 3–5) were Group 1, 59 patients of CKD (stages 4–5) were Group 2. Another 96 patients of CKD (stages 1–3) were Group 3. All patients received general treatments, Group 1 patients received Chinese herb formulation (Chuan Huang Fang-II, CHF-II) simultaneously. These 155 CKD (stages 1–5) without AKI patients were observed for descriptive analysis.

**Results:** HE4 in Group 1 (860.63 $\pm$ 385.40) was higher than that in Group 2 (673.86 $\pm$ 283.58) before treatments. BUN, SCr, UA, NGAL, IL18, HE4 and NT-proBNP in Group 1 were lower, while eGFR was higher ($p < 0.01$, after vs. before treatments). In Group 1, both HE4 and NT-proBNP were positively correlated with SCr (respectively $r = 0.549, 0.464$) before treatments. The diagnostic performance of serum HE4 and NT-proBNP for A on C was 351.5 pmol/L, 274.5 pg/mL as the optimal cutoff value Area Under Curve (AUC) 0.860 (95% CI: 0.808 − 0.913, $p < 0.001$), [AUC 0.775 (95% CI: 0.697 − 0.853, $p < 0.001$), with a sensitivity and specificity of 100% and 66.5%, 87.5% and 48.8%, respectively]. In Group 2, serum HE4 was correlated with SCr ($r = 0.682, p < 0.01$) before treatments. Serum HE4 and NT-proBNP were elevated in advanced CKD stages, and were increased as CKD stages progressed with statistical significance.

**Conclusion:** This work indicated serum HE4 and NT-proBNP should elevate in A on C and CKD patients, HE4 is positively correlated with the disease severity, and

patients with higher HE4 and NT-proBNP usually have poorer prognosis. Thus, serum HE4 and NT-proBNP are impactful predictors of A on C. Additionally, serum HE4 and NT-proBNP have the potential to evaluate clinical efficacy of A on C.

# 1 Introduction

Acute kidney injury (AKI) is a common syndrome characterized by a rapid decline in the glomerular filtration rate (GFR), which is associated with the development of chronic kidney disease (CKD) and poor prognosis. It has become one of the most debilitating complications and a public health problem threatening human health worldwide (Sato et al., 2020; Xie et al., 2020). Approximately 13.3 million AKI cases occur globally every year, leading to approximately 1.7 million deaths annually, and 85% of the patients belong to developing countries (Mehta et al., 2015; Liu et al., 2021). The morbidity rate of AKI is 3%–5% in the general inpatient population and 30%–50% in intensive care units. AKI has been accepted as an important public health problem worldwide. CKD is the common outcome of various kidney diseases and AKI progression, and the number of CKD patients is increasing globally. The prevalence of CKD in China is approximately 10.8% (Cao et al., 2023). The morbidity rate of CKD complicated with AKI accounts for 12.7%–35.5% of the total AKI cases (Prakash et al., 2015). Previously, CKD and AKI were believed to exist independently; however, increasing evidence shows that CKD and AKI are closely linked or have an influence on each other. AKI is an obvious risk factor for accelerating CKD progression to end-stage renal disease (ESRD), and early identification and intervention of A on C patients is crucial (He et al., 2017; Huang, 2018).

Currently, the clinical diagnosis of AKI is based on the serum creatinine (SCr) level and urine volume; however, these parameters are easily affected by the patient's age, body weight, body fluid balance, and other factors. Therefore, early detection of renal injury is difficult. Additionally, patients with CKD have glomerular and renal tubule damage to a certain extent, and common indicators such as SCr and urine volume have limited value in the early prediction of AKI (Huang, 2018). Furthermore, the sensitivity of diagnosing AKI is poor, leading to missed diagnosis. Currently, there is a shortage of specific therapeutic drugs for AKI, and the conventional therapeutic principles of modern medicine focus on controlling the etiology, correcting the internal reversible factors, and alleviating the symptoms. AKI has attracted increasing attention due to its high incidence and poor prognosis. With the improvement of medical resources, researchers expect to find better biomarkers for the early prediction or detection of AKI.

N-terminal pro-B-type natriuretic peptide (NT-proBNP), a member of the diuretic natriuretic peptide family secreted by the heart, regulates the homeostasis of blood pressure and blood volume and has a diuretic effect. NT-proBNP correlates with the occurrence of AKI and may be of great value as a biomarker for the early prediction of AKI (Zhang et al., 2022). HE4, a novel tumor marker, has good predictive value for the progression of ovarian cancer

(DeBoer et al., 2018). Recently, its expression was reported in the kidneys (Huang et al., 2020; Luo et al., 2020). The HE4 level in patients with renal impairment increases significantly, which could be related to the progression of CKD to some extent; however, the test results of HE4 could be influenced by renal function. HE4 indirectly inhibits the degradation of type I collagen (Nagy et al., 2016; Wang et al., 2019) and causes infiltration and polarization of M2 macrophages (Rowswell-Turner et al., 2021), which could promote the progression of renal fibrosis (Jiao et al., 2021a; Jiao et al., 2021b; An et al., 2023). Macrophages are the main immune cells in healthy kidneys and are considered key members in the pathogenesis of AKI (Li and Gong, 2023). HE4 expression is upregulated in renal tissues with fibrosis, and the serum HE4 level of the patients increases significantly (Wang et al., 2018), suggesting that HE4 may be a potential marker for early diagnosis and evaluation of CKD.

Traditional Chinese Medicine (TCM) treatment of AKI and CKD is historical in China. Rhubarb has shown particular efficacy in the clinical treatment of AKI and CKD. In the 1990s, studies showed that rhubarb delayed the progression of chronic renal failure, stabilized renal function, alleviated azotemia, and improved the patient's nutritional status, symptoms, and physical strength (Zheng, 1985; Li, 1991). Our previous data indicated that a Chinese herbal formulation, Chuan Huang Fang (CHF) containing rhubarb, could exert a nephroprotective action in A on C patients (Gong et al., 2020; Gong et al., 2021; Chen et al., 2022). Furthermore, we conducted research on CHF against AKI in animal and cell models. CHF could effectively suppress the clinical dose of trivalent arsenic that causes renal toxicity, and its molecular mechanism was associated with the inhibition of caspase 3-induced renal tubular epithelial cell apoptosis (Gong et al., 2019; Chen and Gong, 2022a). We also investigated the mechanism of the Zhida Huang (prepared rhubarb)-Chuanxiong (Ligusticum wallichii) drug pair on tubular epithelial cell apoptosis in contrast-induced AKI (CI-AKI) rats (Gong et al., 2013). We found that activation of the p38MAPK pathway played an important role in the pathogenesis of CI-AKI, and the Zhida Huang-Chuanxiong drug pair might alleviate renal damage in CI-AKI rats by inhibiting the activation of the pathway. Based on this result, we explored the effect of the drug pair on the nuclear factor erythroid 2-related factor2/hemeoxygenase-1(Nrf2/HO-1) pathway (Gong et al., 2017). The Nrf2/HO-1 pathway was activated and involved in the process of AKI, and the Zhida Huang-Chuanxiong drug pair could activate the nephroprotective effects in the CI-AKI rats by inhibiting this pathway. Our recently published data (Li and Gong, 2023) on Rhizoma Chuanxiong and Radix et Rhizoma Rhei (rhubarb) against AKI and renal fibrosis based on network pharmacology and experimental validation shows that this herbal drug pair might inhibit tubular epithelial cell

apoptosis and improve AKI and renal fibrosis by inhibiting p38 MAPK/p53 signaling.

Rhubarb plays an important role in the process of alleviating the progression of AKI and CKD, and it has been widely used in treating these conditions in China for many years. For instance, the widely used drugs in China, such as Shenkang injection and Shenshuaining capsules, include rhubarb. In order to further improve clinical efficacy, CHF was optimized to form CHF-Ⅱ, and current small-sample clinical efficacy observation was conducted to evaluate the actual effect of CHF-Ⅱ on A on C.

To the best of our knowledge, no study to date has investigated the utility of serum HE4 and NT-proBNP in predicting the incidence of A on C. Accordingly, we aimed to assess the possible predictive ability of serum HE4 and NT-proBNP levels to identify acute deterioration of renal function in CKD patients.

Therefore, this study intends to explore the potential early prediction value of serum HE4 and NT-proBNP in patients with CKD alone and those with A on C. Furthermore, we investigated their expression levels in different clinical stages of CKD and compared them with other renal function indicators.

# 2 Materials and methods

## 2.1 Patients

This single-center, retrospective cohort study included 187 adult CKD patients hospitalized in Shanghai Municipal Hospital of Traditional Chinese Medicine from June 2021 to December 2022. Patients with Grades 1–2 AKI with pre-existing Stages 3–5 CKD were categorized as Group 1 ($n = 32$), those with Stages 4–5 CKD were categorized as Group 2 ($n = 59$), and those with Stages 1–3 CKD were categorized as Group 3 ($n = 96$). All CKD patients underwent general treatment, and the Group 1 patients additionally received the Chinese herbal formulation CHF-Ⅱ.

The clinical data, including age, sex, medical history, blood pressure, and laboratory indices, were obtained by reviewing the medical records. This retrospective study was approved by the Ethics Committee of Shanghai Municipal Hospital of Traditional Chinese Medicine (No. 2020SHL-KYYS-60) and was conducted according to the Declaration of Helsinki principles.

## 2.2 Definition

### 2.2.1 Diagnostic criteria for AKI
According to the "Kidney Disease: Improving Global Outcomes" (KDIGO) standards (KDIGO, 2013), Grade 1 AKI is defined by the following criteria: SCr level 1.5–1.9 times the baseline value or an increase of ≥0.3 mg/dL (26.5 μmol/L), or urine output (UO) < 0.5 mL/kg/h for 6–12 h.

Grade 2 AKI is defined by the following criteria: SCr level 2.0–2.9 times the baseline value, or UO < 0.5 mL/kg/h for ≥12 h.

Grade 3 AKI is defined by the following criteria: SCr level 3.0 times the baseline value or ≥4.0 mg/dL (353.6 μmol/L) or initiation of renal replacement therapy (RRT), or UO < 0.3 mL/kg/h for ≥24 h or anuria for ≥12 h. In patients aged <18 years, Grade 3 AKI is defined by estimated GFR (eGFR) < 35 mL/min/1.73 m².

### 2.2.2 Diagnostic criteria for CKD
CKD was defined as incident CKD during the observation period according to the following KDIGO guideline [16]: "CKD is defined as abnormalities of kidney structure or function present for >3 months."

CKD Stage 1 was defined as eGFR ≥90 mL/min/1.73 m²; CKD Stage 2 as eGFR 60–89 mL/min/1.73 m²; CKD Stage 3 as eGFR 30–59 mL/min/1.73 m²; CKD Stage 4 as eGFR 15–29 mL/min/1.73 m²; and CKD Stage 5 as eGFR <15 mL/min/1.73 m². The CKD-Epidemiology Collaboration formula was used to calculate the eGFR of the CKD patients.

### 2.2.3 Exclusion criteria
Patients with malignancy or acute cerebrovascular disease, those without laboratory measurements or medical records, and pregnant patients were excluded.

### 2.2.4 Interventions
All patients were given a low-salt, high-quality, low-protein diet (protein intake, 0.6–0.8 g/kg/d). They all underwent general treatment to correct water, electrolyte, and acid-base balance disorders, control blood pressure, improve anemia, and correct renal bone diseases. Group 1 patients additionally received CHF-Ⅱ orally, twice a day for 2 weeks. Simultaneously, the concentrated CHF-Ⅱ solution was administered as an enema, once a day for 5 days, followed by rest for 2 days, and then 5 times a week. The pharmaceutical composition of CHF-Ⅱ mainly included prepared Zhida Huang, Chuanxiong, Codonopsis pilosula (Dangshen), Coptidis rhizome (Huanglian), and Smilacis glabrae (Tufuling), etc. The CHF-Ⅱ administered was produced by Jiangyin Tianjiang and Shanghai Wanshicheng Pharmaceutical Co., Ltd.; hence, the quantity and quality of medicine were guaranteed.

## 2.3 Methods

Peripheral venous blood specimens were collected in the early morning within 24 h after admission. For all patients, 10 mL of venous blood was collected and separated for 15 min at 3,500 rpm (14 cm from the core half diameter). The SCr, blood urea nitrogen (BUN), and uric acid (UA) levels were measured using Beckman Coulter chemistry analyzer AU5800 (Beckman Coulter Inc.). The serum HE4 and NT-proBNP levels were measured using electrochemiluminescence immunoassay, while urinary neutrophil gelatinase-associated lipocalin (NGAL) and interleukin (IL)-18 were measured using enzyme-linked immunosorbent assay. All the kits were purchased from Beijing Dingguo Changsheng Biotechnology Co., Ltd.

## 2.4 Statistical methods

All data were analyzed using Statistical Product and SPSS 22.0 statistical software. After data collection, the distribution of each parameter was examined to determine the appropriate statistical method for subsequent analyses. The NGAL and NT-proBNP values did not conform to normal distribution; therefore, they are presented as medians (interquartile ranges). Mann–Whitney $U$ test was used to compare the differences between the groups. The measurement data are expressed as means ± standard deviations (SD). Spearman correlation analysis was used to evaluate the correlation of

**TABLE 1 The causes of AKI and CKD of Group 1 and Group 2.**

| The causes of CKD of Group 1 | Number (%) | The causes of AKI of Group 1 | Number (%) | The causes of CKD of Group 2 | Number (%) |
|---|---|---|---|---|---|
| chronic glomerulonephritis | 11 (35.4%) | poor medication adherence leading to aggravation of existing diseases | 12 (37.5%) | chronic glomerulonephritis | 25 (42.4%) |
| IgA nephropathy | 8 (25.0%) | infectious pneumonia | 5 (15.6%) | IgA nephropathy | 15 (25.4%) |
| diabetic nephropathy | 7 (21.9%) | water-electrolyte imbalance | 5 (15.6%) | diabetic nephropathy | 12 (20.3%) |
| hypertensive nephropathy | 4 (12.5%) | Diuretic, Contrast,NSAIDs-induced renal injury | 4 (12.5%) | hypertensive nephropathy | 5 (8.5%) |
| polycystic kidney disease | 1 (3.2%) | heart failure | 4 (12.5%) | polycystic kidney disease | 2 (3.4%) |
| uric acid nephropathy | 1 (3.2%) | acute gout attack | 2 (6.3%) | | |

**TABLE 2 Baseline characteristics of the participants.**

| Characteristics | Total ($n = 91$) | Group 1 ($n = 32$) | Group 2 ($n = 59$) |
|---|---|---|---|
| Male, n (%) | 62 (68.1%) | 24 (75.0%) | 38 (64.4%) |
| Age (years), mean ± SD | 62.3 ± 12.8 | 62.1 ± 11.9 | 61.9 ± 11.6 |
| Concomitant diseases | 85 (93.4%) | 30 (93.8%) | 55 (93.2%) |
| Hypertension, n (%) | | | |
| Type 2 diabetes mellitus, n (%) | 51 (56.0%) | 18 (56.3%) | 33 (55.9%) |

Group 1: Patients with Grades 1–2 AKI, and pre-existing Stages 3–5 CKD., Group 2: Patients with Stages 4–5 CKD. SD, standard deviation; AKI, acute kidney injury; CKD, chronic kidney disease.

HE4 and NT-proBNP with SCr. The diagnostic value of each indicator for A on C was evaluated using the receiver operating characteristic (ROC) curve; $p$-values < 0.05 were considered statistically significant.

# 3 Results

## 3.1 Participant characteristics

The mean ± SD values of BUN, SCr, and UA did not differ significantly between Group 1 and Group 2. The average age of the participants in Group 1 and Group 2 was 62.1 ± 11.9 and 61.9 ± 11.6 years, respectively, and the number of male participants was 24 and 38, respectively. Poor medication adherence leading to aggravation of existing diseases was the main cause of AKI which accounted for 37.5% (Table 1), the main cause of CKD of both groups was chronic glomerulonephritis which accounted for 35.4% and 42.4% respectively, the causes of AKI and CKD of the two groups are shown in Table 1. The concomitant diseases in Groups 1 and 2 are presented in Table 2. No significant differences were observed in sex, age, and concomitant diseases between these two groups ($p > 0.05$). The baseline characteristics of the patients in Groups 1 and 2 were balanced, and the efficacy of this clinical study was comparable (Table 2).

## 3.2 Comparison of renal function indicators between Groups 1 and 2 before and after treatment

Before treatment, the mean ± SD values of BUN, SCr, and UA did not differ significantly between Group 1 and Group 2. The

mean ± SD SCr values after treatment were 329.16 ± 113.61 μmol/L and 374.24 ± 148.47 μmol/L in Groups 1 and 2, respectively. Compared to the SCr level before treatment in Group 1, a significant decline was observed after treatment ($p < 0.01$); however, Group 2 showed no significant difference in the SCr levels before and after treatment ($p < 0.05$).

The mean ± SD values of BUN after treatment were 17.69 ± 7.14 mmol/L and 20.17 ± 7.06 mmol/L in Groups 1 and 2, respectively. The mean BUN value in Group 1 was significantly lower after treatment than that before treatment ($p < 0.01$). Meanwhile, the mean UA level before treatment in Group 1 was significantly lower than that after treatment ($p < 0.01$). Similarly, the eGFR improved significantly after treatment in Group 1 ($p < 0.01$). However, in Group 2, no significant differences were observed in the BUN, UA, and eGFR values before and after treatment ($p < 0.05$) (Table 3; Figure 1).

No significant differences were observed in the SCr, BUN, and eGFR values between Groups 1 and 2 after treatment ($p > 0.05$).

## 3.3 Various expressions of urine NGAL and IL-18 between Groups 1 and 2

To investigate the prediction performance of the existing AKI biomarkers for A on C, we evaluated the expression of NGAL and IL-18. Both these biomarkers were significantly elevated in Groups 1 and 2. Before treatment, the NGAL and IL-18 levels were significantly elevated in Group 1 when compared with Group 2 ($p < 0.01$).

The median NGAL level was significantly higher in Group 1 than in Group 2 (265.200 ng/mL [138.20–539.50] vs. 151.800 ng/mL [95.00–266.90]; $p < 0.001$); this level decreased

**TABLE 3** Comparison of the renal function indicators between Group 1 and Group 2 before and after treatment.

| Variables | Group 1 (n = 32) | | Group 2 (n = 59) | |
|---|---|---|---|---|
| | Before treatment | After treatment | Before treatment | After treatment |
| SCr (μmol/L) | 404.00 ± 151.18 | 329.16 ± 113.61** | 371.59 ± 141.51 | 374.24 ± 148.47 |
| BUN (mmol/L) | 20.92 ± 7.98 | 17.69 ± 7.14** | 20.34. ± 7.04 | 20.17 ± 7.06 |
| UA (μmol/L) | 440.13 ± 122.69 | 382.56 ± 92.00** | 441.84 ± 94.38 | 439.34 ± 101.29## |
| eGFR (mL/min/1.73m$^2$) | 13.82 ± 4.62 | 18.30 ± 8.67** | 16.93 ± 5.89 | 17.56 ± 6.26 |

Group 1: Patients with Grades 1–2 AKI, and pre-existing Stages 3–5 CKD., Group 2: Patients with Stages 4–5 CKD. SCr, serum creatinine; BUN, blood urea nitrogen; UA, uric acid; eGFR, estimated glomerular filtration rate. **Statistically significant difference from before treatment; $p < 0.01$ considered statistically significant. ##Statistically significant difference from Group 1; $p < 0.01$ considered statistically significant.



**FIGURE 1**
Comparison of the renal function indicators between Group 1 and Group 2 before and after treatment.
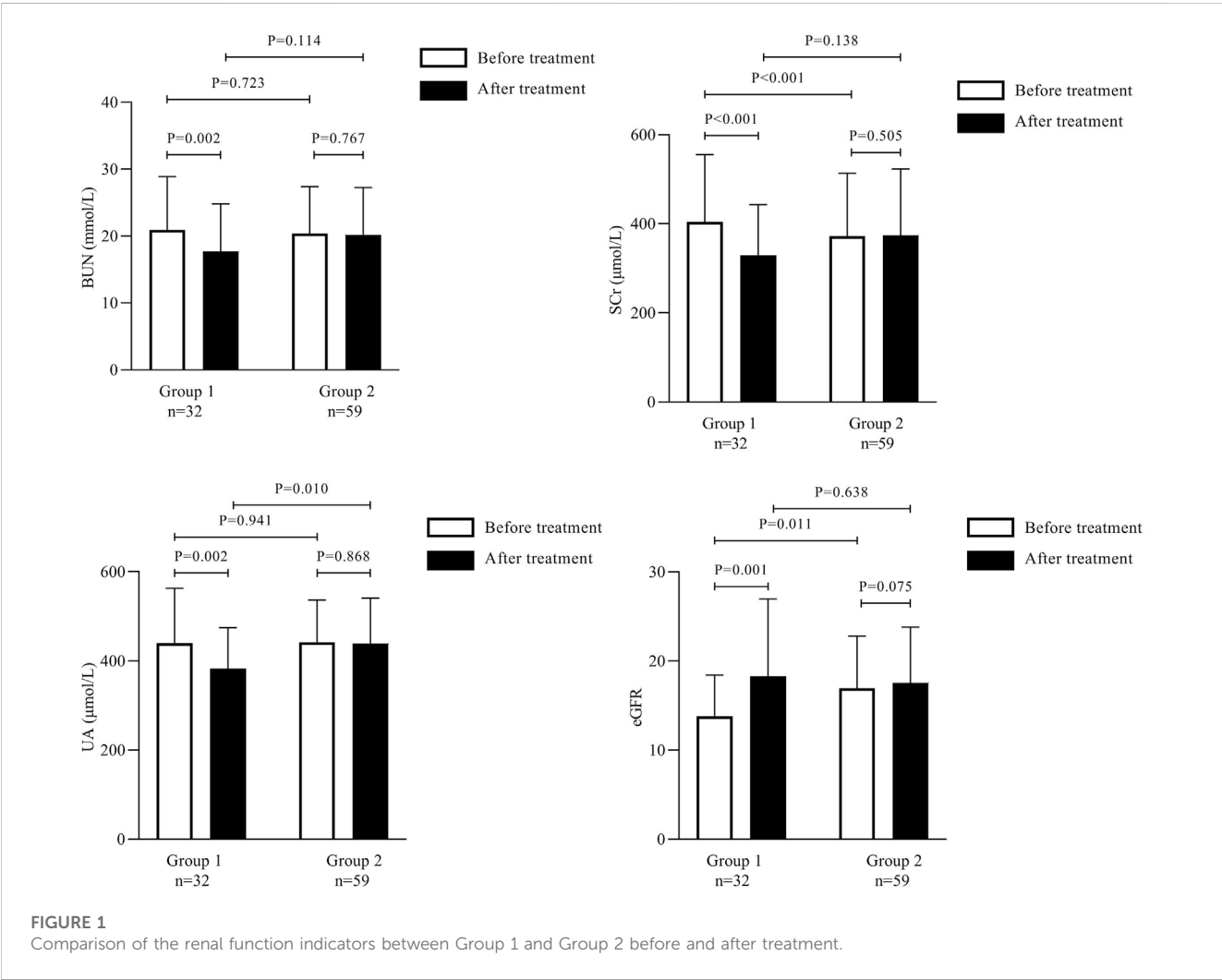
significantly after treatment in Group 1 (203.950 ng/mL [113.50–487.70]; $p < 0.01$).

In contrast, the median NGAL level in Group 2 did not differ significantly before and after treatment (Table 4). The IL-18 levels reduced significantly after treatment in Group 1 (112.06 ± 28.45 pg/mL) and Group 2 (103.63 ± 21.50 pg/mL) as compared to the levels before treatment (127.06 ± 33.01 pg/mL and 109.41 ± 17.65 pg/mL, respectively; $p < 0.001$) (Figure 2).

## 3.4 Various expressions of HE4 and NT-proBNP between Groups 1 and 2

The mean serum HE4 level before treatment was significantly higher in Group 1 than in Group 2 (860.63 ± 385.40 pmol/mL vs. 673.86 ± 283.58 pmol/mL; $p = 0.01$); this level decreased significantly after treatment in Group 1 (737.59 ± 331.49 pmol/mL; $p < 0.001$).

TABLE 4 Comparison of neutrophil gelatinase-associated lipocalin, interleukin-18, human epididymis secretory protein 4, and N-terminal pro-B-type natriuretic peptide between Group 1 and Group 2 before and after treatment.

| Variables | Group 1 (n = 32) | | Group 2 (n = 59) | |
|---|---|---|---|---|
| | Before treatment | After treatment | Before treatment | After treatment |
| NGAL (ng/mL), (P25, P75) | 265.200 (138.2–539.5) | 203.950 (113.5–487.7)** | 151.800 (95.0–266.90)## | 136.000 (93.0–287.7) |
| IL-18 (pg/mL), mean ± SD | 127.06 ± 33.01 | 112.06 ± 28.45** | 109.41 ± 17.65## | 103.63 ± 21.50 |
| HE4 (pmol/mL), mean ± SD | 860.63 ± 385.40 | 737.59 ± 331.49* | 673.86 ± 283.58## | 684.64 ± 310.11 |
| NT-proBNP (pg/mL), (P25, P75) | 613.500 (293.3–3747.0) | 435.000 (278.5–1693.5)** | 529.000 (266.5–1225.5) | 535.000 (331.0–1103.0) |

Group 1: Patients with Grades 1-2 AKI, and pre-existing Stages 3–5 CKD., Group 2: Patients with Stages 4–5 CKD. NGAL, neutrophil gelatinase-associated lipocalin; IL, interleukin; HE4, human epididymis secretory protein 4; NT-proBNP, N-terminal pro-B-type natriuretic peptide; SD, standard deviation. *Statistically significant difference from before treatment; $p = 0.01$. **Statistically significant difference from before treatment; $p < 0.01$. ##Statistically significant difference between Group 1 and Group 2; $p < 0.01$.



FIGURE 2
Comparison of urine neutrophil gelatinase-associated lipocalin and interleukin-18 between Group 1 and Group 2 before and after treatment.



FIGURE 3
Comparison of human epididymis secretory protein 4 and N-terminal pro-B-type natriuretic peptide between Group 1 and Group 2 before and after treatment.
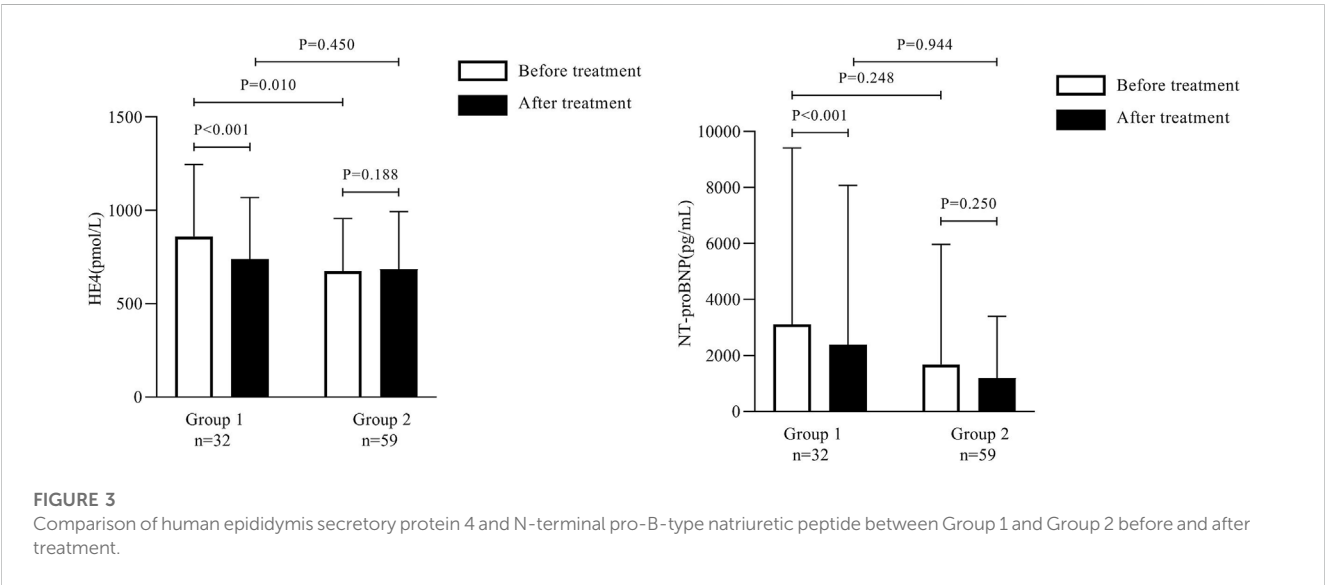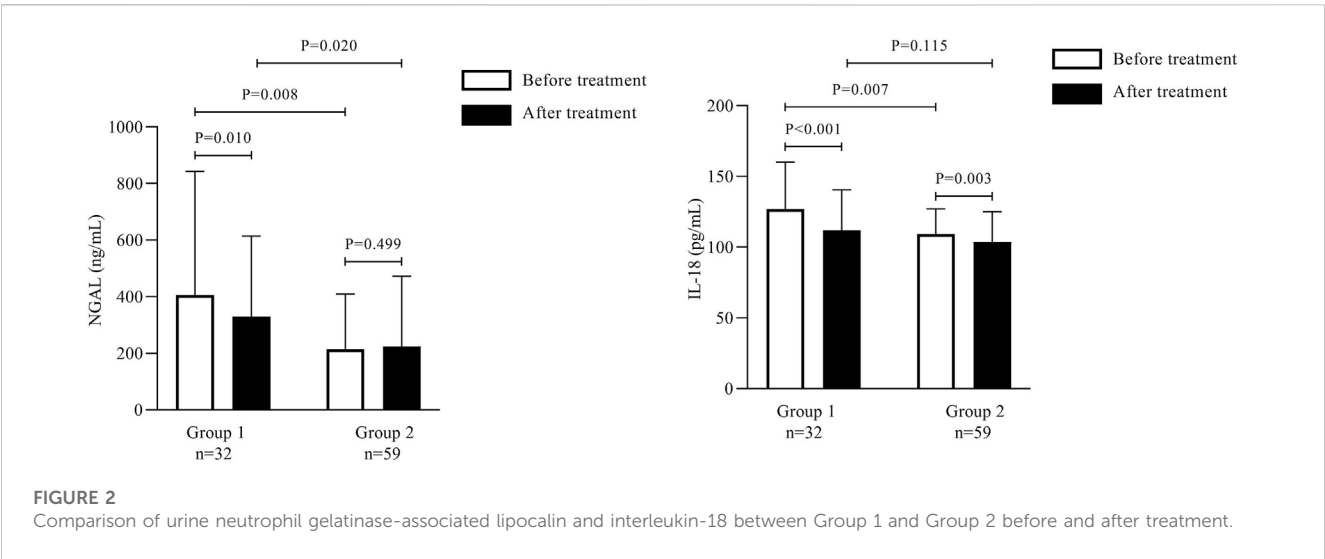
In contrast, the mean HE4 level in Group 2 did not differ significantly before and after treatment (Table 4; Figure 3). The median NT-proBNP level was significantly higher in Group 1 than in Group 2 before treatment (613.500 pg/mL [293.3–3747.0] vs. 529.000 pg/mL [266.5–1225.5]; $p < 0.001$); this level decreased significantly after treatment in Group 1 (435.000 pg/mL [278.5–1693.5]; $p = 0.01$).
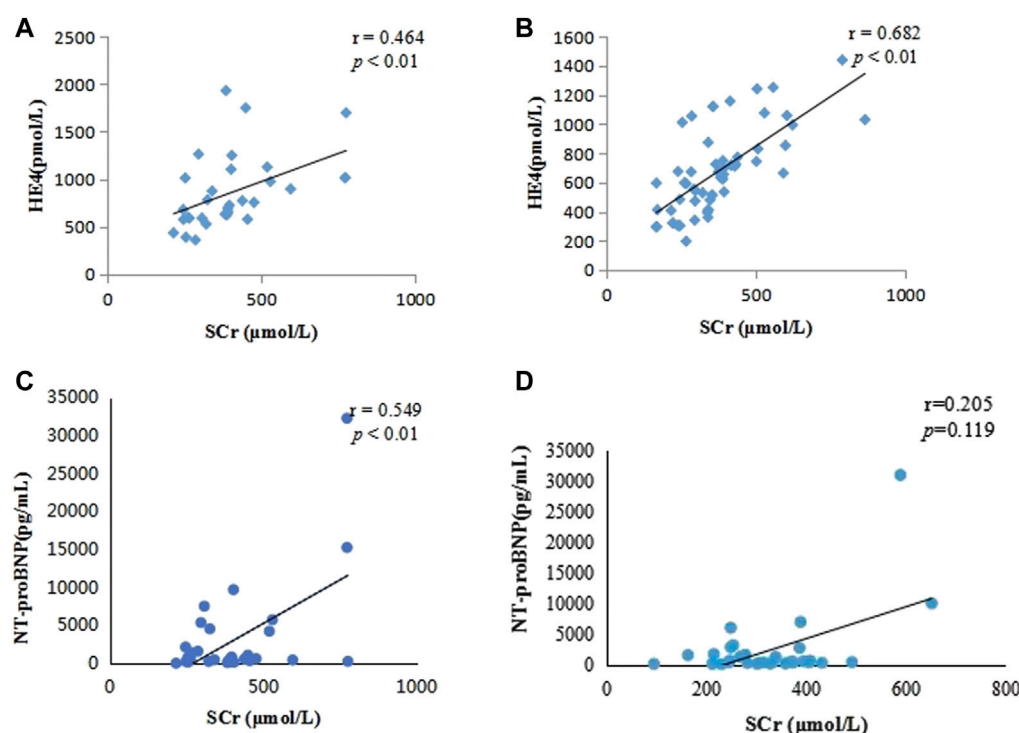
**FIGURE 4**
Scatterplots showing the correlation between human epididymis secretory protein 4 and serum creatinine in Group 1 **(A)** and Group 2 **(B)** and between N-terminal pro-B-type natriuretic peptide and serum creatinine in Group 1 **(C)** and Group 2 **(D)**.

In contrast, the median NT-proBNP level in Group 2 did not differ significantly before and after treatment (Table 4; Figure 3).

Spearman correlation analysis revealed that serum HE4 correlated positively with SCr in Groups 1 and 2 before treatment ($r = 0.464$ and 0.682, respectively; $p < 0.01$). Moreover, NT-proBNP correlated positively with SCr ($r = 0.549$; $p < 0.01$) in Group 1 before treatment but not in Group 2 ($r = 0.205$; $p = 0.119$) (Figure 4).

The ROC curve for diagnostic performance showed that the optimal cutoff value of serum HE4 for A on C was 351.5 pmol/L (area under the curve [AUC], 0.860; 95% confidence interval [CI]: 0.808–0.913; $p < 0.001$), with a sensitivity and specificity of 100% and 66.5%, respectively. The optimal cutoff value of serum NT-proBNP for A on C was 274.5 pg/mL (AUC, 0.775; 95% CI: 0.697–0.853; $p < 0.001$), with a sensitivity and specificity of 87.5% and 48.8%, respectively (Figure 5).

## 3.5 Comparison of renal function indicators and biomarkers in CKD patients

We further categorized the 155 CKD patients (Stage 1, $n = 39$; Stage 2, $n = 28$; Stage 3, $n = 29$; Stage 4, $n = 34$; and Stage 5, $n = 25$) according to their eGFR values. The serum HE4 levels increased as the CKD stages progressed, with a statistically significant difference. Serum HE4 levels were obviously elevated in advanced CKD stages, suggesting serum HE4 as a novel biomarker for predicting the severity of CKD. However, no significant difference was observed in the HE4 levels between Stage 1 and Stage 2 CKD ($p = 0.222$) and between Stage 2 and Stage 3 CKD ($p = 0.112$) (Table 5; Figure 6).

Furthermore, the NT-proBNP levels increased as the CKD stages progressed, with a statistically significant difference. The serum NT-proBNP levels were obviously elevated in advanced CKD stages; however, no significant difference was observed in the serum NT-proBNP levels between Stage 4 and Stage 5 CKD ($p = 0.069$) (Table 5; Figure 6).

## 4 Discussion

To the best of our knowledge, this is the first study investigating the clinical significance of serum HE4 and NT-proBNP levels in A on C patients. This study found that serum HE4 and NT-proBNP levels were elevated in CKD patients, especially in A on C patients. Furthermore, SCr was positively associated with elevated serum HE4 and NT-proBNP levels in A on C patients. Moreover, serum HE4 and NT-proBNP were strongly associated with an increased risk of A on C and could be used as novel biomarkers for A on C diagnosis.

This study showed that CHF-II as part of the integrated TCM and Western medicine has positive clinical efficacy in treating A on C, corroborating our previous findings (Chen and Gong, 2022a; Chen and Gong, 2022b; Chen et al., 2022). This study further

FIGURE 5
Receiver operating characteristic curves of human epididymis secretory protein 4 and N-terminal pro-B-type natriuretic peptide for the diagnosis of acute kidney injury on chronic kidney disease The AUC values of serum HE4 and NT-proBNP for A on C were 0.860 (95% CI: 0.808−0.913; $p$ < 0.001) and 0.775 (95% CI: 0.697−0.853; $p$ < 0.001), respectively, and their optimum cutoff values to predict A on C were 351.5 pmol/L and 274.5 pg/mL, respectively. (AUC, area under the curve; CI, confidence interval; HE4, human epididymis secretory protein 4; NT-proBNP, N-terminal pro-B-type natriuretic peptide; A on C, acute kidney injury on chronic kidney disease).

confirms the clinical value of CHF-Ⅱ and is worthy of further research and promotion of its application. Furthermore, it shows that serum HE4 and NT-proBNP could help evaluate the effectiveness of the drug treatment regimens.

Several studies (Chen et al., 2017; Luo et al., 2018) reported that increased serum HE4 level is associated with decreased renal function in CKD patients. Using the AUC analysis, this study showed that serum HE4 and NT-proBNP are good indicators and predictors of AKI in CKD patients.

AKI and CKD are closely related. Although old age, nephrotoxic drugs, sepsis, chronic heart disease, and diabetes are common risk factors for AKI in clinical practice (Hsu et al., 2016; Liu et al., 2018), the most important risk factor is pre-existing CKD. The incidence of AKI in patients with CKD is nearly 10 times that of patients without CKD (Moo Park, 2014; Wonnacott et al., 2014). AKI can lead to new incidence of CKD, progression of existing CKD, increased risk of long-term morbidity, and increased mortality rate in patients with ESRD. AKI and CKD are risk factors for each other (Chawla et al., 2014); hence, it is crucial to improve the comprehensive understanding of A on C, perform early detection and intervention, and promote recovery of renal function. It is of great clinical significance to strengthen the early detection and diagnosis of A on C.

Privratsky et al. (2022) reported that the risk of postoperative AKI and its severity correlated positively with the risk of developing CKD or ESRD within 1 year after surgery, and preoperative CKD was an independent risk factor for postoperative AKI; however,

there was no correlation with the severity of AKI. Hatakeyama et al. (2017) reported a positive correlation between AKI and glomerular dysfunction. Additionally, the frequency of AKI in patients with CKD is significantly higher than that in patients without CKD, especially after reaching Stage 3b of CKD (Zhang et al., 2019). Therefore, AKI increases the risk of developing CKD and may accelerate the progression of CKD to ESRD. Conversely, CKD itself is one of the main risk factors inducing AKI. Thus, AKI and CKD are interrelated and influence each other. CKD increases susceptibility to AKI, and the prognosis of CKD complicated with AKI is often poor.

The prevention and treatment principle of A on C focuses on reducing the incidence of AKI as much as possible, improving renal function to the greatest extent in the short term, correcting the influence of AKI on CKD, protecting renal function in the long term, and improving the survival rate. In CKD patients who have developed AKI, the cause of AKI should be corrected as soon as possible, and RRT should be performed at the earliest in severe cases. The incidence of A on C has been increasing every year. The interaction between CKD and AKI shows that A on C is a complex clinical syndrome.

The diagnostic means of modern medicine and TCM treatment have their advantages; hence, with the deepening of modern medical research, we must continue to look for sensitive diagnostic markers. Moreover, the continuous research on the curative effects of TCM in treating this disease as well as disease differentiation by Western medicine combined with syndrome differentiation by TCM can maximize the advantages of these two approaches and minimize the recovery time of renal injury, which is the key to treating this disease.

NT-proBNP, which is mainly derived from the ventricle, promotes sodium excretion and urination and has a strong vasodilatory effect, which can counteract the vasodilatory effect of the renin-angiotensin-aldosterone system. Cardiac dysfunction can greatly activate the natriuretic peptide system, and increased ventricular load leads to NT-proBNP release (Wang and Xu, 2020). When AKI occurs, the renal structure is damaged, NT-proBNP receptors are destroyed, and the ability to bind NT-proBNP is decreased, resulting in increased plasma-free NT-proBNP levels. The change in NT-proBNP levels is closely associated with renal function deterioration and prognosis (Wettersten et al., 2019).

NT-proBNP has been extensively studied in patients with cardiovascular disease. It was found that this indicator can predict the progression of AKI in patients with ST-segment elevation myocardial infarction or heart failure (Palazzuoli et al., 2014). In patients with cardiac arrest, NT-proBNP is considered a marker of cardiac and renal load and a risk factor for AKI after cardiac surgery. A prospective trial of ICU patients with non-cardiac causes concluded that NT-proBNP levels could predict the development of AKI (de Cal et al., 2011). Chou et al. (2015) measured the NT-proBNP levels 24 h after admission in 163 critically ill patients and showed that changes in NT-proBNP on the day of admission and after 24 h predicted the development of AKI; however, it did not adjust for disease severity and potential cardiac risk factors. Papanikolaou et al. (2014) measured the NT-proBNP concentrations in patients with sepsis and showed that the levels increased during sepsis and septic shock, which was attributed to the release of pro-inflammatory cytokines and biventricular dysfunction. The results showed that the NT-proBNP concentrations correlated independently with the AKI stage and RRT.

**TABLE 5 Clinical characteristics and laboratory tests of Group 2 and Group 3.**

| Variables | Total (n = 155) | CKD1 (n = 39) | CKD2 (n = 28) | CKD3 (n = 29) | CKD4 (n = 34) | CKD5 (n = 25) |
|---|---|---|---|---|---|---|
| Age (years) | 63.11 ± 14.24 | 59.36 ± 12.90 | 66.71 ± 13.03 | 64.84 ± 15.19 | 61.35 ± 15.89 | 64.64 ± 12.24 |
| Sex (male/female); n | 155 (87/68) | 39 (18/21) | 28 (14/14) | 29 (15/14) | 34 (25/9) | 25 (15/10) |
| **Primary diseases** | | | | | | |
| Diabetes | 77 (49.68%) | 11 (28.21%) | 10 (35.71%) | 11 (37.93%) | 20 (58.82%) | 15 (60%) |
| Hypertension | 106 (68.39%) | 19 (48.72%) | 19 (67.86%) | 21 (72.41%) | 27 (79.41%) | 20 (80%) |
| **Laboratory tests** | | | | | | |
| SCr (μmol/L) | 204.59 ± 131.33 | 61.67 ± 12.76 | 88.11 ± 18.36[aa] | 169.52 ± 41.37[bb] | 299.09 ± 79.23[cc] | 470.20 ± 148.94[d] |
| BUN (mmol/L) | 12.76 ± 6.62 | 5.71 ± 1.81 | 6.98 ± 1.40[aa] | 12.42 ± 3.70[bb] | 17.83 ± 6.65[cc] | 23.76 ± 6.16[d] |
| UA (μmol/L) | 410.62 ± 77.99 | 332.68 ± 76.04 | 406.64 ± 77.41[aa] | 455.78 ± 86.49[b] | 452.09 ± 96.24 | 427.88 ± 91.87 |
| eGFR (mL/min/1.73 m²) | 59.18 ± 38.60 | 127.70 ± 25.40 | 70.59 ± 9.95[aa] | 41.98 ± 9.34[bb] | 20.79 ± 4.51[cc] | 11.68 ± 2.46[d] |
| IL-18 (pg/mL) | 212.86 ± 22.24 | 91.03 ± 18.37 | 102.07 ± 16.57[a] | 99.41 ± 17.39 | 104.00 ± 16.08 | 152.76 ± 65.17[d] |
| NGAL (ng/mL) | 132.20 (78.20–238.00) | 62.50 (38.4–114.00) | 115.50 (83.3–173.0)[aa] | 250.00 (175.5–358.5)[bb] | 123.00 (82.4–159.6)[cc] | 226.00 (165.8–391.6)[d] |
| HE4 (pmol/L) | 323.65 ± 274.65 | 77.34 ± 22.17 | 109.18 ± 61.03 | 149.49 ± 77.02 | 531.09 ± 151.38[cc] | 868.04 ± 277.89[d] |
| NT-proBNP (pg/mL) | 175.00 (75.00–510.00) | 45.40 (36.2–110.0) | 79.20 (64.3–117.8)[aa] | 254.00 (126.5–390.5)[bb] | 477.00 (208.3–1120.5)[c] | 649.00 (295.0–2017.0) |

Data are presented as n (%) or means ± standard deviations for normally distributed continuous variables and as medians (interquartile ranges) for non-normally distributed continuous variables. Group 2: Patients with Stages 4–5 CKD., Group 3: Patients with Stages 1–3 CKD. CKD1 (CKD, Stage 1), patients with eGFR ≥90 mL/min/1.73 m²; CKD2 (CKD, Stage 2), patients with eGFR, 60–89 mL/min/1.73 m²; CKD3 (CKD, Stage 3), patients with eGFR, 30–59 mL/min/1.73 m²; CKD4 (CKD, Stage 4), patients with eGFR, 15–29 mL/min/1.73 m²; CKD5 (CKD, Stage 5), eGFR <15 mL/min/1.73 m². CKD, chronic kidney disease; SCr, serum creatinine; BUN, blood urea nitrogen; UA, uric acid; eGFR, estimated glomerular filtration rate; NGAL, neutrophil gelatinase-associated lipocalin; IL, interleukin; HE4, human epididymis secretory protein 4; NT-proBNP, N-terminal pro-B-type natriuretic peptide. [a]$p < 0.05$. [aa]$p < 0.01$, CKD1 vs. CKD2. [b]$p < 0.05$. [bb]$p < 0.01$, CKD2 vs. CKD3. [c]$p < 0.05$. [cc]$p < 0.01$, CKD3 vs. CKD4. [d]$p < 0.01$, CKD4 vs. CKD5.
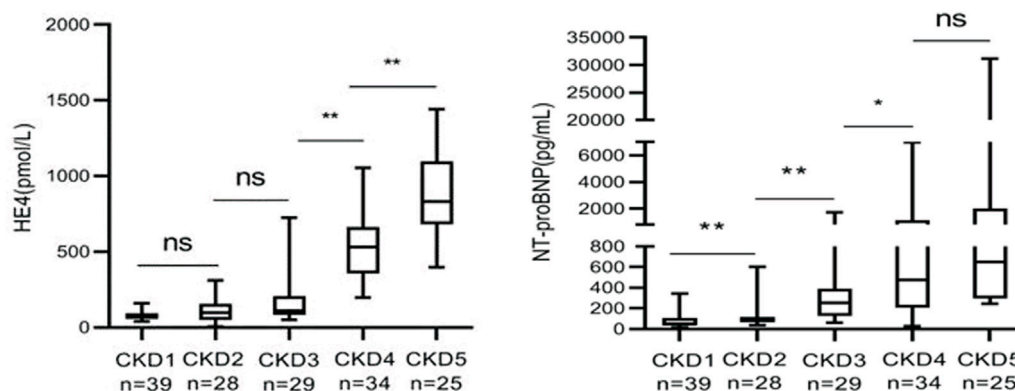


**FIGURE 6**
Comparison of human epididymis secretory protein 4 and N-terminal pro-B-type natriuretic peptide in chronic kidney disease patients (non-significant: $p > 0.05$; *$p < 0.05$; **$p < 0.01$).

In AKI patients, the GFR and urine volume decrease, resulting in excessive volume load, which leads to increased NT-proBNP secretion by the ventricular myocytes. Recently, studies have further verified the threshold value of NT-proBNP for excessive volume load in AKI patients. It was reported that NT-proBNP in patients with AKI had a good correlation with the net ultrafiltration, and NT-proBNP levels were significantly lower in patients with hypotension after continuous RRT than in those without AKI (Cui et al., 2013). Yang et al. (2016) conducted a prospective study to detect serum HE4 levels in CKD patients. The relationship between HE4 and CKD progression was analyzed. Finally, it was confirmed that high expression of serum HE4 is associated with poor renal prognosis in CKD patients, suggesting that HE4 may be a serological marker for CKD progression. Wan et al. (2016) reported that the serum HE4 level in CKD patients was significantly higher than that in healthy individuals. The elevated HE4 level correlated closely with the CKD stage; the higher the HE4 level, the more severe the renal fibrosis. Correlation analysis in a previous study showed that HE4 correlated significantly with the

degree of renal fibrosis (r = 0.938; $p$ < 0.0001); the AUC was 0.99, which was higher than that of SCr (0.89). He et al. (2016) showed that the efficacy of serum HE4 in the early diagnosis of renal injury in male patients with CKD was higher than that of SCr and comparable to that of cystatin-C, which is a sensitive indicator reflecting the eGFR. Based on the results of the existing biological studies, we concluded that serum HE4 level increases significantly in CKD patients with renal fibrosis and correlates with the CKD stage (Lv et al., 2015).

The elevated level of HE4 in CKD patients is attributed to two factors. One is that as a small molecule, HE4 is filtered by the glomerulus, and when eGFR declines, the HE4 level rises inevitably. The other is that HE4 expression level in CKD patients increases significantly (Qu et al., 2016). This provides a new approach for the evaluation of chronic renal function injury.

The HE4 expression is upregulated in patients with renal tissue fibrosis, and the injection of HE4 neutralizing antibody in the mouse renal disease model can inhibit renal fibrosis and delay the progression of CKD in the mice (LeBleu et al., 2013; Wan et al., 2016). Studies have shown that when fibrosis changes occur in the kidneys of CKD patients, the intrinsic cells of the kidney will proliferate and differentiate to form myoblasts (Bai et al., 2019). The HE4 gene in myoblasts is significantly upregulated, resulting in increased HE4 protein secretion. Elevated HE4 inhibits the degradation of collagen I by inhibiting the activity of serine proteases (Prss23 and Prss35) and matrix metalloproteinases (MMP-2 and MMP-9) and accelerates the deposition of type I collagen in the kidneys, leading to renal fibrosis. There are two possible reasons for the increase in HE4 levels in CKD patients. First, the filtration and reabsorption of small molecule substances are significantly affected when the renal function is impaired, and the glomeruli cannot effectively clear HE4, thus the serum HE4 expression level increases significantly (Li et al., 2022). Second, when the kidney changes structurally, the formation of myofibroblasts and secretion of HE4 increases; this increased HE4 expression increases the accumulation of collagen in the extracellular matrix, which promotes the occurrence and development of renal fibrosis (Qu et al., 2016).

## 5 Conclusion

We conducted a retrospective study to investigate the levels of HE4 and NT-proBNP in A on C and CKD patients and of renal function parameters. We also compared the HE4 and NT-proBNP levels in CKD patients according to their clinical stages. Moreover, we analyzed the correlations of HE4 and NT-proBNP with the renal function parameters in A on C and CKD patients. Our study adds additional evidence that serum HE4 and NT-proBNP could be sensitive and specific biomarkers for diagnosing A on C.

This study extended its findings by revealing significant associations between elevated serum HE4 and NT-proBNP levels and the loss of renal function and decreased eGFR in A on C patients. Therefore, these findings suggest that serum HE4 and NT-proBNP levels are elevated as CKD progresses and that they could be valuable biomarkers in patients with a risk of CKD progression. Moreover, HE4 and NT-proBNP may be potential novel biomarkers for assessing treatment efficacy and effectiveness in A on C patients. The HE4 and NT-proBNP levels can help to identify the severity of

A on C or CKD and are powerful predictors of rapid CKD progression.

Our study has certain limitations. First, it was a single-center study with a modest sample size. Second, no information was provided regarding the cause of CKD in the patients. The small number of patients with CKD might be insufficient to determine the reliability and generalizability of serum HE4 and NT-proBNP as biomarkers of A on C. Finally, although this study aimed to identify the potential biomarkers for predicting A on C, the underlying mechanism of these predictors in A on C remains unclear, which requires further investigation. Further investigations with larger samples are warranted to confirm these findings.

## Data availability statement

The original contributions presented in the study are included in the article/Supplementary Material, further inquiries can be directed to the corresponding author.

## Ethics statement

The studies involving humans were approved by the Ethics Committee of Shanghai Municipal Hospital of Traditional Chinese Medicine. The studies were conducted in accordance with the local legislation and institutional requirements. The participants provided their written informed consent to participate in this study. Written informed consent was obtained from the individual(s) for the publication of any potentially identifiable images or data included in this article.

## Author contributions

JS: Data curation, Formal Analysis, Writing–original draft, Writing–review and editing. LC: Project administration, Writing–original draft. ZY: Data curation, Writing–original draft. XG: Methodology, Supervision, Writing–original draft, Writing–review and editing.

## Funding

## Conflict of interest

The authors declare that the research was conducted in the absence of any commercial or financial relationships that could be construed as a potential conflict of interest.

## Publisher's note

All claims expressed in this article are solely those of the authors and do not necessarily represent those of their affiliated organizations, or those of the publisher, the editors and the reviewers. Any product that may be evaluated in this article, or claim that may be made by its manufacturer, is not guaranteed or endorsed by the publisher.

## References

An, C., Jiao, B., Du, H., Tran, M., Song, B., Wang, P., et al. (2023). Jumonji domain-containing protein-3 (JMJD3) promotes myeloid fibroblast activation and macrophage polarization in kidney fibrosis. *Br. J. Pharmacol.* 180 (17), 2250–2265. doi:10.1111/bph.16096

Bai, B., Zhang, D., Wang, P., Huang, J., Jiang, R., and Zhang, H. (2019). The relationship between serum HE4 and disease progression stake in patients with CKD after renal transplantation and its diagnostic value. *Int. J. Lab. Med.* 40 (22), 2767–2770.

Cao, F., Li, S., Li, W., Fu, Y., Xing, H., Sun, Q., et al. (2023). Research progress on risk factors of chronic kidney disease complicated with acute kidney injury and the mechanism of influencing kidney repair. *Chin. Med.* 18 (04), 625–628.

Chawla, L. S., Eggers, P. W., Star, R. A., and Kimmel, P. L. (2014). Acute kidney injury and chronic kidney disease as interconnected syndromes. *N. Engl. J. Med.* 371 (1), 58–66. doi:10.1056/NEJMra1214243

Chen, L., Gong, X., Liu, S., Cao, Y., and Zhu, Z. (2022a). Correction to: Ultrasound-guided supra-inguinal fascia iliaca compartment block for older adults admitted to the emergency department with hip fracture: A randomized controlled, double-blind clinical trial. *Integr. Med. Nephrol. Androl.* 9, 5. doi:10.1186/s12877-021-02698-6

Chen, L., and Gong, X. (2022b). Efficacy and safety of chuan Huang Fang combining reduced glutathione in treating acute kidney injury (grades 1-2) on chronic kidney disease (stages 2-4): Study protocol for a multicenter randomized controlled clinical trial. *Evid. Based Complement. Altern. Med.* 2022, 1099642. doi:10.1155/2022/1099642

Chen, P., Yang, Q., Li, X., and Qin, Y. (2017). Potential association between elevated serum human epididymis protein 4 and renal fibrosis A systemic review and meta-analysis. *Med. Baltim.* 96, e7824. doi:10.1097/MD.0000000000007824

Chen, L., Ye, Z., Wang, D., Liu, J., Wang, Q., Wang, C., et al. (2022). Chuan Huang Fang combining reduced glutathione in treating acute kidney injury (grades 1-2) on chronic kidney disease (stages 2-4): A multicenter randomized controlled clinical trial. *Front. Pharmacol.* 13, 969107. doi:10.3389/fphar.2022.969107

Chou, Y. H., Chen, Y. F., Pan, S. Y., Huang, T. M., Yang, F. J., Shen, W. C., et al. (2015). The role of brain natriuretic peptide in predicting renal outcome and fluid management in critically ill patients. *J. Formos. Med. Assoc.* 114 (12), 1187–1196. doi:10.1016/j.jfma.2015.10.015

Cui, Y., Wan, M., and Zia, P. (2013). The association between BNP and ultrafiltration in patients with CRRT. *Chin. J. Blood Purif.* 12 (12), 657–661.

de Cal, M., Haapio, M., Cruz, D. N., Lentini, P., House, A. A., Bobek, I., et al. (2011). B-type natriuretic Peptide in the critically ill with acute kidney injury. *Int. J. Nephrol.* 2011, 951629. doi:10.4061/2011/951629

DeBoer, M. D., Filipp, S. L., Musani, S. K., Sims, M., Okusa, M. D., and Gurka, M. (2018). Metabolic syndrome severity and risk of CKD and worsened GFR: The jackson heart study. *Kidney Blood Press Res.* 43 (2), 555–567. doi:10.1159/000488829

Gong, X., Wang, Q., Fu, D., Tang, X., Wang, Y., Wang, G., et al. (2013). Research on Radix et Rhizoma Rhei-Rhizoma Ligustici Chuanxiong restraining renal tubular epithelial cell apoptosis in contrast-induced nephropathy rats. *Shanghai J. Trad. Chin. Med.* 47 (03), 69–71. doi:10.16305/j.1007-1334.2013.03.023

Gong, X., Qiu, A., Duan, Y., Ye, Z., Zheng, J., Wang, Q., et al. (2017). Effects of Couplet Medicines of Prepared Radix et Rhizoma Rhei-Rhizoma Ligustici Chuanxiong on Nrf2/HO-1 Signaling Pathway in Renal Tissue of Contrast induced Nephropathy Rats. *J. Shanghai Univ. Trad. Chin. Med. Sci.* 31 (06), 58–61. doi:10.16306/j.1008-861x.2017.06.014

Gong, X., Zheng, J., Duan, Y., and Ye, Z. (2019). Effect of Chuanhuang Fang on apoptosis of renal tubular epithelial cells in rats with trivalent arsenic nephrotoxicity. *Beijing Med. J.* 41, 1089–1093. doi:10.15932/j.0253-9713.2019.12.009

Gong, X., Duan, Y., Wang, Y., Ye, Z., Zheng, J., Lu, W., et al. (2020). Effects of Chuanhuang Decoction on renal function and oxidative stress in patients of chronic kidney disease at stage 2-4 complicated with acute kidney injury. *J. Shanghai Univ. Trad. Chin. Med. Sci.* 34 (1), 11–16. doi:10.16306/j.1008-861x.2020.01.002

Gong, X., Ye, Z., Xu, X., Chen, L., Xu, Y., Yuan, D., et al. (2021). Effects of Chuanhuang Formula combined with prostaglandin E1 in treating patients of chronic kidney disease complicated with acute kidney injury and its influence on NLRP3. *J. Shanghai Univ. Trad. Chin. Med. Sci.* 34 (1), 11–16. 35 (06), 12–16. doi:10.16306/j.1008-861x.2021.06.002

Hatakeyama, Y., Horino, T., Kataoka, H., Matsumoto, T., Ode, K., Shimamura, Y., et al. (2017). Incidence of acute kidney injury among patients with chronic kidney disease: A single-center retrospective database analysis. *Clin. Exp. Nephrol.* 21 (1), 43–48. doi:10.1007/s10157-016-1243-2

He, Y., Qiu, Y., Liu, R., Xu, H., and Zhang, C. (2016). Co-delivery of erlotinib and doxorubicin by pH-sensitive charge conversion nanocarrier for synergistic therapy. *J. Chin. Pract. Diagn Ther.* 30 (01), 80–92. doi:10.1016/j.jconrel.2016.03.001

He, L., Wei, Q., Liu, J., Yi, M., Liu, Y., Liu, H., et al. (2017). AKI on CKD: Heightened injury, suppressed repair, and the underlying mechanisms. *Kidney Int.* 92 (5), 1071–1083. doi:10.1016/j.kint.2017.06.030

Hsu, C. N., Lee, C. T., Su, C. H., Wang, Y. L., Chen, H. L., Chuang, J. H., et al. (2016). Incidence, outcomes, and risk factors of community-acquired and hospital-acquired acute kidney injury: A retrospective cohort study. *Med. Baltim.* 95 (19), e3674. doi:10.1097/md.0000000000003674

Huang, Y., Jiang, H., and Zhu, L. (2020). Human epididymis protein 4 as an indicator of acute heart failure in patients with chronic kidney disease. *Lab. Med.* 51 (2), 169–175. doi:10.1093/labmed/lmz041

Huang, W., Wu, G., Chen, F., Li, M. M., and Li, J. J. (2018). Multi-systemic melioidosis: A clinical, neurological, and radiological case study from hainan province, China. *Chin. J. Blood Purif.* 17 (10), 649–651. doi:10.1186/s12879-018-3569-8

Jiao, B., An, C., Du, H., Tran, M., Wang, P., Zhou, D., et al. (2021a). STAT6 deficiency attenuates myeloid fibroblast activation and macrophage polarization in experimental folic acid nephropathy. *Cells* 10 (11), 3057. doi:10.3390/cells10113057

Jiao, B., An, C., Tran, M., Du, H., Wang, P., Zhou, D., et al. (2021b). Pharmacological inhibition of STAT6 ameliorates myeloid fibroblast activation and alternative macrophage polarization in renal fibrosis. *Front. Immunol.* 12, 735014. doi:10.3389/fimmu.2021.735014

Kidney Disease: Improving Global Outcomes (KDIGO) Chronic Kidney Disease Work Group (2013). KDIGO 2012 clinical practice guideline for the evaluation and management of chronic kidney disease. *Kidney Int. Suppl.* 3 (1), 1–150.

LeBleu, V. S., Teng, Y., O'Connell, J. T., Charytan, D., Müller, G. A., Müller, C. A., et al. (2013). Identification of human epididymis protein-4 as a fibroblast-derived mediator of fibrosis. *Nat. Med.* 19 (2), 227–231. doi:10.1038/nm.2989

Li, J., and Gong, X. (2023). Bibliometric and visualization analysis of kidney repair associated with acute kidney injury from 2002 to 2022. *Front. Pharmacol.* 14, 1101036. doi:10.3389/fphar.2023.1101036

Li, X., Qi, X., Xia, Y., Luo, R., Han, S., and Yu, X. (2022). Clinical value of serum human epididymal protein 4 in the diagnosis of chronic kidney disease. *Chin. J. General Pract.* 20 (05), 789–792.

Li, L. (1991). Curative effect and mechanism of rhubarb in treating chronic renal failure. *J. Clin. inter Med.* (06), 12–13.

Liu, H., Qi, Z., and Li, W. (2018). The risk factors and prognosis of patients with acute kidney injury on the basis of chronic kidney disease. *Hebei Med. J.* 40 (21), 3322–3325.

Liu, Y., Ren, J., Yun, J., Song, Y., and Song, L. (2021). Progress in diagnosis and treatment of acute kidney injury with Chinese and Western medicine. *Acta Chin. Med. Pharmacol.* 49 (12), 89–92.

Luo, J., Wang, F., Wan, J., Ye, Z., Huang, C., Cai, Y., et al. (2018). Serum human epididymis secretory protein 4 as a potential biomarker of renal fibrosis in kidney transplantation recipients. *Clin. Chim. Acta* 483, 216–221. doi:10.1016/j.cca.2018.05.006

Luo, B., Zhang, W., and Meng, F. (2020). Changes and clinical significance of serum human epididymal protein 4 in patients with chronic kidney disease after kidney transplantation. *CHINA Med. Her.* 17 (12), 80–84.

Lv, Y. W., Yang, L., Zhang, M., Jiang, L. H., Niu, J. H., Hou, J., et al. (2015). Increased human epididymis protein 4 in benign gynecological diseases complicated with chronic renal insufficiency patients. *Genet. Mol. Res.* 14 (1), 2156–2161. doi:10.4238/2015.March.27.2

Mehta, R. L., Cerdá, J., Burdmann, E. A., Tonelli, M., García-García, G., Jha, V., et al. (2015). International society of nephrology's 0by25 initiative for acute kidney injury (zero preventable deaths by 2025): A human rights case for nephrology. *Lancet* 385 (9987), 2616–2643. doi:10.1016/s0140-6736(15)60126-x

Moo Park, K. (2014). Experimental evidence that preexisting chronic kidney disease is a risk factor for acute kidney injury. *Kidney Res. Clin. Pract.* 33 (2), 71–72. doi:10.1016/j.krcp.2014.04.005

Nagy, B., Jr., Nagy, B., Fila, L., Clarke, L. A., Gönczy, F., Bede, O., et al. (2016). Human epididymis protein 4: A novel serum inflammatory biomarker in cystic fibrosis. *Chest* 150 (3), 661–672. doi:10.1016/j.chest.2016.04.006

Palazzuoli, A., Masson, S., Ronco, C., and Maisel, A. (2014). Clinical relevance of biomarkers in heart failure and cardiorenal syndrome: The role of natriuretic peptides and troponin. *Heart Fail Rev.* 19 (2), 267–284. doi:10.1007/s10741-013-9391-x

Papanikolaou, J., Makris, D., Mpaka, M., Palli, E., Zygoulis, P., and Zakynthinos, E. (2014). New insights into the mechanisms involved in B-type natriuretic peptide elevation and its prognostic value in septic patients. *Crit. Care* 18 (3), R94. doi:10.1186/cc13864

Prakash, J., Rathore, S., Arora, P., Ghosh, B., Singh, T. B., Gupta, T., et al. (2015). Comparison of clinical characteristics of acute kidney injury versus acute-on-chronic renal failure: Our experience in a developing country. *Hong Kong J. Nephrol.* 17, 14–20. doi:10.1016/j.hkjn.2014.10.001

Privratsky, J. R., Krishnamoorthy, V., Raghunathan, K., Ohnuma, T., Rasouli, M. R., Long, T. E., et al. (2022). Postoperative acute kidney injury is associated with progression of chronic kidney disease independent of severity. *Anesth. Analg.* 134 (1), 49–58. doi:10.1213/ane.0000000000005702

Qu, W., Li, J., Duan, P., Tang, Z., Guo, F., Chen, H., et al. (2016). Physiopathological factors affecting the diagnostic value of serum HE4-test for gynecologic malignancies. *Expert Rev. Mol. Diagn* 16 (12), 1271–1282. doi:10.1080/14737159.2016.1251317

Rowswell-Turner, R. B., Singh, R. K., Urh, A., Yano, N., Kim, K. K., Khazan, N., et al. (2021). HE4 overexpression by ovarian cancer promotes a suppressive tumor immune microenvironment and enhanced tumor and macrophage PD-L1 expression. *J. Immunol.* 206 (10), 2478–2488. doi:10.4049/jimmunol.2000281

Sato, Y., Takahashi, M., and Yanagita, M. (2020). Pathophysiology of AKI to CKD progression. *Semin. Nephrol.* 40 (2), 206–215. doi:10.1016/j.semnephrol.2020.01.011

Wan, J., Wang, Y., Cai, G., Liang, J., Yue, C., Wang, F., et al. (2016). Elevated serum concentrations of HE4 as a novel biomarker of disease severity and renal fibrosis in kidney disease. *Oncotarget* 7 (42), 67748–67759. doi:10.18632/oncotarget.11682

Wang, X., and Xu, M. (2020). An applied study of B type natriuretic peptide in a non-dialysis population with chronic kidney disease. *J. Clin. Nephrol.* 20 (06), 508–512.

Wang, L., Sun, Y., Cai, X., and Fu, G. (2018). The diagnostic value of human epididymis protein 4 as a novel biomarker in patients with renal dysfunction. *Int. Urol. Nephrol.* 50 (11), 2043–2048. doi:10.1007/s11255-018-1930-x

Wang, J., Zhao, H., Xu, F., Zhang, P., Zheng, Y., and Jia, N. (2019). Human epididymis protein 4 (HE4) protects against cystic pulmonary fibrosis associated-inflammation through inhibition of NF-κB and MAPK singnaling. *Genes. Genomics* 41 (9), 1045–1053. doi:10.1007/s13258-019-00836-4

Wettersten, N., Horiuchi, Y., van Veldhuisen, D. J., Mueller, C., Filippatos, G., Nowak, R., et al. (2019). B-type natriuretic peptide trend predicts clinical significance of worsening renal function in acute heart failure. *Eur. J. Heart Fail* 21 (12), 1553–1560. doi:10.1002/ejhf.1627

Wonnacott, A., Meran, S., Amphlett, B., Talabani, B., and Phillips, A. (2014). Epidemiology and outcomes in community-acquired versus hospital-acquired AKI. *Clin. J. Am. Soc. Nephrol.* 9 (6), 1007–1014. doi:10.2215/cjn.07920713

Xie, Z., Li, R., and Liang, X. (2020). Research progress in the pathogenesis of acute renal injury to chronic kidney disease. *Chin. J. Nephrol.* 36 (9), 731–736.

Yang, X., Bai, M., Liu, L., Zhang, L., Zhang, Y., and Sun, S. (2016). Significance of serum human epididymis protein 4 levels in patients with chronic kidney disease. *J. Nephrol. Dialy Transpl.* 25 (02), 128–133.

Zhang, J., Healy, H. G., Baboolal, K., Wang, Z., Venuthurupalli, S. K., Tan, K. S., et al. (2019). Frequency and consequences of acute kidney injury in patients with CKD: A registry study in queensland Australia. *Kidney Med.* 1 (4), 180–190. doi:10.1016/j.xkme.2019.06.005

Zhang, S., Yao, M., Zhou, X., Li, G., Hao, X., Zhou, D., et al. (2022). Serological investigation of Gyrovirus homsa1 infections in chickens in China. *Chin. J. Blood Purif.* 21 (04), 231–234. doi:10.1186/s12917-022-03334-0

Zheng, P. (1985). Treatment of azotemia by rhubarb and its mechanism. *Shanghai J. Trad. Chin. Med.* (08), 46–48. doi:10.16305/j.1007-1334.1985.08.035

frontiers | Frontiers in Pharmacology

# Vancomycin associated acute kidney injury in patients with infectious endocarditis: a large retrospective cohort study

Pan Kunming[1†], Huang Ying[2,3,4†], Xu Chenqi[2,3], Chen Zhangzhang[1], Ding Xiaoqiang[2,3], Li Xiaoyu[1]*, Xu Xialian[2,3]* and Lv Qianzhou[1]*

[1]Department of Pharmacy, Zhongshan Hospital, Fudan University, Shanghai, China, [2]Department of Nephrology, Zhongshan Hospital, Fudan University, Shanghai, China, [3]Shanghai Key Laboratory of Kidney and Blood Purification, Shanghai Medical Center of Kidney Disease, Institute of Kidney Disease and Dialysis, Shanghai, China, [4]Department of Nephrology, Zhongshan Hospital, Fudan University, Xiamen, China

**Background:** Vancomycin remains the cornerstone antibiotic for the treatment of infective endocarditis (IE). Vancomycin has been associated with significant nephrotoxicity. However, vancomycin associated acute kidney injury (AKI) has not been evaluated in patients with IE. We conducted this large retrospective cohort study to reveal the incidence, risk factors, and prognosis of vancomycin-associated acute kidney injury (VA-AKI) in patients with IE.

**Methods:** Adult patients diagnosed with IE and receiving vancomycin were included. The primary outcome was VA-AKI.

**Results:** In total, 435 of the 600 patients were enrolled. Of these, 73.6% were male, and the median age was 52 years. The incidence of VA-AKI was 17.01% (74). Only 37.2% (162) of the patients received therapeutic monitoring of vancomycin, and 30 (18.5%) patients had reached the target vancomycin trough concentration. Multiple logistic regression analysis revealed that body mass index [odds ratio (OR) 1.088, 95% CI 1.004, 1.179], duration of vancomycin therapy (OR 1.030, 95% CI 1.003, 1.058), preexisting chronic kidney disease (OR 2.291, 95% CI 1.018, 5.516), admission to the intensive care unit (OR 2.291, 95% CI 1.289, 3.963) and concomitant radiocontrast agents (OR 2.085, 95% CI 1.093, 3.978) were independent risk factors for VA-AKI. Vancomycin variety (Lai Kexin vs. Wen Kexin, OR 0.498, 95% CI 0.281, 0.885) were determined to be an independent protective factor for VI-AKI. Receiver operator characteristic curve analysis revealed that duration of therapy longer than 10.75 days was associated with a significantly increased risk of VA-AKI (HR 1.927). Kidney function was fully or partially recovered in 73.0% (54) of patients with VA-AKI.

**Conclusion:** The incidence of VA-AKI in patients with IE was slightly higher than in general adult patients. Concomitant contrast agents were the most alarmingly nephrotoxic in patients with IE, adding a 2-fold risk of VA-AKI. In patients with IE, a course of vancomycin therapy longer than 10.75 days was associated with a

significantly increased risk of AKI. Thus, closer monitoring of kidney function and vancomycin trough concentrations was recommended in patients with concurrent contrast or courses of vancomycin longer than 10.75 days.

# 1 Introduction

Vancomycin is a glycopeptide antibiotic that is active against Gram-positive bacteria since its approval in 1958 (Rybak et al., 2009; He et al., 2020; Rybak et al., 2020). Vancomycin remains the cornerstone antibiotic for the treatment of infective endocarditis (IE) and is the drug of first choice for *methicillin-resistant Staphylococcus aureus* (MRSA) infection (Chinese Society of Cardiology, 2014; Habib et al., 2015; Nakatani et al., 2019). The recommended duration of vancomycin therapy for IE is 4–6 weeks, with a target trough concentration of 15–20 mg/L, according to clinical guidelines for IE and guidelines for therapeutic monitoring of vancomycin (Rybak et al., 2009; Chinese Society of Cardiology, 2014; Habib et al., 2015; Nakatani et al., 2019; He et al., 2020; Rybak et al., 2020). However, vancomycin has been associated with significant nephrotoxicity. The incidence of vancomycin-associated acute kidney injury (VA-AKI) ranges from as low as 0% in the absence of concurrent risk factors to 43% (Filippone et al., 2017). Vancomycin is the second most common drug causing drug-induced hospital-acquired acute kidney injury (AKI) in China (Liu et al., 2021). Numerous risk factors have been defined for developing VA-AKI in patients receiving vancomycin, including maximal dose, duration of therapy, concomitant diseases, concomitant nephrotoxic drugs (Filippone et al., 2017; Jeffres, 2017; Kunming et al., 2021). Duration of vancomycin tended to be associated with an increased risk of AKI, and significantly positive durations include ≥7 days, ≥14 days and >15 days (Filippone et al., 2017; Kunming et al., 2021). The mechanism of vancomycin nephrotoxicity is dose dependent, thus high vancomycin target trough concentrations will increase the risk of AKI (Filippone et al., 2017; Jeffres, 2017). The recommended duration of vancomycin therapy for IE is 4–6 weeks, with a target trough concentration of 15–20 mg/L, which we hypothesized would result in an increased risk of VA-AKI in patients with IE. A small sample size retrospective study included 71 patients receiving vancomycin and showed that IE was significantly associated with an increased incidence of VA-AKI (OR = 7.63, 1.02–57.31) (Barberan et al., 2019).

IE is a rare infectious disease, but with high mortality and poor prognosis. The annual incidence ranges from 3 to 7 per 100,000 person-years in the most contemporary population surveys (Baddour et al., 2015). AKI is a common complication of IE and occurs in about 30% of patients (Chinese Society of Cardiology, 2014). Effective antimicrobial therapy such as vancomycin may reduce the complications of IE and the risk of progression to the need for surgery (Chinese Society of Cardiology, 2014; Baddour et al., 2015; Habib et al., 2015).

Gagneux-Brunon A. et al. described the frequency and risk factors for AKI during the course of IE in 112 patients and showed that vancomycin exposure was independently associated

with AKI with an odds ratio of 1.084 (1.084–16.2) (Gagneux-Brunon et al., 2019). Similar results were obtained by Legrand M. et al. in their analysis of post-operative AKI following cardiac surgery for active IE, the use of vancomycin was found to be significantly associated with kidney function impairment (OR: 2.63, 2.07–3.34, $p < 0.001$) (Legrand et al., 2013). The results of most studies tended to support that vancomycin would increase the risk of AKI in patients with IE, however, vancomycin was not always a significant risk factor for AKI in patients with IE (Goenaga Sanchez et al., 2017; Ritchie et al., 2017). Ritchie, B. M., et al. evaluated AKI in 211 patients with IE, and multivariate analysis showed that vancomycin combined with aminoglycosides was significantly associated with an increased risk of kidney failure in patients with bacterial endocarditis, whereas vancomycin alone did not significantly increase the risk (Ritchie et al., 2017). Whether vancomycin increases the risk of AKI in patients with IE remains a minor controversy.

Vancomycin is associated with significant nephrotoxicity, and the risk will be further increased by the long course of treatment and high trough concentrations. Meanwhile, AKI is one of the common complications of IE. Therefore, the risk of AKI in patients with IE who are treated with vancomycin would be of great concern. VA-AKI is associated with prolonged hospital stays, the need for additional antibiotic therapy, and, in rare cases, dialysis treatment, as well as increased medical costs and mortality (Jeffres, 2017). Based on a comprehensive literature search, there are no published studies assessing the characteristics of VA-AKI in this specific group of patients with IE. We conducted this large retrospective cohort study to reveal the incidence, risk factors, and prognosis of VA-AKI in patients with IE in order to provide a clinical reference for the prevention and reduction of VA-AKI in patients with IE.

# 2 Methods

## 2.1 Study design and patients

This was a retrospective observational cohort study conducted at Zhongshan Hospital of Fudan University, a 2005-bed top-tier general teaching hospital in China. This study was reviewed and approved by the Ethics Committee of Zhongshan Hospital, Fudan University (Shanghai, China, approval number: B2019-194 (2)), and no consent was needed. The study is reported according to Strengthening The Reporting of Observational Studies in Epidemiology (STROBE) guidelines (von Elm et al., 2007). All consecutive adult (≥18 years) patients admitted between January 2016 and June 2019 with a diagnosis of IE according to the modified Duke criteria (Chinese Society of Cardiology, 2014; Baddour et al., 2015; Habib et al., 2015) and received vancomycin anti-infective

**TABLE 1 Demographic information, clinical characteristics, medication exposure of patients with and without VA-AKI.**

| Factors | Total N = 435 | Patients without VA-AKI N = 361 | Patients with VA-AKI N = 74 | p-value |
|---|---|---|---|---|
| *Demographic information* | | | | |
| Gender (male) | 320 (73.6) | 267 (74.0) | 54 (71.6) | 0.68 |
| Age (years) | 52.0 (22) | 51.0 (22.0) | 58.0 (22.0) | 0.03 |
| Body Mass Index (kg/m$^2$)[a] | 21.8 (4.2) | 21.48 (4.6) | 22.17 (4.13) | 0.18 |
| Payment mode | | | | 0.13 |
| At one's own expense | 272 (62.5) | 220 (60.9) | 52 (70.3) | |
| National basic medical insurance | 163 (37.5) | 141 (39.1) | 22 (29.7) | |
| *Concomitant underlying diseases* | | | | |
| Preexisting chronic kidney disease | 37 (8.5) | 10 (13.5) | 27 (7.5) | 0.09 |
| Coronary heart disease | 23 (5.3) | 20 (5.5) | 3 (4.1) | 0.81[b] |
| Hypertension | 66 (15.2) | 53 (14.7) | 13 (17.6) | 0.53 |
| Diabetes | 28 (6.4) | 21 (5.8) | 7 (9.5) | 0.37[b] |
| Heart failure | 51 (11.7) | 40 (11.1) | 11 (14.9) | 0.36 |
| Sepsis | 144 (33.1) | 119 (33) | 25 (33.8) | 0.89 |
| Cancer | 43 (9.9) | 36 (10) | 7 (9.5) | 0.89 |
| valvular heart disease | 378 (86.9) | 311 (86.1) | 67 (90.5) | 0.31 |
| *Severity of illness* | | | | |
| Baseline serum creatinine μmol/L | 77 (30.0) | 76.0 (29.9) | 86.3 (41.0) | 0.01 |
| Cardiac surgery | 365 (83.9) | 297 (82.3) | 68 (91.9) | 0.04 |
| Admission to the ICU | 220 (50.6) | 175 (48.5) | 45 (60.8) | 0.053 |
| Mechanical ventilation | 67 (15.4) | 53 (14.7) | 14 (18.9) | 0.36 |
| *Vancomycin exposure* | | | | |
| Vancomycin variety | | | | 0.002 |
| Lai Kexin | 300 (69.0) | 238 (65.9) | 62 (83.8) | |
| Wen Kexin | 135 (31.0) | 123 (34.1) | 12 (16.2) | |
| Duration of vancomycin therapy mean (median), range | 10.0 (9.0), 1.5–56.0 | 9.5 (8.5), 1.5–49.5 | 12.0 (10.6), 1.5–56.5 | 0.04 |
| Daily dose | | | | 0.11 |
| ≤2 g/d | 389 (89.4) | 319 (88.4) | 70 (94.6) | |
| >2 g/d | 46 (10.6) | 42 (11.6) | 4 (5.4) | |
| Trough concentration >15 mg/L[a] | 95 (57.4) | 63 (52.7) | 30 (73.2) | 0.018 |
| *Concomitant nephrotoxic drugs* | 370 (85.1) | 303 (83.9) | 67 (90.5) | 0.15 |
| Loop diuretics | 350 (80.5) | 287 (79.5) | 63 (85.1) | 0.27 |
| Aminoglycosides | 11 (2.5) | 10 (2.8) | 1 (1.4) | 0.76[b] |
| Cephalosporins | 81 (18.6) | 63 (17.5) | 18 (24.3) | 0.17 |
| Carbapenems | 203 (46.7) | 163 (45.2) | 40 (54.1) | 0.16 |
| RAS blockers | 45 (10.3) | 35 (9.7) | 10 (13.5) | 0.33[b] |
| Radiocontrast agents | 62 (14.3) | 45 (12.5) | 17 (23.0) | 0.02 |
| NSAIDs | 25 (5.7) | 21 (5.8) | 4 (5.4) | 1.00[b] |

**TABLE 1 (Continued) Demographic information, clinical characteristics, medication exposure of patients with and without VA-AKI.**

| Factors | Total N = 435 | Patients without VA-AKI N = 361 | Patients with VA-AKI N = 74 | p-value |
|---|---|---|---|---|
| *Concomitant nephroprotective drugs* | | | | |
| Vasopressors | 103 (23.7) | 81 (22.4) | 22 (29.7) | 0.18 |
| Glutathione | 69 (15.9) | 56 (15.5) | 13 (17.6) | 0.66 |
| Coenzyme Q10 | 29 (6.7) | 20 (5.5) | 9 (12.2) | 0.07[b] |

Data are described as mean (SD), n (%), or median (IQR).
[a]There were missing values in the BMI, data. The percentage of missing values for total was 8.8% (8.9%for patients without VA-AKI; 8.1% for patients with VA-AKI). Missing values were filled using the median. *There were missing values in the date of trough concentration >15 mg/L. The percentage of missing values for total was 62.8% (273): 66.5% (240) for patients without VA-AKI; 44.6% (33) for patients with VA-AKI.
[b]Refers to the calibration of the chi-square test. ICU, intensive care unit; NSAIDs , Non-steroidal anti-inflammatory drugs. VA-AKI , vancomycin-associated kidney injury. RAS, blockers = Renin-angiotensin system blockers. Chronic kidney disease is defined as an estimated glomerular filtration rate (eGFR) of less than 60 mL/(min·1.73 m2) (Calculated by the formula of the Chronic Kidney Disease Epidemiology Collaboration equation, CKD-EPI).

therapy were included. Patients were excluded if: 1) they had chronic kidney disease (CKD) stage 5 or were on regular dialysis. 2) their baseline serum creatinine (SCr) was ≥4 mg/dL (353.6 μmol/L). 3) they had AKI at admission. 4) they had a history of nephrectomy, kidney transplantation, or sole kidney. 5) their vancomycin administration was not intravenous. 6) they received less than 4 doses of vancomycin. 7) their SCr measurement was insufficient to determine whether AKI had developed (SCr was not measured within 7 days before receiving vancomycin, or SCr was not measured within 7 days after stopping vancomycin, or SCr was not measured within 7 days before receiving and after stopping vancomycin, or SCr was measured before receiving and after stopping vancomycin, but the interval was longer than 7 days, so as not be able to assess the occurrence of acute kidney injury).

## 2.2 Data collection

Data were collected from the hospital's electronic database between December 2021 and November 2022 using a standardized case report form. Patient information was anonymized by a researcher not involved in the study. Patients were not followed up after discharge. The following variables were collected: demographic information, concomitant underlying diseases, severity of disease, vancomycin exposure, vancomycin variety (Laikexin vs. Wenkexin; trade name: Laikexin, generic name: Vancomycin Hydrochloride for Injection, manufacturers: Zhejiang Medicine Co., Ltd. Xinchang Pharmaceutical Factory, China, specification: 500 mg/bottle; trade name: Wenkexin, generic name: Vancomycin HydrochlorPide for Injection, manufacturer: VIANEX S.A. (PLANT C), Greece, specification: 500 mg/bottle), therapeutic drug monitoring (TDM) during hospitalization, and concomitant nephrotoxic drugs. The detailed items of data collection are presented in Table 1. Missing values were filled using the median. We used the 2012 Kidney Disease: Improving Global Outcomes (KDIGO) Clinical practice guideline for AKI to define and stage AKI, e.g., an increase in SCr by ≥ 0.3 mg/dL (≥26.5 μmol/L) within 48 h or an increase in SCr to ≥1.5 times baseline, which was known or presumed to have occurred within the prior 7 days (Khwaja A., 2012). AKI severity was described by the highest stage of AKI (1, 2, or 3) and receipt of renal replacement therapy (RRT), according to the KDIGO criterion. Preexisting CKD is defined as an estimated glomerular filtration rate (eGFR) of less

than 60 mL/(min·1.73 m²) (Calculated by the formula of the Chronic Kidney Disease Epidemiology Collaboration equation, CKD-EPI). TDM is prescribed by clinicians based on their own experience. Nephrotoxic drugs were documented as loop diuretics, aminoglycosides, cephalosporins, carbapenems, renin-angiotensin system blockers, radiocontrast agents and non-steroidal anti-inflammatory drugs.

## 2.3 Outcome measure

The primary outcome measure was VA-AKI, defined as patients who developed AKI during vancomycin therapy or within 48 h of vancomycin discontinuation. For patients who developed AKI, we further evaluated the 30-day morbidity and recovery of kidney function. Kidney recovery was categorized into three levels: full recovery, partial recovery, and failure to recover. We defined full recovery as a decrease in SCr to baseline at discharge. We defined partial recovery as a decrease in SCr of 25% or more from the peak concentration, but still above baseline. We defined failure to recover as the patient remaining dependent on dialysis or SCr decreasing by less than 25% from peak concentration until discharge (Yang et al., 2015; Pan et al., 2017; Pan et al., 2018).

## 2.4 Data analysis

We used the Kolmogorov-Smirnov test to assess the normality of the variables. Continuous variables were presented as means with standard deviations or medians with interquartile ranges (IQR), and we used independent t-tests or rank-sum tests to compare variables between groups. Qualitative variables are presented as frequencies with corresponding percentages, and we used chi-squared or Fisher's exact tests to compare variables between groups.

We used multivariate logistic regression analysis to assess independent risk factors for the development of VA-AKI, as well as the non-recovery of kidney function. We included all covariates with a p-value ≤ 0.05 in univariate analysis and forced other relevant variables into multivariable models. A backward stepwise regression was used to construct the final model. The following covariates were included in the model to explore the risk factors for the occurrence of VA-AKI: gender (male vs. female), age (years), body mass index

FIGURE 1
Study design.
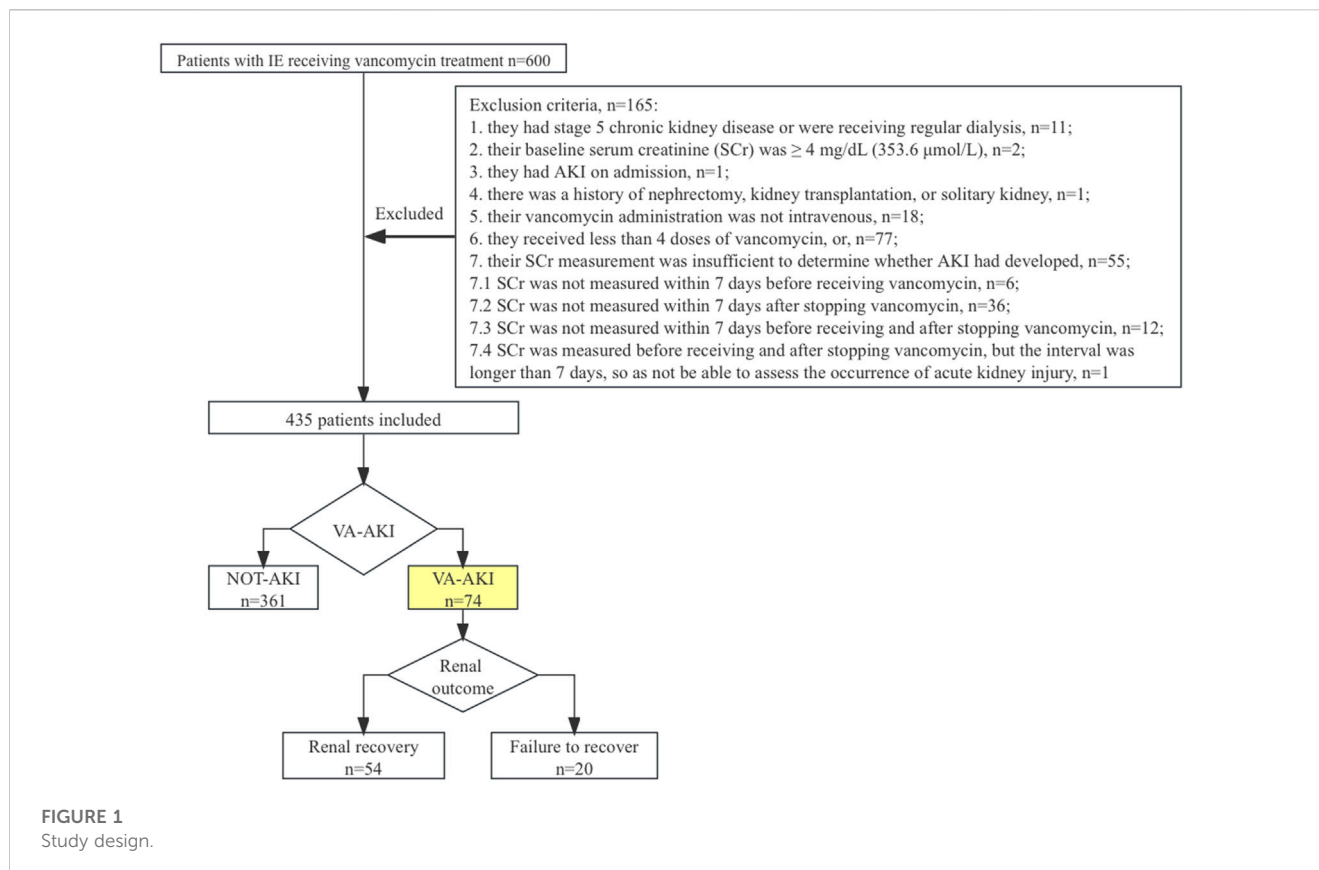
(BMI), preexisting CKD, cardiac surgery (yes or no), admission to the ICU (yes or no), vancomycin variety (Lai Kexin vs. Wen Kexin), length of vancomycin therapy (days), vancomycin daily dose (≤2 g/d vs. > 2 g/d), concomitant nephrotoxic drugs (yes or no), concomitant radiocontrast agents (yes or no). The results of the univariate analysis of factors affecting the recovery of kidney function in patients with VA-AKI were shown in Supplementary Table S1. The following covariates were included in the model to explore the risk factors for non-recovery of kidney function in patients with VA-AKI: age (years), payment mode (At one's own expense vs. National basic medical insurance), concomitant vasopressors (yes or no), and concomitant carbapenems (yes or no). The good of fit was evaluated by the analysis of Hosmer and Lemeshow. Cut-off values for vancomycin trough concentrations and duration of therapy that contributed to the development of VA-AKI were derived by receiver operating characteristic curve (ROC) analysis. All $p$-values were two-sided, and a $p$-value ≤ 0.05 was considered statistically significant. All statistical analyses were performed using SPSS statistics version 26.0 (IBM Inc., Armonk, NY, United States).

## 3 Results

### 3.1 Patients' characteristics

There were 600 patients evaluated for study inclusion. After applying the exclusion criteria, 165 (27.5%) patients were omitted

from the study. Of those excluded, 55 patients lacked SCr measurements, typically within 7 days after stopping vancomycin therapy (Figure 1). In total, 435 patients were included for analysis. Of these, 73.6% were male, and the median age was 52 (IQR = 22) years. A total of 40 patients (8.8%) received heart valve surgery during hospitalization. The remaining patients were treated with vancomycin-based anti-infective therapy only.

Seventy-four patients developed AKI. The incidence of VA-AKI was 17.0% (74), and the time of diagnosis was day 5.9 (IQR = 7.4) after receiving vancomycin therapy. Table 1 displayed patient demographic information, concomitant underlying diseases, and severity of illness. Patients with AKI tend to be older (58.0 vs. 51.0 years, $p$ = 0.028) and were more likely to concomitant preexisting CKD (13.5%vs. 7.5%, $p$ = 0.09) and to undergo cardiac surgery (91.9% vs. 82.3%, $p$ = 0.040), compared to patients without AKI. Table 1 also listed patient vancomycin exposure and concomitant nephrotoxic drugs. There were two varieties of vancomycin from different companies. Patients with VA-AKI were more likely to receive Lai Kexin (Lai Kexin vs. Wen Kexin 83.8% vs. 65.9%, $p$ = 0.002), compared with patients without VA-AKI. Patients with AKI underwent a longer duration of vancomycin treatment (12.0 ± 10.6 days vs. 9.5 ± 8.5 days, $p$ = 0.038), higher proportions of vancomycin concentrations greater than 15 mg/L (73.2% vs. 52.7, $p$ = 0.018) and were more likely to concomitant radiocontrast agents (loversol, iopromid) (23.0% vs. 12.5%, $p$ = 0.019). Twenty-three patients (5.3%) received vancomycin for more than 4 weeks.

TABLE 2 Medical costs and outcomes of patients with and without vancomycin-associated acute kidney injury.

| | Patients without va-AKI N = 361 | Patients with va-AKI N = 74 | *p*-value |
|---|---|---|---|
| Length of hospital stay (day) | 15.1 (10.1) | 18.0 (12.0) | 0.005 |
| Need for Dialysis | 0 0) | 5 (5.4) | <0.001 |
| 30-day mortality | 2 (0.6) | 3 (4.1) | 0.037[f] |
| Total costs (thousand US$) | 98.4 (61.1) | 119.8 (79.3) | 0.001 |
| Medicine costs (thousand US$) | 20.7 (13.7) | 29.4 (17.6) | <0.001 |
| Treatment costs (thousand US$) | 2.9 (2.1) | 3.6 (2.8) | <0.001 |
| medical consumables costs (thousand US$) | 51.9 (52.0) | 61.7 (49.4) | 0.011 |

Data are described as mean (SD), n (%), or median (IQR). VA-AKI, vancomycin-associated kidney injury. F refers to Fisher's exact test.

## 3.2 Therapeutic drug monitoring of patients

One hundred and sixty-two (37.2%) patients received TDM during vancomycin therapy. Of the patients who received TDM, 8% (13) had their initial vancomycin TDM on day 3, in accordance with the guideline recommendations, and 88.3% (143) of patients had delayed first vancomycin trough concentration monitoring. Only 30 (18.5%) patients had vancomycin trough concentrations between 15–20 mg/L and reached the target trough concentration. Besides, 69 (42.6%) patients had vancomycin trough concentrations <15 mg/L and 63 (38.9%) patients had vancomycin trough concentrations >20 mg/L. The incidence of VA-AKI in patients receiving TDM was 25.3% (41) and the risk of VA-AKI increased with higher vancomycin trough concentrations. The VA-AKI rates were 17.3% (4), 15.2% (7), 23.3% (7), and 36.3% (23) for trough concentrations of <10 mg/L, ≥10 - <15 mg/L, ≥15 - ≤20 mg/L, and >20 mg/L, respectively ($p < 0.058$). By binary logistic analysis, the odds ratios (OR) were 0.853 ($p = 0.82$), 1.446 ($p = 0.60$), and 2.731 ($p = 0.099$) for the development of VA-AKI at trough concentrations ≥10 - <15 mg/L, ≥15 - ≤20 mg/L, and >20 mg/L, respectively, compared to trough concentrations <10 mg/L. ROC analysis revealed a cut-off value of 25.5 mg/L for trough concentrations that contributed to the development of VA-AKI (AUC = 0.654, 95% CI 0.557, 0.751, $p = 0.0032$).

## 3.3 Comparison of medical costs and outcomes for patients with and without VA-AKI

Patients who developed AKI had longer hospital stays (18.0 vs. 15.1 days, $p = 0.005$) and a higher 30-day mortality rate (4.4% vs. 0.6%, $p = 0.037$) than those who did not develop AKI. Patients with VA-AKI were more likely to have higher total costs (119.8 vs. 98.4 thousand US dollars, $p = 0.001$), medical costs ($p < 0.001$), treatment costs ($p < 0.001$), and medical consumables costs ($p = 0.011$), compared with patients without VA-AKI (Table 2).

## 3.4 Risk factors for VA-AKI

Multiple logistic regression analysis revealed that BMI (OR 1.085, 95% CI 1.004, 1.179, $p = 0.039$), duration of vancomycin therapy (OR 1.030, 95% CI 1.003, 1.058, $p = 0.032$), preexisting CKD

(OR 2.291, 95% CI 1.018, 5.516, $p = 0.045$), admission to the ICU (OR 2.260, 95% CI 1.289, 3.963, $p = 0.004$) and concomitant radiocontrast agents (OR 2.085, 95% CI 1.093, 3.978, $p = 0.029$) were independent risk factors for VA-AKI; vancomycin variety (Lai Kexin vs. Wen Kexin, OR 0.498, 95% CI 0.281, 0.885, $p = 0.017$) were determined to be an independent protective factor for VI-AKI (Table 3; Figure 2). ROC analysis revealed a cut-off value of 10.75 days for the duration of vancomycin therapy that contributed to the development of VA-AKI. Univariate analysis revealed a significantly higher risk of VA- AKI in patients with a long duration of therapy (longer than 10.75 days) compared to those with a short duration of therapy (shorter than 10.75 days) (HR 1.927, 95% CI 1.159 3.205, $p = 0.011$).

## 3.5 Treatment and outcome of patients with vancomycin-associated acute kidney injury

The 30-day mortality rate in patients with VA-AKI was 4.1% (3). 5.4% (4) of patients were treated with dialysis. Kidney function was fully or partially recovered in 73.0% (54) of patients, and 27.0% (20) failed to recover kidney function until discharge (Table 4). Multiple logistic regression analysis showed payment mode (at one's own expense vs. national basic medical insurance) was the only independent risk factor for non-recovery of kidney function in patients with VA-AKI (OR 4.78, 95% CI 1.59, 14.38, $p = 0.005$).

## 4 Discussion

This study demonstrated the incidence of VA-AKI in patients with IE, which was 17.0%, and further revealed the clinical characteristics, risk factors, and outcomes of VA-AKI. To the best of our knowledge, this is the first study to thematically investigate VA-AKI in patients with IE, and we believe that the results will provide an important reference for the rational use of vancomycin in this special population (Figure 3).

Several studies have focused on the nephrotoxicity of antimicrobial agents used to treat IE, the majority focusing on aminoglycosides such as gentamicin-associated nephrotoxicity (Cosgrove et al., 2009). However, physicians still did not pay enough attention to VA-AKI in patients with IE. The incidence of IE is low, and the sample sizes of published studies are relatively

**TABLE 3 Risk factors for vancomycin-associated acute kidney injury.**

| | B | S.E. | OR | 95% CI. For OR | | p-value |
|---|---|---|---|---|---|---|
| | | | | Lower | Upper | |
| Body Mass Index (kg/m²) | 0.0840 | 0.041 | 1.088 | 1.004 | 1.179 | 0.039 |
| Vancomycin varieties (Lai Kexin vs. Wen Kexin) | −0.696 | 0.293 | 0.498 | 0.281 | 0.885 | 0.017 |
| Daily dose (>2 g/d vs. ≤2 g/d) | −0.911 | 0.554 | 0.402 | 0.136 | 1.190 | 0.010 |
| Length of vancomycin therapy | 0.030 | 0.014 | 1.030 | 1.003 | 1.058 | 0.031 |
| Preexisting chronic kidney disease | 0.829 | 0.414 | 2.291 | 1.018 | 5.516 | 0.045 |
| Admission to the intensive care unit | 0.815 | 0.287 | 2.260 | 1.289 | 3.963 | 0.004 |
| Radiocontrast agents | 0.735 | 0.330 | 2.085 | 1.093 | 3.978 | 0.026 |
| Constant | −4.136 | 0.987 | 0.016 | | | <0.001 |



**FIGURE 2**
Forest-plot figure of risk factors for vancomycin-associated acute kidney injury.
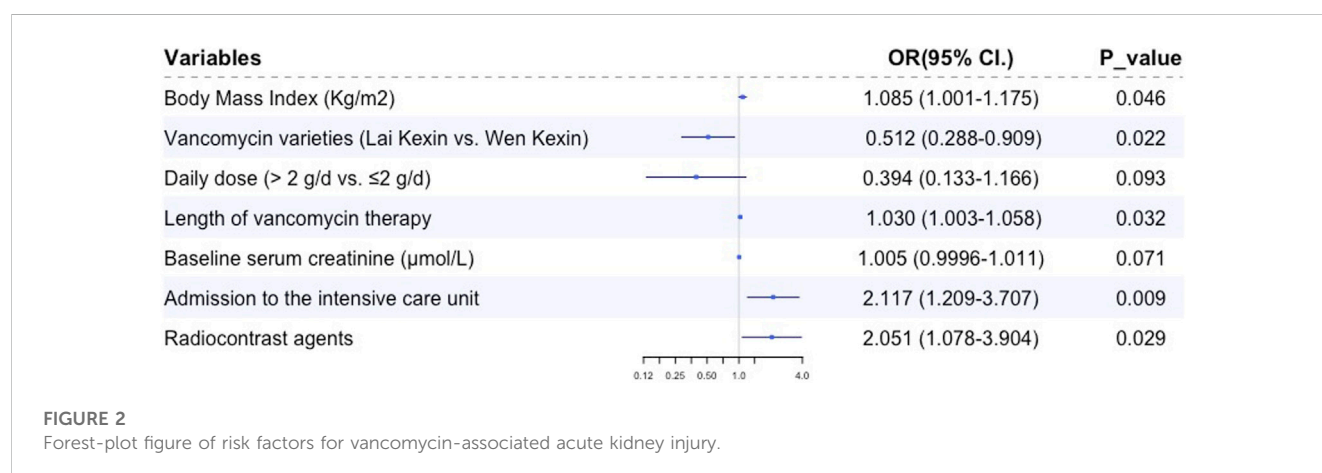
**TABLE 4 Treatment and outcome of patients with vancomycin-associated acute kidney injury.**

| | Total N = 74 | Stage 1 N = 55 | Stage 2 N = 12 | Stage 3 N = 7 | p-Value |
|---|---|---|---|---|---|
| 30-day mortality n (%) | 3 (4.1) | 1 (1.8) | 1 (8.3) | 1 (14.3) | 0.21 |
| Receive dialysis n (%) | 4 (5.4) | 1 (1.8) | 1 (8.3) | 2 (28.6) | 0.011 |
| Kidney recovery n (%) | 54 (73.0) | 40 (72.7) | 10 (83.3) | 4 (57.1) | 0.46[a] |
| Failure to recover n (%) | 20 (27.0) | 15 (27.3) | 2 (16.7) | 3 (42.9) | |
| Full recovery n (%) | 32 (43.2) | 27 (49.1) | 3 (25.0) | 2 (28.6) | — |
| Partial recovery n (%) | 22 (29.7) | 13 (23.6) | 7 (58.3) | 2 (28.6) | — |

[a]Kidney recovery group vs. Failure to recover group.

small, in the range of 100–200 cases (Legrand et al., 2013; Ritchie et al., 2017; Barberan et al., 2019). This study included 435 patients with, IE who were treated with vancomycin, which, to our knowledge, is the largest sample size of any study investigating antibiotic-associated AKI in patients with IE. In previous studies involving vancomycin-associated kidney injury, vancomycin was generally used as conventional therapy or as a control, compared with daptomycin (Barberan et al., 2019). Studies showed vancomycin to be less nephrotoxic than daptomycin, but greater than or closer to other antibiotics such as beta-lactam antibiotics

(Barberan et al., 2019; Blevins et al., 2019; Muklewicz et al., 2021). However, no studies have evaluated the incidence, clinical characteristics, risk factors, and outcomes of VA-AKI in patients with IE.

This study showed a 17.0% prevalence of VA-AKI in adult patients with IE, which is slightly higher than in the general adult population, who are not a special population such as obese, critically ill, or elderly (Pan et al., 2018; Chun et al., 2021; Contejean et al., 2021; Kunming et al., 2021; Muklewicz et al., 2021; Kiley et al., 2022). Data from studies in the United States (11.4%) (Muklewicz et al.,

FIGURE 3
Graphical abstract.
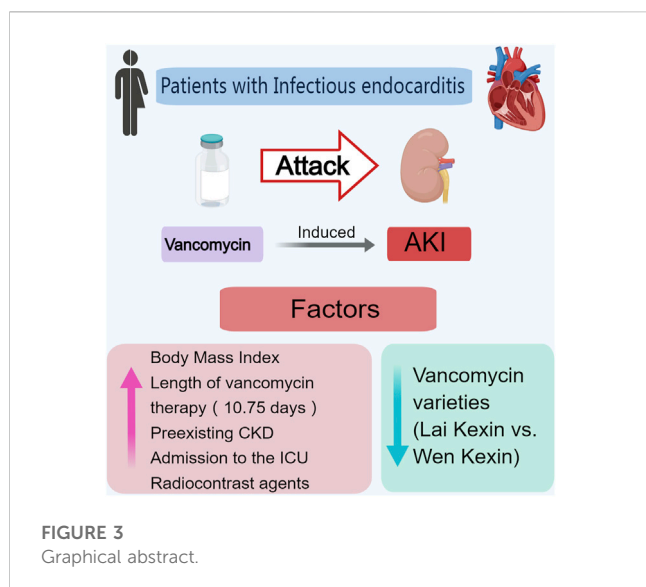
2021), Chinese mainland (14.3%) (Kunming et al., 2021), Taiwan in China (11.5%) (Kiley et al., 2022), South Korea (15.38) (Chun et al., 2021), France (11.2%) (Contejean et al., 2021) and other countries or regions indicated that the incidence of VA-AKI in adult patients was generally around 10%–15%. However, the incidence of VA-AKI in patients with IE is lower than in obese patients and critically ill patients (Filippone et al., 2017). We speculate that there are four causes for the higher incidence of VA-AKI in patients with IE than in the general adult population. First, pathogenic bacteria that infect the endocardium may also invade the kidney and induce AKI through mechanisms such as immune complexes and vasculitis glomerulonephritis (Habib et al., 2015; Ritchie et al., 2017; Gagneux-Brunon et al., 2019). Second, there is a relatively high rate of patients with IE undergoing cardiac surgery, especially valve surgery (Legrand et al., 2013; Gagneux-Brunon et al., 2019). Third, the course of vancomycin for IE is long, usually 4–6 weeks (Chinese Society of Cardiology, 2014; Baddour et al., 2015; Habib et al., 2015). Fourth, a high percentage of patients with IE received vancomycin concomitant contrast agents (Legrand et al., 2013; Mehran et al., 2019). Moreover, these possible contributing factors will also provide an indication for reducing the risk of VA-AKI in patients with IE.

The study showed that 37.2% of patients with IE received vancomycin TDM, 8% of patients were initially monitored on day 3 of vancomycin therapy, and 18.5% of patients achieved target trough concentrations. According to the vancomycin TDM guidelines published by the American Society of Health-System Pharmacists in 2009 and the Chinese Pharmacological Society in 2020 (Rybak et al., 2009; He et al., 2020), there were three deficiencies in vancomycin TDM: low vancomycin TDM rate, inaccurate timing of initial TDM, and low attainment of target trough concentrations. Vancomycin concentration monitoring in most hospitals in China, as exemplified by our hospital, is mainly based on the experience and expertise of clinicians. The technology for TDM of vancomycin is well established and the guidelines are clear in the recommendations for the management of vancomycin monitoring, however, the status of monitoring in clinical practice is not satisfactory. We previously conducted a meta-analysis including

19 studies with 2,598 patients from developed countries such as the United States, Japan, Australia, and New Zealand, and developing countries such as China and India, and showed that the mean vancomycin trough concentration attainment rate was 34.3% under the conventional physician-led model of care (Kunming et al., 2023). Factors contributing to the unsatisfactory status of monitoring under physician-led vancomycin TDM included negative perception towards prescription guidelines, lack of knowledge regarding TDM guidelines, the hierarchy of medication management, work pressure, and ineffective communication among healthcare providers (Abdel Jalil et al., 2023). Our further analysis showed that 64.6% (281) of the patients were given vancomycin at 1g q12 h, which was a conventional dose. Patients with IE may have complex pathophysiological profiles and vancomycin pharmacokinetics; therefore, more precise dosing regimens, more frequent concentration monitoring, and dose adjustments are necessary (Elyasi et al., 2012; Filippone et al., 2017; Rybak et al., 2020). We also found that the hospitalization units for patients with IE were predominantly surgical. Surgeons may be more focused on surgical treatment and pay less attention to drug therapy. The 2020 update of the vancomycin TDM guidelines further recommended area under the curve (AUC)-guided dosing and monitoring regimens, which raised the difficulty of vancomycin monitoring (Rybak et al., 2020). Considering that some medical institutions do not have the technology and professional staff to monitor AUC, and the feasibility of monitoring trough concentration is better than monitoring AUC, thus the evidence-based guideline for therapeutic drug monitoring of vancomycin: 2020 update by the division of therapeutic drug monitoring, Chinese pharmacological society, recommends monitoring trough concentration or AUC (He et al., 2020). We believe that this study reveals the deficiencies in vancomycin prescribing and TDM and suggests that clinicians should pay attention to these issues. In addition, we suggest clinical care teams should increase the involvement of clinical pharmacists. Our previously published study showed that pharmacist intervention in vancomycin treatment significantly decreased the rate of VA-AKI while improving efficacy and reducing mortality (Kunming et al., 2023). Clinical pharmacists are experts in medication therapy management, and many hospitals, mainly in the United States, have established the model of pharmacist managing vancomycin dosing and monitoring, which is worthy of emulation by hospitals in other countries (Kunming et al., 2023).

Concomitant nephrotoxic drugs were risk factors for VA-AKI, especially aminoglycosides and piperacillin-tazobactam (Kim JY et al., 2022; Filippone et al., 2017; O'Callaghan et al., 2020). According to this study, concomitant contrast media was the most alarmingly nephrotoxic agent in patients with IE. Concomitant contrast resulted in a 2.085-fold increased risk of VA-AKI. Contrast-associated AKI was one of the leading causes of iatrogenic kidney insufficiency (Huang et al., 2022). Direct mechanisms of contrast-associated AKI were due to nephrotoxic effects on the tubular epithelium, leading to loss of function, apoptosis, and eventually, necrosis. In addition, contrast can induce ischemic injury through an indirect mechanism of regional or global perfusion reduction (Mehran et al., 2019). The mechanism of vancomycin-associated AKI was suggested to be associated with the oxidative stress effect on proximal kidney

tubular (Elyasi et al., 2012; Jeffres, 2017). Contrast and vancomycin have a synergistic effect on the mechanism of kidney injury; therefore, patients with IE require special attention to the synergistic risk of vancomycin concurrent with contrast. We recommend to postpone tests requiring contrast, such as coronary angiograms and coronary artery imaging, during vancomycin therapy, if conditions permit; or to replace vancomycin with teicoplanin.

The duration of vancomycin therapy was a factor that we focused on. The recommended course of vancomycin for the medical treatment of patients with IE was 4–6 weeks, which was longer than the course of most infections (Chinese Society of Cardiology, 2014; Baddour et al., 2015; Habib et al., 2015). This study suggested that duration of therapy was an independent risk factor for VA-AKI in patients with IE, consistent with previous studies (Jeffres, 2017). However, the HR for duration of vancomycin therapy was only 1.030, showing a weak increased risk of AKI, which was lower than we expected. The risk of developing vancomycin nephrotoxicity significantly increased with a duration ≥7 days, and 14 days (Gagneux-Brunon et al., 2019; Mehran et al., 2019; Rybak et al., 2020). The course of vancomycin in this study was 12 and 9.5 days for patients who developed and did not develop AKI, both greater than 7 and less than 14 days, which may account for the low HR for the vancomycin course. Univariate analysis showed a significantly higher risk of AKI in patients with a long duration of treatment (longer than 10.75 days) compared to those with a short duration of treatment (shorter than 10.75 days) (HR 1.927, $p = 0.011$). In patients with IE, we suggested that the course of vancomycin longer than 10.75 days was associated with a significantly increased risk of AKI and required more frequent monitoring of kidney function and vancomycin trough concentrations.

This study showed that BMI and residence in the ICU were risk factors for VA-AKI in patients with IE, which was consistent with the findings in the general adult patients (Liu et al., 2021; Kim JY et al., 2022). Several studies have shown that obesity or increasing BMI was significantly associated with the development of VA-AKI (Choi et al., 2017). Obese patients have a significantly higher incidence of trough levels >20 mg/L due to complex vancomycin pharmacokinetics (e.g., increased volume of distribution and clearance) and demanding dose adjustment regimens (Elyasi et al., 2012). In addition, a study by Maha S. Assadoon et al. found that obese patients may experience vancomycin accumulation within the first 10 days of treatment (Assadoon et al., 2022). Measures such as actual weight-based dosing, frequent monitoring of vancomycin, and AUC-guided therapy may contribute to the reduction of VA-AKI in obese patients (Choi et al., 2017; Rybak et al., 2020; Assadoon et al., 2022). Severity of illness impacted development of AKI in patients receiving vancomycin. Admission to the ICU indicated that patients were critically ill and more likely to have a combination of multiple risk factors for AKI, thus increasing the nephrotoxicity of vancomycin (Filippone et al., 2017; Blevins et al., 2019; O'Callaghan et al., 2020).

VA-AKI was associated with increased length of hospital stay, need for dialysis, increased mortality, and increased costs, which is consistent with previous studies (Jeffres, 2017). More than 70% of the patient's kidney function can be recovered, which suggests the importance of early intervention and aggressive salvage of VA-AKI. Payment method (at one's own expense vs. national basic medical insurance) was the only risk factor for kidney function recovery, and this was not reported in previous studies. We speculate that patients without medical insurance may limit the choice of measures for improving kidney function due to their weak payment willingness.

This study has several strengths. First, the sample size of this study was relatively large and was the largest sample size studying antibiotic-associated kidney injury in patients with IE. Second, we counted the consequences of VA-AKI, including economic consequences, mortality, and recovery of kidney function. We further analyzed the risk factors affecting the recovery of kidney function in patients with AKI. Third, the economic consequences of VA-AKI were rarely addressed in previous studies. However, the study has several limitations. First, this was a single-center retrospective study, and we could only demonstrate a correlation between vancomycin and AKI, not a causal relationship. Second, vancomycin trough concentrations were not included as a risk factor due to the low percentage of TDM and the small amount of concentration data available for analysis. For the available data, we analyzed the correlation between vancomycin trough concentrations and the risk of AKI occurrence. However, we believe that this deficiency does not affect the quality of this study. Globally, especially in developing countries, hospitals without vancomycin concentration monitoring technology remain in the majority. Vancomycin dose and duration are important bases for assessing vancomycin exposure, and both variables were included in this study. Moreover, even in hospitals where vancomycin monitoring is carried out, its actual monitoring is not satisfactory. Third, this study did not collect data on urine volume, which is an important criterion for the diagnosis of AKI. Due to the retrospective nature of this study, medical record data on urine volume were not or inaccurately recorded, and we will address this shortcoming in a prospective study to be conducted in the future. Fourth, we did not follow up with the patient after discharge. Because the patient's information was anonymized and their contact information was not available.

# 5 Conclusion

The incidence of VA-AKI in patients with IE was slightly higher than in general adult patients, and lower than in special populations such as obese and critically ill. Concomitant contrast agents were the most alarmingly nephrotoxic in patients with IE, adding a 2-fold risk of VA-AKI, and we speculate that this may be due to a synergistic mechanism of nephrotoxicity between contrast agents and vancomycin. In patients with IE, a course of vancomycin therapy longer than 10.75 days was associated with a significantly increased risk of AKI and required more frequent monitoring of kidney function and vancomycin trough concentrations.

# Data availability statement

The raw data supporting the conclusion of this article will be made available by the authors, without undue reservation.

## Ethics statement

The studies involving humans were approved by Ethics Committee of Zhongshan Hospital, Fudan University. The studies were conducted in accordance with the local legislation and institutional requirements. The ethics committee/institutional review board waived the requirement of written informed consent for participation from the participants or the participants' legal guardians/next of kin because This retrospective study obtained data where patient information was anonymized so that the patients themselves could not be contacted.

## Author contributions

## Funding

## Acknowledgments

## Conflict of interest

The authors declare that the research was conducted in the absence of any commercial or financial relationships that could be construed as a potential conflict of interest.

## Publisher's note

All claims expressed in this article are solely those of the authors and do not necessarily represent those of their affiliated organizations, or those of the publisher, the editors and the reviewers. Any product that may be evaluated in this article, or claim that may be made by its manufacturer, is not guaranteed or endorsed by the publisher.

## Supplementary material

The Supplementary Material for this article can be found online at: https://www.frontiersin.org/articles/10.3389/fphar.2023.1260802/full#supplementary-material

## References

Abdel Jalil, M. H., Etaijazeen, R., Khaled Abu-Mahfouz, F., Abu Hammour, K., Hasan Matalqah, M., Saleh Khaleel Albadaineh, J., et al. (2023). Vancomycin prescribing and therapeutic drug monitoring: challenges of real clinical practice. *PLoS One* 18 (5), e0285717. doi:10.1371/journal.pone.0285717

Assadoon, M. S., Pearson, J. C., Kubiak, D. W., Kovacevic, M. P., and Dionne, B. W. (2022). Evaluation of vancomycin accumulation in patients with obesity. *Open Forum Infect. Dis.* 9 (10), ofac491. doi:10.1093/ofid/ofac491

Baddour, L. M., Wilson, W. R., Bayer, A. S., Fowler, V. G., Jr, Tleyjeh, I. M., Rybak, M. J., et al. (2015). Infective endocarditis in adults: diagnosis, antimicrobial therapy, and management of complications: a scientific statement for healthcare professionals from the American heart association. *Circulation* 132 (15), 1435–1486. doi:10.1161/CIR.0000000000000296

Barberan, J., Mensa, J., Artero, A., Epelde, F., Rodriguez, J. C., Ruiz-Morales, J., et al. (2019). Factors associated with development of nephrotoxicity in patients treated with vancomycin versus daptomycin for severe Gram-positive infections: a practice-based study. *Rev. espanola Quimioter.* 32 (1), 22–30.

Blevins, A. M., Lashinsky, J. N., McCammon, C., Kollef, M., Micek, S., and Juang, P. (2019). Incidence of acute kidney injury in critically ill patients receiving vancomycin with concomitant piperacillin-tazobactam, cefepime, or meropenem. *Antimicrob. Agents Chemother.* 64 (5), 026588-18-e2719. doi:10.1128/AAC.02658-18

Chinese Society of Cardiology, (2014). Expert consensus on prevention, diagnosis, and treatment of infective endocarditis in adults. *Chin. J. Cardiovasc. Dis.* 42 (10), 806–816. doi:10.3760/cma.j.issn.0253-3758.2014.10.004

Choi, Y. C. S. S., Soliman, D., Bingham, A. L., Pontiggia, L., Hunter, K., et al. (2017). Intravenous vancomycin associated with the development of nephrotoxicity in patients with class III obesity. *Ann. Pharmacother.* 51 (11), 937–944. doi:10.1177/1060028017720946

Chun, J. Y., Song, K. H., Lee, D. E., Hwang, J. H., Jung, H. G., Heo, E., et al. (2021). Impact of a computerised clinical decision support system on vancomycin loading and the risk of nephrotoxicity. *Int. J. Med. Inf.* 149, 104403. doi:10.1016/j.ijmedinf.2021.104403

Contejean, A., Tisseyre, M., Canoui, E., Treluyer, J. M., Kerneis, S., and Chouchana, L. (2021). Combination of vancomycin plus piperacillin and risk of acute kidney injury: a worldwide pharmacovigilance database analysis. *J. Antimicrob. Chemother.* 76 (5), 1311–1314. doi:10.1093/jac/dkab003

Cosgrove, S. E., Vigliani, G. A., Fowler, V. G., Abrutyn, E., Corey, G. R., Levine, D. P., et al. (2009). Initial low-dose gentamicin for *Staphylococcus aureus* bacteremia and endocarditis is nephrotoxic. *Clin. Infect. Dis.* 48 (6), 713–721. doi:10.1086/597031

Elyasi, S., Khalili, H., Dashti-Khavidaki, S., and Mohammadpour, A. (2012). Vancomycin-induced nephrotoxicity: mechanism, incidence, risk factors and special populations. A literature review. *Eur. J. Clin. Pharmacol.* 68 (9), 1243–1255. doi:10.1007/s00228-012-1259-9

Filippone, E. J., Kraft, W. K., and Farber, J. L. (2017). The nephrotoxicity of vancomycin. *Clin. Pharmacol. Ther.* 102 (3), 459–469. doi:10.1002/cpt.726

Gagneux-Brunon, A., Pouvaret, A., Maillard, N., Berthelot, P., Lutz, M. F., Cazorla, C., et al. (2019). Acute kidney injury in infective endocarditis: a retrospective analysis. *Med. Mal. Infect.* 49 (7), 527–533. doi:10.1016/j.medmal.2019.03.015

Goenaga Sanchez, M. A., Kortajarena Urkola, X., Bouza Santiago, E., Muñoz García, P., Verde Moreno, E., Fariñas Álvarez, M. C., et al. (2017). Aetiology of renal failure in

patients with infective endocarditis. The role of antibiotics. *Med. Clin. Barc.* 149 (8), 331–338. doi:10.1016/j.medcli.2017.03.009

Habib, G., Lancellotti, P., Antunes, M. J., Bongiorni, M. G., Casalta, J. P., Del Zotti, F., et al. (2015). 2015 ESC guidelines for the management of infective endocarditis: the task force for the management of infective endocarditis of the European society of Cardiology (ESC). Endorsed by: European association for cardio-thoracic surgery (EACTS), the European association of nuclear medicine (EANM). *Eur. Heart J.* 36 (44), 3075–3128. doi:10.1093/eurheartj/ehv319

He, N., Su, S., Ye, Z., Du, G., et al. (2020). Evidence-based guideline for therapeutic drug monitoring of vancomycin: 2020 update by the division of therapeutic drug monitoring, Chinese pharmacological society. *Clin. Infect. Dis.* 71 (Suppl. 4), S363–S371. doi:10.1093/cid/ciaa1536

Huang, W. C., Wang, M. T., Lai, T. S., Lee, K. H., Shao, S. C., Chen, C. H., et al. (2022). Nephrotoxins and acute kidney injury - the consensus of the Taiwan acute kidney injury Task Force. *J. Formos. Med. Assoc.* 121 (5), 886–895. doi:10.1016/j.jfma.2021.12.007

Jeffres, M. N. (2017). The whole price of vancomycin: toxicities, troughs, and time. *Drugs* 77 (11), 1143–1154. doi:10.1007/s40265-017-0764-7

Khwaja, A. (2012). KDIGO clinical practice guidelines for acute kidney injury. *Nephron Clin. Pract.* 120 (4), c179–c184. doi:10.1159/000339789

Kiley, P. S. P. A., Hodge, L. A., Kaplan, M. C., Baczek, S. M., Stanley, J. S., et al. (2022). Retrospective cohort study of the incidence of acute kidney injury with vancomycin area under the curve-based dosing with concomitant piperacillin-tazobactam compared to meropenem or cefepime. *Antimicrob. Agents Chemother.* 66 (8), e0004022. doi:10.1128/aac.00040-22

Kim, J. Y., Kim, K. Y., Yee, J., and Gwak, H. S. (2022). Risk scoring system for vancomycin-associated acute kidney injury. *Front. Pharmacol.* 13, 815188. doi:10.3389/fphar.2022.815188

Kunming, P., Can, C., Zhangzhang, C., Wei, W., Qing, X., Xiaoqiang, D., et al. (2021). Vancomycin associated acute kidney injury: a longitudinal study in China. *Front. Pharmacol.* 12, 632107. doi:10.3389/fphar.2021.632107

Kunming, P., Xiaotian, J., Qing, X., Chenqi, X., Xiaoqiang, D., and Qian Zhou, L. (2023). Impact of pharmacist intervention in reducing vancomycin-associated acute kidney injury: a systematic review and meta-analysis. *Br. J. Clin. Pharmacol.* 89 (2), 526–535. doi:10.1111/bcp.15301

Legrand, M., Pirracchio, R., Rosa, Petersen, M. L., Van der Laan, M., Fabiani, J. N., et al. (2013). Incidence, risk factors and prediction of post-operative acute kidney injury following cardiac surgery for active infective endocarditis: an observational study. *Crit. care* 17 (5), R220. doi:10.1186/cc13041

Liu, C., Yan, S., Wang, Y., Wang, J., Fu, X., Song, H., et al. (2021). Drug-induced hospital-acquired acute kidney injury in China: a multicenter cross-sectional survey. *Kidney Dis. (Basel).* 7 (2), 143–155. doi:10.1159/000510455

Mehran, R., Dangas, G. D., and Weisbord, S. D. (2019). Contrast-associated acute kidney injury. *N. Engl. J. Med.* 380 (22), 2146–2155. doi:10.1056/NEJMra1805256

Muklewicz, J. D., Steuber, T. D., and Edwards, J. D. (2021). Evaluation of area under the concentration-time curve-guided vancomycin dosing with or without piperacillin-tazobactam on the incidence of acute kidney injury. *Int. J. Antimicrob. Agents* 57 (1), 106234. doi:10.1016/j.ijantimicag.2020.106234

Nakatani, S., Ohara, T., Ashihara, K., Izumi, C., Iwanaga, S., Eishi, K., et al. (2019). JCS 2017 guideline on prevention and treatment of infective endocarditis. *Circ. J.* 83 (8), 1767–1809. doi:10.1253/circj.CJ-19-0549

O'Callaghan, K., Hay, K., Lavana, J., and McNamara, J. F. (2020). Acute kidney injury with combination vancomycin and piperacillin-tazobactam therapy in the ICU: a retrospective cohort study. *Int. J. Antimicrob. Agents* 56 (1), 106010. doi:10.1016/j.ijantimicag.2020.106010

Pan, K., Ma, L., Xiang, Q., Li, X., Li, H., Zhou, Y., et al. (2017). Vancomycin-associated acute kidney injury: a cross-sectional study from a single center in China. *PLoS One* 12 (4), e0175688. doi:10.1371/journal.pone.0175688

Pan, K. M., Wu, Y., Chen, C., Chen, Z. Z., Xu, J. A., Cao, L., et al. (2018). Vancomycin-induced acute kidney injury in elderly Chinese patients: a single-centre cross-sectional study. *Br. J. Clin. Pharmacol.* 84 (8), 1706–1718. doi:10.1111/bcp.13594

Ritchie, B. M., Hirning, B. A., Stevens, C. A., Cohen, S. A., and DeGrado, J. R. (2017). Risk factors for acute kidney injury associated with the treatment of bacterial endocarditis at a tertiary academic medical center. *J. Chemother.* 29 (5), 292–298. doi:10.1080/1120009X.2017.1296916

Rybak, M., Lomaestro, B., Rotschafer, J. C., Moellering, R., Craig, W., Billeter, M., et al. (2009). Therapeutic monitoring of vancomycin in adult patients: a consensus review of the American society of health-system pharmacists, the infectious diseases society of America, and the society of infectious diseases pharmacists. *Am. J. Health Syst. Pharm.* 66 (1), 82–98. doi:10.2146/ajhp080434

Rybak, M. J., Le, J., Lodise, T. P., Levine, D. P., Bradley, J. S., Liu, C., et al. (2020). Therapeutic monitoring of vancomycin for serious methicillin-resistant *Staphylococcus aureus* infections: a revised consensus guideline and review by the American society of health-system pharmacists, the infectious diseases society of America, the pediatric infectious diseases society, and the society of infectious diseases pharmacists. *Am. J. Health Syst. Pharm.* 77 (11), 835–864. doi:10.1093/ajhp/zxaa036

von Elm, E., Altman, D. G., Egger, M., Pocock, S. J., Gøtzsche, P. C., Vandenbroucke, J. P., et al. (2007). The Strengthening the Reporting of Observational Studies in Epidemiology (STROBE) statement: guidelines for reporting observational studies. *Lancet* 370 (9596), 1453–1457. doi:10.1016/S0140-6736(07)61602-X

Yang, L., Xing, G., Wang, L., Wu, Y., Li, S., Xu, G., et al. (2015). Acute kidney injury in China: a cross-sectional survey. *Lancet* 386 (10002), 1465–1471. doi:10.1016/S0140-6736(15)00344-X

# Huangqi-Danshen decoction protects against cisplatin-induced acute kidney injury in mice

Xinhui Liu[1]*[†], Liwen Gao[2†], Xi Huang[2†], Ruyu Deng[3], Shanshan Wu[2], Yu Peng[2] and Jiandong Lu[1]

[1]Department of Nephrology, Shenzhen Traditional Chinese Medicine Hospital, Guangzhou University of Chinese Medicine, Shenzhen, Guangdong, China, [2]The Fourth Clinical Medical College, Guangzhou University of Chinese Medicine, Shenzhen, Guangdong, China, [3]Shenzhen Traditional Chinese Medicine Hospital Affiliated to Nanjing University of Chinese Medicine, Shenzhen, Guangdong, China

**Background:** Acute kidney injury (AKI) induced by cisplatin remains a major impediment to the clinical application of cisplatin, necessitating urgent exploration for promising solutions. Huangqi-Danshen decoction (HDD), a Chinese herbal preparation, has been shown by our group to have a reno-protective effect in adenine-induced chronic kidney disease mice and diabetic *db/db* mice. However, the effect of HDD on cisplatin-induced AKI and its underlying mechanisms are unknown.

**Methods:** The AKI model was established by intraperitoneal injection of cisplatin (20 mg/kg) in C57BL/6 mice. The mice in the treatment group were administrated with HDD (6.8 g/kg/d) for 5 consecutive days before cisplatin challenge. After 72 h cisplatin injection, blood and kidney tissue were subsequently collected for biochemical detection, histopathological evaluation, Western blot analysis, immunohistochemical staining, and terminal deoxynucleotidyl transferase (TdT)-mediated dUTP nick end labeling assay. Ultra-high-performance liquid chromatography coupled with quadrupole time-of-flight mass spectrometry was used to detect changes in renal metabolites.

**Results:** The results showed that HDD significantly reduced serum creatinine and blood urea nitrogen levels and alleviated renal histopathological injury in cisplatin-induced AKI mice. And HDD treatment demonstrated a significant inhibition in apoptosis, inflammation, and oxidative stress in AKI mice. Moreover, non-target metabolomics revealed that HDD significantly restored 165 altered metabolites in AKI mice. Subsequent enrichment analysis and pathway analysis of these metabolites indicated that nicotinate and nicotinamide metabolism was the primary pathway affected by HDD intervention. Further investigation showed that HDD could upregulate nicotinamide adenine dinucleotide (NAD$^+$) biosynthesis-related enzymes quinolinate phosphoribosyltransferase, nicotinamide mononucleotide adenylyltransferase 1, and nicotinamide phosphoribosyltransferase to replenish NAD$^+$ content in the kidney of AKI mice.

**Abbreviations:** AKI, Acute kidney injury; ATP, Adenosine triphosphate; BUN, Blood urea nitrogen; CHM, Chinese herbal medicine; CKD, Chronic kidney disease; NA, Nicotinic acid; NAD+, Nicotinamide adenine dinucleotide; NAM, Nicotinamide; NAMPT, Nicotinamide phosphoribosyltransferase; NGAL, Neutrophil gelatinase-associated lipocalin; NMN, Nicotinamide mononucleotide; NMNAT1, Nicotinamide mononucleotide adenylyltransferase 1; NR, Nicotinamide riboside; QPRT, Quinolinate phosphoribosyltransferase; ROS, Reactive oxygen species; Scr, Serum creatinine; TCM, Traditional Chinese medicine.

**Conclusion:** In summary, HDD exerted a protective effect against cisplatin-induced AKI and suppressed apoptosis, inflammation, and oxidative stress in the kidney of AKI mice, which may be attributed to the modulation of NAD$^+$ biosynthesis.

## Introduction

Acute kidney injury (AKI) is a sharp decrease in glomerular filtration function over a short period of time due to various aetiologies (Hoste et al., 2018). AKI is associated with considerable morbidity and mortality and has a high risk of development of chronic kidney disease (CKD) or end-stage kidney disease (ESKD) (Lameire et al., 2013). Cisplatin [*cis*-diamminedichloroplatinum (II)], an inorganic platinum derivative, is widely used to treat solid tumors including those of the head, neck, lung, breast, ovary, and testis (Dasari and Tchounwou, 2014; Zhang et al., 2021). Cisplatin is mainly cleared by the kidneys and therefore has a high risk of causing acute and chronic nephrotoxicity. It was reported that AKI occurred in 31.5% of patients with cancer who received cisplatin for treatment across multiple tumor types (Latcha et al., 2016). AKI is the dose-limiting side effect of cisplatin that limits its clinical application in cancer patients (Karasawa and Steyger, 2015). Therefore, it is urgent to further explore the underlying mechanism and effective therapeutic regimens of cisplatin-induced AKI.

In recent years, accumulating evidence elucidates the reno-protective effect of Chinese herbal medicine (CHM) in multiple AKI models via different mechanisms of inhibiting inflammation, cell apoptosis, necroptosis, ferroptosis, and restraining oxidative stress etc., (Li H. D. et al., 2019; Li J. et al., 2023). Chen *et al.* included 15 randomized controlled trials to evaluate the efficacy of CHM as an adjunctive therapy for patients with AKI. The results showed that patients randomly assigned to CHM plus Western treatment had a statistically significant reduction in in-hospital mortality compared with those randomly assigned to Western treatment alone (Chen et al., 2016). In traditional Chinese medicine (TCM) theory, AKI is caused by qi deficiency, blood stasis, and toxin accumulation. Huangqi-Danshen decoction (HDD) is composed of Astragalus membranaceus (Huangqi) and Salvia miltiorrhiza (Danshen) and has the effect of invigorating qi and promoting blood circulation. According to TCM theory, HDD would be beneficial in treating AKI. Our previous studies have found that HDD had reno-protective effect in adenine-induced CKD mice and *db/db* diabetic mice (Liu et al., 2019a; Liu et al., 2019b; Liu et al., 2020). However, the protective effects and underlying mechanisms of HDD against cisplatin-induced AKI are unknown.

Metabolomics provides a tool to qualitatively and quantitatively analyze small molecular metabolites (typically <1,500 Da) in specific tissues, organs or biological fluids (German et al., 2005). Metabolomics, with its high-throughput and high-resolution characteristics, allows accurate analysis of metabolite changes in body fluids or tissues, thus helping to understand the development and progression of diseases (Abbiss et al., 2019). Several studies have used metabolomics analysis to identify novel biomarkers for the development, progression and prognosis of AKI and to reveal specific mechanisms of AKI (Cui et al., 2021; Ping et al., 2021; Tan et al., 2021; Yuan et al., 2022).

Metabolomics reflects the overall changes of the organism by studying the changes of metabolites, which is similar to the holistic view of TCM and provides new ideas and methods for the research of CHM. The application of metabonomics is helpful to further clarify the mechanism of action of CHM (Wang et al., 2017; Wang et al., 2021). In this study, we first evaluated the protective effect of HDD on cisplatin-induced AKI, and secondly, we used ultra-high-performance liquid chromatography coupled with quadrupole time-of-flight mass spectrometry (UHPLC-QTOF/MS) to detect changes in renal metabolites to clarify the mechanism of action of HDD.

## Materials and methods

### Chemicals and antibodies

Cisplatin was purchased from Sigma-Aldrich (St. Louis, MO, United States). The primary antibodies used in this study were neutrophil gelatinase-associated lipocalin (NGAL), Bax, 4-hydroxynonenal (4-HNE), nicotinamide mononucleotide adenylyltransferase 1 (NMNAT1) (Abcam, Cambridge, MA, United States); nicotinamide phosphoribosyltransferase (NAMPT) (Proteintech, Wuhan, China); 8-hydroxy-2′-deoxyguanosine (8-OHdG) (Santa CruzBiotechnology, Santa Cruz, CA, United States); cleaved caspase-3, F4/80, p53, p-p53 (Cell Signaling Technology, Beverly, MA, United States); quinolinic acidphosphoribosyltransferase (QPRT), and β-actin (Sigma-Aldrich, St Louis, MO, United States). The horseradish peroxidase (HRP)-conjugated secondary antibodies were obtained from Thermo Fisher Scientific (Waltham, MA, United States).

### HDD preparation

HDD was composed of 2 herbs: *Astragalus mongholicus* Bunge [Fabaceae] and *Salvia miltiorrhiza* Bunge [Lamiaceae], in the ratio of 2:1. These two herbs were extracted twice with 8 times of ddH$_2$O (volume/weight) for 1 h each time. The extracts obtained twice were mixed together, filtered and concentrated to obtain an HDD extract with a final concentration of 1 g of raw herbs per mL of extract. High performance liquid chromatography-mass spectrometry (HPLC-MS) analysis was conducted to confirm the quality of HDD extract (Supplementary Figure S1).

### Animals and treatment

Eighteen male C57BL/6 mice (6–8 weeks old) were purchased from Guangdong Medical Laboratory Animal Center (Foshan,

China). After 1 week of adaptive feeding, all mice were randomly divided into 3 groups: the control group (*n* = 6), the AKI group (*n* = 6), and the AKI + HDD group (*n* = 6). The AKI mice received single intraperitoneal injection of cisplatin (20 mg/kg) (Yu et al., 2018), while AKI + HDD group was pretreated with HDD at the dose of 6.8 g/kg/d for 5 consecutive days before cisplatin challenge. After 72 h cisplatin injection, all mice were sacrificed. After clotting, the blood was centrifuged at 1,500 rpm for 10 min at 4°C to isolate serum. A portion of kidneys were fixed with 4% paraformaldehyde for pathological staining, and the remaining kidneys were frozen at −80°C for protein expression analysis.

## Biochemical assay

The serum creatinine (Scr) and blood urea nitrogen (BUN) concentrations were measured by using specific kits (StressMarq Biosciences, British Columbia, Canada) in accordance with manufacturer's instructions.

## Histological assessment

To evaluate renal pathological injury, periodic acid-Schiff (PAS) staining was conducted on paraffin-embedded kidney sections. Quantitative analysis of tubular injury was performed according to the following scoring criteria: normal tubules = 0; less than 25% tubular injury = 1; 25%–50% tubular injury = 2; 50%–75% tubular injury = 3; more than 75% tubular injury = 4 (Weidemann et al., 2008).

## Western blotting

Kidney tissues were homogenized in RIPA lysis buffer on ice. Then, the supernatants were separated and the protein concentrations were determined by Bradford method. Equal amounts of protein were electrophoresed in 10% or 15% SDS-PAGE gels, transferred to nitrocellulose or polyvinylidene difluoride membranes, and blocked with 5% non-fat milk. Next, these membranes were incubated with the corresponding primary and secondary antibodies. To visualize protein bands, these membranes were treated with ECL luminescent solution. The gray values of protein bands were calculated by Image Lab software version 5.1 (Bio-Rad Laboratories, Hercules, CA, United States).

## Terminal deoxynucleotidyl transferase (TdT)-mediated dUTP nick end labeling (TUNEL)

Detection of apoptotic cells in paraffin-embedded kidney sections was performed by using One Step TUNEL Apoptosis Assay Kit (Beyotime, Shanghai, China). In brief, kidney tissue sections were dewaxed, hydrated, and treated with DNase-free proteinase K. After washing with PBS, the sections were incubated with TUNEL detection solution at 37°C for 60 min in the dark. The numbers of TUNEL positive cells per field were counted under ×200 microscopic fields.

## Immunohistochemistry

Paraffin-embedded kidney tissues were cut into 6 μm sections. After deparaffinization and hydration, the sections were sequentially treated with citrate antigen retrieval solution, 3% hydrogen peroxide, and goat serum. Then, the sections were incubated with primary antibodies against F4/80, 4-HNE, and 8-OHdG at 4°C overnight. The brown positive staining area was visualized by using diaminobenzidine (DAB) solution. The numbers of F4/80 positive cells per field were counted under ×400 microscopic fields. The integrated optical density (IOD) values of 4-HNE and 8-OHdG positive staining areas were calculated by ImagePro Plus 6.0 software (Media Cybernetics, CA, United States).

## UHPLC-QTOF/MS analysis

A 25 mg kidney tissue sample was grinded with 1 mL of extract solution (methanol: acetonitrile: water = 2:2:1). After centrifugation at 10,000 rpm for 15 min at 4°C, the supernatant was collected for vacuum drying. Then, the dried samples were reconstituted with 200 μL of 50% acetonitrile and centrifuged at 13,000 rpm for 15 min at 4°C. The supernatant was used for on-board detection. Chromatographic separation was carried out on Agilent 1290 UHPLC system (Agilent Technologies, Santa Clara, CA, United States). The chromatographic parameters were: column, BEH Amide (2.1 × 100 mm, 1.7 μm, Waters, Milford, MA, United States); mobile phase, 25 mmol/L ammonium acetate and 25 mmol/L ammonia (A) and acetonitrile (B); gradient elution conditions, 0–0.5 min, 95%B; 0.5–7.0 min, 95%–65% B; 7.0–8.0 min, 65%–40% B; 8.0–9.0 min, 40% B; 9.0–9.1 min, 40%–95% B; 9.1–12.0 min, 95% B; column temperature: 25°C; auto-sampler temperature, 4°C; injection volume, 1 μL. MS spectra were acquired using TripleTOF 6,600 mass spectrometry (AB Sciex, Framingham, MA, United States). The electrospray ionization interface (ESI) source conditions were: source temperature, 600°C; gas 1, 60 psi; gas 2, 60 psi; curtain gas, 35 psi; declustering potential, 60 V; ion spray voltage floating, 5 kV (pos) or −4 kV (neg).

The raw data were processed by R package XCMS (version 3.2), including retention time correction, peak identification, peak extraction, peak integration, peak alignment, etc. Then, the data matrices were imported into MetaboAnalyst for statistical and pathway analysis. Principal component analysis (PCA), partial least squares-discriminant analysis (PLS-DA), sparse partial least squares-discriminant analysis (sPLS-DA), and orthogonal partial least squares-discriminant analysis (orthoPLS-DA) were used to show differences in metabolite profiles between groups. Pathway analysis was performed based on Kyoto Encyclopedia of Genes and Genomes (KEGG).

## Statistical analysis

Data were expressed as mean ± standard error of mean (SEM). Statistical differences were calculated using one-way ANOVA, and the method for multiple comparisons was Tukey (SPSS 16.0, Chicago, IL, United States). $p < 0.05$ was considered statistically significant.
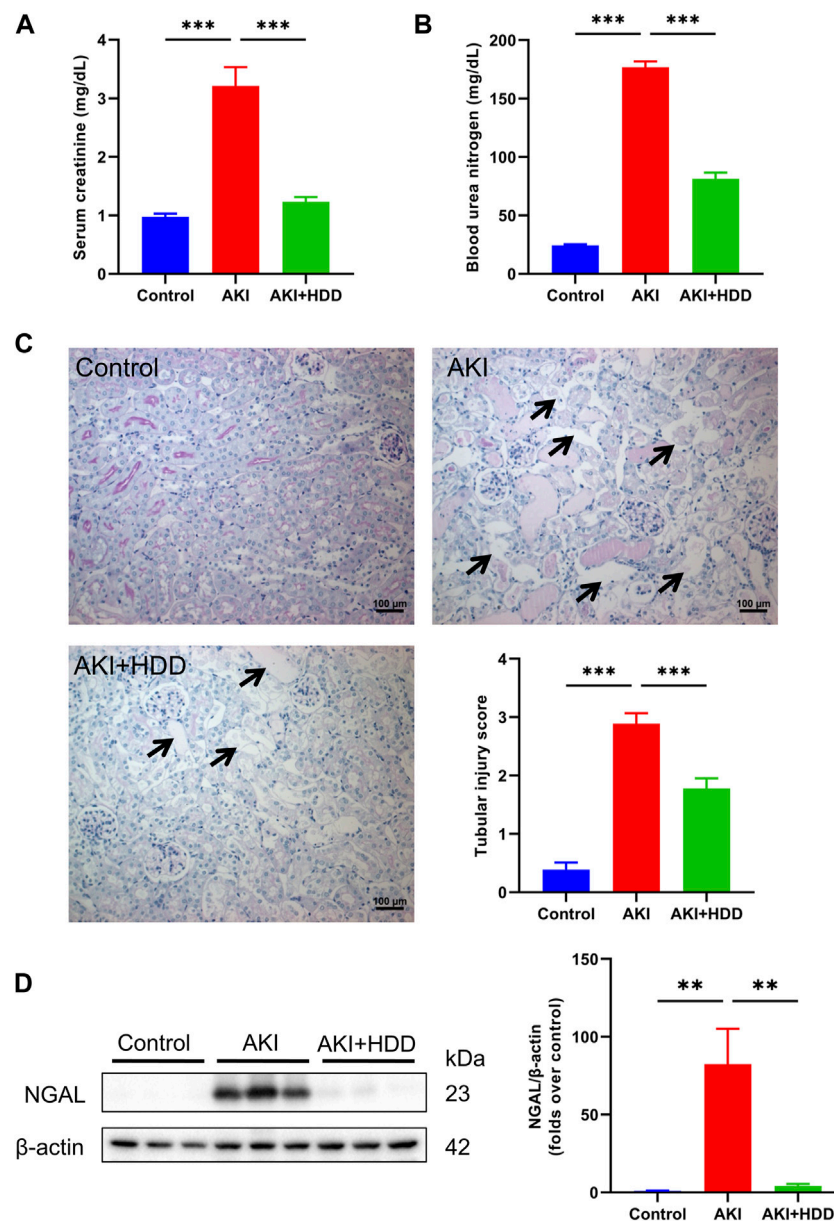
**FIGURE 1**
Effects of HDD on cisplatin-induced acute kidney injury in mice. **(A)** Serum creatinine levels. **(B)** Blood urea nitrogen levels. **(C)** Representative images of renal PAS staining (scale bars = 100 μm, magnification = ×200, arrows indicate tubule degeneration) and quantitative analysis of renal tubular injury. **(D)** Western blot analysis of NGAL expression in the kidneys of each group. Data are expressed as mean ± SEM, $n$ = 6 mice per group, one-way ANOVA followed by Tukey's *post hoc* test was used for calculating statistical differences, \*\*$p$ < 0.01, \*\*\*$p$ < 0.001.

# Results

## HDD attenuated cisplatin-induced AKI in mice

AKI is characterized by a dramatic decline in kidney function over a short period of time, resulting in elevated Scr and BUN levels. In this study, the levels of Scr and BUN of model mice increased 3-fold and 7-fold, respectively, after 3 days of cisplatin challenge. Pretreatment with HDD could prevent the significant elevation of Scr and BUN in AKI mice ($p$ < 0.001, Figures 1A, B). PAS staining indicated obvious tubular injury in AKI mice, including tubular epithelial cell necrosis, shedding,

and tubular dilation. In contrast, these tubular injuries were significantly attenuated in mice pretreated with HDD (Figure 1C). In addition, the expression of NGAL, a renal tubular injury marker, was strikingly increased in the kidney of AKI mice, and was significantly blunted after HDD pretreatment (Figure 1D). Collectively, these data demonstrated that HDD protected against cisplatin-induced AKI in mice.

## HDD decreased apoptosis in AKI mice

Renal tubular epithelial cell apoptosis was detected through TUNEL staining. As shown in Figures 2A, B, there were rare TUNEL-positive cells
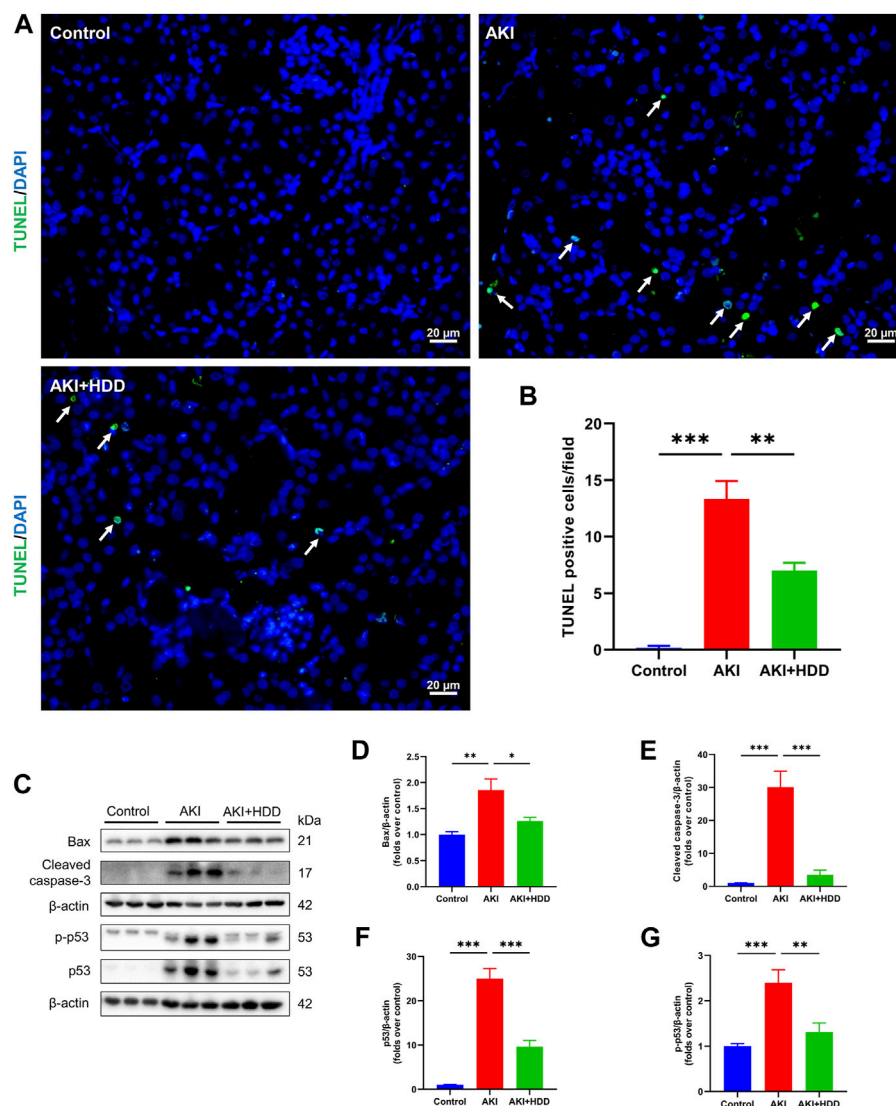
**FIGURE 2**
Effects of HDD on apoptosis in AKI mice. **(A)** Representative images of TUNEL staining of apoptotic cells in the kidney of each group (scale bars = 20 μm, magnification = ×400, arrows indicate apoptotic tubular cells). **(B)** Quantitative analysis of TUNEL-positive cells. **(C)** Representative Western blot images of Bax, cleaved caspase-3, p53, and p-p53 expression in the kidneys of each group. **(D−G)** Densitometric analysis of Bax, cleaved caspase-3, p53, and p-p53 expression, normalized to β-actin. Data are expressed as mean ± SEM, $n = 6$ mice per group, one-way ANOVA followed by Tukey's *post hoc* test was used for calculating statistical differences, *$p < 0.05$, **$p < 0.01$, ***$p < 0.001$.

in the kidneys of mice in the control group. The number of TUNEL-positive cells was increased significantly in the kidney of AKI mice, which was notably decreased by HDD pretreatment. Moreover, Western blot analysis showed that the enhanced protein expressions of Bax, cleaved caspase-3, p53, and p-p53 in the kidneys of AKI mice were markedly suppressed by HDD pretreatment (Figures 2C–G). These findings suggested that HDD decreased apoptosis in cisplatin-induced AKI mice.

## HDD alleviated inflammation and oxidative stress in AKI mice

Inflammatory response and oxidative stress are significant pathological features of cisplatin-induced AKI (McSweeney et al., 2021). IHC staining of F4/80, a macrophage marker, revealed that

cisplatin injection significantly increased the number of F4/80-positive cells in the mouse kidney, which was reduced by HDD administration (Figure 3). Oxidative stress was assessed by lipid peroxidation product 4-HNE and DNA oxidation marker 8-OHdG. As shown in Figure 3, cisplatin-induced increase of 4-HNE and 8-OHdG in mice kidneys was reduced by 61.5% and 31.7% ($p < 0.001$), respectively, after HDD pretreatment. These data suggested the anti-inflammatory and anti-oxidative stress effects of HDD in cisplatin-induced AKI mice.

## HDD regulated renal metabolite profiles in AKI mice

To further explore the underlying mechanism by which HDD protected against AKI, we performed non-target metabolomics to
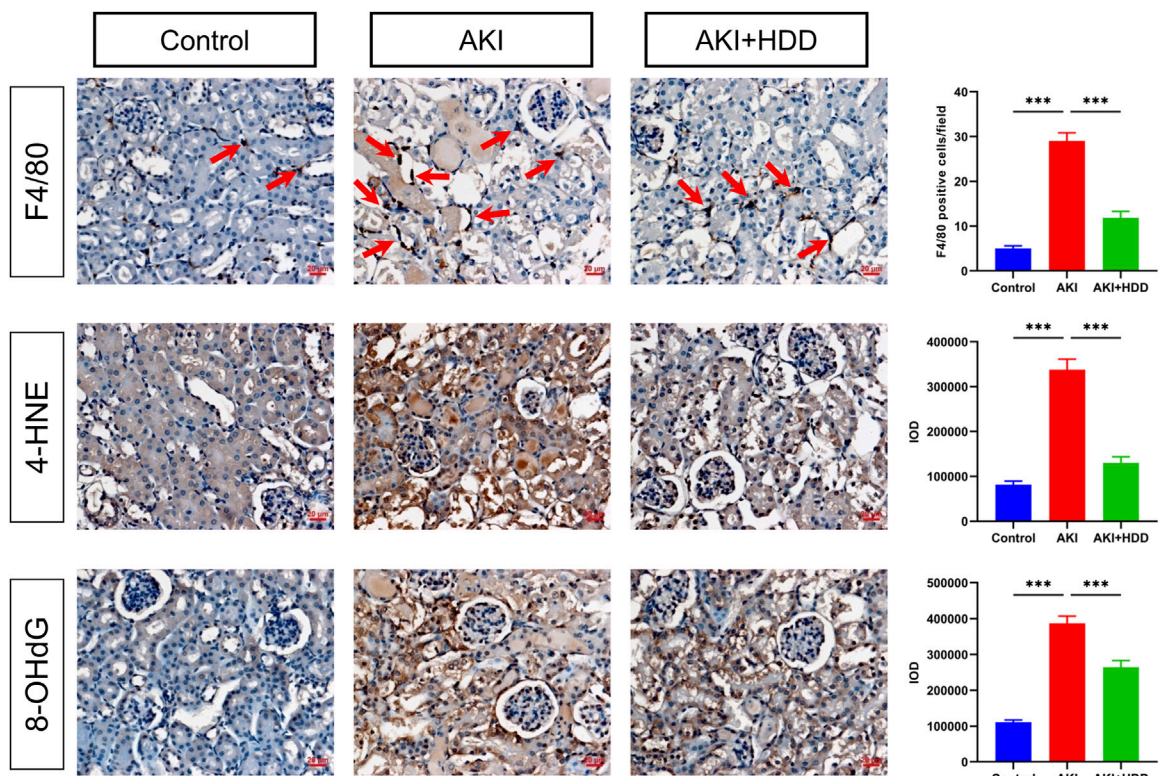
**FIGURE 3**
Effects of HDD on inflammation and oxidative stress in AKI mice. Immunohistochemical staining and quantitative analysis of F4/80, 4-HNE, and 8-OHdG in the kidneys of each group. Scale bars = 20 μm, magnification = ×400, arrows indicate F4/80-positive cells. Data are expressed as mean ± SEM, $n = 3$ mice per group, one-way ANOVA followed by Tukey's *post hoc* test was used for calculating statistical differences, ***$p < 0.001$.
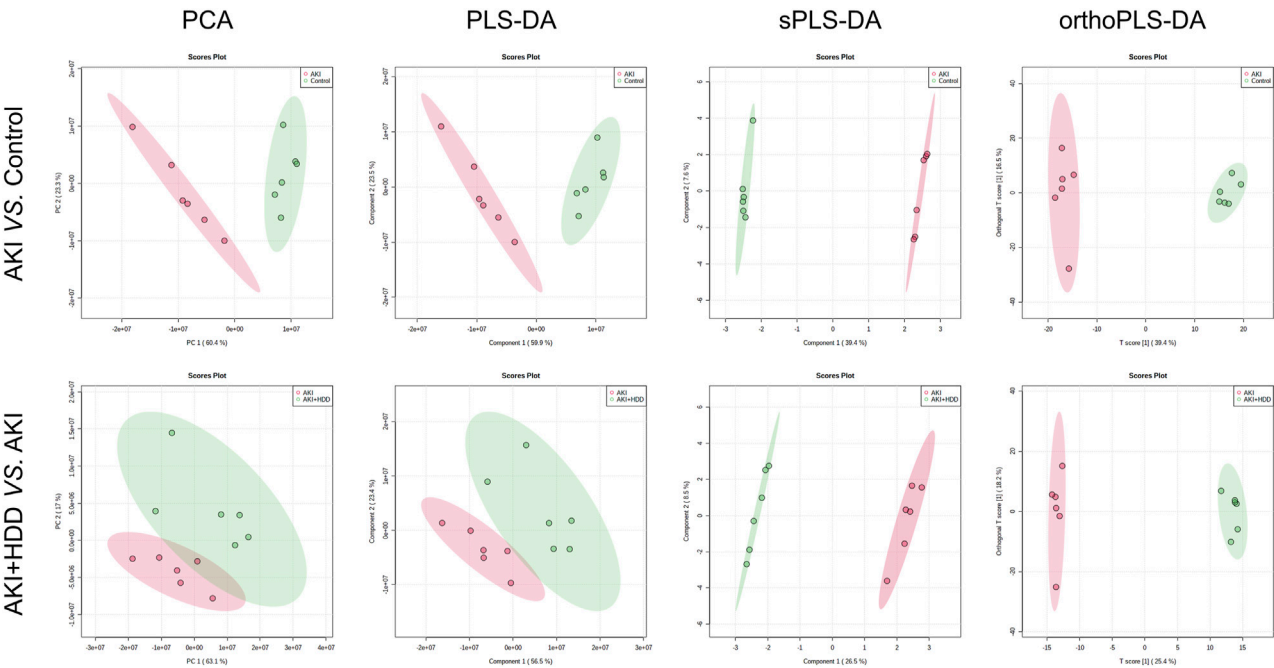


**FIGURE 4**
Effects of HDD on renal metabolic profile in AKI mice. PCA, PLS-DA, sPLS-DA, and orthoPLS-DA analyses showed differences in renal metabolic profiles when comparing AKI to control and AKI + HDD to AKI.
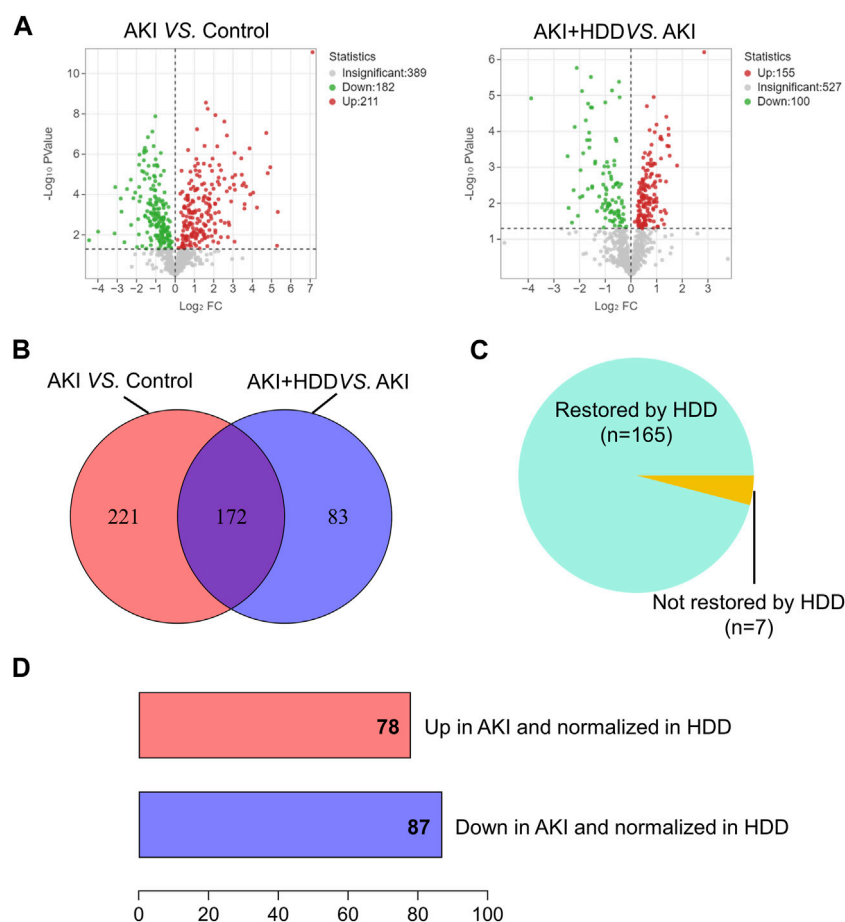
**FIGURE 5**
Identification of significantly restored metabolites by HDD in AKI mice. **(A)** Volcano plots of metabolite distribution when comparing AKI to control and AKI + HDD to AKI. **(B)** Venn diagram of the significantly altered metabolites after comparison. **(C)** Pie chart of the proportion of metabolites that could be restored by HDD or not in AKI mice. **(D)** Numbers of metabolites upregulated and downregulated in AKI and normalized in HDD.

detect changes in renal metabolites. In multivariate analysis, there was a clear metabolites separation between the AKI and the control group in PCA, PLS-DA, sPLS-DA, and orthoPLS-DA models. Metabolites in the AKI + HDD and AKI groups had partial overlap in the PCA and PLS-DA models, while they were completely separated in the sPLS-DA and orthoPLS-DA models (Figure 4). Compared to controls, cisplatin challenge significantly increased 211 and decreased 182 metabolites in the kidneys of mice. Administration of HDD regulated renal metabolite profiles by upregulating 155 and downregulating 100 metabolites in AKI mice (Figure 5A). Comparing the metabolites that changed significantly in the two comparison groups yielded 172 overlapping metabolites (Figure 5B), 165 of which could be reversed by HDD treatment and 7 of which did not respond to HDD treatment (Figure 5C). Of the 165 metabolites normalized by HDD, 78 were upregulated and 87 were downregulated in AKI (Figure 5D). Details of these 165 metaboliteswere summarized in Supplementary Table S1. Both enrichment analysis and pathway analysis of these 165 metabolites that responded to HDD treatment revealed that nicotinate and nicotinamide metabolism was the main pathway that was significantly altered (Figure 6). Taken together, these data indicated that HDD could regulate renal metabolite profiles in

AKI mice, with a primary focus on nicotinate and nicotinamide metabolism.

## HDD corrected disturbed nicotinamide adenine dinucleotide (NAD$^+$) metabolism in AKI mouse kidneys

We then focused on metabolites associated with nicotinate and nicotinamide metabolism because this pathway showed the highest enrichment and had been reported to participate in various kidney diseases (Ralto et al., 2020). Levels of nicotinamide (NAM), nicotinic acid adenine dinucleotide (NAAD), and NAD$^+$ were lower in the kidney of AKI mice and could be significantly restored by HDD except for NAAD. Levers of quinolinic acid (QA) and QA/tryptophan in the *de novo* NAD$^+$ synthesis pathway were markedly increased in AKI mouse kidneys and were normalized by HDD treatment ($p < 0.001$, Figure 7A). Correlation analysis showed that NAM, NAAD, and NAD$^+$ were negatively correlated with Scr ($p < 0.01$), while QA and QA/tryptophan were positively correlated with Scr ($p < 0.001$, Figure 7B). These data suggested that renal NAD$^+$ metabolism in AKI mice was disturbed and associated with renal function, which could be corrected by HDD treatment.
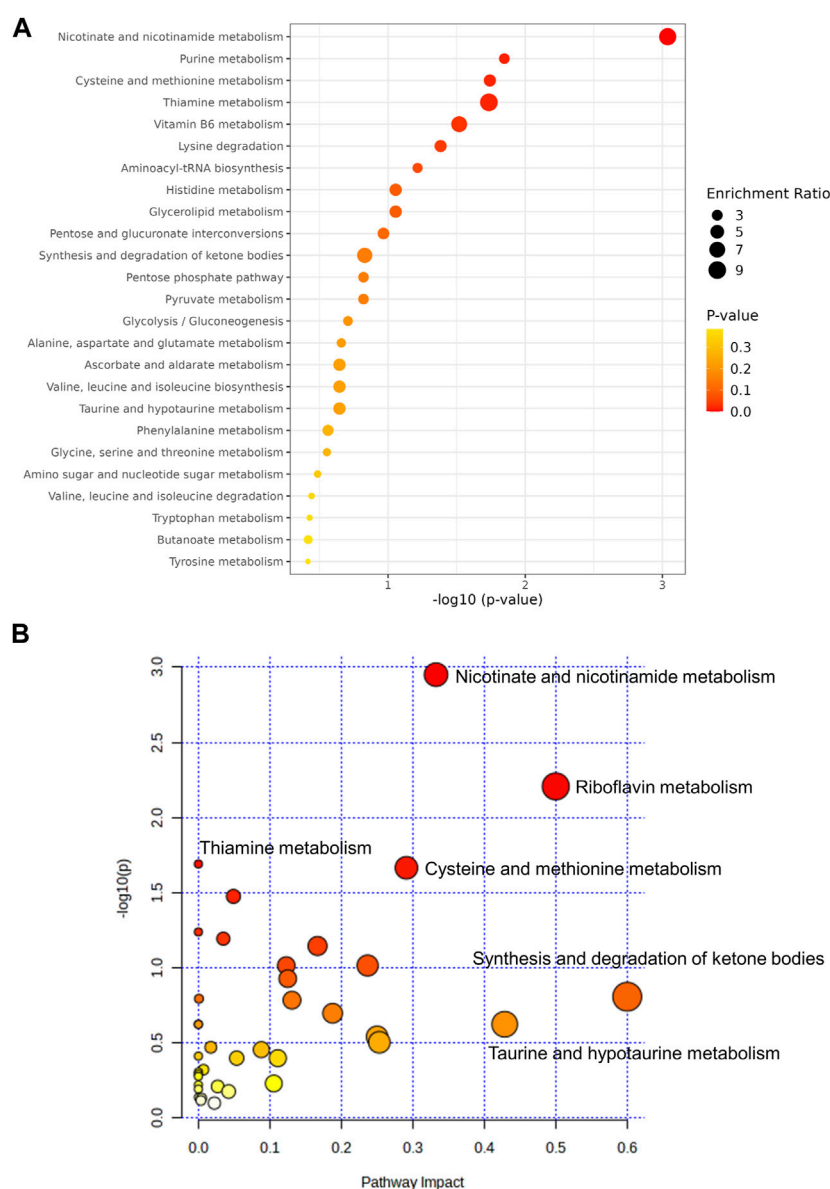
**FIGURE 6**
Analysis of the 165 metabolitesrestored by HDD. **(A)** Enrichment analysis. **(B)** Pathway analysis.

## HDD regulated the expression of enzymes involved in NAD$^+$ synthesis in AKI mice

NAMPT, QPRT, and NMNAT are key enzymes for NAD$^+$ synthesis (Zapata-Pérez et al., 2021). Western blot found that the expression of QPRT and NMNAT1 were all downregulated in the kidney of AKI mice ($p < 0.05$). Administration of HDD partially restored the expression of these two enzymes. Although no significant difference was observed in NAMPT expression between the AKI kidney and the control, HDD treatment significantly upregulated NAMPT expression in AKI mice ($p < 0.01$, Figures 8A–D). Summary of NAD$^+$ biosynthesis-related metabolites content and enzymes expression was showed in Figure 8E.

## Discussion

In the present study, we explored whether HDD had a reno-protective effect on cisplatin-induced AKI, as well as its underlying mechanism. The results showed that HDD protected against cisplatin-induced renal dysfunction and tubular injury and suppressed apoptosis, inflammation, and oxidative stress in the kidney of AKI mice. Non-target metabolomics revealed that HDD regulated renal metabolite profiles in AKI mice, with a primary focus on nicotinate and nicotinamide metabolism. Furthermore, HDD administration was found to effectively restore the levels of NAD$^+$ biosynthesis-related metabolites and enzymes expression in the kidney of AKI mice.
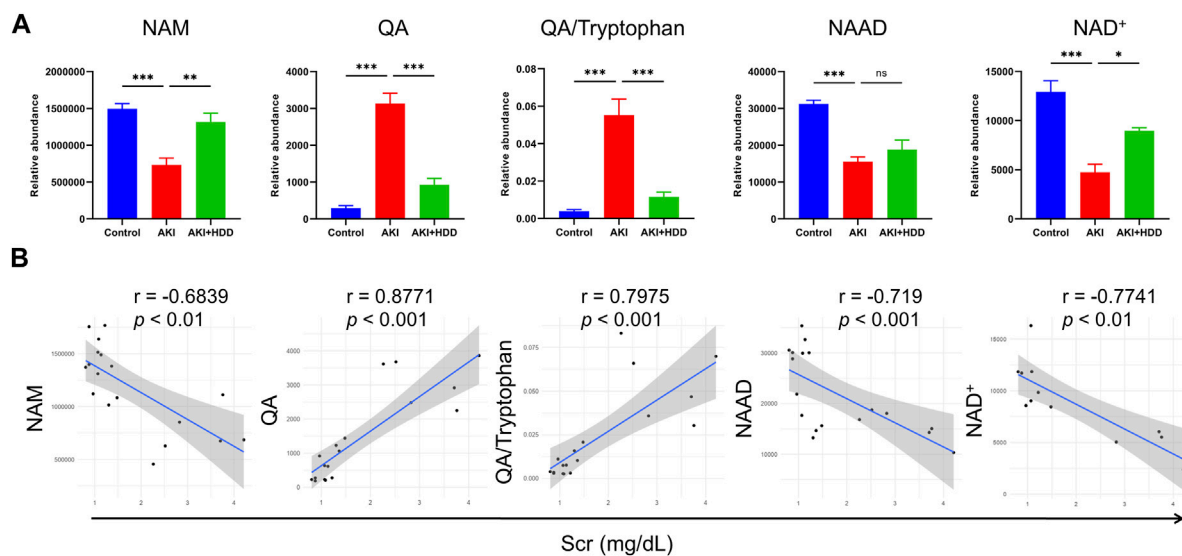
**FIGURE 7**
Levels and correlation analyses of metabolites related to NAD$^+$ metabolism. **(A)** Relative abundance of NAM, QA, QA/Tryptophan, NAAD, and NAD$^+$ in the control, AKI and AKI + HDD group. **(B)** Correlation analyses of NAM, QA, QA/Tryptophan, NAAD, and NAD$^+$ with Scr. Data are expressed as mean $\pm$ SEM, $n$ = 4-6 mice per group, one-way ANOVA followed by Tukey's *post hoc* test was used for calculating statistical differences, *$p < 0.05$, **$p < 0.01$, ***$p < 0.001$, ns, not significant.

NAD$^+$ is referred to as an "electron carrier" due to its capacity for accepting and donating electrons in cellular oxidation-reduction reactions (White and Schenk, 2012). This process is necessary for adenosine triphosphate (ATP) synthesis involved in cellular energy metabolism (Morevati et al., 2022). The kidney necessitates a substantial amount of energy to execute reabsorption function, and it is inherently one of the organs with the highest demand for NAD$^+$ content (Zapata-Pérez et al., 2021). Apart from its function as an essential cofactor in energy metabolism, NAD$^+$ also acts as a co-substrate for NAD$^+$-consuming enzymes (Ralto et al., 2020; Zapata-Pérez et al., 2021; Morevati et al., 2022). The sirtuins (SIRTs), a family of NAD$^+$-dependent histone deacetylases, are implicated in various physiological and pathological processes, including energy metabolism, aging, mitochondrial biogenesis, inflammation, DNA repairment, and stress resistance, etc .,(Vachharajani et al., 2016; Majeed et al., 2021; Rasti et al., 2023; Xu et al., 2023). The protective effects of SIRT1, SIRT3, and SIRT5 against cisplatin-induced kidney injury have been reported (Hasegawa et al., 2010; Kim et al., 2011; Morigi et al., 2015; Li W. et al., 2019). SIRT1 indirectly modulates peroxisome proliferator-activated receptor-γ coactivator-1-α (PGC-1α), whose diminished activity in kidney increases susceptibility to AKI (Fontecha-Barriuso et al., 2020). Pathologically activated NAD$^+$-consuming poly (ADP-ribose) polymerases (PARPs) are implicated in renal ischaemia-reperfusion injury (IRI) (Martin et al., 2000), as evidenced by the increased resistance to renal IRI observed in *Parp1*-knockout mice (Zheng et al., 2005) and the protective effect against IRI provided by a PARP1 inhibitor (Ralto et al., 2020). NAD$^+$ depletion has been observed in both cisplatin-induced and IRI models (Guan et al., 2017; Katsyuba et al., 2018). The reduction of renal NAD$^+$ appears to inhibit certain reno-protective enzymes and trigger a series of reactions in the initiation and progression of AKI. Evidence to date suggests that AKI prognosis may be related to the capacity of NAD$^+$

replenishment to buffer against pathological stress induced by reduced NAD$^+$ levels (Ralto et al., 2020). In mammals, NAD$^+$ is synthesized through three pathways: the *de novo* pathway from tryptophan, the salvage pathway from nicotinamide (NAM) and nicotinamide riboside (NR), and the Preiss-Handler pathway from nicotinic acid (NA) (Zapata-Pérez et al., 2021). Of note, impaired *de novo* NAD$^+$ biosynthesis pathway was found in AKI (Poyan Mehr et al., 2018). The research also proposed that elevated urinary quinolinate/tryptophan could serve as an indicator for predicting AKI and other adverse outcomes. Our findings were in line with these results, as we observed an increase in both QA and QA/tryptophan levels in the kidneys induced by cisplatin. Since QA only participates in NAD$^+$ *de novo* synthesis after being catalyzed by QPRT and not in other metabolic reactions (Poyan Mehr et al., 2018), QA accumulation indicates a reduction in QPRT activity. Further results from Western blot confirmed that the expression of QPRT was reduced in kidney induced by cisplatin and HDD significantly restored QPRT expression, reversing the elevated QA and QA/tryptophan levels. Besides, reduced intracellular NAD$^+$ contents and a decreased ratio of NAD$^+$: NADH were observed in cisplatin-treated renal tissue, resulting in reactive oxygen species (ROS) accumulation, inflammation, and kidney injury (Oh et al., 2014). NAM, a precursor of NAD$^+$, exhibits potent antioxidant properties and can significantly mitigate the damage caused by ROS production under oxidative stress (Mejía et al., 2018). In our study, we observed a significant reversal of reduced levels of NAM and NAD$^+$ in the kidneys of AKI mice with HDD treatment. NMNAT1 and NAMPT, two important enzymes in NAD$^+$ synthesis pathways, were also upregulated upon HDD treatment.

Due to the potent nephrotoxicity of cisplatin, its clinical application as an anticancer agent for solid tumors is considerably restricted (Tang et al., 2023). Given that cisplatin is excreted through the kidneys, high doses or prolonged exposure to cisplatin leads to its accumulation in

**FIGURE 8**
Effects of HDD on the expression of NAD+ biosynthesis-related enzymes in AKI mice. **(A)** Representative Western blot images of NAMPT, QPRT, and NMNAT1 expression in the kidneys of each group. **(B–D)** Densitometric analysis of NAMPT, QPRT, and NMNAT1 expression, normalized to β-actin. **(E)** Summary of NAD+ biosynthesis-related metabolites content and enzymes expression. Data are expressed as mean ± SEM, $n = 6$ mice per group, one-way ANOVA followed by Tukey's *post hoc* test was used for calculating statistical differences, *$p < 0.05$, **$p < 0.01$, ***$p < 0.001$, ns, not significant.

renal tubular cells (Zhang et al., 2021). This accumulation triggers diverse cellular stress responses, including apoptosis, inflammation, oxidative stress, DNA damage, and mitochondrial pathology (Wei et al., 2007; Basu and Krishnamurthy, 2010; Tang et al., 2021; Tang et al., 2023). Macrophages have critical roles in renal inflammation and repair. Our results found obvious macrophage infiltration in the kidneys of AKI mice and could be alleviated by HDD treatment (Figure 3). Macrophages are highly heterogeneous and can differentiate into two phenotypes, pro-inflammatory M1 macrophages and anti-inflammatory M2 macrophages. Previous studies have indicated that macrophage polarization played essential roles in renal fibrosis and folic acid nephropathy (Jiao et al., 2021a; Jiao et al., 2021b; An et al., 2023). However, the phenotype of macrophages and their response to HDD treatment in the present study need further investigation. NAD+ plays a crucial role in anti-aging, anti-inflammation, anti-oxidation, and DNA repair processes (Hershberger et al., 2017; Zapata-Pérez et al., 2021). The NAD+ precursor, NAM, has been reported to enhance mitochondrial metabolism and reduce ROS, implying that NAM supplementation may be a potential reno-protective approach against cisplatin nephrotoxicity (Tran et al., 2016). Combined with the results of our experiment, we have discovered that HDD could significantly restore NAM levels in cisplatin-induced kidney. Taken together, HDD may exert reno-protective effects against cisplatin-induced AKI through

restoring NAD+ biosynthesis and thus replenish NAD+ content, thereby promoting a cascade of responses.

Although targeting NAD+ biosynthesis has been found to confer reno-protection (Allison, 2019) and improve health (Katsyuba et al., 2018), its effectiveness is limited due to the lack of renal targeting ability (Duan et al., 2023). It has been reported that natural products can modulate NAD+ homeostasis and exhibit various biological activities, including anti-apoptosis, anti-inflammation, anti-oxidation, improving energy metabolism, and neuroprotection. And most of them increase the content of NAD+, which is for preventing and treating diseases (Guo et al., 2023). Huangqi-Danshen, a classic combination of CHM, exerts invigorating effects on qi, promotes blood circulation, and facilitates detoxification. A plethora of studies have revealed that both Huangqi and Danshen possess beneficial improvements on diverse diseases by inhibiting inflammatory response, reducing cell apoptosis, alleviating oxidative stress, and activating immunomodulation (Ko et al., 2005; Qin et al., 2012; Shahrajabian et al., 2019; Li R. et al., 2023; Luo et al., 2023; Yang et al., 2023). Several components of Danshen have been reported to target NAD+ metabolism for therapeutic effects. Salvianolic acid B reversed the depletion of cellular NAD+ induced by angiotensin II to protect cardiomyocyte (Liu et al., 2014). Apigenin could increase NAD+ level and suppress neurodegeneration (Roboon et al., 2021) and protect against obesity and metabolic syndrome (Escande et al., 2013). The regulation of NAD+ metabolism by these components in models of kidney disease has not been reported. TCM adheres to the concept of disease prevention should take priority over disease onset. The results of our present study implied that HDD pretreatment could effectively counteract the nephrotoxic side effects induced by cisplatin to a certain extent, which was in line with the concept of disease prevention. However, the downstream effects of enhancing NAD+ availability and precise mechanisms by which HDD modulates NAD+ metabolism remain unclear and necessitate further investigation.

## Conclusion

In summary, HDD exerted a protective effect against cisplatin-induced AKI and suppressed apoptosis, inflammation, and oxidative stress in the kidney of AKI mice, which may be attributed to the modulation of NAD+ biosynthesis.

## Data availability statement

The datasets presented in this study can be found in online repositories. The link to the repository and accession number can be found below: https://www.ebi.ac.uk/metabolights - MTBLS8876.

## Ethics statement

The animal study was approved by the Experimental Animal Ethics Committee of Guangzhou University of Chinese Medicine.

The study was conducted in accordance with the local legislation and institutional requirements.

## Author contributions

XL and JL contributed to conception and design of the study. LG and XH carried out animal experiment. RD conducted the pathological analysis. SW and YP performed the experiments and analyzed the data. XL and LG prepared figures and wrote the manuscript. All authors contributed to the article and approved the submitted version.

## Funding

## Conflict of interest

The authors declare that the research was conducted in the absence of any commercial or financial relationships that could be construed as a potential conflict of interest.

## Publisher's note

All claims expressed in this article are solely those of the authors and do not necessarily represent those of their affiliated organizations, or those of the publisher, the editors and the reviewers. Any product that may be evaluated in this article, or claim that may be made by its manufacturer, is not guaranteed or endorsed by the publisher.

## Supplementary material

The Supplementary Material for this article can be found online at: https://www.frontiersin.org/articles/10.3389/fphar.2023.1236820/full#supplementary-material

## References

Abbiss, H., Maker, G. L., and Trengove, R. D. (2019). Metabolomics approaches for the diagnosis and understanding of kidney diseases. *Metabolites* 9 (2), 34. doi:10.3390/metabo9020034

Allison, S. J. (2019). Targeting NAD(+) synthesis to boost mitochondrial function and protect the kidney. *Nat. Rev. Nephrol.* 15 (1), 1. doi:10.1038/s41581-018-0086-3

An, C., Jiao, B., Du, H., Tran, M., Song, B., Wang, P., et al. (2023). Jumonji domain-containing protein-3 (JMJD3) promotes myeloid fibroblast activation and macrophage polarization in kidney fibrosis. *Br. J. Pharmacol.* 180 (17), 2250–2265. doi:10.1111/bph.16096

Basu, A., and Krishnamurthy, S. (2010). Cellular responses to Cisplatin-induced DNA damage. *J. Nucleic Acids* 2010, 201367. doi:10.4061/2010/201367

Chen, T., Zhan, L., Fan, Z., Bai, L., Song, Y., and Lu, X. (2016). Efficacy of Chinese herbal medicine as an adjunctive therapy on in-hospital mortality in patients with acute kidney injury: a systematic review and meta-analysis. *Evid. Based Complement. Altern. Med.* 2016, 7592705. doi:10.1155/2016/7592705

Cui, H., Shu, S., Li, Y., Yan, X., Chen, X., Chen, Z., et al. (2021). Plasma metabolites-based prediction in cardiac surgery-associated acute kidney injury. *J. Am. Heart Assoc.* 10 (22), e021825. doi:10.1161/jaha.121.021825

Dasari, S., and Tchounwou, P. B. (2014). Cisplatin in cancer therapy: molecular mechanisms of action. *Eur. J. Pharmacol.* 740, 364–378. doi:10.1016/j.ejphar.2014.07.025

Duan, R., Li, Y., Zhang, R., Hu, X., Wang, Y., Zeng, J., et al. (2023). Reversing acute kidney injury through coordinated interplay of anti-inflammation and iron supplementation. *Adv. Mater* 35, e2301283. doi:10.1002/adma.202301283

Escande, C., Nin, V., Price, N. L., Capellini, V., Gomes, A. P., Barbosa, M. T., et al. (2013). Flavonoid apigenin is an inhibitor of the NAD+ ase CD38: implications for cellular NAD+ metabolism, protein acetylation, and treatment of metabolic syndrome. *Diabetes* 62 (4), 1084–1093. doi:10.2337/db12-1139

Fontecha-Barriuso, M., Martin-Sanchez, D., Martinez-Moreno, J. M., Monsalve, M., Ramos, A. M., Sanchez-Niño, M. D., et al. (2020). The role of PGC-1α and mitochondrial biogenesis in kidney diseases. *Biomolecules* 10 (2), 347. doi:10.3390/biom10020347

German, J. B., Hammock, B. D., and Watkins, S. M. (2005). Metabolomics: building on a century of biochemistry to guide human health. *Metabolomics* 1 (1), 3–9. doi:10.1007/s11306-005-1102-8

Guan, Y., Wang, S. R., Huang, X. Z., Xie, Q. H., Xu, Y. Y., Shang, D., et al. (2017). Nicotinamide mononucleotide, an NAD(+) precursor, rescues age-associated susceptibility to AKI in a sirtuin 1-dependent manner. *J. Am. Soc. Nephrol.* 28 (8), 2337–2352. doi:10.1681/asn.2016040385

Guo, C., Huang, Q., Wang, Y., Yao, Y., Li, J., Chen, J., et al. (2023). Therapeutic application of natural products: NAD(+) metabolism as potential target. *Phytomedicine* 114, 154768. doi:10.1016/j.phymed.2023.154768

Hasegawa, K., Wakino, S., Yoshioka, K., Tatematsu, S., Hara, Y., Minakuchi, H., et al. (2010). Kidney-specific overexpression of Sirt1 protects against acute kidney injury by

retaining peroxisome function. *J. Biol. Chem.* 285 (17), 13045–13056. doi:10.1074/jbc.M109.067728

Hershberger, K. A., Martin, A. S., and Hirschey, M. D. (2017). Role of NAD(+) and mitochondrial sirtuins in cardiac and renal diseases. *Nat. Rev. Nephrol.* 13 (4), 213–225. doi:10.1038/nrneph.2017.5

Hoste, E. A. J., Kellum, J. A., Selby, N. M., Zarbock, A., Palevsky, P. M., Bagshaw, S. M., et al. (2018). Global epidemiology and outcomes of acute kidney injury. *Nat. Rev. Nephrol.* 14 (10), 607–625. doi:10.1038/s41581-018-0052-0

Jiao, B., An, C., Du, H., Tran, M., Wang, P., Zhou, D., et al. (2021a). STAT6 deficiency attenuates myeloid fibroblast activation and macrophage polarization in experimental folic acid nephropathy. *Cells* 10 (11), 3057. doi:10.3390/cells10113057

Jiao, B., An, C., Tran, M., Du, H., Wang, P., Zhou, D., et al. (2021b). Pharmacological inhibition of STAT6 ameliorates myeloid fibroblast activation and alternative macrophage polarization in renal fibrosis. *Front. Immunol.* 12, 735014. doi:10.3389/fimmu.2021.735014

Karasawa, T., and Steyger, P. S. (2015). An integrated view of cisplatin-induced nephrotoxicity and ototoxicity. *Toxicol. Lett.* 237 (3), 219–227. doi:10.1016/j.toxlet.2015.06.012

Katsyuba, E., Mottis, A., Zietak, M., De Franco, F., van der Velpen, V., Gariani, K., et al. (2018). De novo NAD(+) synthesis enhances mitochondrial function and improves health. *Nature* 563 (7731), 354–359. doi:10.1038/s41586-018-0645-6

Kim, D. H., Jung, Y. J., Lee, J. E., Lee, A. S., Kang, K. P., Lee, S., et al. (2011). SIRT1 activation by resveratrol ameliorates cisplatin-induced renal injury through deacetylation of p53. *Am. J. Physiol. Ren. Physiol.* 301 (2), F427–F435. doi:10.1152/ajprenal.00258.2010

Ko, J. K., Lam, F. Y., and Cheung, A. P. (2005). Amelioration of experimental colitis by Astragalus membranaceus through anti-oxidation and inhibition of adhesion molecule synthesis. *World J. Gastroenterol.* 11 (37), 5787–5794. doi:10.3748/wjg.v11.i37.5787

Lameire, N. H., Bagga, A., Cruz, D., De Maeseneer, J., Endre, Z., Kellum, J. A., et al. (2013). Acute kidney injury: an increasing global concern. *Lancet* 382 (9887), 170–179. doi:10.1016/s0140-6736(13)60647-9

Latcha, S., Jaimes, E. A., Patil, S., Glezerman, I. G., Mehta, S., and Flombaum, C. D. (2016). Long-term renal outcomes after cisplatin treatment. *Clin. J. Am. Soc. Nephrol.* 11 (7), 1173–1179. doi:10.2215/cjn.08070715

Li, H. D., Meng, X. M., Huang, C., Zhang, L., Lv, X. W., and Li, J. (2019a). Application of herbal traditional Chinese medicine in the treatment of acute kidney injury. *Front. Pharmacol.* 10, 376. doi:10.3389/fphar.2019.00376

Li, J., Li, T., Li, Z., Song, Z., and Gong, X. (2023a). Potential therapeutic effects of Chinese meteria medica in mitigating drug-induced acute kidney injury. *Front. Pharmacol.* 14, 1153297. doi:10.3389/fphar.2023.1153297

Li, R., Shi, C., Wei, C., Wang, C., Du, H., Hong, Q., et al. (2023b). Fufang shenhua tablet, astragali radix and its active component astragaloside IV: research progress on anti-inflammatory and immunomodulatory mechanisms in the kidney. *Front. Pharmacol.* 14, 1131635. doi:10.3389/fphar.2023.1131635

Li, W., Yang, Y., Li, Y., Zhao, Y., and Jiang, H. (2019b). Sirt5 attenuates cisplatin-induced acute kidney injury through regulation of Nrf2/HO-1 and bcl-2. *Biomed. Res. Int.* 2019, 4745132. doi:10.1155/2019/4745132

Liu, M., Ye, J., Gao, S., Fang, W., Li, H., Geng, B., et al. (2014). Salvianolic acid B protects cardiomyocytes from angiotensin II-induced hypertrophy via inhibition of PARP-1. *Biochem. Biophys. Res. Commun.* 444 (3), 346–353. doi:10.1016/j.bbrc.2014.01.045

Liu, X., Huang, S., Wang, F., Zheng, L., Lu, J., Chen, J., et al. (2019a). Huangqi-danshen decoction ameliorates adenine-induced chronic kidney disease by modulating mitochondrial dynamics. *Evid. Based Complement. Altern. Med.* 2019, 9574045. doi:10.1155/2019/9574045

Liu, X., Lu, J., Liu, S., Huang, D., Chen, M., Xiong, G., et al. (2020). Huangqi-Danshen decoction alleviates diabetic nephropathy in db/db mice by inhibiting PINK1/Parkin-mediated mitophagy. *Am. J. Transl. Res.* 12 (3), 989–998.

Liu, X., Zhang, B., Huang, S., Wang, F., Zheng, L., Lu, J., et al. (2019b). Metabolomics analysis reveals the protection mechanism of huangqi-danshen decoction on adenine-induced chronic kidney disease in rats. *Front. Pharmacol.* 10, 992. doi:10.3389/fphar.2019.00992

Luo, L., Xue, J., Shao, Z., Zhou, Z., Tang, W., Liu, J., et al. (2023). Recent developments in Salvia miltiorrhiza polysaccharides: isolation, purification, structural characteristics and biological activities. *Front. Pharmacol.* 14, 1139201. doi:10.3389/fphar.2023.1139201

Majeed, Y., Halabi, N., Madani, A. Y., Engelke, R., Bhagwat, A. M., Abdesselem, H., et al. (2021). SIRT1 promotes lipid metabolism and mitochondrial biogenesis in adipocytes and coordinates adipogenesis by targeting key enzymatic pathways. *Sci. Rep.* 11 (1), 8177. doi:10.1038/s41598-021-87759-x

Martin, D. R., Lewington, A. J., Hammerman, M. R., and Padanilam, B. J. (2000). Inhibition of poly(ADP-ribose) polymerase attenuates ischemic renal injury in rats. *Am. J. Physiol. Regul. Integr. Comp. Physiol.* 279 (5), R1834–R1840. doi:10.1152/ajpregu.2000.279.5.R1834

McSweeney, K. R., Gadanec, L. K., Qaradakhi, T., Ali, B. A., Zulli, A., and Apostolopoulos, V. (2021). Mechanisms of cisplatin-induced acute kidney injury: pathological mechanisms, pharmacological interventions, and genetic mitigations. *Cancers (Basel)* 13 (7), 1572. doi:10.3390/cancers13071572

Mejía, S., Gutman, L. A. B., Camarillo, C. O., Navarro, R. M., Becerra, M. C. S., Santana, L. D., et al. (2018). Nicotinamide prevents sweet beverage-induced hepatic steatosis in rats by regulating the G6PD, NADPH/NADP(+) and GSH/GSSG ratios and reducing oxidative and inflammatory stress. *Eur. J. Pharmacol.* 818, 499–507. doi:10.1016/j.ejphar.2017.10.048

Morevati, M., Fang, E. F., Mace, M. L., Kanbay, M., Gravesen, E., Nordholm, A., et al. (2022). Roles of NAD(+) in acute and chronic kidney diseases. *Int. J. Mol. Sci.* 24 (1), 137. doi:10.3390/ijms24010137

Morigi, M., Perico, L., Rota, C., Longaretti, L., Conti, S., Rottoli, D., et al. (2015). Sirtuin 3-dependent mitochondrial dynamic improvements protect against acute kidney injury. *J. Clin. Invest.* 125 (2), 715–726. doi:10.1172/jci77632

Oh, G. S., Kim, H. J., Choi, J. H., Shen, A., Choe, S. K., Karna, A., et al. (2014). Pharmacological activation of NQO1 increases NAD$^+$ levels and attenuates cisplatin-mediated acute kidney injury in mice. *Kidney Int.* 85 (3), 547–560. doi:10.1038/ki.2013.330

Ping, F., Li, Y., Cao, Y., Shang, J., Zhang, Z., Yuan, Z., et al. (2021). Metabolomics analysis of the development of sepsis and potential biomarkers of sepsis-induced acute kidney injury. *Oxid. Med. Cell Longev.* 2021, 6628847. doi:10.1155/2021/6628847

Poyan Mehr, A., Tran, M. T., Ralto, K. M., Leaf, D. E., Washco, V., Messmer, J., et al. (2018). *De novo* NAD(+) biosynthetic impairment in acute kidney injury in humans. *Nat. Med.* 24 (9), 1351–1359. doi:10.1038/s41591-018-0138-z

Qin, Q., Niu, J., Wang, Z., Xu, W., Qiao, Z., and Gu, Y. (2012). Astragalus membranaceus inhibits inflammation via phospho-P38 mitogen-activated protein kinase (MAPK) and nuclear factor (NF)-κB pathways in advanced glycation end product-stimulated macrophages. *Int. J. Mol. Sci.* 13 (7), 8379–8387. doi:10.3390/ijms13078379

Ralto, K. M., Rhee, E. P., and Parikh, S. M. (2020). NAD(+) homeostasis in renal health and disease. *Nat. Rev. Nephrol.* 16 (2), 99–111. doi:10.1038/s41581-019-0216-6

Rasti, G., Becker, M., Vazquez, B. N., Espinosa-Alcantud, M., Fernández-Duran, I., Gámez-García, A., et al. (2023). SIRT1 regulates DNA damage signaling through the PP4 phosphatase complex. *Nucleic Acids Res.* 51 (13), 6754–6769. doi:10.1093/nar/gkad504

Roboon, J., Hattori, T., Ishii, H., Takarada-Iemata, M., Nguyen, D. T., Heer, C. D., et al. (2021). Inhibition of CD38 and supplementation of nicotinamide riboside ameliorate lipopolysaccharide-induced microglial and astrocytic neuroinflammation by increasing NAD<sup/>. *J. Neurochem.* 158 (2), 311–327. doi:10.1111/jnc.15367

Shahrajabian, M. H., Sun, W., and Cheng, Q. (2019). A review of Astragalus species as foodstuffs, dietary supplements, A traditional Chinese medicine and A part of modern pharmaceutical science. *Appl. Ecol. Environ. Res.* 17 (6), 13371–13382. doi:10.15666/aeer/1706_1337113382

Tan, B., Chen, J., Qin, S., Liao, C., Zhang, Y., Wang, D., et al. (2021). Tryptophan pathway-targeted metabolomics study on the mechanism and intervention of cisplatin-induced acute kidney injury in rats. *Chem. Res. Toxicol.* 34 (7), 1759–1768. doi:10.1021/acs.chemrestox.1c00110

Tang, C., Cai, J., Yin, X. M., Weinberg, J. M., Venkatachalam, M. A., and Dong, Z. (2021). Mitochondrial quality control in kidney injury and repair. *Nat. Rev. Nephrol.* 17 (5), 299–318. doi:10.1038/s41581-020-00369-0

Tang, C., Livingston, M. J., Safirstein, R., and Dong, Z. (2023). Cisplatin nephrotoxicity: new insights and therapeutic implications. *Nat. Rev. Nephrol.* 19 (1), 53–72. doi:10.1038/s41581-022-00631-7

Tran, M. T., Zsengeller, Z. K., Berg, A. H., Khankin, E. V., Bhasin, M. K., Kim, W., et al. (2016). PGC1α drives NAD biosynthesis linking oxidative metabolism to renal protection. *Nature* 531 (7595), 528–532. doi:10.1038/nature17184

Vachharajani, V. T., Liu, T., Wang, X., Hoth, J. J., Yoza, B. K., and McCall, C. E. (2016). Sirtuins link inflammation and metabolism. *J. Immunol. Res.* 2016, 8167273. doi:10.1155/2016/8167273

Wang, M., Chen, L., Liu, D., Chen, H., Tang, D. D., and Zhao, Y. Y. (2017). Metabolomics highlights pharmacological bioactivity and biochemical mechanism of traditional Chinese medicine. *Chem. Biol. Interact.* 273, 133–141. doi:10.1016/j.cbi.2017.06.011

Wang, T., Liu, J., Luo, X., Hu, L., and Lu, H. (2021). Functional metabolomics innovates therapeutic discovery of traditional Chinese medicine derived functional compounds. *Pharmacol. Ther.* 224, 107824. doi:10.1016/j.pharmthera.2021.107824

Wei, Q., Dong, G., Franklin, J., and Dong, Z. (2007). The pathological role of Bax in cisplatin nephrotoxicity. *Kidney Int.* 72 (1), 53–62. doi:10.1038/sj.ki.5002256

Weidemann, A., Bernhardt, W. M., Klanke, B., Daniel, C., Buchholz, B., Campean, V., et al. (2008). HIF activation protects from acute kidney injury. *J. Am. Soc. Nephrol.* 19 (3), 486–494. doi:10.1681/ASN.2007040419

White, A. T., and Schenk, S. (2012). NAD(+)/NADH and skeletal muscle mitochondrial adaptations to exercise. *Am. J. Physiol. Endocrinol. Metab.* 303 (3), E308–E321. doi:10.1152/ajpendo.00054.2012

Xu, H., Liu, Y. Y., Li, L. S., and Liu, Y. S. (2023). Sirtuins at the crossroads between mitochondrial quality control and neurodegenerative diseases: structure, regulation, modifications, and modulators. *Aging Dis.* 14 (3), 794–824. doi:10.14336/ad.2022.1123

Yang, Y., Shao, M., Cheng, W., Yao, J., Ma, L., Wang, Y., et al. (2023). A pharmacological review of tanshinones, naturally occurring monomers from Salvia miltiorrhiza for the treatment of cardiovascular diseases. *Oxid. Med. Cell Longev.* 2023, 3801908. doi:10.1155/2023/3801908

Yu, X., Meng, X., Xu, M., Zhang, X., Zhang, Y., Ding, G., et al. (2018). Celastrol ameliorates cisplatin nephrotoxicity by inhibiting NF-κB and improving mitochondrial function. *EBioMedicine* 36, 266–280. doi:10.1016/j.ebiom.2018.09.031

Yuan, H., Gao, Z., Chen, G., Peng, C., Sun, Y., Jiang, B., et al. (2022). An integrative proteomics metabolomics based strategy reveals the mechanisms involved in wasp sting induced acute kidney injury. *Toxicon* 205, 1–10. doi:10.1016/j.toxicon.2021.11.005

Zapata-Pérez, R., Wanders, R. J. A., van Karnebeek, C. D. M., and Houtkooper, R. H. (2021). NAD(+) homeostasis in human health and disease. *EMBO Mol. Med.* 13 (7), e13943. doi:10.15252/emmm.202113943

Zhang, J., Ye, Z. W., Tew, K. D., and Townsend, D. M. (2021). Cisplatin chemotherapy and renal function. *Adv. Cancer Res.* 152, 305–327. doi:10.1016/bs.acr.2021.03.008

Zheng, J., Devalaraja-Narashimha, K., Singaravelu, K., and Padanilam, B. J. (2005). Poly(ADP-ribose) polymerase-1 gene ablation protects mice from ischemic renal injury. *Am. J. Physiol. Ren. Physiol.* 288 (2), F387–F398. doi:10.1152/ajprenal.00436.2003

# The nuclear factor kappa B signaling pathway is a master regulator of renal fibrosis

Na Ren[1], Wen-Feng Wang[2], Liang Zou[3], Yan-Long Zhao[4]*, Hua Miao[5]* and Ying-Yong Zhao[5]*

[1]The First School of Clinical Medicine, Shaanxi University of Chinese Medicine, Xianyang, Shaanxi, China, [2]School of Pharmacy, Heilongjiang University of Chinese Medicine, Harbin, China, [3]School of Food and Bioengineering, Chengdu University, Chengdu, Sichuan, China, [4]Dialysis Department of Nephrology Hospital, Shaanxi Traditional Chinese Medicine Hospital, Xi'an, Shaanxi, China, [5]School of Pharmacy, Zhejiang Chinese Medical University, Hangzhou, Zhejiang, China

Renal fibrosis is increasingly recognized as a global public health problem. Acute kidney injury (AKI) and chronic kidney disease (CKD) both result in renal fibrosis. Oxidative stress and inflammation play central roles in progressive renal fibrosis. Oxidative stress and inflammation are closely linked and form a vicious cycle in which oxidative stress induces inflammation through various molecular mechanisms. Ample evidence has indicated that a hyperactive nuclear factor kappa B (NF-kB) signaling pathway plays a pivotal role in renal fibrosis. Hyperactive NF-kB causes the activation and recruitment of immune cells. Inflammation, in turn, triggers oxidative stress through the production of reactive oxygen species and nitrogen species by activating leukocytes and resident cells. These events mediate organ injury through apoptosis, necrosis, and fibrosis. Therefore, developing a strategy to target the NF-kB signaling pathway is important for the effective treatment of renal fibrosis. This Review summarizes the effect of the NF-kB signaling pathway on renal fibrosis in the context of AKI and CKD (immunoglobulin A nephropathy, membranous nephropathy, diabetic nephropathy, hypertensive nephropathy, and kidney transplantation). Therapies targeting the NF-kB signaling pathway, including natural products, are also discussed. In addition, NF-kB-dependent non-coding RNAs are involved in renal inflammation and fibrosis and are crucial targets in the development of effective treatments for kidney disease. This Review provides a clear pathophysiological rationale and specific concept-driven therapeutic strategy for the treatment of renal fibrosis by targeting the NF-kB signaling pathway.

KEYWORDS

nuclear factor kappa B, renal fibrosis, inflammation, acute kidney injury, chronic kidney disease, natural products

## 1 Introduction

Renal fibrosis has become a significant public health problem because of its high morbidity and mortality worldwide (Mantovani and Zusi, 2020; Kalantar-Zadeh et al., 2021; Yu et al., 2022). Acute kidney injury (AKI) and chronic kidney disease (CKD) are the most common kidney diseases that can lead to renal fibrosis (hAinmhire and Humphreys, 2017). AKI is an extraordinarily dangerous clinical syndrome due to the rapid decline in kidney function and tubulointerstitial inflammatory cell infiltration, which leads to the

accumulation of end products such as creatinine and urea, resulting in a decrease in urine output (Reid and Scholey, 2021). Accumulating evidence indicates that renal tubular cells have an impact on AKI-mediated inflammation, which often results in increased mortality rates, hospitalization time, and medical-related costs (Hoste et al., 2018). Importantly, episodes of AKI are associated with short-term adverse outcomes, and advanced AKI may also result in the development of CKD and even end-stage renal disease (ESRD) (Song et al., 2021). ESRD is a worldwide socioeconomic burden, and patients require renal replacement therapy through dialysis or kidney transplantation (Webster et al., 2017; Choueiri et al., 2022). Moreover, AKI and CKD cause chronic inflammation, which can lead to renal fibrosis (Jin et al., 2021; Nikolic-Paterson et al., 2021). In fact, renal fibrosis is accompanied by the excessive accumulation of extracellular matrix (ECM) proteins, such as fibronectin (FN) and various collagens, in the glomerulus and renal tubulointerstitium (Zhao et al., 2020; Ren et al., 2023b). Regardless of the etiology, renal fibrosis is a chronic and progressive process that leads to a decline in renal function during CKD (Miao et al., 2020; Miao et al., 2022a). Oxidative stress and inflammation play central roles in progressive renal fibrosis. Oxidative stress and inflammation are closely linked and form a vicious cycle in which oxidative stress induces inflammation through various underlying molecular mechanisms (Wang et al., 2023b). Nuclear factor kappa B (NF-ƙB) affects various types of cells and is important for inflammation, the immune response, the cell cycle, and cell survival (Shih et al., 2015). Numerous publications have suggested that the NF-ƙB signaling pathway regulates the inflammatory response and is associated with the pathogenesis of renal fibrosis (Zhang and Sun, 2015; Song et al., 2019). Thus, the potential of NF-ƙB as a drug target for the treatment of renal fibrosis could lead to more specific concept-driven therapeutic strategies. This Review discusses the roles of the NF-ƙB signaling pathway in both AKI and CKD, as well as the possibility of therapeutically targeting the NF-ƙB signaling pathway in renal fibrosis.

# 2 Renal fibrosis

Fibrosis is an enormous burden that affects 25% of the world's population and can contribute to the failure of organ structural integrity, functional impairment, and even death (Chen T. K. et al., 2019; Rashid et al., 2022). The annualized incidence of major fibrosis-related conditions is nearly 1 in 20 (Zhao et al., 2020). Approximately 45% of total disease-related deaths are associated with abnormal fibroblast activation and fibrosis (Distler et al., 2019). Similarly, renal fibrosis is a final common stage in most CKD cases and results from renal injury when the wound healing and repair processes are dysregulated (Ren et al., 2023a). It involves inflammatory cell infiltration, intrinsic renal cell damage and apoptosis, cell phenotypic transition to fibroblasts and myofibroblasts, abnormal secretion of inflammatory cytokines, and ECM deposition (Yang et al., 2019). Physiologically, the phenotypic transition between epithelial cells and fibroblasts/myofibroblasts is fundamental for tissue development and homeostasis. However, abnormal epithelial-mesenchymal crosstalk results in the formation of a profibrotic milieu, which inhibits the normal wound repair process. Repetitive or persistent injury to the epithelium initiates

HYPERLINK "https://www.sciencedirect.com/topics/pharmacology-toxicology-and-pharmaceutical-science/fibrosis" \o "Learn more about fibrosis from ScienceDirect's AI-generated Topic Pages" fibrosis (Prasad et al., 2014). The kidney can be divided into three main compartments, the tubulointerstitial system, glomerular system and vascular system, each of which may be exposed to fibrosis such as glomerulosclerosis, tubulointerstitial fibrosis, vasculoarterial sclerosis, and perivascular fibrosis (Djudjaj and Boor, 2019). Sclerotic lesions in the glomerular tuft predominantly consist of capillary basement membrane proteins with smaller amounts of fibrillar collagens III and V, whereas periglomerular fibrosis and fibrosis within glomerular crescents typically contain higher levels of collagen I (Duffield, 2014). Interstitial fibrosis is defined as the excessive synthesis and deposition of ECM components and is associated with inflammatory cell infiltration, tubular epithelial cell damage, fibroblast activation and proliferation, and rarefaction of the peritubular microvasculature (Yu et al., 2022). In most cases, renal fibrosis is closely associated with tubular cell injury, which can progress to tubular atrophy, as shown by renal biopsy. At this stage, we consider tubular (and nephron) damage irreversible. In many cases, interstitial fibrosis and tubular atrophy occur in parallel, which leads to interstitial fibrosis (Djudjaj and Boor, 2019). Vasculoarterial sclerosis and perivascular fibrosis are fibrous thickenings of the intima and extima of the vascular network, respectively (Djudjaj and Boor, 2019). Fibrosis involves nearly all types of cells in the kidneys (pericytes, endothelial cells, mesangial cells, and podocytes), as well as macrophages and fibroblasts, and different pathways are involved in the pathogenesis of renal fibrosis, illustrating the immense complexity of this process (Liu, 2011; Feng et al., 2020). In summary, excessive fibrosis is a key factor in the development of kidney disease, and it is an irreversible progression that can impair renal function and cause severe organ failure (Li et al. , 2021).

## 2.1 Mechanisms of renal fibrosis

Renal fibrosis is a characteristic final stage of inflammation that occurs in almost all renal diseases (Lin et al., 2020). Fibrosis affects all areas of the kidney, eventually leading to renal parenchymal destruction and ESRD (Gusev et al., 2021; Malaki, 2022). The process of renal fibrosis involves five stages. First, inflammation and massive mononuclear/macrophage infiltration activate the renal tubular epithelium. Macrophages are divided into M0, M1, and M2 types. M1 macrophages promote the Th1-type inflammatory response by secreting inflammatory factors such as interleukin-1 (IL-1), interleukin-6 (IL-6), interleukin-12, and tumor necrosis factor-alpha (TNF-α) (Yang et al., 2021). Second, excessive production of fibrogenic cytokines and growth factors, such as transforming growth factor (TGF)-β and connective tissue growth factor (CTGF), occurs (Nastase et al., 2018). Third, an imbalance in the compounding and degrading of ECM occurs, and excessive ECM accumulates in the renal interstitium, which is the main stage of renal structural and functional damage. Key mediators that drive EMT conversion, such as TGF-β/Smads, interleukins, Wnt/β-catenin, Twist1, and Snail1, are activated in renal tubular epithelial cells after injury (Sun et al., 2016). Fourth, intrinsic renal cell interstitial alterations occur, which are accompanied by a reduction in the number of intrinsic kidney
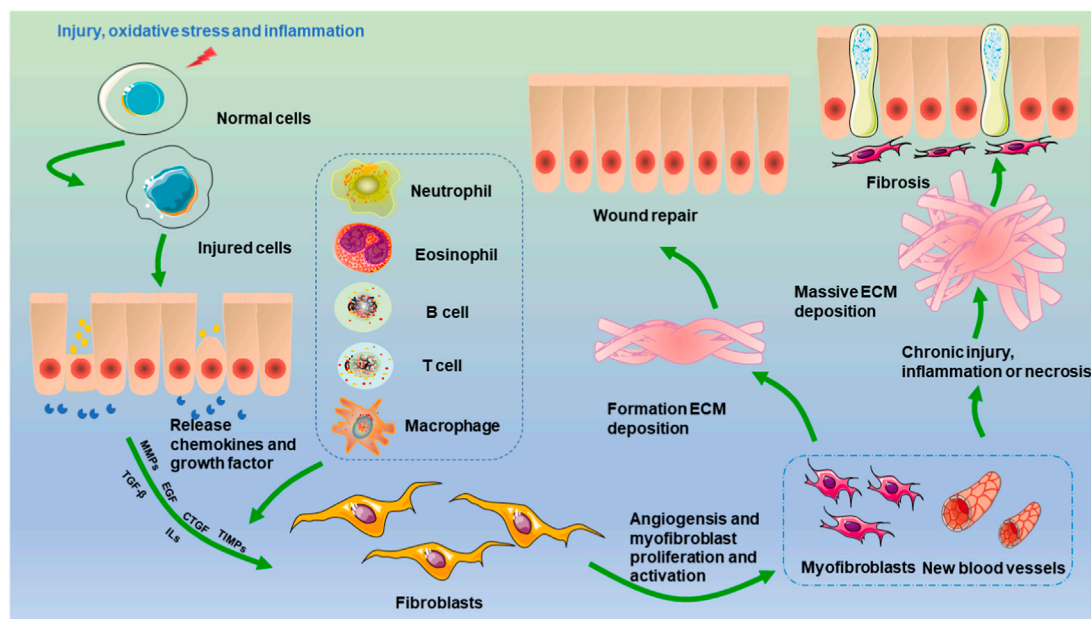
**FIGURE 1**
Mechanisms of renal fibrosis. Injury, oxidative stress, and inflammation stimulate the transformation of epithelial cells, endothelial cells, and pericytes. The activation of monocytes and macrophages leads to the production of cytokines and chemokines, which stimulate the activation of fibroblasts. Two events occur once activated fibroblasts are changed into myofibroblasts. One is the healing of damaged tissue, which is followed by wound contraction and regrowth of the epithelium. On the other hand, when persistent damage, an inflammatory response, and necrosis occur, myofibroblasts become permanently active, excessive ECM is produced, and renal fibrosis ultimately occurs.

cells. Finally, renal microangiopathy results in renal interstitial ischemia and hypoxia (Wei et al., 2022). Renal fibrosis is characterized by tubular loss and ECM accumulation, and myofibroblasts, which are a potent and effective form of fibroblast, are often regarded as the primary source of ECM production during renal fibrosis (Wu et al., 2022). During fibrosis, aberrant fibroblast activation and the expression of α-SMA indicate that myofibroblasts contribute significantly to the pathogenesis of kidney fibrosis. After injury, inflammatory cells infiltrate renal tissue, and the subsequent production of inflammatory cytokines activates fibroblasts to proliferate and produce extracellular matrix proteins, such as collagen I, III, IV, and FN (Sun et al., 2016). Damaged renal tubules and invading inflammatory cells produce profibrotic factors, resulting in the activation of myofibroblasts through paracrine or autocrine mechanisms (Quan et al., 2020). In addition to immunological factors, a wide array of non-immunologic elements, such as reactive oxygen species (ROS) and advanced glycation end products (AGEs), as well as diseases such as hyperglycemia, hypertension, and hypoxia, influence the development of renal fibrosis (Meng et al., 2014; Wu et al., 2021; Wang et al., 2023c). Oxidative stress is enhanced in CKD patients, especially those with diabetic kidney disease. An imbalance between ROS production and scavenging occurs through dysfunctional mitochondrial respiration (Honda et al., 2019). AGEs are slowly degraded with blood glucose control under hyperglycemic conditions. Furthermore, receptor for advanced glycation end products (RAGE) expression is increased in aging kidneys and DN, and the increase in RAGE expression mediates the sustained activation of oxidative stress and inflammation via the NF-ƙB signaling pathway (Rungratanawanich et al., 2021).

## 2.2 Renal fibrosis and inflammation

A wide range of noxious irritants, such as dysmetabolism, inflammation, autoimmune infection, and trauma, may lead to the dysregulation of various molecular pathways that initiate and drive fibrosis (Feng et al., 2019b; Djudjaj and Boor, 2019; Wang et al., 2023c; Rashid et al., 2023). Extensive evidence has suggested that the inflammatory response plays an integral role in the development of renal fibrosis (Chen et al., 2016; Luo et al., 2021) (Figure 1). Acute inflammation, which is the initial period of inflammation, is mediated by the activation of the immune system, is an essential part of the innate defense mechanism, is short in duration, and is typically beneficial to the host (Sobhon, 2023a). In the context of acute inflammation, the initiation of an inflammatory response occurs because of a stimulus, which subsequently leads to the release of various cytokines and chemokines, such as IL-1, IL-6, interferon gamma, and TNF. These molecules play pivotal roles in driving localized and systemic responses. Additionally, immune cells, particularly macrophages and neutrophils, are recruited and proliferate. Ultimately, the threat is eliminated, allowing for the restoration of baseline conditions and subsequent tissue repair (Bennett et al., 2018). However, if acute inflammation worsens and cannot be controlled, a second phase (chronic inflammation) is triggered, which may predispose the host to a number of chronic diseases, including fibrosis (Bennett et al., 2018; Tan et al., 2022; Sobhon, 2023b). Although acute inflammation is beneficial in the early stages of kidney injury, chronic inflammation leads to renal fibrosis. Kidney injury induces an inflammatory response that is protective, and a sustained inflammatory response can contribute to renal fibrosis. During this process, leukocytes and fibrotic cells are
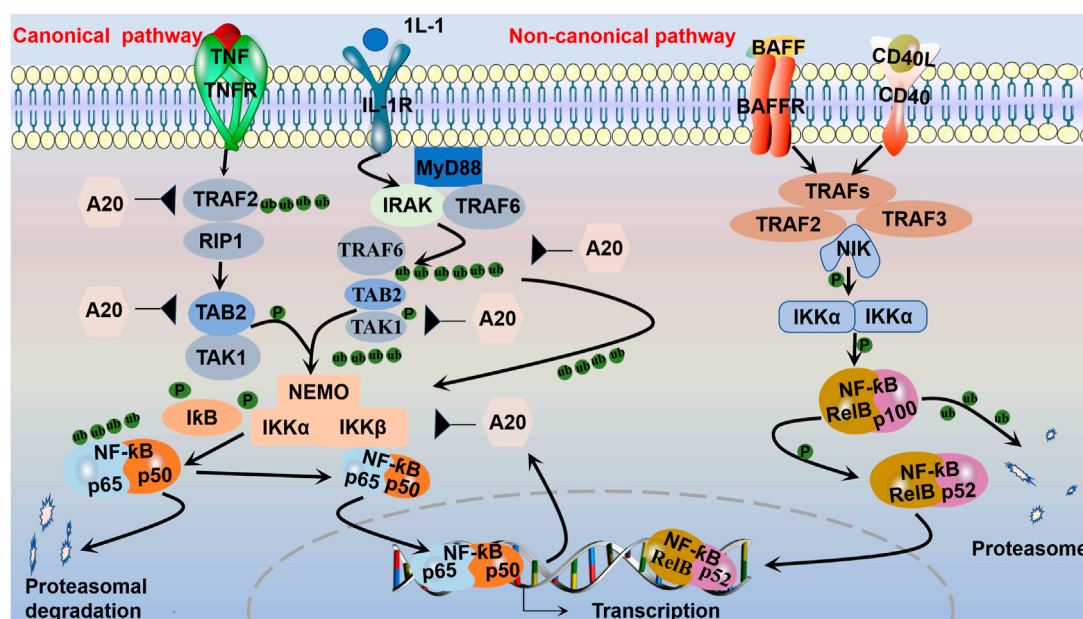
**FIGURE 2**
Canonical and non-canonical NF-ƙB pathways. The canonical pathway, which is triggered by TLRs and proinflammatory cytokines, such as TNF-α and IL-1, is activated by the kinase complex composed of IKKα, IKKβ, and regulatory NEMO, which are activated via TRAF complexes to ubiquitinate transforming growth factor beta-activated kinase (TAK1, TAB2). The activated IKKα-IKKβ-NEMO complex phosphorylates and leads to the ubiquitination of IƙB bound to NF-ƙB dimers (such as p50-p65). Then, the p50-p65 complex translocates to the nucleus to activate the transcription of target genes. After activation, the synthesized IƙB proteins and TRAF bind to and inhibit NF-ƙB activity and traffic it back to form a negative feedback loop. The non-canonical pathway is activated by receptors and their corresponding ligands, such as the ligand for CD40 (CD40L) and the ligand for BAFFR (BAFF). Inhibitory IKKα then phosphorylates p100, marking it for partial proteasomal degradation into p52. RelB-bound p52 is subsequently translocated to the nucleus to regulate gene transcription.

recruited to the glomerulus and renal interstitium and activate resident renal immune cells, and this recruitment contributes to increased levels of proinflammatory cytokine production (Chung et al., 2023). The chemokine gradient further drives the infiltration of monocytes/macrophages, T cells, and B cells toward the site of injury. Moreover, chemokines are mediators of angiogenesis, fibroblast recruitment, and epithelial-to-mesenchymal transition (Lv et al., 2018). In addition, a proportion of bone marrow-derived macrophages are transformed into myofibroblasts through macrophage-to-myofibroblast transition (MMT), and these cells coexpress a macrophage marker (CD68) and alpha-smooth muscle actin, produce collagen I, and promote renal fibrosis (Lan, 2022). A recent study suggested that bone marrow-derived macrophages could also lead directly to renal fibrosis via MMT. For instance, *in vitro* and *in vivo* experiments have indicated that macrophages infiltrating the glomerulus in patients with diabetic nephropathy can be converted to myofibroblasts through MMT, ultimately leading to renal fibrosis (Wei et al., 2022). Currently, several approaches to protecting against renal fibrosis through an anti-inflammatory pathway have recently attracted increased attention (Stenvinkel et al., 2021).

# 3 NF-ƙB signaling pathway-mediated inflammation

It is well established that NF-ƙB belongs to the Rel family of transcription factors, and there are five distinct members of the NF-

ƙB family that share similar amino acid sequences: p50/p105 (NF-ƙB1), p52/p100 (NF-ƙB2), RelB, c-Rel, and p65 (RelA) (Xiao et al., 2001). NF-ƙB activation has been shown to play a role in promoting cell proliferation and regulating cell survival. It is generally observed that NF-ƙB possesses antiapoptotic properties. Notably, RelA-null mice exhibited significant TNF-mediated liver apoptosis. Both TNF and TNF-related apoptosis-induced ligand have been shown to activate concurrent death and NF-ƙB-dependent survival signals in renal cells. When NF-ƙB is inhibited, cell death is promoted. However, NF-ƙB/RelA activation is implicated in podocyte apoptosis in HIV-transgenic mice, which is mediated by NF-ƙB-dependent Fas and Fas ligand expression in nephrotoxin- and ischemia-induced tubular cell apoptosis (Sanz et al., 2010). The aggregation of activated NF-ƙB subunits into heterodimeric transcription factor complexes results in DNA-binding capacity and transactional activation potential. NF-ƙB, which is a heterodimer of p50 and p65, is a powerful activator of gene transcription (Song et al., 2019). NF-ƙB is an important signaling factor that regulates gene transcription and controls various processes, such as immunity, inflammation, cell growth, and apoptosis. The regulation of these genes is crucial for maintaining immune and inflammatory balance. Two different NF-ƙB pathways, the canonical and non-canonical NF-ƙB pathways, have different activation mechanisms (Lawrence, 2009) (Figure 2). Apparently, variations in NF-ƙB transcriptional activity are generated by multiple kinases phosphorylating the p50 subunit in response to various stimuli (Vermeulen et al., 2002). Activation of the canonical NF-ƙB pathway is mediated by the receptor, which

does not require new protein synthesis and takes place within a few minutes, as opposed to activation of the non-canonical NF-ƙB pathway, which requires the synthesis of new proteins and is activated over a longer time period (Zarnegar et al., 2008). The release of various cellular stress factors, including cytokines such as TNF-α, IL-1, and growth factors, as well as neurotrophic factors or viral infections, promotes the cellular stress response by causing the transcription of certain genes that activate NF-ƙB (Singh and Singh, 2020). The inhibition of NF-ƙB entry into the nucleus or transcriptional alterations in the absence of stimulation by binding to inhibitor of kappa B (IƙB) maintains the inactive state of NF-ƙB dimers (Singh and Singh, 2020). The family of IƙB proteins consists of IƙBα, IƙBβ, and B-cell lymphoma-3; IƙBα can bind to heterodimeric (p50/Rel A) protein complexes (Yu et al., 2020). IƙBα can be divided into three structural domains: a 70-amino-acid N-terminal region, a 205-amino-acid internal region that is composed of ankyrin repeats, and a 42-amino-acid C-terminal region that contains a so-called PEST region. Mutation and protease sensitivity studies indicate that deletion of the N-terminal or C-terminal region does not inhibit the ability of IƙBα to interact with NF-ƙB. However, deletion of the C-terminus blocks the ability of IƙBα to inhibit the DNA binding of NF-ƙB. Mutations within the ankyrin repeat block interactions with NF-ƙB (Baldwin, 1996).

## 3.1 Canonical and non-canonical NF-ƙB signaling pathway

### 3.1.1 Activation of the canonical NF-ƙB signaling pathway

Phosphorylation of the inhibitor of kappa B kinase (IKK) complex is the critical step in canonical NF-ƙB activation (Chen and Stark, 2019; Yu et al., 2020). Central to the activation of the canonical pathway is signal-induced IƙB phosphorylation by IKK. The IKK complex contains two kinase subunits, IKKα (IKK1) and IKKβ (IKK2), as well as the regulatory subunit IKKγ (NEMO) (Eluard et al., 2020). IKKβ modulates canonical pathway activation via phosphorylation of IƙB and requires the IKKγ subunit. By contrast, IKKα is essential for substitution pathway activation through the phosphorylation and processing of p100, which is isolated from both IKKβ and IKKγ (Sivandzade et al., 2019; Yu et al., 2020). IKKγ has no known intrinsic kinase activity but contains helix-loop-helix and leucine-zipper motifs that are known to be involved in protein-protein interactions. Without two IKKs or NEMO in MEFs, NF-ƙB activation is completely blocked after induction with various stimuli (Li and Verma, 2002). The IƙB protein keeps RelA and p50 away from the cytoplasm under stable conditions. By contrast, the inhibitor protein IƙB degrades IKK, allowing the transfer of heterodimers (e.g., p50/p65) from the cytosol to the nucleus, where they associate with DNA to enable the transcription of some genes encoding proinflammatory mediators (Song et al., 2019). This activation is rapid and transient, and the gene is simultaneously expressed with negative regulators such as IƙBα, p105, and A20, which are subsequently transported back to form a negative feedback loop (Blanchett et al., 2021). Deubiquitination is also essential for the inhibition of NF-ƙB. A20 inhibits NF-ƙB activity by deubiquitinating a few

intermediary NF-ƙB signaling proteins, such as receptor-interacting protein 1 and tumor necrosis factor receptor associated factor. A20 is an important negative feedback regulator of NF-ƙB that is required for immune homeostasis. Early studies suggested that A20 may target the upstream receptor proximal molecule RIP1 in the TNF receptor and the ubiquitin-activating enzyme (E3) ligase TNF receptor-associated factor 6 in the IL-1 receptor signaling pathway to inhibit NF-ƙB activation (Pujari et al., 2013). During ubiquitination, the carboxy-terminal end of ubiquitin is covalently attached to a lysine in the target protein. Ubiquitination consists of a three-step enzymatic cascade initiated by the activation of ubiquitin by a ubiquitin-activating enzyme (E1) followed by the transfer of the activated ubiquitin to the active cysteine of a ubiquitin-conjugating enzyme (E2); ultimately, with the assistance of a ubiquitin-activating enzyme (E3) or ubiquitin ligase, the ubiquitin is transferred to a lysine on a substrate protein to form an isopeptide bond (Harhaj and Dixit, 2011). After the first ubiquitin molecule is added to a target protein, further ubiquitin molecules can attach to the first ubiquitin molecule, generating polyubiquitin chains (Napetschnig and Wu, 2013). The NF-ƙB pathway is negatively regulated by additional deubiquitinases in specific cells, including cylindromatosis, ovarian tumor domain deubiquitinase with linear linkage specificity (OTULIN), and cellular zinc finger anti-NF-ƙB (Cezanne) (Chen and Stark, 2019; Song et al., 2019).

### 3.1.2 Activation of the non-canonical NF-ƙB signaling pathway

TNF cytokines and their corresponding TNF receptors activate atypical signaling pathways. Although alternative receptors are available to mediate the non-canonical NF-ƙB pathway, TNF receptors are commonly recognized. The TNF receptor family includes the lymphotoxin-β receptor, fibroblast growth factor-inducible factor 1, and B-cell activating factor receptor. NF-ƙB-inducible kinase (NIK) is activated by TNF or other relevant receptors, initiating the atypical pathway. In response to activation, the E3 ubiquitin ligase, which is a cellular inhibitor of apoptosis, degrades tumor necrosis factor receptor-associated factor 3 and contributes to NIK accumulation. When the accumulated levels are sufficient, NIK phosphorylates and activates IKKα in the IKK complex, and IKKα phosphorylates p100, a precursor subunit of NF-ƙB. Moreover, the SCF$^{bTrCP}$ ubiquitin ligase complex phosphorylates p100, which is subsequently converted by the proteasome into p52, an NF-ƙB subunit with transcriptional functions. Genetic evidence has indicated that NIK is a core and specialized component of the non-canonical NF-ƙB pathway (Sun S. C., 2017).

## 3.2 Regulation of inflammation in renal fibrosis by the NF-ƙB signaling pathway

Inflammatory responses are characterized by the coordinated triggering of various pathways that regulate the expression of proinflammatory and anti-inflammatory mediators in resident tissue cells and blood-borne leukocytes (Lawrence, 2009). NF-ƙB has been proven to activate more than 500 genes that have been linked to inflammation-related

**FIGURE 3**
Oxidative stress and NF-ƙB-mediated inflammation in renal fibrosis and injury. Injurious stimuli trigger oxidative stress and inflammation and the secretion of inflammatory factors such as IL-1 and TNF-α. Inflammation activates TLR4 and stimulates quiescence in NF-ƙB in the renal tubular epithelium. Subsequently, excessive amounts of fibrogenesis-associated cytokines and growth factors, such as TGF-β, are produced. The chemokine gradient further drives cells to the site of injury. After injury, inflammatory cells infiltrate the renal tubular epithelium, and subsequent inflammatory cytokines activate myofibroblasts to proliferate and produce ECM. This eventually leads to renal fibrosis.

responses (Gupta et al., 2010). NF-ƙB, which is a crucial regulator of inflammation and cell survival, is part of a classic pathway associated with the inflammatory response and a promising target for the diagnosis and treatment of kidney disease (Lawrence, 2009; Song et al., 2019). Inflammation is regulated at the molecular level by a variety of factors and molecules, including adhesion molecules such as intercellular adhesion molecules, chemokines such as monocyte chemoattractant protein 1 and interleukin-8, cytokines such as IL-6, TNF-α, and tumor necrosis factor-beta, proinflammatory enzymes such as cyclooxygenase-2 (COX-2) and 5-lipoxygenase, vascular endothelial growth factor, and the proinflammatory transcription factor NF-ƙB (Aggarwal, 2004). Among these mediators, NF-ƙB is a crucial regulator of inflammation (Ahn and Aggarwal, 2005). Peng et al. reported that autophagy-related protein 5 (ATG5) was essential for controlling inflammation during kidney fibrosis development. By limiting NF-ƙB signaling, ATG5 reduced the inflammatory response induced by wounded tubular epithelial cells in an autophagy-dependent manner (Peng et al., 2019). Garcinol suppressed NF-ƙB and proinflammatory cytokines such as TNF-α and IL-6, which preserved the nuclear expression of nuclear factor erythroid-derived 2-related factor 2 (Nrf2) and the levels of Nrf2-dependent antioxidants, including heme oxygenase-1 (HO-1), catalase, superoxide dismutase 1, and nicotinamide adenine dinucleotide phosphate quinone dehydrogenase 1 (NQO1), in tubulointerstitial fibrosis induced by non-diabetic unilateral ureteral obstruction (UUO). The administration of garcinol, a p300/CBP-associated factor (PCAF) inhibitor, effectively reversed the UUO-induced upregulation of total PCAF

expression and histone 3 lysine 9 acetylation in the kidney. Additionally, it led to reductions in trichrome-positive staining areas, α-smooth muscle actin, and collagen. Furthermore, treatment with garcinol decreased the mRNA levels of TGF-β, matrix metalloproteinase-2, matrix metalloproteinase-9, and FN (Chung et al., 2019). These discoveries suggest that NF-ƙB is crucial for the progression of chronic inflammation in the kidney (Tak and Firestein, 2001).

# 4 The NF-ƙB signaling pathway in renal disease

Aseptic inflammation, which occurs in the absence of infection or particular immunogens, plays an essential role in the inhibition of renal fibrosis (Lopez-De La Mora et al., 2015). The complex interplay between many intracellular signaling pathways influences the process of renal fibrosis. In the context of kidney damage, NF-ƙB is a significant transcriptional driver of inflammation and fibrosis (Reid and Scholey, 2021) (Figure 3). UUO is a classic model of renal fibrosis. Activation of the NF-ƙB signaling pathway has been demonstrated in the obstructed kidneys of UUO mice (Wang et al., 2020). Inflammation, including macrophage infiltration and the generation of proinflammatory cytokines, is the primary etiology of renal interstitial fibrosis following ureteral obstruction (Chevalier et al., 2009). Ongoing inflammation can lead to gradual kidney damage and eventually permanent renal parenchymal damage (Xianyuan et al., 2019).

## 4.1 The NF-ƙB signaling pathway in AKI

AKI is a condition with a wide range of pathologies (Siew and Davenport, 2015; Ma et al., 2023). AKI is characterized by a rapid decrease in kidney function and a high level of morbidity and mortality. Sepsis, ischemia-reperfusion injury (IRI), and nephrotoxicity (radiographic agents and non-steroidal anti-inflammatory drugs) are the main factors involved in the development of AKI (Amrouche et al., 2017; Wang J. et al., 2022). Increasing evidence suggests that AKI-associated renal inflammation can be sustained even following the remission of acute injury and the recovery of renal function, resulting in the slow progression of renal fibrosis (Andrade-Oliveira et al., 2019). AKI etiologies are categorized as prerenal, intrinsic renal, or postrenal. Type 1 cardiorenal syndrome and hepatorenal syndrome decrease the effective circulating volume and increase central venous pressure, further leading to renal dysfunction and the development of prerenal AKI. If early intervention is not timely, renal parenchymal ischemia worsens, and renal tubular cell damage in prerenal AKI can further develop into AKI (Turgut et al., 2023). By contrast, AKI is an ischemic injury to the kidney, and the etiology of AKI can be divided into glomerular, tubulointerstitial, and vascular diseases. Among these conditions, acute tubular necrosis (ATN) is the major known cause of intrarenal AKI, which can include renal ischemia and nephrotoxicity and can cause harm to tubular endothelial and epithelial cells, leading to the development of ATN. Ischemic ATN is caused by persistent hypotension, hypovolemia, and low renal irrigation and is most common in patients with severe hypotension. Postrenal AKI is mainly caused by obstruction; 5%–10% of AKI cases are caused by urinary tract obstruction and it is more common in elderly individuals, and the most common types of obstruction are prostate cancer, prostate hypertrophy, cervical cancer, and retroperitoneal disease (Mercado et al., 2019).

AKI causes inflammation that exacerbates kidney damage, and controlling inflammation has been shown to mitigate further deterioration of kidney injury and promote slow recovery (Bonventre and Zuk, 2004). The systematic regulation of the NF-ƙB pathway, an important component of AKI pathogenesis, can influence the severity of AKI (Song et al., 2019). A previous study showed that calcium dobesilate mitigated renal impairment and inflammation in sepsis-associated AKI by downregulating the NF-ƙB signaling pathway in lipopolysaccharide (LPS)-induced mice (Xie et al., 2022). Additional studies have suggested that inhibiting miR-494 by blocking the NF-ƙB pathway, which reduces apoptosis in renal tubular epithelial cells, could attenuate the inflammatory response and oxidative stress in the kidney tissues of rats with LPS-induced AKI (Lu et al., 2022). Fisetin, a naturally occurring flavonoid, reduces inflammation in the kidney and apoptosis in mice with LPS-induced septic AKI by inhibiting the Src-mediated NF-ƙB p65 signaling pathway (Ren et al., 2020). Additionally, NF-ƙB can induce COX-2 expression, which is pivotal in the development of AKI (Ranganathan et al., 2013). Thalidomide attenuates glycerol-induced AKI in rats by inhibiting NF-ƙB and COX-2 (Amirshahrokhi, 2021). In addition, IRI is a common factor in the AKI-to-CKD transition and renal fibrosis. Postischemic fibrosis involves the AKI-to-CKD transition and is subsequently influenced by oxidative stress and inflammation.

## 4.2 The NF-ƙB signaling pathway in CKD

CKD is a progressive disease that affects between 8% and 16% of the global population and is a major cause of death (Chen T. K. et al., 2019; Rashid et al., 2022). A glomerular filtration rate less than 60 mL/min/1.73 m², an albuminuria level of at least 30 mg/24 h, or symptoms of kidney disease (such as hematuria or structural abnormalities such as polycystic or dysplastic kidneys) that persist for more than 3 months are considered indicators of kidney damage (Kalantar-Zadeh et al., 2021; Zhao, 2022). Multiple factors are involved in the inflammatory state of CKD, including oxidative stress, increased production of proinflammatory cytokines, dysbiosis of the gut flora, altered adipose tissue metabolism, acidosis, and chronic and recurrent infections (Rapa et al., 2019; Yang and Wu, 2021; Zhao, 2022; Liu et al., 2023). Oxidative stress and inflammation play significant roles in the pathophysiology of CKD. Oxidative stress and inflammation strongly interact to create a vicious cycle, and oxidative stress triggers inflammation through a number of processes, including the transcriptional activation of NF-ƙB, leading to immune cell activation and recruitment. Oxidative stress mediates inflammation through the generation of proinflammatory oxidized lipids, advanced oxidation protein products, and AGEs (Duni et al., 2019). Conversely, inflammation induces oxidative stress through the production of ROS and nitrogen species through the activation of leukocytes and resident cells. These incidents enhance renal injury by causing renal necrosis and fibrosis (Chen et al., 2017). Moreover, various studies have substantiated the anti-inflammatory effects of Nrf2 by inhibiting the expression of inflammatory genes, including those responsible for the TNF-α-induced production of monocyte chemoattractant protein-1 (MCP-1) and vascular cell adhesion molecule-1. Dysfunctional Nrf2 activation, which is observed in CKD, renders the kidneys susceptible to the impacts of oxidative stress. Furthermore, this dysfunctional activation exacerbates intrarenal inflammation by mediating the accumulation of hydroperoxides and lipoperoxides, which are potent activators of NF-ƙB (Duni et al., 2019). Globally, the most commonly reported causes of CKD are diabetes and/or hypertension, but other conditions, such as cardiovascular disease and kidney transplantation, can lead to CKD development (Luyckx et al., 2020). Next, we summarize the effect of the NF-ƙB signaling pathway on renal fibrosis in CKD (immunoglobulin A nephropathy, membranous nephropathy, diabetic nephropathy, hypertensive nephropathy, and kidney transplantation).

### 4.2.1 Immunoglobulin A nephropathy (IgAN)

Glomerular diseases present as a spectrum of clinical syndromes and include various glomerular cell types, such as mesangial cells (MCs), endothelial cells, podocytes, parietal epithelial cells, and infiltrating inflammatory cells (Scindia et al., 2010). Glomerular disease is characterized by inflammation, and activation of the NF-ƙB and TGF-β signaling pathways is important for disease progression. Immunoglobulin aggregates activate MCs by signaling through surface Fc receptors. Mesangial alterations observed after glomerular injury involve the production of chemoattractants for inflammatory cells, the proliferation of MCs, the loss of mesangial matrix (mesangiolysis), and the excessive production of ECM, which leads to mesangial

expansion (Scindia et al., 2010). Notably, drugs that target the NF-ƙB pathway in animal models have renoprotective effects, indicating that these agents may be viable treatments for glomerulopathy. IgAN is the most prevalent primary glomerulonephritis in the world (Möller-Hackbarth et al., 2021). Currently, IgAN is considered an immune-mediated disease characterized by immunoglobulin A deposition in the mesangial area (Coppo and Amore, 2004). The deposition of IgA triggers MC proliferation and monocyte/macrophage infiltration, resulting in the activation of the complement system. Subsequently, activated MCs release ECM proteins, growth factors, and proinflammatory cytokines (Apeland et al., 2020). IgAN is identified in approximately 50% of kidney biopsies in Asia and up to 45% of biopsies in China (Zhang J. et al., 2020). In particular, 30%–40% of patients with IgAN progress to ESRD within 20 years (Bai et al., 2019). A study showed the levels of 37 different inflammation-related factors in IgAN patients with stage 1–4 CKD. The IgAN group had elevated levels of nine inflammation-related factors according to univariate analysis. However, multivariate analysis revealed five important factors that were characteristic of patients with IgAN: osteopontin, a proinflammatory mediator, proliferation-inducing ligand, matrix metalloproteinase-3, TNF receptor-1, and TNF-like weak inducer of apoptosis, which are members of the TNF receptor-2 non-canonical NF-ƙB pathway. This pathway may be activated in a slow and persistent manner, and dysregulated pathway activation contributes to the pathogenesis of various inflammatory diseases (Sun S.-C., 2017). Apolipoprotein C1 is thought to be a central secretory gene associated with IgAN, and mechanistic studies have indicated that knockdown of apolipoprotein C1 can ameliorate IgAN and renal fibrosis by inhibiting the NF-ƙB pathway (Yu et al., 2023). In addition, a study revealed the increased expression of toll-like receptor 4 (TLR4) in mesangial cells, which subsequently activated the MyD88-NF-ƙB signaling pathway. This signaling cascade ultimately results in the production of proinflammatory cytokines such as TNF-α, IL-6, and MCP-1, contributing to kidney damage in secretory IgA-mediated human renal mesangial cells (Zhang J. et al., 2020).

## 4.2.2 Membranous nephropathy

The most prevalent form of adult nephrotic syndrome, which is known as membranous nephropathy (MN), is a primary glomerular disease that develops following kidney transplantation (Hua et al., 2023; Li et al., 2023). In approximately 80% of patients, MN has no root cause (primary MN), and 20% of cases are related to drugs or other diseases, such as malignancy, hepatitis virus infection, or systemic lupus erythematosus (Ronco et al., 2021; Zhao et al., 2023). MN patients are diagnosed by the presence of the phospholipase $A_2$ receptor before they progress to renal failure (Wang et al., 2022b; Salvadori and Tsalouchos, 2022). However, the subepithelium-like immunocomplex deposit-mediated downstream molecular pathways are poorly understood (Miao et al., 2023a; Miao et al., 2023b). A recent study suggested that patients with primary MN exhibited significant upregulation of CD3, NF-ƙB p65, and COX-2 protein expression and significant downregulation of Nrf2 and HO-1 protein expression in kidney tissues (Wang et al., 2023b), indicating activation of the NF-ƙB signaling pathway and impairment of the Nrf2 signaling pathway. This was further demonstrated by the significant upregulation of the protein expression of the phosphorylated inhibitors kappa B alpha, NF-ƙB p65, and downstream gene products, including COX-2,

MCP-1, inducible nitric oxide synthases, 12-lipoxygenase, $p47^{phox}$, and $p67^{phox}$; additionally, the protein expression of Nrf2 and its downstream gene products, including HO-1, catalase, the glutamate-cysteine ligase catalytic subunit, glutamate-cysteine ligase modifier subunit, manganese superoxide dismutase, and NQO1, was significantly downregulated in the kidney tissues of CBSA-induced rats (Wang et al., 2023b). These results were further verified in zymosan activation serum (ZAS)-stimulated podocytes (Wang et al., 2023b). By contrast, treatment with the NF-ƙB inhibitor BAY 11-7082 and NF-ƙB p65 siRNA inhibited the protein expression of NF-ƙB p65 and COX-2 and preserved the protein expression of Nrf2 and HO-1 in ZAS-induced podocytes (Wang et al., 2023b). Tian et al. reported that CBSA injection led to the deposition of C3 and immunoglobulin G and reduced the protein expression of podocin and synaptopodin, which are associated with the NF-ƙB signaling pathway (Miao et al., 2022b). The NF-ƙB signaling pathway plays an important role in immune modulation. Previous studies revealed that the NF-ƙB pathway is involved in the pathogenesis of MN (Wang et al., 2022b). These findings suggest the activation of oxidative stress and inflammation in MN.

## 4.2.3 Diabetic nephropathy (DN)

Diabetes mellitus occurs regardless of age, sex, ethnicity, education level, or economic status. Up to 20% of diabetic patients develop diabetic nephropathy (DN) (Hung et al., 2021; Rangel et al., 2021). DN is characterized by a thickened basal lamina, renal fibrosis, proteinuria, and the accumulation of mesangial cells (Wang H. et al., 2021). DN is related to hyperglycemia-induced metabolic changes leading to glomerular hypertrophy, glomerulosclerosis, tubulointerstitial inflammation and fibrosis, and renal remodeling, which includes glomerular and tubular hypertrophy, inflammation, and extracellular matrix accumulation (Sun et al., 2020; Wang and Chen, 2022). One of the main pathological factors in renal fibrosis linked to DN is thought to be inflammation. Infiltrating cells are also a source of cytokines and other mediators that promote the onset and progression of renal injury, as well as amplify and perpetuate a preexisting inflammatory response (Samsu, 2021). Under diabetic pathological conditions, high levels of glucose induce cells to generate massive amounts of ROS, thereby activating multiple downstream inflammatory signaling pathways and leading to the induction and accelerated development of inflammatory fibrosis (Zhuang et al., 2020). After hyperglycemic therapy, TLR4 activates high mobility group box 1, which in turn mediates the development of tubulointerstitial inflammation in DN patients. Additionally, TLR4 participates in the production of TRAF and IL-1 receptor-related kinase via myeloid differentiation factor 88, which eventually results in the production of NF-ƙB and mediates the development of DN (Zhou et al., 2021). Notably, NF-ƙB is involved in DN by regulating inflammatory factors, chemokines, and cell adhesion proteins (Navarro-González et al., 2011). By preventing the activation of the NF-ƙB pathway in a rat model of DN, silencing paternally expressed gene 3 could minimize renal fibrosis in DN (Guan et al., 2020). The NF-ƙB signaling pathway is involved in DN.

## 4.2.4 Hypertensive nephropathy

Hypertension and CKD are strongly related to pathophysiological states, and sustained hypertension leads to the

deterioration in renal function and an ongoing decrease in renal function, which leads to the deterioration in blood pressure control (Abraham et al., 2022). Chronic arterial hypertension can cause the development of renal-angiosclerosis, which is a critical cause of ESRD, and CKD might be aggravated by arterial hypertension due to different pathogenetic mechanisms, such as sympathetic hyperactivity, endocannabinoid dysfunction, and volume overload (Cice et al., 2020). According to previously published studies, the levels of C-reactive protein, TNF-α, IL-6, MCP-1, plasminogen activator inhibitor-1, and adhesion molecules are elevated in individuals with hypertension (Montecucco et al., 2011). It has been reported that $H_2S$ administration alleviates IRI by decreasing local and systemic intercellular adhesion molecule expression and NF-ĸB levels in the kidneys of normotensive and L-nitro-arginine-methyl-ester (L-NAME)-induced hypertensive rats (Hashmi et al., 2021). These findings indicate the involvement of inflammation in hypertension.

### 4.2.5 Kidney transplantation

A consistent decrease in the glomerular filtration rate is linked to the progression of CKD to ESRD (Wishahi and Kamal, 2022). Stage 5 CKD and ESRD patients require peritoneal or programmed hemodialysis or renal transplantation. Renal transplantation results in better survival for ESRD patients than dialysis treatment (Gadelkareem et al., 2023). Renal transplantation provides a better quality of life and better affordability (Cabezas et al., 2022). However, the majority of transplants experience chronic renal allograft dysfunction (CAD), which negatively impacts long-term graft survival (Zhou et al., 2022). CAD, which was previously mentioned as chronic allograft nephropathy, is a polyfactorial disease related to the progression of renal interstitial fibrosis (Gui et al., 2021). Under certain circumstances, grafts may exhibit dysfunction regardless of the immunosuppressive regimen used. The local and systemic proinflammatory state in patients worsens with the development of renal graft failure. According to the Banff classification, significant pathomorphological features of most variants of this dysfunction can reflect the molecular mechanisms involved in tissue stress that leads to fibrin formation and inflammation (Gusev et al., 2021). Kidney transplants unavoidably experience ischemia once they have been removed from the donor. Ischemia is regarded as an unavoidable event after kidney transplantation. IRI reduces the prolongation of graft survival, which has been recognized as an unavoidable event after renal transplantation. Early after surgery, IRI can lead to end-stage graft loss through a reduction in renal function clumps, which can cause graft vascular injury, chronic hypoxia, and subsequent fibrosis (Zhao et al., 2018). Consequently, an effective strategy to alleviate the IRI-induced inflammatory response and oxidative stress injury during postrenal transplantation is needed.

## 5 Therapeutic strategies targeting the NF-ĸB signaling pathway in renal fibrosis

In the clinical setting, treatments for renal fibrosis are ineffective or unsafe (Breyer and Susztak, 2016). Although numerous therapeutic strategies to prevent and treat renal fibrosis have been explored, the prognosis of patients is still poor (Salvadori and Tsalouchos, 2022). Thus, there is an urgent need for the development of specific and efficacious antifibrotic drugs to improve AKI and CKD (Tanemoto and Mimura, 2022; Allinson et al., 2023; Habshi et al., 2023; Song and Gong, 2023). Accordingly, renal fibrosis can be efficiently treated by inhibiting the NF-ĸB signaling pathway. Regardless of the underlying etiology, various strategies have been used to protect against renal fibrosis by targeting the NF-ĸB signaling pathway in this context (Table 1).

## 5.1 Chemical agents for treating renal fibrosis

For more than 50 years, metformin has been used as an antihyperglycemic medication with few negative side effects. More recently, advances have shown its antifibrotic effects on several organs, such as the kidney, liver, and other tissues (Sun et al., 2022). Glomerular tenascin-C (TNC) levels in DN rats were measured, and the effect of TNC expression on inflammatory and fibrogenic factors was examined in high glucose-cultured rat mesangial cells. After administering an miR-155-5p inhibitor to selectively suppress the expression of miR-155-5p for 6 h, the culture medium was replaced, and the cells were incubated with normal or high glucose for 24 h. This intervention reduced the levels of the fibrogenic factors FN and CTGF. Following the targeted silencing of TNC expression, there was a decrease in TLR4 expression and the phosphorylation of the inflammatory factor NF-ĸB p65. Additionally, miR-155-5p expression was downregulated, and the expression of the fibrotic factors CTGF and FN was decreased in high-glucose-treated rat mesangial cells (Zhou et al., 2021). Compared with normal rats, diabetic rats had significantly higher serum TNC levels. The levels of phosphorylated NF-ĸB p65 and miR-155-5p were significantly decreased when TNC was downregulated, indicating that TNC controlled miR-155-5p expression via the NF-ĸB signaling pathway, which controls inflammation and fibrosis in DN rats. Metformin treatment may relieve inflammation and fibrosis in individuals with DN by reducing the protein levels of TNC, p-NF-ĸB p65, CTGF, and FN (Zhou et al., 2021). Additionally, telbivudine is an orally bioavailable L-nucleoside with potent and specific antiviral activity against the hepatitis B virus, and it has been used widely to treat chronic HBV infection. Clinical findings indicate that telbivudine therapy improves renal function. A study showed that the UUO group had decreased levels of the inhibitor IĸBα and increased levels of p-IĸBα compared with those in the control group. In the telbivudine-treated group, TLR4 activation was inhibited; IKKα, p-IKKα, and p-IĸBα expression was significantly attenuated; and the decrease in IĸBα was reversed to a level that was significantly higher than that in UUO rats. These findings indicated that the NF-ĸB signaling pathway allows telbivudine to reduce renal fibrosis and inflammation in UUO patients (Chen and Li, 2018). Nifuroxazide is a safe nitrofuran antibacterial drug that is used clinically to treat acute diarrhea and infectious traveler's diarrhea or colitis. Recent studies revealed that nifuroxazide has multiple pharmacological effects, including anticancer, antioxidant, and

TABLE 1 Summary of small molecular inhibitors of NF-ĸB signaling in renal fibrosis.

| Agents | Targets | Outcomes | References |
|---|---|---|---|
| Metformin | NF-ĸB pathways | Reliving the processes of inflammation and fibrosis in individuals with DN | Zhou et al. (2021) |
| Telbivudine | NF-ĸB pathways | Reducing renal fibrosis and inflammation | Chen and Li (2018) |
| Tacrolimus | NF-ĸB pathways | Suppressing intrarenal inflammation | Kim et al. (2021) |
| Bortezomib | NF-ĸB-TNF-α-Akt-mTOR-P70S6K-Smurf2 pathway | Improving renal allograft tubulointerstitial fibrosis | Suo et al. (2021) |
| Pioglitazone | NF-ĸB pathways | Suppressing renal IRI-induced inflammation | Zou et al. (2021) |
| 5-MTP | NF-ĸB and Nrf2 pathways | Attenuating tubulointerstitial fibrosis | Chen et al. (2019a) |
| TPH-1 | NF-ĸB and Nrf2 pathways | Exacerbating renal injury and fibrosis | Chen et al. (2019a) |
| Shenkang injection | NF-ĸB and Nrf2 pathways | Ameliorating renal fibrosis by inhibiting oxidative stress and inflammation | Xu et al. (2016) |
| Chrysophanol | NF-ĸB pathways | Improving renal fibrosis | Gu et al. (2022) |
| *Poria cocos* | NF-ĸB pathway, COX-2, MCP-1, HO-1, catalase and NQO1 | Ameliorating renal fibrosis | Feng et al. (2019a) |
| Poricoic acid A | Gas6-Axl-NF-ĸB-Nrf2 pathway | Inhibiting AKI-to-CKD transition | Chen et al. (2019b) |
| Ergone *Polyporusumbellatus* | NF-ĸB and Nrf2pathways | Ameliorating tubulointerstitial fibrosis | Chen et al. (2019c) |
| | NF-ĸB and Nrf2 pathways | Ameliorating tubulointerstitial fibrosis | Chen et al. (2019c) |
| Isoliquiritigenin | NF-ĸB pathway | Lowering kidney inflammation and fibrosis | Liao et al. (2020) |
| Artemisinin | NF-ĸB pathway | Attenuating tubulointerstitial inflammation and fibrosis | Wen et al. (2019) |
| Ferulic acid | NF-ĸB pathway | Reduced podocyte damage | Qi et al. (2020) |
| Quercetin | Mincle-Syk-NF-ĸB pathway | Lessening AKI-induced kidney inflammation and damage | Tan et al. (2020) |
| Red ginseng | NF-ĸB and PI3K-Akt pathways | Improving inflammation and the oxidative stress response | Li et al. (2019) |
| Zhen-wu-tang | NF-ĸB pathway and NLRP3 inflammasome | Inhibiting kidney inflammation and improving podocyte injury and structure in MN rats | Liu et al. (2019) |
| Baicalin | TLR4-NF-ĸB pathway | Retarding renal fibrosis | Zhang et al. (2020b) |
| MiR-21-5p | NF-ĸB pathway | Progressing renal fibrosis and enhancing renal inflammation | Liu et al. (2021) |
| MiR-103a-3p | NF-ĸB p65 pathway | Leading to renal inflammation and fibrosis | Lu et al. (2019) |
| LncRNAKCNQ1OT1 | NF-ĸB pathway | Modulating DN cell proliferation, apoptosis, and fibrosis | Jie et al. (2020) |

anti-inflammatory effects (Althagafy et al., 2023). Nifuroxazide decreased the levels of proinflammatory cytokines, including TGF-β1, TNF-α, IL-1β, and MCP-1, and macrophage infiltration in a UUO rat model. Additionally, it improved renal function, decreased tissue injury and fibrosis, and reduced renal oxidative damage and inflammation, which were associated with inhibiting the NF-ĸB signaling pathway (Hassan et al., 2021). In a classical model of lupus nephritis, the administration of MRL/lpr, which are hydrophobically modified glycol chitosan nanomicelles loaded with tacrolimus, decreased glomerulosclerosis and suppressed intrarenal inflammation via the NF-ĸB signaling pathway (Kim et al., 2021). Suo et al. (2021) reported that bortezomib improved renal allograft tubulointerstitial fibrosis by inhibiting the NF-ĸB-TNF-α-Akt-mTOR-P70S6K-Smurf2 pathway via IĸBα protein stabilization. Suo et al. reported that TNF-α and MCP-1 expression was reduced in the renal tissue of rats with renal IRI, indicating that

pioglitazone suppressed the renal IRI-induced inflammatory response by inhibiting the NF-ĸB signaling pathway (Zou et al., 2021).

Our previous studies revealed that 5-methoxytryptophan (5-MTP) levels strongly correlated with clinical marker levels in patients with progressive CKD (Chen et al., 2019a). The level of 5-MTP decreased with the progression of CKD and in the obstructed kidneys of UUO mice. Treatment with 5-MTP slowed tubulointerstitial fibrosis, inhibited the NF-ĸB signaling pathway, and enhanced the Nrf2 signaling pathway in mice with UUO or IRI, as well as in HK-2 cells (Chen et al., 2019a). Our examination of the biological effects of 5-MTP on UUO mice, as well as HK-2 cells and human mesangial cells, revealed that 5-MTP mitigated the proinflammatory factor NF-ĸB p65. Additionally, it decreased the expression of its target gene products, MCP-1 and COX-2, while enhancing the expression of the anti-inflammatory and antioxidant

transcription factor Nrf2. Furthermore, there was an increase in the expression of its target gene products, HO-1 and NQO-1 (Chen et al., 2019a). Tryptophan hydroxylase-1 (TPH-1) is a key enzyme involved in 5-MTP synthesis. TPH-1 overexpression ameliorated renal damage by suppressing renal inflammation and fibrosis, whereas TPH-1 deficiency exacerbated renal injury and fibrosis by activating NF-ƙB and inhibiting the Nrf2 signaling pathway (Chen et al., 2019a). Our results indicated that TPH-1 could be a target in the treatment of CKD. Collectively, these findings suggest that the NF-ƙB signaling pathway is a critical therapeutic target for the treatment of renal fibrosis.

## 5.2 Natural products for treating renal fibrosis

Many publications have demonstrated that natural products have beneficial effects on renal fibrosis and that natural products are a promising source of new medicines (Newman and Cragg, 2020; Wang et al., 2023a). A growing body of evidence has revealed the molecular mechanisms of natural products, and numerous natural products suppress renal fibrosis though the NF-ƙB pathway (Chen et al., 2018). With the advantages of multiple pathways, multiple targets, and few side effects, Chinese medicine compounds have the potential to be used in therapeutic and adjunctive therapy for nephrogenic fibrosis. According to Chinese medicine, kidney deficiency and blood stasis are not isolated but are interrelated and coexist; kidney deficiency must be accompanied by blood stasis, and blood stasis exacerbates kidney deficiency. As a result, kidney deficiency and blood stasis coexist throughout the course of the disease. The main mechanism of CKD and the root cause of renal fibrosis is the "interior retention of damp heat and toxin stasis." Shenkang injection is widely used to treat patients with CKD (Wang et al., 2022c). Our study demonstrated that Shenkang injection and its main components, chrysophanol, emodin, and rhein, ameliorated renal fibrosis by inhibiting oxidative stress and inflammation by improving the NF-ƙB and Nrf2 signaling pathways in adenine-induced CKD rats (Xu et al., 2016). In addition, Gu et al. showed that chrysophanol improved renal fibrosis by regulating the NF-ƙB pathway (Gu et al., 2022). *Poria cocos* is a well-known medicinal mushroom that is widely used in Asia and North America. *Poria cocos* has diverse biological activities, such as anti-inflammatory, antioxidant, antitumor, and lipid-lowering effects. Our previous study demonstrated that *Poria cocos* extracts ameliorated renal fibrosis by regulating redox signaling, as indicated by the downregulated protein expression of NF-ƙB and its downstream target gene products (*COX-2* and *MCP-1*) and the upregulated protein expression of Nrf2 and its downstream target gene products (*HO-1*, catalase, and *NQO1*) in 5/6 nephrectomized rats (Feng et al., 2019a). Similarly, our study showed that poricoic acid ZM and poricoic acid ZP isolated from the surface layer of *Poria cocos* ameliorated renal fibrosis by regulating the NF-ƙB and Nrf2 signaling pathways in TGF-β1-induced HK-2 cells and UUO mice (Wang et al., 2020). Poricoic acid A is a major component of the surface layer of *Poria cocos*. Our previous study demonstrated that poricoic acid A inhibited the

AKI-to-CKD transition by regulating the Gas6-Axl-NF-ƙB-Nrf2 signaling cascade in IRI rats (Chen et al., 2019b). *Polyporus umbellatus* is commonly used for its diuretic activity and to treat renal disease (Zhao Y. Y. et al., 2009; Zhao, 2013). Ergone, one of the main components of *Polyporus umbellatus* (Zhao Y. et al., 2009; Zhao et al., 2010a; Zhao et al., 2010b), has been shown to slow renal fibrosis (Zhao et al., 2011; Chen et al., 2016). Our previous study demonstrated that the extracts of *Polyporus umbellatus* and ergone ameliorated tubulointerstitial fibrosis by activating IƙBα/NF-ƙB, which was accompanied by the significant upregulation of inflammatory genes, including *MCP-1* and *COX-2*, and the downregulation of genes in the antioxidant system, including Nrf2 and its downstream gene products (including *HO-1*, catalase, and *NQO1*) (Chen L. et al., 2019).

Isoliquiritigenin is a chalcone flavonoid found in licorice and shallots. Isoliquiritigenin has anti-inflammatory, antifibrotic, and antitumor properties. Treatment with isoliquiritigenin improved UUO-induced renal dysfunction by significantly downregulating the mRNA expression and secretion of IL-1β, IL-6, TNF-α, and MCP-1, inhibiting the phosphorylation of Syk and NF-ƙB and reducing the expression of α-SMA and Col III *in vitro and in vivo*. Isoliquiritigenin decreased kidney inflammation and fibrosis by suppressing the NF-ƙB signaling pathway in UUO mice (Liao et al., 2020). Artemisinin is known as the most powerful drug for treating malaria. Clinical research has suggested that artemisinin possesses anti-inflammatory and immunomodulatory characteristics in addition to its antimalarial effect. Artemisinin plays a protective role in attenuating renal tubulointerstitial inflammation and fibrosis by reducing the protein levels of fibrosis markers, such as TGF-β1 and CTGF, by inhibiting the NF-ƙB pathway in 5/6 nephrectomized rats (Wen et al., 2019). Ferulic acid is a phenolic compound that exists in both fruits and plants and has various pharmacological activities, such as regulating blood glucose and blood lipids and antioxidant, anti-inflammatory, and antifibrotic activities. Furthermore, prolonged administration of ferulic acid significantly downregulated the protein expression of p-NF-ƙB p65, TNF-α, TGF-β1, and collagen IV. Moreover, it upregulated the expression of the nephrin and podocin proteins in renal tissues by inhibiting the NF-ƙB signaling pathway in DN rats (Qi et al., 2020). Quercetin is a common flavonoid that is abundant in the leaves, stems, and fruits of several plant species. It has a variety of biological activities, such as antioxidant, anticancer, and anti-inflammatory effects. Tan et al. reported that quercetin significantly ameliorated the serum levels of creatinine, IL-1, IL-6, and TNF-α and reduced inflammatory factor production by inhibiting Mincle-Syk-NF-ƙB signaling axis-mediated macrophage inflammation, consequently decreasing AKI-induced kidney inflammation and damage (Tan et al., 2020). Red ginseng possesses a variety of biological benefits, including the ability to prevent tumor formation, lower blood sugar levels, and increase antioxidant activity. 1-Aminyl-fructosyl-glucose is a significant and typical non-saponin component of red ginseng. Tan et al. demonstrated that treatment with 1-arginine-fructosyl-glucose improved cisplatin-induced acute kidney injury by inhibiting oxidative stress, NF-ƙB-mediated inflammation, and PI3K-Akt-induced apoptotic signaling pathways (Li et al., 2019). Tan et al. showed that Zhen-wu-tang, a Chinese compound formula,

has good therapeutic effects on MN by enhancing kidney function in an MN rat model triggered by cationic bovine serum albumin, inhibiting kidney inflammation and improving podocyte injury and structure, which was associated with inhibiting the NF-ƙB pathway and NLRP3 inflammasome (Liu et al., 2019). In addition, baicalin protected against renal fibrosis by augmenting miR-124 and silencing the downstream TLR4-NF-ƙB pathway in streptozotocin-induced DN mice (Zhang S. et al., 2020). Therefore, baicalin may serve as a renoprotective agent. There are a variety of natural products. Further in-depth studies of the underlying mechanism by which natural products affect the NF-ƙB signaling pathway would be beneficial for the popularization and application of natural products.

## 5.3 Targeting non-coding RNAs to treat renal fibrosis

MicroRNAs (miRNAs), which are a large family of small and highly conserved non-coding RNAs, regulate gene expression through translational repression or mRNA degradation (Zou et al., 2017). MiRNAs are RNAs of approximately 22 nucleotides in length that drive the post-transcriptional repression of target mRNA in a variety of eukaryotic lineages (Bartel, 2018). The dysregulation of miRNAs is associated with many disorders, including renal fibrosis (Chung and Lan, 2015). MiR-21 is a frequently referenced miRNA in the renal fibrosis field. It was found to be dysregulated in several renal fibrosis models and human specimens. A study revealed that an increase in miR-21-5p expression levels in ureteral obstruction led to ECM deposition and progressive renal fibrosis by targeting sprouty receptor tyrosine kinase signaling antagonist 1, which activated the NF-ƙB signaling pathway and enhanced renal inflammation (Liu et al., 2021). Lu et al. reported that angiotensin II increased circulating miR-103a-3p levels, which reduced serine/threonine-protein kinase levels in glomerular endothelial cells, resulting in the overactivation of NF-ƙB p65 and leading to renal inflammation and fibrosis (Lu et al., 2019). Therefore, these findings suggest that microRNAs are associated with inflammation in renal injury.

Research has shown that long non-coding RNAs (lncRNAs) are closely related to the development and prognosis of renal fibrosis (Jia et al., 2020). LncRNAs are more than 200 nucleotides in length and do not encode proteins in most instances (Wang Y. N. et al., 2021). LncRNAKCNQ1OT1 is an lncRNA, and studies have shown that KCNQ1OT1 is upregulated in DN patients, human glomerular mesangial cells (HGMCs), and human renal glomerular endothelial cells (HRGECs) in response to high glycemic induction. Treatment with 30 mM glucose to simulate DN conditions resulted in an increase in KCNQ1OT1 in both HGMCs and HRGECs compared with that in the normal group. Moreover, in the high glucose group, there was a significant increase in cell viability and a notable decrease in the rate of apoptosis compared with those in the normal group. These findings indicate that KCNQ1OT1 promotes DN progression. MTT assays also showed that KCNQ1OT1 knockdown suppressed proliferation in both HGMCs and HRGECs. Apoptosis was promoted in HGMCs and HRGECs transfected with siKCNQ1OT1, and this effect was reversed by co-transfection with pcDNA-SORBS2. In addition, the expression levels of the

fibrosis-related proteins FN, Col-4, and TGF-β1 were markedly downregulated by transfection with siKCNQ1OT1, and overexpression of SORBS2 reversed the changes in fibrosis-related proteins caused by KCNQ1OT1 knockdown. Moreover, the mRNA and protein levels of NF-ƙB were decreased in HGMCs. In brief, KCNQ1OT1 knockdown inhibited cell proliferation and fibrosis and induced apoptosis, suggesting that KCNQ1OT1 modulated DN cell proliferation, apoptosis, and fibrosis through the NF-ƙB signaling pathway (Jie et al., 2020).

In a clinical setting, CKD patients receiving hemodialysis were treated with curcumin for 3 months, and inflammatory markers, NF-ƙB mRNA expression, and high-sensitivity C-reactive protein levels decreased. This finding suggested that oral curcumin may have anti-inflammatory effects on these patients (Alvarenga et al., 2020). A study enrolled patients with stage 3 to 5 CKD into α-ketoacid tablet and non-α-ketoacid tablet groups according to their medications. After adjusting for basic demographic factors, the rate of the decrease in the eGFR in stage 4 and stage 5 patients in the α-ketoacid tablet group was much lower than that in the non-α-ketoacid group, indicating the positive role of α-ketoacid in preventing CKD progression (Wang et al., 2019).

In summary, a growing body of evidence confirms that the NF-ƙB signaling pathway plays an important role in renal fibrosis. Inhibitors, including chemical agents, natural products and non-coding RNAs, are available to protect against renal fibrosis progression.

## 6 Conclusion

The common pathway of the progression of all types of AKI and CKD is renal fibrosis; therefore, every attempt to prevent the progression of renal fibrosis could be effective at reducing the burden on the world's economy. NF-ƙB signaling is considered a pivotal pathway in the progression of renal fibrosis. A growing number of studies suggest that NF-ƙB is a critical mediator of renal fibrosis. In particular, hyperactivation of the NF-ƙB signaling pathway contributes to renal fibrosis. Therefore, inhibiting NF-ƙB signaling may be a prospective approach for the treatment of renal fibrosis. We described a number of lines of evidence indicating that NF-ƙB signaling is a target of renal fibrosis in AKI and CKD as well as in the AKI-to-CKD transition. Unresolved renal inflammation can drive progressive fibrosis. This means that we will face greater challenges in the future to identify more powerful treatments for renal fibrosis. Moreover, natural products are uniquely suited to suppress renal fibrosis, and many isolated compounds have been shown to inhibit the NF-ƙB signaling pathway. This Review covers a variety of strategies for treating renal fibrosis by inhibiting NF-ƙB signaling. Considering the essential role of NF-ƙB in the development of renal fibrosis, the development of therapeutic medicines that inhibit abnormal NF-ƙB signaling is critical for identifying effective therapeutic approaches for treating patients with kidney fibrosis. Future research should focus on the development of new NF-ƙB inhibitors that could prevent and treat renal fibrosis. It is worth noting that the majority of these studies were based on animal and cell experiments. Further research should be conducted to investigate the underlying mechanisms

involved to confirm the safety and effectiveness of these treatments in the clinic. Existing studies have focused primarily on inflammation and oxidative stress, as well as the TGF-β-Smad and NF-κB signaling pathways. However, there are limitations, including a lack of diversity in treatment targets. Additional research is needed to explore other cellular and molecular pathways that may be involved.

## Author contributions

NR: Writing–original draft. W-FW: Writing–review and editing. LZ: Writing–review and editing. Y-LZ: Writing–review and editing. HM: Writing–review and editing. Y-YZ: Writing–original draft, Writing–review and editing.

## Funding

## Conflict of interest

The authors declare that the research was conducted in the absence of any commercial or financial relationships that could be construed as a potential conflict of interest.

The author(s) declared that they were an editorial board member of Frontiers, at the time of submission. This had no impact on the peer review process and the final decision.

## Publisher's note

All claims expressed in this article are solely those of the authors and do not necessarily represent those of their affiliated organizations, or those of the publisher, the editors and the reviewers. Any product that may be evaluated in this article, or claim that may be made by its manufacturer, is not guaranteed or endorsed by the publisher.

## References

Abraham, G., Almeida, A., Gaurav, K., Khan, M. Y., Patted, U. R., and Kumaresan, M. (2022). Reno protective role of amlodipine in patients with hypertensive chronic kidney disease. *World J. Nephrol.* 11, 86–95. doi:10.5527/wjn.v11.i3.86

Aggarwal, B. B. (2004). Nuclear factor-kappaB: the enemy within. *Cancer Cell* 6, 203–208. doi:10.1016/j.ccr.2004.09.003

Ahn, K. S., and Aggarwal, B. B. (2005). Transcription factor NF-kappaB: a sensor for smoke and stress signals. *Ann. N. Y. Acad. Sci.* 1056, 218–233. doi:10.1196/annals.1352.026

Allinson, C. S., Pollock, C. A., and Chen, X. (2023). Mesenchymal stem cells in the treatment of acute kidney injury (AKI), chronic kidney disease (CKD) and the AKI-to-CKD transition. *Integr. Med. Nephrol. Androl.* 10, e00014. doi:10.1097/imna-d-22-00014

Althagafy, H. S., El-Aziz, M. K. A., Ibrahim, I. M., Abd-Alhameed, E. K., and Hassanein, E. H. M. (2023). Pharmacological updates of nifuroxazide: promising preclinical effects and the underlying molecular mechanisms. *Eur. J. Pharmacol.* 951, 175776. doi:10.1016/j.ejphar.2023.175776

Alvarenga, L., Salarolli, R., Cardozo, L., Santos, R. S., De Brito, J. S., Kemp, J. A., et al. (2020). Impact of curcumin supplementation on expression of inflammatory transcription factors in hemodialysis patients: a pilot randomized, double-blind, controlled study. *Clin. Nutr.* 39, 3594–3600. doi:10.1016/j.clnu.2020.03.007

Amirshahrokhi, K. (2021). Thalidomide reduces glycerol-induced acute kidney injury by inhibition of NF-κB, NLRP3 inflammasome, COX-2 and inflammatory cytokines. *Cytokine* 144, 155574. doi:10.1016/j.cyto.2021.155574

Amrouche, L., Desbuissons, G., Rabant, M., Sauvaget, V., Nguyen, C., Benon, A., et al. (2017). MicroRNA-146a in human and experimental ischemic AKI: CXCL8-dependent mechanism of action. *J. Am. Soc. Nephrol.* 28, 479–493. doi:10.1681/ASN.2016010045

Andrade-Oliveira, V., Foresto-Neto, O., Watanabe, I. K. M., Zatz, R., and Câmara, N. O. S. (2019). Inflammation in renal diseases: new and old players. *Front. Pharmacol.* 10, 1192. doi:10.3389/fphar.2019.01192

Apeland, T., Mansoor, M. A., Furriol, J., Ushakova, A., Jonsson, G., Stangeland, K. W., et al. (2020). Circulating inflammation-related factors are correlated with systemic redox status in IgA nephropathy; a case-control study. *Free Radic. Biol. Med.* 155, 10–18. doi:10.1016/j.freeradbiomed.2020.05.005

Bai, L., Li, J., Li, H., Song, J., Zhou, Y., Lu, R., et al. (2019). Renoprotective effects of artemisinin and hydroxychloroquine combination therapy on IgA nephropathy via suppressing NF-κB signaling and NLRP3 inflammasome activation by exosomes in rats. *Biochem. Pharmacol.* 169, 113619. doi:10.1016/j.bcp.2019.08.021

Baldwin, A. S., Jr. (1996). The NF-kappa B and I kappa B proteins: new discoveries and insights. *Annu. Rev. Immunol.* 14, 649–683. doi:10.1146/annurev.immunol.14.1.649

Bartel, D. P. (2018). Metazoan microRNAs. *Cell* 173, 20–51. doi:10.1016/j.cell.2018.03.006

Bennett, J. M., Reeves, G., Billman, G. E., and Sturmberg, J. P. (2018). Inflammation–nature's way to efficiently respond to all types of challenges: implications for understanding and managing "the epidemic" of chronic diseases. *Front. Med.* 5, 316. doi:10.3389/fmed.2018.00316

Blanchett, S., Boal-Carvalho, I., Layzell, S., and Seddon, B. (2021). NF-κB and extrinsic cell death pathways - entwined do-or-die decisions for T cells. *Trends Immunol.* 42, 76–88. doi:10.1016/j.it.2020.10.013

Bonventre, J. V., and Zuk, A. (2004). Ischemic acute renal failure: an inflammatory disease? *Kidney Int.* 66, 480–485. doi:10.1111/j.1523-1755.2004.761_2.x

Breyer, M. D., and Susztak, K. (2016). The next generation of therapeutics for chronic kidney disease. *Nat. Rev. Drug Discov.* 15, 568–588. doi:10.1038/nrd.2016.67

Cabezas, L., Jouve, T., Malvezzi, P., Janbon, B., Giovannini, D., Rostaing, L., et al. (2022). Tocilizumab and active antibody-mediated rejection in kidney transplantation: a literature review. *Front. Immunol.* 13, 839380. doi:10.3389/fimmu.2022.839380

Chen, D. Q., Cao, G., Chen, H., Argyopoulos, C. P., Yu, H., Su, W., et al. (2019a). Identification of serum metabolites associating with chronic kidney disease progression and anti-fibrotic effect of 5-methoxytryptophan. *Nat. Commun.* 10, 1476. doi:10.1038/s41467-019-09329-0

Chen, D. Q., Cao, G., Chen, H., Liu, D., Su, W., Yu, X. Y., et al. (2017). Gene and protein expressions and metabolomics exhibit activated redox signaling and wnt/β-catenin pathway are associated with metabolite dysfunction in patients with chronic kidney disease. *Redox Biol.* 12, 505–521. doi:10.1016/j.redox.2017.03.017

Chen, D. Q., Feng, Y. L., Cao, G., and Zhao, Y. Y. (2018). Natural products as a source for antifibrosis therapy. *Trends Pharmacol. Sci.* 39, 937–952. doi:10.1016/j.tips.2018.09.002

Chen, D. Q., Feng, Y. L., Chen, L., Liu, J. R., Wang, M., Vaziri, N. D., et al. (2019b). Poricoic acid A enhances melatonin inhibition of AKI-to-CKD transition by regulating Gas6/AxlNFκB/Nrf2 axis. *Free Radic. Biol. Med.* 134, 484–497. doi:10.1016/j.freeradbiomed.2019.01.046

Chen, H., Cao, G., Chen, D. Q., Wang, M., Vaziri, N. D., Zhang, Z. H., et al. (2016). Metabolomics insights into activated redox signaling and lipid metabolism dysfunction in chronic kidney disease progression. *Redox Biol.* 10, 168–178. doi:10.1016/j.redox.2016.09.014

Chen, J., and Li, D. (2018). Telbivudine attenuates UUO-induced renal fibrosis via TGF-β/Smad and NF-κB signaling. *Int. Immunopharmacol.* 55, 1–8. doi:10.1016/j.intimp.2017.11.043

Chen, J., and Stark, L. A. (2019). Insights into the relationship between nucleolar stress and the NF-κB pathway. *Trends Genet.* 35, 768–780. doi:10.1016/j.tig.2019.07.009

Chen, L., Chen, D. Q., Liu, J. R., Zhang, J., Vaziri, N. D., Zhuang, S., et al. (2019c). Unilateral ureteral obstruction causes gut microbial dysbiosis and metabolome disorders contributing to tubulointerstitial fibrosis. *Exp. Mol. Med.* 51, 1–18. doi:10.1038/s12276-019-0234-2

Chen, T. K., Knicely, D. H., and Grams, M. E. (2019d). Chronic kidney disease diagnosis and management: a review. *Jama* 322, 1294–1304. doi:10.1001/jama.2019.14745

Chevalier, R. L., Forbes, M. S., and Thornhill, B. A. (2009). Ureteral obstruction as a model of renal interstitial fibrosis and obstructive nephropathy. *Kidney Int.* 75, 1145–1152. doi:10.1038/ki.2009.86

Choueiri, R., Faddoul, J., Ghorra, C., Al Najjar, J., Akiki, B.-B., Boustany, S., et al. (2022). A case report: 19-year-old male diagnosed with C1q nephropathy requiring renal replacement therapy. *Explor. Med.* 3, 386–392. doi:10.37349/emed.2022.00101

Chung, A.C.-K., and Lan, H. Y. (2015). MicroRNAs in renal fibrosis. *Front. physiology* 6, 50. doi:10.3389/fphys.2015.00050

Chung, J.Y.-F., Zhang, Y.-Y., Ji, Z.Z.-Y., Tang, T., Chen, J.-Y., Tang, S.C.-W., et al. (2023). Immunodynamics of macrophages in renal fibrosis. *Integr. Med. Nephrol. Androl.* 10, e00001. doi:10.1097/imna-d-23-00001

Chung, S., Kim, S., Son, M., Kim, M., Koh, E. S., Shin, S. J., et al. (2019). Inhibition of p300/CBP-associated factor attenuates renal tubulointerstitial fibrosis through modulation of NF-κB and Nrf2. *Int. J. Mol. Sci.* 20, 1554. doi:10.3390/ijms20071554

Cice, G., Monzo, L., and Calo, L. (2020). The uraemic hypertensive patient: a therapeutic challenge-right you are (if you think so). *Eur. Heart J. Suppl.* 22, L44–l48. doi:10.1093/eurheartj/suaa133

Coppo, R., and Amore, A. (2004). Aberrant glycosylation in IgA nephropathy (IgAN). *Kidney Int.* 65, 1544–1547. doi:10.1111/j.1523-1755.2004.05407.x

Distler, J. H. W., Györfi, A. H., Ramanujam, M., Whitfield, M. L., Königshoff, M., and Lafyatis, R. (2019). Shared and distinct mechanisms of fibrosis. *Nat. Rev. Rheumatol.* 15, 705–730. doi:10.1038/s41584-019-0322-7

Djudjaj, S., and Boor, P. (2019). Cellular and molecular mechanisms of kidney fibrosis. *Mol. Asp. Med.* 65, 16–36. doi:10.1016/j.mam.2018.06.002

Duffield, J. S. (2014). Cellular and molecular mechanisms in kidney fibrosis. *J. Clin. investigation* 124, 2299–2306. doi:10.1172/JCI72267

Duni, A., Liakopoulos, V., Roumeliotis, S., Peschos, D., and Dounousi, E. (2019). Oxidative stress in the pathogenesis and evolution of chronic kidney disease: untangling Ariadne's thread. *Int. J. Mol. Sci.* 20, 3711. doi:10.3390/ijms20153711

Eluard, B., Thieblemont, C., and Baud, V. (2020). NF-κB in the new era of cancer therapy. *Trends Cancer* 6, 677–687. doi:10.1016/j.trecan.2020.04.003

Feng, Y. L., Cao, G., Chen, D. Q., Vaziri, N. D., Chen, L., Zhang, J., et al. (2019a). Microbiome-metabolomics reveals gut microbiota associated with glycine-conjugated metabolites and polyamine metabolism in chronic kidney disease. *Cell Mol. Life Sci.* 76, 4961–4978. doi:10.1007/s00018-019-03155-9

Feng, Y. L., Chen, D. Q., Vaziri, N. D., Guo, Y., and Zhao, Y. Y. (2020). Small molecule inhibitors of epithelial-mesenchymal transition for the treatment of cancer and fibrosis. *Med. Res. Rev.* 40, 54–78. doi:10.1002/med.21596

Feng, Y. L., Chen, H., Chen, D. Q., Vaziri, N. D., Su, W., Ma, S. X., et al. (2019b). Activated NF-κB/Nrf2 and Wnt/β-catenin pathways are associated with lipid metabolism in CKD patients with microalbuminuria and macroalbuminuria. *Biochim. Biophys. Acta Mol. Basis Dis.* 1865, 2317–2332. doi:10.1016/j.bbadis.2019.05.010

Gadelkareem, R. A., Abdelgawad, A. M., Reda, A., Azoz, N. M., Zarzour, M. A., Mohammed, N., et al. (2023). Preemptive living donor kidney transplantation: access, fate, and review of the status in Egypt. *World J. Nephrol.* 12, 40–55. doi:10.5527/wjn.v12.i3.40

Gu, M., Zhou, Y., Liao, N., Wei, Q., Bai, Z., Bao, N., et al. (2022). Chrysophanol, a main anthraquinone from Rheum palmatum L. (rhubarb), protects against renal fibrosis by suppressing NKD2/NF-κB pathway. *Phytomedicine* 105, 154381. doi:10.1016/j.phymed.2022.154381

Guan, T., Fang, F., Su, X., Lin, K., and Gao, Q. (2020). Silencing PEG3 inhibits renal fibrosis in a rat model of diabetic nephropathy by suppressing the NF-κB pathway. *Mol. Cell Endocrinol.* 513, 110823. doi:10.1016/j.mce.2020.110823

Gui, Z., Suo, C., Wang, Z., Zheng, M., Fei, S., Chen, H., et al. (2021). Impaired atg16l-dependent autophagy promotes renal interstitial fibrosis in chronic renal graft dysfunction through inducing EndMT by NF-κB signal pathway. *Front. Immunol.* 12, 650424. doi:10.3389/fimmu.2021.650424

Gupta, S. C., Kim, J. H., Prasad, S., and Aggarwal, B. B. (2010). Regulation of survival, proliferation, invasion, angiogenesis, and metastasis of tumor cells through modulation of inflammatory pathways by nutraceuticals. *Cancer Metastasis Rev.* 29, 405–434. doi:10.1007/s10555-010-9235-2

Gusev, E., Solomatina, L., Zhuravleva, Y., and Sarapultsev, A. (2021). The pathogenesis of End-Stage renal disease from the standpoint of the theory of general pathological processes of inflammation. *Int. J. Mol. Sci.* 22, 11453. doi:10.3390/ijms222111453

Habshi, T., Shelke, V., Kale, A., Lech, M., and Gaikwad, A. B. (2023). Hippo signaling in acute kidney injury to chronic kidney disease transition: current understandings and future targets. *Drug Discov. Today* 28, 103649. doi:10.1016/j.drudis.2023.103649

hAinmhire, E. Ó., and Humphreys, B. D. (2017). Fibrotic changes mediating acute kidney injury to chronic kidney disease transition. *Nephron* 137, 264–267. doi:10.1159/000474960

Harhaj, E. W., and Dixit, V. M. (2011). Deubiquitinases in the regulation of NF-κB signaling. *Cell Res.* 21, 22–39. doi:10.1038/cr.2010.166

Hashmi, S. F., Rathore, H. A., Sattar, M. A., Johns, E. J., Gan, C. Y., Chia, T. Y., et al. (2021). Hydrogen sulphide treatment prevents renal ischemia-reperfusion injury by inhibiting the expression of ICAM-1 and NF-kB concentration in normotensive and hypertensive rats. *Biomolecules* 11, 1549. doi:10.3390/biom11101549

Hassan, N. M. E., Said, E., and Shehatou, G. S. G. (2021). Nifuroxazide suppresses UUO-induced renal fibrosis in rats via inhibiting STAT-3/NF-κB signaling, oxidative stress and inflammation. *Life Sci.* 272, 119241. doi:10.1016/j.lfs.2021.119241

Honda, T., Hirakawa, Y., and Nangaku, M. (2019). The role of oxidative stress and hypoxia in renal disease. *Kidney Res. Clin. Pract.* 38, 414–426. doi:10.23876/j.krcp.19.063

Hoste, E. a.J., Kellum, J. A., Selby, N. M., Zarbock, A., Palevsky, P. M., Bagshaw, S. M., et al. (2018). Global epidemiology and outcomes of acute kidney injury. *Nat. Rev. Nephrol.* 14, 607–625. doi:10.1038/s41581-018-0052-0

Hua, M. R., Zhao, Y. L., Yang, J. Z., Zou, L., Zhao, Y. Y., and Li, X. (2023). Membranous nephropathy: mechanistic insights and therapeutic perspectives. *Int. Immunopharmacol.* 120, 110317. doi:10.1016/j.intimp.2023.110317

Hung, P. H., Hsu, Y. C., Chen, T. H., and Lin, C. L. (2021). Recent advances in diabetic kidney diseases: from kidney injury to kidney fibrosis. *Int. J. Mol. Sci.* 22, 11857. doi:10.3390/ijms222111857

Jia, H., Ma, T., and Hao, C. (2020). Identification of candidate lncRNA biomarkers for renal fibrosis: a systematic review. *Life Sci.* 262, 118566. doi:10.1016/j.lfs.2020.118566

Jie, R., Zhu, P., Zhong, J., Zhang, Y., and Wu, H. (2020). LncRNA KCNQ1OT1 affects cell proliferation, apoptosis and fibrosis through regulating miR-18b-5p/SORBS2 axis and NF-κB pathway in diabetic nephropathy. *Diabetol. Metab. Syndr.* 12, 77. doi:10.1186/s13098-020-00585-5

Jin, L., Yu, B., Armando, I., and Han, F. (2021). Mitochondrial DNA-mediated inflammation in acute kidney injury and chronic kidney disease. *Oxid. Med. Cell Longev.* 2021, 9985603. doi:10.1155/2021/9985603

Kalantar-Zadeh, K., Jafar, T. H., Nitsch, D., Neuen, B. L., and Perkovic, V. (2021). Chronic kidney disease. *Lancet* 398, 786–802. doi:10.1016/S0140-6736(21)00519-5

Kim, C. S., Mathew, A. P., Vasukutty, A., Uthaman, S., Joo, S. Y., Bae, E. H., et al. (2021). Glycol chitosan-based tacrolimus-loaded nanomicelle therapy ameliorates lupus nephritis. *J. Nanobiotechnology* 19, 109. doi:10.1186/s12951-021-00857-w

Lan, H.-Y. (2022). Macrophage-myofibroblast transition in kidney disease. *Integr. Med. Nephrol. Androl.* 9, 12. doi:10.4103/2773-0387.358225

Lawrence, T. (2009). The nuclear factor NF-kappaB pathway in inflammation. *Cold Spring Harb. Perspect. Biol.* 1, a001651. doi:10.1101/cshperspect.a001651

Li, Q., and Verma, I. M. (2002). NF-kappaB regulation in the immune system. *Nat. Rev. Immunol.* 2, 725–734. doi:10.1038/nri910

Li, R. Y., Zhang, W. Z., Yan, X. T., Hou, J. G., Wang, Z., Ding, C. B., et al. (2019). Arginyl-fructosyl-glucose, a major maillard reaction product of red ginseng, attenuates cisplatin-induced acute kidney injury by regulating nuclear factor κB and phosphatidylinositol 3-kinase/protein kinase B signaling pathways. *J. Agric. Food Chem.* 67, 5754–5763. doi:10.1021/acs.jafc.9b00540

Li, S., Yan, B., and Liu, F. (2023). Diagnosis of fibrillary glomerulonephritis with positive immunoglobulin A-κ deposits presenting as membranous nephropathy using immunoelectron microscopy: a case report and literature review. *Integr. Med. Nephrol. Androl.* 10, e00028. doi:10.1097/imna-d-22-00028

Li, S. S., Sun, Q., Hua, M. R., Suo, P., Chen, J. R., Yu, X. Y., et al. (2021). Targeting the Wnt/β-Catenin signaling pathway as a potential therapeutic strategy in renal tubulointerstitial fibrosis. *Front. Pharmacol.* 12, 719880. doi:10.3389/fphar.2021.719880

Liao, Y., Tan, R. Z., Li, J. C., Liu, T. T., Zhong, X., Yan, Y., et al. (2020). Isoliquiritigenin attenuates UUO-induced renal inflammation and fibrosis by inhibiting mincle/syk/NF-kappa B signaling pathway. *Drug Des. Devel Ther.* 14, 1455–1468. doi:10.2147/DDDT.S243420

Lin, J., Jiang, Z., Liu, C., Zhou, D., Song, J., Liao, Y., et al. (2020). Emerging roles of long non-coding RNAs in renal fibrosis. *Life (Basel)* 10, 131. doi:10.3390/life10080131

Liu, B., Lu, R., Li, H., Zhou, Y., Zhang, P., Bai, L., et al. (2019). Zhen-Wu-tang ameliorates membranous nephropathy rats through inhibiting NF-κB pathway and NLRP3 inflammasome. *Phytomedicine* 59, 152913. doi:10.1016/j.phymed.2019.152913

Liu, E., Lv, L., Zhan, Y., Ma, Y., Feng, J., He, Y., et al. (2021). METTL3/N6-methyladenosine/miR-21-5p promotes obstructive renal fibrosis by regulating inflammation through SPRY1/ERK/NF-κB pathway activation. *J. Cell Mol. Med.* 25, 7660–7674. doi:10.1111/jcmm.16603

Liu, H. J., Miao, H., Yang, J. Z., Liu, F., Cao, G., and Zhao, Y. Y. (2023). Deciphering the role of lipoproteins and lipid metabolic alterations in ageing and ageing-associated renal fibrosis. *Ageing Res. Rev.* 85, 101861. doi:10.1016/j.arr.2023.101861

Liu, Y. (2011). Cellular and molecular mechanisms of renal fibrosis. *Nat. Rev. Nephrol.* 7, 684–696. doi:10.1038/nrneph.2011.149

Lopez-De La Mora, D. A., Sanchez-Roque, C., Montoya-Buelna, M., Sanchez-Enriquez, S., Lucano-Landeros, S., Macias-Barragan, J., et al. (2015). Role and new Insights of pirfenidone in fibrotic diseases. *Int. J. Med. Sci.* 12, 840–847. doi:10.7150/ijms.11579

Lu, P., Zhang, L., Liu, T., Fan, J. J., Luo, X., and Zhu, Y. T. (2022). MiR-494-mediated effects on the NF-κB signaling pathway regulate lipopolysaccharide-induced acute kidney injury in mice. *Immunol. Invest.* 51, 1372–1384. doi:10.1080/08820139.2021.1944184

Lu, Q., Ma, Z., Ding, Y., Bedarida, T., Chen, L., Xie, Z., et al. (2019). Circulating miR-103a-3p contributes to angiotensin II-induced renal inflammation and fibrosis via a SNRK/NF-κB/p65 regulatory axis. *Nat. Commun.* 10, 2145. doi:10.1038/s41467-019-10116-0

Luo, L. P., Suo, P., Ren, L. L., Liu, H. J., Zhang, Y., and Zhao, Y. Y. (2021). Shenkang injection and its three anthraquinones ameliorates renal fibrosis by simultaneous targeting IκB/NF-κB and Keap1/Nrf2 signaling pathways. *Front. Pharmacol.* 12, 800522. doi:10.3389/fphar.2021.800522

Luyckx, V. A., Cherney, D. Z. I., and Bello, A. K. (2020). Preventing CKD in developed countries. *Kidney Int. Rep.* 5, 263–277. doi:10.1016/j.ekir.2019.12.003

Lv, W., Booz, G. W., Wang, Y., Fan, F., and Roman, R. J. (2018). Inflammation and renal fibrosis: recent developments on key signaling molecules as potential therapeutic targets. *Eur. J. Pharmacol.* 820, 65–76. doi:10.1016/j.ejphar.2017.12.016

Ma, F. Y., Tesch, G. H., Grynberg, K., Ozols, E., Mulley, W. R., and Nikolic-Paterson, D. J. (2023). A model of ischaemia-induced renal interstitial fibrosis in mice with established diabetes. *Integr. Med. Nephrol. Androl.* 10, e00032. doi:10.1097/imna-d-22-00032

Malaki, M. (2022). Adenine-rich diet: a potential mechanism for renal fibrosis progression. *Explor. Med.* 3, 314–316. doi:10.37349/emed.2022.00095

Mantovani, A., and Zusi, C. (2020). PNPLA3 gene and kidney disease. *Explor. Med.* 1, 42–50. doi:10.37349/emed.2020.00004

Meng, X. M., Nikolic-Paterson, D. J., and Lan, H. Y. (2014). Inflammatory processes in renal fibrosis. *Nat. Rev. Nephrol.* 10, 493–503. doi:10.1038/nrneph.2014.114

Mercado, M. G., Smith, D. K., and Guard, E. L. (2019). Acute kidney injury: diagnosis and management. *Am. Fam. Physician* 100, 687–694.

Miao, H., Cao, G., Wu, X. Q., Chen, Y. Y., Chen, D. Q., Chen, L., et al. (2020). Identification of endogenous 1-aminopyrene as a novel mediator of progressive chronic kidney disease via aryl hydrocarbon receptor activation. *Br. J. Pharmacol.* 177, 3415–3435. doi:10.1111/bph.15062

Miao, H., Wang, Y. N., Su, W., Zou, L., Zhuang, S. G., Yu, X. Y., et al. (2023a). Sirtuin 6 protects against podocyte injury by blocking the renin-angiotensin system by inhibiting the Wnt1/β-catenin pathway. *Acta Pharmacol. Sin.* 45, 137–149. doi:10.1038/s41401-023-01148-w

Miao, H., Wang, Y. N., Yu, X. Y., Zou, L., Guo, Y., Su, W., et al. (2023b). Lactobacillus species ameliorate membranous nephropathy through inhibiting the aryl hydrocarbon receptor pathway via tryptophan-produced indole metabolites. *Br. J. Pharmacol.* 181, 162–179. doi:10.1111/bph.16219

Miao, H., Wu, X. Q., Wang, Y. N., Chen, D. Q., Chen, L., Vaziri, N. D., et al. (2022a). 1-Hydroxypyrene mediates renal fibrosis through aryl hydrocarbon receptor signalling pathway. *Br. J. Pharmacol.* 179, 103–124. doi:10.1111/bph.15705

Miao, H., Zhang, Y., Yu, X., Zou, L., and Zhao, Y. (2022b). Membranous nephropathy: systems biology-based novel mechanism and traditional Chinese medicine therapy. *Front. Pharmacol.* 13, 969930. doi:10.3389/fphar.2022.969930

Möller-Hackbarth, K., Dabaghie, D., Charrin, E., Zambrano, S., Genové, G., Li, X., et al. (2021). Retinoic acid receptor responder1 promotes development of glomerular diseases via the Nuclear Factor-κB signaling pathway. *Kidney Int.* 100, 809–823. doi:10.1016/j.kint.2021.05.036

Montecucco, F., Pende, A., Quercioli, A., and Mach, F. (2011). Inflammation in the pathophysiology of essential hypertension. *J. Nephrol.* 24, 23–34. doi:10.5301/jn.2010.4729

Napetschnig, J., and Wu, H. (2013). Molecular basis of NF-κB signaling. *Annu. Rev. Biophys.* 42, 443–468. doi:10.1146/annurev-biophys-083012-130338

Nastase, M. V., Zeng-Brouwers, J., Wygrecka, M., and Schaefer, L. (2018). Targeting renal fibrosis: mechanisms and drug delivery systems. *Adv. Drug Deliv. Rev.* 129, 295–307. doi:10.1016/j.addr.2017.12.019

Navarro-González, J. F., Mora-Fernández, C., Muros De Fuentes, M., and García-Pérez, J. (2011). Inflammatory molecules and pathways in the pathogenesis of diabetic nephropathy. *Nat. Rev. Nephrol.* 7, 327–340. doi:10.1038/nrneph.2011.51

Newman, D. J., and Cragg, G. M. (2020). Natural products as sources of new drugs over the nearly four decades from 01/1981 to 09/2019. *J. Nat. Prod.* 83, 770–803. doi:10.1021/acs.jnatprod.9b01285

Nikolic-Paterson, D. J., Grynberg, K., and Ma, F. Y. (2021). JUN amino terminal kinase in cell death and inflammation in acute and chronic kidney disease. *Integr. Med. Nephrol. Androl.* 8, 10. doi:10.4103/imna.imna_35_21

Peng, X., Wang, Y., Li, H., Fan, J., Shen, J., Yu, X., et al. (2019). ATG5-mediated autophagy suppresses NF-κB signaling to limit epithelial inflammatory response to kidney injury. *Cell Death Dis.* 10, 253. doi:10.1038/s41419-019-1483-7

Prasad, S., Hogaboam, C. M., and Jarai, G. (2014). Deficient repair response of IPF fibroblasts in a co-culture model of epithelial injury and repair. *Fibrogenesis tissue repair* 7, 7–14. doi:10.1186/1755-1536-7-7

Pujari, R., Hunte, R., Khan, W. N., and Shembade, N. (2013). A20-mediated negative regulation of canonical NF-κB signaling pathway. *Immunol. Res.* 57, 166–171. doi:10.1007/s12026-013-8463-2

Qi, M. Y., Wang, X. T., Xu, H. L., Yang, Z. L., Cheng, Y., and Zhou, B. (2020). Protective effect of ferulic acid on STZ-induced diabetic nephropathy in rats. *Food Funct.* 11, 3706–3718. doi:10.1039/c9fo02398d

Quan, Y., Park, W., Jin, J., Kim, W., Park, S. K., and Kang, K. P. (2020). Sirtuin 3 activation by honokiol decreases unilateral ureteral obstruction-induced renal inflammation and fibrosis via regulation of mitochondrial dynamics and the renal NF-κBTGF-β1/Smad signaling pathway. *Int. J. Mol. Sci.* 21, 402. doi:10.3390/ijms21020402

Ranganathan, P. V., Jayakumar, C., Mohamed, R., Dong, Z., and Ramesh, G. (2013). Netrin-1 regulates the inflammatory response of neutrophils and macrophages, and suppresses ischemic acute kidney injury by inhibiting COX-2-mediated PGE2 production. *Kidney Int.* 83, 1087–1098. doi:10.1038/ki.2012.423

Rangel, P. X. M., Priyadarshini, A., and Tian, X. (2021). New insights into the immunity and podocyte in glomerular health and disease: from pathogenesis to therapy in proteinuric kidney disease. *Integr. Med. Nephrol. Androl.* 8, 5. doi:10.4103/imna.imna_26_21

Rapa, S. F., Di Iorio, B. R., Campiglia, P., Heidland, A., and Marzocco, S. (2019). Inflammation and oxidative stress in chronic kidney disease-potential therapeutic role of minerals, vitamins and plant-derived metabolites. *Int. J. Mol. Sci.* 21, 263. doi:10.3390/ijms21010263

Rashid, I., Katravath, P., Tiwari, P., D'cruz, S., Jaswal, S., and Sahu, G. (2022). *Hyperuricemiaa serious complication among patients with chronic kidney disease: a systematic review and meta-analysis.* China: Open Exploration.

Rashid, I., Tiwari, P., D'cruz, S., and Jaswal, S. (2023). Prognostic importance of neutrophil-lymphocyte ratio in non-dialysis chronic kidney disease patients—a hospital-based prospective cohort. *Explor. Med.* 4, 299–313. doi:10.37349/emed.2023.00141

Reid, S., and Scholey, J. W. (2021). Recent approaches to targeting canonical NFκB signaling in the early inflammatory response to renal IRI. *J. Am. Soc. Nephrol.* 32, 2117–2124. doi:10.1681/ASN.2021010069

Ren, L. L., Li, X. J., Duan, T. T., Li, Z. H., Yang, J. Z., Zhang, Y. M., et al. (2023a). Transforming growth factor-β signaling: from tissue fibrosis to therapeutic opportunities. *Chem. Biol. Interact.* 369, 110289. doi:10.1016/j.cbi.2022.110289

Ren, L. L., Miao, H., Wang, Y. N., Liu, F., Li, P., and Zhao, Y. Y. (2023b). TGF-β as a master regulator of aging-associated tissue fibrosis. *Aging Dis.* 14, 1633–1650. doi:10.14336/ad.2023.0222

Ren, Q., Guo, F., Tao, S., Huang, R., Ma, L., and Fu, P. (2020). Flavonoid fisetin alleviates kidney inflammation and apoptosis via inhibiting Src-mediated NF-κB p65 and MAPK signaling pathways in septic AKI mice. *Biomed. Pharmacother.* 122, 109772. doi:10.1016/j.biopha.2019.109772

Ronco, P., Beck, L., Debiec, H., Fervenza, F. C., Hou, F. F., Jha, V., et al. (2021). Membranous nephropathy. *Nat. Rev. Dis. Prim.* 7, 69. doi:10.1038/s41572-021-00303-z

Rungratanawanich, W., Qu, Y., Wang, X., Essa, M. M., and Song, B. J. (2021). Advanced glycation end products (AGEs) and other adducts in aging-related diseases and alcohol-mediated tissue injury. *Exp. Mol. Med.* 53, 168–188. doi:10.1038/s12276-021-00561-7

Salvadori, M., and Tsalouchos, A. (2022). New antigens involved in membranous nephropathy beyond phospholipase A2 receptor. *World J. Nephrol.* 11, 115–126. doi:10.5527/wjn.v11.i4.115

Samsu, N. (2021). Diabetic nephropathy: challenges in pathogenesis, diagnosis, and treatment. *Biomed. Res. Int.* 2021, 1497449. doi:10.1155/2021/1497449

Sanz, A. B., Sanchez-Niño, M. D., Ramos, A. M., Moreno, J. A., Santamaria, B., Ruiz-Ortega, M., et al. (2010). NF-kappaB in renal inflammation. *J. Am. Soc. Nephrol.* 21, 1254–1262. doi:10.1681/ASN.2010020218

Scindia, Y. M., Deshmukh, U. S., and Bagavant, H. (2010). Mesangial pathology in glomerular disease: targets for therapeutic intervention. *Adv. Drug Deliv. Rev.* 62, 1337–1343. doi:10.1016/j.addr.2010.08.011

Shih, R. H., Wang, C. Y., and Yang, C. M. (2015). NF-kappaB signaling pathways in neurological inflammation: a mini review. *Front. Mol. Neurosci.* 8, 77. doi:10.3389/fnmol.2015.00077

Siew, E. D., and Davenport, A. (2015). The growth of acute kidney injury: a rising tide or just closer attention to detail? *Kidney Int.* 87, 46–61. doi:10.1038/ki.2014.293

Singh, S., and Singh, T. G. (2020). Role of nuclear factor kappa B (NF-κB) signalling in neurodegenerative diseases: an mechanistic approach. *Curr. Neuropharmacol.* 18, 918–935. doi:10.2174/1570159X18666200207120949

Sivandzade, F., Prasad, S., Bhalerao, A., and Cucullo, L. (2019). NRF2 and NF-κB interplay in cerebrovascular and neurodegenerative disorders: molecular mechanisms and possible therapeutic approaches. *Redox Biol.* 21, 101059. doi:10.1016/j.redox.2018.11.017

Sobhon, P., Gavin, S., and Sawaek, W. (2023a). Oxidative stress and inflammation: the root causes of aging. *Explor. Med.* 4, 127–156. doi:10.37349/emed.2023.00129

Sobhon, P., Savedvanich, G., and Weerakiet, S. (2023b). Oxidative stress, inflammation, dysfunctional redox homeostasis and autophagy cause age-associated diseases. *Explor. Med.* 4, 45–70. doi:10.37349/emed.2023.00124

Song, N., Thaiss, F., and Guo, L. (2019). NFκB and kidney injury. *Front. Immunol.* 10, 815. doi:10.3389/fimmu.2019.00815

Song, Y., Mao, D., Zou, R., Hu, Y., Luo, D., Liu, H., et al. (2021). Patients with chronic kidney disease have higher acute kidney injury morbidity than those without after SARS-CoV-2 infection. *Integr. Med. Nephrol. Androl.* 8, 12–18. doi:10.4103/imna.imna_24_21

Song, Z., and Gong, X. (2023). Research progress on the potential mechanisms of acute kidney injury and chronic kidney disease induced by proton pump inhibitors. *Integr. Med. Nephrol. Androl.* 10, e00027. doi:10.1097/imna-d-22-00027

Stenvinkel, P., Chertow, G. M., Devarajan, P., Levin, A., Andreoli, S. P., Bangalore, S., et al. (2021). Chronic inflammation in chronic kidney disease progression: role of Nrf2. *Kidney Int. Rep.* 6, 1775–1787. doi:10.1016/j.ekir.2021.04.023

Sun, H., Shi, K., Zuo, B., Zhang, X., Liu, Y., Sun, D., et al. (2022). Kidney-targeted drug delivery system based on metformin-grafted chitosan for renal fibrosis therapy. *Mol. Pharm.* 19, 3075–3084. doi:10.1021/acs.molpharmaceut.1c00827

Sun, S.-C. (2017a). The non-canonical NF-κB pathway in immunity and inflammation. *Nat. Rev. Immunol.* 17, 545–558. doi:10.1038/nri.2017.52

Sun, S. C. (2017b). The non-canonical NF-κB pathway in immunity and inflammation. *Nat. Rev. Immunol.* 17, 545–558. doi:10.1038/nri.2017.52

Sun, T., Liu, Y., Liu, L., and Ma, F. (2020). MicroRNA-544 attenuates diabetic renal injury via suppressing glomerulosclerosis and inflammation by targeting FASN. *Gene* 723, 143986. doi:10.1016/j.gene.2019.143986

Sun, Y. B., Qu, X., Caruana, G., and Li, J. (2016). The origin of renal fibroblasts/myofibroblasts and the signals that trigger fibrosis. *Differentiation* 92, 102–107. doi:10.1016/j.diff.2016.05.008

Suo, C., Gui, Z., Wang, Z., Zhou, J., Zheng, M., Chen, H., et al. (2021). Bortezomib limits renal allograft interstitial fibrosis by inhibiting NF-κB/TNF-α/Akt/mTOR/P70S6K/Smurf2 pathway via IκBα protein stabilization. *Clin. Sci. (Lond)* 135, 53–69. doi:10.1042/CS20201038

Tak, P. P., and Firestein, G. S. (2001). NF-kappaB: a key role in inflammatory diseases. *J. Clin. Invest.* 107, 7–11. doi:10.1172/JCI11830

Tan, R. Z., Wang, C., Deng, C., Zhong, X., Yan, Y., Luo, Y., et al. (2020). Quercetin protects against cisplatin-induced acute kidney injury by inhibiting Mincle/Syk/NF-κB signaling maintained macrophage inflammation. *Phytother. Res.* 34, 139–152. doi:10.1002/ptr.6507

Tan, Y. Q., Wang, Y. N., Feng, H. Y., Guo, Z. Y., Li, X., Nie, X. L., et al. (2022). Host/microbiota interactions-derived tryptophan metabolites modulate oxidative stress and inflammation via aryl hydrocarbon receptor signaling. *Free Radic. Biol. Med.* 184, 30–41. doi:10.1016/j.freeradbiomed.2022.03.025

Tanemoto, F., and Mimura, I. (2022). Therapies targeting epigenetic alterations in acute kidney injury-to-chronic kidney disease transition. *Pharm. (Basel)* 15, 123. doi:10.3390/ph15020123

Turgut, F., Awad, A. S., and Abdel-Rahman, E. M. (2023). Acute kidney injury: medical causes and pathogenesis. *J. Clin. Med.* 12, 375. doi:10.3390/jcm12010375

Vermeulen, L., De Wilde, G., Notebaert, S., Vanden Berghe, W., and Haegeman, G. (2002). Regulation of the transcriptional activity of the nuclear factor-kappaB p65 subunit. *Biochem. Pharmacol.* 64, 963–970. doi:10.1016/s0006-2952(02)01161-9

Wang, H., Zhang, R., Wu, X., Chen, Y., Ji, W., Wang, J., et al. (2021a). The Wnt signaling pathway in diabetic nephropathy. *Front. Cell Dev. Biol.* 9, 701547. doi:10.3389/fcell.2021.701547

Wang, J., Shen, F., Liu, F., and Zhuang, S. (2022a). Histone modifications in acute kidney injury. *Kidney Dis. (Basel)* 8, 466–477. doi:10.1159/000527799

Wang, M., Hu, H. H., Chen, Y. Y., Chen, L., Wu, X. Q., and Zhao, Y. Y. (2020). Novel poricoic acids attenuate renal fibrosis through regulating redox signalling and aryl hydrocarbon receptor activation. *Phytomedicine* 79, 153323. doi:10.1016/j.phymed.2020.153323

Wang, M., Xu, H., Chong Lee Shin, O. L., Li, L., Gao, H., Zhao, Z., et al. (2019). Compound α-keto acid tablet supplementation alleviates chronic kidney disease progression via inhibition of the NF-κB and MAPK pathways. *J. Transl. Med.* 17, 122. doi:10.1186/s12967-019-1856-9

Wang, Y., and Chen, H. (2022). Ferroptosis in diabetic nephropathy: a narrative review. *Integr. Med. Nephrol. Androl.* 9, 1. doi:10.4103/imna.imna_2_22

Wang, Y. N., Feng, H. Y., Nie, X., Zhang, Y. M., Zou, L., Li, X., et al. (2022b). Recent advances in clinical diagnosis and pharmacotherapy options of membranous nephropathy. *Front. Pharmacol.* 13, 907108. doi:10.3389/fphar.2022.907108

Wang, Y. N., Liu, H. J., Ren, L. L., Suo, P., Zou, L., Zhang, Y. M., et al. (2022c). Shenkang injection improves chronic kidney disease by inhibiting multiple renin-angiotensin system genes by blocking the Wnt/β-catenin signalling pathway. *Front. Pharmacol.* 13, 964370. doi:10.3389/fphar.2022.964370

Wang, Y. N., Miao, H., Hua, M. R., Yang, J. Z., Pei, M., Yu, H. X., et al. (2023a). Moshen granule ameliorates membranous nephropathy by blocking intrarenal renin-angiotensin system signalling via the Wnt1/β-catenin pathway. *Phytomedicine* 114, 154763. doi:10.1016/j.phymed.2023.154763

Wang, Y. N., Miao, H., Yu, X. Y., Guo, Y., Su, W., Liu, F., et al. (2023b). Oxidative stress and inflammation are mediated via aryl hydrocarbon receptor signalling in idiopathic membranous nephropathy. *Free Radic. Biol. Med.* 207, 89–106. doi:10.1016/j.freeradbiomed.2023.07.014

Wang, Y. N., Yang, C. E., Zhang, D. D., Chen, Y. Y., Yu, X. Y., Zhao, Y. Y., et al. (2021b). Long non-coding RNAs: a double-edged sword in aging kidney and renal disease. *Chem. Biol. Interact.* 337, 109396. doi:10.1016/j.cbi.2021.109396

Wang, Y. N., Zhang, Z. H., Liu, H. J., Guo, Z. Y., Zou, L., Zhang, Y. M., et al. (2023c). Integrative phosphatidylcholine metabolism through phospholipase A(2) in rats with chronic kidney disease. *Acta Pharmacol. Sin.* 44, 393–405. doi:10.1038/s41401-022-00947-x

Webster, A. C., Nagler, E. V., Morton, R. L., and Masson, P. (2017). Chronic kidney disease. *Lancet* 389, 1238–1252. doi:10.1016/S0140-6736(16)32064-5

Wei, J., Xu, Z., and Yan, X. (2022). The role of the macrophage-to-myofibroblast transition in renal fibrosis. *Front. Immunol.* 13, 934377. doi:10.3389/fimmu.2022.934377

Wen, Y., Pan, M. M., Lv, L. L., Tang, T. T., Zhou, L. T., Wang, B., et al. (2019). Artemisinin attenuates tubulointerstitial inflammation and fibrosis via the NF-κB/NLRP3 pathway in rats with 5/6 subtotal nephrectomy. *J. Cell Biochem.* 120, 4291–4300. doi:10.1002/jcb.27714

Wishahi, M., and Kamal, N. M. (2022). Multidisciplinary basic and clinical research of acute kidney injury with COVID-19: pathophysiology, mechanisms, incidence, management and kidney transplantation. *World J. Nephrol.* 11, 105–114. doi:10.5527/wjn.v11.i3.105

Wu, W., Wang, X., Yu, X., and Lan, H. Y. (2022). Smad3 signatures in renal inflammation and fibrosis. *Int. J. Biol. Sci.* 18, 2795–2806. doi:10.7150/ijbs.71595

Wu, X. Q., Zhang, D. D., Wang, Y. N., Tan, Y. Q., Yu, X. Y., and Zhao, Y. Y. (2021). AGE/RAGE in diabetic kidney disease and ageing kidney. *Free Radic. Biol. Med.* 171, 260–271. doi:10.1016/j.freeradbiomed.2021.05.025

Xianyuan, L., Wei, Z., Yaqian, D., Dan, Z., Xueli, T., Zhanglu, D., et al. (2019). Anti-renal fibrosis effect of asperulosidic acid via TGF-β1/smad2/smad3 and NF-κB signaling pathways in a rat model of unilateral ureteral obstruction. *Phytomedicine* 53, 274–285. doi:10.1016/j.phymed.2018.09.009

Xiao, G., Harhaj, E. W., and Sun, S. C. (2001). NF-kappaB-inducing kinase regulates the processing of NF-kappaB2 p100. *Mol. Cell* 7, 401–409. doi:10.1016/s1097-2765(01)00187-3

Xie, Z., Wei, L., Chen, J., and Chen, Z. (2022). Calcium dobesilate alleviates renal dysfunction and inflammation by targeting nuclear factor kappa B (NF-κB) signaling in sepsis-associated acute kidney injury. *Bioengineered* 13, 2816–2826. doi:10.1080/21655979.2021.2024394

Xu, S., Lv, Y., Zhao, J., Wang, J., Zhao, X., and Wang, S. (2016). Inhibitory effects of Shenkang injection and its main component emodin on the proliferation of high glucose-induced renal mesangial cells through cell cycle regulation and induction of apoptosis. *Mol. Med. Rep.* 14, 3381–3388. doi:10.3892/mmr.2016.5631

Yang, H., Liao, D., Tong, L., Zhong, L., and Wu, K. (2019). MiR-373 exacerbates renal injury and fibrosis via NF-κB/MatrixMetalloproteinase-9 signaling by targeting Sirtuin1. *Genomics* 111, 786–792. doi:10.1016/j.ygeno.2018.04.017

Yang, M., Liu, J. W., Zhang, Y. T., and Wu, G. (2021). The role of renal macrophage, AIM, and TGF-β1 expression in renal fibrosis progression in IgAN patients. *Front. Immunol.* 12, 646650. doi:10.3389/fimmu.2021.646650

Yang, Y., and Wu, C. (2021). Traditional Chinese medicine in ameliorating diabetic kidney disease via modulating gut microbiota. *Integr. Med. Nephrol. Androl.* 8, 8. doi:10.4103/imna.imna_28_21

Yu, H., Lin, L., Zhang, Z., Zhang, H., and Hu, H. (2020). Targeting NF-κB pathway for the therapy of diseases: mechanism and clinical study. *Signal Transduct. Target Ther.* 5, 209. doi:10.1038/s41392-020-00312-6

Yu, K., Ding, L., An, X., Yang, Y., Zhang, X., Li, L., et al. (2023). APOC1 exacerbates renal fibrosis through the activation of the NF-κB signaling pathway in IgAN. *Front. Pharmacol.* 14, 1181435. doi:10.3389/fphar.2023.1181435

Yu, X. Y., Sun, Q., Zhang, Y. M., Zou, L., and Zhao, Y. Y. (2022). TGF-β/Smad signaling pathway in tubulointerstitial fibrosis. *Front. Pharmacol.* 13, 860588. doi:10.3389/fphar.2022.860588

Zarnegar, B. J., Wang, Y., Mahoney, D. J., Dempsey, P. W., Cheung, H. H., He, J., et al. (2008). Noncanonical NF-kappaB activation requires coordinated assembly of a regulatory complex of the adaptors cIAP1, cIAP2, TRAF2 and TRAF3 and the kinase NIK. *Nat. Immunol.* 9, 1371–1378. doi:10.1038/ni.1676

Zhang, H., and Sun, S. C. (2015). NF-κB in inflammation and renal diseases. *Cell Biosci.* 5, 63. doi:10.1186/s13578-015-0056-4

Zhang, J., Mi, Y., Zhou, R., Liu, Z., Huang, B., Guo, R., et al. (2020a). The TLR4-MyD88-NF-κB pathway is involved in sIgA-mediated IgA nephropathy. *J. Nephrol.* 33, 1251–1261. doi:10.1007/s40620-020-00722-3

Zhang, S., Xu, L., Liang, R., Yang, C., and Wang, P. (2020b). Baicalin suppresses renal fibrosis through microRNA-124/TLR4/NF-κB axis in streptozotocin-induced diabetic nephropathy mice and high glucose-treated human proximal tubule epithelial cells. *J. Physiol. Biochem.* 76, 407–416. doi:10.1007/s13105-020-00747-z

Zhao, H., Alam, A., Soo, A. P., George, A. J. T., and Ma, D. (2018). Ischemia-reperfusion injury reduces long term renal graft survival: mechanism and beyond. *EBioMedicine* 28, 31–42. doi:10.1016/j.ebiom.2018.01.025

Zhao, S., Jia, L., Cui, C., Chen, Z., Duan, Z., Gao, J., et al. (2023). Combination therapy of low-dose steroids, tacrolimus and mycophenolate mofetil in primary membranous nephropathy: a single-center retrospective cohort study. *Integr. Med. Nephrol. Androl.* 10, e00012. doi:10.1097/imna-d-22-00012

Zhao, X., Kwan, J. Y. Y., Yip, K., Liu, P. P., and Liu, F. F. (2020). Targeting metabolic dysregulation for fibrosis therapy. *Nat. Rev. Drug Discov.* 19, 57–75. doi:10.1038/s41573-019-0040-5

Zhao, Y., Yang, L., Wang, M., Wang, L., Cheng, X.-L., Zhang, Y., et al. (2009a). 1β-hydroxylfriedelin, a new natural pentacylic triterpene from the sclerotia of Polyporus umbellatus. *J. Chem. Res.* 2009, 699–701. doi:10.3184/030823409x12562954717147

Zhao, Y. Y. (2013). Traditional uses, phytochemistry, pharmacology, pharmacokinetics and quality control of Polyporus umbellatus (Pers.) Fries: a review. *J. Ethnopharmacol.* 149, 35–48. doi:10.1016/j.jep.2013.06.031

Zhao, Y.-Y. (2022). Recent advances of gut microbiota in chronic kidney disease patients. *Explor. Med.* 3, 260–274. doi:10.37349/emed.2022.00090

Zhao, Y. Y., Chao, X., Zhang, Y., Lin, R. C., and Sun, W. J. (2010a). Cytotoxic steroids from Polyporus umbellatus. *Planta Med.* 76, 1755–1758. doi:10.1055/s-0030-1249926

Zhao, Y. Y., Cheng, X. L., Zhang, Y., Zhao, Y., Lin, R. C., and Sun, W. J. (2010b). Simultaneous determination of eight major steroids from Polyporus umbellatus by high-performance liquid chromatography coupled with mass spectrometry detections. *Biomed. Chromatogr.* 24, 222–230. doi:10.1002/bmc.1277

Zhao, Y. Y., Xie, R. M., Chao, X., Zhang, Y., Lin, R. C., and Sun, W. J. (2009b). Bioactivity-directed isolation, identification of diuretic compounds from Polyporus umbellatus. *J. Ethnopharmacol.* 126, 184–187. doi:10.1016/j.jep.2009.07.033

Zhao, Y. Y., Zhang, L., Mao, J. R., Cheng, X. H., Lin, R. C., Zhang, Y., et al. (2011). Ergosta-4,6,8(14),22-tetraen-3-one isolated from Polyporus umbellatus prevents early renal injury in aristolochic acid-induced nephropathy rats. *J. Pharm. Pharmacol.* 63, 1581–1586. doi:10.1111/j.2042-7158.2011.01361.x

Zhou, Q., Li, J., Xiang, Z., Zou, H., and Shao, X. (2022). Amelioration of renal injury by resveratrol in a rat renal transplantation model via activation of the SIRT1/NF-κB signaling pathway. *Biomed. Res. Int.* 2022, 7140961. doi:10.1155/2022/7140961

Zhou, Y., Ma, X. Y., Han, J. Y., Yang, M., Lv, C., Shao, Y., et al. (2021). Metformin regulates inflammation and fibrosis in diabetic kidney disease through TNC/TLR4/NF-κB/miR-155-5p inflammatory loop. *World J. Diabetes* 12, 19–46. doi:10.4239/wjd.v12.i1.19

Zhuang, K., Jiang, X., Liu, R., Ye, C., Wang, Y., Wang, Y., et al. (2020). Formononetin activates the Nrf2/ARE signaling pathway via Sirt1 to improve diabetic renal fibrosis. *Front. Pharmacol.* 11, 616378. doi:10.3389/fphar.2020.616378

Zou, G., Zhou, Z., Xi, X., Huang, R., and Hu, H. (2021). Pioglitazone ameliorates renal ischemia-reperfusion injury *via* inhibition of NF-κB activation and inflammation in rats. *Front. Physiol.* 12, 707344. doi:10.3389/fphys.2021.707344

Zou, X. Z., Liu, T., Gong, Z. C., Hu, C. P., and Zhang, Z. (2017). MicroRNAs-mediated epithelial-mesenchymal transition in fibrotic diseases. *Eur. J. Pharmacol.* 796, 190–206. doi:10.1016/j.ejphar.2016.12.003

Ren et al.                                                              10.3389/fphar.2023.1335094

# Glossary

| | |
|---|---|
| **AGEs** | advanced glycation end-products |
| **AKI** | acute kidney injury |
| **ATN** | acute tubular necrosis |
| **CAD** | chronic renal allograft dysfunction |
| **CKD, COX-2** | chronic kidney disease, cyclooxygenase-2 |
| **CTGF** | connective tissue growth factor |
| **DN** | diabetic nephropathy |
| **ESRD** | end-stage renal disease |
| **ECM** | extracellular matrix |
| **FN** | fibronectin |
| **HO-1** | heme oxygense-1 |
| **HGMCs** | human glomerular mesangial cells |
| **HRGECs** | human renal glomerular endothelial cells |
| **IL-1** | interleukin-1 |
| **IL-6** | interleukin-6 |
| **IKK** | inhibitor of kappa B kinases |
| **IĸB** | inhibitor of kappa B |
| **IRI** | ischemia-reperfusion injury |
| **IgAN** | immunoglobulin A nephropathy |
| **LncRNAs** | long non-coding RNAs |
| **LPS** | lipopolysaccharide |
| **MCP-1** | monocyte chemoattractant protein-1 |
| **MCs** | mesangial cells |
| **MMT** | macrophage-to-myofibroblast transition |
| **MN** | membranous nephropathy |
| **MiRNAs** | microRNAs |
| **NF-ĸB** | nuclear factor kappa B |
| **Nrf2** | nuclear factor erythroid-derived 2-related factor 2 |
| **NQO1** | nicotinamide adenine dinucleotide phosphate quinone dehydrogenase 1 |
| **ROS** | reactive oxygen species |
| **PCAF** | p300/CBP-associate factor |
| **TCR4** | toll-like receptor 4 |
| **TGF-β** | transforming growth factor-β |
| **TNC** | tenascin-C |
| **TNF-α** | tumor necrosis factor-alpha |
| **TPH-1** | tryptophan hydroxylase-1 |
| **UUO** | unilateral ureteral obstruction |
| **ZAS** | zymosan activation serum |
| **5-MTP** | 5-methoxytryptophan |

Frontiers in Pharmacology

# Kidney derived apolipoprotein M and its role in acute kidney injury

Line S. Bisgaard[1,2], Pernille M. Christensen[1,2], Jeongah Oh[3], Federico Torta[3,4], Ernst-Martin Füchtbauer[5], Lars Bo Nielsen[6] and Christina Christoffersen[1,2]*

[1]Department of Clinical Biochemistry, Copenhagen University Hospital—Rigshospitalet, Copenhagen, Denmark, [2]Department of Biomedical Sciences, University of Copenhagen, Copenhagen, Denmark, [3]Singapore Lipidomics Incubator, Life Sciences Institute, National University of Singapore, Singapore, Singapore, [4]Precision Medicine Translational Research Programme and Department of Biochemistry, Yong Loo Lin School of Medicine, National University of Singapore, Singapore, Singapore, [5]Department of Molecular Biology and Genetics, Aarhus University, Aarhus, Denmark, [6]The Faculty of Health Sciences, Aarhus University, Aarhus, Denmark

**Aim:** Apolipoprotein M (apoM) is mainly expressed in liver and in proximal tubular epithelial cells in the kidney. In plasma, apoM associates with HDL particles via a retained signal peptide and carries sphingosine-1-phosphate (S1P), a small bioactive lipid. ApoM is undetectable in urine from healthy individuals but lack of megalin receptors in proximal tubuli cells induces loss of apoM into the urine. Besides this, very little is known about kidney-derived apoM. The aim of this study was to address the role of apoM in kidney biology and in acute kidney injury.

**Methods:** A novel kidney-specific human apoM transgenic mouse model (RPTEC-hapoM[TG]) was generated and subjected to either cisplatin or ischemia/reperfusion injury. Further, a stable transfection of HK-2 cells overexpressing human apoM (HK-2-hapoM[TG]) was developed to study the pattern of apoM secretion in proximal tubuli cells.

**Results:** Human apoM was present in plasma from RPTEC-hapoM[TG] mice (mean 0.18 µM), with a significant increase in plasma S1P levels. *In vitro* apoM was secreted to both the apical (urine) and basolateral (blood) compartment from proximal tubular epithelial cells. However, no differences in kidney injury score was seen between RPTEC-hapoM[TG] and wild type (WT) mice upon kidney injury. Further, gene expression of inflammatory markers (i.e., IL6, MCP-1) was similar upon ischemia/reperfusion injury.

**Conclusion:** Our study suggests that kidney-derived apoM is secreted to plasma, supporting a role for apoM in sequestering molecules from excretion in urine. However, overexpression of human apoM in the kidney did not protect against acute kidney injury.

**Abbreviations:** apoM, apolipoprotein M; hapoM, human apoM; mapoM, mouse apoM; apoM-Tg[H], apoM-transgenic High; apoM-Tg[N], apoM-transgenic Normal; apoM-KO, apoM knockout; HDL, high density lipoprotein; LDL, low density lipoprotein; S1P, sphingosine-1-phosphate; Sglt2, sodium/glucose cotransporter 2; RPTEC-hapoM[TG], renal proximal tubule epithelial cell specific apoM-transgenic mice; WT, wild type; I/R, ischemia reperfusion; HK-2-hapoM[TG], HK-2 cells with stable overexpression of hapoM; Papp, Passive permeability.

## Introduction

Human apolipoprotein M (hapoM) is a 21 kDa (non-glycosylated) or 25 kDa (glycosylated) apolipoprotein (Xu and Dahlback, 1999). Murine apoM (mapoM) is only detectable in the non-glycosylated form (Faber et al., 2004). ApoM in plasma is mainly associated with HDL particles and to a lesser extent with LDL and triglyceride-rich lipoproteins (Christoffersen et al., 2006). Approximately 5% of all HDL particles contain an apoM molecule (Christoffersen et al., 2006). ApoM is anchored to lipoproteins by a retained hydrophobic 21 amino acid signal peptide, which prevents rapid clearance of apoM in the kidneys (Christoffersen et al., 2008a). Thus, apoM does not circulate without association to lipoproteins in plasma.

ApoM is expressed in the liver and kidney in both humans (Zhang et al., 2003) and mice (Faber et al., 2004). The expression of apoM in the kidney is conferred primarily to the proximal tubular cells and to a lesser extent to the cells of the distal tubules and the glomeruli (Zhang et al., 2003). It is assumed that apoM in plasma is derived from the liver and due to its association with lipoproteins, apoM is not believed to be able to pass the healthy glomerular filtration barrier. Structurally, apoM contain a characteristic eight-stranded anti-parallel beta-barrel conformation surrounding a hydrophobic binding pocket (Duan et al., 2001). Sphingosine-1-phosphate (S1P), retinoic acids, and oxidized phospholipids have been identified as ligands for apoM (Ahnström et al., 2007; Christoffersen et al., 2011; Elsoe et al., 2012). At present, it is mainly the liver-derived plasma apoM/S1P-axis that has been investigated. Thus, studies have shown that the apoM/S1P-axis is necessary to maintain the endothelial barrier via S1P and the S1P receptors, play a role in lipid turnover and are involved in fibrosis formation (Christoffersen et al., 2011; Ding et al., 2016; Christoffersen et al., 2018; Ding et al., 2020; Hajny et al., 2021). Importantly, several studies have in addition indicated that besides being a transporter of small hydrophobic molecules, apoM might also modulate HDL particles and affect the turnover of apoB containing lipoproteins (Wolfrum et al., 2005; Christoffersen et al., 2008b; Kurano et al., 2013; Liu et al., 2014).

Due to the lack of appropriate animal models, the role of apoM specifically derived from the kidney is more speculative. *In vitro*, apoM binds the megalin receptor on proximal tubular cells and subsequently gets internalized (Faber et al., 2006), while apoM is undetectable in the urine from healthy wild type (WT) mice and humans (Faber et al., 2006). However, mice with kidney-specific megalin-deficiency loose apoM in the urine (Faber et al., 2006; Sutter et al., 2014). Therefore, it is hypothesized that kidney-derived apoM is secreted into the pre-urine where it binds S1P or other small molecules and subsequently gets endocytosed into the tubular cells via binding to megalin receptors. Thereby, apoM prevents urinary loss of S1P or other small hydrophobic molecules, which have been filtered in the glomeruli. This hypothesis is supported by a study with transgenic mice expressing human apoM without the signal peptide (Christoffersen et al., 2008a). These mice have undetectable levels of human apoM in plasma due to its rapid filtration in the kidney. However, human apoM was not found in the urine but was shown to be taken up by the proximal tubular cells in the kidney (Christoffersen et al., 2008a). Furthermore, apoM-deficient mice loose S1P in the urine (Sutter et al., 2014), but it is unknown whether

this is due to lack of apoM in plasma or caused by lack of apoM in the kidney.

Besides megalin-deficiency, ischemia reperfusion (I/R) injury in rat kidneys also lead to rapid apoM excretion in urine (Xu et al., 2013). Further, knock out of S1P receptor 1 in proximal tubular epithelial cells leads to increased kidney injury upon both I/R and cisplatin induced acute kidney injury (Bajwa et al., 2010; Bajwa et al., 2015). This prompted the suggestion of kidney derived apoM as an important modulator of acute kidney injury.

To characterize the role of apoM on atherosclerosis and lipid metabolism, a panel of apoM gene-modified mice has been generated using the endogenous promoter (express apoM in liver and kidney) (Christoffersen et al., 2008b), the apoE promoter (express apoM primarily in liver) (Liu et al., 2014), and adenovirus (express apoM in liver) (Kurano et al., 2013). These models are not suitable for studying the specific function of kidney-derived apoM. Therefore, the purpose of this study was to generate a novel kidney-specific apoM transgenic mouse and subsequently to determine if kidney-derived apoM contributes to the plasma pool of apoM as well as its role in acute kidney injury.

## Materials and methods

### Animals

Mice were housed in a temperature-controlled facility with a 12-h light/dark cycle at the Panum Institute, University of Copenhagen, Denmark. They had free access to standard chow diet (Altromin 1314, Brogaarden) and water. Renal proximal tubule epithelial cell specific apoM-transgenic (RPTEC-hapoM[TG]) mice were backcrossed at least twice onto a C57BL6/J background for the basic characteristic of the model, while they were backcrossed at least three times for the injury studies. ApoM-transgenic Normal (apoM-Tg[N]) (Christoffersen et al., 2008b), apoM-transgenic High (apoM-Tg[H]) (Christoffersen et al., 2008b) and apoM knockout (apoM-KO) (Christoffersen et al., 2008b) mice were backcrossed >10 times. All animal experiments were approved by the Animal Experiments Inspectorate, Danish Veterinary and Food Administration, Ministry of Food, Agriculture and Fisheries, Denmark.

### Cloning and generation of kidney-specific human apoM transgenic mice

DNA containing the coding region of human apoM, 1729 bp 3′ to the polyA site and 3 bp 5′ to the ATG site was amplified from the Bacterial Artificial Chromosome (BAC) DNA (RP11-201G24, NCBI sequence AF129756, BACPAC) with PCR using Phusion HotStart High-Fidelity DNA Polymerase (F540, Thermo Scientific). Primer sequences were: 5′-CCGCGGATACCGTCGACCCTGAAGATG TTCCA-3′ and 5′-TCTAGAGACGGCTTGGTGGCTGGCTA-3′. PCR products were purified with illustra GFX PCR DNA and Gel Band Purification kit (GE Healthcare), cloned into pCR-BluntII-TOPO (Life Technologies) and transfected into *E. coli* (*Escherichia coli*). Plasmid DNA was isolated with QIAPrep Spin Miniprep kit (27106, Qiagen), digested with *SacII* and *SalI* and

isolated on an agarose gel and purified with illustra GFX PCR DNA and Gel Band Purification kit (GE Healthcare).The Sglt2 promotor was isolated from pGEM-sglt2 5 pr-mut (Rubera et al., 2004) kindly provided by Dr. Isabelle Rubera by digestion with *SacII* and *SalI*, agarose gel electrophoresis and purification with illustra GFX PCR DNA and Gel Band Purification kit (GE Healthcare). The isolated fragment was ligated with the digested pCR-BluntII vector containing hapoM. The plasmid was transfected into *E. coli* and plasmid DNA was isolated with QIAPrep Spin Miniprep kit (27106, Qiagen). The correctness of the plasmid was assured by digestion with *ApaI* and sequencing of 700 bp surrounding the 5′ and 3′ end of human apoM and the 5′ end of Sglt2, respectively. The fragment containing the Sglt2 promotor and human apoM was isolated by digestion with *NsiI*, agarose gel electrophoresis and purification with illustra GFX PCR DNA and Gel Band Purification kit (GE Healthcare). Pronuclear injections of the isolated transgenes into fertilized mouse oocytes (B6D2F2 embryos) were done by Danish Genetically Modified Animal Resource, Aarhus University, Denmark, providing a novel mouse line with the following gene code: Tg(Sglt2-hsapoM)EMFU, and strain name: B6.D2-Tg(Sglt2-hsapoM)EMFU1.

## Genotyping

DNA was isolated and amplified from ear snips using REDExtract-N-Amp Tissue PCR Kit (XNAT, Sigma-Aldrich) according to the manufacturer's protocol. Primers used were forward: 5′-GGGACTTGAATTCCTCCACA-3′ and reverse: 5′-TGAAGGGAGCACAGATCTCA-3′. The primers span exon 3-5 of the human apoM gene. PCR products were analyzed with agarose gel electrophoresis.

## Kidney injury models

Mice were given a single injecting of cisplatin (20 mg/kg, *i.p.*) to induce kidney injury in RPTEC-hapoM[TG] and WT mice. Following the injection, mice were monitored closely for the rest of the study, weighed once daily and given 1 mL of NaCl. 3 days after the cisplatin injection, a urine sample was collected, and mice were anesthetized with Zoletil (tiletamin 1.63 mg/mL, zolazepam 1.63 mg/mL, xylazin, 2.61 mg/mL, butorphanoltartrat 0.065 mg/mL) at a dose of 0.01 mL/ g mouse. A blood sample was collected, and the mice were perfused with ice-cold saline after which the kidneys were excised and saved for histological and qPCR evaluation.

For I/R injury in RPTEC-hapoM[TG], apoM-KO and WT mice, the right kidney was exteriorized via a dorsal incision. The blood vessels were exposed by carefully removing fat and connective tissue and the blood supply to the kidney was clamped at the renal pedicle for 30 min using a non-traumatic vascular clamp. During the procedure the kidney was covered with the skin and vet sterile gaze to avoid desiccation. After 30 min, the clamp was removed, and the kidney was gently pushed back into its retroperitoneal location. Mice were anesthetized with Zoletil during the procedure, and analgesia was administered by subcutaneous injection of buprenorphine (0.05 mg/kg mouse) during the procedure, and every 8 h after the procedure. 24 h of reperfusion was allowed

after which a urine sample was collected, and mice were anesthetized. A blood sample was taken, mice were perfused with ice-cold saline and kidneys were saved for histological and qPCR evaluation.

## Blood samples and plasma measurements

Blood samples were taken either from the mandibular vein or retro-orbital (at termination of the mice). Blood was collected in EDTA microtubes and centrifuged at 3,500 rpm for 10 min at 4°C. Plasma urea and creatinine were measured with a Cobas1 8000 modular analyzer series (Roche A/S).

## Cell culture and transfection

HK-2 cells (ATCC, CRL-2190) were cultured on collagen coated wells (Type 1 Collagen, 5 μg/cm² overnight, Sigma), in DMEM/ F12 without phenol red (21041–025, Gibco) supplemented with 1 × GlutaMAX (Gibco), 1 × P/S (Gibco), 20 mM Hepes (Gibco), 25 ng/ mL Hydrocortizone (H6909, Sigma) and 1 × ITS supplement (41400045, Gibco). 200 μg/mL Zeocin (45–0430, Invitrogen) was added for selection.

A stable cell line overexpressing human apoM (HK-2-hapoM[TG]) was established by transfecting the HK-2 cells with full length human apoM under the control of the human cytomegalovirus (CMV) promotor using the Flp-In system (Invitrogen). For experiments, cells were plated on collagen coated polycarbonate transwells (3401, Costar) and cultured until confluency. At day 4 after confluency was reached, cells were washed ones with PBS and the medium was changed to medium without FBS but with 0.05 mM BSA (A7030, Sigma).

## Transepithelial electrical resistance measurement

TEER was determined using an EndOhm Chamber 12G connected to an EVOM2 Meter (World Precision Instrument, England, United Kingdom). The measurements were done at room temperature. For data analysis, the resistance of an empty well was subtracted from the resistance in each of the wells and the data was adjusted for well size by multiplying with the well area of the insert.

## Permeability assay

Passive permeability (Papp) was determined using Cascade blue labelled 10 kDa dextrans (D1976, Invitrigen) and Fluorescein labelled 40 kDa dextrans (D1845, Invitrogen). The two dextrans were added directly to the apical wells for a final concentration of 0.5 mg/mL and 100 μL medium was collected from the basolateral (receiver) compartment at time point 15, 30, 45, 60, 90, 120, and 180 min. Each time the 100 μL medium was replaced with clean cell medium. At 180 min, a donor sample from the apical compartment was collected. During the

procedure the plates were placed on a shaking table with a speed of 90 rpm, and in a controlled temperature of 37°C in atmospheric air between the sampling.

The receiver and the donor samples (diluted 1:100) as well as a control sample (0.5 mg/mL of each of the dextrans in clean medium) were pipetted to a black 96-well plate and the fluorescence signal was determined (EnSpire™ Multimode Plate Reader, PerkinElmer, Inc.; Cascade blue: excitation 400 nm, emission 440 nm; Fluorescein excitation 494 nm, emission 521 nm).

The apparent permeability ($P_{app}$) was determined as previously described (Hubatsch et al., 2007; Tornabene et al., 2019). Briefly, Papp was calculated using the formula: $P_{app} = J/(C_{donor}*A)$, with J being the flux at steady state ($\mu mol * sec^{-1}$), $C_{donor}$ the initial concentration of the relevant marker molecule in the donor compartment ($\mu M$), and A the surface area of the filter ($cm^2$). To determine J, the accumulation of the tested compound in the receiver chamber was plotted as a function of time and the slope in the linear region was determined.

## RNA extraction and gene expression analysis

RNA was extracted with TRIzol Reagent (15596–018, Life Technologies) according to the manufacturer's protocol. cDNA was generated from 1 μg RNA using High-Capacity cDNA Reverse Transcription Kit (4368814, Applied Biosystems) and gene expression was determined by quantitative real-time PCR on TaqMan (Life Technologies). 18S, GAPDH, B2M and TBP was used as housekeeping (HK) genes.
Primer sequences:
Human apoM forward: 5′-GGGACTTGAATTCCTCCACA-3′
Human apoM reverse: 5′-TGAAGGGAGCACAGATCTCA-3′
Mouse apoM forward: 5′-CCTGGGCCTGTGGTACTTTA-3′
Mouse apoM reverse: 5′-CCATGTTTCCTTTCCCTTCA-3′
Mouse TNFα forward: 5′-CTGGCCCAAGGCGCCACATC-3′
Mouse TNFα reverse: 5′-TGGGGACCGATCACCCCGAAG-3′
Mouse ICAM forward: 5′-ATGCCGACCCAGGAGAGCACAA-3′
Mouse ICAM reverse: 5′-TCGACGCCGCTCAGAAGAACCA-3′
Mouse VCAM forward: 5′-CTTCATCCCCACCATTGAAG-3′
Mouse VCAM reverse: 5′-TGAGGAGGTCAGGTTCACAG-3′
Mouse IL-6 forward: 5′-ACAAAGCCAGAGTCCTTCAGAGAGA-3′
Mouse IL-6 reverse: 5′-GGCATAACGCACTAGGTTTGCCG-3′
Mouse S1P1 forward: 5′-TCGCGCGGTGTACCCAGA-3′
Mouse S1P1 reverse: 5′-CCAGGCAAACGCTAGAGGGCG-3′
Mouse S1P2 forward: 5′-TTACTGGCTATCGTGGCTCTG-3′
Mouse S1P2 reverse: 5′-ATGGTGACCGTCTTGAGCAG-3′
Mouse S1P3 forward: 5′-AAGCCTAGCGGGAGAGAAAC-3′
Mouse S1P3 reverse: 5′-TCAGGGAACAATTGGGAGAG-3′
Mouse 18s forward: 5′-CGCGGTTCTATTTTGTTGGT-3′
Mouse 18s reverse: 5′-AGTCGGCATCGTTTATGGTC-3′
GAPDH forward: 5′-GTGGTTCACACCCATCACAA-3′
GAPDH reverse: 5′-GGTGCTGAGTATGTCGTGGA-3′
B2M forward: 5′-TCTCACTGACCGGCCTGTAT -3′
B2M reverse: 5′-TTTCAATGTGAGGCGGGTGG-3′
TBP forward: 5′-TAATCCCAAGCGATTTGCTGC-3′
TBP reverse: 5′-CTTCACATCACAGCTCCCCA-3′

## Lipid analyses

Cholesterol in plasma samples and gel filtration chromatography fractions from both plasma and conditioned cell medium was analyzed enzymatically (11491458-216, Roche). Triglycerides were determined in plasma samples enzymatically according to the manufacturer's protocols (TR0100, Sigma Aldrich).

## Gel filtration chromatography

Plasma samples were pooled ($n = 2–4$) and diluted 1:3.2 with PBS containing 0.01% EDTA and 500 μL were run at a Superose 6 10/300 GL column (17-5172-01, GE Healthcare). Fractions of 6 drops (~280 μL) were collected. Protein profiles were determined by the absorbance read at 280 nm and cholesterol determined in individual fractions. Pools corresponding to the VLDL, LDL, and HDL peaks were collected for WB analysis of apoM.

Conditioned cell medium from respectively the apical (diluted 1: 3) and the basolateral compartment was concentrated x6 using spin columns (10 k, Umicon Ultra, Merck) and pooled (medium from 3 wells). 500 μL of each sample were run at a Superose 6 10/300 GL column (17-5172-01, GE Healthcare) and fractions of 3 drops (~140 μL) were collected. Also, a human plasma sample was run as reference material, and cholesterol determined in the fractions.

## Western blot

Gel filtration samples (15.6 μL) were run on 12% SDS-gels and blotted on PVDF membranes with iBlot Gel Transfer Device (Invitrogen). Membranes were blocked with 5% skim milk solution and incubated O/N with primary antibody at 4°C (rabbit anti-hapoM EPR2904, Genetex or goat anti-hapoM C54523, Life Span). After washing, membranes were incubated with secondary antibodies (anti-goat P0160, Dako or anti-rabbit P0448, Dako) for minimum 1 h at RT. Membranes were visualized with SuperSignal West Pico Chemiluminescent Substrate (34080, Thermo Scientific).

For urine samples, the analysis of mouse apoM (rabbit antibody EPR2904, Abcam) and mouse ApoA1 (K23001R, Biosite) were done as described above. The analysis of human apoM was done with an in-house apoM antibody (Christensen et al., 2017) directly labelled with IRDye 800CW High MW (LICOR). For this analysis membranes were blocked with Oddesey 927–40000 4°C O/N and visualized directly.

## Human apoM ELISA

Human apoM in plasma (10 μL) and urine (30 μL) samples from mice as well as conditioned medium (30 μL) and FPLC fractions (30 μL) of concentrated conditioned medium was analyzed with a specific human apoM ELISA as previously described (Bosteen et al., 2015). Briefly, samples were reduced with DTT and alkylated with iodoacetamide before addition to the sandwich ELISA. The monoclonal mouse antibody clone 1G9 (Abnova) was used as
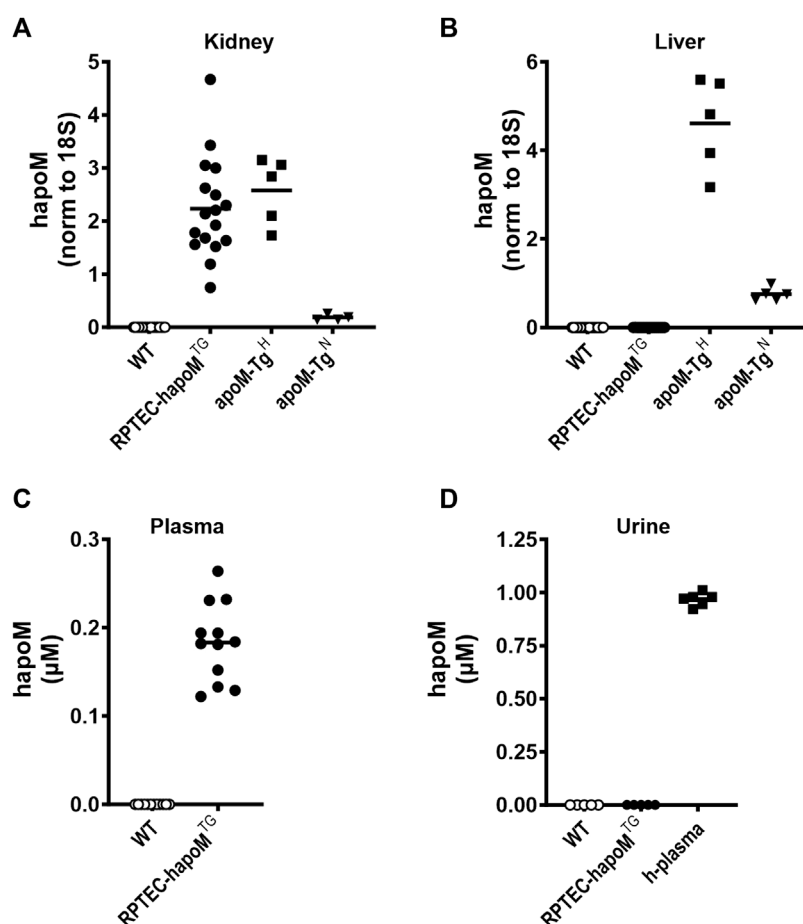
**FIGURE 1**
Expression of human apoM in liver and kidney, as well as plasma and urine concentration. Gene expression of human apoM were analyzed in kidney **(A)** and liver **(B)** from WT, PTEC-hapoM[TG], apoM-Tg[H] (10 times higher plasma apoM levels) and apoM-Tg[N] (2 times higher plasma apoM levels) mice with qPCR and normalized to the expression of 18S. Human apoM in plasma from PTEC-hapoM[TG] and their WT littermates **(C)** was measured with ELISA. Human apoM in urine samples from PTEC-hapoM[TG], WT and human plasma samples **(D)** was measured with ELISA. For samples with an absorbance below the lowest standard in the standard curve, the concentration is noted as 0. Each symbol represents an individual mouse or human sample, and horizontal lines represent the mean.

capture antibody and the rabbit antibody EPR2904 (Abcam) was used as detection antibody. Standard curve concentrations for the assay are 3.481, 2.660, 2.024, 1.369, 0.922, 0.695, 0.465, 0.234 nM. Urine samples were diluted 1:1000 while plasma samples were diluted 1:500 or 1:250. The apoM concentration detected is the same for dilution in water and urine.

## S1P extraction and quantification

Plasma S1P was determined as previously described (Burla et al., 2018). Briefly, lipids were extracted by mixing 20 µL of plasma with 200 µL butanol/methanol (1:1, v/v) solution containing an internal S1P d18:1 [13]C2D2 standard (Toronto Research Chemicals, S681502), followed by derivatization of the lipids by a trimethylsilyl-diazomethane derivatization step (Narayanaswamy et al., 2014). Lipids were then separated on an Agilent 1290 UHPLC, using a Waters ACQUITY UPLC BEH HILIC, C18 (130 Å, 2.1 × 100 mm, 1.7 µm) column, and measured in an Agilent 6495 QQQ MS. The mobile phase A consisted of acetonitrile and 25 mM ammonium formate buffer (50:50, v/v) and mobile phase B was composed of acetonitrile and 25 mM ammonium formate buffer (95:5, v/v).

The Agilent MassHunter software was used to analyze the data, with lipid peaks being identified based on the specific precursor and product ion transitions, as well as the retention time. Finally, normalization to the internal standards was carried out as previously discussed (Burla et al., 2018).

## Histology

Kidneys were fixated in 4% formalin, embedded in paraffin, and 3 or 4 µm sections were collected and stained with PAS staining according to standard protocols.

Injury in both disease models was defined as: Tubular dilation, cell necrosis, loss of brush borders, protein casts formation. For the cisplatin model, kidney injury score was assessed by two blinded observers in at
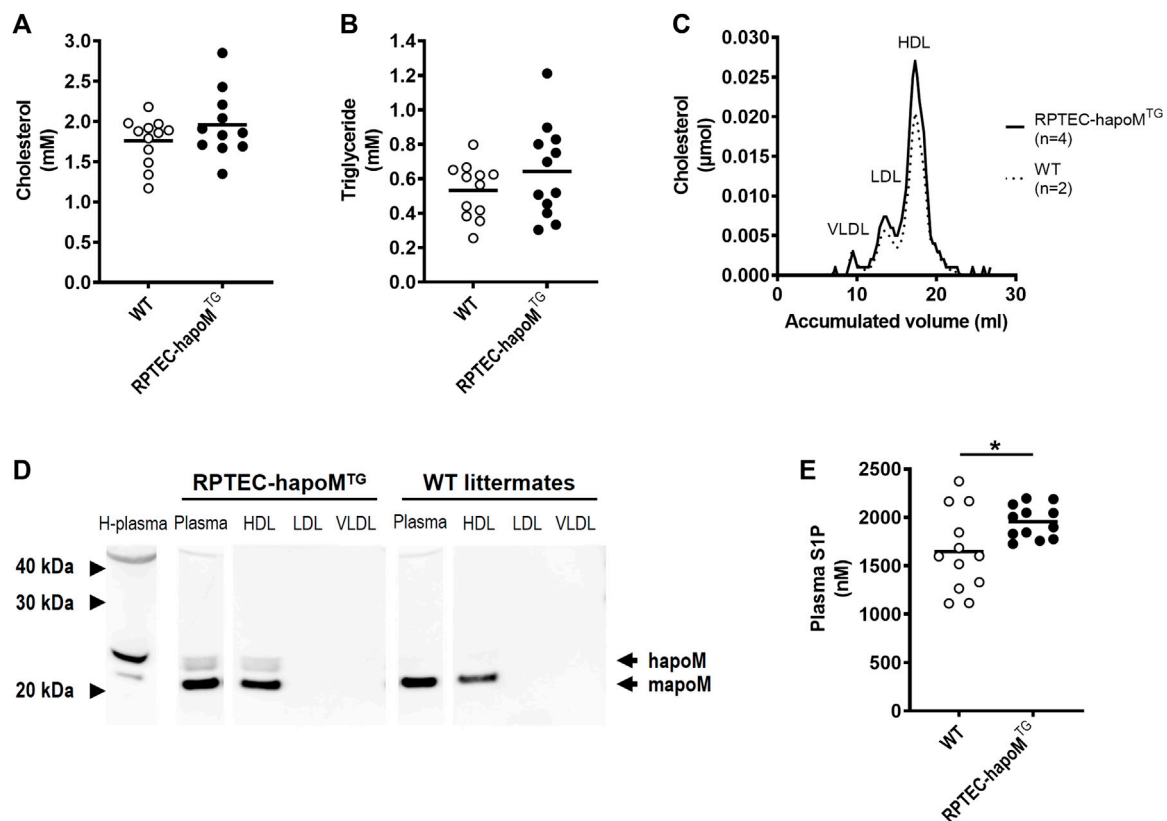
FIGURE 2
Characterization of the lipid profile and S1P levels in plasma. Plasma levels of cholesterol (A) and triglycerides (B) were measured in PTEC-hapoM (TG) and WT mice (littermates). Plasma from PTEC-hapoM^TG was analyzed by gel filtration chromatography and fractions were analyzed for cholesterol (C). Pools of fractions corresponding to VLDL, LDL, and HDL (marked in C) were analyzed with Western blot against apoM (D). Plasma S1P was analyzed by LC-MS (E). Each point in A, B and E represents an individual mouse and lines represent the mean. Statistical analysis for A, B and E was done with Student's t-test. *p < 0.05.

least 15 random pictures from the cortex area of the kidney taken from one section per mouse. Areas of kidney injury were marked on each picture using the Visiopharm software (Visiopharm, Denmark), and the values were then converted into a score from 0–4 (0 = no abnormalities, 1 = < 10% of picture affected, 2 = 11–25% of picture affected, 3 = 26–50% of picture affected, 4 = 51–75% of picture affected, 5 = > 76% of picture affected). For the I/R injury model, injury was assessed in 4 random selected pictures from the cortex area of both the injured and the control kidney taken from one section per mouse in a ×10 magnification. For each kidney a score from 1 to 3 was given, with 1 being small changes and 3 being major changes.

## Statistics

All statistical analyses, except analysis of qPCR data on kidneys from the I/R injury study, were performed using GraphPad Prism version 4.03 (GraphPad Software, Inc.). Groups of two were compared using Student's t-test with welch correction or paired analysis when appropriate. Mann-Whitney test was used when one or two of the groups were not normally distributed. Groups of 3 were compared using one-way ANOVA with the Holm-Šídák post hoc test. p-values ≤0.05 were considered statistically significant. For analysis of qPCR data on

kidneys from the I/R injury study, SPSS was used. Data was analyzed using mixed ANOVA.

## Results

### Generation of kidney-specific human apoM transgenic mice

A new transgenic mouse line only expressing human apoM in proximal tubular epithelial cells of the kidney, RPTEC-hapoM^TG mice, was generated by expressing human apoM under the control of the Sodium/glucose cotransporter 2 (Sglt2) promoter (Rubera et al., 2004). Six positive founders were generated and one founder with ~38 genomic copies, as determined by real time PCR, was selected. The distribution between gender in the N3 generation contained equal numbers of positive and negative RPTEC-hapoM^TG males and females.

### Plasma apoM levels are increased in mice with kidney specific overexpression of apoM

Gene expression analysis of kidney and liver tissue revealed tissue-specific expression of human apoM in kidneys from RPTEC-
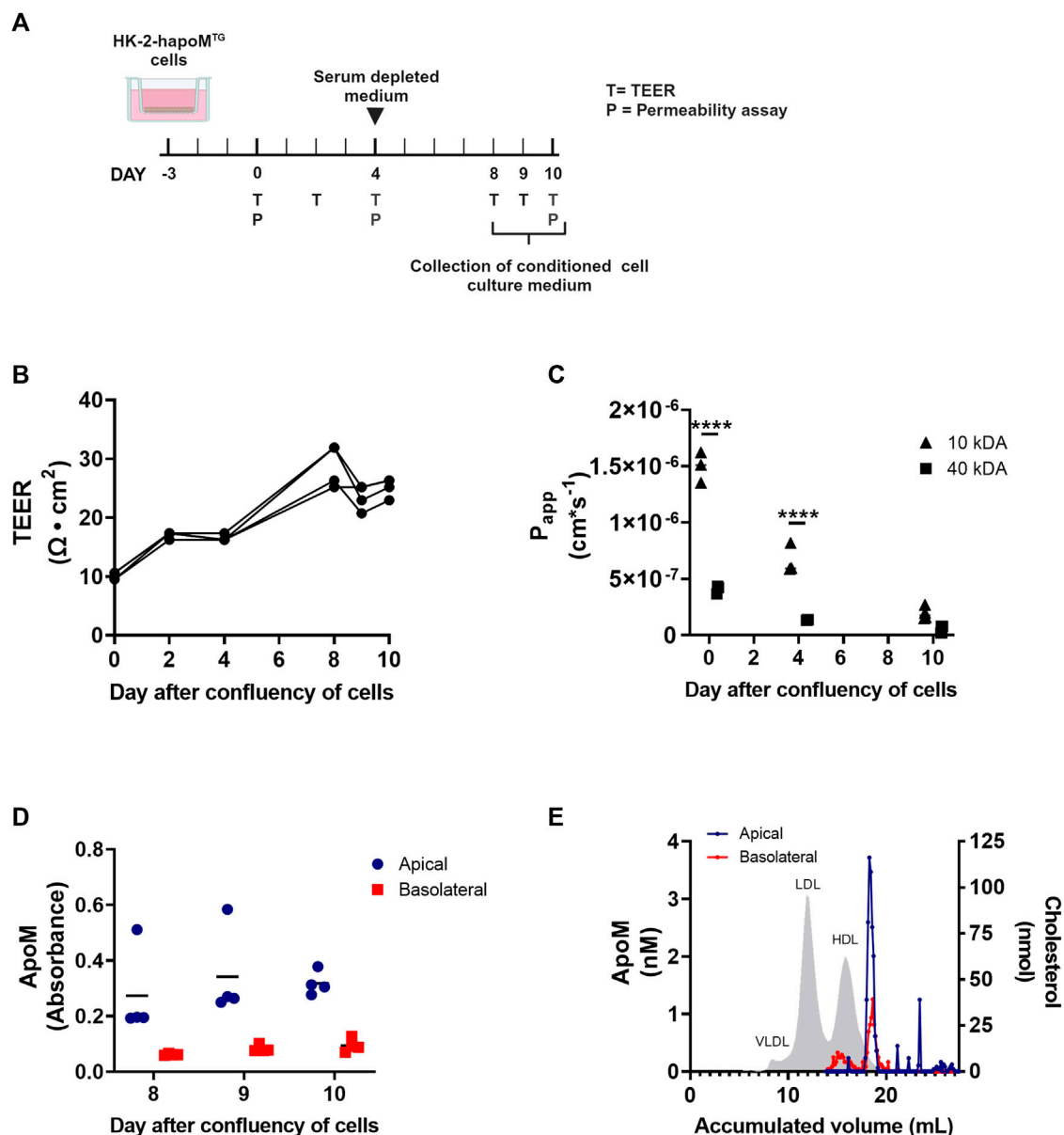
**FIGURE 3**
*In vitro* analysis of apoM secretion from proximal tubular epithelial cells. HK-2 cells overexpressing human apoM (HK-2-hapoM^TG) was used to address the secretion of apoM to respectively the apical and basolateral compartment **(A)**. Teer measurement **(B)** as well as determination of permeability **(C)** was performed to confirm that the cells were confluent at day 8–10 after confluency. The apoM concentration in respectively the apical and basolateral compartment **(D)** was measured at day 8–10 after confluency. Medium from the apical and basolateral compartment was pooled, separated by FPLC and the apoM concentration in each of the fractions was determined **(E)**. Grey area depicts the cholesterol profile in human plasma. Each point in B-D represents an individual well ($n = 3$) and lines represent the mean. Statistical analysis for C was done using 2-way ANOVA with the Holm-Šídák *post hoc* test testing the difference between the two dextran sizes at each time point. Both the within factor (time) and the between factor (dextran size) was significant. ****$p < 0.0001$.

hapoM^TG mice (Figure 1A), while there, as expected, was no expression in the liver (Figure 1B). The expression level of human apoM in kidneys from RPTEC-hapoM^TG mice was comparable to the expression levels seen in kidneys from apoM-Tg^H mice (mice with global overexpression of human apoM) (Figure 1A). Human apoM was undetectable in brain, heart, lung, skeletal muscle, duodenum, small intestine, colon, ventricle, ovaries, subcutaneous white adipose tissue, epididymal white adipose tissue, and interscapular brown adipose tissue in both

lines (data not shown). Further, gene expression of endogenous mouse apoM was not affected by the overexpression of human apoM (Supplementary Figure S1).

No major phenotypes were observed in RPTEC-hapoM^TG mice. Weight-curves obtained over 10 weeks were identical for transgenic mice and their WT littermates (Supplementary Figure S2), no major differences were found in terms of organ weight or development between transgenic mice and WT littermates (Supplementary Figure S3), and there was no
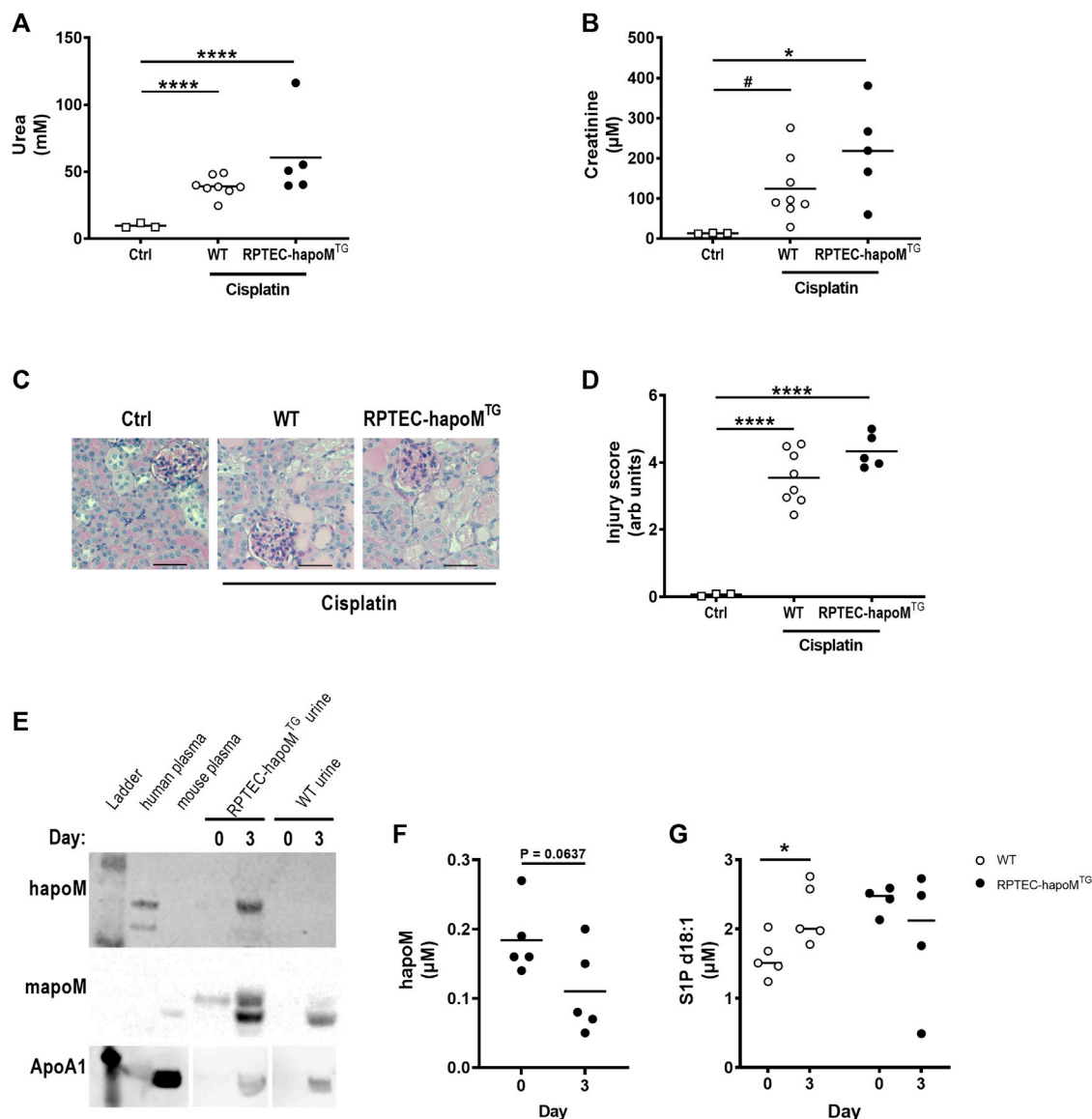
**FIGURE 4**
Characterization of kidney injury after cisplatin induced acute kidney injury. Plasma levels of urea **(A)** and creatinine **(B)** were measured in PTEC-hapoM[TG], WT and ctrl mice. Kidney sections from PTEC-hapoM[TG], WT and ctrl mice were stained with PAS stain **(C)**, representative pictures), and kidney injury was scores semi-quantitivly **(D)**. Human apoM, mouse apoM and ApoA1 in urine from PTEC-hapoM[TG] and WT mice was determined by Western blot before and after cisplatin injury **(E)**. The human apoM **(F)** and the S1P concentration **(G)** in plasma from PTEC-hapoM[TG] and WT mice was analyzed before and after injury. Each point in A, B, D, F, and G represents an individual mouse and lines represent the mean. Statistical analysis for A, B and D was done using one-way ANOVA with the Holm-Šídák *post hoc* test. For F and G, statistics was done using paired Student's t-test. *$p < 0.05$, ****$p < 0.0001$ #$p < 0.05$ analyzed by Student's t-test with Welch's correction.

difference in the plasma concentration of urea (a marker for kidney injury) between RPTEC-hapoM[TG] and WT mice (Supplementary Figure S4).

To test if kidney-derived apoM is secreted to plasma or is conserved in the kidney, plasma levels of human apoM were measured in RPTEC-hapoM[TG] mice and WT littermates. Human apoM was present in plasma from RPTEC-hapoM[TG] mice (range 0.12–0.26 μM, mean 0.18 μM), whereas human apoM as expected, was undetectable in WT littermates (Figure 1C). Further, human apoM was undetectable in urine samples from RPTEC-hapoM[TG] mice and WT littermates (Figure 1D).

## Plasma S1P levels are increased in RPTEC-hapoM[TG] mice

Global overexpression of apoM affects plasma lipids and lipoprotein metabolism (Christoffersen et al., 2008b). To address whether similar findings are present in the kidney specific overexpression model, the lipid profile of the mice was determined. Plasma levels of cholesterol and triglycerides were assessed in RPTEC-hapoM[TG] mice and their WT littermates and the lipoprotein profile in plasma was determined by gel filtration chromatography. No difference was found in either total plasma cholesterol (Figure 2A), triglyceride concentration (Figure 2B) or
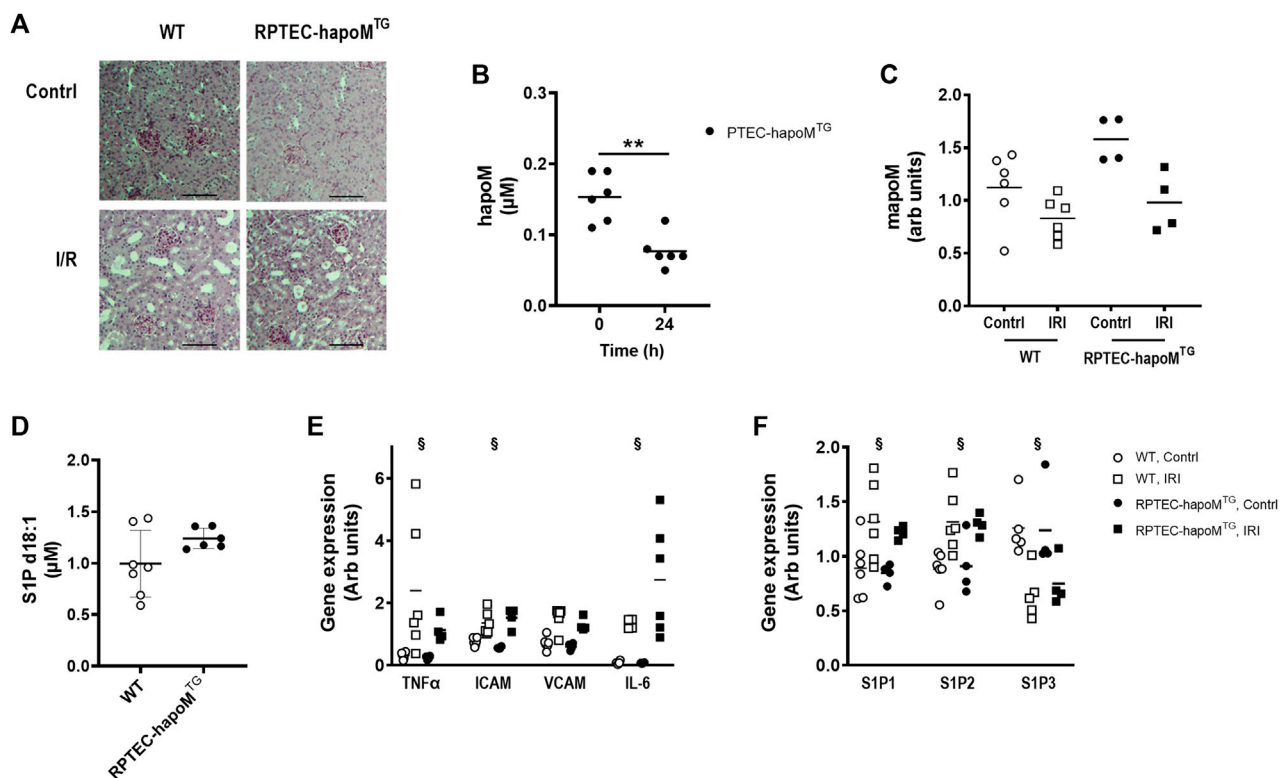
FIGURE 5
Characterization of kidney injury after I/R induced acute kidney injury. Kidney sections from both the injured and control kidney from PTEC-hapoM[TG] and WT were stained with PAS. Representative pictures are shown in **(A)**. Plasma concentration of human apoM before and after IR injury was analyzed in PTEC-hapoM[TG] by elisa **(B)**. Gene expression of mouse apoM was determined in both the kidney subjected to injury (IRI) and the contralateral control kidney (contrl) from PTEC-hapoM[TG] and WT mice and normalized to M2B and TBP **(C)**. Plasma level of S1P d18:1 was determined after 24 h of reperfusion in both WT and PTEC-hapoM[TG] mice **(D)**. Gene expression of inflammatory markers **(E)** as well as S1PR1-3 **(F)** was determined in both the kidney subjected to injury (IRI) and the contralateral control kidney (contrl) from PTEC-hapoM[TG] and WT mice and normalized to verified housekeeping genes. Each point in B, C, D, and E represents an individual mouse and lines represent the mean. Statistical analysis for B was done with paired $t$-test, while mixed ANOVA was used for C, D and **(E)**. There were no interaction for any of the genes in either C, E or **(F)**. The within factor (injury) was significant for TNFα, ICAM, IL-6 and S1P1-3, while the between factor (genotype) was non-significant for all genes. **$p < 0.05$ $^{§}p < 0.05$ for the withing factor (injury).

lipoprotein composition measured as the cholesterol (Figure 2C) and protein (Supplementary Figure S5) profile. Normally, apoM is found exclusively in lipoproteins, where the majority is bound to HDL particles and smaller amounts are found in non-HDL particles. To test the distribution of human apoM among lipoproteins in RPTEC-hapoM[TG] mice, pools corresponding to the VLDL, LDL, and HDL peaks from the gel filtration chromatography were analyzed with Western blot against human apoM (Figure 2D). Human apoM (~25 kDa) was detectable in the HDL peak, while no human apoM was detectable in the LDL and VLDL fraction. In mice with a global overexpression of human apoM plasma, S1P is increased (Christoffersen et al., 2008b; Christoffersen et al., 2011). Interestingly, we found a significant increase in plasma S1P levels in the RPTEC-hapoM[TG] mice compared to WT littermates (Figure 2E).

## ApoM is secreted both to the apical and basolateral compartment of proximal tubular epithelial cells

To address whether the human apoM measured in plasma is directly secreted to the blood compartment, or occur secondary to the secretion into the pre-urine, a transwell model of human proximal

epithelial cells were established. A stable transfection of HK-2 cells with human apoM (HK-2-hapoM[TG]) was made and the cells were cultured on transwell inserts to collect conditioned medium from both the basolateral (comparable to blood) and apical compartment (comparable to pre-urine) (Figure 3A). To test the confluency of the cells, the resistance of the cell monolayer was tested at day 2, 4 8, 9, and 10 after confluency of the cells. As expected, the transepithelial electrical resistance (TEER) increased slowly from day 0–8 where it stabilized around $25\ \Omega \times cm^2$ (Figure 3B). The passive permeability of fluorescence labelled dextrans was assessed at day 0, 4 and 10 after confluency. The permeability of both 10 kDA and 40 kDa dextrans decreased over time, with especially the permeability for 10 kDa dextrans being markedly reduced from day 0–10, suggesting establishment of a tighter monolayer (Figure 3C).

To evaluate the secretion pattern of apoM from proximal tubular epithelial cells, apoM concentration in respectively the apical and basolateral compartment, was determined at day 8, 9, and 10. ApoM was present in the conditioned medium from both the apical as well as the basolateral well, with the concentration being higher in the apical compartment (Figure 3D). ApoM is secreted with its hydrophobic signal peptide and thus needs to be associated with lipids in plasma. To elucidate what particles apoM is secreted

with, the lipoprotein profile was determined using FPLC. Interestingly, we found that while apoM is only present in a very specific subfraction corresponding to small HDL particles in the apical compartment, apoM in the basolateral compartment were found on two distinct populations, one with a size similar to the one found in the apical compartment and one with a size similar to large HDL particles (Figure 3E).

## Overexpression of apoM in RPTECs does not protect against acute kidney injury

Low apoM levels have been associated with increased fibrosis formation, hence we investigated whether overexpression of human apoM in proximal tubular epithelial cells would protect against kidney damage. Acute kidney injury was induced in the mice by a single injection of cisplatin inducing damage to the proximal tubular cells. To assess kidney injury, plasma urea and creatinine levels were measured 3 days post-injection. As expected, cisplatin injection significantly increased both urea and creatinine but there was no difference between RPTEC-hapoM[TG] mice and their WT littermates (Figures 4A,B). Further, we performed histological evaluation of kidney injury on PAS-stained kidney sections (Figure 4C). Here we again found a significant increase in kidney injury after cisplatin injections but no difference between RPTEC-hapoM[TG] mice and WT littermates (Figure 4D). No apoM was detected in urine before cisplatin injury (time 0) but both human and mouse apoM was present in urine at termination (Figure 4E). Further, we found a trend towards a reduction of human apoM in plasma upon cisplatin injury (Figure 4F). In contrast, the S1P concentration in plasma was increased for WT mice upon injury while no difference was found in the transgenic mice (Figure 4G).

The effect of apoM on acute kidney injury was in addition assessed in a model of I/R injury. Kidney injury was induced by clamping of one kidney for 30 min followed by reperfusion for 24 h. The contralateral kidney served as control. As for cisplatin, no difference was found for either urea or creatinine between RPTEC-hapoM[TG] mice and their WT littermates (data not shown). To address kidney injury, kidney sections were stained with PAS-staining (representative pictures are shown in Figure 5A). Histological evaluation of the kidneys revealed a significant injury of the tissue (e.g., tubular dilation and protein casts formation) in the kidney subjected to I/R injury compared to the contralateral control. However, we did not find any clear morphological differences between the injury seen in RPTEC-hapoM[TG] mice and WT littermates (data not shown).

Plasma concentration of human apoM was significantly reduced after I/R injury (Figure 5B), as well as the gene expression of both human and mouse apoM in the kidney, without any difference between WT and RPTEC-hapoM[TG] mice (Figure 5C). The S1P plasma levels between the two genotypes was unchanged.

To assess whether overexpression of human apoM affected the inflammatory status of the kidney, gene expression analysis on kidney tissue was performed. TNFα, ICAM and IL-6 were significantly increased in the kidney subjected to I/R injury compared to the contralateral kidney, with VCAM having the same trend (Figure 5E). However, no difference between RPTEC-hapoM[TG] mice and their WT littermates was seen for any of the genes. We also assessed the expression level of genes involved in the

apoM/S1P-axis (Figure 5F). Here we found that S1P receptor 1 and S1P receptor 2 were upregulated in the injured kidney compared to the control kidney while S1P receptor 3 was downregulated. However, overexpression of apoM did not affect gene expression of any of the analyzed genes involved in the apoM/S1P-axis.

To further address the role of apoM in acute kidney injury, gene expression of inflammatory markers as well as genes involved in the apoM/S1P-axis was determined in apoM-KO mice (mice with global deletion of apoM) subjected to I/R injury (Supplementary Figure S6). Similar to the results from RPTEC-hapoM[TG] mice, ICAM and VCAM was significantly increased in kidneys subjected to I/R injury, with TNFα and IL-6 having the same trend. Further, S1P receptor 1 and 2 was upregulated while S1P receptor 3 was downregulated. For none of the genes was there an effect of genotype when comparing apoM-KO and WT mice.

## Discussion

ApoM is mainly produced by the liver and the proximal tubular epithelial cells in the kidney. While the role of liver derived apoM has been studied extensively, the role of kidney derived apoM is much more elusive. In this study, we have generated a novel transgenic mouse model with kidney-specific overexpression of human apoM. We show for the first time that kidney-derived apoM contributes to the plasma pool of apoM. This finding is supported by in vitro data showing that apoM is secreted to both the apical and basolateral compartment from proximal tubular epithelial cells. Finally, we show that overexpression of apoM locally in the kidney is not able to protect against either cisplatin or I/R induced acute kidney injury.

Unexpectedly, human apoM is detectable in plasma from RPTEC-hapoM[TG] transgenic mice. This is highly important as it suggests that apoM is not only secreted to the apical (urine) site from the proximal tubular cells as earlier hypothesized, but also to the basolateral (plasma) compartment. It should be noted that, despite the overexpression of human apoM in this model, the concentration found is low compared to the apoM levels found in human plasma (~0.9 μM) (Axler et al., 2007), suggesting that kidney-derived apoM is not a major contributor of plasma apoM levels. However, the presence of kidney-derived apoM in plasma raises a fundamental question of how and why kidney-derived apoM is transported from the proximal tubular cells into plasma.

In healthy individuals, apoM is not detectable in urine. Faber et al. have shown that apoM, in the pre-urine, is taken up by megalin-receptors in the proximal tubular cells, and secondly that megalin deficiency leads to apoM excretion in the urine (Faber et al., 2006). The apoM excreted into the urine is likely kidney-derived, since plasma-apoM is bound to lipoproteins, which are too large to undergo glomerular filtration. Once in the pre-urine, it has been suggested that apoM binds ligands, which have been filtered in the glomerulus. Subsequently, apoM transports them back to the proximal tubular cells, where they bind the megalin-receptor and are endocytosed into the proximal tubular cells (Faber et al., 2006). This hypothesis is supported by the finding that apoM without its signal peptide (and thus, without binding to HDL) are taken up by the proximal tubular cells (Christoffersen et al., 2008a). After endocytosis, at least two possible routes can explain how kidney-derived apoM is transferred to plasma. Either apoM

bound to megalin can pass through the epithelial cells of the proximal tubule via transcytosis and enter the bloodstream on the basolateral side of the cell, or apoM are endocytosed after binding to megalin and subsequently degraded in the lysosomes. Newly formed apoM could then be transported to the basolateral side of the proximal tubular cells through the Golgi apparatus and be released to the bloodstream by exocytosis. Both processes have been described for retinol-binding protein (Christensen et al., 1999; Marino et al., 2001), which is structurally and functionally related to apoM. In this paper, we find that apoM secreted to the apical side of the proximal tubular cells associates to particles with a relative defined size that is smaller than HDL, similar to what is found by Faber et al., 2006. In contrast, the particles at the basolateral side associated with apoM seem to have two distinct sizes, one similar to the size found in the apical compartment and another with a broader size span in the HDL size range. This finding at least suggest that the secretion pathway for apoM differs between the apical and basolateral compartment, or that the particles are somehow modified before secretion to the basolateral side. Further studies are however needed to reveal the precise secretion pathway.

In plasma, apoM serves as an important carrier of S1P and plays a significant role in vascular barrier functions, lipid turnover, and fibrosis (Christoffersen et al., 2011; Ding et al., 2016; Christoffersen et al., 2018; Ding et al., 2020; Hajny et al., 2021). The role of apoM in the kidney is less explored. One possible role of kidney-derived apoM is to help preserve glomeruli-filtered ligands. In the pre-urine apoM could bind S1P or other small molecules such as retinoic acids or oxidized phospholipids and assist re-uptake of ligands into the proximal tubular cells. The hypothesis is supported by findings from Sutter et al. who measure S1P in the urine from apoM-deficient mice (Sutter et al., 2014), and now also by our data showing that plasma S1P levels are increased in mice with kidney specific overexpression of human apoM. However, proximal tubular epithelial cells are also able to de novo synthesize S1P (Blanchard et al., 2018). The increased S1P levels found in our study could therefore also be a result of an increased secretion of endogenously produced S1P with apoM from the proximal tubular cells in the kidney. Further studies will be needed to unravel this. At this point it is also not clear whether apoM might sequester other molecules than S1P from the urine. This would again be important to address to fully elucidate the role of kidney derived apoM.

A number of studies have shown that modulation of S1P signaling affects the outcome after acute kidney injury. Thus, stimulation with FTY720 (an S1P analogue) or SEW-2827 (specific S1P receptor 1 agonist) leads to less injury after both cisplatin and I/R injury (Awad et al., 2006; Bajwa et al., 2010; Bajwa et al., 2015). Further, kidney injury induced by both cisplatin and I/R injury are increased in mice with local knockout of the S1P receptor 1 in proximal tubular epithelial cells (Bajwa et al., 2010; Bajwa et al., 2015). A recent publication suggest that the detrimental effects of IL-1 signaling during acute kidney injury are mediated via suppression of apoM expression in proximal tubular epithelial cells highlighting the possible important role of apoM in kidney functionality (Ren et al., 2023). To our knowledge the present study is, however, the first to look directly at the role of apoM locally produced in the kidney on acute kidney injury. Despite the increased plasma S1P levels we see in the naïve RPTEC-hapoM[TG] mice, we do not find any protective effect of kidney specific overexpression of apoM on the degree of kidney injury. Why this is the case when S1P modulation does protect against kidney injury, is at this

point elusive, but one explanation might be that the S1P increase is relatively modest or the impact of S1P via the family of S1P-receptors are counteracted. Similar, our observations in apoM-KO mice support that a change in apoM levels does not affect inflammatory markers after I/R induced acute kidney injury.

It is here, however, also important to notice that increased S1P levels are not always protective. Thus, mutations in the sphingosine phosphate lyase gene, the enzyme that mediates the degradation of S1P, have been shown to result in development of severe illness including risk of kidney failure, suggesting that accumulation of S1P intracellularly is critical (Janecke et al., 2017; Lovric et al., 2017; Prasad et al., 2017). A possible explanation for the lack of effect of apoM overexpression on kidney injury observed in the present study, could therefore be that locally produced apoM levels in proximal tubuli cells sequesters S1P intracellularly followed by detrimental intracellular effects. Such a hypothesis will need further investigation.

Some limitations need to be mentioned. In both kidney injury models, we did see a decrease in apoM levels, both in plasma and in the kidney tissue. This might decrease any protective effects of the overexpression of apoM. Also, despite the overexpression nature of the mouse model, we only see modest increases in plasma apoM levels. A more potent increase in plasma apoM levels, could still be protective.

In conclusion, we have developed a unique mouse model with overexpression of apoM in the proximal tubular epithelial cells. With this model we have shown that apoM can be secreted to the basolateral site and thus into the blood compartment in the kidney, which was confirmed in vitro. Further, we find that the overexpression of apoM also results in increased S1P plasma levels. The increased apoM levels do, however, not protect against acute kidney injury.

We believe that this unique mouse model will be highly valuable for future studies exploring the role of apoM/S1P in the kidney, both in the normal setting and in pathophysiological conditions such as chronic kidney injury, where only a few studies so far have looked at the role of apoM and none of these have addressed the specific role of kidney-derived apoM.

## Data availability statement

The raw data supporting the conclusion of this article will be made available by the authors, without undue reservation.

## Ethics statement

## Author contributions

LB: Conceptualization, Investigation, Methodology, Writing–original draft, Funding acquisition, Visualization, Writing–review and editing. PC:

## Conflict of interest

The authors declare that the research was conducted in the absence of any commercial or financial relationships that could be construed as a potential conflict of interest.

## Publisher's note

All claims expressed in this article are solely those of the authors and do not necessarily represent those of their affiliated organizations, or those of the publisher, the editors and the reviewers. Any product that may be evaluated in this article, or claim that may be made by its manufacturer, is not guaranteed or endorsed by the publisher.

## Supplementary material

The Supplementary Material for this article can be found online at: https://www.frontiersin.org/articles/10.3389/fphar.2024.1328259/full#supplementary-material

## References

Ahnström, J., Faber, K., Axler, O., and Dahlbäck, B. (2007). Hydrophobic ligand binding properties of the human lipocalin apolipoprotein M. *J. Lipid Res.* 48, 1754–1762. doi:10.1194/jlr.m700103-jlr200

Awad, A. S., Ye, H., Huang, L., Li, L., Foss, F. W., Jr., Macdonald, T. L., et al. (2006). Selective sphingosine 1-phosphate 1 receptor activation reduces ischemia-reperfusion injury in mouse kidney. *Am. J. Physiol. Ren. Physiol.* 290, F1516–F1524. doi:10.1152/ajprenal.00311.2005

Axler, O., Ahnstrom, J., and Dahlback, B. (2007). An ELISA for apolipoprotein M reveals a strong correlation to total cholesterol in human plasma. *J. Lipid Res.* 48, 1772–1780. doi:10.1194/jlr.M700113-JLR200

Bajwa, A., Jo, S. K., Ye, H., Huang, L., Dondeti, K. R., Rosin, D. L., et al. (2010). Activation of sphingosine-1-phosphate 1 receptor in the proximal tubule protects against ischemia-reperfusion injury. *J. Am. Soc. Nephrol.* 21, 955–965. doi:10.1681/ASN.2009060662

Bajwa, A., Rosin, D. L., Chroscicki, P., Lee, S., Dondeti, K., Ye, H., et al. (2015). Sphingosine 1-phosphate receptor-1 enhances mitochondrial function and reduces cisplatin-induced tubule injury. *J. Am. Soc. Nephrol.* 26, 908–925. doi:10.1681/asn.2013121351

Blanchard, O., Stepanovska, B., Starck, M., Erhardt, M., Römer, I., Meyer Zu Heringdorf, D., et al. (2018). Downregulation of the S1P transporter spinster homology protein 2 (Spns2) exerts an anti-fibrotic and anti-inflammatory effect in human renal proximal tubular epithelial cells. *Int. J. Mol. Sci.* 19, 1498. doi:10.3390/ijms19051498

Bosteen, M. H., Dahlback, B., Nielsen, L. B., and Christoffersen, C. (2015). Protein unfolding allows use of commercial antibodies in an apolipoprotein M sandwich ELISA. *J. Lipid Res.* 56, 754–759. doi:10.1194/jlr.D055947

Burla, B., Muralidharan, S., Wenk, M. R., and Torta, F. (2018). Sphingolipid analysis in clinical research. *Methods Mol. Biol.* 1730, 135–162. doi:10.1007/978-1-4939-7592-1_11

Christensen, E. I., Moskaug, J. O., Vorum, H., Jacobsen, C., Gundersen, T. E., Nykjaer, A., et al. (1999). Evidence for an essential role of megalin in transepithelial transport of retinol. *J. Am. Soc. Nephrol.* 10, 685–695. doi:10.1681/ASN.V104685

Christensen, P. M., Bosteen, M. H., Hajny, S., Nielsen, L. B., and Christoffersen, C. (2017). Apolipoprotein M mediates sphingosine-1-phosphate efflux from erythrocytes. *Sci. Rep.* 7, 14983. doi:10.1038/s41598-017-15043-y

Christoffersen, C., Ahnström, J., Axler, O., Christensen, E. I., Dahlbäck, B., and Nielsen, L. B. (2008a). The signal peptide anchors apolipoprotein M in plasma lipoproteins and prevents rapid clearance of apolipoprotein M from plasma. *J. Biol. Chem.* 283, 18765–18772. doi:10.1074/jbc.m800695200

Christoffersen, C., Federspiel, C. K., Borup, A., Christensen, P. M., Madsen, A. N., Heine, M., et al. (2018). The apolipoprotein M/S1P Axis controls triglyceride metabolism and Brown fat activity. *Cell Rep.* 22, 175–188. doi:10.1016/j.celrep.2017.12.029

Christoffersen, C., Jauhiainen, M., Moser, M., Porse, B., Ehnholm, C., Boesl, M., et al. (2008b). Effect of apolipoprotein M on high density lipoprotein metabolism and atherosclerosis in low density lipoprotein receptor knock-out mice. *J. Biol. Chem.* 283, 1839–1847. doi:10.1074/jbc.M704576200

Christoffersen, C., Nielsen, L. B., Axler, O., Andersson, A., Johnsen, A. H., and Dahlback, B. (2006). Isolation and characterization of human apolipoprotein M-containing lipoproteins. *J. Lipid Res.* 47, 1833–1843. doi:10.1194/jlr.M600055-JLR200

Christoffersen, C., Obinata, H., Kumaraswamy, S. B., Galvani, S., Ahnstrom, J., Sevvana, M., et al. (2011). Endothelium-protective sphingosine-1-phosphate provided by HDL-associated apolipoprotein M. *Proc. Natl. Acad. Sci. U. S. A.* 108, 9613–9618. doi:10.1073/pnas.1103187108

Ding, B. S., Liu, C. H., Sun, Y., Chen, Y., Swendeman, S. L., Jung, B., et al. (2016). HDL activation of endothelial sphingosine-1-phosphate receptor-1 (S1P1) promotes regeneration and suppresses fibrosis in the liver. *JCI Insight* 1, e87058. doi:10.1172/jci.insight.87058

Ding, B. S., Yang, D., Swendeman, S. L., Christoffersen, C., Nielsen, L. B., Friedman, S. L., et al. (2020). Aging suppresses sphingosine-1-phosphate chaperone ApoM in circulation resulting in maladaptive organ repair. *Dev. Cell* 53, 677–690. doi:10.1016/j.devcel.2020.05.024

Duan, J., Dahlback, B., and Villoutreix, B. O. (2001). Proposed lipocalin fold for apolipoprotein M based on bioinformatics and site-directed mutagenesis. *FEBS Lett.* 499, 127–132. doi:10.1016/s0014-5793(01)02544-3

Elsoe, S., Ahnstrom, J., Christoffersen, C., Hoofnagle, A. N., Plomgaard, P., Heinecke, J. W., et al. (2012). Apolipoprotein M binds oxidized phospholipids and increases the antioxidant effect of HDL. *Atherosclerosis* 221, 91–97. doi:10.1016/j.atherosclerosis.2011.11.031

Faber, K., Axler, O., Dahlback, B., and Nielsen, L. B. (2004). Characterization of apoM in normal and genetically modified mice. *J. Lipid Res.* 45, 1272–1278. doi:10.1194/jlr.M300451-JLR200

Faber, K., Hvidberg, V., Moestrup, S. K., DahlbaCk, B. R., and Nielsen, L. B. (2006). Megalin is a receptor for apolipoprotein M, and kidney-specific megalin-deficiency confers urinary excretion of apolipoprotein M. *Mol. Endocrinol.* 20, 212–218. doi:10.1210/me.2005-0209

Hajny, S., Borup, A., Elsoe, S., and Christoffersen, C. (2021). Increased plasma apoM levels impair triglyceride turnover in mice. *Biochim. Biophys. Acta Mol. Cell Biol. Lipids* 1866, 158969. doi:10.1016/j.bbalip.2021.158969

Hubatsch, I., Ragnarsson, E. G. E., and Artursson, P. (2007). Determination of drug permeability and prediction of drug absorption in Caco-2 monolayers. *Nat. Protoc.* 2, 2111–2119. doi:10.1038/nprot.2007.303

Janecke, A. R., Xu, R., Steichen-Gersdorf, E., Waldegger, S., Entenmann, A., Giner, T., et al. (2017). Deficiency of the sphingosine-1-phosphate lyase SGPL1 is associated with congenital nephrotic syndrome and congenital adrenal calcifications. *Hum. Mutat.* 38, 365–372. doi:10.1002/humu.23192

Kurano, M., Tsukamoto, K., Ohkawa, R., Hara, M., Iino, J., Kageyama, Y., et al. (2013). Liver involvement in sphingosine 1-phosphate dynamism revealed by adenoviral hepatic overexpression of apolipoprotein M. *Atherosclerosis* 229, 102–109. doi:10.1016/j.atherosclerosis.2013.04.024

Liu, M., Seo, J., Allegood, J., Bi, X., Zhu, X., Boudyguina, E., et al. (2014). Hepatic apolipoprotein M (ApoM) overexpression stimulates formation of larger ApoM/sphingosine 1-Phosphate-enriched plasma high density lipoprotein. *J. Biol. Chem.* 289, 2801–2814. doi:10.1074/jbc.m113.499913

Lovric, S., Goncalves, S., Gee, H. Y., Oskouian, B., Srinivas, H., Choi, W. I., et al. (2017). Mutations in sphingosine-1-phosphate lyase cause nephrosis with ichthyosis and adrenal insufficiency. *J. Clin. Invest.* 127, 912–928. doi:10.1172/JCI89626

Marino, M., Andrews, D., Brown, D., and Mc, C. R. (2001). Transcytosis of retinol-binding protein across renal proximal tubule cells after megalin (gp 330)-mediated endocytosis. *J. Am. Soc. Nephrol.* 12, 637–648. doi:10.1681/ASN.V124637

Narayanaswamy, P., Shinde, S., Sulc, R., Kraut, R., Staples, G., Thiam, C. H., et al. (2014). Lipidomic "deep profiling": an enhanced workflow to reveal new molecular species of signaling lipids. *Anal. Chem.* 86, 3043–3047. doi:10.1021/ac4039652

Prasad, R., Hadjidemetriou, I., Maharaj, A., Meimaridou, E., Buonocore, F., Saleem, M., et al. (2017). Sphingosine-1-phosphate lyase mutations cause primary adrenal insufficiency and steroid-resistant nephrotic syndrome. *J. Clin. Invest.Invest.* 127, 942–953. doi:10.1172/JCI90171

Ren, J., Liu, K., Wu, B., Lu, X., Sun, L., Privratsky, J. R., et al. (2023). Divergent actions of renal tubular and endothelial type 1 IL-1 receptor signaling in toxin-induced AKI. *J. Am. Soc. Nephrol.* 34, 1629–1646. doi:10.1681/ASN.0000000000000191

Rubera, I., Poujeol, C., Bertin, G., Hasseine, L., Counillon, L., Poujeol, P., et al. (2004). Specific Cre/Lox recombination in the mouse proximal tubule. *J. Am. Soc. Nephrol.* 15, 2050–2056. doi:10.1097/01.ASN.0000133023.89251.01

Sutter, I., Park, R., Othman, A., Rohrer, L., Hornemann, T., Stoffel, M., et al. (2014). Apolipoprotein M modulates erythrocyte efflux and tubular reabsorption of sphingosine-1-phosphate. *J. Lipid Res.* 55, 1730–1737. doi:10.1194/jlr.m050021

Tornabene, E., Helms, H. C. C., Pedersen, S. F., and Brodin, B. (2019). Effects of oxygen-glucose deprivation (OGD) on barrier properties and mRNA transcript levels of selected marker proteins in brain endothelial cells/astrocyte co-cultures. *PLOS ONE* 14, e0221103. doi:10.1371/journal.pone.0221103

Wolfrum, C., Poy, M. N., and Stoffel, M. (2005). Apolipoprotein M is required for prebeta-HDL formation and cholesterol efflux to HDL and protects against atherosclerosis. *Nat. Med.* 11, 418–422. doi:10.1038/nm1211

Xu, N., and Dahlback, B. (1999). A novel human apolipoprotein (apoM). *J. Biol. Chem.* 274, 31286–31290. doi:10.1074/jbc.274.44.31286

Xu, X. L., Mao, Q. Y., Luo, G. H., Nilsson-Ehle, P., He, X. Z., and Xu, N. (2013). Urinary apolipoprotein M could be used as a biomarker of acute renal injury: an ischemia-reperfusion injury model of kidney in rat. *Transpl. Proc.* 45, 2476–2479. doi:10.1016/j.transproceed.2013.04.009

Zhang, X. Y., Dong, X., Zheng, L., Luo, G. H., Liu, Y. H., Ekstrom, U., et al. (2003). Specific tissue expression and cellular localization of human apolipoprotein M as determined by *in situ* hybridization. *Acta histochem.* 105, 67–72. doi:10.1078/0065-1281-00687

frontiers | Frontiers in Medicine

# Urinary liver-type fatty acid-binding protein levels may be associated with the occurrence of acute kidney injury induced by trauma

Ryu Yasuda[1†], Keiko Suzuki[2,3†], Hideshi Okada[1,4]*,
Takuma Ishihara[5], Toru Minamiyama[1], Ryo Kamidani[1],
Yuichiro Kitagawa[1], Tetsuya Fukuta[1], Kodai Suzuki[1,2],
Takahito Miyake[1], Shozo Yoshida[1,6], Nobuyuki Tetsuka[2] and
Shinji Ogura[1]

[1]Department of Emergency and Disaster Medicine, Gifu University Graduate School of Medicine, Gifu,
Japan, [2]Department of Infection Control, Gifu University Graduate School of Medicine, Gifu, Japan,
[3]Department of Pharmacy, Gifu University Hospital, Gifu, Japan, [4]Center for One Medicine Innovative
Translational Research, Gifu University Institute for Advanced Study, Gifu, Japan, [5]Innovative
and Clinical Research Promotion Center, Gifu University Hospital, Gifu, Japan, [6]Abuse Prevention
Emergency Medicine, Gifu University Graduate School of Medicine, Gifu, Japan

**Introduction:** Acute kidney injury (AKI), with a fatality rate of 8.6%, is one of the most common types of multiorgan failure in the intensive care unit (ICU). Thus, AKI should be diagnosed early, and early interventions should be implemented. Urinary liver-type fatty acid-binding protein (L-FABP) could aid in the diagnosis of AKI.

**Methods:** In this prospective, single-center, observational study, we included 100 patients with trauma. Urinary L-FABP levels were measured using a semi-quantitative rapid assay kit 6 and 12 h after injury. Negative, weakly positive, and strongly positive urinary L-FABP levels were examined using two protocols. Using protocol 1, measurements were performed at 6 h after injury negative levels were considered "negative," and weakly positive and strongly positive levels were considered "positive." Using protocol 2, strongly positive levels at 6 h after injury were considered "positive," and negative or weakly positive levels at 6 h after injury were considered "positive" if they were weakly positive or positive at 12 h after injury.

**Results:** Fifteen patients were diagnosed with AKI. Using protocol 1, the odds ratio (OR) was 20.55 ($p = 0.001$) after adjustment for the injury severity score (ISS), contrast media use, and shock index. When the L-FABP levels at 6 and 12 h were similarly adjusted for those three factors, the OR was 18.24 ($p < 0.001$). The difference in ORs for protocols 1 and 2 was 1.619 ($p = 0.04$).

**Discussion:** Associations between urinary L-FABP and AKI can be examined more precisely by performing measurements at 6 and 12 h after injury than only one time at 6 h.

# 1 Introduction

Acute kidney injury (AKI) is one of the most common types of multiorgan failure in the intensive care unit (ICU), with a reported fatality rate of 8.6% (1). Therefore, to improve its prognosis, AKI should be diagnosed early, and early interventions should be implemented (1). However, the current diagnostic criteria for AKI, such as an increased serum creatinine level and decreased urine output, include changes that occur as a result of renal injury and may delay intervention; therefore, new biomarkers have been proposed as potentially useful tools for its diagnosis (2, 3). However, which biomarkers should be used and when they should be used have not yet been established. Urinary liver-type fatty acid-binding protein (L-FABP) is expressed in the renal proximal tubules, and its increased expression attributable to ischemia or oxidative stress increases urinary excretion, suggesting that it may be a marker for diagnosing AKI. L-FABP levels are increased early after cardiovascular surgery for patients with AKI (3). Recently, a semiquantitative evaluation kit for urinary L-FABP levels that can be easily performed at the bedside has been developed and reported to be useful in predicting the development of AKI (4, 5). However, many of its target patients have endogenous diseases or developed such after surgery (4, 5), and AKI occurs in approximately 20% of patients even when urinary L-FABP is negative, making this study a sensitivity issue (4). One possible reason for this issue is L-FABP testing is performed after ICU admission, which includes many endogenous diseases for which time since disease onset is difficult to estimate.

A previous meta-analysis reported a 13% complication rate of acute kidney injury in moderate trauma with a median ISS of 14 (6). In addition, trauma often has a more definite onset time than endogenous disease, making it easier to examine the association between the development of AKI and L-FABP levels.

In this study, we investigated whether a urinary L-FABP semiquantitative kit could predict the subsequent onset of AKI in trauma patients 6 and 12 h after trauma injury.

# 2 Materials and methods

## 2.1 Patients

From October 2019 to February 2020, trauma patients 20 years of age or older who were transported directly or by referral and admitted to the ICU of Gifu University Hospital (Gifu, Gifu Prefecture) were included in this study. At our hospital, an arterial access is placed in trauma patients who are deemed to require hemodynamic monitoring upon admission, and a urethral catheter is inserted when urine output measurement is deemed necessary. Therefore, trauma patients who did not require these insertions were considered to have mild trauma and very unlikely to develop AKI; therefore, patients without an implanted intra-arterial pressure line or urethral balloon were excluded from the study. In addition, patients in which more than 6 h had elapsed at the time of transport to our hospital and patients in which specimens could not be collected during emergency surgery or other procedures were excluded from the study. Furthermore, patients of early death in the emergency room, or patients in which the attending physician

expected early death, even after admission, patients who could not give study consent, patients with chronic hemodialysis, and patients undergoing renal replacement therapy within 24 h of admission or renal transplantation were also excluded.

## 2.2 Ethics approval and consent to participate

This study conformed to the principles outlined in the Declaration of Helsinki (7). Ethical approval was obtained from the medical ethics committee of Gifu University Graduate School of Medicine, Gifu, Japan (institutional review board approval no. 2018-173). Patients provided written informed consent prior to all study-related procedures. Before initiation, the study was registered with the UMIN Clinical Trials Registry (registry number: UMIN 000038306).

## 2.3 Data collection and study design

This was a single-center, prospective, observational study conducted at Gifu University Hospital, Gifu, Japan. On admission to the ICU, the following clinical variables were evaluated: age, sex, body mass index, presence of chronic diseases, international injury severity score (ISS), shock index (within 6 h of injury), use of contrast media within 6 h of injury acute surgery within 24 h of injury, blood infusion within 24 h of injury, use of rapid renal replacement therapy, and mortality at 28 days. All laboratory data, except patient attributes, were extracted from the hospital's electronic medical records.

## 2.4 Measurement of L-FABP levels and other tests

Urinary L-FABP levels in urine collected from urethral catheters were evaluated at 6 and 12 h after injury using the RENAPRO® semi-quantitative rapid assay kit (CMIC Pharmaceutical Services Corporation, 1-1-1, Tokyo, Japan). This kit considers the levels negative when they are less than 12.5 ng/mL, weakly positive when 12.5–100 ng/mL, and strongly positive levels at more than 100 ng/mL.

The investigators performed examinations at 6 and 12 h after injury and used two protocols for each patient. Using protocol 1, measurements were performed at 6 h after injury negative levels were considered "negative" and weakly positive and strongly positive levels were considered "positive."

Using protocol 2, strongly positive levels at 6 h after injury were considered "positive," and negative or weakly positive levels at 6 h after injury were considered "positive" if they were weakly positive or positive at 12 h after injury. In contrast, negative and weakly positive levels at 6 h after injury were considered "negative" if they were negative at 12 h after injury.

The protocol and indication criteria for this study were thoroughly communicated to all responsible physicians before study commencement. Patients who met the criteria were admitted to the hospital, and if consent was obtained, they were asked

to contact the study coordinator, who stored urine samples at 6 and 12 h post-injury in a designated area. The results were not communicated to the treating physician, who was asked to treat the patient to avoid any bias regarding the diagnosis of AKI or intervention.

Blood and urine samples necessary for systemic management were collected at 6 h after injury. respectively, and the data were recorded. The following clinical data were evaluated: creatinine, urea nitrogen, uric acid, cystatin C, and albumin levels; electrolytes (sodium, potassium, hydrogen chloride, calcium, magnesium, and phosphorus in serum); pH level, base excess, and bicarbonate levels in the arteries; hemoglobin levels; platelet count; fibrinogen in whole blood; and pH and specific gravity of urine.

## 2.5 Outcomes

The primary study outcome was the development of AKI within 7 days. The development of AKI was determined by the baseline serum creatinine level within 7 days of injury according to the Kidney Disease Improving Global Outcomes classification ([8]). Patients with stage 1 or higher disease were considered to have AKI.

## 2.6 Statistical analysis

Patient characteristics and laboratory data were summarized using the median and interquartile range (IQR) for continuous variables and the number and percentage for categorical variables. The association between AKI and each protocol was confirmed using a multivariate logistic regression analysis. Explanatory variables in the logistic regression model (protocol, ISS, contrast media use within 6 h of injury and shock index) were adjusted. Overfitting was possible because of the large number of explanatory variables relative to the number of AKI cases. Therefore, overfitting was avoided by estimating the shrinkage of the regression coefficients. Specifically, we penalized the estimation of the regression coefficients such that the optimism parameter obtained from the 150 bootstrap validations did not exceed 0.2. An association between the protocol and AKI was recognized if the results of the statistical tests of the shrinkage-estimated regression coefficients of the protocol were significant. Because protocols 1 and 2 were used for each patient (paired data), generalized estimating equations were used for comparisons between protocols. The sensitivity and specificity of protocols 1 and 2 for AKI and their 95% confidence intervals (CIs) were calculated. The two-sided significance level was set at 5%. R version 4.3.1 (The R Project for Statistical Computing)[1] was used for all statistical analyses.

## 3 Results

### 3.1 Patient characteristics

From October 2019 to February 2020, there were 342 trauma patients. Of these, 194 patients without an intra-arterial pressure

---

[1] www.r-project.org

line or urethral balloon in place, 6 patients who were unable to provide a blood or urine sample within 6 h of injury 9 patients deemed early death in the emergency room, or in which the attending physician expected early death even after admission, 31 patients who were unable to provide research consent, and 2 patients on chronic maintenance dialysis were excluded. None of the 100 patients (67 men and 33 women) dropped out of the study (Figure 1). The patients had a median age of 67.0 years (IQR, 46.0–77.0 years), body mass index of 22.0 (IQR, 19.1–24.2), ISS of 17 (IQR, 9–25), and shock index at 6 hours after injury of 0.74 (IQR, 0.6–0.88). Additionally, 73 patients were administered contrast media within 6 h of injury (Table 1). The clinical data at 6 h after injury are shown in Table 2. Twenty-eight patients underwent acute surgery within 24 h of injury Forty-three patients received blood transfusions within 24 h of injury. Two patients required renal replacement therapy and two patients died within 28 days.

## 3.2 Urinary L-FABP levels and AKI according to two different protocols

Fifteen patients were diagnosed with AKI. At 6 h after injury, urinary L-FABP levels were strongly positive in 12 patients, weakly positive in 17 patients, and negative in 71 patients. At 12 h after injury, urinary L-FABP levels were strongly positive in 9 patients, weakly positive in 12 patients, and negative in 79 patients.

Using protocol 1, during which L-FABP was semi-quantitatively measured at only one time point (6 h after injury), the odds ratio (OR) was 20.55 ($p = 0.001$) after adjusting for the ISS, contrast media use within 6 h after injury, and shock index. However, when the L-FABP levels at two time points, 6 and 12 h after injury, were similarly adjusted for the ISS, contrast use within 6 h after injury, and shock index, the OR was 18.24 ($p < 0.001$) (Table 3). The difference in ORs for protocols 1 and 2 was 1.619 ($p = 0.04$) (Table 4). The sensitivities and specificities of protocols 1 and 2 for AKI were calculated (Table 5). The sensitivity of protocol 1, which was evaluated at only one time point, 6 h after injury, was higher than that of protocol 2; however, the specificity of protocol 2, which was evaluated at two time points, 6 and 12 h after injury, was higher than that of protocol 1 (Table 6).

## 4 Discussion

Recently, several urinary biomarkers have been investigated to determine their use for early detection of and intervention for AKI in critically ill patients. Urinary N-acetyl-β-D-glucosaminidase and β-microglobulin have been used to differentiate whether AKI is renal in origin; however, they are affected by many factors, including chronic kidney disease, and their sensitivity and specificity for the diagnosis of AKI are not high ([9]). Subsequently, IL-18 ([10], [11]), kidney molecule-1 (KIM-1) ([11], [12]), and neutrophil gelatinase-associated lipocalin (NGAL) ([11], [13]) have been investigated; however, which of these biomarkers should be used and when they should be used have not yet been established. Of these biomarkers, NGAL correlates with AKI severity, but L-FABP was previously reported to be more useful

**FIGURE 1**
Patients who met the eligibility criteria.
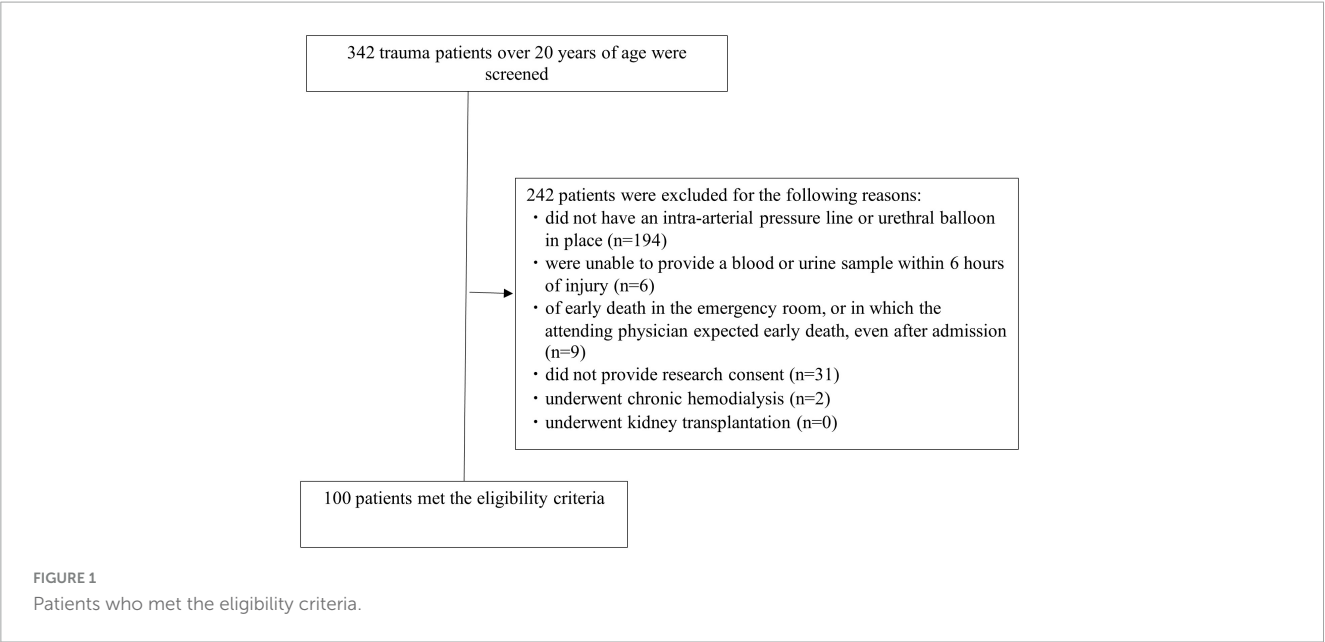
**TABLE 1** Patient characteristics.

| General information | |
|---|---|
| Age, years, median (IQR) | 67 (46–77) |
| Sex, male, n (%) | 67 (67%) |
| BMI, median (IQR) | 22.0 (19.1–24.2) |
| **Chronic disease (multiple reported per study)** | **n (%)** |
| Hypertension | 25 (25%) |
| Diabetes | 11 (11%) |
| Stroke | 9 (9%) |
| Coronary artery syndrome | 6 (6%) |
| Hyperuricemia | 4 (4%) |
| Aortic disease | 4 (4%) |
| Urological disorders | 2 (2%) |
| **Associated injuries (multiple reported per study)** | **n (%)** |
| Head or neck injuries | 25 (25%) |
| Facial injuries | 15 (15%) |
| Chest injuries | 53 (53%) |
| Abdominal or pelvic injuries | 32 (32%) |
| Extremities or pelvic girdle injuries | 62 (62%) |
| External and other trauma injuries | 17 (17%) |
| **Others** | |
| Injury severity score, median (IQR) | 17 (9–25) |
| Shock index, median (IQR) | 0.74 (0.60–0.88) |
| Use of contract media within 6 h of injury, n (%) | 73 (73%) |

All data are presented as the median and $25^{th}$–$75^{th}$ percentile unless otherwise indicated. BMI: body mass index; ICU: intensive care unit; IQR: interquartile range.

**TABLE 2** Laboratory data at 6 h after ICU admission.

| Laboratory data | Median (IQR) |
|---|---|
| **Cre (mg/dL)** | 0.71 (0.58–0.86) |
| **BUN (mg/dL)** | 16.1 (11.45–19.3) |
| **UA (mg/dL)** | 4.9 (3.97–5.9) |
| **CysC (mg/dL)** | 0.71 (0.62–0.87) |
| **Alb (g/dL)** | 3.3 (2.9–3.6) |
| **Na (mmol/L)** | 139 (137–140) |
| **K (mmol/L)** | 4 (3.8–4.3) |
| **Cl (mmol/L)** | 107 (105–108) |
| **Ca (mmol/L)** | 8.3 (8–8.6) |
| **P (mmol/L)** | 3.4 (3–4) |
| **Mg (mmol/L)** | 1.9 (1.8–2) |
| **pH** | 7.39 (7.37–7.43) |
| **BE** | −0.1 (−2.5–0.8) |
| **$HCO_3^-$ (mmol/L)** | 23.8 (21.8–24.7) |
| **Hb (g/dL)** | 10.1 (9.05–11.6) |
| **Plt × $10^3$/μL** | 157 (101–197) |
| **FIB (mg/dL)** | 195 (162–234.5) |
| **Urine pH** | 6.25 (5.5–7.5) |
| **Urine gravity** | 1.02 (1.01–1.02) |

All data are presented as the median and $25^{th}$–$75^{th}$ percentile unless otherwise indicated. Alb: albumin; BE: base excess; BUN: blood urea nitrogen; Ca: calcium; Cl: hydrogen chloride; Cre: creatinine; FIB: fibrinogen in whole blood; $HCO_3^-$: bicarbonate in the artery; Hb: hemoglobin; ICU: intensive care unit; CysC: cystatin C; K: potassium; Mg: magnesium; Na: sodium; P: phosphorus; Plt: platelets; UA: uric acid.

in discriminating between non-AKI and AKI ([10]). Both can also predict in-hospital mortality, although L-FABP has been reported to be more predictive ([14]). In terms of pathophysiology, NGAL tends to increase with inflammation and is useful for early diagnosis of sepsis-related AKI, for example. On the other hand, L-FABP increases with decreased renal blood flow, so L-FABP may be

TABLE 3 Odds ratio for protocol 1.

| Variable | Odds ratio | 95% LCI | 95% UCI | p-value |
|---|---|---|---|---|
| Protocol 1 | 20.55 | 3.62 | 116.76 | 0.001 |

LCL: lower confidence limit; UCL: upper confidence limit. The odds ratio was calculated using a logistic regression model with the injury severity score, contrast use within 6 h after injury, and shock index as adjusted factors.

TABLE 4 Odds ratio for protocol 2.

| Variable | Odds ratio | 95% LCI | 95% UCI | p-value |
|---|---|---|---|---|
| Protocol 2 | 18.24 | 4.21 | 79.02 | < 0.001 |

LCL: lower confidence limit; UCL: upper confidence limit. The odds ratio was calculated using a logistic regression model with the injury severity score, contrast use within 6 h after injury, and shock index as the adjusted factors.

TABLE 5 Difference between odds ratios for protocol 1 and protocol 2.

| Variable | Odds ratio | 95% LCI | 95% UCI | p-value |
|---|---|---|---|---|
| Protocol 2 | 1.619 | 1.023 | 2.562 | 0.04 |

LCL: lower confidence limit; UCL: upper confidence limit. The odds ratio was calculated using a logistic regression model with the injury severity score, contrast use within 6 h after injury, and shock index as the adjusted factors.

TABLE 6 Sensitivity and specificity of protocol 1 and protocol 2 for acute kidney injury.

| Sensitivity | | |
|---|---|---|
| Variable | n = 15 | 95% CI |
| **Protocol 1** | 12 (80.0%) | 51%, 95% |
| **Protocol 2** | 11 (73.3%) | 45%, 91% |
| Specificity | | |
| Variable | n = 85 | 95% CI |
| **Protocol 1** | 68 (81.0%) | 71%, 88% |
| **Protocol 2** | 75 (88.2%) | 79%, 94% |

Data are presented as n (%) unless otherwise indicated. CI: confidence interval.

suitable for the early diagnosis of trauma-induced AKI, as it can detect decreased renal blood flow at the time of trauma, as in this study. However, other studies have compared L-FABP, NGAL, and KIM-1 and found no difference in predicting the onset of AKI (2). Unlike L-FABP; however, simple test kits, such as those used in this study, are not yet widely available for KIM-1 and NGAL. Thus, L-FABP may be a marker that could be studied in the future as an indicator for early diagnosis of AKI.

L-FABP is a 14-kDa low-molecular-weight protein localized in the cytoplasm of renal proximal tubular cells. Under normal conditions, L-FABP binds to free fatty acids reabsorbed in the tubules and transports them to mitochondria and peroxisomes to promote beta-oxidation, thus contributing to energy production and homeostasis (15).

In tubules with impaired blood flow leading to tubular dysfunction, oxidative stress and increased production of reactive oxygen species convert free fatty acids to highly cytotoxic lipid peroxides, which also increase L-FABP expression. Therefore, it has been suggested that increased urinary L-FABP levels may be useful

indicators during the evaluation of AKI associated with tubular dysfunction (10, 16, 17).

Increased L-FABP levels at 4 h after cardiac surgery have been reported (3) and are useful for predicting AKI development with a wide range of diseases in patients who require intensive care (2, 5, 10), those who require emergency care (4), those with sepsis (18), and those with contrast-induced nephropathy (19). Compared to other markers, L-FABP is also associated with the disease prognosis (5, 11). The use of L-FABP to predict chronic kidney disease (20) has been reported, and patients with chronic kidney disease were included in this study. Additionally, L-FABP has been semi-quantitatively evaluated, with negative, weakly positive, and strongly positive levels observed at 15 minutes, and it is useful in general practice (4, 5, 21).

Because no study has examined the association between AKI and urinary L-FABP with trauma using a semi-quantitative kit, it was necessary to establish the timing of L-FABP measurements after trauma. Previous studies have reported that L-FABP can predict the patient prognosis when assessed using a semi-quantitative kit at two time points: at injury and 6 h after injury (4). This two-point measurement method is advantageous because changes can be analyzed. For example, if the first measurement is positive and the second measurement is negative, then tubular ischemia is improved; however, if the first measurement is negative and the second measurement is positive, then the condition is worse. During the present study, L-FABP was measured at two time points; however, unlike previous reports, L-FABP was evaluated at 6 and 12 h after injury (21). This is because bleeding is often uncontrolled immediately after injury, and L-FABP is evaluated after confirming hemostasis by transarterial embolization or other means at the time of arrival at the hospital.

L-FABP, which indicates the blood flow status of the proximal renal tubule, may be an appropriate biomarker reflecting the dynamically changing hemodynamics and acute phase status of systemic lesions. At 6 h after injury a positive result (including a weakly positive result) indicated that the blood flow in the proximal renal tubule was impaired. In contrast, a weakly positive result at 6 h after injury and a negative result at 12 h may indicate that blood flow has improved; however, a weakly positive or positive result at 12 h may indicate that blood flow in the renal tubules is still impaired. Based on these results, it is considered appropriate to perform repeat testing at 12 h if the level is negative or weakly positive at 6 h.

This study had some limitations. First, it was a single-center study. Second, although urinary L-FABP levels are increased in patients with abdominal trauma (22), the number of patients was insufficient to allow a subgroup analysis or strict confounding adjustments. Third, interventions prior to arrival at the hospital were variable. We included both patients who were directly transported from the trauma scene to our hospital as well as those who were transported to our hospital after being admitted to another hospital and receiving interventions such as intravenous fluid infusion. Finally, comparisons with other urinary markers were not performed.

# 5 Conclusion

The results of a semi-quantitative kit used to measure urinary L-FABP were associated with the development of AKI after trauma. Although it was suggested that this association may be more accurately examined by performing measurements at 6 h and again at 12 h after injury, multiple markers should be examined simultaneously to allow a more comprehensive investigation of markers that allow for the early diagnosis of AKI.

## Data availability statement

The raw data supporting the conclusions of this article will be made available by the authors, without undue reservation.

## Ethics statement

The studies involving humans were approved by the medical ethics committee of Gifu University Graduate School of Medicine, Gifu, Japan (institutional review board approval no. 2018-173). The studies were conducted in accordance with the local legislation and institutional requirements. The participants provided their written informed consent to participate in this study.

## Author contributions

RY: Conceptualization, Writing – original draft. KeS: Conceptualization, Data curation, Writing – original draft. HO: Conceptualization, Writing – review and editing. TI: Formal analysis, Writing – review and editing. ToM: Data curation, Writing – review and editing. RK: Data curation, Writing – review and editing. YK: Data curation, Writing – review and editing. TF: Investigation, Writing – review and editing. KoS: Investigation,

Writing – review and editing. TaM: Investigation, Writing – review and editing. SY: Supervision, Writing – review and editing. NT: Data curation, Writing – review and editing. SO: Supervision, Writing – review and editing.

## Conflict of interest

The authors declare that the research was conducted in the absence of any commercial or financial relationships that could be construed as a potential conflict of interest.

## Publisher's note

All claims expressed in this article are solely those of the authors and do not necessarily represent those of their affiliated organizations, or those of the publisher, the editors and the reviewers. Any product that may be evaluated in this article, or claim that may be made by its manufacturer, is not guaranteed or endorsed by the publisher.

# References

1. Vaara S, Pettilä V, Kaukonen K, Bendel S, Korhonen A, Bellomo R, et al. The attributable mortality of acute kidney injury: a sequentially matched analysis*. *Crit Care Med* (2014) 42:878–85. doi: 10.1097/CCM.0000000000000045

2. Nickolas T, Schmidt-Ott K, Canetta P, Forster C, Singer E, Sise M, et al. Diagnostic and prognostic stratification in the emergency department using urinary biomarkers of nephron damage: a multicenter prospective cohort study. *J Am Coll Cardiol* (2012) 59:246–55. doi: 10.1016/j.jacc.2011.10.854

3. Portilla D, Dent C, Sugaya T, Nagothu K, Kundi I, Moore P, et al. Liver fatty acid-binding protein as a biomarker of acute kidney injury after cardiac surgery. *Kidney Int* (2008) 73:465–72. doi: 10.1038/sj.ki.5002721

4. Suzuki G, Ichibayashi R, Yamamoto S, Nakamichi Y, Watanabe M, Honda M. Clinical significance of urinary L-FABP in the emergency department. *Int J Emerg Med* (2019) 12:24. doi: 10.1186/s12245-019-0244-9

5. Suzuki G, Ichibayashi R, Yamamoto S, Serizawa H, Nakamichi Y, Watanabe M, et al. Urinary liver-type fatty acid-binding protein variation as a predictive value of short-term mortality in intensive care unit patients. *Ren Fail* (2021) 43:1041–8. doi: 10.1080/0886022X.2021.1943439

6. Harrois A, Soyer B, Gauss T, Hamada S, Raux M, Duranteau J, et al. Prevalence and risk factors for acute kidney injury among trauma patients: a multicenter cohort study. *Crit Care* (2018) 22:344. doi: 10.1186/s13054-018-2265-9

7. Rickham P. Human experimentation. Code of ethics of the World Medical Association. *Declaration of Helsinki. Br Med J* (1964) 2:177. doi: 10.1136/bmj.2.5402.177

8. Khwaja A. KDIGO clinical practice guidelines for acute kidney injury. *Nephron Clin Pract* (2012) 120:c179–84. doi: 10.1159/000339789

9. Chew S, Lins R, Daelemans R, Nuyts G, De Broe M. Urinary enzymes in acute renal failure. *Nephrol Dial Transplant* (1993) 8:507–11. doi: 10.1093/ndt/8.6.507

10. Doi K, Negishi K, Ishizu T, Katagiri D, Fujita T, Matsubara T, et al. Evaluation of new acute kidney injury biomarkers in a mixed intensive care unit. *Crit Care Med* (2011) 39:2464–9. doi: 10.1097/CCM.0b013e318225761a

11. Parr S, Clark A, Bian A, Shintani A, Wickersham N, Ware L, et al. Urinary L-FABP predicts poor outcomes in critically ill patients with early acute kidney injury. *Kidney Int* (2015) 87:640–8. doi: 10.1038/ki.2014.301

12. Tanase D, Gosav E, Radu S, Costea C, Ciocoiu M, Carauleanu A, et al. The predictive role of the biomarker Kidney Molecule-1 (KIM-1) in acute kidney injury (AKI) cisplatin-induced nephrotoxicity. *Int J Mol Sci* (2019) 20:5238. doi: 10.3390/ijms20205238

13. Liu S, Che M, Xue S, Xie B, Zhu M, Lu R, et al. Urinary L-FABP and its combination with urinary NGAL in early diagnosis of acute kidney injury after cardiac

surgery in adult patients. *Biomarkers* (2013) 18:95–101. doi: 10.3109/1354750X.2012. 740687

14. Haase M, Bellomo R, Devarajan P, Schlattmann P, Haase-Fielitz A, Ngal Meta-analysis Investigator Group. Accuracy of neutrophil gelatinase-associated lipocalin (NGAL) in diagnosis and prognosis in acute kidney injury: a systematic review and meta-analysis. *Am J Kidney Dis* (2009) 54:1012-24. doi: 10.1053/j.ajkd.2009.07.020

15. Kamijo A, Sugaya T, Hikawa A, Okada M, Okumura F, Yamanouchi M, et al. Urinary excretion of fatty acid-binding protein reflects stress overload on the proximal tubules. *Am J Pathol* (2004) 165:1243–55. doi: 10.1016/S0002-9440(10) 63384-6

16. McMahon B, Galligan M, Redahan L, Martin T, Meaney E, Cotter E, et al. Biomarker predictors of adverse acute kidney injury outcomes in critically ill patients: the Dublin acute biomarker group evaluation study. *Am J Nephrol* (2019) 50:19–28. doi: 10.1159/000500231

17. Noiri E, Doi K, Negishi K, Tanaka T, Hamasaki Y, Fujita T, et al. Urinary fatty acid-binding protein 1: an early predictive biomarker of kidney injury. *Am J Physiol Ren Physiol* (2009) 296:F669–79. doi: 10.1152/ajprenal.905 13.2008

18. Doi K, Noiri E, Maeda-Mamiya R, Ishii T, Negishi K, Hamasaki Y, et al. Urinary L-type fatty acid-binding protein as a new biomarker of sepsis complicated with acute kidney injury. *Crit Care Med* (2010) 38:2037–42. doi: 10.1097/CCM.0b013e3181eedac0

19. Nakamura T, Sugaya T, Node K, Ueda Y, Koide H. Urinary excretion of liver-type fatty acid-binding protein in contrast medium-induced nephropathy. *Am J Kidney Dis* (2006) 47:439–44. doi: 10.1053/j.ajkd.2005.11.006

20. Kamijo-Ikemori A, Sugaya T, Yasuda T, Kawata T, Ota A, Tatsunami S, et al. Clinical significance of urinary liver-type fatty acid-binding protein in diabetic nephropathy of type 2 diabetic patients. *Diabetes Care* (2011) 34:691–6. doi: 10.2337/dc10-1392

21. Sato R, Suzuki Y, Takahashi G, Kojika M, Inoue Y, Endo S. A newly developed kit for the measurement of urinary liver-type fatty acid-binding protein as a biomarker for acute kidney injury in patients with critical care. *J Infect Chemother* (2015) 21:1659. doi: 10.1016/j.jiac.2014.10.017

22. Voth M, Holzberger S, Auner B, Henrich D, Marzi I, Relja B. I-FABP and L-FABP are early markers for abdominal injury with limited prognostic value for secondary organ failures in the post-traumatic course. *Clin Chem Lab Med* (2015) 53:771–80. doi: 10.1515/cclm-2014-0354

# Arachidonic acid metabolism as a therapeutic target in AKI-to-CKD transition

Xiao-Jun Li[1,2†], Ping Suo[1†], Yan-Ni Wang[1], Liang Zou[3], Xiao-Li Nie[2]*, Ying-Yong Zhao[1]* and Hua Miao[1]*

[1]School of Pharmacy, Zhejiang Chinese Medical University, Hangzhou, Zhejiang, China, [2]Department of Nephrology, Integrated Hospital of Traditional Chinese Medicine, Southern Medical University, Guangzhou, Guangdong, China, [3]School of Food and Bioengineering, Chengdu University, Chengdu, Sichuan, China

Arachidonic acid (AA) is a main component of cell membrane lipids. AA is mainly metabolized by three enzymes: cyclooxygenase (COX), lipoxygenase (LOX) and cytochrome P450 (CYP450). Esterified AA is hydrolysed by phospholipase $A_2$ into a free form that is further metabolized by COX, LOX and CYP450 to a wide range of bioactive mediators, including prostaglandins, lipoxins, thromboxanes, leukotrienes, hydroxyeicosatetraenoic acids and epoxyeicosatrienoic acids. Increased mitochondrial oxidative stress is considered to be a central mechanism in the pathophysiology of the kidney. Along with increased oxidative stress, apoptosis, inflammation and tissue fibrosis drive the progressive loss of kidney function, affecting the glomerular filtration barrier and the tubulointerstitium. Recent studies have shown that AA and its active derivative eicosanoids play important roles in the regulation of physiological kidney function and the pathogenesis of kidney disease. These factors are potentially novel biomarkers, especially in the context of their involvement in inflammatory processes and oxidative stress. In this review, we introduce the three main metabolic pathways of AA and discuss the molecular mechanisms by which these pathways affect the progression of acute kidney injury (AKI), diabetic nephropathy (DN) and renal cell carcinoma (RCC). This review may provide new therapeutic targets for the identification of AKI to CKD continuum.

**Abbreviations:** AA, Arachidonic acid; AKI, acute kidney injury; Ang II, angiotensin II; COX, cyclooxygenases; CYP450, cytochrome P450; CKD, chronic kidney disease; ccRCC, clear cell renal cell carcinoma; CREB, cAMP-responsive element-binding; DN, diabetic nephropathy; EET, epoxyeicosatrienoic acids; HETE, hydroxyeicosatetraenoic acids; IRI, ischemia-reperfusion injury; GFR, glomerular filtration rate; GSK3β, glycogen synthase kinase 3β; LOX, lipoxygenases; LX, lipoxins; LT, leukotrienes; MC, mesangial cells; PG, prostaglandins; p38, MAPK, p38 mitogen-activated protein kinase; RCC, renal cell carcinoma; ROS, reactive oxygen species; RBF, renal blood flow; STZ, streptozotocin; TGF-β, transforming growth factor-β; TX, thromboxanes.

# 1 Introduction

Arachidonic acid (AA) is an n-6 essential fatty acid that exists in an esterified form in the membrane phospholipids of all mammalian cells and plays an important role in human and animal growth and development (Badimon et al., 2021; Huang et al., 2021). Studies have shown that phospholipase $A_2$ ($PLA_2$) catalyses the hydrolysis of sn-2 acyl ester bonds in phospholipids to produce active metabolites, including lysophospholipids and AA, which alter various cell functions (Turolo et al., 2021). Free AA is further metabolized by cyclooxygenase (COX), lipoxygenase (LOX) and cytochrome P450

(CYP450) to a wide range of bioactive mediators, including prostaglandin (PG), lipoxin (LX), thromboxane (TX), leukotriene (LT), hydroxyeicosatetraenoic acid (HETE) and epoxyeicosatrienoic acid (EET) (Huang et al., 2021) (Figure 1). These AA metabolites, which are collectively known as eicosanoids, are potent autocrine and paracrine mediators with a variety of biological activities that play critical roles in normal and various pathophysiological functions (Kopp et al., 2019; Wang et al., 2023). AA and its metabolites have attracted much attention in kidney and cancer biology, especially in relation to inflammatory processes and disease (Fishbein et al., 2021). COX, LOX and CYP450 metabolites are



FIGURE 1
AA metabolism. AA is released from the cell membrane by $PLA_2$. AA is mainly metabolized by three enzymes: COX, LOX and CYP450. The COX pathway **(A)** converts AA to prostaglandins and thromboxanes. The LOX pathway **(B)** metabolizes AA to LT, HETE and LX. AA is mainly metabolized into EET and HETE through the CYP450 pathway **(C)**. EET is converted to dihydroxyeicosatrienoic acids by sEH.

important lipid mediators of renal function and contribute significantly to kidney dysfunction in diseases such as diabetes, hypertension, acute kidney injury (AKI) and chronic kidney disease (CKD) (Imig, 2015). Metabolic enzymes and their products in the AA pathway regulate inflammatory responses and modulate multiple cellular processes, such as angiogenesis, cell proliferation, survival, invasion and metastasis, which promote carcinogenesis (Yarla et al., 2016). COX, LOX and CYP450 and their inhibitors are widely used in the treatment of inflammation and cancer and are new targets for cancer prevention and treatment (Fishbein et al., 2021). This review will discuss the role of the AA pathway in the pathogenesis of AKI, diabetic nephropathy (DN) and renal cell carcinoma (RCC).

## 2 The subtypes and clinical features of diverse kidney diseases

Before summarizing the role of the AA signalling pathway in kidney pathogenesis, we will briefly review the subtypes and clinical features of the different kidney diseases and their different classifications. AKI is characterized by a sudden decrease in the glomerular filtration rate (GFR), which is characterized by a rapid increase in serum creatinine concentrations and/or oliguria (Ronco et al., 2019). This type of injury occurs in approximately 30%–60% of critically ill patients, and the major complications include electrolyte disorders, volume overload, uraemic complications, and drug toxicity, which are associated with acute morbidity and mortality (Pickkers et al., 2021). Even if patients with AKI survive the acute stage, AKI can develop to CKD and progress to end-stage renal disease, which causes a huge social burden (Chen et al., 2018; Chen D. Q. et al., 2019; Chen L. et al., 2019). Renal ischaemia–reperfusion injury (IRI) has been considered an appropriate model for examining the impact of therapeutic interventions on the transition from AKI to CKD. Potential mechanisms of kidney IRI are associated with the initiation of inflammation and oxidative stress (Shuvy et al., 2011; Xiao et al., 2016).

The morbidity and mortality rates of type 1 and type 2 diabetes, both of which are costly to healthcare systems, have risen rapidly worldwide in recent decades (Zhao et al., 2019; Wu et al., 2021). DN is one of the most common microvascular complications and the leading cause of chronic and end-stage renal disease worldwide, requiring dialysis or kidney transplantation and increasing the risk of cardiovascular disease (Reidy et al., 2014; Lytvyn et al., 2020). The clinical features of DN are proteinuria and a progressive reduction in kidney function (Umanath and Lewis, 2018). Pathologically, DN is characterized by basement membrane thickening, mesangial matrix expansion, foot process effacement, nodular glomerulosclerosis and tubulointerstitial fibrosis (Anders et al., 2018). There is growing evidence that inflammation and oxidative stress are the major pathophysiological mechanisms of DN (Reidy et al., 2014; Yan, 2021).

Kidney cancer is one of the top ten cancers diagnosed in the United States in both men and women (Chen et al., 2020; Siegel et al., 2020). Kidney cancer includes a diverse spectrum of tumours. RCC is a common and fatal disease, and there are 400,000 estimated new cases and 175,000 deaths worldwide in 2018 (Linehan and Ricketts, 2019; Feng et al., 2020). RCC is the most common solid kidney tumour, originates in renal tubular epithelial cells and accounts for 87% of all renal malignancies (Bhatt and Finelli, 2014). RCC is divided into different subtypes, with clear cell RCC (ccRCC) accounting for approximately 85% of all RCC tumors, making it the most common subtype (Makhov et al., 2018). Papillary RCC and chromophobe RCC are the most common remaining histological subtypes, with incidences of 7%–14% and 6%–11%, respectively (Shuch et al., 2015). Currently, surgical resection is the first-line treatment for RCC (Wang et al., 2020). In addition, most RCCs are resistant to chemotherapy and radiotherapy once they have recurred or metastasized.

## 3 Overview of AA metabolism

AA is metabolized mainly by three enzymes: COX, LOX and CYP450. The different metabolic pathways are described separately in the following sections.

## 3.1 COX pathway

COX refers to enzymes known as prostaglandin G/H synthases (PGHS), which catalyse AA into $PGH_2$, $PGG_2$ and TXA. COX enzymes exist in two isoforms called COX-1 (PGHS-1) and COX-2 (PGHS-2), which are the products of two different genes (Alvarez and Lorenzetti, 2021). COX-1 is a constitutive housekeeping enzyme that is found in almost all cells and tissues, maintains baseline levels of PGs and is vital for protecting the stomach by producing mucus and maintaining renal blood flow (Burian and Gelisslinger, 2005; Hyde and Missailids, 2009). Furthermore, COX-2 is hardly or not expressed under normal physiological conditions but increases dramatically in a variety of inflammatory and cancerous states (Garavito et al., 2002). The first step in the COX metabolic pathway is the oxygenation of AA through its cyclooxygenase activity to produce $PGG_2$, followed by the rapid conversion of $PGG_2$ through its peroxidase activity into $PGH_2$ (Hyde and Missailidis, 2009). $PGH_2$ is an unstable endoperoxide that is metabolized by specific synthases to $PGI_2$, $PGD_2$, $PGE_2$, $PGF_{2\alpha}$ and $TXA_2$ (Honda and Kabashima, 2015). PGs exert their effects by specific membrane-localized G protein-coupled receptors on the plasma membrane, and these prostanoid receptors are classified into five basic types: the PGD receptor (DP), the PGE receptor (EP1-4), the PGF receptor (FP), the PGI receptor (IP), and the thromboxane receptor (TP) (Narumiya and Fitzgerald, 2001). $PGE_2$ is the most abundant PG and has complex pathophysiological effects on the inflammatory response pathway, which is composed of four distinct and tissue-specific E prostanoid families of GPCRs: EP1-4 (Yarla et al., 2016; Wang et al., 2019). TXA synthase is a downstream enzyme of COX that catalyses the conversion of $PGH_2$ to $TXA_2$ (Schneider and Pozzi, 2011).

## 3.2 LOX pathway

Current research has confirmed that at least four types of enzymes in the LOX pathway (5-LOX, 8-LOX, 12-LOX, and 15-LOX) participate in the metabolism of AA (Wang et al., 2019). The

four distinct LOX enzymes insert molecular oxygen at carbons 5, 8, 12, or 15 in AA, generating 5-, 8-, 12-, or 15-hydroperoxyeicosatetraenoic acid (5-, 8-, 12-, and 15-HPETE), respectively. HPETEs can be further reduced by glutathione peroxidase to HETE or converted to other biologically active compounds, such as LT and LX (Borin et al., 2017). Specifically, human 5-LOX plays a crucial role in the progression of kidney inflammation, exerting its effects across a spectrum that spans from the kidney tubules to the glomeruli (Wang et al., 2019). $LTA_4$ formation is facilitated when 5-LOX interacts with the 5-LOX activating protein FLAP. FLAP is necessary for the conversion of AA to $LTA_4$ because it is a membrane-spanning protein with three transmembrane domains (Rådmark et al., 2015). $LTA_4$ is an unstable intermediate LT that can be converted into either $LTB_4$ or cysteinyl LT ($LTC_4$, $LTD_4$, and $LTE_4$) by specific downstream enzymes. These LTs exert physiological effects through GPCR-mediated signalling pathways (Haeggström and Funk, 2011). Regarding signalling, $LTC_4$ and $LTD_4$ exert their effects on vascular smooth muscle cell contraction to increase vascular permeability through CysLT1 and CysLT2 receptors. On the other hand, $LTB_4$ is a potent chemotactic substance that acts via $LTB_4R$ (BLT1) and $LTB_4R2$ (BLT2) receptors (Samuelsson et al., 1987; Hoxha, 2019). Interleukin 1β, tumour necrosis factor α, and histamine signalling have been shown to stimulate 5-LOX activity, ultimately leading to reactive oxygen species (ROS)-mediated NF-κB activation (Bonizzi et al., 1999; Anthonsen et al., 2001). In addition to 5-LOX, other LOX enzymes expressed in mammalian cells are 12-LOX, 15-LOX-1 and 15-LOX-2, which are mainly involved in the generation of HETE, LXA and LXB (Porro et al., 2014; Witola et al., 2014). The biosynthetic pathway of LX includes 5-LOX in neutrophils and 12-LOX in platelets. In neutrophils, 5-LOX generates $LTA_4,$ which is then transferred to platelets, where 12-LOX generates $LXA_4$ or $LXB_4$ (Green et al., 2018; Zheng et al., 2020). Unlike the majority of LOX products, LXs are proresolving molecules with anti-inflammatory properties. LX binding to the G-protein coupled receptor ALX/FPR2 contributes to neutrophil migration and promotes the resolution of inflammation by delaying apoptosis in macrophages (Sodin-Semrl et al., 2004). 15-LOX-1 is encoded by the arachidonate 15-LOX gene, which metabolizes AA to $LXA_4$, $LXB_4$, and 15-oxo-ETE, while 15-LOX-2 metabolizes AA into 8(S)-HETE and 15-oxo-ETE (Dobrian et al., 2019; Singh and Rao, 2019).

## 3.3 CYP450 pathway

The CYP450 metabolic pathway is divided into ω-hydroxylases (CYP4 isoforms) and epoxygenases (CYP2 isoforms) (Sausville et al., 2019). Proximal straight tubules convert AA to 20-HETE and 19(S)-HETE in the kidney via ω-hydroxylase (Quigley et al., 2000). Xu et al. reported the expression of several ω-hydroxylases involved in AA metabolism in human tissues, including CYP4A11, CYP4F11, CYP4F2, CYP4F8 and CYP4F12 (Xu et al., 2013). Immunohistochemical studies have shown that the CYP4A and CYP4F isoforms are principally localized in proximal tubule cells and exhibit low immunoreactivity in collecting tubules and thick ascending limbs (Ito et al., 2006). Additionally, 20-HETE can be further oxidized to 20-carboxy-AA by ethanol dehydrogenase (Collins et al., 2005). The epoxidation of AA by

CYP450 epoxygenase yields four EET system isomers: 5,6-EET, 8,9-EET, 11,12-EET and 14,15-EET. sEH hydrolyses EET to 5,6-DHET, 8,9-DHET, 11,12-DHET and 14,15-DHET, all of which are lipids with weak biological effects (Wang et al., 2019). sEH is one of the key enzymes in EET metabolism that regulates EET activity and levels *in vivo* (Wang et al., 2019). EET, an AA metabolite, is a highly polarizing factor in endothelial cells and is produced mainly in vascular endothelial cells and tissues such as the heart, muscle, kidney, pancreas, lung, gastrointestinal tract and brain (Hamzaoui et al., 2018; Pallàs et al., 2020). Thus, sEH is expressed in these organs. In most cases, a reduction in EET or increased sEH activity is associated with and contributes to kidney and cardiovascular diseases (Imig, 2018). The pattern is related to water and electrolyte homeostasis and blood pressure control (Imig et al., 2020). The physiological properties of vascular, renal, and heart EET increase blood flow, induce vasodilation, inhibit platelets, promote angiogenesis and the hyperpolarization of vascular smooth muscles, inhibit apoptosis, inhibit fibrosis and exert powerful anti-inflammatory effects (Aliwarga et al., 2018).

# 4 AA metabolites in AKI

In this section, we discuss the role of certain AA metabolites generated by COX, LOX and CYP450 in the development and progression of AKI (Table 1).

## 4.1 Role of COX enzymes and their products in AKI

AKI is defined as an abrupt decrease in GFR leading to tubular necrosis and has a high morbidity and mortality rate (Imig, 2006; Kawakami et al., 2013). AKI is often associated with the use of β-lactam antibiotics and nonsteroidal anti-inflammatory drugs and may be mediated by allergy mechanisms (Yuan et al., 2020). COX metabolites have been implicated because COX inhibitor and NSAID treatment has been associated with AKI in patients (Imig, 2006). It has long been acknowledged that COX-derived PGs play a key role in the regulation of renal blood flow (RBF) and GFR (Walshe et al., 1984; DiBona, 1986). Under normal conditions, PGs have little effect on RBF and GFR. However, in certain pathophysiological conditions, especially in the volume contracted state, such as cirrhotic ascites and nephrotic syndrome, the maintenance of normal kidney function is dependent on PG (Huerta and Rodriguez, 2001; Hao and Breyer, 2007). Under volume-contracting conditions, substances such as catecholamines, vasopressin, and angiotensin cause constriction of the kidneys and peripheral arteries. In the kidneys, PGs act as vasodilators, countering the effects of these vasoconstrictors and thus helping to maintain RBF from falling (Yared et al., 1985). In addition, in volume-contracted conditions, COX-2 expression is dramatically increased in the macula densa and cortical thick ascending limb in humans and rodents (Kömhoff et al., 2000). $PGE_2$ is the predominant and most active product of the COX-2 pathway and can maintain GFR by dilating afferent small arteries (Edwards, 1985). The receptors that mediate vasodilatory effects include cAMP-coupled prostanoid receptors: the EP2, EP4 and IP

TABLE 1 AA metabolites and related receptors in renal diseases.

| Diseases | Pathway | Product or receptor | Impact | References |
|---|---|---|---|---|
| AKI | COX | PGs | Counteracted the effects of vasoconstrictors, thereby helping to maintain RBF from decreasing | Yared et al. (1985) |
| AKI | COX | PGE$_2$ | Mediated oxidative stress-induced ferroptosis in renal tubular epithelial cells, exacerbating kidney damage | Liu et al. (2023) |
| AKI | COX | EP4/EP2 | Enhanced PGE$_2$-induced renal vasodilatation | Meurer et al. (2018) |
| AKI | COX | EP4 | Modulated macrophage polarization impedes the progression of AKI to CKD | Guan et al. (2022) |
| AKI | LOX | 12-HETE and 12/15 LOX | Stimulated inflammatory processes, oxidative stress, and apoptosis exacerbates AKI | Kar et al. (2020), Sharma et al. (2022), Mohamed and Sullivan (2023) |
| AKI | P450 | 20-HETE | Increased oxidative stress and the release of inflammatory cytokines, and intensifying IRI in renal epithelial cells | Nilakantan et al. (2008) |
| AKI | P450 | 20-HETE | Reduced cell swelling, tubular necrosis, and the physical obstruction of adjacent vasa recta capillaries, preventing a secondary decrease in medullary blood flow following IRI | Linkermann et al. (2014) |
| AKI | P450 | 14 (15)-EET | Inhibited hypoxia/reoxygenation-induced apoptosis in murine renal tubular epithelial cells | Deng et al. (2017), Hoff et al. (2019) |
| DN | COX | EP1 | Associated with glomerular hypertrophy and proteinuria in DN, as well as the transcriptional activation of TGF-β and fibronectin | Makino et al. (2002) |
| DN | COX | PGE$_2$-EP4 | Alleviated fibrosis and markers of inflammation/fibrosis as well as apoptosis in mice | Nasrallah et al. (2016) |
| DN | COX | TXA-TP | Associated with the upregulation of TGF-β1, and related to markers of oxidative stress and inflammation | Xu et al. (2006), Cai et al. (2020) |
| DN | COX | PGI$_2$ | Altered matrix proteins and matrix metalloproteinases | Nasrallah and Hébert (2004) |
| DN | LOX | 12-LOX/12(S)-HETE | Induced Ang II-related fibrogenic effects by increasing p38 MAPK and CREB transcriptional activity, and enhanced the expression of TGF-β | Guo et al. (2011), Sutariya et al. (2016), Xu et al. (2016), Dong et al. (2020) |
| DN | CYP450 | 20-HETE | Prevented Palb changes caused by focal segmental glomerulosclerosis factor and the increase in Palb induced by TGF-β1, reducing proteinuria and kidney injury | Sharma et al. (2000), Schiffer et al. (2001), Dahly-Vernon et al. (2005), Luo et al. (2009) |
| DN | CYP450 | 20-HETE | Enhanced NADPH-dependent superoxide anion production, upregulated Nox1 and Nox4 protein expression, and induced apoptosis in podocytes. Reduced inflammation, oxidative stress, and endothelial dysfunction | Eid et al. (2009) |
| DN | CYP450 | EET | Reduced inflammation, oxidative stress, and endothelial dysfunction | Elmarakby et al. (2013), Imig, 2015; Imig and Khan (2015), Roche et al. (2015) |
| DN | CYP450 | sEH | Impaired renal function, associated with the expression of renal inflammatory markers COX-2, vascular cell adhesion molecule-1 protein, and monocyte chemoattractant protein-1 mRNA in DN | Roche et al. (2015) |
| RCC | COX | COX-2-PGE$_2$-EP2 | Mediated the migration of Caki cells through the G protein-dependent PKA pathway | Woo et al. (2015) |
| RCC | COX | COX-2-PGE$_2$-EP4 | Promoted tumor cell migration and invasion by activating the PI3K-AKT signaling pathway | Chen et al. (2011), Wu et al. (2011), Zhang et al. (2017), Ching et al. (2020) |
| RCC | LOX | 5/12-LOX | Crucial for the growth of RCC cells and may serve as a biomarker for RCC | Yoshimura et al. (2004a), Faronato et al. (2007) |

TABLE 1 (*Continued*) AA metabolites and related receptors in renal diseases.

| Diseases | Pathway | Product or receptor | Impact | References |
|---|---|---|---|---|
| RCC | CYP450 | 20-HETE | Related to the activation of MAPK, PI3K/Akt, and ROS pathways, leading to the progression of RCC. | Muthalif et al. (1998), Guo et al. (2008), Yu et al. (2011) |
| RCC | CYP450 | EET | Activated multiple signaling pathways, including MAPK and PI3K/Akt, promoting cell proliferation, epithelial-mesenchymal transition, and anti-apoptotic processes | Zhang et al. (1997), Murai et al. (2006), Jiang et al. (2007), Nithipatikom et al. (2010) |

(Breyer and Breyer, 2001). EP4 and/or EP2 agonists increase the survival rate and restore lost kidney function in the mercury chloride model of AKI, supporting the protective role of EP2/4 in maintaining kidney function (Vukicevic et al., 2006). The kidney $PGI_2/TXB_2$ ratio is reduced in patients with antibiotic-induced AKI, and treatment with the $PGI_2$ analogue iloprost or a $TXA_2$ synthase inhibitor attenuates the decline in GFR and tubular injury that occurs during AKI (Papanikolaou et al., 1992). Interestingly, deletion of the IP receptor does not result in the same kidney damage as $PGI_2$ deletion, suggesting that other signalling mechanisms may be responsible for the beneficial effects of $PGI_2$ on RBF (Murata et al., 1997). Most patients with AKI associated with COX inhibitors have additional risk factors, including CKD, hypertension, congestive heart failure, chronic liver disease, and plasma volume depletion. Therefore, avoiding the use of COX-2 inhibitors in patients with AKI risk factors is vitally important to lower the incidence of COX inhibitor-associated AKI (Jia et al., 2015). However, in some specific cases, COX inhibitors have a protective effect on AKI. Feitoza et al. reported that indomethacin (a nonselective COX inhibitor) protected against ischaemia/reperfusion-induced kidney injury in rats (Feitoza et al., 2005). Selective COX-2 inhibitors can also attenuate cisplatin-induced AKI (Jia et al., 2011). Due to the complexity and diversity of AKI pathogenesis, this effect might depend on differences in pathogenic mechanisms or pathological damage in kidney disease.

## 4.2 Role of LOX enzymes and their products in AKI

It is noteworthy that while the COX pathway and its metabolites like prostaglandins have been extensively studied, the LOX pathway also plays a significant role in renal physiology and pathology. Research indicates that in gentamicin-induced AKI, ROS-mediated lipid peroxidation is significantly increased, which correlates with the enhanced expression of Arachidonate 12-lipoxygenase and production of 12-HETE (Sharma et al., 2022). Further studies suggest that sustained activation of 12/15 LOX aids in the recovery of renal damage post-ischemic injury in hypertensive rats, potentially linked to reduced inflammation and lowered levels of 12-HETE (Mohamed and Sullivan, 2023). Similarly, inhibitors of 12/15 LOX can protect against I/R-induced AKI by modulating inflammatory processes, oxidative stress, and apoptosis (Kar et al., 2020). This elaboration highlights the critical role of the LOX pathway in AKI, especially in the context of oxidative stress and inflammation, demonstrating its potential as a target for therapeutic intervention in renal diseases.

## 4.3 Role of CYP450 and their products in AKI

AA is mainly metabolized into EET and HETE through the CYP450 pathway. In this section, we discuss the role of CYP450-generated HETE and EET in AKI.

### 4.3.1 CYP450-derived HETE in AKI

IRI is the most common cause of AKI (Muroya et al., 2015). 20-HETE has numerous effects on the regulation of kidney tubular and vascular function that have been implicated in IRI (Fan and Roman, 2017). Kidney ischaemia increases 20-HETE formation and/or release in the kidney cortex and outer medulla, but the levels of other eicosanoids are unaffected. Cortical levels of 20-HETE return to normal within 1 h of reperfusion, but kidney medullary levels remain elevated (Muroya et al., 2015). IRI is associated with vasocongestion and prolonged hypoxia in the kidney outer medulla. Intrarenal 20-HETE production is elevated after kidney ischaemia (Regner et al., 2009; Hoff et al., 2011). 20-HETE constricts the afferent arteriole and can reduce RBF and worsen IRI (Fan and Roman, 2017). 20-HETE increases oxidative stress and the release of inflammatory cytokines and potentiates IRI in kidney epithelial cells (Nilakantan et al., 2008). However, 20-HETE can also attenuate IRI. The increase in 20-HETE inhibits sodium transport in the proximal tubule and the thick ascending loop of Henle. Therefore, it may prevent the secondary decrease in medullary blood flow by reducing cell swelling, tubular necrosis and the physical occlusion of adjacent vasa recta capillaries after kidney IRI (Linkermann et al., 2014). Regner et al. reported that a 20-HETE agonist mimetic protected the secondary decrease in medullary blood flow and reduced IRI after bilateral kidney ischaemia (Regner et al., 2009). Kidney IRI is enhanced in Dahl salt-sensitive rats, which are deficient in the CYP4A protein and the production of 20-HETE. By transferring chromosome 5, which contains the CYP4A gene that is responsible for the production of 20-HETE, from Norwegian Brown rats to Dahl salt-sensitive rats, the levels of 20-HETE in the kidneys of the recipient rats were increased. This increase in 20-HETE levels provided partial protection against IRI (Muroya et al., 2015). However, another study indicated that a 20-HETE inhibitor (HET0016) or a 20-HETE antagonist (6,15–20-HEDE) protected against kidney IRI in uninephrectomized male rats (Fan et al., 2015). Further research has discovered that 20-HETE aggravates, whereas EETs ameliorate ischemia/reperfusion (I/R)-induced organ damage. However, EETs are rapidly metabolized by sEH. Therefore, in mice lacking the sEH gene, there is an increase in endogenous EET levels, but this increase leads to elevated 20-HETE levels, resulting in more severe kidney damage. This diminishes the potential beneficial effects of reduced EET degradation (Zhu et al., 2016). This

TABLE 2 Potential therapeutic targets/strategies in the pathogenesis of DN.

| Targets | Strategies | Mechanism of action | Effect on DN | References(s) |
|---|---|---|---|---|
| COX | COX-2 inhibition | Reduces glomerular hyperfiltration | Reduces glomerulosclerosis | Komers et al. (2001), Dey et al. (2004) |
| | EP1 receptor inhibition | Inhibits transcriptional activation of TGF-β and fibronectin | Reduces mesangial expansion, improves kidney and glomerular hypertrophy | Makino et al. (2002) |
| | TX synthase inhibition | Decreases the production of plasminogen activator inhibitor-1 | Reduces the incidence of intraglomerular thrombi and glomerulosclerosis | Xu et al. (2006) |
| | TP receptor inhibition | Attenuates various markers of oxidative stress and inflammation | Improves histological changes | Xu et al. (2006) |
| LOX | LOX inhibition | Reduces p38 MAPK protein and collagen a5(IV) mRNA in podocyte | Reduces ECM expansion, glomerular hypertrophy and albuminuria | Yuan et al. (2008) |
| CYP450 | CYP4A inhibition | Downregulates of Nox1 and Nox4 protein and mRNA expression and inhibits of NADPH oxidase activity | Attenuates albuminuria and reduces podocyte loss, apoptosis and foot process effacement | Williams et al. (2007) |

indicates the complexity of the research, necessitating more comprehensive and in-depth investigations.

### 4.3.2 CYP450-derived EET in AKI

Glycogen synthase kinase 3β (GSK3β) has been identified as a key enzyme involved in AKI. The pathogenesis of AKI is associated with a significant decrease in GSK3β phosphorylation and a significant increase in GSK3β activity (Deng et al., 2017). 14 (15)-EET significantly upregulated the expression of phosphorylated GSK3β in kidney cells and tissues and dose-dependently inhibited hypoxia/reoxygenation-induced apoptosis in murine renal tubular epithelial cells (Deng et al., 2017; Hoff et al., 2019). 14 (15)-EET also significantly attenuated the decrease in creatinine clearance induced by ischemia/reperfusion in mice (Hoff et al., 2019). Therefore, GSK3β may be an effective target for the treatment of AKI. In addition, EET analogues significantly induce GSK-3β inactivation, attenuate inflammatory cell infiltration and reduce the development of kidney tubular apoptosis (Hoff et al., 2019). The administration of EET or EET analogues is a promising therapeutic and preventive strategy for the treatment of AKI and other kidney injuries.

## 5 AA metabolites in DN

In this section, we discuss the role of some AA metabolites generated by COX, LOX and CYP450 in the development and progression of DN (Table 1). We summarize potential therapeutic targets in the pathogenesis of DN (Table 2).

### 5.1 Role of COX enzymes and their metabolites in DN

DN is characterized by glomerular hypertrophy, glomerular basement membrane thickening, expansion of the mesangium, arteriolar hyalinosis, and global glomerular sclerosis, which ultimately lead to proteinuria and kidney failure (Vivian and Rubinstein, 2002; Breyer et al., 2005). Increased GFR and ultrafiltration is a typical sign of early DN (McGowan et al., 2001). Several studies have connected diabetes with enhanced

kidney COX-2 production of PG. In streptozotocin (STZ)-induced type I diabetic rats, kidney COX-2 protein expression is increased (Cheng et al., 2002). Kidney COX-2 expression is also strikingly upregulated in the thick ascending limbs and macula densa in type II diabetic models in Zucker rats and db/db mice (Komers et al., 2005; Sun et al., 2013). In diabetic patients, urinary $PGE_2$ levels are increased in parallel with COX-2 activation (Jia et al., 2014). Selective COX-2 inhibition dramatically reduces glomerular hyperfiltration in STZ-induced diabetic rats, which is consistent with an increase in RBF in diabetic kidneys induced by COX-2-derived PGs (Komers et al., 2001). Refecoxib, a specific COX-2 inhibitor, reduced glomerulosclerosis and restored proteinuria to normal levels in obese Zucker rats without affecting hyperglycaemia (Dey et al., 2004). These findings strongly suggest that COX-2 may be an important therapeutic target for DN.

As mentioned previously, there is a strong interest in targeting EP receptors to better control the kidney complications of diabetes, but the properties of these homologous receptors have not been completely characterized. The role of EP receptors in DN and their potential as therapeutic targets are reviewed below. The EP1 receptor is thought to be an essential mediator of angiotensin II (Ang II)-induced hypertrophy in mesangial cells (MCs) (Qian et al., 2009). Treatment with EP1 receptor antagonists improves kidney and glomerular hypertrophy, inhibits transcriptional activation of transforming growth factor-β (TGF-β) and fibronectin, reduces mesangial expansion and prevents diabetic kidney injury in rats (Makino et al., 2002). Similarly, markers of injury and altered kidney function were attenuated in diabetic EP1-knockout mice. It has been suggested that selective inhibition of the EP1 receptor inhibits glomerular hypertrophy and proteinuria and TGF-β and fibronectin transcriptional activation, preventing the development of diabetic kidney injury in rats. $PGE_2$ acts on the EP4 receptor and is closely associated with matrix turnover, the fibrotic response and apoptosis in kidney cells. Intrarenal EP4 was shown to attenuate tubulointerstitial fibrosis in unilateral ureteral obstruction mice, and EP4-knockout mice had increased fibrosis and inflammation/fibrosis markers, which was prevented by EP4 agonists (Nakagawa et al., 2012). Antagonizing the EP1 receptors or agonizing EP4 may reduce kidney injury associated with growth/apoptosis, inflammation, oxidative stress, and fibrosis and control dysfunction in diabetic patients, thereby reducing the

need for kidney replacement therapies (Nasrallah et al., 2016). Furthermore, Coffman et al. showed that activation of TP by TXA₂ increased the production of plasminogen activator inhibitor-1 and plasminogen activators by MC, which regulated glomerular thrombosis and fibrosis in inflammatory diseases. Consistent with this effect, Okumura et al. reported a reduction in intraglomerular thrombi and glomerulosclerosis following TXA₂ inhibition in diabetic rats (Okumura et al., 2003). TP receptor antagonist treatment attenuated various markers of oxidative stress and inflammation in diabetic apolipoprotein E-deficient mice and ameliorated histological changes in DN (Xu et al., 2006). Interestingly, a general decrease in IP levels was found in cultured MCs exposed to high glucose. In addition, PGI₂ analogues altered matrix proteins and matrix metalloproteinases, indicating that targeting IP might be a therapeutic approach to decrease matrix changes related to DN or other kidney diseases (Nasrallah and Hebert, 2004). At present, the identity of these COX-derived PGs and their receptors in the pathogenesis of DN has not been fully established, and much work is needed to clarify the exact pathways involved.

## 5.2 Role of LOX enzymes and their products in DN

There is growing evidence that LOX-derived products are involved in the pathogenesis of diabetes, including DN. High glucose levels directly increase the expression levels of 12-LOX in the MCs obtained from type I and type II diabetic mouse models (Yoshimura et al., 2004b). In rats with STZ-induced DN, podocyte-specific mRNA levels, as well as fibronectin and collagen a5(IV) protein levels, are increased, which correlate with increased 12-LOX mRNA and protein expression, increased p38 mitogen-activated protein kinase (MAPK) mRNA expression, and p38 MAPK protein activation (Ma et al., 2005; Watanabe et al., 2018). Inhibition of high glucose-induced podocyte 12-LOX activation by the 12-LOX inhibitor cinnamyl-3,4-dihydroxy-a-cyanocinnamate (CDC) decreased podocyte p38 MAPK and collagen a5(IV) mRNA and protein expression (Kang et al., 2003). An in vitro study demonstrated that MCs obtained from 12-LOX knockout mice grew more slowly than wild-type cells. This was associated with suppression of the responses of the downstream signalling molecules p38 MAPK, activator protein-1 and cAMP-responsive element-binding protein (CREB) (Kim et al., 2003). Thus, ample evidence suggests that activation of the 12-LOX and p38 MAPK signalling pathways can stimulate downstream immediate early genes and key signalling kinase molecules that mediate cytokine and growth factor activity and induce DN (Ma et al., 2005).

Considering the key role of Ang II and TGF-β in the pathogenesis of DN, the interrelationship among Ang II, TGF-β and 12-LOX in the fibrotic changes in the diabetic kidney was investigated (Figure 2). Ang II can stimulate MC hypertrophy and ECM production, directly increasing the activity and expression of leukocyte-type 12-LOX in MCs (August and Suthanthiran, 2003). In contrast, 12-LOX-derived 12(S)-HETE induces Ang II-related fibrogenic effects by increasing p38 MAPK and CREB transcriptional activity (Dong et al., 2020). 12(S)-HETE may potentiate the effects of Ang II by upregulating the expression of AT1 receptors on the glomerulus, podocytes and the mesangium

(Dong et al., 2020). The p38 MAPK inhibitor SB202190 significantly inhibits 12(S)-HETE-mediated AT1 receptor expression on rat MCs (Xu et al., 2016). These events may ultimately reduce P-cadherin expression, promote interstitial expansion, and induce proteinuria, which is a key event in DN (Guo et al., 2011). Additionally, 12(S)-HETE can cross-talk with TGF-β in an interactive manner to induce fibrotic changes in DN. It was shown that treatment of rat MCs with TGF-β increased 12(S)-HETE synthesis (Sutariya et al., 2016). Conversely, the 12-LOX product 12(S)-HETE can increase the mRNA and protein expression of TGF-β and induce TGF-β promoter activity (Kim et al., 2005). Cholesterol-tagged siRNAs targeting 12(S)-HETE ameliorated glomerular dysfunction and the expression of renal TGF-β and profibrotic genes in DN (Yuan et al., 2008). 12-LOX knockdown attenuated TGF-β-induced increases in SET7 (histone methyltransferase), histone modifications and profibrotic gene expression in mesangial cells. Transfection of MCs with siRNA targeting SET7 resulted in the silencing of SET7 and the suppression of 12(S)-HETE-induced profibrotic gene expression (Yuan et al., 2016). Thus, 12-LOX and TGF-β can interfere with and activate each other to induce the development of nephropathy in diabetic conditions.

## 5.3 Role of CYP450 and its products in DN

AA is mainly metabolized into EET and HETE through the CYP450 pathway. In this section, we discuss the role of HETE and EET produced by CYP450 in DN.

### 5.3.1 CYP450-derived HETE in DN

Increased pressure transmission to the glomerular capillaries has an important role in the development of glomerulosclerosis. Increased glomerular capillary pressure is thought to contribute to the development of proteinuria, but the mechanisms are unclear. The increase in glomerular capillary pressure can promote the development of kidney injury by increasing TGF-β production (Williams et al., 2007). However, TGF-β has a disruptive effect on glomerular filtration, leading to glomerular damage in the early stage of DN and directly increasing the permeability of the glomerulus to albumin (Palb), which is associated with a decrease in 20-HETE formation (Sharma et al., 2000; Schiffer et al., 2001; Luo et al., 2009). 20-HETE is produced in the glomerulus and cultured podocytes. McCarthy et al. recently reported that 20-HETE has a protective effect on the glomerulus and prevents Palb changes caused by focal segmental glomerulosclerotic factor (Dahly-Vernon et al., 2005). It was found that adding a stable 20-HETE agonist (WIT003) or a 20-HETE mimetic prevented the decrease in 20-HETE levels and protected against the increase in Palb induced by TGF-β1. In addition, glomerular 20-HETE production is decreased in diabetic rats, and the induction of 20-HETE formation with fibrates decreases proteinuria and kidney injury (Fan and Roman, 2017). Overall, 20-HETE has a protective effect on the glomerular permeability barrier, in part because it can reduce transmural pressure gradients across glomerular capillaries secondary to the constriction of afferent arterioles to oppose the development of proteinuria and glomerular disease.

Oxidative stress is thought to be a key factor in the development of DN. ROS have been demonstrated to play a critical role in DN
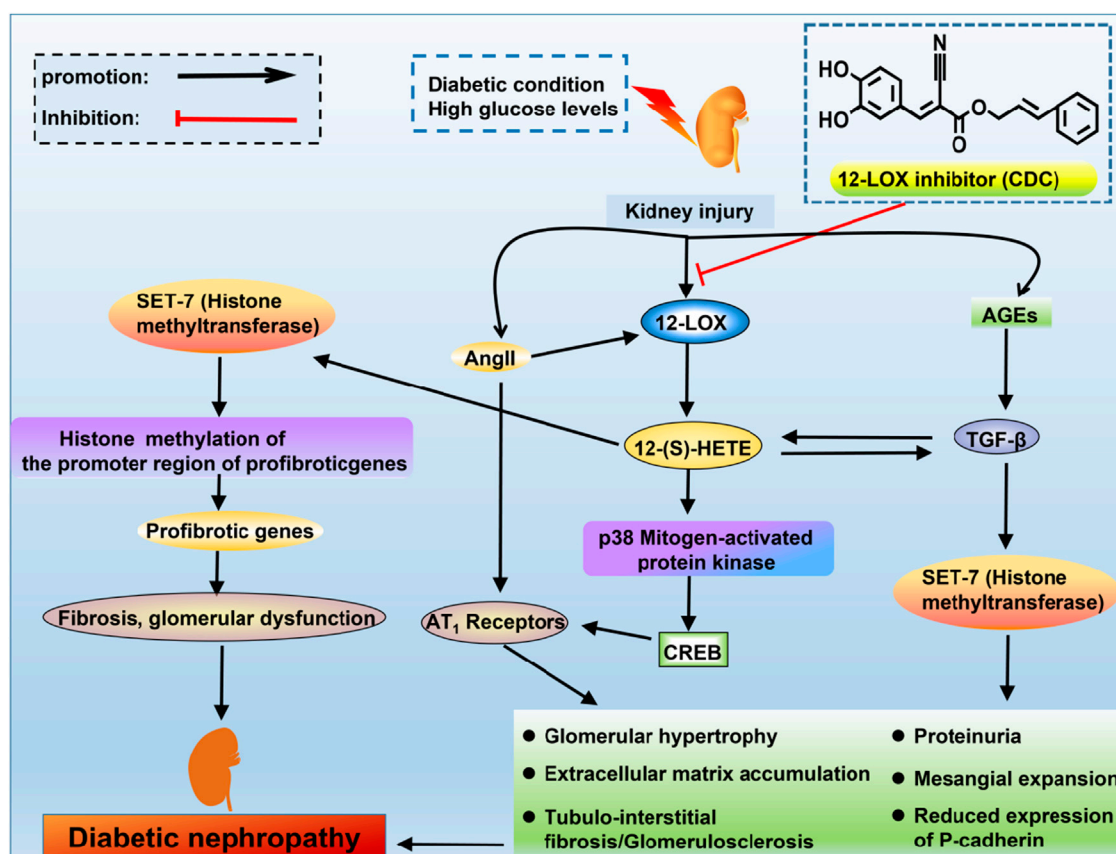
**FIGURE 2**
The interrelationship of TGF-β, Ang II and 12-LOX in DN. High glucose levels or diabetic conditions can activate the expression of 12-LOX, and there is a subsequent increase in the production of 12(S)-HETE. 12(S)-HETE activates p38 mitogen-activated protein kinase and CREB to increase the expression of AT1 receptors. Ang II can increase the levels of 12-LOX, which can potentiate the effects of Ang II by upregulating the expression of AT1 receptors. 12(S)-HETE can interact with TGF-β. These signals can ultimately reduce P-cadherin expression, promote mesangial expansion and induce proteinuria, which are the key events in DN. 12(S)-HETE also increases SET7 (histone methyltransferase), which can increase the expression of profibrotic genes.

(Eid et al., 2013). However, the exact sources of ROS, as well as the molecular mechanisms of oxidative stress, have not been fully elucidated. NADPH oxidase, CYP450 and the mitochondrial electron transport chain are major sources of ROS in cells and tissues (McCarthy et al., 2015). The NADPH oxidases Nox1, Nox2 and Nox4 have recently been identified as the major sources of ROS in the glomeruli and kidney cortex in type 1 diabetic rats (Eid et al., 2009). CYP450 is a potential source of ROS in many cells and tissues (Puntarulo and Cederbsum, 1998; Fleming et al., 2001). Intracellular ROS mediate apoptosis in podocytes in response to high glucose or Ang II (Susztak et al., 2006). High glucose induces apoptosis in cultured podocytes by sequentially upregulating CYP4A, Nox1 and Nox4 to produce ROS (Bedard and Krause, 2007). 20-HETE is the major product of CYP4A and the hydroxylated product of AA, one of the major CYP450 eicosanoids produced in the kidney cortex. 20-HETE enhanced NADPH-dependent superoxide anion production, upregulated Nox1 and Nox4 protein expression, and induced apoptosis in podocytes. The type 1 diabetic mouse model OVE26 shows morphological and structural changes characteristic of human DN. Similarly, OVE26 mice exhibited glomerular basement membrane thickening, podocyte apoptosis,

foot process effacement and podocyte loss (Fan et al., 2015). Injection of the specific 20-HETE production inhibitor HET0016 attenuated albuminuria and reduced podocyte loss, apoptosis and foot process effacement. CYP4A inhibition also led to the downregulation of Nox1 and Nox4 protein and mRNA expression and significant inhibition of NADPH oxidase activity (Williams et al., 2007). Collectively, these data indicate that increased release of CYP4A and 20-HETE induces podocyte injury, and this biological effect may be mediated by enhanced ROS production.

In summary, while 20-HETE exhibits a protective role in maintaining glomerular permeability and preventing proteinuria in DN, its involvement in podocyte injury through enhanced ROS production presents a complex paradox. This duality highlights the intricate balance within renal pathophysiology. Further studies are needed to unravel these conflicting roles of 20-HETE, aiming to harness its beneficial effects while mitigating the adverse outcomes related to oxidative stress and podocyte damage in diabetic nephropathy.

### 5.3.2 CYP450-derived EET in DN

EET has been shown to be renoprotective by reducing inflammation, oxidative stress, and endothelial dysfunction in

experimental animal models of diabetes and hypertension. Knockout of sEH increases the production of EET, lowers blood pressure, proteinuria, kidney inflammation and glomerular injury in animals with diabetic- and obesity-induced nephropathy and reduces renal Ang II levels and DOCA-salt-induced hypertension (Elmarakby et al., 2013; Imig, 2015; Imig and Khan, 2015; Roche et al., 2015). Recently, the production of EET was reduced in the kidney and glomeruli of STZ-treated animals, as well as in the glomeruli exposed to high glucose (Chen et al., 2012; Eid et al., 2013). Increased expression of EET or the administration of EET agonists in CYP2J2 transgenic mice or the administration of a CYP2J2 viral vector reduced proteinuria, glomerular injury and inflammation in STZ diabetic mice (Zhao et al., 2012; Hye Khan et al., 2014). In summary, the common protective effects of EET involve reducing oxidative stress and inflammation. Therefore, sEH inhibitors and EET agonists can be promising therapeutic agents for the treatment of DN.

Numerous *in vivo* and *in vitro* studies have associated the beneficial effects of EET with antiapoptotic pathways. Studies have shown that EET is not only an important regulator of apoptosis in kidney proximal tubular cells but also an effective antiapoptotic factor in the kidney (Chen et al., 2012). TNF-α-induced apoptotic HK-2 cells were treated with synthetic EET, which significantly upregulated basal antiapoptotic proteins B-cell lymphoma 2 (Bcl-2) and B-cell lymphoma-extra large (Bcl-XL) expression levels and downregulated the proapoptotic Bcl-2-associated X protein (Bax) protein expression levels (Yang et al., 2007; Hutchinson et al., 2008). Treatment of HK-2 cells with synthetic EET stimulated the phosphorylation of phosphatidylinositol 3-kinase PI3K/Akt and extracellular signal-regulated protein kinase 1/2 (ERK1/2), suggesting that kidney EET can activate the PI3K-Akt-NOS3 and AMP-activated protein kinase (AMPK) signalling pathways (Wender-Ozegowska and Biczysko, 2004; Wang et al., 2005; Xu et al., 2010). STZ-induced diabetic mice had significantly increased the levels of blood glucose, BUN, plasma creatinine, and urinary albumin and the kidney weight-to-body weight ratio. Interestingly, sEH inhibition decreased the levels of blood glucose, BUN, plasma creatinine, and urinary albumin and the kidney weight-to-body weight ratio (Chen et al., 2012). Additionally, sEH inhibition increased kidney levels of the NF-κB inhibitor IκB in the HFD mouse model of DN, resulting in decreased mRNA expression of the kidney inflammatory markers COX-2, vascular cell adhesion molecule-1 protein and monocyte chemoattractant protein-1 (Roche et al., 2015).

# 6 AA metabolites in RCC

In this section, we discuss the role of some AA metabolites generated by COX, LOX and CYP450 in the development and progression of RCC (Table 1).

## 6.1 Role of COX enzymes and their metabolites in RCC

Kidney tumour mass is sustained by the release of circulating and topically produced factors that act on cellular receptors to convert susceptible quiescent kidney cells to an activated state (Wu et al., 2011). COX-2 plays a critical pathophysiological role

in the progression of RCC (Kaminska et al., 2014). Several previous studies have reported higher levels of COX-2 expression in RCC than in normal kidney (Lee et al., 2012). Currently, it is widely accepted that COX-2 is overexpressed in some human RCC cell lines and plays a key role in the carcinogenesis of human RCC by promoting PGE$_2$ production and inhibiting apoptosis to subsequently enhance tumorigenesis and angiogenesis *in vivo* (Chen et al., 2004). Because of its important role in kidney tumour migration and metastasis, COX-2 is considered a promising target for cancer treatment (Woo et al., 2015). Specific COX-2 inhibitors have been used to treat cancer patients, but undesirable side effects, including cardiovascular and kidney problems, have limited their use (Ohba et al., 2011). Therefore, there is still a need for more effective and safer strategies to inhibit tumorigenesis.

COX-2 is a key enzyme in the production of PGs, and PGE$_2$ is the major PG in the kidney; there is evidence of elevated PGE$_2$ levels in patients diagnosed with cancer (Asano et al., 2002; Wang et al., 2006). Previous pharmacological and animal studies have reported that the primary antitumour effects of COX-2 inhibitors are mediated through the inhibition of PGE$_2$. Therefore, further understanding the pathological function of PGE$_2$ will be useful for future cancer treatment strategies (Hansen-Petrik et al., 2002; Zweifel et al., 2002). PGE$_2$ exerts its biological effects through the G protein-coupled receptors EP1, EP2, EP3 and EP4, which can stimulate the migration of epithelial cells (Woo et al., 2015). EP2 and EP4 but not EP1 and EP3 contribute to RCC development, and different receptors mediate different signalling pathways with somewhat different outcomes. Therefore, PGE$_2$ transduces multiple receptor-specific signalling events in target kidney cells.

### 6.1.1 COX-2-PGE$_2$-EP2 axis in RCC

In the Caki cell line, the PGE$_2$-EP2 axis is activated the G protein-dependent PKA pathway and the G protein-independent Src-STAT3 pathway, which promotes Caki cell migration (Woo et al., 2015) (Figure 3). The PGE$_2$-EP2 axis induces G protein-dependent CREB phosphorylation through the PKA signalling pathway. In this model, treatment with the PKA pathway inhibitor H89 suppressed PGE$_2$-induced EP2 mRNA and protein levels, which inhibited PGE$_2$-mediated migration. Similarly, a Src inhibitor (saracatinib) significantly reduced PGE$_2$-mediated migration (Kaminska et al., 2014). Downregulating EP2 by knockdown and an EP2 antagonist (AH6809) reduced PGE$_2$-induced Caki cell migration. In contrast, the EP2 agonist butaprost increased cell migration (Woo et al., 2015). Silymarin reduced PGE$_2$-induced CREB/Src-STAT3 phosphorylation, suggesting that its inhibitory effect on PGE$_2$-induced cell migration may be related to the G protein-dependent PKA-CREB and G protein-independent Src-STAT3 signalling pathways (Woo et al., 2015).

### 6.1.2 COX-2-PGE$_2$-EP4 axis in RCC

In most cell types, activated EP4 receptors are regulated by lipids and intracellular messengers such as cAMP (Fong et al., 2021) (Figure 3). The PGE$_2$-EP4-mediated signalling pathway induces the dose-dependent accumulation of cAMP in RCC7 cells, which is inhibited by the ligand antagonist AH23848 (Wu et al., 2011). The
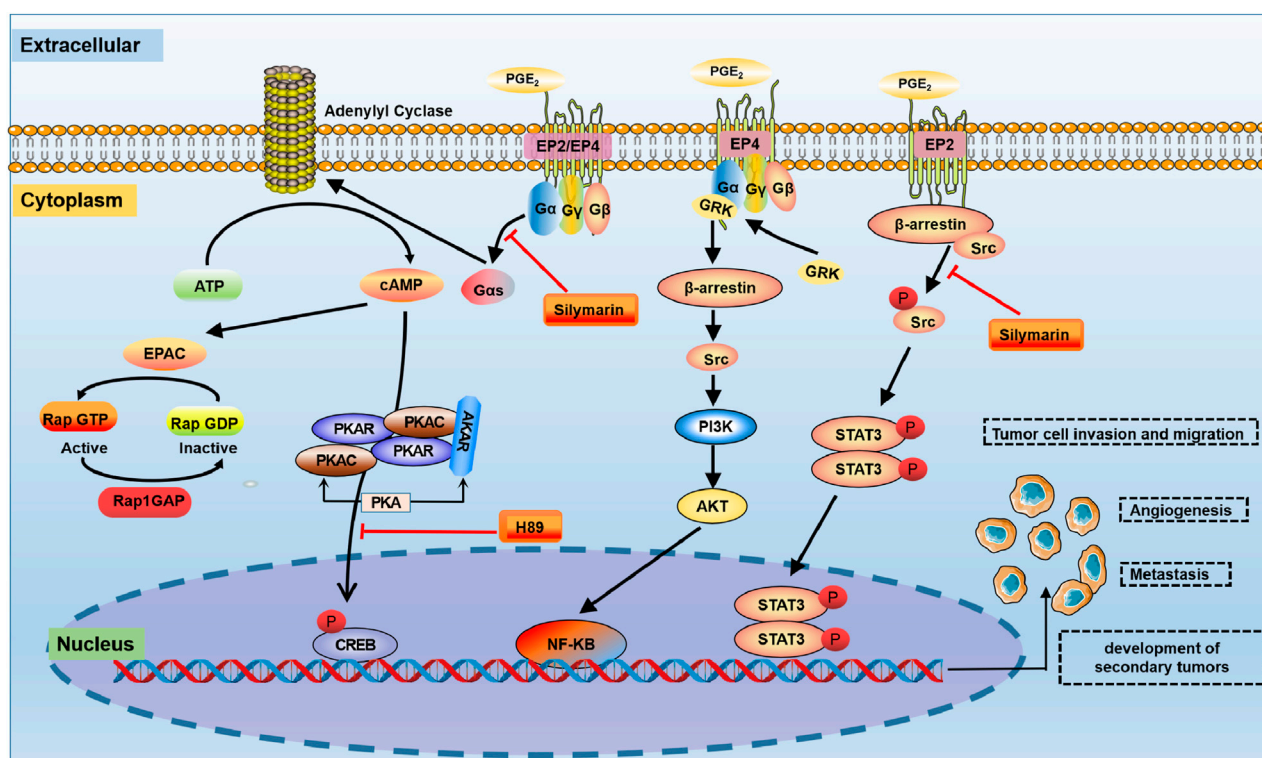
**FIGURE 3**
The COX-2-PGE$_2$ signalling pathway in RCC. In the tumour microenvironment, PGE$_2$ is involved in the regulation of a variety of signalling pathways, such as PKA, PI3K/Akt and Src–STAT3. PKA: protein kinase A; STAT3: signal transducer and activator of transcription 3.

actions of cAMP are mediated by PKA, ion channels and Epac. Epac is a guanine-nucleotide-exchange factor for the small GTPase Rap (Tengholm and Gylfe, 2017). There is evidence that PKA does not impact PGE$_2$-regulated RCC7 cell invasion. However, Epac mediates the effects of EP4-induced RCC7 cell invasion (Wu et al., 2011). PGE$_2$ induces Epac activation in RCC7 cells ectopically expressing Epac1 (Ponsioen et al., 2004). In addition, the PGE$_2$-EP4 signalling pathway induced a marked increase in the level of Rap GTP-binding protein (Rap1). The accumulation of Rap1 correlated with the PGE$_2$ concentration and was necessary for the increased invasion of RCC7 cells (Kim et al., 2012). Notably, the accumulation of Rap1 was inhibited when cells were treated with the EP4 antagonist AH23848. Under physiological conditions, the invasion signal is balanced by the Rap inactivator Rap1GAP, the expression of which has been lost in RCC cell lines (Zhang et al., 2017). Therefore, combined targeted inhibition of EP4 activation and the restoration of Rap1GAP expression may be a new strategy to control advanced kidney cancer.

In RCC, the EP4 receptor plays a pivotal role in cell migration and invasion. This is primarily mediated through the PI3K-AKT signaling pathway. Studies have shown that using small molecule EP4 antagonists, such as ONO-AE3-208 and AH23848, or silencing the EP4 gene, can significantly reduce the metastatic potential of RCC in preclinical models. This effect is attributed to the direct inhibition of tumor cell migration (Ching et al., 2020). Furthermore, the EP4 receptor's involvement in the PI3K-Akt pathway extends to the activation of Ral GTPase activating protein complex 2 (RGC2)

and the small GTPase RalA. These components serve as drug-targeting intermediates, offering therapeutic potential for patients with advanced RCC (Chen et al., 2011). Activation of EP4 has been observed to elevate the phosphorylation levels of Akt and RGC2, leading to increased RalA GTP levels and enhanced invasion capability of RCC cells (Zhang et al., 2017). This demonstrated a critical role of activated Akt in EP4-induced cancer cell migration and invasion (Dillon and Muller, 2010). However, the inhibition of the PI3K activation or downregulation of endogenous Akt expression results in decreased RGC2 phosphorylation. This, in turn, leads to reduced RalA GTP levels and attenuates RCC cell invasion (Li et al., 2013). These findings collectively underscore the importance of the EP4-PI3K-AKT-RGC2-RalA GTP signalling cascade in promoting RCC cell migration and invasion.

## 6.2 Role of LOX enzymes and their metabolites in RCC

There is increasing evidence that immunoreactive 5-LOX and 12-LOX are highly expressed in RCC tissues due to an alteration in normal tissue homeostasis (Yoshimura et al., 2004a; Wettersten, 2020). Transcriptional and translational levels of 5-LOX and 12-LOX were significantly upregulated in the majority of RCC compared with normal kidney tissue. Therefore, 5-LOX plays a significant role in the carcinogenesis of renal cell carcinoma and may serve as a biomarker for kidney cancer (Faronato et al., 2007). The 5-

LOX protein is readily detectable in RCC cell lines Caki-1, Caki-2, and CRBM-1990. In contrast, it is undetectable in HK-2 cells derived from proximal tubules. The 12-LOX protein is significantly and strongly expressed in RCC cells A498, Caki-1, and RC-1, whereas its expression is very weak in normal kidney cells. Additionally, studies indicate that inhibitors of 5-LOX and 12-LOX have a dose- and time-dependent inhibitory effect on renal cancer cells. (Yoshimura et al., 2004a). This finding suggests that 5-LOX and 12-LOX are necessary for the growth of RCC cells. 5-LOX inhibitors may be more effective than 12-LOX inhibitors. A large amount of data suggests that 5-LOX inhibitors may be more effective than 12-LOX inhibitors in preventing the growth of cancer cells in the kidney because the specific relationship of the 5-LOX pathway is more closely related to carcinogenesis than that of the 12-LOX pathway (Matsuyama et al., 2004).

## 6.3 Role of CYP450 and its products in RCC

AA is mainly metabolized into EET and HETE through the CYP450 pathway. In this section, we discuss the role of HETE and EET produced by CYP450 in RCC.

### 6.3.1 CYP450-derived HETE in RCC

Kidney epithelial cells typically express high levels of CYP4504A and CYP4F family enzymes and robustly produce 20-HETE, and it is likely that RCC can produce 20-HETE (Alexanian et al., 2009). The addition of HET0016 (20-HETE synthesis-selective inhibitor) and WIT002 (20-HETE antagonist) inhibited the proliferation of the human renal cell adenocarcinoma lines 786-O and 769-P but had minimal effects on the proliferation of primary human proximal tubular epithelial cells (Evangelista et al., 2020). Guo et al. showed that the CYP4/20-HETE pathway could influence tumour volume (Guo et al., 2007). The signalling mechanisms of 20-HETE-induced kidney cancer progression are mainly related to activation of the MAPK, PI3K/Akt and ROS pathways (Muthalif et al., 1998; Guo et al., 2008; Yu et al., 2011). In conclusion, targeted inhibition of 20-HETE synthesis could have renoprotective effects and reduce tumour growth in RCC.

### 6.3.2 CYP450-derived EET in RCC

EET plays a pivotal role in promoting the cancer phenotype of RCC (Figure 4). EET has been implicated in a wide variety of physiological processes associated with cancer pathogenesis, including the regulation of intracellular signalling pathways, cell proliferation, gene expression and inflammation (Jiang et al., 2005). The molecular mechanism of the effect of EET on cancer cell proliferation is achieved in part through significantly enhanced phosphorylation of the epidermal growth factor receptor (EGFR) and the activation of downstream signalling cascades, including the MAPK and PI3K/Akt pathways (Jiang et al., 2007; Nithipatikom et al., 2010). EET promotes epithelial-mesenchymal transition and resistance through the PI3K/Akt pathway, and this activation upregulates the metastasis-related genes MMPs and CD44. MMP activation can promote cancer cell growth and stimulate angiogenesis (Zhang et al., 1997; Murai et al., 2006). CD44 is an adhesion molecule that can activate the NF-kB signalling pathway and upregulate various prometastatic genes to further promote

cancer metastasis (Fitzgerald et al., 2000). EET also inhibits apoptosis in cancer cells by upregulating the antiapoptotic proteins Bcl-2 and Bcl-XL and downregulating the proapoptotic protein Bax (Chen et al., 2009). This suggests that targeting EET signaling pathways could offer new therapeutic strategies in the treatment of RCC.

## 7 Concluding remarks

Recent advances in understanding the AA pathway highlight its significance in AKI development. COX-2 is an important physiological mediator of kidney function. COX enzymes and their products also have several beneficial renal effects by mediating processes such as RBF and renal salt handling. COX-2-derived PGs may be essential for afferent arteriolar vasodilation. During AKI, the COX product PG may act as a vasodilator to balance the constriction of renal and peripheral arteries caused by elevated levels of catecholamines, pressors and angiotensins. PG receptors can mediate vasodilatory effects and play a renoprotective role to maintain RBF. In addition, ischaemia triggers an imbalance in 20-HETE and EET in the kidney, suggesting that this imbalance plays a key role in the cascade of events that leads to renal I/R injury. 20-HETE constricts the afferent arteriole, and increased kidney 20-HETE levels can reduce RBF and worsen IRI. 20-HETE can attenuate AKI by reducing cellular swelling, tubular necrosis and the physical occlusion of adjacent vasa recta capillaries after kidney IRI. A 20-HETE agonist mimetic can protect against the secondary decrease in medullary blood flow and reduce IRI after bilateral renal ischaemia. Furthermore, the administration of EET or an EET analogue in the initiation phase of renal I/R injury may prevent ischaemic AKI.

Significant advancements have been made in understanding the AA pathway's impact on DN. DN is associated with enhanced production of COX enzymes and the product PG. COX-2 and the product PG may be important therapeutic targets for DN. In experimental models of diabetic kidney injury, long-term treatment with selective COX-2 inhibitors and $PGE_2$ receptor antagonists improves functional and structural kidney injury in these conditions. However, the identity of these COX-derived PGs and their receptors in the pathogenesis of DN has not been fully established, and much work is needed to clarify the exact pathways involved in the future. In addition, 12-LOX and its metabolite 12(S)-HETE play essential roles in the pathogenesis of DN. 12(S)-HETE may interact with angiotensin II and TGF-β to induce fibrosis in the diabetic kidney. The 12-LOX inhibitor CDC inhibited the renal 12-LOX pathway in diabetic rats *in vivo*. Therefore, the discovery of a strategy for 12-LOX inhibition with a drug regimen capable of sustained 12-LOX inhibition is important for the treatment of DN in future studies. Furthermore, EET has been shown to be renoprotective by reducing inflammation, oxidative stress, and endothelial dysfunction in experimental animal models of diabetes and hypertension. sEH inhibitors and agonists of EET can be promising therapeutic agents for the treatment of DN.

Advances in the AA pathway have shed light on its role in RCC development. COX-2 is overexpressed in some human RCC cell lines and plays a key role in the carcinogenesis of human RCC by
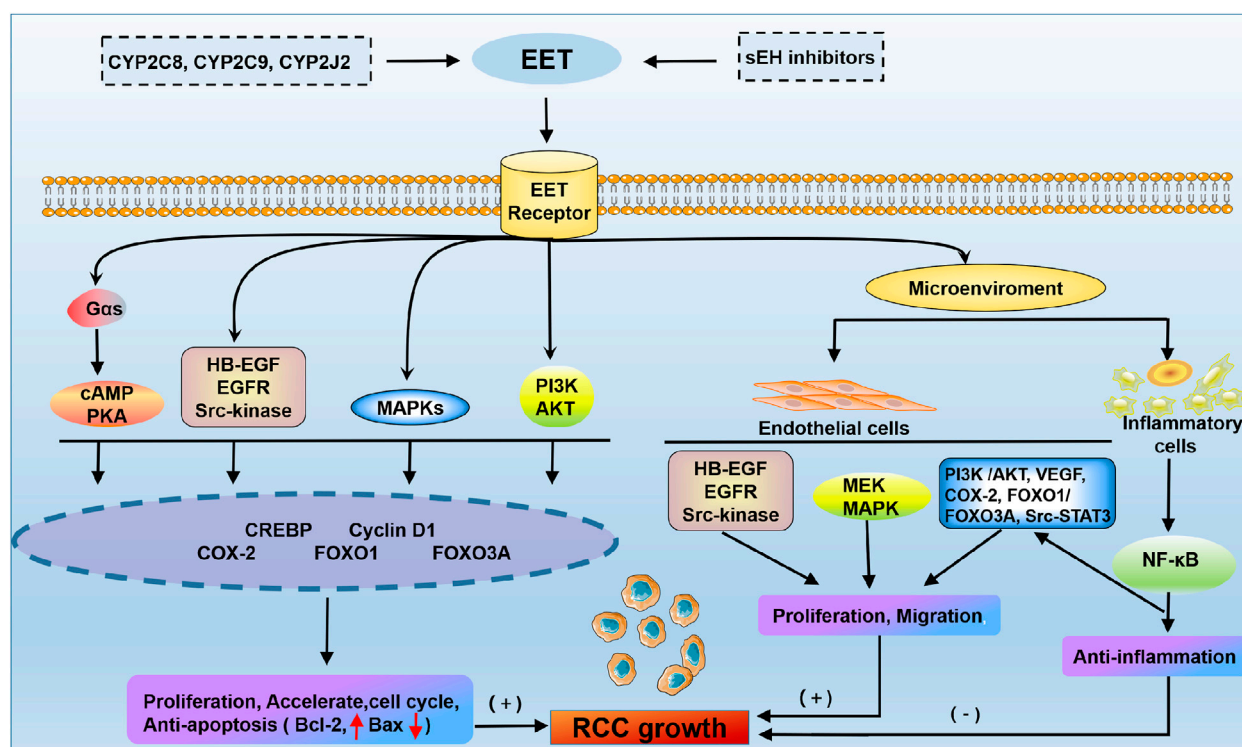
**FIGURE 4**
Membrane receptor mechanism of EET in RCC. The cAMP-PKA, phosphoinositide 3-kinase (PI3K)-Akt, MAPK and Src kinase pathways promote RCC growth through the activation of gene expression. EET accelerates proliferation and the cell cycle and protects carcinoma cells from apoptosis through multiple signal transduction pathways. In addition, EET has been shown to regulate multiple cells in the microenvironment by promoting endothelial cell angiogenesis and inhibiting inflammation. HB-EGF, heparin-binding epidermal growth factor-like growth factor; CREBP, cAMP response-element binding protein; VEGF, vascular endothelial growth factor.

promoting $PGE_2$ production, inhibiting apoptosis and subsequently enhancing tumorigenesis and angiogenesis *in vivo*. Therefore, COX-2 may become a new target gene for RCC treatment. Specific COX-2 inhibitors have been used to treat cancer patients, but undesirable side effects, including cardiovascular and kidney problems, have limited their use. Therefore, COX downstream products and their receptors are now targets. EP2 activates the G protein-dependent PKA pathway and the G protein-independent Src-STAT3 pathway to promote RCC invasion and migration. EP4 promoted a marked increase in Akt and RGC2 phosphorylation levels, which in turn led to an increase in RalA GTP levels and increased the invasion of RCC. EP4 signalling also reduced Rap1 GAP expression and promoted RCC invasion. Therefore, the $PGE_2$ receptors EP2 and EP4 could provide new therapeutic targets for RCC. Based on the reduced expression of EP4 in normal kidney tissue compared to RCC cells and the potential role of EP4 but not EP2 in malignancy aggressiveness, EP4 may be a safer and more effective target in RCC patients. In addition, the evaluation of 5-LOX and 12-LOX in preclinical studies indicates that these pathways may be more potent than COX-2, and inhibition may be a more effective therapeutic strategy (Matsuyama et al., 2004; Matsuyama et al., 2005). As a result, many new LOX inhibitors are undergoing trials for the treatment of inflammatory diseases to address the shortage of LOX inhibitors.

Many natural compounds have been shown to regulate a variety of enzymes in the AA pathway; in addition, natural compounds are readily accepted by the public and could play an important role in complementary therapies for advanced cancers.

In summary, current and ongoing studies provide directional insight into numerous unanswered questions. Future studies will gain further understanding of the role of AA metabolites in mediating oxidative stress and inflammation, as well as the overall complexity of the AA pathway and eicosanoid lipid mediators in the treatment of AKI, DKD and RCC. These findings can provide new diagnostic and prognostic methods for AKI, DKD and RCC and may establish novel therapeutic strategies for AA signalling pathway activation. Undoubtedly, future investigations will identify additional eicosanoid targets and therapies for kidney injury.

## Author contributions

X-JL: Data curation, Investigation, Project administration, Supervision, Validation, Visualization, Writing–review and editing. PS: Conceptualization, Resources, Software, Visualization, Writing–original draft. Y-NW: Conceptualization, Methodology, Project administration, Software, Writing–review and editing. LZ: Methodology, Writing–review and editing, Investigation, Validation. X-LN: Methodology, Writing–review and editing, Data curation, Formal Analysis, Project administration, Software. Y-YZ: Conceptualization, Funding acquisition, Methodology,

Visualization, Investigation, Writing–original draft. HM: Conceptualization, Funding acquisition, Methodology, Validation, Visualization, Writing–review and editing, Formal Analysis.

## Funding

## Conflict of interest

The authors declare that the research was conducted in the absence of any commercial or financial relationships that could be construed as a potential conflict of interest.

## Publisher's note

All claims expressed in this article are solely those of the authors and do not necessarily represent those of their affiliated organizations, or those of the publisher, the editors and the reviewers. Any product that may be evaluated in this article, or claim that may be made by its manufacturer, is not guaranteed or endorsed by the publisher.

## References

Alexanian, A., Rufanova, V. A., Miller, B., Flasch, A., Roman, R. J., and Sorokin, A. (2009). Down-regulation of 20-HETE synthesis and signaling inhibits renal adenocarcinoma cell proliferation and tumor growth. *Anticancer Res.* 29, 3819–3824.

Aliwarga, T., Evangelista, E. A., Sotoodehnia, N., Lemaitre, R. N., and Totah, R. A. (2018). Regulation of CYP2J2 and EET levels in cardiac disease and diabetes. *Int. J. Mol. Sci.* 19, 1916. doi:10.3390/ijms19071916

Alvarez, M. L., and Lorenzetti, F. (2021). Role of eicosanoids in liver repair, regeneration and cancer. *Biochem. Pharmacol.* 192, 114732. doi:10.1016/j.bcp.2021.114732

Anders, H. J., Huber, T. B., Isermann, B., and Schiffer, M. (2018). CKD in diabetes: diabetic kidney disease versus nondiabetic kidney disease. *Nat. Rev. Nephrol.* 14, 361–377. doi:10.1038/s41581-018-0001-y

Anthonsen, M. W., Andersen, S., Solhaug, A., and Johansen, B. (2001). Atypical λ/ι PKC conveys 5-lipoxygenase/leukotriene B4-mediated cross-talk between phospholipase A2s regulating NF-κB activation in response to tumor necrosis factor-α and interleukin-1β. *J. Biol. Chem.* 276, 35344–35351. doi:10.1074/jbc.M105264200

Asano, T., Shoda, J., Ueda, T., Kawamoto, T., Todoroki, T., Shimonishi, M., et al. (2002). Expressions of cyclooxygenase-2 and prostaglandin E-receptors in carcinoma of the gallbladder: crucial role of arachidonate metabolism in tumor growth and progression. *Clin. Cancer Res.* 8, 1157–1167.

August, P., and Suthanthiran, M. (2003). Transforming growth factor beta and progression of renal disease. *Kidney Int.* Suppl, S99–S104. doi:10.1046/j.1523-1755.64.s87.15.x

Badimon, L., Vilahur, G., Rocca, B., and Patrono, C. (2021). The key contribution of platelet and vascular arachidonic acid metabolism to the pathophysiology of atherothrombosis. *Cardiovasc. Res.* 117, 2001–2015. doi:10.1093/cvr/cvab003

Bedard, K., and Krause, K. H. (2007). The NOX family of ROS-generating NADPH oxidases: physiology and pathophysiology. *Physiol. Rev.* 87, 245–313. doi:10.1152/physrev.00044.2005

Bhatt, J. R., and Finelli, A. (2014). Landmarks in the diagnosis and treatment of renal cell carcinoma. *Nat. Rev. Urol.* 11, 517–525. doi:10.1038/nrurol.2014.194

Bonizzi, G., Piette, J., Schoonbroodt, S., Greimers, R., Havard, L., Merville, M. P., et al. (1999). Reactive oxygen intermediate-dependent NF-κB activation by interleukin-1β requires 5-lipoxygenase or NADPH oxidase activity. *Mol. Cell. Biol.* 19, 1950–1960. doi:10.1128/mcb.19.3.1950

Borin, T. F., Angara, K., Rashid, M. H., Achyut, B. R., and Arbab, A. S. (2017). Arachidonic acid metabolite as a novel therapeutic target in breast cancer metastasis. *Int. J. Mol. Sci.* 18, 2661. doi:10.3390/ijms18122661

Breyer, M. D., Böttinger, E., Brosius, F. C., Coffman, T. M., Fogo, A., Harris, R. C., et al. (2005). Diabetic nephropathy: of mice and men. *Adv. Chronic Kidney Dis.* 12, 128–145. doi:10.1053/j.ackd.2005.01.004

Breyer, M. D., and Breyer, R. M. (2001). G protein-coupled prostanoid receptors and the kidney. *Annu. Rev. Physiol.* 63, 579–605. doi:10.1146/annurev.physiol.63.1.579

Burian, M., and Geisslinger, G. (2005). COX-dependent mechanisms involved in the antinociceptive action of NSAIDs at central and peripheral sites. *Pharmacol. Ther.* 107, 139–154. doi:10.1016/j.pharmthera.2005.02.004

Cai, J., Liu, B., Guo, T., Zhang, Y., Wu, X., Leng, J., et al. (2020). Effects of thromboxane prostanoid receptor deficiency on diabetic nephropathy induced by high fat diet and streptozotocin in mice. *Eur. J. Pharmacol.* 882, 173254. doi:10.1016/j.ejphar.2020.173254

Chen, C., Li, G., Liao, W., Wu, J., Liu, L., Ma, D., et al. (2009). Selective inhibitors of CYP2J2 related to terfenadine exhibit strong activity against human cancers *in vitro* and *in vivo*. *J. Pharmacol. Exp. Ther.* 329, 908–918. doi:10.1124/jpet.109.152017

Chen, D. Q., Feng, Y. L., Chen, L., Liu, J. R., Wang, M., Vaziri, N. D., et al. (2019a). Poricoic acid A enhances melatonin inhibition of AKI-to-CKD transition by regulating Gas6/AxlNFκB/Nrf2 axis. *Free Radic. Biol. Med.* 134, 484–497. doi:10.1016/j.freeradbiomed.2019.01.046

Chen, D. Q., Hu, H. H., Wang, Y. N., Feng, Y. L., Cao, G., and Zhao, Y. Y. (2018). Natural products for the prevention and treatment of kidney disease. *Phytomedicine* 50, 50–60. doi:10.1016/j.phymed.2018.09.182

Chen, G., Xu, R., Wang, Y., Wang, P., Zhao, G., Xu, X., et al. (2012). Genetic disruption of soluble epoxide hydrolase is protective against streptozotocin-induced diabetic nephropathy. *Am. J. Physiol. Endocrinol. Metab.* 303, E563–E575. doi:10.1152/ajpendo.00591.2011

Chen, L., Chen, D. Q., Liu, J. R., Zhang, J., Vaziri, N. D., Zhuang, S., et al. (2019b). Unilateral ureteral obstruction causes gut microbial dysbiosis and metabolome disorders contributing to tubulointerstitial fibrosis. *Exp. Mol. Med.* 51, 38. doi:10.1038/s12276-019-0234-2

Chen, Q., Shinohara, N., Abe, T., Watanabe, T., Nonomura, K., and Koyanagi, T. (2004). Significance of COX-2 expression in human renal cell carcinoma cell lines. *Int. J. Cancer* 108, 825–832. doi:10.1002/ijc.11646

Chen, X. W., Leto, D., Xiong, T., Yu, G., Cheng, A., Decker, S., et al. (2011). A Ral GAP complex links PI3-kinase/Akt signaling to RalA activation in insulin action. *Mol. Biol. Cell.* 22, 141–152. doi:10.1091/mbc.E10-08-0665

Chen, Y. Y., Hu, H. H., Wang, Y. N., Liu, J. R., Liu, H. J., Liu, J. L., et al. (2020). Metabolomics in renal cell carcinoma: from biomarker identification to pathomechanism insights. *Arch. Biochem. Biophys.* 695, 108623. doi:10.1016/j.abb.2020.108623

Cheng, H. F., Wang, C. J., Moeckel, G. W., Zhang, M. Z., Mckanna, J. A., and Harris, R. C. (2002). Cyclooxygenase-2 inhibitor blocks expression of mediators of renal injury in a model of diabetes and hypertension. *Kidney Int.* 62, 929–939. doi:10.1046/j.1523-1755.2002.00520.x

Ching, M. M., Reader, J., and Fulton, A. M. (2020). Eicosanoids in cancer: prostaglandin E₂ receptor 4 in cancer therapeutics and immunotherapy. *Front. Pharmacol.* 11, 819. doi:10.3389/fphar.2020.00819

Collins, X. H., Harmon, S. D., Kaduce, T. L., Berst, K. B., Fang, X., Moore, S. A., et al. (2005). Omega-oxidation of 20-hydroxyeicosatetraenoic acid (20-HETE) in cerebral microvascular smooth muscle and endothelium by alcohol dehydrogenase 4. *J. Biol. Chem.* 280, 33157–33164. doi:10.1074/jbc.M504055200

Dahly-Vernon, A. J., Sharma, M., Mccarthy, E. T., Savin, V. J., Ledbetter, S. R., and Roman, R. J. (2005). Transforming growth factor-β, 20-HETE interaction, and glomerular injury in Dahl salt-sensitive rats. *Hypertension* 45, 643–648. doi:10.1161/01.HYP.0000153791.89776.43

Deng, B. Q., Luo, Y., Kang, X., Li, C. B., Morisseau, C., Yang, J., et al. (2017). Epoxide metabolites of arachidonate and docosahexaenoate function conversely in acute kidney injury involved in GSK3β signaling. *Proc. Natl. Acad. Sci. U. S. A.* 114, 12608–12613. doi:10.1073/pnas.1705615114

Dey, A., Maric, C., Kaesemeyer, W. H., Zaharis, C. Z., Stewart, J., Pollock, J. S., et al. (2004). Rofecoxib decreases renal injury in obese Zucker rats. *Clin. Sci. (Lond)* 107, 561–570. doi:10.1042/CS20040125

Dibona, G. F. (1986). Prostaglandins and nonsteroidal anti-inflammatory drugs. Effects on renal hemodynamics. *Am. J. Med.* 80, 12–21. doi:10.1016/0002-9343(86)90928-9

Dillon, R. L., and Muller, W. J. (2010). Distinct biological roles for the akt family in mammary tumor progression. *Cancer Res.* 70, 4260–4264. doi:10.1158/0008-5472. CAN-10-0266

Dobrian, A. D., Morris, M. A., Taylor-Fishwick, D. A., Holman, T. R., Imai, Y., Mirmira, R. G., et al. (2019). Role of the 12-lipoxygenase pathway in diabetes pathogenesis and complications. *Pharmacol. Ther.* 195, 100–110. doi:10.1016/j. pharmthera.2018.10.010

Dong, R., Bai, M., Zhao, J., Wang, D., Ning, X., and Sun, S. (2020). A comparative study of the gut microbiota associated with immunoglobulin A nephropathy and membranous nephropathy. *Front. Cell. Infect. Microbiol.* 10, 557368. doi:10.3389/fcimb. 2020.557368

Edwards, R. M. (1985). Effects of prostaglandins on vasoconstrictor action in isolated renal arterioles. *Am. J. Physiol.* 248, F779–F784. doi:10.1152/ajprenal.1985.248.6.F779

Eid, A. A., Gorin, Y., Fagg, B. M., Maalouf, R., Barnes, J. L., Block, K., et al. (2009). Mechanisms of podocyte injury in diabetes: role of cytochrome P450 and NADPH oxidases. *Diabetes* 58, 1201–1211. doi:10.2337/db08-1536

Eid, S., Maalouf, R., Jaffa, A. A., Nassif, J., Hamdy, A., Rashid, A., et al. (2013). 20-HETE and EETs in diabetic nephropathy: a novel mechanistic pathway. *PLoS One* 8, e70029. doi:10.1371/journal.pone.0070029

Elmarakby, A. A., Faulkner, J., Pye, C., Rouch, K., Alhashim, A., Maddipati, K. R., et al. (2013). Role of haem oxygenase in the renoprotective effects of soluble epoxide hydrolase inhibition in diabetic spontaneously hypertensive rats. *Clin. Sci. (Lond)* 125, 349–359. doi:10.1042/CS20130003

Evangelista, E. A., Cho, C. W., Aliwarga, T., and Totah, R. A. (2020). Expression and function of eicosanoid-producing cytochrome P450 enzymes in solid tumors. *Front. Pharmacol.* 11, 828. doi:10.3389/fphar.2020.00828

Fan, F., Muroya, Y., and Roman, R. J. (2015). Cytochrome P450 eicosanoids in hypertension and renal disease. *Curr. Opin. Nephrol. Hypertens.* 24, 37–46. doi:10.1097/ MNH.0000000000000088

Fan, F., and Roman, R. J. (2017). Effect of cytochrome P450 metabolites of arachidonic acid in nephrology. *J. Am. Soc. Nephrol.* 28, 2845–2855. doi:10.1681/ ASN.2017030252

Faronato, M., Muzzonigro, G., Milanese, G., Menna, C., Bonfigli, A. R., Catalano, A., et al. (2007). Increased expression of 5-lipoxygenase is common in clear cell renal cell carcinoma. *Histol. Histopathol.* 22, 1109–1118. doi:10.14670/HH-22.1109

Feitoza, C. Q., Câmara, N. O., Pinheiro, H. S., Gonçalves, G. M., Cenedeze, M. A., Pacheco-Silva, A., et al. (2005). Cyclooxygenase 1 and/or 2 blockade ameliorates the renal tissue damage triggered by ischemia and reperfusion injury. *Int. Immunopharmacol.* 5, 79–84. doi:10.1016/j.intimp.2004.09.024

Feng, Y. L., Chen, D. Q., Vaziri, N. D., Guo, Y., and Zhao, Y. Y. (2020). Small molecule inhibitors of epithelial-mesenchymal transition for the treatment of cancer and fibrosis. *Med. Res. Rev.* 40, 54–78. doi:10.1002/med.21596

Fishbein, A., Hammock, B. D., Serhan, C. N., and Panigrahy, D. (2021). Carcinogenesis: failure of resolution of inflammation? *Pharmacol. Ther.* 218, 107670. doi:10.1016/j.pharmthera.2020.107670

Fitzgerald, K. A., Bowie, A. G., Skeffington, B. S., and O'neill, L. A. (2000). Ras, protein kinase Cζ, and IκB kinases 1 and 2 are downstream effectors of CD44 during the activation of NF-κB by hyaluronic acid fragments in T-24 carcinoma cells. *J. Immunol.* 164, 2053–2063. doi:10.4049/jimmunol.164.4.2053

Fleming, I., Michaelis, U. R., Bredenkötter, D., Fisslthaler, B., Dehghani, F., Brandes, R. P., et al. (2001). Endothelium-derived hyperpolarizing factor synthase (Cytochrome P450 2C9) is a functionally significant source of reactive oxygen species in coronary arteries. *Circ. Res.* 88, 44–51. doi:10.1161/01.res.88.1.44

Fong, Z., Griffin, C. S., Large, R. J., Hollywood, M. A., Thornbury, K. D., and Sergeant, G. P. (2021). Regulation of P2X1 receptors by modulators of the cAMP effectors PKA and EPAC. *Proc. Natl. Acad. Sci. U. S. A.* 118, e2108094118. doi:10.1073/pnas. 2108094118

Garavito, R. M., Malkowski, M. G., and Dewitt, D. L. (2002). The structures of prostaglandin endoperoxide H synthases-1 and -2. *Prostaglandins Other Lipid Mediat.* 68-69, 129–152. doi:10.1016/s0090-6980(02)00026-6

Green, A. R., Freedman, C., Tena, J., Tourdot, B. E., Liu, B., Holinstat, M., et al. (2018). 5S,15S-dihydroperoxyeicosatetraenoic acid (5,15-diHpETE) as a lipoxin intermediate: reactivity and kinetics with human leukocyte 5-lipoxygenase, platelet 12-lipoxygenase, and reticulocyte 15-lipoxygenase-1. *Biochemistry* 57, 6726–6734. doi:10.1021/acs. biochem.8b00889

Guan, X., Liu, Y., Xin, W., Qin, S., Gong, S., Xiao, T., et al. (2022). Activation of EP4 alleviates AKI-to-CKD transition through inducing CPT2-mediated lipophagy in renal macrophages. *Front. Pharmacol.* 13, 1030800. doi:10.3389/fphar.2022.1030800

Guo, A. M., Arbab, A. S., Falck, J. R., Chen, P., Edwards, P. A., Roman, R. J., et al. (2007). Activation of vascular endothelial growth factor through reactive oxygen species mediates 20-hydroxyeicosatetraenoic acid-induced endothelial cell proliferation. *J. Pharmacol. Exp. Ther.* 321, 18–27. doi:10.1124/jpet.106.115360

Guo, A. M., Sheng, J., Scicli, G. M., Arbab, A. S., Lehman, N. L., Edwards, P. A., et al. (2008). Expression of CYP4A1 in U251 human glioma cell induces hyperproliferative phenotype *in vitro* and rapidly growing tumors *in vivo*. *J. Pharmacol. Exp. Ther.* 327, 10–19. doi:10.1124/jpet.108.140889

Guo, Q. Y., Miao, L. N., Li, B., Ma, F. Z., Liu, N., Cai, L., et al. (2011). Role of 12-lipoxygenase in decreasing P-cadherin and increasing angiotensin II type 1 receptor expression according to glomerular size in type 2 diabetic rats. *Am. J. Physiol. Endocrinol. Metab.* 300, E708–E716. doi:10.1152/ajpendo.00624.2010

Haeggström, J. Z., and Funk, C. D. (2011). Lipoxygenase and leukotriene pathways: biochemistry, biology, and roles in disease. *Chem. Rev.* 111, 5866–5898. doi:10.1021/ cr200246d

Hamzaoui, M., Guerrot, D., Djerada, Z., Duflot, T., Richard, V., and Bellien, J. (2018). Cardiovascular consequences of chronic kidney disease, impact of modulation of epoxyeicosatrienoic acids. *Ann. Cardiol. Angeiol. (Paris)* 67, 141–148. doi:10.1016/j. ancard.2018.04.018

Hansen-Petrik, M. B., Mcentee, M. F., Jull, B., Shi, H., Zemel, M. B., and Whelan, J. (2002). Prostaglandin E$_2$ protects intestinal tumors from nonsteroidal anti-inflammatory drug-induced regression in Apc(Min/+) mice. *Cancer Res.* 62, 403–408.

Hao, C. M., and Breyer, M. D. (2007). Physiologic and pathophysiologic roles of lipid mediators in the kidney. *Kidney Int.* 71, 1105–1115. doi:10.1038/sj.ki.5002192

Hoff, U., Bubalo, G., Fechner, M., Blum, M., Zhu, Y., Pohlmann, A., et al. (2019). A synthetic epoxyeicosatrienoic acid analogue prevents the initiation of ischemic acute kidney injury. *Acta Physiol. (Oxf)* 227, e13297. doi:10.1111/apha.13297

Hoff, U., Lukitsch, I., Chaykovska, L., Ladwig, M., Arnold, C., Manthati, V. L., et al. (2011). Inhibition of 20-HETE synthesis and action protects the kidney from ischemia/ reperfusion injury. *Kidney Int.* 79, 57–65. doi:10.1038/ki.2010.377

Honda, T., and Kabashima, K. (2015). Prostanoids in allergy. *Allergol. Int.* 64, 11–16. doi:10.1016/j.alit.2014.08.002

Hoxha, M. (2019). Duchenne muscular dystrophy: focus on arachidonic acid metabolites. *Biomed. Pharmacother.* 110, 796–802. doi:10.1016/j.biopha.2018.12.034

Huang, N., Wang, M., Peng, J., and Wei, H. (2021). Role of arachidonic acid-derived eicosanoids in intestinal innate immunity. *Crit. Rev. Food Sci. Nutr.* 61, 2399–2410. doi:10.1080/10408398.2020.1777932

Huerta, C., and Rodríguez, L. A. (2001). Incidence of ocular melanoma in the general population and in glaucoma patients. *J. Epidemiol. Community Health* 55, 338–339. doi:10.1136/jech.55.5.338

Hutchinson, D. S., Summers, R. J., and Bengtsson, T. (2008). Regulation of AMP-activated protein kinase activity by G-protein coupled receptors: potential utility in treatment of diabetes and heart disease. *Pharmacol. Ther.* 119, 291–310. doi:10.1016/j. pharmthera.2008.05.008

Hyde, C. A., and Missailidis, S. (2009). Inhibition of arachidonic acid metabolism and its implication on cell proliferation and tumour-angiogenesis. *Int. Immunopharmacol.* 9, 701–715. doi:10.1016/j.intimp.2009.02.003

Hye Khan, M. A., Pavlov, T. S., Christain, S. V., Neckář, J., Staruschenko, A., Gauthier, K. M., et al. (2014). Epoxyeicosatrienoic acid analogue lowers blood pressure through vasodilation and sodium channel inhibition. *Clin. Sci. (Lond)* 127, 463–474. doi:10. 1042/CS20130479

Imig, J. D. (2006). Eicosanoids and renal vascular function in diseases. *Clin. Sci. (Lond)* 111, 21–34. doi:10.1042/CS20050251

Imig, J. D. (2015). Epoxyeicosatrienoic acids, hypertension, and kidney injury. *Hypertension* 65, 476–482. doi:10.1161/HYPERTENSIONAHA.114.03585

Imig, J. D. (2018). Prospective for cytochrome P450 epoxygenase cardiovascular and renal therapeutics. *Pharmacol. Ther.* 192, 1–19. doi:10.1016/j.pharmthera.2018.06.015

Imig, J. D., Jankiewicz, W. K., and Khan, A. H. (2020). Epoxy fatty acids: from salt regulation to kidney and cardiovascular therapeutics: 2019 Lewis K. Dahl memorial lecture. *Hypertension* 76, 3–15. doi:10.1161/HYPERTENSIONAHA.120.13898

Imig, J. D., and Khan, M. A. (2015). Cytochrome P450 and lipoxygenase metabolites on renal function. *Compr. Physiol.* 6, 423–441. doi:10.1002/cphy.c150009

Ito, O., Nakamura, Y., Tan, L., Ishizuka, T., Sasaki, Y., Minami, N., et al. (2006). Expression of cytochrome P-450 4 enzymes in the kidney and liver: regulation by PPAR and species-difference between rat and human. *Mol. Cell. Biochem.* 284, 141–148. doi:10.1007/s11010-005-9038-x

Jia, Z., Sun, Y., Liu, S., Liu, Y., and Yang, T. (2014). COX-2 but not mPGES-1 contributes to renal PGE2 induction and diabetic proteinuria in mice with type-1 diabetes. *PLoS One* 9, e93182. doi:10.1371/journal.pone.0093182

Jia, Z., Wang, N., Aoyagi, T., Wang, H., Liu, H., and Yang, T. (2011). Amelioration of cisplatin nephrotoxicity by genetic or pharmacologic blockade of prostaglandin synthesis. *Kidney Int.* 79, 77–88. doi:10.1038/ki.2010.331

Jia, Z., Zhang, Y., Ding, G., Heiney, K. M., Huang, S., and Zhang, A. (2015). Role of COX-2/mPGES-1/prostaglandin E2 cascade in kidney injury. *Mediat. Inflamm.* 2015, 147894. doi:10.1155/2015/147894

Jiang, J. G., Chen, C. L., Card, J. W., Yang, S., Chen, J. X., Fu, X. N., et al. (2005). Cytochrome P450 2J2 promotes the neoplastic phenotype of carcinoma cells and is up-regulated in human tumors. *Cancer Res.* 65, 4707–4715. doi:10.1158/0008-5472.CAN-04-4173

Jiang, J. G., Ning, Y. G., Chen, C., Ma, D., Liu, Z. J., Yang, S., et al. (2007). Cytochrome p450 epoxygenase promotes human cancer metastasis. *Cancer Res.* 67, 6665–6674. doi:10.1158/0008-5472.CAN-06-3643

Kaminska, K., Szczylik, C., Lian, F., and Czarnecka, A. M. (2014). The role of prostaglandin E$_2$ in renal cell cancer development: future implications for prognosis and therapy. *Future Oncol.* 10, 2177–2187. doi:10.2217/fon.14.152

Kang, S. W., Natarajan, R., Shahed, A., Nast, C. C., Lapage, J., Mundel, P., et al. (2003). Role of 12-lipoxygenase in the stimulation of p38 mitogen-activated protein kinase and collagen α5(IV) in experimental diabetic nephropathy and in glucose-stimulated podocytes. *J. Am. Soc. Nephrol.* 14, 3178–3187. doi:10.1097/01.asn.0000099702.16315.de

Kar, F., Hacioglu, C., Senturk, H., Donmez, D. B., Kanbak, G., and Uslu, S. (2020). Curcumin and LOXblock-1 ameliorate ischemia-reperfusion induced inflammation and acute kidney injury by suppressing the semaphorin-plexin pathway. *Life Sci.* 256, 118016. doi:10.1016/j.lfs.2020.118016

Kawakami, T., Ren, S., and Duffield, J. S. (2013). Wnt signalling in kidney diseases: dual roles in renal injury and repair. *J. Pathol.* 229, 221–231. doi:10.1002/path.4121

Kim, W. J., Gersey, Z., and Daaka, Y. (2012). Rap1GAP regulates renal cell carcinoma invasion. *Cancer Lett.* 320, 65–71. doi:10.1016/j.canlet.2012.01.022

Kim, Y. S., Reddy, M. A., Lanting, L., Adler, S. G., and Natarajan, R. (2003). Differential behavior of mesangial cells derived from 12/15-lipoxygenase knockout mice relative to control mice. *Kidney Int.* 64, 1702–1714. doi:10.1046/j.1523-1755.2003.00286.x

Kim, Y. S., Xu, Z. G., Reddy, M. A., Li, S. L., Lanting, L., Sharma, K., et al. (2005). Novel interactions between TGF-β1 actions and the 12/15-lipoxygenase pathway in mesangial cells. *J. Am. Soc. Nephrol.* 16, 352–362. doi:10.1681/ASN.2004070568

Komers, R., Lindsley, J. N., Oyama, T. T., Schutzer, W. E., Reed, J. F., Mader, S. L., et al. (2001). Immunohistochemical and functional correlations of renal cyclooxygenase-2 in experimental diabetes. *J. Clin. Invest.* 107, 889–898. doi:10.1172/JCI10228

Komers, R., Zdychová, J., Cahová, M., Kazdová, L., Lindsley, J. N., and Anderson, S. (2005). Renal cyclooxygenase-2 in obese Zucker (fatty) rats. *Kidney Int.* 67, 2151–2158. doi:10.1111/j.1523-1755.2005.00320.x

Kömhoff, M., Jeck, N. D., Seyberth, H. W., Gröne, H. J., Nüsing, R. M., and Breyer, M. D. (2000). Cyclooxygenase-2 expression is associated with the renal macula densa of patients with Bartter-like syndrome. *Kidney Int.* 58, 2420–2424. doi:10.1046/j.1523-1755.2000.00425.x

Kopp, B. T., Thompson, R., Kim, J., Konstan, R., Diaz, A., Smith, B., et al. (2019). Secondhand smoke alters arachidonic acid metabolism and inflammation in infants and children with cystic fibrosis. *Thorax* 74, 237–246. doi:10.1136/thoraxjnl-2018-211845

Lee, J. W., Park, J. H., Suh, J. H., Nam, K. H., Choe, J. Y., Jung, H. Y., et al. (2012). Cyclooxygenase-2 expression and its prognostic significance in clear cell renal cell carcinoma. *Korean J. Pathol.* 46, 237–245. doi:10.4132/KoreanJPathol.2012.46.3.237

Li, Z., Zhang, Y., Kim, W. J., and Daaka, Y. (2013). PGE2 promotes renal carcinoma cell invasion through activated RalA. *Oncogene* 32, 1408–1415. doi:10.1038/onc.2012.161

Linehan, W. M., and Ricketts, C. J. (2019). The Cancer Genome Atlas of renal cell carcinoma: findings and clinical implications. *Nat. Rev. Urol.* 16, 539–552. doi:10.1038/s41585-019-0211-5

Linkermann, A., Chen, G., Dong, G., Kunzendorf, U., Krautwald, S., and Dong, Z. (2014). Regulated cell death in AKI. *J. Am. Soc. Nephrol.* 25, 2689–2701. doi:10.1681/ASN.2014030262

Liu, Y., Zhou, L., Lv, C., Liu, L., Miao, S., Xu, Y., et al. (2023). PGE2 pathway mediates oxidative stress-induced ferroptosis in renal tubular epithelial cells. *FEBS J.* 290, 533–549. doi:10.1111/febs.16609

Luo, P., Zhou, Y., Chang, H. H., Zhang, J., Seki, T., Wang, C. Y., et al. (2009). Glomerular 20-HETE, EETs, and TGF-β1 in diabetic nephropathy. *Am. J. Physiol. Renal. Physiol.* 296, F556–F563. doi:10.1152/ajprenal.90613.2008

Lytvyn, Y., Bjornstad, P., Van Raalte, D. H., Heerspink, H. L., and Cherney, D. Z. I. (2020). The new biology of diabetic kidney disease-mechanisms and therapeutic implications. *Endocr. Rev.* 41, 202–231. doi:10.1210/endrev/bnz010

Ma, J., Natarajan, R., Lapage, J., Lanting, L., Kim, N., Becerra, D., et al. (2005). 12/15-lipoxygenase inhibitors in diabetic nephropathy in the rat. *Prostaglandins Leukot. Essent. Fatty Acids* 72, 13–20. doi:10.1016/j.plefa.2004.06.004

Makhov, P., Joshi, S., Ghatalia, P., Kutikov, A., Uzzo, R. G., and Kolenko, V. M. (2018). Resistance to systemic therapies in clear cell renal cell carcinoma: mechanisms and management strategies. *Mol. Cancer Ther.* 17, 1355–1364. doi:10.1158/1535-7163.MCT-17-1299

Makino, H., Tanaka, I., Mukoyama, M., Sugawara, A., Mori, K., Muro, S., et al. (2002). Prevention of diabetic nephropathy in rats by prostaglandin E receptor EP1-selective antagonist. *J. Am. Soc. Nephrol.* 13, 1757–1765. doi:10.1097/01.asn.0000019782.37851.bf

Matsuyama, M., Yoshimura, R., Mitsuhashi, M., Tsuchida, K., Takemoto, Y., Kawahito, Y., et al. (2005). 5-Lipoxygenase inhibitors attenuate growth of human renal cell carcinoma and induce apoptosis through arachidonic acid pathway. *Oncol. Rep.* 14, 73–79.

Matsuyama, M., Yoshimura, R., Tsuchida, K., Takemoto, Y., Segawa, Y., Shinnka, T., et al. (2004). Lipoxygenase inhibitors prevent urological cancer cell growth. *Int. J. Mol. Med.* 13, 665–668. doi:10.3892/ijmm.13.5.665

Mccarthy, E. T., Zhou, J., Eckert, R., Genochio, D., Sharma, R., Oni, O., et al. (2015). Ethanol at low concentrations protects glomerular podocytes through alcohol dehydrogenase and 20-HETE. *Prostaglandins Other Lipid Mediat.* 116, 88–98. doi:10.1016/j.prostaglandins.2014.10.006

Mcgowan, T., Mccue, P., and Sharma, K. (2001). Diabetic nephropathy. *Clin. Lab. Med.* 21, 111–146.

Meurer, M., Ebert, K., Schweda, F., and Höcherl, K. (2018). The renal vasodilatory effect of prostaglandins is ameliorated in isolated-perfused kidneys of endotoxemic mice. *Pflugers Arch.* 470, 1691–1703. doi:10.1007/s00424-018-2183-3

Mohamed, R., and Sullivan, J. C. (2023). Sustained activation of 12/15 lipoxygenase (12/15 LOX) contributes to impaired renal recovery post ischemic injury in male SHR compared to females. *Mol. Med.* 29, 163. doi:10.1186/s10020-023-00762-y

Murai, T., Miyauchi, T., Yanagida, T., and Sako, Y. (2006). Epidermal growth factor-regulated activation of Rac GTPase enhances CD44 cleavage by metalloproteinase disintegrin ADAM10. *Biochem. J.* 395, 65–71. doi:10.1042/BJ20050582

Murata, T., Ushikubi, F., Matsuoka, T., Hirata, M., Yamasaki, A., Sugimoto, Y., et al. (1997). Altered pain perception and inflammatory response in mice lacking prostacyclin receptor. *Nature* 388, 678–682. doi:10.1038/41780

Muroya, Y., Fan, F., Regner, K. R., Falck, J. R., Garrett, M. R., Juncos, L. A., et al. (2015). Deficiency in the formation of 20-hydroxyeicosatetraenoic acid enhances renal ischemia-reperfusion injury. *J. Am. Soc. Nephrol.* 26, 2460–2469. doi:10.1681/ASN.2014090868

Muthalif, M. M., Benter, I. F., Karzoun, N., Fatima, S., Harper, J., Uddin, M. R., et al. (1998). 20-Hydroxyeicosatetraenoic acid mediates calcium/calmodulin-dependent protein kinase II-induced mitogen-activated protein kinase activation in vascular smooth muscle cells. *Proc. Natl. Acad. Sci. U. S. A.* 95, 12701–12706. doi:10.1073/pnas.95.21.12701

Nakagawa, N., Yuhki, K., Kawabe, J., Fujino, T., Takahata, O., Kabara, M., et al. (2012). The intrinsic prostaglandin E2-EP4 system of the renal tubular epithelium limits the development of tubulointerstitial fibrosis in mice. *Kidney Int.* 82, 158–171. doi:10.1038/ki.2012.115

Narumiya, S., and Fitzgerald, G. A. (2001). Genetic and pharmacological analysis of prostanoid receptor function. *J. Clin. Invest.* 108, 25–30. doi:10.1172/JCI13455

Nasrallah, R., Hassouneh, R., and Hébert, R. L. (2016). PGE$_2$, kidney disease, and cardiovascular risk: beyond hypertension and diabetes. *J. Am. Soc. Nephrol.* 27, 666–676. doi:10.1681/ASN.2015050528

Nasrallah, R., and Hébert, R. L. (2004). Reduced IP receptors in STZ-induced diabetic rat kidneys and high-glucose-treated mesangial cells. *Am. J. Physiol. Renal. Physiol.* 287, F673–F681. doi:10.1152/ajprenal.00025.2004

Nilakantan, V., Maenpaa, C., Jia, G., Roman, R. J., and Park, F. (2008). 20-HETE-mediated cytotoxicity and apoptosis in ischemic kidney epithelial cells. *Am. J. Physiol. Renal. Physiol.* 294, F562–F570. doi:10.1152/ajprenal.00387.2007

Nithipatikom, K., Brody, D. M., Tang, A. T., Manthati, V. L., Falck, J. R., Williams, C. L., et al. (2010). Inhibition of carcinoma cell motility by epoxyeicosatrienoic acid (EET) antagonists. *Cancer Sci.* 101, 2629–2636. doi:10.1111/j.1349-7006.2010.01713.x

Ohba, K., Miyata, Y., Watanabe, S., Hayashi, T., Kanetake, H., Kanda, S., et al. (2011). Clinical significance and predictive value of prostaglandin E2 receptors (EPR) 1 - 4 in patients with renal cell carcinoma. *Anticancer Res.* 31, 597–605.

Okumura, M., Imanishi, M., Okamura, M., Hosoi, M., Okada, N., Konishi, Y., et al. (2003). Role for thromboxane A2 from glomerular thrombi in nephropathy with type 2 diabetic rats. *Life Sci.* 72, 2695–2705. doi:10.1016/s0024-3205(03)00180-2

Pallàs, M., Vázquez, S., Sanfeliu, C., Galdeano, C., and Griñán-Ferré, C. (2020). Soluble epoxide hydrolase inhibition to face neuroinflammation in Parkinson's Disease: a new therapeutic strategy. *Biomolecules* 10, 703. doi:10.3390/biom10050703

Papanikolaou, N., Peros, G., Morphake, P., Gkikas, G., Maraghianne, D., Tsipas, G., et al. (1992). Does gentamicin induce acute renal failure by increasing renal TXA$_2$ synthesis in rats? *Prostagl. Leukot. Essent. Fat. Acids* 45, 131–136. doi:10.1016/0952-3278(92)90229-c

Pickkers, P., Darmon, M., Hoste, E., Joannidis, M., Legrand, M., Ostermann, M., et al. (2021). Acute kidney injury in the critically ill: an updated review on pathophysiology and management. *Intensive Care Med.* 47, 835–850. doi:10.1007/s00134-021-06454-7

Ponsioen, B., Zhao, J., Riedl, J., Zwartkruis, F., Van Der Krogt, G., Zaccolo, M., et al. (2004). Detecting cAMP-induced Epac activation by fluorescence resonance energy transfer: Epac as a novel cAMP indicator. *EMBO Rep.* 5, 1176–1180. doi:10.1038/sj.embor.7400290

Porro, B., Songia, P., Squellerio, I., Tremoli, E., and Cavalca, V. (2014). Analysis, physiological and clinical significance of 12-HETE: a neglected platelet-derived 12-lipoxygenase product. *J. Chromatogr. B Anal. Technol. Biomed. Life Sci.* 964, 26–40. doi:10.1016/j.jchromb.2014.03.015

Puntarulo, S., and Cederbaum, A. I. (1998). Production of reactive oxygen species by microsomes enriched in specific human cytochrome P450 enzymes. *Free Radic. Biol. Med.* 24, 1324–1330. doi:10.1016/s0891-5849(97)00463-2

Qian, Q., Kassem, K. M., Beierwaltes, W. H., and Harding, P. (2009). PGE$_2$ causes mesangial cell hypertrophy and decreases expression of cyclin D3. *Nephron Physiol.* 113, p7–p14. doi:10.1159/000232399

Quigley, R., Baum, M., Reddy, K. M., Griener, J. C., and Falck, J. R. (2000). Effects of 20-HETE and 19(S)-HETE on rabbit proximal straight tubule volume transport. *Am. J. Physiol. Renal. Physiol.* 278, F949–F953. doi:10.1152/ajprenal.2000.278.6.F949

Rådmark, O., Werz, O., Steinhilber, D., and Samuelsson, B. (2015). 5-Lipoxygenase, a key enzyme for leukotriene biosynthesis in health and disease. *Biochim. Biophys. Acta* 1851, 331–339. doi:10.1016/j.bbalip.2014.08.012

Regner, K. R., Zuk, A., Van Why, S. K., Shames, B. D., Ryan, R. P., Falck, J. R., et al. (2009). Protective effect of 20-HETE analogues in experimental renal ischemia reperfusion injury. *Kidney Int.* 75, 511–517. doi:10.1038/ki.2008.600

Reidy, K., Kang, H. M., Hostetter, T., and Susztak, K. (2014). Molecular mechanisms of diabetic kidney disease. *J. Clin. Invest.* 124, 2333–2340. doi:10.1172/JCI72271

Roche, C., Guerrot, D., Harouki, N., Duflot, T., Besnier, M., Rémy-Jouet, I., et al. (2015). Impact of soluble epoxide hydrolase inhibition on early kidney damage in hyperglycemic overweight mice. *Prostaglandins Other Lipid Mediat.* 120, 148–154. doi:10.1016/j.prostaglandins.2015.04.011

Ronco, C., Bellomo, R., and Kellum, J. A. (2019). Acute kidney injury. *Lancet* 394, 1949–1964. doi:10.1016/S0140-6736(19)32563-2

Samuelsson, B., Dahlén, S. E., Lindgren, J. A., Rouzer, C. A., and Serhan, C. N. (1987). Leukotrienes and lipoxins: structures, biosynthesis, and biological effects. *Science* 237, 1171–1176. doi:10.1126/science.2820055

Sausville, L. N., Williams, S. M., and Pozzi, A. (2019). Cytochrome P450 epoxygenases and cancer: a genetic and a molecular perspective. *Pharmacol. Ther.* 196, 183–194. doi:10.1016/j.pharmthera.2018.11.009

Schiffer, M., Bitzer, M., Roberts, I. S., Kopp, J. B., Ten Dijke, P., Mundel, P., et al. (2001). Apoptosis in podocytes induced by TGF-β and Smad7. *J. Clin. Invest.* 108, 807–816. doi:10.1172/JCI12367

Schneider, C., and Pozzi, A. (2011). Cyclooxygenases and lipoxygenases in cancer. *Cancer Metastasis Rev.* 30, 277–294. doi:10.1007/s10555-011-9310-3

Sharma, I., Liao, Y., Zheng, X., and Kanwar, Y. S. (2022). Modulation of gentamicin-induced acute kidney injury by myo-inositol oxygenase via the ROS/ALOX-12/12-HETE/GPR31 signaling pathway. *JCI Insight* 7, e155487. doi:10.1172/jci.insight.155487

Sharma, R., Khanna, A., Sharma, M., and Savin, V. J. (2000). Transforming growth factor-β1 increases albumin permeability of isolated rat glomeruli via hydroxyl radicals. *Kidney Int.* 58, 131–136. doi:10.1046/j.1523-1755.2000.00148.x

Shuch, B., Amin, A., Armstrong, A. J., Eble, J. N., Ficarra, V., Lopez-Beltran, A., et al. (2015). Understanding pathologic variants of renal cell carcinoma: distilling therapeutic opportunities from biologic complexity. *Eur. Urol.* 67, 85–97. doi:10.1016/j.eururo.2014.04.029

Shuvy, M., Abedat, S., Beeri, R., Valitsky, M., Daher, S., Kott-Gutkowski, M., et al. (2011). Raloxifene attenuates Gas6 and apoptosis in experimental aortic valve disease in renal failure. *Am. J. Physiol. Heart Circ. Physiol.* 300, H1829–H1840. doi:10.1152/ajpheart.00240.2010

Siegel, R. L., Miller, K. D., and Jemal, A. (2020). Cancer statistics, 2020. *CA Cancer J. Clin.* 70, 7–30. doi:10.3322/caac.21590

Singh, N. K., and Rao, G. N. (2019). Emerging role of 12/15-lipoxygenase (ALOX15) in human pathologies. *Prog. Lipid Res.* 73, 28–45. doi:10.1016/j.plipres.2018.11.001

Sodin-Semrl, S., Spagnolo, A., Barbaro, B., Varga, J., and Fiore, S. (2004). Lipoxin A4 counteracts synergistic activation of human fibroblast-like synoviocytes. *Int. J. Immunopathol. Pharmacol.* 17, 15–25. doi:10.1177/039463200401700103

Sun, Y., Jia, Z., Liu, G., Zhou, L., Liu, M., Yang, B., et al. (2013). PPARγ agonist rosiglitazone suppresses renal mPGES-1/PGE2 pathway in db/db mice. *PPAR Res.* 2013, 612971. doi:10.1155/2013/612971

Susztak, K., Raff, A. C., Schiffer, M., and Böttinger, E. P. (2006). Glucose-induced reactive oxygen species cause apoptosis of podocytes and podocyte depletion at the onset of diabetic nephropathy. *Diabetes* 55, 225–233. doi:10.2337/diabetes.55.01.06.db05-0894

Sutariya, B., Jhonsa, D., and Saraf, M. N. (2016). TGF-β: the connecting link between nephropathy and fibrosis. *Immunopharmacol. Immunotoxicol.* 38, 39–49. doi:10.3109/08923973.2015.1127382

Tengholm, A., and Gylfe, E. (2017). cAMP signalling in insulin and glucagon secretion. *Diabetes Obes. Metab.* 19 (Suppl. 1), 42–53. doi:10.1111/dom.12993

Turolo, S., Edefonti, A., Mazzocchi, A., Syren, M. L., Morello, W., Agostoni, C., et al. (2021). Role of arachidonic acid and its metabolites in the biological and clinical manifestations of idiopathic nephrotic syndrome. *Int. J. Mol. Sci.* 22, 5452. doi:10.3390/ijms22115452

Umanath, K., and Lewis, J. B. (2018). Update on diabetic nephropathy: core curriculum 2018. *Am. J. Kidney Dis.* 71, 884–895. doi:10.1053/j.ajkd.2017.10.026

Vivian, E. M., and Rubinstein, G. B. (2002). Pharmacologic management of diabetic nephropathy. *Clin. Ther.* 24, 1741–1756. doi:10.1016/s0149-2918(02)80076-5

Vukicevic, S., Simic, P., Borovecki, F., Grgurevic, L., Rogic, D., Orlic, I., et al. (2006). Role of EP2 and EP4 receptor-selective agonists of prostaglandin E2 in acute and chronic kidney failure. *Kidney Int.* 70, 1099–1106. doi:10.1038/sj.ki.5001715

Walshe, J. J., Brentjens, J. R., Costa, G. G., Andres, G. A., and Venuto, R. C. (1984). Abdominal pain associated with IgA nephropathy. Possible mechanism. *Am. J. Med.* 77, 765–767. doi:10.1016/0002-9343(84)90382-6

Wang, D., Wang, H., Brown, J., Daikoku, T., Ning, W., Shi, Q., et al. (2006). CXCL1 induced by prostaglandin E2 promotes angiogenesis in colorectal cancer. *J. Exp. Med.* 203, 941–951. doi:10.1084/jem.20052124

Wang, T., Fu, X., Chen, Q., Patra, J. K., Wang, D., Wang, Z., et al. (2019). Arachidonic acid metabolism and kidney inflammation. *Int. J. Mol. Sci.* 20, 3683. doi:10.3390/ijms20153683

Wang, Y., Wei, X., Xiao, X., Hui, R., Card, J. W., Carey, M. A., et al. (2005). Arachidonic acid epoxygenase metabolites stimulate endothelial cell growth and angiogenesis via mitogen-activated protein kinase and phosphatidylinositol 3-kinase/Akt signaling pathways. *J. Pharmacol. Exp. Ther.* 314, 522–532. doi:10.1124/jpet.105.083477

Wang, Y., Zhang, Y., Wang, P., Fu, X., and Lin, W. (2020). Circular RNAs in renal cell carcinoma: implications for tumorigenesis, diagnosis, and therapy. *Mol. Cancer* 19, 149. doi:10.1186/s12943-020-01266-7

Wang, Y. N., Zhang, Z. H., Liu, H. J., Guo, Z. Y., Zou, L., Zhang, Y. M., et al. (2023). Integrative phosphatidylcholine metabolism through phospholipase A2 in rats with chronic kidney disease. *Acta Pharmacol. Sin.* 44, 393–405. doi:10.1038/s41401-022-00947-x

Watanabe, Y., Yamaguchi, T., Ishihara, N., Nakamura, S., Tanaka, S., Oka, R., et al. (2018). 7-Ketocholesterol induces ROS-mediated mRNA expression of 12-lipoxygenase, cyclooxygenase-2 and pro-inflammatory cytokines in human mesangial cells: potential role in diabetic nephropathy. *Prostaglandins Other Lipid Mediat.* 134, 16–23. doi:10.1016/j.prostaglandins.2017.11.002

Wender-Ozegowska, E., and Biczysko, R. (2004). Vascular complications and their effect on fetal-maternal outcome and therapeutic approach in diabetic women. *Ginekol. Pol.* 75, 385–396.

Wettersten, H. I. (2020). Reprogramming of metabolism in kidney cancer. *Semin. Nephrol.* 40, 2–13. doi:10.1016/j.semnephrol.2019.12.002

Williams, J. M., Sharma, M., Anjaiahh, S., Falck, J. R., and Roman, R. J. (2007). Role of endogenous CYP450 metabolites of arachidonic acid in maintaining the glomerular protein permeability barrier. *Am. J. Physiol. Renal. Physiol.* 293, F501–F505. doi:10.1152/ajprenal.00131.2007

Witola, W. H., Liu, S. R., Montpetit, A., Welti, R., Hypolite, M., Roth, M., et al. (2014). ALOX12 in human toxoplasmosis. *Infect. Immun.* 82, 2670–2679. doi:10.1128/IAI.01505-13

Woo, S. M., Min, K. J., Chae, I. G., Chun, K. S., and Kwon, T. K. (2015). Silymarin suppresses the PGE2 -induced cell migration through inhibition of EP2 activation; G protein-dependent PKA-CREB and G protein-independent Src-STAT3 signal pathways. *Mol. Carcinog.* 54, 216–228. doi:10.1002/mc.22092

Wu, J., Zhang, Y., Frilot, N., Kim, J. I., Kim, W. J., and Daaka, Y. (2011). Prostaglandin E2 regulates renal cell carcinoma invasion through the EP4 receptor-Rap GTPase signal transduction pathway. *J. Biol. Chem.* 286, 33954–33962. doi:10.1074/jbc.M110.187344

Wu, X. Q., Zhang, D. D., Wang, Y. N., Tan, Y. Q., Yu, X. Y., and Zhao, Y. Y. (2021). AGE/RAGE in diabetic kidney disease and ageing kidney. *Free Radic. Biol. Med.* 171, 260–271. doi:10.1016/j.freeradbiomed.2021.05.025

Xiao, L., Zhou, D., Tan, R. J., Fu, H., Zhou, L., Hou, F. F., et al. (2016). Sustained activation of Wnt/β-catenin signaling drives AKI to CKD progression. *J. Am. Soc. Nephrol.* 27, 1727–1740. doi:10.1681/ASN.2015040449

Xu, H. Z., Cheng, Y. L., Wang, W. N., Wu, H., Zhang, Y. Y., Zang, C. S., et al. (2016). 12-Lipoxygenase inhibition on microalbuminuria in type-1 and type-2 diabetes is associated with changes of glomerular angiotensin II type 1 receptor related to insulin resistance. *Int. J. Mol. Sci.* 17, 684. doi:10.3390/ijms17050684

Xu, M., Ju, W., Hao, H., Wang, G., and Li, P. (2013). Cytochrome P450 2J2: distribution, function, regulation, genetic polymorphisms and clinical significance. *Drug Metab. Rev.* 45, 311–352. doi:10.3109/03602532.2013.806537

Xu, S., Jiang, B., Maitland, K. A., Bayat, H., Gu, J., Nadler, J. L., et al. (2006). The thromboxane receptor antagonist S18886 attenuates renal oxidant stress and proteinuria in diabetic apolipoprotein E-deficient mice. *Diabetes* 55, 110–119. doi:10.2337/diabetes.55.01.06.db05-0831

Xu, X., Zhao, C. X., Wang, L., Tu, L., Fang, X., Zheng, C., et al. (2010). Increased CYP2J3 expression reduces insulin resistance in fructose-treated rats and db/db mice. *Diabetes* 59, 997–1005. doi:10.2337/db09-1241

Yan, L. J. (2021). NADH/NAD+ redox imbalance and diabetic kidney disease. *Biomolecules* 11, 730. doi:10.3390/biom11050730

Yang, S., Lin, L., Chen, J. X., Lee, C. R., Seubert, J. M., Wang, Y., et al. (2007). Cytochrome P-450 epoxygenases protect endothelial cells from apoptosis induced by tumor necrosis factor-α via MAPK and PI3K/Akt signaling pathways. *Am. J. Physiol. Heart Circ. Physiol.* 293, H142–H151. doi:10.1152/ajpheart.00783.2006

Yared, A., Kon, V., and Ichikawa, I. (1985). Mechanism of preservation of glomerular perfusion and filtration during acute extracellular fluid volume depletion. Importance of intrarenal vasopressin-prostaglandin interaction for protecting kidneys from constrictor action of vasopressin. *J. Clin. Invest.* 75, 1477–1487. doi:10.1172/JCI111851

Yarla, N. S., Bishayee, A., Sethi, G., Reddanna, P., Kalle, A. M., Dhananjaya, B. L., et al. (2016). Targeting arachidonic acid pathway by natural products for cancer prevention and therapy. *Semin. Cancer Biol.* 40-41, 48–81. doi:10.1016/j.semcancer.2016.02.001

Yoshimura, R., Inoue, K., Kawahito, Y., Mitsuhashi, M., Tsuchida, K., Matsuyama, M., et al. (2004a). Expression of 12-lipoxygenase in human renal cell carcinoma and growth prevention by its inhibitor. *Int. J. Mol. Med.* 13, 41–46. doi:10.3892/ijmm.13.1.41

Yoshimura, R., Matsuyama, M., Mitsuhashi, M., Takemoto, Y., Tsuchida, K., Kawahito, Y., et al. (2004b). Relationship between lipoxygenase and human testicular cancer. *Int. J. Mol. Med.* 13, 389–393. doi:10.3892/ijmm.13.3.389

Yu, W., Chen, L., Yang, Y. Q., Falck, J. R., Guo, A. M., Li, Y., et al. (2011). Cytochrome P450 ω-hydroxylase promotes angiogenesis and metastasis by upregulation of VEGF and MMP-9 in non-small cell lung cancer. *Cancer Chemother. Pharmacol.* 68, 619–629. doi:10.1007/s00280-010-1521-8

Yuan, C., Ni, L., Zhang, C., and Wu, X. (2020). The role of Notch3 signaling in kidney disease. *Oxid. Med. Cell. Longev.* 2020, 1809408. doi:10.1155/2020/1809408

Yuan, H., Lanting, L., Xu, Z. G., Li, S. L., Swiderski, P., Putta, S., et al. (2008). Effects of cholesterol-tagged small interfering RNAs targeting 12/15-lipoxygenase on parameters of diabetic nephropathy in a mouse model of type 1 diabetes. *Am. J. Physiol. Renal. Physiol.* 295, F605–F617. doi:10.1152/ajprenal.90268.2008

Yuan, H., Reddy, M. A., Deshpande, S., Jia, Y., Park, J. T., Lanting, L. L., et al. (2016). Epigenetic histone modifications involved in profibrotic gene regulation by 12/15-lipoxygenase and its oxidized lipid products in diabetic nephropathy. *Antioxid. Redox Signal.* 24, 361–375. doi:10.1089/ars.2015.6372

Zhang, M., Wang, M. H., Singh, R. K., Wells, A., and Siegal, G. P. (1997). Epidermal growth factor induces CD44 gene expression through a novel regulatory element in mouse fibroblasts. *J. Biol. Chem.* 272, 14139–14146. doi:10.1074/jbc.272.22.14139

Zhang, Y., Thayele Purayil, H., Black, J. B., Fetto, F., Lynch, L. D., Masannat, J. N., et al. (2017). Prostaglandin E2 receptor 4 mediates renal cell carcinoma intravasation and metastasis. *Cancer Lett.* 391, 50–58. doi:10.1016/j.canlet.2017.01.007

Zhao, G., Tu, L., Li, X., Yang, S., Chen, C., Xu, X., et al. (2012). Delivery of AAV2-CYP2J2 protects remnant kidney in the 5/6-nephrectomized rat via inhibition of apoptosis and fibrosis. *Hum. Gene Ther.* 23, 688–699. doi:10.1089/hum.2011.135

Zhao, H., Chen, L., Yang, T., Feng, Y. L., Vaziri, N. D., Liu, B. L., et al. (2019). Aryl hydrocarbon receptor activation mediates kidney disease and renal cell carcinoma. *J. Transl. Med.* 17, 302. doi:10.1186/s12967-019-2054-5

Zheng, Z., Li, Y., Jin, G., Huang, T., Zou, M., and Duan, S. (2020). The biological role of arachidonic acid 12-lipoxygenase (ALOX12) in various human diseases. *Biomed. Pharmacother.* 129, 110354. doi:10.1016/j.biopha.2020.110354

Zhu, Y., Blum, M., Hoff, U., Wesser, T., Fechner, M., Westphal, C., et al. (2016). Renal ischemia/reperfusion injury in soluble epoxide hydrolase-deficient mice. *PLoS One* 11, e0145645. doi:10.1371/journal.pone.0145645

Zweifel, B. S., Davis, T. W., Ornberg, R. L., and Masferrer, J. L. (2002). Direct evidence for a role of cyclooxygenase 2-derived prostaglandin E2 in human head and neck xenograft tumors. *Cancer Res.* 62, 6706–6711.

Check for updates

*CORRESPONDENCE
Mingcheng Huang,
✉ huangmch6@mail.sysu.edu.cn
Zhihua Zheng,
✉ zhzhihua@mail.sysu.edu.cn
Ling Hong,
✉ hongling5@mail2.sysu.edu.cn

†These authors have contributedequally to
this work

# Myricitrin inhibited ferritinophagy-mediated ferroptosis in cisplatin-induced human renal tubular epithelial cell injury

Jiawen Lin[1†], Yangyang Zhang[1†], Hui Guan[2†], Shuping Li[3],
Yuan Sui[4], Ling Hong[1]*, Zhihua Zheng[1]* and Mingcheng Huang[1]*

[1]Department of Nephrology, Kidney and Urology Center, The Seventh Affiliated Hospital, Sun Yat-sen University, Shenzhen, China, [2]Department of Radiation Oncology, The First Affiliated Hospital of Zhengzhou University, Zhengzhou, China, [3]Department of Physiology, University of Oklahoma Health Sciences Center, Oklahoma City, OK, United States, [4]Molecular and Cellular Biology Laboratory, The Salk Institute for Biological Studies, La Jolla, CA, United States

Cisplatin-induced acute kidney injury (AKI) increases the patient mortality dramatically and results in an unfavorable prognosis. A strong correlation between AKI and ferroptosis, which is a notable type of programmed cell death, was found in recent studies. Myricitrin is a natural flavonoid compound with diverse pharmacological properties. To investigate the protective effect of myricitrin against cisplatin induced human tubular epithelium (HK-2) cell injury and the underlying anti-ferroptic mechanism by this study. Firstly, a pharmacology network analysis was proposed to explore the myricitrin's effect. HK-2 cells were employed for *in vitro* experiments. Ferroptosis was detected by cell viability, quantification of iron, malondialdehyde, glutathione, lipid peroxidation fluorescence, and glutathione peroxidase (GPX4) expression. Ferritinophagy was detected by related protein expression (NCOA4, FTH, LC3II/I, and SQSTM1). In our study, GO enrichment presented that myricitrin might be effective in eliminating ferroptosis. The phenomenon of ferroptosis regulated by ferritinophagy was observed in cisplatin-activated HK-2 cells. Meanwhile, pretreatment with myricitrin significantly rescued HK-2 cells from cell death, reduced iron overload and lipid peroxidation biomarkers, and improved GPX4 expression. In addition, myricitrin downregulated the expression of LC3II/LC3I and NCOA4 and elevated the expression of FTH and SQTM. Furthermore, myricitrin inhibited ROS production and preserved mitochondrial function with a lower percentage of green JC-1 monomers. However, the protection could be reserved by the inducer of ferritinophagy rapamycin. Mechanically, the Hub genes analysis reveals that AKT and NF-κB are indispensable mediators in the anti-ferroptic process. In conclusion, myricitrin ameliorates cisplatin induced HK-2 cells damage by attenuating ferritinophagy mediated ferroptosis.

KEYWORDS

acute kidney injury, myricitrin, renal tubular epithelial cell, ferroptosis, ferritinophagy, oxidative stress

# 1 Introduction

Acute kidney injury (AKI) is a critical medical illness with high mortality and morbidity, which is observed among approximately 5%–15% of hospitalized patients (Al-Jaghbeer et al., 2018; Martin-Cleary et al., 2021). AKI is clinically characterized by an abrupt decline in renal function. Known as a common cause of AKI, cisplatin is widely used as a chemotherapeutic drug in the management of solid malignant tumors (Tang C. et al., 2023). Nevertheless in prolonged, accumulating cisplatin could elicit renal dysfunction. The nephrotoxic responses to cisplatin not only limit its therapeutic potential but also affect the life quality of individuals with malignancies adversely.

Programmed cell death, including apoptosis and necrosis, has been identified as pivotal events in the pathological course of AKI, which manifests tremendous tubular cell damage in terms of histology (Sanz et al., 2023; Wu et al., 2022). As firstly proposed in 2012 by Dixon et al., ferroptosis is a form of novel programmed cell death placed on excessive iron production and overwhelming lipid peroxidation (Dixon et al., 2012). It has been showed in numerous studies that ferroptosis exists in both AKI patients and animal models established by different stimuli, such as LPS, cisplatin, ischemia-refusion, and folic acid (Bayır et al., 2023; Liang et al., 2022; Friedmann Angeli et al., 2014; Martin-Sanchez et al., 2017).

Iron metabolism is an essential biological activity responsible for ferroptosis. Generally, overloaded free iron could easily undergo the Fenton reaction, arousing massive oxidative damage to cell membrane lipid peroxidation (Fuhrmann and Brüne, 2022). Ferritinophagy is the process of autophagic degradation of ferritin and the release of extensive iron (Tang et al., 2018). While appropriate autophagy has emerged as a favorable cellular survival mechanism, excessive ferritin autophagy might be responsible for ferroptosis (Liu et al., 2020). It was found by Joseph D et al. that nuclear receptor coactivator 4 (NCOA4) was a specific receptor, which encouraged ferritin to be transported to the autophagosome and degraded eventually (Mancias et al., 2014). In brief, there is considerable intrigue in investigating the likely participation of NCOA4-mediated ferritinophagy in the progression of AKI.

Myricitrin, a bioactive component of bayberry, is a naturally occurring flavonoid with a diverse range of biological activities, which provides protections for multiple systems (Geng et al., 2023). Meanwhile, myricitrin exerts an immense impact on anti-oxidation and elimination of free radicals. Evidences provided by Sun et al. support the inhibitory effects of myricitrin on endothelial apoptosis induced by ox-LDL mediated ROS in the atherosclerosis mouse model (Qin et al., 2015). It has been demonstrated by animal studies that myricitrin can minimize liver I/R injury by preventing oxidative stress as well as inflammatory responses and boosting NO synthase activation (Shen et al., 2020). Currently, it was reported by Bin Zhao et al. that myricitrin attenuated cisplatin-induced kidney injury, mechanically eliminated reactive oxygen species, and inhibited apoptosis (Li et al., 2020). It is commonly recognized that reactive oxygen species triggers lipid peroxidation, which is the foundation of ferroptosis development (Pope and Dixon, 2023). However, there is a scarcity of published information concerning the anti-ferroptosis efficacy of myricitrin, whose mechanism of modulating AKI remains limitedly explored.

In the present investigation, we postulated that NOA4-mediated ferritinophagy contributed to ferroptosis in the context of cisplatin-induced renal tubular cells. Furthermore, we plan to investigate the potential role of myricitrin in the cell death of renal tubular cells and elucidate the underlying protective mechanism of myricitrin.

# 2 Methods

## 2.1 Reagent and antibody

The chemical reagents were purchased as below: Myricitrin (Myr): Selleck, S2327; Cisplatin (CDDP): MCE, HY-17394; 3-Methyladenine (3-MA): MCE, HY-19312; Chloroquine (CQ): MCE, HY-17589A; acetylcysteine (NAC): MCE, HY-B0215. All other chemicals were of high-grade purity available from commercial sources.

The antibodies were obtained as below: GPX4 (Abcam, ab125066), FTH (proteintech, 10727-1-AP), LC3A/B (CST, 4108), NCOA4 (abclonal, A5695), SQSTM1 (CST, 5,114), GAPDH (abclonal, AC001) and HRP-conjugated Goat Anti Rabbit IgG (proteintech, SA0001-2).

The relevant materials were provided as following: Cell Counting Kit-8 Kit (Beyotime, C0038), Annexin V/PI Apoptosis Analysis Kit (KeyGEN, KGA1013), Cell Ferrous Iron Colorimetric Assay Kit (Biosharp, BL1147A), Lipid Peroxidation MDA Assay Kit (Beyotime, S0131M), GSH Assay Kit (Jiancheng Bioengineering, A006-2-1), Bodipy 581/591 C11 (abclonal, RM02821), Reactive oxygen species Assay Kit (Beyotime, S0033S), MitoSox (ThermoFisher, M36008), and JC-1 applied to detect mitochondrial membrane potential (MCE, S0131M).

## 2.2 Construction of Myricitrin's prediction targets network and GO function enrichment analysis

The SMILES format and structure of myricitrin were obtained from PubChem and we imported these information to SwissTargetPrediction database, comparative toxicogenomics database (CTD), and PharmMapper database (Daina et al., 2019; Davis et al., 2023; Wang et al., 2017). The gene interaction network was established by using STRING database (Szklarczyk et al., 2023). Furthermore, the identified genes were imported into Cytoscape to construct a protein-protein interaction (PPI) network for analysis by utilizing the CytoNCA method (Shannon et al., 2003; Tang et al., 2015). It is our aim to identify and evaluate the potential main targets of myricitrin in this study. In addition, the biological process of the key genes was enriched by using online Metascape database and visualized as a chordal graph by the application of bioinformatics (Zhou et al., 2019; Tang D. et al., 2023).

## 2.3 Pharmacodynamic mechanism analysis of myricitrin on cisplatin induced acute kidney injury

To explore the pharmacodynamic mechanism of myricitrin on acute kidney injury stimulated by cisplatin, the disease-related

targets were collected at first from the following three databases: GenCards, Online Mendelian Inheritance in Man (OMIM) database, and DisGeNET (Stelzer et al., 2016; Amberger et al., 2015; Piñero et al., 2021). The two key phrases "cisplatin induced acute kidney injury" and "cisplatin nephrotoxicity" were used for searching, and only "*Homo sapiens*" proteins linked to the disease from results were selected. Finally, the targets were obtained from the overlaps between the myricitrin-related targets and the disease-related targets.

The "myricitrin on cisplatin acute kidney injury" perdition target network was constructed by using Cytoscape software. In the network, proteins were represented as nodes, and interactions between those molecular species were represented as edges. Functional annotation of target genes was analyzed by using the online Metascape database. The statistical significances were defined as $p < 0.05$ and the gene sets containing more than five genes were significant as well. Based on the online Metascape database, the GO and KEGG analysis projects were employed to explore the predicted action targets.

## 2.4 Cell culture

Human kidney epithelial tubular HK-2 cells were grown in F12 medium with 10% fetal bovine serum and 1% streptomycin/penicillin mixture. A humidified 5% $CO_2$ atmosphere was applied to maintain all cell cultures at 37°C. After seeded in plates and cultured for 24 h, the HK-2 cells were incubated with fresh complete culture medium, and exposed to different treatments.

## 2.5 Cells model establishment and treatment

To establish cisplatin (CDDP) activated cells, HK-2 cells were exposed to different concentrations of cisplatin (2.5 or 5 ug/mL) for 24 h. To explore whether ferritinophagy occurs and is involved, we first employed the autophagy inhibitor, 3-MA (5, 10 uM) and CQ (10, 20 uM), to the HK-2 cells with cisplatin co-treatment for 24 h. To observe the effect of myricitrin on cisplatin activated cells, HK-2 cells were divided into four groups: the normal control, the CDDP group exposed to 5 ug/mL cisplatin, the Myr group cultured in medium containing 5 uM myricitrin for 24 h, and the CDDP + Myr group incubated with 5 uM myricitrin for 1 h prior to cisplatin stimulation for sequentially 24 h. Then, known as the autophagy inducer, 100 nM rapamycin (Rapa) was applied to the HK-2 cells 30 min before the administration of both myricitrin and cisplatin.

## 2.6 Cell viability assays

Cell viability was measured by using the Cell Counting Kit-8 (CCK8) assay. Cells were inoculated in a 96-well plate with a density of 5,000 cells per well. After overnight incubation the cells were treated by cisplatin and myricitrin for 24 h described above. The cells were incubated for 4 h after we applied 10 ul CCK8 solution in each well. Finally, the absorbance value was measured at 450 nm by a microreader.

## 2.7 Annexin V-PI assays

To explore the apoptosis level, the HK-2 cells from treatment groups and controls were harvested for different experimental needs, and then incubated by Annexin V-FITC and PI in the dark for at least 10 min according to the manufacturer's protocols. Afterward, flow cytometry was utilized to examine the cells. Early apoptotic cells were determined by counting the percentage of Annexin V+/PI− cells; progressed apoptotic cells were obtained by counting the percentage of Annexin V+/PI + cells; necrotic cells were detected by counting the percentage of Annexin V-/PI + cells, and Annexin V−/PI− cells were considered as surviving cells.

## 2.8 Measurement of iron content

According to the manufacturer's guidelines, an iron assay kit was employed to quantify the iron content in the HK-2 cells from treatment groups and controls. Briefly, cells were harvested and further lysed in iron lysis buffer by ultrasound. After centrifuged at 12,000 rpm for 10 min, the supernatant mixed with the working reagent was incubated for 15 min at room temperature. A microreader was employed to detect the absorbance at a wavelength of 562 nm.

## 2.9 Assessment of malondialdehyde (MDA)

To investigate the MDA concentration, the HK-2 cells from treatment groups and controls were subjected to lysis by using Western & IP lysis buffer. In accordance with manufacturer's instructions, the resulting lysate was centrifuged at 12,000 rpm for 10 min and then measured by MDA Assay Kit which implemented TBA approach. Thereafter, 532 nm absorbance was recorded by using a microplate reader.

## 2.10 Assessment of glutathione (GSH)

The HK-2 cells from treatment groups and controls were homogenized by using an ultrasonic crusher and centrifuged at 12,000 rpm for 10 min after they were gathered. Then, the supernatant was collected for the following examination of GSH level. The experiment involved the process of the addition of samples mixed with GSH working mixture in the 96-well plate, which was incubated for 5 min at room temperature. The absorbance was determined at the wavelength of 405 nm.

## 2.11 Lipid peroxidation assay

The evaluation of lipid peroxidation was conducted by incubating different samples with 10uM Bodipy 581/591 for 1 h at 37 C in the dark. After the incubation was completed, the cells were washed twice with PBS to eliminate any surplus dye. The phenomenon of oxidized Bodipy was noticed by using a fluorescence microscope.

FIGURE 1
Screening and analysis of potential targets of myricitrin. **(A)** The Protein Interaction (PPI) network of myricitrin's targets was gathered from the String database. **(B)** Network diagram of the most important targets of the myricitrin's potential genes was made by using CytoNCA calculation. **(C)** Top enriched GO process of myricitrin's targets was acquired from Metascape database, and the chordal diagram was constructed by representing enrichment items and their relevant genes.

## 2.12 Intracellular ROS assay and mitochondrial ROS assay

The intracellular ROS production was observed by using reactive species oxygen Assay Kit. The HK-2 cells from treatment groups and controls were incubated with 1: 2000 DCFH-DA at 37°C for 15 min in the dark. Then, after being washed twice by PBS, the HK-2 cells were resuspended in stain buffer and measured immediately by flow cytometry. Mitochondrial ROS level was detected by Mitosox stained. After incubated with 5 uM MitoSox for 60 min, the HK-2 cells were observated in fluorescence microscope.

## 2.13 Measurement of mitochondrial membrane potential

The Mito Probe JC-1 Assay Kit was used to detect the changes in mitochondrial membrane potential (MMP). The HK-2 cells from treatment groups and controls were collected and incubated in 10 uM JC-1 working solution for 30 min in the dark. Then, the cells were washed twice by staining buffer and

analyzed by flow cytometry within 1 h. The red aggregation showed normal MMP, while the green monomer indicated a reduction in MMP due to mitochondrial dysfunction. Results were presented as the percentage of green monomer stained by JC-1.

## 2.14 Western blot

Western blotting was employed to detect the protein expression of GPX4, FTH, NCOA4, LC3, and SQSTM1 in the cells from treatment groups and controls. The proteins obtained from the lysate of HK-2 cells were employed in RIPA buffer on ice and then the concentration was quantified by adopting the BCA protein assay kit. After the addition of 15 μg of distinct samples into each individual well, the proteins were separated by using 10%–12% SDS-PAGE gel and transferred onto a PVDF membrane. The membrane was blocked for 2 h at room temperature in the 5% non-fatty milk. The membranes were sectioned into different portions based on the molecular weight of the target protein. Subsequently, the pieces were subjected to overnight incubation with primary antibody under the

temperature condition of 4℃. After using a suitable secondary antibody for incubation, the immunoblots were eventually detected by super ECL reagent. All protein bands' intensity was measured by ImageJ.

## 2.15 Statistical analysis

All experiments were conducted three to five times, with each repetition carried out independently. Data was expressed as mean + standard deviation and analyzed by using GraphPad Prism 8. Data analysis and comparison between groups used one-way ANOVA and two-tailed Student's t-test. Values of $p < 0.05$ were considered statistically significant.

# 3 Results

## 3.1 Screening and analysis of potential targets of myricitrin

As shown in Figure 1A, a total of 242 target genes of myricitrin were obtained by searching three online databases (PharmMapper database, SwissTargetPrediction database, and superpre database). With the help of the STRING database, a pharmacological target of the myricitrin network was constructed. According to Cytoscape by applying CytoNCA calculation, Figure 1B showed that a network of top 27 interactional genes is obtained by setting parameters (Degree ≥18, Betweenness Centrality ≥370, Closeness Centrality ≥0.248). Then, with analysis results of the 27 genes via Metascape database, it was surprisingly noted that the biological process of the top gene was mainly enriched in cellular response to cytokines stimulus, regulation of reactive oxygen species metabolic, cellular response to lipid, and so on. In addition, it was fascinating to mention that when conducting a search in the ferroptosis database and the related literature, a significant majority of the top 27 genes were identified as hallmark indicators of ferroptosis. These genes contain PTGS2, NFE2L2, KEAP1, SLC2A1, and so on (Figure 1C). To sum up, it can be speculated that administration of myricitrin was intricately countering the incidence and progression of ferroptosis.

## 3.2 Ferroptosis occurs on cisplatin induced renal tubular cells

HK-2 cells were treated with different doses and by different times of cisplatin to determine the exact concentrations that inhibiting the cell growth. As shown in Figure 2A, cisplatin significantly inhibited the cell viability compared with the control group. Furthermore, confirmed with the above results, Figure 2B depicted that cisplatin increased the cell death-rate, which was detected by Annexin-V flow cytometry based on dose dependence. Known as specific markers for ferroptosis, Western blot was used to examine the GPX4 protein expression. The results showed that GPX4, a crucial enzyme against lipid peroxidation and ferroptosis, was also suppressed in the cisplatin group (Figure 2C). Furthermore, our results showed

that cisplatin exposure led to enhanced accumulation of intracellular iron content. Lipid peroxidation was considered as a key component involved in the cell death cascade driven by ferroptosis. The amount of MDA could reflect the degree of intracellular lipid peroxidation. It was observed that cisplatin could significantly increase MDA levels in HK-2 cells (Figure 2D). C11-BOPIDY staining showed that the level of oxidation C11-BODIPY was significantly increased in the cisplatin group compared with the control group (Figure 2E).

## 3.3 Ferritinophagy Contributes to ferroptosis in cisplatin induced renal tubular cells

It has been confirmed in an increasing number of studies that autophagy participates in the occurrence and development of cisplatin-related renal tubular cell injury. Moreover, ferritinophagy is an autophagy mode of ferritin degradation mediated by NCOA4, which can regulate ferroptosis. Therefore, it was speculated that ferritinophagy might be involved in HK-2 cell injury caused by cisplatin. Meanwhile, it was speculated that NCOA4, FTH1, SQTM1, and LC3II/LC3I protein-related expression were obtained by applying Western blot. Compared with the CDDP group, the expressions of NCOA4 and LC3II/LC3I were downregulated in myricitrin pretreatment group, while the FTH1 and SQTMQ expression were increasing (Figures 3A,B). However, the classical autophagy inhibitors, specifically 3-methyladenine (3-MA) and chloroquine (CQ), were all employed to suppress the ferritinophagy activity. As illustrated in Figures 3C,D, high concentrations of 3-MA and CQ pretreatment could enhance the cell viability and diminish the cell damage. These results indicated that ferritinophagy might have participated in the progress of the injury of renal tubular cells with cisplatin administration.

## 3.4 Myricitrin significantly reduced ferroptosis upon cisplatin induction in renal tubular cells

First of all, according to the results of cell viability (Figure 4A), myricitrin at a concentration between 0.5 and 10 uM stimulation of 24 h showed no cytotoxicity effect on HK-2 cells. Therefore, 5 uM myricitrin incubation was selected for subsequent cell experiments. Secondly, we found that the decreased cell viability induced by cisplatin could be alleviated by myricitrin pretreatment (Figure 4B). In addition, it was observed that myricitrin could promote cell survival whereas cisplatin stimulated the apparent apoptosis of HK-2 cells (Figure 4C).

In Figure 4D, the HK-2 cells with myricitrin incubation showed a dramatic increase in GPX4 expression compared with the cisplatin induction group, which showed the depletion of GPX4. Meanwhile, the contents of intracellular iron in myricitrin treatment group were obviously lower than the cisplatin group (Figure 4E). As illustrated in Figure 4F, after myricitrin intervention, the increase of MDA content stimulated by cisplatin was partially reserved, whereas the levels of GSH inhibited by cisplatin were effectively restored. At the same time, the oxidation of C11-BODIPY fluorescent intensity was
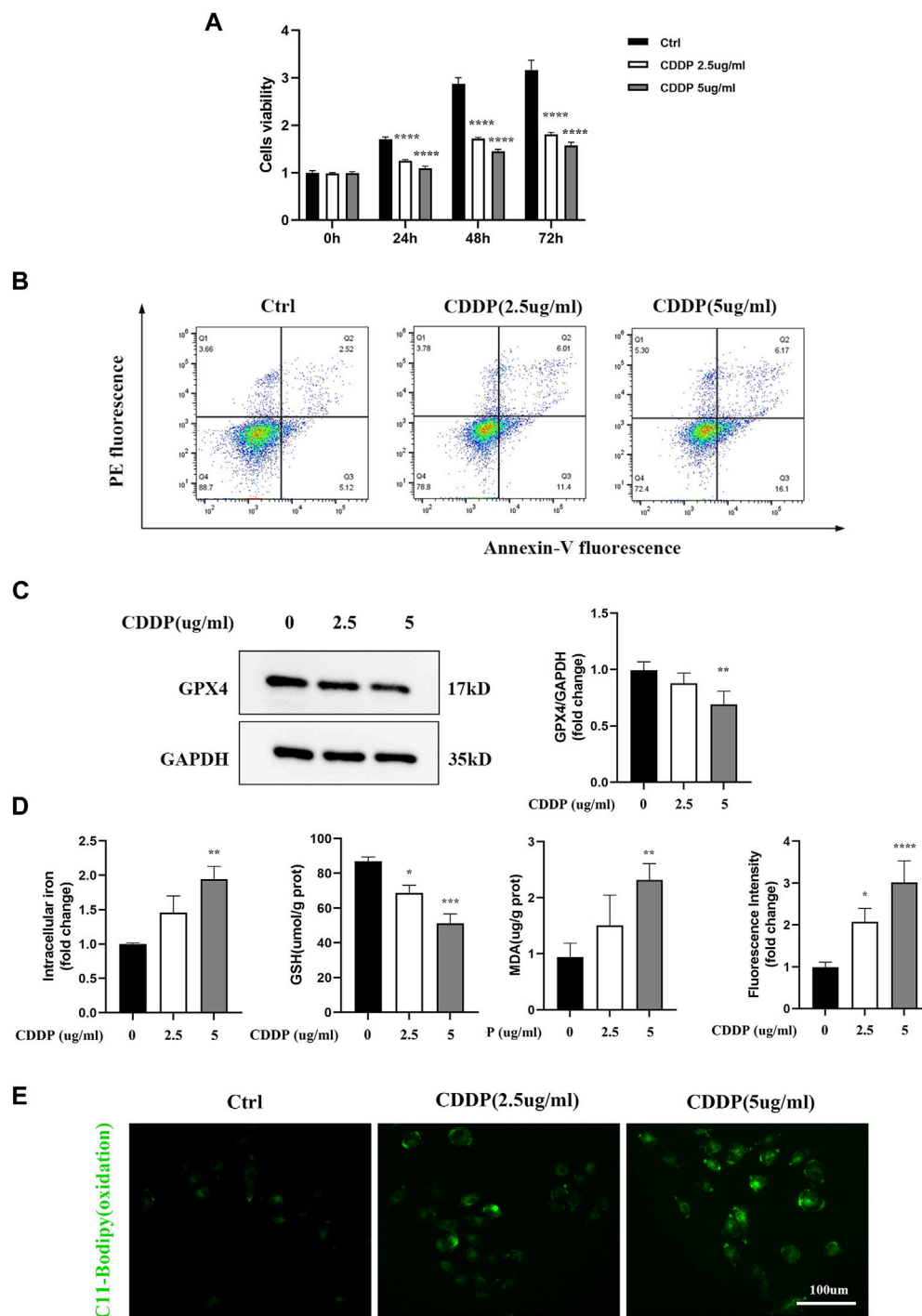
**FIGURE 2**
Renal tubular cells induced by Ferroptosis occurs on Cisplatin. *In vitro*, HK-2 cells were treated with different concentrations of cisplatin (0, 2.5, 5ug/mL). **(A)** Cell viability of HK-2 cells was determined by CCK-8 assays. **(B)** Annexin V-PI assay was used to determine the apoptosis cells. **(C)** Western blot was used to examine the expression of ferroptosis-related proteins GPX4. Protein levels were measured by using densitometry and normalized with GAPDH. **(D)** Intracellular iron was examined by Colorimetric Assay Kits. MDA and GSH were examined and normalized with the protein concentration. **(E)** Oxidation C11 BODIPY staining of the cisplatin activation HK-2 cells (scale bar = 100um). Compared with the control group, Data were presented as mean ± SD. (n = 3–4). *$p < 0.05$, **$p < 0.01$, ***$p < 0.005$, ****$p < 0.001$.

suppressed by myricitrin administration, indicating a decrease in lipid peroxidation and inhibition of ferroptosis, which was in alignment with the results mentioned before. In short, these

results demonstrated that myricitrin ameliorated lipid peroxidation and ferroptosis against cisplatin-induced HK-2 cell injury.
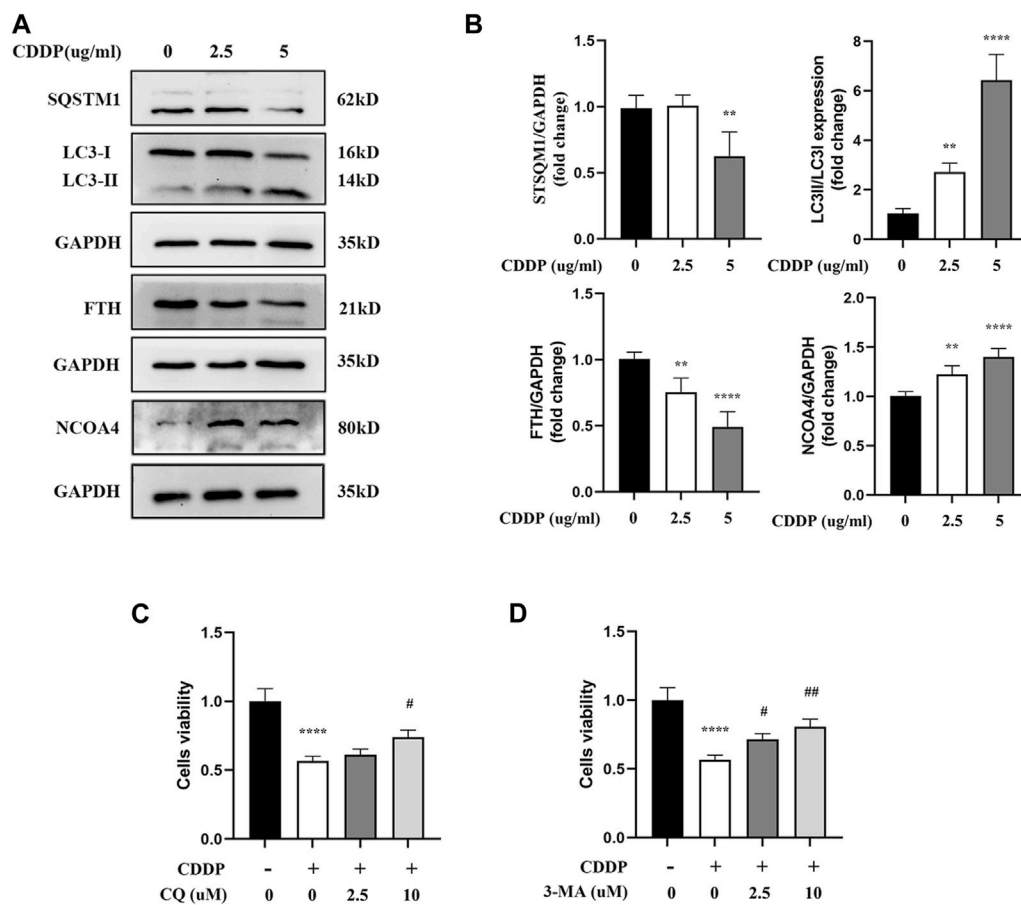
**FIGURE 3**
Ferritinophagy Contributes to Ferroptosis in Cisplatin induced Renal Tubular Cells. The HK-2 cell were stimulated with 2.5ug/mL or 5ug/mL cisplatin for 24 h. **(A)** The representative images of Western blot showed the expression of ferritinophagy-related proteins (LC3II/LC3I, FTH, NCOA4, SQSTM1) in cells (n = 4). **(B)** Protein levels were measured by using densitometry and normalized with GAPDH. **(C), (D)** Cell viability of cisplatin activated HK-2 cells with co-incubation of different concentrations CQ (2.5, 10uM) and 3-MA (2.5, 10uM) was determined by CCK-8 assays (n = 3). Data were presented as mean $\pm$ SD. $**p < 0.01$, $****p < 0.001$, compared with the control group and $\#p < 0.05$, $\#\#p < 0.01$, compared with the CDDP group.

## 3.5 Myricitrin attenuated ROS production and persevered mitochondrial function in cisplatin activated kidney tubular cells

Previous research suggested the acetylcysteine, the oxidatve stress inhibitor, could attenuated the ferroptosis in various disease. The CCK-8 assays showed that does independed acetylcysteine could improved the cell viability of cisplatin induced cells (Figure 5A). Furthermore, intracellular iron content and MDA were lower in acetylcysteine group compare to the cisplatin group. Acetylcysteine could also increased the anti-oxidant GSH level (Figure 5B). In summary, we validated the positive role of ROS in the occurrence of ferrpotosis. To determine the effect of myricitrin on oxidative stress in renal tubular cells, the intracellular ROS levels were measured by using flow cytometry to detect the HK-2 cells stained with DCFDA. As shown in Figure 5C, ROS levels were significantly higher in cisplatin group, whereas both myricitrin and acetylcysteine could reverse oxidative stress via reducing intracellular ROS production. In addition, myricitrin could reduce the increased level of mitochondrial ROS, which induced by cisplatin (Figure 5D).

As the main organelle of energy metabolism and ROS production, mitochondria plays an important role in renal proximal tubular epithelial cells. In our study, it was found that cisplatin intervention in HK-2 cells resulted in a decrease in the percentage of JC-1 monomers, indicating MMP reduction and mitochondrial damage. However, lower percentage of green monomers was detected in the cisplatin-induced cells with myricitrin treatment (Figure 5E). These results manifested that myricitrin had an antioxidant effect as well as a protective function of mitochondria.

## 3.6 Myricitrin mitigated ferroptosis in cisplatin activated tubular epithelium cells via inhibiting NCOA4 mediated ferritinophagy

It has been demonstrated in our earlier research that the autophagic degradation of ferritin, a process referred to as ferritinophagy, can promote ferroptosis in activated HK-2 cells with cisplatin stimulation. Additionally, NCOA4 is a specific cargo receptor that facilitates ferritin degradation in lysosomes. Herein, we investigated whether the
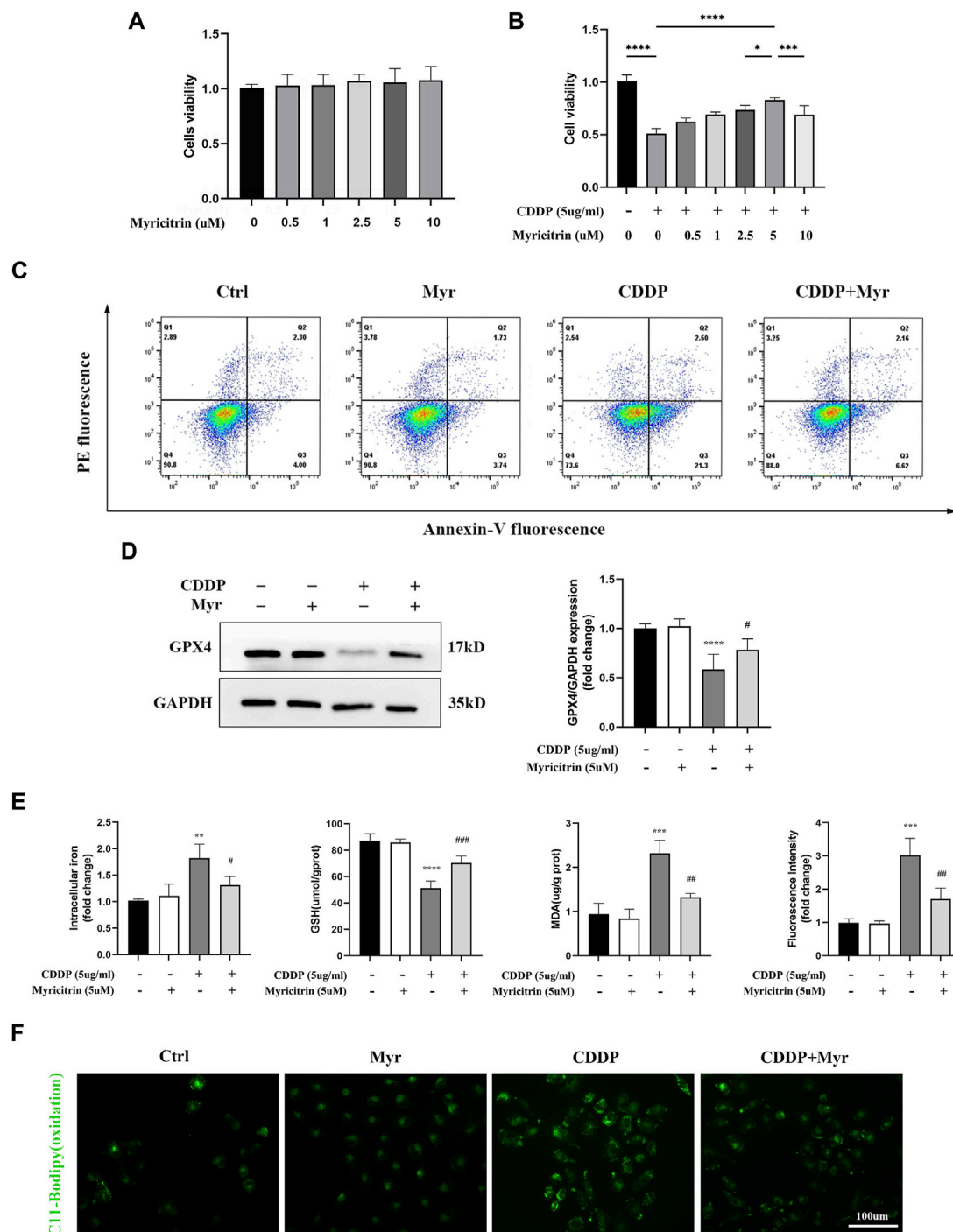
**FIGURE 4**
Myricitrin significantly reduced Ferroptosis upon cisplatin induction in renal tubular cells. **(A)** Cell viability of HK-2 cells treated with different concentrations of myricitrin (0, 0.5, 1, 2.5, 5, 10uM) for 24 h (n = 6). **(B)** Cell viability of cisplatin induced HK-2 cells treated with different concentrations of myricitrin (0, 0.5, 1, 2.5, 5, 10uM) for 24 h (n = 6). **(C)** The HK-2 cells were incubated with 5uM myritrin, 5ug/mL cisplatin or the combination for the following experiments in this section. Annexin V-PI assay determined the apoptosis cells. **(D)** Western blot was employed to examine the expression of ferroptosis-related proteins (GPX4). Protein levels were measured by using densitometry and normalized with GAPDH (n = 4). **(E)** Intracellular iron content was detected by Colorimetric Assay Kits. MDA and GSH, were examined and normalized with the protein concentration (n = 3–4). **(F)** Oxidation C11 BODIPY staining of the cisplatin activation HK-2 cells (n = 3), scale bar = 100um. Data were presented as mean $\pm$ SD. **$p < 0.01$, ***$p < 0.005$, ***$p < 0.001$, compared with the control group, and #$p < 0.05$, ##$p < 0.01$, ###$p < 0.005$, compared with the CDDP group.

NCOA4 mediated degradation of ferritin was associated with myricitrin's protective mechanism against ferroptosis induced by cisplatin in renal tubular cells. Western blotting revealed that the expression of vital

ferritinophagy makers LC3II/LC3I and NCOA4 were downregulated, while FTH as well as SQTM1 expression were upregulated by myricitrin treatment (Figure 6A).
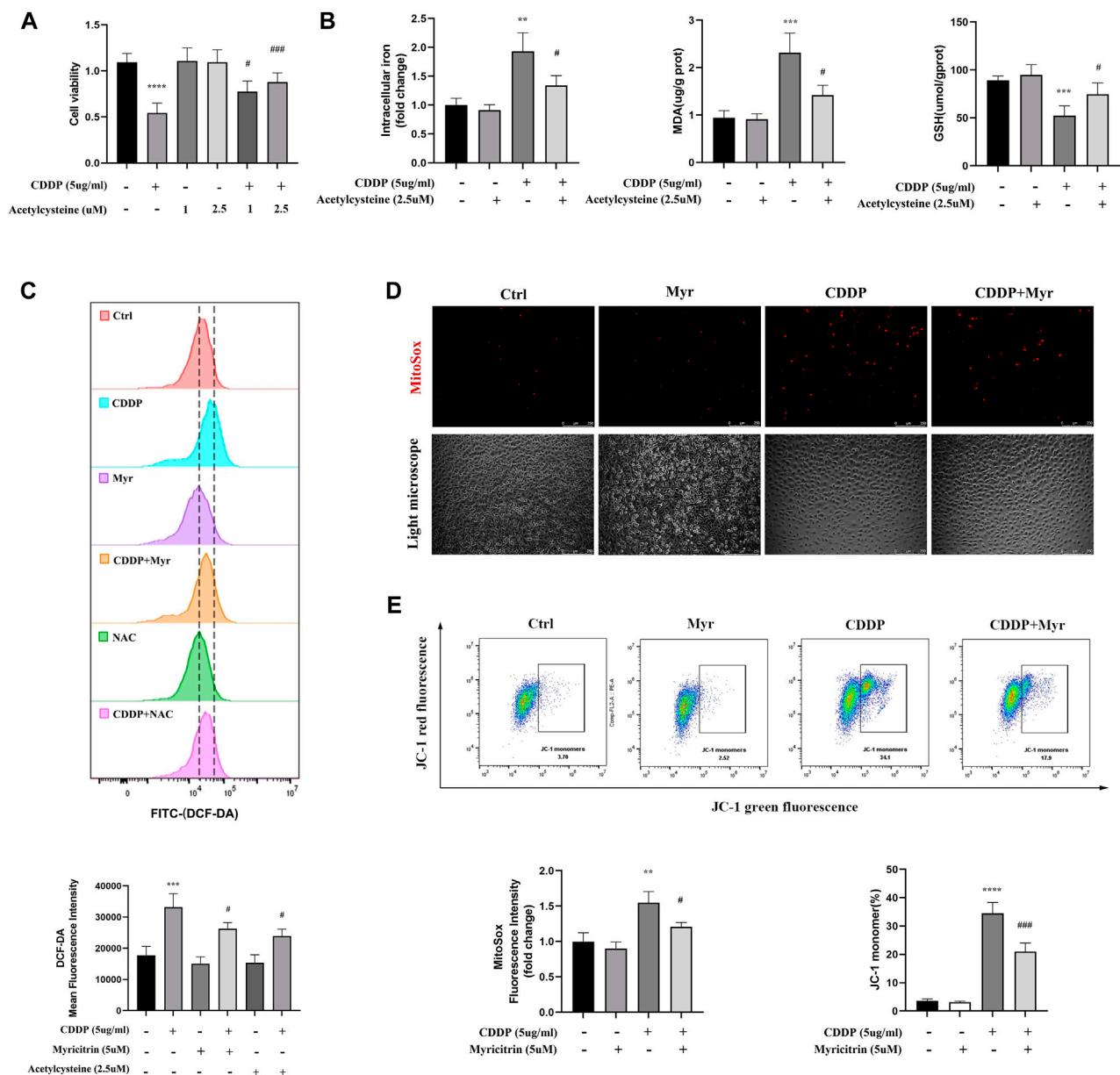
FIGURE 5
Myricitrin attenuated the ROS production and preserved the mitochondrial function. **(A)** CCK8 assays measured cell viability of HK-2 cells treated with indicated dose acetylcysteine or cisplatin or the combination for 24 h (n = 6). **(B)** Intracellular iron conten, MDA and GSH were detected in HK-2 cells incubated with 2.5uM acetylcysteine, or cisplatin, or the combination for 24 h (n = 4). **(C)** Cells were divided into six groups. HK-2 cells were stimulated with 2.5uM acetylcysteine or 5uM myritrin individually, and then treated with cisplatin for 24 h. Evaluation of ROS generation by using flow cytometry with DCFDA probe. The results were analyzed by quantification of mean fluorescence intensity (MFI) of DCFDA staining (n = 3). **(D)** Immunofluorescence analysis and quantification analysis of MitoSox in HK-2 cells (scale bar = 250um), the results were calculated by quantification of MFI (n = 3). **(E)** Flow cytometry was used to detect the mitochondrial membrane potential (Ψm) of HK-2 cells stained with JC-1. The dot plot illustrates the gate represented for JC-1 (green) monomer populations (n = 3). Data were presented as mean $\pm$ SD. ****$p < 0.005$, compared with the control group; ##$p < 0.01$, ###$p < 0.005$, compared with the CDDP group.

To further investigate the role of ferritinophagy in cisplatin-induced renal tubular cell injury, activated HK-2 cells were pretreated with the ferritinophagy inducer and rapamycin (Rapa), and co-treated with myricitrin for 24 h. Our results demonstrated that myricitrin alleviated ferroptosis by promoting the cell viability and survival (Figures 6B,C), decreasing intracellular iron level and MDA content, and

increasing GSH content, which was reversed by Rapa co-treatment (Figure 6D). In addition, results from C11-BODIPY immunofluorescence showed that myricitrin significantly decreased the level of lipid peroxidation, while co-incubation with Rapa deteriorated this influence (Figure 6E). Overall, these findings revealed that myricitrin suppressed the activated HK-2 cells ferroptosis by inhibiting NCOA4-mediated ferritinophagy.
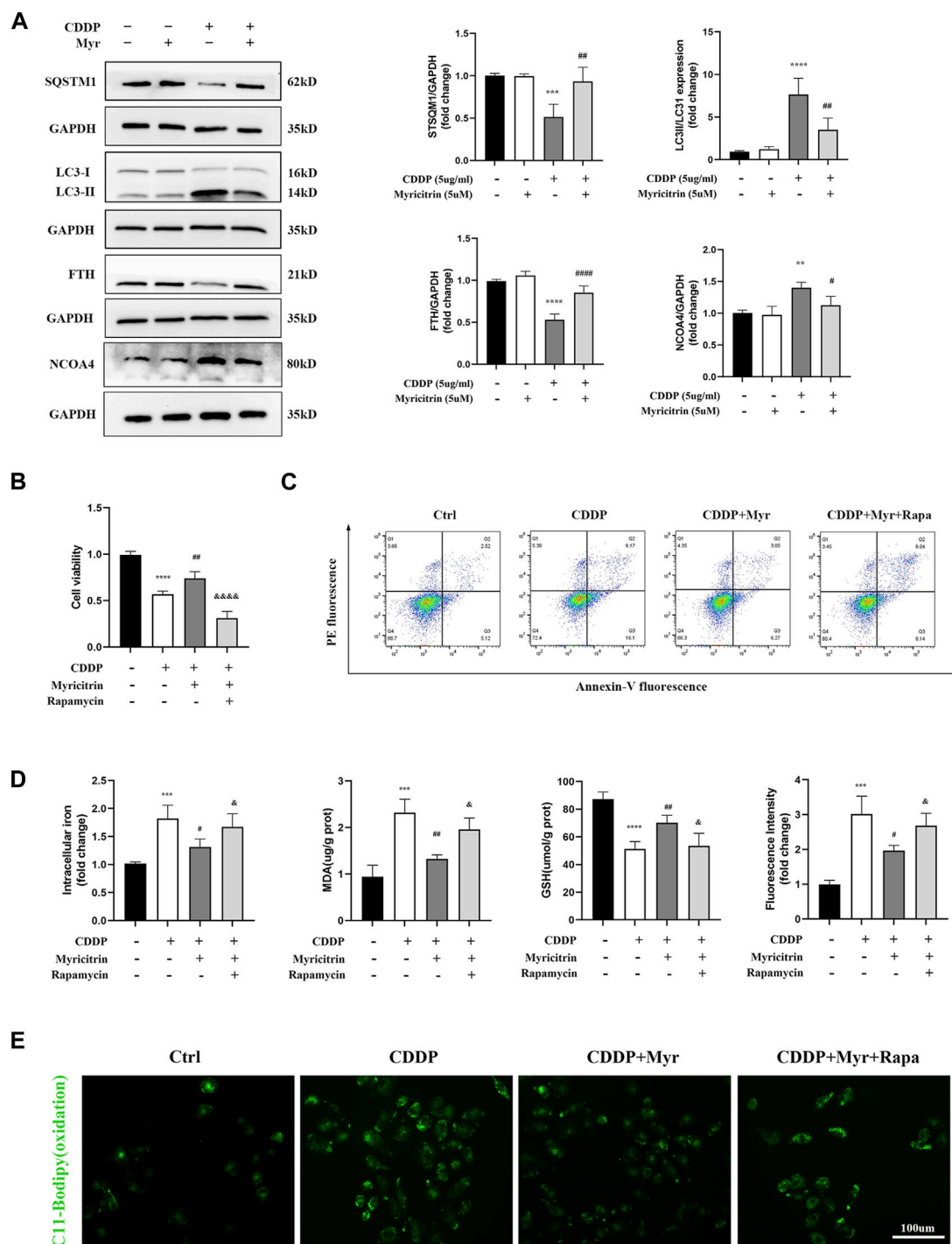
**FIGURE 6**
Myricitrin mitigated ferroptosis in cisplatin activated tubular epithelium cells via inhibiting NCOA4 mediated ferritinophagy. **(A)** Western blot examined the expression of ferritinophagy-related proteins (LC3II/LC3I, FTH, NCOA4, SQSTM1) from HK-2 cells treated with 5uM myricitrin (Myr), 5ug/mL cisplatin (CDDP), myricitrin + cisplatin (CDDP + Myr), or without both drugs (Ctrl) for 24 h. Protein levels were measured by using densitometry and normalized with GAPDH (n = 4). **(B)** After rapamycin appllied to HK-2 cells 30 min, both myricitrin and cisplatin were added to stimulated cells for 24 h. Cell viability of cisplatin activated HK-2 cells with co-treatment of rapamycin and myricitri (n = 5). **(C)** Annexin V-PI assay was used to determine apoptosis cells. **(D)** Intracellular iron content, MDA and GSH were examined and normalized with the protein concentration (n = 5). **(E)** Oxidation C11 BODIPY staining of the cisplatin activation HK-2 cells (scale bar = 100um). Data were presented as mean $\pm$ SD. $*p < 0.05$, $**p < 0.01$, $****p < 0.005$, compard with the control group; $\#p < 0.05$, $\#\#p < 0.01$, $\#\#\#p < 0.005$, compared with the CDDP group; $\&p < 0.05$, $\&\&\&\&p < 0.001$, compared with the CDDP + Myr group.

FIGURE 7
Potential targets of the action targets of Myricitrin on Cisplatin induced acute kidney injury. **(A)** Venn diagram illustrated the cross-section between cisplatin-induce acute kidney injury target and myricitrin target. **(B)** Network diagram of the predictive targets was constructed and visualized using Cytoscape software. **(C)** GO and KEGG pathway enrichment analysis were obtained from online Metascape database. **(D)** The 10 hubs genes were identified by utilizing CytoNCA algorithm. **(E)** The HK-2 cells were incubated with 5uM myritrin as monotherapy or in combination with 5ug/mL cisplatin for 24 h. Western blot showed the AKT and NF-κB protein phosphorylation expression of different group of HK-2 cells (n = 5). Data are presented as mean ± SD. ***$p < 0.005$, compare to the control group; #$p < 0.05$, compare to the CDDP group.

## 3.7 Potential targets of the action targets of myricitrin on cisplatin induced acute kidney injury

From GeneCards and OMIM, 2005 related targets for cisplatin-induced acute kidney injury were retrieved. Figure 7A displayed 94 putative targets for myricitrin acting on cisplatin induced acute kidney injury that derived from gene mapping. After removing the irrelevant genes from STRING

database, the protein interaction network was created and enhanced by Cytoscape software. Figure 7B illustrated the construction of the targets of "myricitrin—cisplatin induced AKI" network. As shown in Figure 7C, the GO and KEGG pathway analysis results obtained from Metascape database, showed the enrichment in the process of response to lipid and reactive oxygen species metabolism, which was closely related to ferroptosis mechanism. Subsequently, the CytoNCA algorithm was utilized to identify the key proteins, including AKT1, SRC,

EGFR, NFKB1, STAT1, PPARG, HIF1A, MTOR, ESR1, TNF, and so on (Figure 7D). Hence, it seemed sensible to assume that the AKT and NF-κB pathway might be implicated in myricitrin's anti-ferroptosis effect on cisplatin-induced acute kidney injury.

# 4 Discussions

At present, our pharmacology network analysis demonstrated that myricitrin might display potential efficacy in preventing ferroptosis. In the meantime, it was observed that ferroptosis regulated by ferritinophagy participated in the damage of cisplatin activated HK-2 cells. Additionally, myricitrin significantly suppressed the cell damage by reducing ferroptosis and ferritinophagy, as well as preserving the mitochondrial function. In summary, these results revealed that inhibiting ferritinophagy-mediated ferroptosis might serve as the underlying mechanism of myricitrin against cisplatin-induced HK-2 cell injury.

Cisplatin is extensively employed as a chemotherapeutic drug for the treatment of solid tumors. With the rising use of this antineoplastic medication, acute kidney injury is known as one of the inevitable complications which deserves our attention. Recent studies have reported that inflammation, oxidative stress, vascular injury, endoplasmic reticulum stress, and tubular cell death are all involved in the pathogenesis of cisplatin-induced nephrotoxicity (McSweeney et al., 2021; Holditch et al., 2019).

Ferroptosis, an emerging type of regulatory cell death, is characterized by iron accumulation and excessive lipid peroxidation. There are mounting researches showing that ferroptosis plays a role in the field of renal disease, including diabetic nephropathy, renal fibrosis, and acute kidney injury caused by diverse factors (Wang Y. et al., 2022; Li et al., 2021; Tonnus et al., 2021; Wang J. et al., 2022). In our research, the renal proximal tubular epithelium cell was applied to establish the vitro models. Firstly, it was found that cisplatin could induce cell viability reduction and the process of cell death. Moreover, Fe2+ and lipid peroxidation accumulation were detected in HK-2 cells stimulated by cisplatin. GPX4 is recognized as a central repressor of ferroptosis in limiting lipid peroxidation (Seibt et al., 2019; Chen et al., 2023; Miao et al., 2023). The dysregulation of GPX4 is implicated in the ferroptosis execution. As western blotting illustrated, cisplatin reduced the expression of GPX4 expression of HK-2 cells, suggesting that ferroptosis contributes to cell injury related to cisplatin, aligning with earlier findings reported in the literature.

Intracellular iron homeostasis is critical for governing ferroptosis. Mechanistically, ferritinophagy facilitates the autophagic degradation of ferritin, resulting in iron release and Fe2+ dependent lipid peroxidation. NCOA4 is an essential factor regulating ferritinophagy by governing the autolysosome formation and ferritin degradation. It was observed that the protein level of FTH and SQTMQ1 dramatically decreased, while the NCOA4 protein level and the ratio of LC3II/LC3I increased in the presence of cisplatin. However, ferritinophagy inhibitor 3-MA or CQ significantly promoted cisplatin activated the cell viability. In these experiments, it had been discovered that ferritinophagy was reinforced in cisplatin activated HK-2 cells and this process ultimately led to ferroptosis condition.

Myricitrin is a flavonoid compound with several feasible medicinal activities, including regulating oxidative stress, inflammatory response, and apoptosis. More significant researches are required to explore the myricitrin's molecular mechanisms. The pharmacology network method offers a systematic observation of the process of medications, focusing on the interaction network among disease, gene, and drug (Nogales et al., 2022). Therefore, we leveraged this approach and performed a GO enrichment study to evaluate the identified 27 hub genes obtained from network analysis. Interestingly, these genes exhibited enrichment in the biological process of regulating reactive oxygen species metabolic and cellular response to lipids, which was associated with ferroptosis. It is noteworthy that PTGS2, NFE2L2, KEAP1, and SLC2A1 are recognized as crucial biomarkers for ferroptosis, which suggest a promising potential for therapeutic intervention in mitigating this process. There have been reports about the myricitrin's preventive effect on various kidney diseases (Dua et al., 2021; Weng et al., 2019). It was found by Zhao et al. that myricitrin played a protective role against cisplatin-induced acute kidney injury through the inhibition of oxidative stress and inflammation (Li et al., 2020). However, whether myricitrin could mitigate cisplatin-induced renal tubular epithelial cell impairment via inhibiting ferroptosis remains uncertain. In the following study, we explored the function of myricitrin in cisplatin-induced renal tubular epithelial cell damage. While 5uM myricitrin was administered as a pretreatment to cisplatin activated HK-2 cells, it was found that myricitrin greatly prevented the cell damage by reducing ferroptosis, with regards to the phenomenon of Fe2+, lipid peroxidation reduction, and GPX4 expression escalation compared with the model group. Along with the detection of ferritinophagy protein, it was found that myricitrin not only mitigated the expression of NCOA4 and the ratio of LC3II/LC3I, but it also improved FTH and SQTMQ1 levels. However, ferritinophagy inducer rapamycin co-incubation reversed the protection against ferroptosis mentioned above partially. In short, it was revealed in these results that the inhibition of ferritinophagy mediated ferroptosis might serve as the underlying mechanism of myricitrin against cell injury.

Oxidative stress is characterized by the overproduction of ROS and depletion of endogenous antioxidant defense function. Oxidative stress could exacerbate cellular metabolic homeostasis, and ultimately cause malfunctioning mitochondria to generate lower ATP (Forman and Zhang, 2021). Our study herein demonstrated that myricitrin attenuated the abundant ROS generation induced by cisplatin and maintained the mitochondrial function by preserving a higher level of MMP.

Finally, the pharmacological network analysis was applied to investigate the possible mechanism of how myricitrin influences renal tubular cells induced by cisplatin. The activation of AKT and NF-κB was determined to be an important target of myricitrin for cisplatin-related nephrotoxicity. AKT is widely recognized as a major autophagic blocker by exerting its influence on inactivating ULK1 and VPS34 complex, which are responsible for cellular digestion initiation (Yu et al., 2015; Zhang et al., 2020). Activation of the mTORC1 complex, epigenetic modification of FOXO, and direct regulation of autophagic protein are the main mechanisms of AKT silencing autophagy (Cheng, 2019; Bach et al.,

2011). Interestingly, it has been shown in emerging evidences that activation of AKT could attenuate the effect of ferritinophagy modulation significantly. It was reported by Scott et al. that apolipoprotein E potently blocked the degradation of ferritin in murine mesencephalic neurons by stimulating the PI3K/AKT pathway and inducing AKT phosphorylation (Belaidi et al., 2022). Yi Cai et al. demonstrated that the activation of p38/AKT signaling in the host's macrophages was the initiation of the ferritin degradation cascade provoked by *mycobacterium tuberculosis* (Dai et al., 2023). Besides, it was reported that autophagy was associated with NF-κB activation in acute kidney injury both *in vivo* and *in vitro* (Pan et al., 2021; Wu et al., 2015). In combination with the previous researches, we recognized myricitrin as an inhibitor against ferroptosis by conducting the phosphorylation modification of AKT and NF-κB.

## 5 Conclusion

This study presents novel findings which indicate the involvement of ferritinophagy in the process of ferroptosis in cisplatin-induced renal tubular cell damage. Furthermore, myricitrin ameliorates cisplatin induced HK-2 cells damage and restores proper mitochondrial function by mitigating ferritinophagy mediated ferroptosis via NCOA4. Moreover, the pharmacological network analysis shows that myricitrin might possibly regulate the AKT and NF-κB pathways to provide anti-ferroptosis effects. Hence, myricitrin could be considered as a viable therapeutic intervention for treatment on cisplatin induced AKI.

## Data availability statement

The original contributions presented in the study are included in the article/Supplementary material, further inquiries can be directed to the corresponding authors.

## Author contributions

MH: Writing–review and editing, Conceptualization. JL: Writing–original draft, Investigation. YZ: Writing–original draft. HG: Writing–original draft, Data curation. SL: Writing–original draft, Formal Analysis. YS: Writing–original draft, Methodology. LH: Writing–review and editing. ZZ: Writing–review and editing, Funding acquisition.

## Funding

## Conflict of interest

The authors declare that the research was conducted in the absence of any commercial or financial relationships that could be construed as a potential conflict of interest.

## Publisher's note

All claims expressed in this article are solely those of the authors and do not necessarily represent those of their affiliated organizations, or those of the publisher, the editors and the reviewers. Any product that may be evaluated in this article, or claim that may be made by its manufacturer, is not guaranteed or endorsed by the publisher.

## References

Al-Jaghbeer, M., Dealmeida, D., Bilderback, A., Ambrosino, R., and Kellum, J. A. (2018). Clinical decision support for in-hospital AKI. *J. Am. Soc. Nephrol. JASN* 29, 654–660. doi:10.1681/ASN.2017070765

Amberger, J. S., Bocchini, C. A., Schiettecatte, F., Scott, A. F., and Hamosh, A. (2015). OMIM.org: online Mendelian Inheritance in Man (OMIM®), an online catalog of human genes and genetic disorders. *Nucleic Acids Res.* 43, D789–D798. doi:10.1093/nar/gku1205

Bach, M., Larance, M., James, D. E., and Ramm, G. (2011). The serine/threonine kinase ULK1 is a target of multiple phosphorylation events. *Biochem. J.* 440, 283–291. doi:10.1042/BJ20101894

Bayır, H., Dixon, S. J., Tyurina, Y. Y., Kellum, J. A., and Kagan, V. E. (2023). Ferroptotic mechanisms and therapeutic targeting of iron metabolism and lipid peroxidation in the kidney. *Nat. Rev. Nephrol.* 19, 315–336. doi:10.1038/s41581-023-00689-x

Belaidi, A. A., Masaldan, S., Southon, A., Kalinowski, P., Acevedo, K., Appukuttan, A. T., et al. (2022). Apolipoprotein E potently inhibits ferroptosis by blocking ferritinophagy. *Mol. Psychiatry*. doi:10.1038/s41380-022-01568-w

Chen, L., Ma, Y., Ma, X., Liu, L., Jv, X., Li, A., et al. (2023). TFEB regulates cellular labile iron and prevents ferroptosis in a TfR1-dependent manner. *Free Radic. Biol. Med.* 208, 445–457. doi:10.1016/j.freeradbiomed.2023.09.004

Cheng, Z. (2019). The FoxO-autophagy Axis in health and disease. *Trends Endocrinol. Metab.* 30, 658–671. doi:10.1016/j.tem.2019.07.009

Dai, Y., Zhu, C., Xiao, W., Chen, X., and Cai, Y. (2023). *Mycobacterium tuberculosis* induces host autophagic ferritin degradation for enhanced iron bioavailability and bacterial growth. *Autophagy* 20, 943–945. doi:10.1080/15548627.2023.2213983

Daina, A., Michielin, O., and Zoete, V. (2019). SwissTargetPrediction: updated data and new features for efficient prediction of protein targets of small molecules. *Nucleic Acids Res.* 47, W357-W364–W364. doi:10.1093/nar/gkz382

Davis, A. P., Wiegers, T. C., Johnson, R. J., Sciaky, D., Wiegers, J., and Mattingly, C. J. (2023). Comparative toxicogenomics database (CTD): update 2023. *Nucleic Acids Res.* 51, D1257–D1262. doi:10.1093/nar/gkac833

Dixon, S. J., Lemberg, K. M., Lamprecht, M. R., Skouta, R., Zaitsev, E. M., Gleason, C. E., et al. (2012). Ferroptosis: an iron-dependent form of nonapoptotic cell death. *Cell.* 149, 1060–1072. doi:10.1016/j.cell.2012.03.042

Dua, T. K., Joardar, S., Chakraborty, P., Bhowmick, S., Saha, A., De Feo, V., et al. (2021). Myricitrin, a glycosyloxyflavone in *Myrica esculenta* bark ameliorates diabetic nephropathy via improving glycemic status, reducing oxidative stress, and suppressing inflammation. *Mol. Basel, Switz.* 26, 258. doi:10.3390/molecules26020258

Forman, H. J., and Zhang, H. (2021). Targeting oxidative stress in disease: promise and limitations of antioxidant therapy. *Nat. Rev. Drug Discov.* 20, 689–709. doi:10.1038/s41573-021-00233-1

Friedmann Angeli, J. P., Schneider, M., Proneth, B., Tyurina, Y. Y., Tyurin, V. A., Hammond, V. J., et al. (2014). Inactivation of the ferroptosis regulator Gpx4 triggers acute renal failure in mice. *Nat. Cell. Biol.* 16, 1180–1191. doi:10.1038/ncb3064

Fuhrmann, D. C., and Brüne, B. (2022). A graphical journey through iron metabolism, microRNAs, and hypoxia in ferroptosis. *Redox Biol.* 54, 102365. doi:10.1016/j.redox.2022.102365

Geng, Y., Xie, Y., Li, W., Mou, Y., Chen, F., Xiao, J., et al. (2023). Toward the bioactive potential of myricitrin in food production: state-of-the-art green extraction and trends in biosynthesis. *Crit. Rev. Food Sci. Nutr.*, 1–27. doi:10.1080/10408398.2023.2227262

Holditch, S. J., Brown, C. N., Lombardi, A. M., Nguyen, K. N., and Edelstein, C. L. (2019). Recent advances in models, mechanisms, biomarkers, and interventions in cisplatin-induced acute kidney injury. *Int. J. Mol. Sci.* 20, 3011. doi:10.3390/ijms20123011

Li, R., Hu, L., Hu, C., Wang, Q., Lei, Y., and Zhao, B. (2020). Myricitrin protects against cisplatin-induced kidney injury by eliminating excessive reactive oxygen species. *Int. Urol. Nephrol.* 52, 187–196. doi:10.1007/s11255-019-02334-8

Li, S., Zheng, L., Zhang, J., Liu, X., and Wu, Z. (2021). Inhibition of ferroptosis by up-regulating Nrf2 delayed the progression of diabetic nephropathy. *Free Radic. Biol. Med.* 162, 435–449. doi:10.1016/j.freeradbiomed.2020.10.323

Liang, N.-N., Zhao, Y., Guo, Y.-Y., Zhang, Z.-H., Gao, L., Yu, D.-X., et al. (2022). Mitochondria-derived reactive oxygen species are involved in renal cell ferroptosis during lipopolysaccharide-induced acute kidney injury. *Int. Immunopharmacol.* 107, 108687. doi:10.1016/j.intimp.2022.108687

Liu, J., Kuang, F., Kroemer, G., Klionsky, D. J., Kang, R., and Tang, D. (2020). Autophagy-dependent ferroptosis: machinery and regulation. *Cell. Chem. Biol.* 27, 420–435. doi:10.1016/j.chembiol.2020.02.005

Mancias, J. D., Wang, X., Gygi, S. P., Harper, J. W., and Kimmelman, A. C. (2014). Quantitative proteomics identifies NCOA4 as the cargo receptor mediating ferritinophagy. *Nature* 509, 105–109. doi:10.1038/nature13148

Martin-Cleary, C., Molinero-Casares, L. M., Ortiz, A., and Arce-Obieta, J. M. (2021). Development and internal validation of a prediction model for hospital-acquired acute kidney injury. *Clin. Kidney J.* 14, 309–316. doi:10.1093/ckj/sfz139

Martin-Sanchez, D., Ruiz-Andres, O., Poveda, J., Carrasco, S., Cannata-Ortiz, P., Sanchez-Niño, M. D., et al. (2017). Ferroptosis, but not necroptosis, is important in nephrotoxic folic acid-induced AKI. *J. Am. Soc. Nephrol. JASN* 28, 218–229. doi:10.1681/ASN.2015121376

McSweeney, K. R., Gadanec, L. K., Qaradakhi, T., Ali, B. A., Zulli, A., and Apostolopoulos, V. (2021). Mechanisms of cisplatin-induced acute kidney injury: pathological mechanisms, pharmacological interventions, and genetic mitigations. *Cancers (Basel)* 13, 1572. doi:10.3390/cancers13071572

Miao, R., Fang, X., Zhang, Y., Wei, J., Zhang, Y., and Tian, J. (2023). Iron metabolism and ferroptosis in type 2 diabetes mellitus and complications: mechanisms and therapeutic opportunities. *Cell. Death Dis.* 14, 186. doi:10.1038/s41419-023-05708-0

Nogales, C., Mamdouh, Z. M., List, M., Kiel, C., Casas, A. I., and Schmidt, HHHW (2022). Network pharmacology: curing causal mechanisms instead of treating symptoms. *Trends Pharmacol. Sci.* 43, 136–150. doi:10.1016/j.tips.2021.11.004

Pan, P., Liu, X., Wu, L., Li, X., Wang, K., Wang, X., et al. (2021). TREM-1 promoted apoptosis and inhibited autophagy in LPS-treated HK-2 cells through the NF-κB pathway. *Int. J. Med. Sci.* 18, 8–17. doi:10.7150/ijms.50893

Piñero, J., Saüch, J., Sanz, F., and Furlong, L. I. (2021). The DisGeNET cytoscape app: exploring and visualizing disease genomics data. *Comput. Struct. Biotechnol. J.* 19, 2960–2967. doi:10.1016/j.csbj.2021.05.015

Pope, L. E., and Dixon, S. J. (2023). Regulation of ferroptosis by lipid metabolism. *Trends Cell. Biol.* 33, 1077–1087. doi:10.1016/j.tcb.2023.05.003

Qin, M., Luo, Y., Meng, X.-b., Wang, M., Wang, H.-w., Song, S.-y., et al. (2015). Myricitrin attenuates endothelial cell apoptosis to prevent atherosclerosis: an insight into PI3K/Akt activation and STAT3 signaling pathways. *Vasc. Pharmacol.* 70, 23–34. doi:10.1016/j.vph.2015.03.002

Sanz, A. B., Sanchez-Niño, M. D., Ramos, A. M., and Ortiz, A. (2023). Regulated cell death pathways in kidney disease. *Nat. Rev. Nephrol.* 19, 281–299. doi:10.1038/s41581-023-00694-0

Seibt, T. M., Proneth, B., and Conrad, M. (2019). Role of GPX4 in ferroptosis and its pharmacological implication. *Free Radic. Biol. Med.* 133, 144–152. doi:10.1016/j.freeradbiomed.2018.09.014

Shannon, P., Markiel, A., Ozier, O., Baliga, N. S., Wang, J. T., Ramage, D., et al. (2003). Cytoscape: a software environment for integrated models of biomolecular interaction networks. *Genome Res.* 13, 2498–2504. doi:10.1101/gr.1239303

Shen, Y., Shen, X., Cheng, Y., and Liu, Y. (2020). Myricitrin pretreatment ameliorates mouse liver ischemia reperfusion injury. *Int. Immunopharmacol.* 89, 107005. doi:10.1016/j.intimp.2020.107005

Stelzer, G., Rosen, N., Plaschkes, I., Zimmerman, S., Twik, M., Fishilevich, S., et al. (2016). The GeneCards suite: from gene data mining to disease genome sequence analyses. *Curr. Protoc. Bioinforma.* 54, 1. doi:10.1002/cpbi.5

Szklarczyk, D., Kirsch, R., Koutrouli, M., Nastou, K., Mehryary, F., Hachilif, R., et al. (2023). The STRING database in 2021: customizable protein-protein networks, and functional characterization of user-uploaded gene/measurement sets. *Nucleic Acids Res.* 51, D605–D612. doi:10.1093/nar/gkaa1074

Tang, C., Livingston, M. J., Safirstein, R., and Dong, Z. (2023a). Cisplatin nephrotoxicity: new insights and therapeutic implications. *Nat. Rev. Nephrol.* 19, 53–72. doi:10.1038/s41581-022-00631-7

Tang, D., Chen, M., Huang, X., Zhang, G., Zeng, L., Zhang, G., et al. (2023b). SRplot: a free online platform for data visualization and graphing. *PloS One* 18, e0294236. doi:10.1371/journal.pone.0294236

Tang, M., Chen, Z., Wu, D., and Chen, L. (2018). Ferritinophagy/ferroptosis: iron-related newcomers in human diseases. *J. Cell. Physiol.* 233, 9179–9190. doi:10.1002/jcp.26954

Tang, Y., Li, M., Wang, J., Pan, Y., and Wu, F.-X. (2015). CytoNCA: a cytoscape plugin for centrality analysis and evaluation of protein interaction networks. *Biosystems* 127, 67–72. doi:10.1016/j.biosystems.2014.11.005

Tonnus, W., Meyer, C., Steinebach, C., Belavgeni, A., von Mässenhausen, A., Gonzalez, N. Z., et al. (2021). Dysfunction of the key ferroptosis-surveilling systems hypersensitizes mice to tubular necrosis during acute kidney injury. *Nat. Commun.* 12, 4402. doi:10.1038/s41467-021-24712-6

Wang, J., Wang, Y., Liu, Y., Cai, X., Huang, X., Fu, W., et al. (2022b). Ferroptosis, a new target for treatment of renal injury and fibrosis in a 5/6 nephrectomy-induced CKD rat model. *Cell. Death Discov.* 8, 127. doi:10.1038/s41420-022-00931-8

Wang, X., Shen, Y., Wang, S., Li, S., Zhang, W., Liu, X., et al. (2017). PharmMapper 2017 update: a web server for potential drug target identification with a comprehensive target pharmacophore database. *Nucleic Acids Res.* 45, W356-W360–W360. doi:10.1093/nar/gkx374

Wang, Y., Zhang, M., Bi, R., Su, Y., Quan, F., Lin, Y., et al. (2022a). ACSL4 deficiency confers protection against ferroptosis-mediated acute kidney injury. *Redox Biol.* 51, 102262. doi:10.1016/j.redox.2022.102262

Weng, W., Wang, Q., Wei, C., Man, N., Zhang, K., Wei, Q., et al. (2019). Preparation, characterization, pharmacokinetics and anti-hyperuricemia activity studies of myricitrin-loaded proliposomes. *Int. J. Pharm.* 572, 118735. doi:10.1016/j.ijpharm.2019.118735

Wu, Y., Zhang, Y., Wang, L., Diao, Z., and Liu, W. (2015). The role of autophagy in kidney inflammatory injury via the NF-κB route induced by LPS. *Int. J. Med. Sci.* 12, 655–667. doi:10.7150/ijms.12460

Wu, Z., Deng, J., Zhou, H., Tan, W., Lin, L., and Yang, J. (2022). Programmed cell death in sepsis associated acute kidney injury. *Front. Med.* 9, 883028. doi:10.3389/fmed.2022.883028

Yu, X., Long, Y. C., and Shen, H.-M. (2015). Differential regulatory functions of three classes of phosphatidylinositol and phosphoinositide 3-kinases in autophagy. *Autophagy* 11, 1711–1728. doi:10.1080/15548627.2015.1043076

Zhang, Y., Hu, B., Li, Y., Deng, T., Xu, Y., Lei, J., et al. (2020). Binding of Avibirnavirus VP3 to the PIK3C3-PDPK1 complex inhibits autophagy by activating the AKT-MTOR pathway. *Autophagy* 16, 1697–1710. doi:10.1080/15548627.2019.1704118

Zhou, Y., Zhou, B., Pache, L., Chang, M., Khodabakhshi, A. H., Tanaseichuk, O., et al. (2019). Metascape provides a biologist-oriented resource for the analysis of systems-level datasets. *Nat. Commun.* 10, 1523. doi:10.1038/s41467-019-09234-6

**frontiers** | Frontiers in Pharmacology

# Targeting pyruvate kinase M2 for the treatment of kidney disease

Dan-Qian Chen[1]*†, Jin Han[1,2]†, Hui Liu[1], Kai Feng[1] and Ping Li[3]*

[1]College of Life Sciences, Northwest University, Xi'an, Shaanxi, China, [2]Department of Nephrology, Xi'an Chang'an District Hospital, Xi'an, Shaanxi, China, [3]Beijing Key Lab for Immune-Mediated Inflammatory Diseases, Institute of Clinical Medical Sciences, China-Japan Friendship Hospital, Beijing, China

Pyruvate kinase M2 (PKM2), a rate limiting enzyme in glycolysis, is a cellular regulator that has received extensive attention and regards as a metabolic regulator of cellular metabolism and energy. Kidney is a highly metabolically active organ, and glycolysis is the important energy resource for kidney. The accumulated evidences indicates that the enzymatic activity of PKM2 is disturbed in kidney disease progression and treatment, especially diabetic kidney disease and acute kidney injury. Modulating PKM2 post-translational modification determines its enzymatic activity and nuclear translocation that serves as an important interventional approach to regulate PKM2. Emerging evidences show that PKM2 and its post-translational modification participate in kidney disease progression and treatment through modulating metabolism regulation, podocyte injury, fibroblast activation and proliferation, macrophage polarization, and T cell regulation. Interestingly, PKM2 activators (TEPP-46, DASA-58, mitapivat, and TP-1454) and PKM2 inhibitors (shikonin, alkannin, compound 3k and compound 3h) have exhibited potential therapeutic property in kidney disease, which indicates the pleiotropic effects of PKM2 in kidney. In the future, the deep investigation of PKM2 pleiotropic effects in kidney is urgently needed to determine the therapeutic effect of PKM2 activator/inhibitor to benefit patients. The information in this review highlights that PKM2 functions as a potential biomarker and therapeutic target for kidney diseases.

KEYWORDS

pyruvate kinase M2, diabetic kidney disease, acute kidney injury, post-translational modification, glycolysis

## 1 Introduction

Kidney is a highly metabolically active organ. The metabolic programing in the kidney is different in the distinct regions of kidney. The cortex has high rates of gluconeogenesis and fatty acid oxidation, while the medulla mainly relies on glycolysis, which indicates that oxygen requirement reduces gradually from cortex to medulla in kidney. In the cortex, proximal tubules are highly aerobic and mainly responsible for fluid reabsorption, while in the medulla, distal nephron segments have lower oxygen tension. Under physiological condition, the medulla papilla and distal convoluted tubules has high glycolytic activity (Tang and Wei, 2023), and glycolysis is also the major energy source of podocytes (Brinkkoetter et al., 2019). Even proximal tubular cells have low glycolytic activity, glycolysis plays an important role in maintaining phosphate homeostasis (Zhou et al., 2022; Zhou et al., 2023). Since emerging evidences demonstrated that glycolysis is significantly disturbed during kidney disease (Nakagawa et al., 2020; Gu et al., 2022; Ito et al., 2022), glycolysis is the potential therapeutic target for kidney disease.
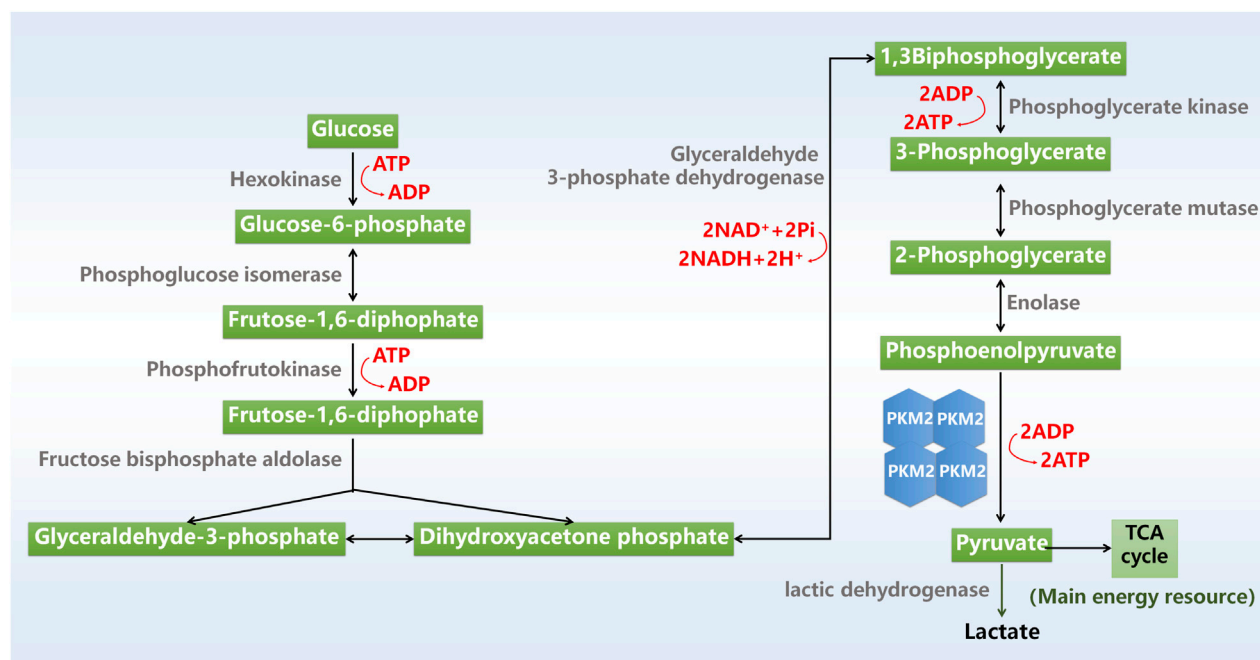
FIGURE 1
Glycolysis process. ADP, adenosine triphosphate; ATP, adenosine triphosphate; NAD, nicotinamide adenine dinucleotide; TCA cycle, tricarboxylic acid cycle.

Glycolysis is a major metabolic process that converts glucose into pyruvate with the production of adenosine triphosphate (ATP) and nicotinamide adenine dinucleotide. Glycolysis is mediated by a series of cellular enzymes, and hexokinase, phosphofructokinase and pyruvate kinase (PK) serves as key rate-limiting enzymes. The final product of glycolysis pyruvate is converted to lactic acid or acetyl-coenzyme A (CoA) for utilization in tricarboxylic acid cycle by mitochondria, which produces energy precursors for oxidative phosphorylation (Figure 1).

PK mediates its substrate phosphoenolpyruvate (PEP) to pyruvate. PK has four different subtypes including L, R, M1, and M2 (Zhang et al., 2019). PKL isoforms are mainly distributed in liver, pancreas and kidney, and PKR is distributed in erythrocytes (Puckett et al., 2021). PKM1 are predominantly expressed in muscle, mature spermatozoa and central nervous system, while PKM2 is expressed in brain, kidney, lung and spleen (Alquraishi et al., 2019; Puckett et al., 2021). PKM2 is the dominant form of PK in kidney tissue (Alquraishi et al., 2019), and a lot of researches have revealed that regulating PKM2 affects kidney disease progression and treatment (Li et al., 2020a; Chen et al., 2023; Xie et al., 2023), highlighting the important role of PKM2 in kidney disease.

In this review, we describe some important research progresses of PKM2 in recent 5 years, from its structure and post-translational modifications to its role in kidney, and introduce the potential intervention effects of PKM2 agonists and antagonists. We further present clinical application of PKM2 in kidney disease, with the goal of highlighting the therapeutic potential of PKM2 in kidney disease. Finally, we discuss the major opportunities and obstacles of PKM2 in kidney disease to facilitate the clinical treatment.

# 2 PKM2 structure and its post-translational modifications

## 2.1 PKM2 structure

Human PKM2 protein consists of 531 amino acids that is subdivided as N (43aa), A (244aa), B (102aa) and C (142aa) domains according to their characteristic features (Figure 2A). The catalytic active site locates at the adjoining region between the A1 and B domains, while the intersubunit contact domain (ISCD) locates at the adjoining region between the A2 and C domains. Nuclear localization signal sequence and the binding site of the allosteric activator (FBP) locate at C domain. The A domain mediates the subunits interaction to form a dimer and functions as the core of monomer, while the formation of the tetramer form of PKM2 is assembled through the binding of two dimers' C-subunits in ISCD.

The enzyme activity of PKM2 is affected by its oligomeric state. PKM2 has four different enzymatic states: an inactive monomer, a nearly inactive dimer, an inactive T state tetramer, and an active R state tetramer (Prakasam et al., 2018; Alquraishi et al., 2019). The tetrameric form has a high PEP affinity, while the dimeric form has a low affinity for PEP and is almost inactive under physiological conditions.

## 2.2 PKM2 post-translational modification

Numerous conserved post-translational modification sites exist in PKM2 protein, including phosphorylation, acetylation,
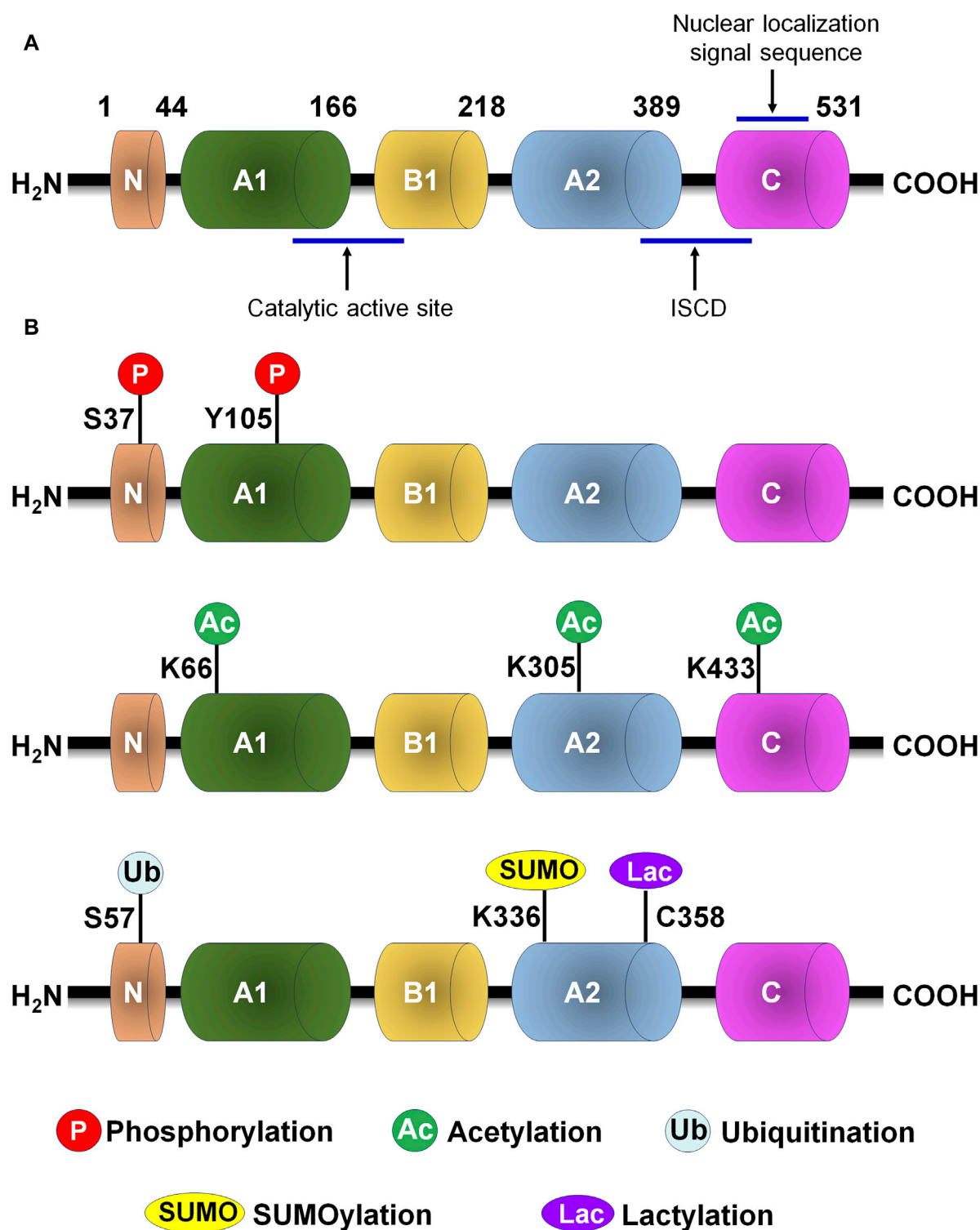
FIGURE 2
PKM2 protein structure and post-translational modification of PKM2. **(A)** PKM2 protein structure. **(B)** The major post-translational modification sites of PKM2, including phosphorylation, acetylation, ubiquitination, SUMOylation and lactylation. C, cysteine; ISCD, intersubunit contact domain; K, lysine; S, serine; Y, tyrosine.

methylation, SUMOylation and oxidation (Figure 2B; Table 1). Post-translational modification of PKM2 determines its structural and functional properties, including oligomeric state, catalytic activity, protein stability, binding of allosteric activators, conditional protein interaction, and subcellular localization, which influences disease progression and therapeutic effect.

The Tyr105 and Ser37 are the common phosphorylation site of PKM2 phosphorylation, which mainly control PKM2 active tetramer

**TABLE 1 Post-translational modifications of PKM2 and their effects in kidney and other disease.**

| Modification | Specific site | Effects | Disease | Proposed function | References |
|---|---|---|---|---|---|
| Phosphorylation | Tyr105 | Increasing glycolysis | Autoimmune diseases | Modulating Th17 cell metabolic reprograming | Chen et al. (2022) |
| | | Facilitating tetramer formation | Nonalcoholic steatohepatotis | Modulating macrophage polarization | Xu et al. (2020) |
| | | Promoting dimer formation | AKI | Promoting mitochondrial fragmentation and suppresses renal tubular injury and cell death | Xie et al. (2023) |
| | | Suppressing glycolysis | Osteoclast | Suppressing osteoclastic bone loss and modulating osteoclast differentiation | Kim et al. (2023) |
| | Ser37 | Decreasing nuclear translocation | Breast cancer | Reducing cell invasion, impairing redox balance, and triggering cancer cell death | Apostolidi et al. (2021) |
| | — | Promoting nuclear translocation | Liver fibrosis | Enhancing glycolysis and M1 polarization | Rao et al. (2022) |
| Acetylation | Lys433 | Promoting detetramerization and nuclear translocation | Aberrant immune responses | Regulating dendritic cell activation, promoting glycolysis and fatty acid synthesis | Jin et al. (2020), Wu et al. (2023) |
| | | Promoting nuclear translocation | Lung cancer | Promoting cell migration | Biyik-Sit et al. (2021) |
| | | Promoting glycolysis | Innate immune cell-mediated inflammation | Inhibiting inflammatory effect | Das Gupta et al. (2020) |
| | | Stabilizing Bcl-2 | Lung ischemia/reperfusion injury | Increasing apoptosis | Zhao et al. (2022b) |
| | Lys305 | Suppressing PKM2 nuclear translocation | Heaptocellular carcinoma | Activating dendritic cell, and facilitating glycolysis and fatty acid synthesis | Wu et al. (2023) |
| | Lys66 | Increasing PKM2 expression | Hematologic diseases | Promoting hematopoietic imbalance | Zhang et al. (2022) |
| SUMOylation | — | Promoting PKM2 phosphorylation and nuclear translocation and reducing enzymatic activity | Rheumatoid arthritis | Reducing glycolysis, aggressive phenotype, and inflammation | Wang et al. (2020) |
| | — | Increasing Ectosomal PKM2 excretion | Heaptocellular carcinoma | Inducing monocyte-to-macrophage differentiation and tumor microenvironment remodeling | Hou et al. (2020) |
| | Lys270 | Promoting dimeric formation and and nuclear translocation | Leukemia | Promoting the blockage of myeloid differentiation | Xia et al. (2021) |
| | Lys336 | Increasing glycolysis | Lung cancer | Enhancing glycolysis and cell proliferation | An et al. (2018) |
| | — | Increasing glycolysis | Heaptocellular carcinoma | Promoting glycolytic reprogramming, growth and metastasis | Zhou et al. (2022a) |
| Ubiquitination | — | Facilitating degradation | Colorectal cancer | Modulating growth and metastasis | Zhao et al. (2022a) |
| | — | | Intrahepatic cholangiocarcinoma | Suppressing tumor cell migration, invasion, and proliferation | Chen et al. (2021) |
| Deubiquitination | Ser57 | Preventing degradation | — | Functioning as a HAUSP binding substrate | Choi et al. (2020) |
| | — | Increasing enzymatic activity | Colorectal cancer | Increasing glucose consumption, lactate production, and cellular ATP production | Yu et al. (2022) |

TABLE 1 (*Continued*) Post-translational modifications of PKM2 and their effects in kidney and other disease.

| Modification | Specific site | Effects | Disease | Proposed function | References |
|---|---|---|---|---|---|
| Lactylation | Lys62 | Promoting dimer formation and inhibiting nuclear translocation | Metabolic adaptation | Modulating metabolic adaptions in pro-inflammatory macrophages | Wang et al. (2022a) |
| O-GlcNAcylation | — | Suppressing enzymatic activity | Tumor cells | Promoting aerobic glycolysis and tumor growth | Singh et al. (2020) |
| S-nitrosylation | — | Suppressing enzymatic activity | AKI | Aggravating kidney injury | Zhou et al. (2023a) |
| Modification by acrolein | Cys358 | Suppressing enzymatic activity | DKD | Facilitating epithelial-mesenchymal transition | Kuo et al. (2023) |

AKI, acute kidney injury; DKD, diabetic kidney disease.

formation and nuclear translocation. CoA binds to PKM2 to block its Tyr105 phosphorylation and nuclear translocation, resulting in reduced glycolysis in Th17 cell. These data indicate that targeting Th17 cell metabolic reprograming via PKM2 functions as a potential therapeutic intervention for Th17 cell-associated autoimmune diseases (Chen et al., 2022). Annexin A5 has the ability to switch metabolic reprogramming from glycolysis to oxidative phosphorylation in activated macrophages by modulating PKM2 post-translational modification. Mechanistically, Annexin A5 directly interacts with PKM2 and further reduces Tyr105 phosphorylation to facilitate tetramer formation in macrophage polarization (Xu et al., 2020). The phosphorylation of PKM2 at Tyr105 promotes its dimer formation and translocation into the mitochondria after treatment with staurosporine or cisplatin in acute kidney injury (AKI). Mitochondrial PKM2 binds myosin heavy chain 9 to facilitate dynamin-related protein 1-mediated mitochondrial fragmentation, and the loss of PKM2 attenuates mitochondrial fragmentation and suppresses renal tubular injury and cell death (Xie et al., 2023). Immunoglobulin superfamily 11 suppresses PKM2 activity through promoting PKM2 phosphorylation at Tyr105 to modulate osteoclast differentiation. Modulating PKM2 activity is considered as a metabolic switch that is necessary for optimal osteoclast maturation (Kim et al., 2023). The phosphorylation of PKM2 at Tyr105 and Ser37 can be activated by an allosteric activator, TEPP-46, results in PKM2 tetramerization and inhibits its nuclear translocation to prevent glycolysis, which reduces CD4+ T cell pathogenicity and inhibits autoimmunity (Angiari et al., 2020). PKM2 phosphorylation involves in aggressive breast cancer cell phenotypes, and PKM2 phosphorylation at Ser37 functions as an effective therapeutic target for triple-negative breast cancer treatment (Apostolidi et al., 2021). Follistatin-like protein 1 (FSTL1), a secreted glycoprotein, could directly bound to PKM2 through its FK domain. FSTL1 facilitates PKM2 phosphorylation and nuclear translocation and inhibits PKM2 ubiquitination to enhance PKM2-dependent glycolysis and M1 polarization to promote liver fibrosis (Rao et al., 2022). In addition, succinate stimulates PKM2 dimerization that further translocate into the nucleus and mitochondria to accelerate fibroblast activation and apoptosis resistance in heart (Wang et al., 2023).

The acetylation of PKM2 occurs in Lys433, Lys305, and Lys66, and this process can be reversed by the deacetylase. JNK induces the acetylation of PKM2 at Lys433, resulting in PKM2 detetramerization and nuclear translocation during dendritic cell activation through modulating glycolysis and fatty acid synthesis (Jin et al., 2020).

Testes-specific protease 50 (TSP50) maintains the low activity of PKM2 to control aerobic glycolysis in heaptocellular carcinoma (HCC) cells. Mechanistically, TSP50 enhances the acetylation of PKM2 at Lys433, while the acetyl-insensitive mutation of PKM2 K433R obviously counteracts TSP50-induced aerobic glycolysis (Gao et al., 2021). Phosphoserine aminotransferase 1 (PSAT1) accumulates nuclear PKM2 translocation to facilitate lung cancer cell migration, while the acetyl-mimetic mutant of PKM2 (K433Q) affected PSAT1-mediated cell migration (Biyik-Sit et al., 2021). Class IIa histone deacetylase HDAC7 mediates the deacetylation of PKM2 at Lys433 to aggravate its proinflammatory property (Das Gupta et al., 2020). Sirt3 mediates the deacetylation of PKM2 at Lys433 in A549 cells, which process significantly alleviates apoptosis against lung ischemia/reperfusion injury (Zhao et al., 2022). Phosphoglycerate dehydrogenase (PHGDH) increases the stability and activity of PKM2 through interacting with PKM2 to facilitate Lys433 acetylation and prevent Lys305 acetylation, which leading to PKM2 nuclear translocation and ultimately prevents premature senescence (Wu et al., 2023). A common environmental carcinogen, 1,4-benzoquinone, results in the acetylation of PKM2 at Lys66 that contributes to the upregulation of PKM2. However, the acetyltransferase general control non-derepressible 5 could reverse the acetylation of PKM2 at Lys66 (Zhang et al., 2022). Besides, Sirt2 mediates PKM2 deacetylation, which is the potential therapeutic approach for psoriasis therapy (Hao et al., 2021).

The SUMOylation often occurs in lysine residue in PKM2. Small ubiquitin-like modifier-activating (SUMO-activating) enzyme 1/ubiquitin like modifier activating enzyme 2 mediates the SUMOylation of PKM2 that facilitates PKM2 phosphorylation and nuclear translocation and reduces enzymatic activity (Wang et al., 2020). HCC-derived ectosomal PKM2 induced metabolic reprogramming in monocytes to accelerate HCC progression. In HCC cells, the SUMOylation of PKM2 facilitates its plasma membrane targeting and subsequent ectosomal excretion. Ectosomal PKM2 is clearly detected in the plasma of HCC patients and functions as a potential diagnostic marker for HCC (Hou et al., 2020). The SUMOylation of PKM2 at Lys270 induces PKM2 from tetrameric to dimeric formation, and nuclear translocation. The replacement of wild type PKM2 to a SUMOylation-deficient mutant (K270R) weakens PKM2 effect on RUNX1 in leukemia cells (Xia et al., 2021). The knockdown of small ubiquitin-like modifier 1 (SUMO1) causes the downregulation of

**FIGURE 3**
The role of PKM2 in kidney. In tubular epithelial cell, podocyte, fibroblast, macrophage and T cell, PKM2 participate in kidney disease and treatment. Drp-1, dynamin-related protein-1; ERK, extracellular regulated protein kinase; HIF-1α, hypoxia inducible factor-1; HSP90, heat shock protein 90; ICAM-1, intercellular cell adhesion molecule-1; IFN-γ, interferon gamma; IL-17A, interleukin-17A; MYH9, myosin heavy chain 9; NF-κB, nuclear factor kappa-B; NLRP3, NOD-like receptor thermal protein domain associated protein 3; PCNA, proliferating cell nuclear antigen; STAT3, signal transducer and activator of transcription 3; TNF-α, tumor necrosis factor-α; USP25, ubiquitin specific peptidase 25; WT-1, Wilm's tumor-1.

PKM2 protein in A549 cells. SUMO1 directly mediates the SUMO1 modification of PKM2 at Lys336 that enhances glycolysis and cell proliferation (An et al., 2018). The activated guanosine triphosphate binding protein 4 (GTPBP4) promotes PKM2 SUMOylation via facilitating SUMO1 protein activation and functioning as a linker between SUMO1 and PKM2 protein, which process accelerates aerobic glycolysis in HCC (Zhou et al., 2022).

The ubiquitination and deubiquitination of PKM2 are reported in plenty of researches. DExD-box helicase 39B (DDX39B) directly

interacts with PKM2 and stabilizes PKM2 by competitively suppressing STIP1 homology and U-box-containing protein 1 (STUB1)-mediated PKM2 ubiquitination and degradation. DDX39B accelerates the nuclear translocation of PKM2 to promote the activation of oncogenes and glycolysis-related genes, which process is independent of ERK1/2-mediated phosphorylation of PKM2 at Ser37 (Zhao et al., 2022). CNRIP1 overexpression activates Parkin (an E3 ubiquitin ligase), and triggers the protein degradation of PKM2 in intrahepatic cholangiocarcinoma cells (Chen et al., 2021). In addition, the deubiquitinating enzyme,

herpesvirus-associated ubiquitin-specific protease (HAUSP), interacts with PKM2 at Ser57 to deubiquitinate PKM2, while HAUSP knockdown increases PKM2 ubiquitination (Choi et al., 2020). OTUB2, an OTU deubiquitinase, directly interacts with PKM2 and suppresses its ubiquitination via weakening the interaction of PKM2 and Parkin to increase PKM2 activity and glycolysis in colorectal cancer (Yu et al., 2022).

Additionally, the lactylation of PKM2 is found in macrophages, and Lys62 site is responsible for PKM2 lactylation to inhibit inflammatory metabolic adaptation. Lactate facilitates PKM2 lactylation that delays the transition from tetramer to dimer, and increase its enzymatic activity and suppress nuclear distribution (Wang et al., 2022). O-GlcNAc transferase mediates PKM2 O-GlcNAcylation to suppress PKM2 catalytic activity that increases aerobic glycolysis and tumor growth (Singh et al., 2020). The S-nitrosylation of PKM2 by JSD26 intraperitoneal injection protects against AKI in mice (Zhou et al., 2023). The modification at Cys358 by acrolein leads to PKM2 inactivation and aberrant glycolysis to promote renal fibrosis progression in high-fat diet-streptozotocin-induced diabetic kidney disease (DKD) mice. Treatment with acrolein scavengers (hydralazine and carnosine) obviously attenuates PKM2 activity and renal fibrosis (Kuo et al., 2023). Inhibiting neddylation modification by MLN4924 treatment induces tetramerization and activates PKM2 to increase glycolysis against cancer cell growth (Zhou et al., 2019). These data demonstrate that targeting post-translational modification of PKM2 is a promising therapeutic approach to treat renal and various diseases.

# 3 The role of PKM2 in kidney disease

## 3.1 Metabolism regulation

PKM2 plays a vital role in regulating the glycolytic reprogramming in multiple renal cells and various kidney diseases (Figure 3). In tubular epithelial cell, the phosphorylation of PKM2 at Tyr105 promotes its dimer formation and translocation into the mitochondria after treatment with staurosporine or cisplatin in AKI. Hsp90 triggers the activation of PKM2-Akt signaling pathway to exhibit antiapoptotic effect against heat-stress injury in AKI (Chen et al., 2020). Mitochondrial PKM2 binds myosin heavy chain 9 to facilitate dynamin-related protein 1-mediated mitochondrial fragmentation, and the loss of PKM2 attenuates mitochondrial fragmentation and suppresses renal tubular injury and cell death by cisplatin (Xie et al., 2023). PKM2 interacts with mitofusin 2 to enhance mitochondrial fusion and oxidative phosphorylation, and suppress glycolysis (Li et al., 2019). Metabolomic study reveals that in cisplatin-induced normal kidney tubular epithelial NRK-52E cells, the excretion of PKM2 is significantly elevated in the media (Kim et al., 2022). PKM2 serves as the direct target of miR-144-5p. The long non-coding RNA (lncRNA) Opa-interacting protein 5 antisense RNA 1 targets miR-144-5p/PKM2 axis to attenuate the apoptosis of renal epithelial cells induced by cisplatin (Chang et al., 2022). Additionally, the activation of ERK modulated glycolysis and resulted in the reduced reserve respiratory capacity during cisplatin treatment (Suman et al., 2024).

PKM2 is significantly increased in glomeruli of patients with DKD and corelated with estimated glomerular filtration rate, which involves in preserving kidney function. The elevated PKM2 in circulation functions as biomarkers in DKD (Gordin et al., 2019). PKM2 protein is highly detected in the urine of DKD patients but not found in the urine of normal subjects. PKM2 is identified as the new biomarker for the early diagnosis of DKD (Park et al., 2023). DKD process is accompanied with Sirt3 suppression and PKM2 dimer formation. Sirt3 deficiency-induced abnormal glycolysis facilitates renal fibrosis (Srivastava et al., 2018). Sodium glucose cotransporter 2 inhibitor, empagliflozin, induces PKM2 dimer formation to normalize aberrant glycolysis, and eventually exhibits renal protection against DKD in proximal tubules (Li et al., 2020a). Besides, in the present of aminylation, tissue transglutaminase modulates glycolysis in normal and indoxyl sulfate-induced endothelial cell injury via activating PKM2 (Lin et al., 2023).

## 3.2 Podocyte injury

PKM2 is identified as a vital metabolic regulator for podocyte development (Figure 3). PKM2 is downregulated in podocytes from kidney biopsies of patients with DKD and hypertensive nephropathy (Luo et al., 2022; Chen et al., 2023). The injured glycolysis in podocytes enhances ornithine catabolism under diabetic conditions, and podocyte-specific loss of PKM2 aggravates ornithine catabolism to modulate cytoskeletal remodeling in podocytes in DKD (Luo et al., 2022). Podocyte-specific deletion of PKM2 in mice promotes angiotensin II-induced glomerular and podocyte injury with foot process effacement and proteinuria. Mechanistically, angiotensin II-induced glycolysis impairment aggravates an insufficient energy supply to the foot process and leads to podocyte injury (Chen et al., 2023). Podocyte-specific overexpression of PKM2 exhibits potent therapeutic effects on albumin/creatinine ratio, mesangial expansion, basement membrane thickness, and podocyte foot process effacement in streptozotocin-induced DKD mice (Fu et al., 2022). Podocyte-specific deletion of Smad4 alleviates DKD. Mechanistically, hyperglycaemia causes Smad4 localization to mitochondria in podocytes, and Smad4 directly binds to PKM2 and reduces the formation of active tetrameric form to decrease glycolysis (Li et al., 2020b).

In adriamycin-induced mice, podocyte-specific deletion of PKM2 exhibits limited energy metabolism that induces cell differentiation defects. Podocyte-specific knockout of PKM2 in mice worsens albuminuria and podocyte injury in adriamycin-induced mice (Yuan et al., 2020). Metadherin triggers the deaggregation of PKM2 tetramers and facilitates PKM2 monomers to enter the nucleus in podocyte to accelerate podocyte injury and proteinuria. Podocyte-specific knockout of metadherin attenuates proteinuria, podocyte injury and glomerulosclerosis after advanced oxidation protein products challenge or in adriamycin-induced mice (Chen et al., 2023).

In AKI, podocyte-specific deletion of PKM2 alleviates LPS-induced inflammation and apoptosis via the activation of β-catenin and the loss of Wilms' Tumor 1 and nephrin. These data reveals PKM2 as a promising therapeutic target for AKI (Alquraishi et al., 2022). The elevated PKM2 and increased glycolysis is detected

during renal fibrosis. These contribute to hypoxic and acidic environment, and eventually suppress podocyte proliferation and differentiation and accelerate renal interstitial fibrosis. These results elicit that increased glycolysis-induced energy metabolism recodification influences podocyte number and function and aggravates fibrosis (Li et al., 2018).

PKM2 also participate in podocyte death. Podocyte-specific deletion of PKM2 contributes to glomerular and podocyte injury that involves in reduced glycolysis, cytoskeletal remodeling and podocyte apoptosis (Chen et al., 2023). The inhibition of dihydroxyacetone phosphate exhibits protective property on podocyte pyroptosis via downregulating PKM2 expression (Zhang et al., 2023).

## 3.3 Fibroblast activation and proliferation

Fibroblast-specific loss of PKM2 inhibits fibroblast proliferation and triggers tubular epithelial cell death during AKI process (Figure 3). PKM2-mediated fibroblast proliferation activates pro-survival signals to reduce tubular cell death (Ye et al., 2021). Overexpression of PKM2 triggers fibroblast activation and renal interstitial fibrosis that is accompanied by elevated glycometabolism, which elicits the important role of metabolic reprogramming in renal interstitial fibrosis (Yin et al., 2018). The knock-out of a multifunctional E3 ubiquitin-protein ligase, WWP2, facilitates myofibroblast proliferation and suppresses its activation. The loss of WWP2 sacrifices glycolysis and boosts mitochondrial respiration to activate fatty acid oxidation and the pentose phosphate pathway, which is the promising therapeutic target for renal fibrosis (Chen et al., 2024).

## 3.4 Macrophage polarization

Ubiquitin-specific protease 25 (USP25)-PKM2-aerobic glycolysis axis positively modulates M1-like polarization and accelerates ischemic AKI in mice, indicating potential therapeutic targets for AKI treatment (Figure 3). Mechanistically, USP25 controls aerobic glycolysis and lactate production during M1-like polarization via PKM2 (Yang et al., 2023). Besides, the regulation of PKM2 modulates inflammation by phosphorylating STAT3 and NF-κB in DKD that delays the differentiation of macrophages to M1 cells, and the downregulation of phosphorylated PKM2 is beneficial for DKD treatment (Li et al., 2020).

## 3.5 T cell regulation

Even few researches report the effect of PKM2 on T cell regulation in the kidney, the regulatory role of PKM2 on T cell regulation is confirmed in other tissues (Figure 3). PKM2 participates in T cell biology, and the upregulation, phosphorylation and nuclear accumulation of PKM2 is observed in CD4$^+$ T cells. The activation of PKM2 by TEPP-46 treatment restricts T helper 17 and T helper 1 cells development and alleviates experimental autoimmune encephalomyelitis (Angiari et al., 2020).

PRAK-Nrf2-mediated antioxidant signaling is a metabolic checkpoint that controls Th17 cell glycolysis and differentiation via restoring PKM2 phosphorylation to exhibit potent Th17 cell antitumor immunity (Zhao et al., 2023). Specific deletion of PKM2 in inflammatory hepatic CXCR3$^+$ Th17 cells has ability to reverse inflammatory vigor and non-alcoholic fatty liver disease severity (Moreno-Fernandez et al., 2021). PKM2 is increased in infiltrated T lymphocytes of vascular lesions. Extracellular vesicles (EVs) from PKM2-activated T lymphocyte triggers abdominal aortic aneurysm progression through facilitating macrophage redox imbalance and migration (Dang et al., 2022). These data confirm the regulatory effect of PKM2 on T cell.

# 4 The activators and inhibitors of PKM2 in kidney disease

## 4.1 Activators

TEPP-46, a small-molecule PKM2 activator, leads to PKM2 tetramer formation through enhancing PKM2 subunit interactions and increasing PKM2 enzymatic activity (Table 2). Several studies reveal the protective role of TEPP-46 in DKD. The PKM2 activator TEPP-46 increases the glycolytic activity and lactate production in the kidney against DKD, suggesting targeting PKM2 as a promising therapeutic target for DKD treatment (Bertelsen et al., 2021). PKM2 activator TEPP-46 that promotes tetramerization enhances the interaction of endocytic trafficking through the versatile networks of Hsp70s and rewrites the crosstalk of EGFR signal transduction circuits and metabolic stress to promote resilience in DKD (Wang et al., 2022). PKM2 activation by TEPP-46 treatment improves tubular phenotype through suppressing the epithelial-mesenchymal transition program and normalizing aberrant glycolysis in high glucose-induced renal tubular epithelial cell and DKD model (Liu et al., 2021).

DASA-58 is able to induce PKM2 activation by promoting PKM2 tetramerization and reducing lactate secretion (Table 2). Pharmacological activation of PKM2 by DASA-58 partially counters glycolysis and inflammation during liver fibrosis process (Rao et al., 2022). DASA-58 treatment facilitates the proliferation of vascular resident endothelial progenitor cell and enhances PKM2 activity via promoting glycolysis and mitochondrial fusion (Ren et al., 2020). Besides, treatment with TEPP-46 or DASA-58 obviously hinders IL-17-producing T helper cell 17 development against multiple sclerosis (Seki et al., 2020). Even if few studies report the effect of DASA-58 in kidney disease, the above-mentioned data provide a promising prospect for DASA-58 in kidney disease treatment.

Mitapivat, also called AG-348, is the first-line oral small molecule allosteric activator of PK (Table 2). Several clinical trials have confirmed the beneficial role of mitapivat in pyruvate kinase deficiency (PKD) treatment, and mitapivat has been granted orphan drug designation by the FDA for PKD. A phase 3, randomized, placebo-controlled clinical trial demonstrates that mitapivat substantially elevates hemoglobin level, reduces hemolysis, and improves patient-reported outcomes in patients with PKD (Al-Samkari et al., 2022). Another multicentre, open-label, single-

TABLE 2 The roles of PKM2 activators and inhibitors in kidney and other diseases.

| Compound | Effects | Disease | Proposed function | References |
|---|---|---|---|---|
| Activators | | | | |
| TEPP-46 | Promoting PKM2 tetramer formation and increasing PKM2 enzymatic activity | DKD | Increasing the glycolytic activity and lactate production | Bertelsen et al. (2021) |
| | | DKD | Promoting tetramerization enhances the interaction of endocytic trafficking | Wang et al. (2022b) |
| | | DKD | Suppressing the epithelial-mesenchymal transition program and normalizing aberrant glycolysis | Liu et al. (2021) |
| DASA-58 | Promoting PKM2 tetramerization and reducing lactate secretion | Liver fibrosis | Suppressing glycolysis and inflammation | Rao et al. (2022) |
| | | Angiogenesis | Promoting glycolysis and mitochondrial fusion | Ren et al. (2020) |
| | | Multiple sclerosis | Suppressing IL-17-producing T helper cell 17 development | Seki et al. (2020) |
| Mitapivat | Promoting PKM2 tetramer formation and increasing PKM2 enzymatic activity | PKD | Restoring activity of the red blood cell PK enzyme | Al-Samkari et al. (2022), Glenthøj et al. (2022) |
| | | α-Thalassaemia and β-thalassaemia | Increasing haemoglobin concentration | Kuo et al. (2022) |
| TP-1454 | Promoting PKM2 tetramer formation and increasing PKM2 enzymatic activity | Advanced solid tumors | Modulating cellular metabolism and enhancing response to checkpoint inhibitors | Weagel et al. (2022) |
| Celastrol | Altering the spatial conformation to reduce the enzyme activity | Non-alcoholic fatty liver disease | Suppressing lipid accumulation, inflammation and fibrosis | Fan et al. (2022) |
| Modified Hu-lu-ba-wan | Increasing PKM2 protein expression | DKD | Facilitateing mitochondrial dynamic homeostasis | Gong et al. (2023) |
| Inhibitors | | | | |
| Shikonin | Decreasing PKM2 enzymatic activity | AKI | Decreasing the histopathological symptoms and apoptosis | Wu et al. (2021) |
| | | AKI | Inhibiting renal oxidative stress, inflammatory and tubular epithelial cell apoptosis | Peng et al. (2022) |
| | | Unilateral ureteral obstruction | Inhibiting renal fibrosis | Wei et al. (2019) |
| | | NRK-52E cells | Modulating mitochondrial membrane potential | Tong et al. (2018) |
| | | DKD | Inhibiting renal oxidative stress and inflammation | Balaha et al. (2023), Zhu et al. (2023) |
| | | Liver fibrosis | Modulating PKM2-mediated aerobic glycolysis | Zheng et al. (2020) |
| Compound 3k | Triggering PKM2 tetramer disruption | Idiopathic pulmonary fibrosis | Stabilizing TGF-β1 receptor I and enhancing TGF-β1 signaling | Gao et al. (2022) |
| | | Ovarian cancer | Inhibiting glycolysis and reprograms metabolism | Park et al. (2021) |
| Compound 3h | | Prostate cancer | Attenuating apoptotic and autophagic cell death | Jiang et al. (2022) |
| Microcystin-RR | Inhibiting PKM2 expression and phosphorylation | Unilateral ureteral obstruction | Restoring the inhibited expression of MMP-7 and MMP-13, and reducing the upregulated expression of MMP-9 | Ren et al. (2022) |
| Dendropanax morbifera | Reducing PKM2 expression | DKD | Suppressing oxidative stress and inflammation | Sachan et al. (2020) |

(Continued on following page)

TABLE 2 (*Continued*) The roles of PKM2 activators and inhibitors in kidney and other diseases.

| Compound | Effects | Disease | Proposed function | References |
|---|---|---|---|---|
| Huangqi-Danshen decoction | Reducing PKM2 expression | Adenine-induced CKD | Reshaping glucose metabolism profiles | Huang et al. (2023) |
| Qian Yang Yu Yin granule | Reducing PKM2 expression | Hypertensive nephropathy | Modulating metabolic reprogramming | Qian et al. (2021) |
| Tianshu capsule | Reducing serum PKM2 expression | Spontaneous hypertension | Normalizing energy metabolism | Gao et al. (2019) |
| LncRNA ARAP1 | Promoting tetrameric PKM2 formation | DKD | Normalizing aberrant glycolysis and fibrosis | Li et al. (2023a) |

AKI, acute kidney injury; CKD, chronic kidney disease; DKD, diabetic kidney disease.

arm, phase 3 trial shows that mitapivat functions as a novel therapy and becomes first disease-modifying agent for PKD that alleviates transfusion burden in adult patients who accepts regular transfusions (Glenthøj et al., 2022). Besides, an open-label, multicentre, phase 2 study reveals that mitapivat also exhibits potent therapeutic effect against α-thalassaemia and β-thalassaemia, and haemoglobin concentration significantly increases after treatment (Kuo et al., 2022).

TP-1454, derived from SGI-9380, enhances the bind of two dimer PKM2 as a glue of monomer PKM2 (Xu et al., 2014). TP-1454 is a potent PKM2 activator and has enter clinical trials as the first oral PKM2 activator for advanced solid tumors treatment (Weagel et al., 2022). In addition, PKM2 is identified as a major celastrol-bound protein, and celastrol binds to the residue Cys31 and further alters the spatial conformation to reduce the enzyme activity of PKM2 in hepatic macrophages against non-alcoholic fatty liver disease (Fan et al., 2022).

PKM2 is also the therapeutic target of traditional medicine against kidney disease. Modified Hu-lu-ba-wan exhibits beneficial effect on DKD patients and animal model through facilitating mitochondrial dynamic homeostasis. The one of its components, berberine, has a high affinity with PKM2, and prevent apoptosis by enhancing PKM2-mediated mitochondrial dynamic homeostasis (Gong et al., 2023).

## 4.2 Inhibitors

Shikonin and alkannin, enantiomeric pair of pigments derived from *Lithospermum erythrorhizon* roots, are identified as potent and highly selective PKM2 inhibitor (Table 2). The protective role of shikonin has been confirmed in kidney diseases (Wei et al., 2019; Wu et al., 2021; Peng et al., 2022). The inhibition of PKM2 by shikonin notably suppresses the expression of HIF-1α and apoptosis-related factors such as BNIP3, Bax, and caspase-3, while the inhibition of PKM2 by shikonin significantly improves the histopathological symptoms of LPS-induced AKI. The inhibition of PKM2 by shikonin significantly ameliorates the histopathological symptoms in LPS-induced AKI mice and inhibits apoptosis via downregulating BNIP3, Bax, and caspase-3 (Wu et al., 2021). Shikonin inhibits renal oxidative stress, inflammatory and tubular epithelial cell apoptosis through regulating NOX4/PTEN/AKT pathway against sepsis-induced AKI rat model (Peng et al., 2022). The blockade of glycolysis by shikonin obviously attenuates renal fibrosis through modulating PKM2 in unilateral ureteral obstruction mice (Wei et al.,

2019). Shikonin effectively controls mitochondrial membrane potential to exhibit renal protection in high glucose-induced NRK-52E cells (Tong et al., 2018). Shikonin suppresses DKD progression and gentamicin-induced renal injury through inhibiting renal oxidative stress and inflammation (Balaha et al., 2023; Zhu et al., 2023). In addition, PKM2 antagonist (shikonin) and its allosteric agent (TEPP-46) substantially attenuates liver fibrosis by modulating PKM2-mediated aerobic glycolysis (Zheng et al., 2020). As for alkannin, few studies investigate its renal protection, but alkannin exhibits potent therapeutic property on Alzheimer's disease and anti-cancer treatment (Chang et al., 2020; Hosoi et al., 2023).

The selectivity of compound 3k is higher than shikonin for PKM2 (Gao et al., 2022). Compound 3k triggers PKM2 tetramer disruption to delay fibrosis progression in idiopathic pulmonary fibrosis (Gao et al., 2022). Treatment with compound 3k hinders glycolysis and reprograms metabolism against ovarian cancer (Park et al., 2021). Besides, comparing with compound 3k, compound 3h has a higher affinity with PKM2. Treatment with compound 3h hinders glycolytic pathways to attenuate apoptotic and autophagic cell death against prostate cancer cells (Jiang et al., 2022).

PKM2 severs as a potential therapeutic target for natural product and antisense against kidney diseases. Microcystin-RR directly binds to PKM2 and suppresses phosphorylated PKM2 at Lys105 to impair PKM2-HIF-1α pathway against chronic kidney disease (CKD) (Ren et al., 2022). The aquatic extract of *Dendropanax morbifera* alleviates PKM2 expression against DKD and renal fibrosis via ameliorating oxidative stress and inflammation (Sachan et al., 2020). Huangqi-Danshen decoction, a Chinese herbal preparation, attenuates PKM2 expression to reshape glucose metabolism profiles against adenine-induced CKD (Huang et al., 2023). Qian Yang Yu Yin granule suppresses PKM2 expression in hypertensive nephropathy rat model and modulates metabolic reprogramming via HIF-1α/PKM2 positive feedback loop (Qian et al., 2021). Tianshu capsule alleviates serum PKM2 expression to normalize energy metabolism in spontaneously hypertensive rat model (Gao et al., 2019). Besides, natural antisense lncRNA ARAP1 knock-down suppresses dimeric PKM2 expression and restores tetrameric PKM2 formation to normalize aberrant glycolysis and fibrosis in DKD models (Li et al., 2023).

## 5 Conclusion and perspectives

Glycolysis is the key energy resource for kidney, and PKM2 plays a vital role in glycolysis. PKM2 is not only the rate-limiting enzyme that

mediates PEP to pyruvate, also functions as a co-transcription factor that triggers the upregulation of glycolysis-related genes including MYC, SLC2A1, LDHA and PDK1 (Li et al., 2023). PKM2 monomer has 531 amino acids and owns four domains (N, A, B and C). The inactive monomer, nearly inactive dimer, inactive T state tetramer, and active R state tetramer are four states of PKM2 protein. The post-translational modification of PKM2 modulates its enzymatic activity and nuclear localization. PKM2 phosphorylation at Tyr105 and Ser37 inhibits active tetramer formation and induces nuclear translocation, and the acetylation of PKM2 at Lys433, Lys305 and Lys66 also influences its enzymatic activity and nuclear translocation. The SUMOylation at Lys270 triggers PKM2 dimeric formation and nuclear translocation, while the SUMOylation at Lys336 enhances PKM2 enzymatic activity. The deubiquitination of PKM2 at Ser57 by HAUSP protects PKM2 from degradation. Besides, the lactylation and the modification at Cys358 by acrolein also affects PKM2 enzymatic activity to regulate glycolysis. These data indicates that the post-translational modification of PKM2 is responsible for PKM2 enzymatic activity and nuclear translocation that is the promising therapeutic target.

Emerging evidences show that the aberrant glycolysis contributes to kidney disease progression accompanying PKM2 dysfunction. PKM2 participates in kidney disease and treatment through modulating metabolism regulation, podocyte injury, fibroblast activation and proliferation, macrophage polarization, and T cell regulation. Notably, the expression and enzymatic activity of PKM2 is substantially disturbed in kidney and targeting PKM2 has been proved a promising therapeutic target, especially in DKD and AKI that is consistent with previous study (Rabelink and Carmeliet, 2018). Notably, DKD and AKI accompany with the accumulation of glycolytic intermediate products (Rabelink and Carmeliet, 2018). The obvious elevation of PKM2 is observed in glomeruli of patients with DKD (Gordin et al., 2019), and the knock-down of PKM2 in podocyte aggravates glomerular injury and albuminuria in DKD mice (Qi et al., 2017). In AKI, PKM2 severs as a novel biomarker for early detection (Cheon et al., 2016), and the deletion of PKM2 in several kidney cells is beneficial in AKI. The deletion of PKM2 in podocyte attenuates AKI, and the deletion of PKM2 in fibroblast triggers fibroblast activation and AKI progression. Besides, PKM2 also controls macrophage polarization to participate in AKI. The possible reason that PKM2 is more important in DKD and AKI than other kidney diseases is that DKD and AKI suffer aberrant glycolysis and energy metabolism more during their progression. These results reveal that targeting PKM2 is emerging as a promising therapeutic approach for DKD and AKI treatment.

Interestingly, both PKM2 activator TEPP-46 and PKM2 inhibitor shikonin exhibits protective effect on kidney diseases, suggesting the importance of PKM2 during kidney disease progression. Importantly, these results remind us that the deep investigation of PKM2 pleiotropic effects are urgent before the application in clinical. The novel positron emission tomography [$^{18}$F]DASA-23 helps to determine PKM2 level in human to visualize intracranial malignancies that is a useful tool to explore of PKM2 pleiotropic effects in kidney (Beinat et al., 2020). Both the regulation of PKM2 post-translational modification and pharmacological modulation of PKM2 is the promising approach to control PKM2 activity and kidney disease progression. PKM2 activator (TEPP-46, DASA-58, mitapivat and TP-1454) and PKM2 inhibitor (shikonin, alkannin, compound 3k and

compound 3h) have exhibited potential therapeutic property in kidney disease, which provides candidates for kidney disease in further pre-clinical and clinical investigation. Another limitation that hinders PKM2 as a therapeutic target is restricted clinical trials in kidney disease and other disease. Clinical trials demonstrates that PKM2 is the potential biomarker in inflammatory bowel disease and Crohn's disease (Almousa et al., 2018), and elevated plasma PKM2 is associated with poorer prognosis of pancreatic and peri-ampullary cancer in clinical (Bandara et al., 2018). The increased PKM2 expression are more frequent in cirrhotic liver than non-cirrhotic liver, and is associated with poor survival rates in both cirrhotic liver and non-cirrhotic liver (Liu et al., 2017). Although the clinical and related renal studies referring PKM2 are limited, the promising potential of PKM2 has been verified, which provides the candidates for kidney disease treatment.

Overall, PKM2 is the promising therapeutic target for kidney disease. The deep investigation of PKM2 pleiotropic effects in kidney and clinical trial are urgently needed to verify the therapeutic effect of PKM2 activator/inhibitor to benefit patients.

## Author contributions

D-QC: Funding acquisition, Writing-original draft, Writing-review and editing. JH: Writing-review and editing. HL: Writing-review and editing. KF: Writing-review and editing. PL: Writing-review and editing.

## Funding

## Conflict of interest

The authors declare that the research was conducted in the absence of any commercial or financial relationships that could be construed as a potential conflict of interest.

## Publisher's note

All claims expressed in this article are solely those of the authors and do not necessarily represent those of their affiliated organizations, or those of the publisher, the editors and the reviewers. Any product that may be evaluated in this article, or claim that may be made by its manufacturer, is not guaranteed or endorsed by the publisher.

# References

Almousa, A. A., Morris, M., Fowler, S., Jones, J., and Alcorn, J. (2018). Elevation of serum pyruvate kinase M2 (PKM2) in IBD and its relationship to IBD indices. *Clin. Biochem.* 53, 19–24. doi:10.1016/j.clinbiochem.2017.12.007

Alquraishi, M., Chahed, S., Alani, D., Puckett, D. L., Dowker, P. D., Hubbard, K., et al. (2022). Podocyte specific deletion of PKM2 ameliorates LPS-induced podocyte injury through beta-catenin. *Cell Commun.* 20 (1), 76. doi:10.1186/s12964-022-00884-6

Alquraishi, M., Puckett, D. L., Alani, D. S., Humidat, A. S., Frankel, V. D., Donohoe, D. R., et al. (2019). Pyruvate kinase M2: a simple molecule with complex functions. *Free Radic. Biol. Med.* 143, 176–192. doi:10.1016/j.freeradbiomed.2019.08.007

Al-Samkari, H., Galactéros, F., Glenthøj, A., Rothman, J. A., Andres, O., Grace, R. F., et al. (2022). Mitapivat versus placebo for pyruvate kinase deficiency. *N. Engl. J. Med.* 386 (15), 1432–1442. doi:10.1056/NEJMoa2116634

An, S., Huang, L., Miao, P., Shi, L., Shen, M., Zhao, X., et al. (2018). Small ubiquitin-like modifier 1 modification of pyruvate kinase M2 promotes aerobic glycolysis and cell proliferation in A549 human lung cancer cells. *Onco. Targets Ther.* 11, 2097–2109. doi:10.2147/ott.S156918

Angiari, S., Runtsch, M. C., Sutton, C. E., Palsson-McDermott, E. M., Kelly, B., Rana, N., et al. (2020). Pharmacological activation of pyruvate kinase M2 Inhibits CD4(+) T cell pathogenicity and suppresses autoimmunity. *Cell Metab.* 31 (2), 391–405. doi:10.1016/j.cmet.2019.10.015

Apostolidi, M., Vathiotis, I. A., Muthusamy, V., Gaule, P., Gassaway, B. M., Rimm, D. L., et al. (2021). Targeting pyruvate kinase M2 Phosphorylation reverses aggressive cancer phenotypes. *Cancer Res.* 81 (16), 4346–4359. doi:10.1158/0008-5472.Can-20-4190

Balaha, M. F., Alamer, A. A., Eisa, A. A., and Aljohani, H. M. (2023). Shikonin alleviates gentamicin-induced renal injury in rats by targeting renal endocytosis, SIRT1/Nrf2/HO-1, TLR-4/NF-κB/MAPK, and PI3K/Akt cascades. *Antibiotics* 12 (5), 826. doi:10.3390/antibiotics12050826

Bandara, I. A., Baltatzis, M., Sanyal, S., and Siriwardena, A. K. (2018). Evaluation of tumor M2-pyruvate kinase (Tumor M2-PK) as a biomarker for pancreatic cancer. *World J. Surg. Oncol.* 16 (1), 56. doi:10.1186/s12957-018-1360-3

Beinat, C., Patel, C. B., Haywood, T., Shen, B., Naya, L., Gandhi, H., et al. (2020). Human biodistribution and radiation dosimetry of [[(18)F]DASA-23, a PET probe targeting pyruvate kinase M2. *Eur. J. Nucl. Med. Mol. Imaging* 47 (9), 2123–2130. doi:10.1007/s00259-020-04687-0

Bertelsen, L. B., Hansen, E. S. S., Sadowski, T., Ruf, S., and Laustsen, C. (2021). Hyperpolarized pyruvate to measure the influence of PKM2 activation on glucose metabolism in the healthy kidney. *NMR Biomed.* 34 (11), e4583. doi:10.1002/nbm.4583

Biyik-Sit, R., Kruer, T., Dougherty, S., Bradley, J. A., Wilkey, D. W., Merchant, M. L., et al. (2021). Nuclear Pyruvate kinase M2 (PKM2) contributes to phosphoserine aminotransferase 1 (PSAT1)-mediated cell migration in EGFR-Activated lung cancer cells. *Cancers* 13 (16), 3938. doi:10.3390/cancers13163938

Brinkkoetter, P. T., Bork, T., Salou, S., Liang, W., Mizi, A., Özel, C., et al. (2019). Anaerobic glycolysis maintains the glomerular filtration barrier independent of mitochondrial metabolism and dynamics. *Cell Rep.* 27 (5), 1551–1566. doi:10.1016/j.celrep.2019.04.012

Chang, M., Wang, H., Niu, J., Song, Y., and Zou, Z. (2020). Alkannin-induced oxidative DNA damage synergizes with PARP inhibition to cause cancer-specific cytotoxicity. *Front. Pharmacol.* 11, 610205. doi:10.3389/fphar.2020.610205

Chang, S., Chang, M., Liu, G., Xu, D., Wang, H., Sun, R., et al. (2022). LncRNA OIP5-AS1 reduces renal epithelial cell apoptosis in cisplatin-induced AKI by regulating the miR-144-5p/PKM2 axis. *Biomed. J.* 45 (4), 642–653. doi:10.1016/j.bj.2021.07.005

Chen, B., Yang, B., Zhu, J., Wu, J., Sha, J., Sun, J., et al. (2020). Hsp90 relieves heat stress-induced damage in mouse kidneys: involvement of antiapoptotic PKM2-AKT and autophagic HIF-1α signaling. *Int. J. Mol. Sci.* 21 (5), 1646. doi:10.3390/ijms21051646

Chen, C., Zhang, W., Zhou, T., Liu, Q., Han, C., Huang, Z., et al. (2022). Vitamin B5 rewires Th17 cell metabolism via impeding PKM2 nuclear translocation. *Cell Rep.* 41 (9), 111741. doi:10.1016/j.celrep.2022.111741

Chen, D., Wu, H., Feng, X., Chen, Y., Lv, Z., Kota, V. G., et al. (2021). DNA methylation of cannabinoid receptor interacting protein 1 promotes pathogenesis of intrahepatic cholangiocarcinoma through suppressing parkin-dependent pyruvate kinase M2 ubiquitination. *Hepatology* 73 (5), 1816–1835. doi:10.1002/hep.31561

Chen, H., You, R., Guo, J., Zhou, W., Chew, G., Devapragash, N., et al. (2024). WWP2 regulates kidney fibrosis and the metabolic reprogramming of profibrotic myofibroblasts. *J. Am. Soc. Nephrol.* doi:10.1681/asn.0000000000000328

Chen, X., Xiao, J., Tao, D., Liang, Y., Chen, S., Shen, L., et al. (2023a). Metadherin orchestrates PKA and PKM2 to activate β-catenin signaling in podocytes during proteinuric chronic kidney disease. *Transl. Res.* 266, 68–83. doi:10.1016/j.trsl.2023.11.006

Chen, Y., Bai, X., Chen, J., Huang, M., Hong, Q., Ouyang, Q., et al. (2023b). Pyruvate kinase M2 regulates kidney fibrosis through pericyte glycolysis during the progression from acute kidney injury to chronic kidney disease. *Cell Prolif.* 57, e13548. doi:10.1111/cpr.13548

Chen, Z., Zhu, Z., Liang, W., Luo, Z., Hu, J., Feng, J., et al. (2023c). Reduction of anaerobic glycolysis contributes to angiotensin II-induced podocyte injury with foot process effacement. *Kidney Int.* 103 (4), 735–748. doi:10.1016/j.kint.2023.01.007

Cheon, J. H., Kim, S. Y., Son, J. Y., Kang, Y. R., An, J. H., Kwon, J. H., et al. (2016). Pyruvate kinase M2: a novel biomarker for the early detection of acute kidney injury. *Toxicol. Re.s* 32 (1), 47–56. doi:10.5487/tr.2016.32.1.047

Choi, H. S., Pei, C. Z., Park, J. H., Kim, S. Y., Song, S. Y., Shin, G. J., et al. (2020). Protein stability of pyruvate kinase isozyme M2 is mediated by HAUSP. *Cancers* 12 (6), 1548. doi:10.3390/cancers12061548

Dang, G., Li, T., Yang, D., Yang, G., Du, X., Yang, J., et al. (2022). T lymphocyte-derived extracellular vesicles aggravate abdominal aortic aneurysm by promoting macrophage lipid peroxidation and migration via pyruvate kinase muscle isozyme 2. *Redox Biol.* 50, 102257. doi:10.1016/j.redox.2022.102257

Das Gupta, K., Shakespear, M. R., Curson, J. E. B., Murthy, A. M. V., Iyer, A., Hodson, M. P., et al. (2020). Class IIa histone deacetylases drive toll-like receptor-inducible glycolysis and macrophage inflammatory responses via pyruvate kinase M2. *Cell Rep.* 30 (8), 2712–2728. doi:10.1016/j.celrep.2020.02.007

Fan, N., Zhang, X., Zhao, W., Zhao, J., Luo, D., Sun, Y., et al. (2022). Covalent inhibition of pyruvate kinase M2 reprograms metabolic and inflammatory pathways in hepatic macrophages against non-alcoholic fatty liver disease. *Int. J. Biol. Sci.* 18 (14), 5260–5275. doi:10.7150/ijbs.73890

Fu, J., Shinjo, T., Li, Q., St-Louis, R., Park, K., Yu, M. G., et al. (2022). Regeneration of glomerular metabolism and function by podocyte pyruvate kinase M2 in diabetic nephropathy. *JCI Insight* 7 (5), e155260. doi:10.1172/jci.insight.155260

Gao, F., Zhang, X., Wang, S., Zheng, L., Sun, Y., Wang, G., et al. (2021). TSP50 promotes the Warburg effect and hepatocyte proliferation via regulating PKM2 acetylation. *Cell Death Dis.* 12 (6), 517. doi:10.1038/s41419-021-03782-w

Gao, J., Wang, T., Wang, C., Wang, S., Wang, W., Ma, D., et al. (2019). Effects of Tianshu capsule on spontaneously hypertensive rats as revealed by (1)H-NMR-based metabolic profiling. *Front. Pharmacol.* 10, 989. doi:10.3389/fphar.2019.00989

Gao, S., Li, X., Jiang, Q., Liang, Q., Zhang, F., Li, S., et al. (2022). PKM2 promotes pulmonary fibrosis by stabilizing TGF-β1 receptor I and enhancing TGF-β1 signaling. *Sci. Adv.* 8 (38), eabo0987. doi:10.1126/sciadv.abo0987

Glenthøj, A., van Beers, E. J., Al-Samkari, H., Viprakasit, V., Kuo, K. H. M., Galactéros, F., et al. (2022). Mitapivat in adult patients with pyruvate kinase deficiency receiving regular transfusions (ACTIVATE-T): a multicentre, open-label, single-arm, phase 3 trial. *Lancet Haematol.* 9 (10), e724–e732. doi:10.1016/s2352-3026(22)00214-9

Gong, M., Guo, Y., Dong, H., Wu, F., He, Q., Gong, J., et al. (2023). Modified Hu-lu-ba-wan protects diabetic glomerular podocytes via promoting PKM2-mediated mitochondrial dynamic homeostasis. *Phytomedicine* 123, 155247. doi:10.1016/j.phymed.2023.155247

Gordin, D., Shah, H., Shinjo, T., St-Louis, R., Qi, W., Park, K., et al. (2019). Characterization of glycolytic enzymes and pyruvate kinase M2 in type 1 and 2 diabetic nephropathy. *Diabetes Care* 42 (7), 1263–1273. doi:10.2337/dc18-2585

Gu, M., Tan, M., Zhou, L., Sun, X., Lu, Q., Wang, M., et al. (2022). Protein phosphatase 2Acα modulates fatty acid oxidation and glycolysis to determine tubular cell fate and kidney injury. *Kidney Int.* 102 (2), 321–336. doi:10.1016/j.kint.2022.03.024

Hao, L., Park, J., Jang, H. Y., Bae, E. J., and Park, B. H. (2021). Inhibiting protein kinase activity of pyruvate kinase M2 by SIRT2 deacetylase attenuates psoriasis. *J. Invest. Dermatol.* 141 (2), 355–363.e6. doi:10.1016/j.jid.2020.06.024

Hosoi, T., Yazawa, K., Imada, M., Tawara, A., Tohda, C., Nomura, Y., et al. (2023). Alkannin attenuates Amyloid β aggregation and Alzheimer's disease pathology. *Mol. Pharmacol.* 103 (5), 266–273. doi:10.1124/molpharm.121.000468

Hou, P. P., Luo, L. J., Chen, H. Z., Chen, Q. T., Bian, X. L., Wu, S. F., et al. (2020). Ectosomal PKM2 promotes HCC by inducing macrophage differentiation and remodeling the tumor microenvironment. *Mol. Cell* 78 (6), 1192–1206. doi:10.1016/j.molcel.2020.05.004

Huang, X., Gao, L., Deng, R., Peng, Y., Wu, S., Lu, J., et al. (2023). Huangqi-Danshen decoction reshapes renal glucose metabolism profiles that delays chronic kidney disease progression. *Biomed. Pharmacother.* 164, 114989. doi:10.1016/j.biopha.2023.114989

Ito, M., Gurumani, M. Z., Merscher, S., and Fornoni, A. (2022). Glucose- and non-glucose-induced mitochondrial dysfunction in diabetic kidney disease. *Biomolecules* 12 (3), 351. doi:10.3390/biom12030351

Jiang, C., Zhao, X., Jeong, T., Kang, J. Y., Park, J. H., Kim, I. S., et al. (2022). Novel specific pyruvate kinase M2 inhibitor, compound 3h, induces apoptosis and autophagy through suppressing Akt/mTOR signaling pathway in LNCaP cells. *Cancers* 15 (1), 265. doi:10.3390/cancers15010265

Jin, X., Zhang, W., Wang, Y., Liu, J., Hao, F., Li, Y., et al. (2020). Pyruvate kinase M2 promotes the activation of dendritic cells by enhancing IL-12p35 expression. *Cell Rep.* 31 (8), 107690. doi:10.1016/j.celrep.2020.107690

Kim, H., Takegahara, N., and Choi, Y. (2023). IgSF11-mediated phosphorylation of pyruvate kinase M2 regulates osteoclast differentiation and prevents pathological bone loss. *Bone Res.* 11 (1), 17. doi:10.1038/s41413-023-00251-2

Kim, H. R., Park, J. H., Lee, S. H., Kwack, S. J., Lee, J., Kim, S., et al. (2022). Using intracellular metabolic profiling to identify novel biomarkers of cisplatin-induced acute kidney injury in NRK-52E cells. *J. Toxicol. Environ. Health A* 85 (1), 29–42. doi:10.1080/15287394.2021.1969305

Kuo, C. W., Chen, D. H., Tsai, M. T., Lin, C. C., Cheng, H. W., Tsay, Y. G., et al. (2023). Pyruvate kinase M2 modification by a lipid peroxidation byproduct acrolein contributes to kidney fibrosis. *Front. Med.* 10, 1151359. doi:10.3389/fmed.2023.1151359

Kuo, K. H. M., Layton, D. M., Lal, A., Al-Samkari, H., Bhatia, J., Kosinski, P. A., et al. (2022). Safety and efficacy of mitapivat, an oral pyruvate kinase activator, in adults with non-transfusion dependent α-thalassaemia or β-thalassaemia: an open-label, multicentre, phase 2 study. *Lancet* 400 (10351), 493–501. doi:10.1016/s0140-6736(22)01337-x

Li, J., Liu, H., Takagi, S., Nitta, K., Kitada, M., Srivastava, S. P., et al. (2020a). Renal protective effects of empagliflozin via inhibition of EMT and aberrant glycolysis in proximal tubules. *JCI Insight* 5 (6), e129034. doi:10.1172/jci.insight.129034

Li, J., Sun, Y. B. Y., Chen, W., Fan, J., Li, S., Qu, X., et al. (2020b). Smad4 promotes diabetic nephropathy by modulating glycolysis and OXPHOS. *EMBO Rep.* 21 (2), e48781. doi:10.15252/embr.201948781

Li, L., Tang, L., Yang, X., Chen, R., Zhang, Z., Leng, Y., et al. (2020c). Gene regulatory effect of pyruvate kinase M2 is involved in renal inflammation in type 2 diabetic nephropathy. *Exp. Clin. Endocrinol. Diabetes* 128 (9), 599–606. doi:10.1055/a-1069-7290

Li, M., Jia, F., Zhou, H., Di, J., and Yang, M. (2018). Elevated aerobic glycolysis in renal tubular epithelial cells influences the proliferation and differentiation of podocytes and promotes renal interstitial fibrosis. *Eur. Rev. Med. Pharmacol. Sci.* 22 (16), 5082–5090. doi:10.26355/eurrev_201808_15701

Li, T., Han, J., Jia, L., Hu, X., Chen, L., and Wang, Y. (2019). PKM2 coordinates glycolysis with mitochondrial fusion and oxidative phosphorylation. *Protein Cell* 10 (8), 583–594. doi:10.1007/s13238-019-0618-z

Li, X., Ma, T. K., Wang, M., Zhang, X. D., Liu, T. Y., Liu, Y., et al. (2023a). YY1-induced upregulation of LncRNA-ARAP1-AS2 and ARAP1 promotes diabetic kidney fibrosis via aberrant glycolysis associated with EGFR/PKM2/HIF-1α pathway. *Front. Pharmacol.* 14, 1069348. doi:10.3389/fphar.2023.1069348

Li, Y. J., Zhang, C., Martincuks, A., Herrmann, A., and Yu, H. (2023b). STAT proteins in cancer: orchestration of metabolism. *Nat. Rev. Cancer* 23 (3), 115–134. doi:10.1038/s41568-022-00537-3

Lin, C. J., Chiu, C. Y., Liao, E. C., Wu, C. J., Chung, C. H., Greenberg, C. S., et al. (2023). S-nitrosylation of tissue transglutaminase in modulating glycolysis, oxidative stress, and inflammatory responses in normal and indoxyl-sulfate-induced endothelial cells. *Int. J. Mol. Sci.* 24 (13), 10935. doi:10.3390/ijms241310935

Liu, H., Takagaki, Y., Kumagai, A., Kanasaki, K., and Koya, D. (2021). The PKM2 activator TEPP-46 suppresses kidney fibrosis via inhibition of the EMT program and aberrant glycolysis associated with suppression of HIF-1α accumulation. *J. Diabetes Investig.* 12 (5), 697–709. doi:10.1111/jdi.13478

Liu, Y., Wu, H., Mei, Y., Ding, X., Yang, X., Li, C., et al. (2017). Clinicopathological and prognostic significance of PKM2 protein expression in cirrhotic hepatocellular carcinoma and non-cirrhotic hepatocellular carcinoma. *Sci. Rep.* 7 (1), 15294. doi:10.1038/s41598-017-14813-y

Luo, Q., Liang, W., Zhang, Z., Zhu, Z., Chen, Z., Hu, J., et al. (2022). Compromised glycolysis contributes to foot process fusion of podocytes in diabetic kidney disease: role of ornithine catabolism. *Metabolism* 134, 155245. doi:10.1016/j.metabol.2022.155245

Moreno-Fernandez, M. E., Giles, D. A., Oates, J. R., Chan, C. C., Damen, M., Doll, J. R., et al. (2021). PKM2-dependent metabolic skewing of hepatic Th17 cells regulates pathogenesis of non-alcoholic fatty liver disease. *Cell Metab.* 33 (6), 1187–1204.e9. doi:10.1016/j.cmet.2021.04.018

Nakagawa, T., Johnson, R. J., Andres-Hernando, A., Roncal-Jimenez, C., Sanchez-Lozada, L. G., Tolan, D. R., et al. (2020). Fructose production and metabolism in the kidney. *J. Am. Soc. Nephrol.* 31 (5), 898–906. doi:10.1681/asn.2019101015

Park, J. H., Kundu, A., Lee, S. H., Jiang, C., Lee, S. H., Kim, Y. S., et al. (2021). Specific pyruvate kinase M2 inhibitor, compound 3K, induces autophagic cell death through disruption of the glycolysis pathway in ovarian cancer cells. *Int. J. Biol. Sci.* 17 (8), 1895–1908. doi:10.7150/ijbs.59855

Park, Y. S., Han, J. H., Park, J. H., Choi, J. S., Kim, S. H., and Kim, H. S. (2023). Pyruvate kinase M2: a new biomarker for the early detection of diabetes-induced nephropathy. *Int. J. Mol. Sci.* 24 (3), 2683. doi:10.3390/ijms24032683

Peng, Y., Li, Y., Li, H., and Yu, J. (2022). Shikonin attenuates kidney tubular epithelial cells apoptosis, oxidative stress, and inflammatory response through nicotinamide adenine dinucleotide phosphate oxidase 4/PTEN pathway in acute kidney injury of sepsis model. *Drug Dev. Res.* 83 (5), 1111–1124. doi:10.1002/ddr.21936

Prakasam, G., Iqbal, M. A., Bamezai, R. N. K., and Mazurek, S. (2018). Posttranslational modifications of pyruvate kinase M2: tweaks that benefit cancer. *Front. Oncol.* 8, 22. doi:10.3389/fonc.2018.00022

Puckett, D. L., Alquraishi, M., Chowanadisai, W., and Bettaieb, A. (2021). The role of PKM2 in metabolic reprogramming: insights into the regulatory roles of non-coding RNAs. *Int. J. Mol. Sci.* 22 (3), 1171. doi:10.3390/ijms22031171

Qi, W., Keenan, H. A., Li, Q., Ishikado, A., Kannt, A., Sadowski, T., et al. (2017). Pyruvate kinase M2 activation may protect against the progression of diabetic glomerular pathology and mitochondrial dysfunction. *Nat. Med.* 23 (6), 753–762. doi:10.1038/nm.4328

Qian, L., Ren, S., Xu, Z., Zheng, Y., Wu, L., Yang, Y., et al. (2021). Qian Yang Yu Yin granule improves renal injury of hypertension by regulating metabolic reprogramming mediated by HIF-1α/PKM2 positive feedback loop. *Front. Pharmacol.* 12, 667433. doi:10.3389/fphar.2021.667433

Rabelink, T. J., and Carmeliet, P. (2018). Renal metabolism in 2017: glycolytic adaptation and progression of kidney disease. *Nat. Rev. Nephrol.* 14 (2), 75–76. doi:10.1038/nrneph.2017.173

Rao, J., Wang, H., Ni, M., Wang, Z., Wang, Z., Wei, S., et al. (2022). FSTL1 promotes liver fibrosis by reprogramming macrophage function through modulating the intracellular function of PKM2. *Gut* 71 (12), 2539–2550. doi:10.1136/gutjnl-2021-325150

Ren, R., Guo, J., Shi, J., Tian, Y., Li, M., and Kang, H. (2020). PKM2 regulates angiogenesis of VR-EPCs through modulating glycolysis, mitochondrial fission, and fusion. *J. Cell Physiol.* 235 (9), 6204–6217. doi:10.1002/jcp.29549

Ren, Y., Wang, J., Guo, W., Chen, J., Wu, X., Gu, S., et al. (2022). Renoprotection of microcystin-RR in unilateral ureteral obstruction-induced renal fibrosis: targeting the PKM2-HIF-1α pathway. *Front. Pharmacol.* 13, 830312. doi:10.3389/fphar.2022.830312

Sachan, R., Kundu, A., Dey, P., Son, J. Y., Kim, K. S., Lee, D. E., et al. (2020). Dendropanax morbifera protects against renal fibrosis in streptozotocin-Induced diabetic rats. *Antioxidants* 9 (1), 84. doi:10.3390/antiox9010084

Seki, S. M., Posyniak, K., McCloud, R., Rosen, D. A., Fernández-Castañeda, A., Beiter, R. M., et al. (2020). Modulation of PKM activity affects the differentiation of T(H)17 cells. *Sci. Signal.* 13 (655), eaay9217. doi:10.1126/scisignal.aay9217

Singh, J. P., Qian, K., Lee, J. S., Zhou, J., Han, X., Zhang, B., et al. (2020). O-GlcNAcase targets pyruvate kinase M2 to regulate tumor growth. *Oncogene* 39 (3), 560–573. doi:10.1038/s41388-019-0975-3

Srivastava, S. P., Li, J., Kitada, M., Fujita, H., Yamada, Y., Goodwin, J. E., et al. (2018). SIRT3 deficiency leads to induction of abnormal glycolysis in diabetic kidney with fibrosis. *Cell Death Dis.* 9 (10), 997. doi:10.1038/s41419-018-1057-0

Suman, I., Šimić, L., Čanadi Jurešić, G., Buljević, S., Klepac, D., and Domitrović, R. (2024). The interplay of mitophagy, autophagy, and apoptosis in cisplatin-induced kidney injury: involvement of ERK signaling pathway. *Cell Death Discov.* 10 (1), 98. doi:10.1038/s41420-024-01872-0

Tang, W., and Wei, Q. (2023). The metabolic pathway regulation in kidney injury and repair. *Front. Physiol.* 14, 1344271. doi:10.3389/fphys.2023.1344271

Tong, Y., Chuan, J., Bai, L., Shi, J., Zhong, L., Duan, X., et al. (2018). The protective effect of shikonin on renal tubular epithelial cell injury induced by high glucose. *Biomed. Pharmacother.* 98, 701–708. doi:10.1016/j.biopha.2017.12.112

Wang, C., Xiao, Y., Lao, M., Wang, J., Xu, S., Li, R., et al. (2020). Increased SUMO-activating enzyme SAE1/UBA2 promotes glycolysis and pathogenic behavior of rheumatoid fibroblast-like synoviocytes. *JCI Insight* 5 (18), e135935. doi:10.1172/jci.insight.135935

Wang, J., Yang, P., Yu, T., Gao, M., Liu, D., Zhang, J., et al. (2022a). Lactylation of PKM2 suppresses inflammatory metabolic adaptation in pro-inflammatory macrophages. *Int. J. Biol. Sci.* 18 (16), 6210–6225. doi:10.7150/ijbs.75434

Wang, Z., Yang, S., Ping, Z., Li, Y., Jiang, T., Zheng, X., et al. (2023). Age-induced accumulation of succinate promotes cardiac fibrogenesis. *Circ. Res.* 134 (5), 1–23. doi:10.1161/circresaha.123.323651

Wang, Z., Yu, J., Hao, D., Liu, X., and Wang, X. (2022b). Transcriptomic signatures responding to PKM2 activator TEPP-46 in the hyperglycemic human renal proximal epithelial tubular cells. *Front. Endocrinol.* 13, 965379. doi:10.3389/fendo.2022.965379

Weagel, E. G., Foulks, J. M., Siddiqui, A., and Warner, S. L. (2022). Molecular glues: enhanced protein-protein interactions and cell proteome editing. *Med. Chem. Res.* 31 (7), 1068–1087. doi:10.1007/s00044-022-02882-2

Wei, Q., Su, J., Dong, G., Zhang, M., Huo, Y., and Dong, Z. (2019). Glycolysis inhibitors suppress renal interstitial fibrosis via divergent effects on fibroblasts and tubular cells. *Am. J. Physiol. Ren. Physiol.* 316 (6), F1162–f1172. doi:10.1152/ajprenal.00422.2018

Wu, J., Rong, S., Zhou, J., and Yuan, W. (2021). The role and mechanism of PKM2 in the development of LPS-induced acute kidney injury. *Histol. Histopathol.* 36 (8), 845–852. doi:10.14670/hh-18-343

Wu, Y., Tang, L., Huang, H., Yu, Q., Hu, B., Wang, G., et al. (2023). Phosphoglycerate dehydrogenase activates PKM2 to phosphorylate histone H3T11 and attenuate cellular senescence. *Nat. Commun.* 14 (1), 1323. doi:10.1038/s41467-023-37094-8

Xia, L., Jiang, Y., Zhang, X. H., Wang, X. R., Wei, R., Qin, K., et al. (2021). SUMOylation disassembles the tetrameric pyruvate kinase M2 to block myeloid

differentiation of leukemia cells. *Cell Death Dis.* 12 (1), 101. doi:10.1038/s41419-021-03400-9

Xie, W., He, Q., Zhang, Y., Xu, X., Wen, P., Cao, H., et al. (2023). Pyruvate kinase M2 regulates mitochondrial homeostasis in cisplatin-induced acute kidney injury. *Cell Death Dis.* 14 (10), 663. doi:10.1038/s41419-023-06195-z

Xu, F., Guo, M., Huang, W., Feng, L., Zhu, J., Luo, K., et al. (2020). Annexin A5 regulates hepatic macrophage polarization via directly targeting PKM2 and ameliorates NASH. *Redox Biol.* 36, 101634. doi:10.1016/j.redox.2020.101634

Xu, Y., Liu, X. H., Saunders, M., Pearce, S., Foulks, J. M., Parnell, K. M., et al. (2014). Discovery of 3-(trifluoromethyl)-1H-pyrazole-5-carboxamide activators of the M2 isoform of pyruvate kinase (PKM2). *Bioorg. Med. Chem. Lett.* 24 (2), 515–519. doi:10.1016/j.bmcl.2013.12.028

Yang, Y., Zhan, X., Zhang, C., Shi, J., Wu, J., Deng, X., et al. (2023). USP25-PKM2-glycolysis axis contributes to ischemia reperfusion-induced acute kidney injury by promoting M1-like macrophage polarization and proinflammatory response. *Clin. Immunol.* 251, 109279. doi:10.1016/j.clim.2023.109279

Ye, Y., Xu, L., Ding, H., Wang, X., Luo, J., Zhang, Y., et al. (2021). Pyruvate kinase M2 mediates fibroblast proliferation to promote tubular epithelial cell survival in acute kidney injury. *Faseb J.* 35 (7), e21706. doi:10.1096/fj.202100040R

Yin, X. N., Wang, J., Cui, L. F., and Fan, W. X. (2018). Enhanced glycolysis in the process of renal fibrosis aggravated the development of chronic kidney disease. *Eur. Rev. Med. Pharmacol. Sci.* 22 (13), 4243–4251. doi:10.26355/eurrev_201807_15419

Yu, S., Zang, W., Qiu, Y., Liao, L., and Zheng, X. (2022). Deubiquitinase OTUB2 exacerbates the progression of colorectal cancer by promoting PKM2 activity and glycolysis. *Oncogene* 41 (1), 46–56. doi:10.1038/s41388-021-02071-2

Yuan, Q., Miao, J., Yang, Q., Fang, L., Fang, Y., Ding, H., et al. (2020). Role of pyruvate kinase M2-mediated metabolic reprogramming during podocyte differentiation. *Cell Death Dis.* 11 (5), 355. doi:10.1038/s41419-020-2481-5

Zhang, W., Guo, X., Ren, J., Chen, Y., Wang, J., and Gao, A. (2022). GCN5-mediated PKM2 acetylation participates in benzene-induced hematotoxicity through regulating glycolysis and inflammation via p-Stat3/IL17A axis. *Environ. Pollut.* 295, 118708. doi:10.1016/j.envpol.2021.118708

Zhang, Z., Deng, X., Liu, Y., Liu, Y., Sun, L., and Chen, F. (2019). PKM2, function and expression and regulation. *Cell Biosci.* 9, 52. doi:10.1186/s13578-019-0317-8

Zhang, Z., Hu, H., Luo, Q., Yang, K., Zou, Z., Shi, M., et al. (2023). Dihydroxyacetone phosphate accumulation leads to podocyte pyroptosis in diabetic kidney disease. *J. Cell. Mol. Med.* 28 (3), e18073. doi:10.1111/jcmm.18073

Zhao, G., Yuan, H., Li, Q., Zhang, J., Guo, Y., Feng, T., et al. (2022a). DDX39B drives colorectal cancer progression by promoting the stability and nuclear translocation of PKM2. *Signal Transduct. Target Ther.* 7 (1), 275. doi:10.1038/s41392-022-01096-7

Zhao, J., Wang, G., Han, K., Wang, Y., Wang, L., Gao, J., et al. (2022b). Mitochondrial PKM2 deacetylation by procyanidin B2-induced SIRT3 upregulation alleviates lung ischemia/reperfusion injury. *Cell Death Dis.* 13 (7), 594. doi:10.1038/s41419-022-05051-w

Zhao, Z., Wang, Y., Gao, Y., Ju, Y., Zhao, Y., Wu, Z., et al. (2023). The PRAK-NRF2 axis promotes the differentiation of Th17 cells by mediating the redox homeostasis and glycolysis. *Proc. Natl. Acad. Sci. U. S. A.* 120 (19), e2212613120. doi:10.1073/pnas.2212613120

Zheng, D., Jiang, Y., Qu, C., Yuan, H., Hu, K., He, L., et al. (2020). Pyruvate kinase M2 tetramerization protects against hepatic stellate cell activation and liver fibrosis. *Am. J. Pathol.* 190 (11), 2267–2281. doi:10.1016/j.ajpath.2020.08.002

Zhou, H. L., Hausladen, A., Anand, P., Rajavel, M., Stomberski, C. T., Zhang, R., et al. (2023a). Identification of a selective SCoR2 inhibitor that protects against acute kidney injury. *J. Med. Chem.* 66 (8), 5657–5668. doi:10.1021/acs.jmedchem.2c02089

Zhou, Q., Li, H., Li, Y., Tan, M., Fan, S., Cao, C., et al. (2019). Inhibiting neddylation modification alters mitochondrial morphology and reprograms energy metabolism in cancer cells. *JCI Insight* 4 (4), e121582. doi:10.1172/jci.insight.121582

Zhou, Q., Yin, Y., Yu, M., Gao, D., Sun, J., Yang, Z., et al. (2022a). GTPBP4 promotes hepatocellular carcinoma progression and metastasis via the PKM2 dependent glucose metabolism. *Redox Biol.* 56, 102458. doi:10.1016/j.redox.2022.102458

Zhou, W., Simic, P., and Rhee, E. P. (2022b). Fibroblast growth factor 23 regulation and acute kidney injury. *Nephron* 146 (3), 239–242. doi:10.1159/000517734

Zhou, W., Simic, P., Zhou, I. Y., Caravan, P., Vela Parada, X., Wen, D., et al. (2023b). Kidney glycolysis serves as a mammalian phosphate sensor that maintains phosphate homeostasis. *J. Clin. Invest.* 133 (8), e164610. doi:10.1172/jci164610

Zhu, F., Song, Z., Zhang, S., Zhang, X., and Zhu, D. (2023). The renoprotective effect of shikonin in a rat model of diabetic kidney disease. *Transpl. Proc.* 55 (7), 1731–1738. doi:10.1016/j.transproceed.2023.04.039

Frontiers | Frontiers in Pharmacology

# Bibliometric and visual analysis of immunisation associated with acute kidney injury from 2003 to 2023

Ling Chen[1,2], Jing Hu[1], Jianrao Lu[1]* and Xuezhong Gong[2]*

[1]Department of Nephrology, Seventh People's Hospital of Shanghai University of Traditional Chinese Medicine, Shanghai, China, [2]Department of Nephrology, Shanghai Municipal Hospital of Traditional Chinese Medicine, Shanghai University of Traditional Chinese Medicine, Shanghai, China

**Objective:** This study aims to conduct a detailed bibliometric and visual analysis of acute kidney injury (AKI) and immune-related research conducted over the past two decades, focusing on identifying emerging trends and key areas of interest.

**Methods:** The Web of Science Core Collection (WoSCC) was utilised for the meticulous examination of various parameters including publication volume, authorship, geographic distribution, institutional contributions, journal sources, prevalent keywords and citation frequencies. Data were intricately visualised and interpreted using VOSviewer, CiteSpace and Excel 365 software.

**Results:** Analysis of the WoSCC database revealed 3,537 articles on AKI and immunisation, originating from 94 countries and regions, involving 3,552 institutions and authored by 18,243 individuals. Notably, the top five countries contributing to this field were the United States, China, Germany, Italy and the United Kingdom, with the United States leading with 35.76% of total publications. Among the 3,552 contributing institutions, those in the United States were predominant, with Harvard University leading with 134 papers and 3,906 citations. Key journals driving productivity included Frontiers in Immunology, Kidney International, Journal of the American Society of Nephrology and International Journal of Molecular Sciences, with Kidney International being the most cited, followed by Journal of the American Society of Nephrology and New England Journal of Medicine. Prominent authors in the field included Ronco Claudio, Okusa Mark D and Anders, Hans-Joachim. Co-citation clustering and timeline analysis highlighted recent research foci such as COVID-19, immune checkpoint inhibitors, regulated necrosis, cirrhosis and AKI. Keyword analysis identified "inflammation," "ischaemia-reperfusion injury," "sepsis," "covid-19," and "oxidative stress" as prevalent terms.

**Conclusion:** This study provides the first bibliometric analysis of AKI and immune research, offering a comprehensive overview of research hotspots and evolving trends within the field.

KEYWORDS

advanced bibliometric analysis, acute kidney injury, immunisation, Web of Science Core Collection, CiteSpace, VOSviewer

# 1 Introduction

Acute kidney injury (AKI), characterised by a sudden and rapid decline in renal function, stems from various physiological and pathological factors (Eisenstein, 2023; Zarbock et al., 2023; Zhao et al., 2023). Moreover, patients with AKI face a potential risk of developing chronic kidney disease (CKD) (Kurata and Nangaku, 2023). Despite considerable advancements in the detection and treatment of AKI, along with research into its pathophysiological mechanisms, the morbidity and mortality rates of AKI continue to rise (Fortrie et al., 2019; Joannidis et al., 2023; Kashani et al., 2023; Zhong et al., 2023). Immunopathophysiological responses can lead to disturbances in both macrocirculatory and microcirculatory functions in the kidney, resulting in functional impairment (Okusa et al., 2017; Inoue et al., 2019). Simultaneous activation of innate immunity components drives kidney inflammation, glomerular and tubular damage and blood–urine barrier disruption (Messerer et al., 2021). Previous studies (Gumbert et al., 2020; Sprangers et al., 2022; Sanz et al., 2023) have demonstrated the critical role of the immune microenvironment and immune response resulting in AKI, offering a promising avenue for novel therapeutic research. Consequently, there is a growing interest in AKI induced by immune dysfunction.

Bibliometric analysis, a scientific knowledge system employed to elucidate further development trends and guide research directions (Liu W.-C. et al., 2023; Xu et al., 2023; Tao et al., 2024), has been utilised in previous studies to explore topics such as ferroptosis (Liu C. et al., 2023), kidney repair (Li and Gong, 2023), global biomarkers trends (Fan and Xu, 2023) and the intellectual base along with global trends (Wang et al., 2023) in AKI research. However, none of these studies have specifically delved into immunisation associated with AKI, an area that has exhibited significant research direction recently. Therefore, this study aims to a comprehensive bibliometric analysis in the field of immunisation associated with AKI, thereby elucidating the hotspots and frontiers of potential researches concerning this area.

# 2 Materials and methods

## 2.1 Data acquisition and search protocol

The Web of Science Core Collection (WoSCC) database was selected for its superior accuracy in document type annotation, making it the optimal choice for literature analysis. A search was conducted on 10th December 2023, within WoSCC, for articles related to the use of immunisation in AKI between 1st January 2004 and 10th December 2023. The search query employed the following formula (((((((((((((((((((((((TS = (Acute Kidney Injury)) OR TS = (Acute Kidney Injuries)) OR TS = (Kidney Injuries, Acute)) OR TS = (Kidney Injury, Acute)) OR TS = (Acute Renal Injury)) OR TS = (Acute Renal Injuries)) OR TS = (Renal Injuries, Acute)) OR TS = (Renal Injury, Acute)) OR TS = (Renal Insufficiency, Acute)) OR TS = (Acute Renal Insufficiencies)) OR TS = (Renal Insufficiencies, Acute)) OR TS = (Acute Renal Insufficiency)) OR TS = (Kidney Insufficiency, Acute)) OR TS = (Acute Kidney Insufficiencies)) OR TS = (Kidney Insufficiencies, Acute)) OR TS = (Acute Kidney Insufficiency)) OR TS = (Kidney Failure,

Acute)) OR TS = (Acute Kidney Failures)) OR TS = (Kidney Failures, Acute)) OR TS = (Acute Renal Failure)) OR TS = (Acute Renal Failures)) OR TS = (Renal Failures, Acute)) OR TS = (Renal Failure, Acute)) OR TS = (Acute Kidney Failure) AND TS = (immune).

## 2.2 Bibliometric examination and visual depiction

GraphPad prism (version 8.0.2) was utilised to analyse and visualise annual paper counts, national publication trends and percentages. Additionally, CtieSpace (6.2.4R (64-bit) Premium Edition) and VOSviewer (version 1.6.18) were employed for data analysis and visualisation. Created in 2009 by van Eck and Waltman, (2010), VOSviewer (version 1.6.18) is a Java-based free software facilitating the analysis of extensive literature data by presenting it in map format. CiteSpace (6.2.4R) (Synnestvedt et al., 2005), devised by Prof. Chen Chaomei, enables the construction of literature co-citation network maps, aiding in the visualisation of research outcomes within a specific field. It offers insights into knowledge areas, research frontiers trends and future research trajectories.

## 2.3 Inclusion and exclusion parameters

Inclusion criteria for references in this study comprised: 1) Full text of publications related to the use of immunisation associated with AKI; 2) Articles and reviews written in English; 3) Articles published between 1st January 2004 and 10th December 2023. Exclusion criteria were: 1) irrelevance to the utilisation of immunisation associated with AKI; 2) The articles were conference abstracts, news or briefings.

# 3 Results

## 3.1 Evolution of global publications

During the period of 1st January 2004 to 10th December 2023, the WoSCC database contained 3,537 articles focusing on the application of AKI and immunisation (Figure 1). Among these, 2,371 articles (67.03%) and 1,166 reviews (32.97%) were identified. The literature encompassed contributions from 94 countries and regions, involving 3,552 institutions and 18,243 authors.

The number of papers published annually exhibited a gradual increase since 2004 (Figure 2A), delineated into three stages. From 2004 to 2010, the growth was modest, with annual publications remaining below 100. Subsequently, from 2011 to 2019, there was a gradual rise in publications. Post-2020, there was a notable surge in publications in this field, reaching a peak in 2021.

## 3.2 International collaborations and contributions

Studies on the application of immunisation in AKI spanned 94 countries and regions (Figures 2B,C,D). Figure 3A illustrates the

**FIGURE 1**
Flow chart of literature screening.
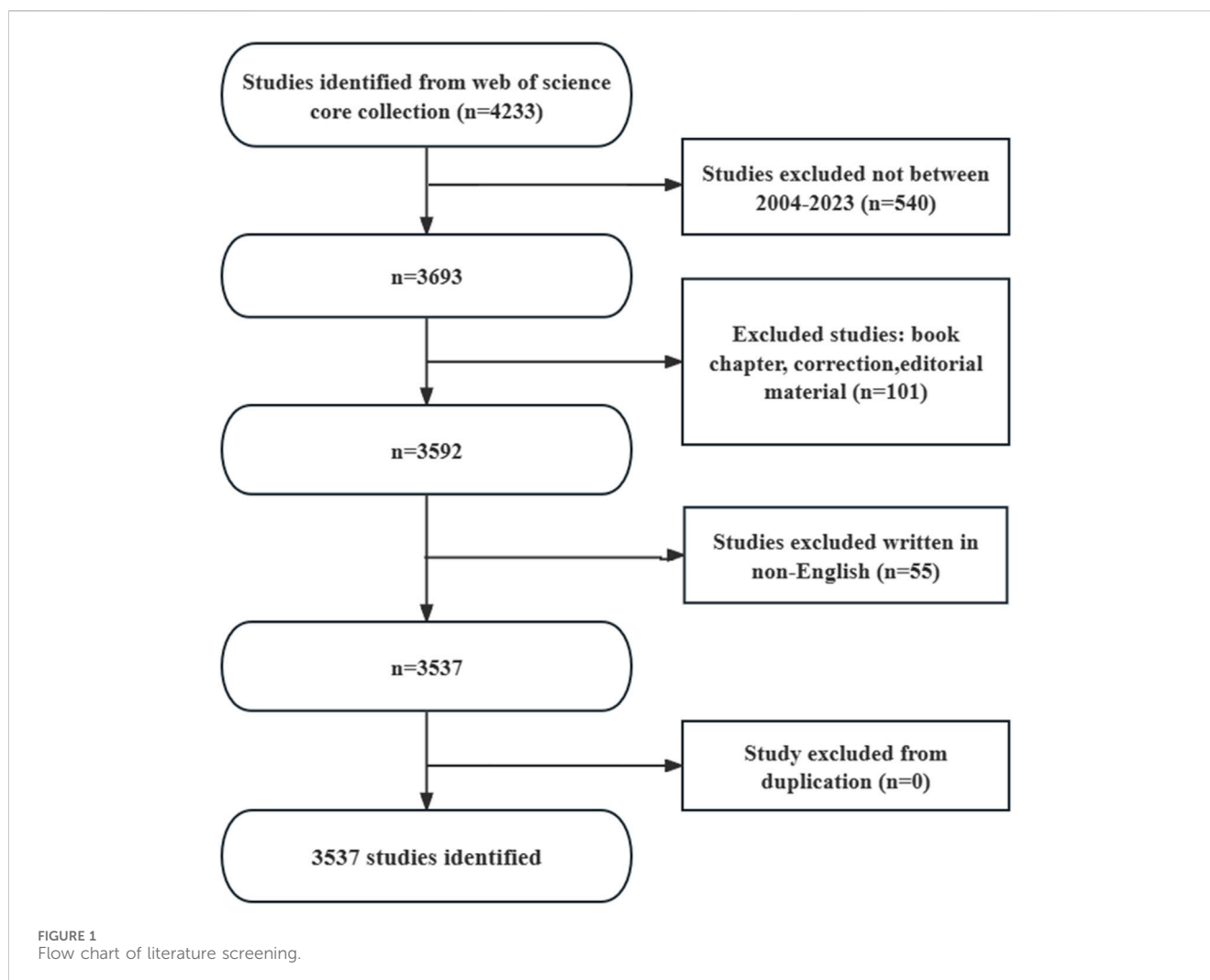
annual publication volume in the top 10 countries over the past decade, with the United States, China, Germany, Italy and the United Kingdom emerging as the leading contributors. The United States accounted for 35.76% of the total published papers, significantly surpassing other countries. The United States garnered 66,444 citations (Table 1), surpassing other countries and ranking fifth in the citations/publications ratio (52.52%). China ranked second in published papers (603) and number of citations (16,477), with the lowest citation/publication ratio (14.89), suggestive of varying publication quality. The United States demonstrated close collaboration with the United Kingdom, Japan, Italy and Germany, while China exhibited closer collaboration with France, the Netherlands, South Korea and Australia. With high publication numbers, citation frequencies and centrality (0.40), the United States emerged as a pivotal contributor.

## 3.3 Institutional research dynamics

A total of 3,552 institutions contributed to publications in this field. Among the top 10 publications, six from the United States, 3 from France and 1 from the United Kingdom (Table 2; Figure 3B).

Harvard University led with the most publications (134 papers, 3,906 citations, 29.15 citations per paper), followed by Harvard Medical School (95 papers, 2,937 citations, 30.92 citations per paper) and Institut National de la Sante et de la Recherche Medicale (Inserm) (92 papers, 1,549 citations, 16.84 citations per paper).

## 3.4 Enhanced analysis of journals

Table 3 and Figure 4A present the top 10 most prolific and cited journals. Frontiers in Immunology (133 articles, 3.76%) led in publications, followed by Kidney International (83 articles, 2.35%), Journal of the American Society of Nephrology (78 articles, 2.21%) and International Journal of Molecular Sciences (69 articles, 1.95%). Among these journals, Kidney International boasted the highest impact factor (IF) of 19.6. Furthermore, 90% of these journals were classified as either Q1 or Q2.

Journal influence is determined by co-citations, reflecting its impact on the scientific community. As indicated in Table 4 and Figure 4B, KIDNEY INT (2,205 co-citations) ranked highest in co-citations, followed by J AM SOC NEPHROL (2,017) and NEW ENGL J MED (1,781). Among the top 10 journals, NEW ENGL J
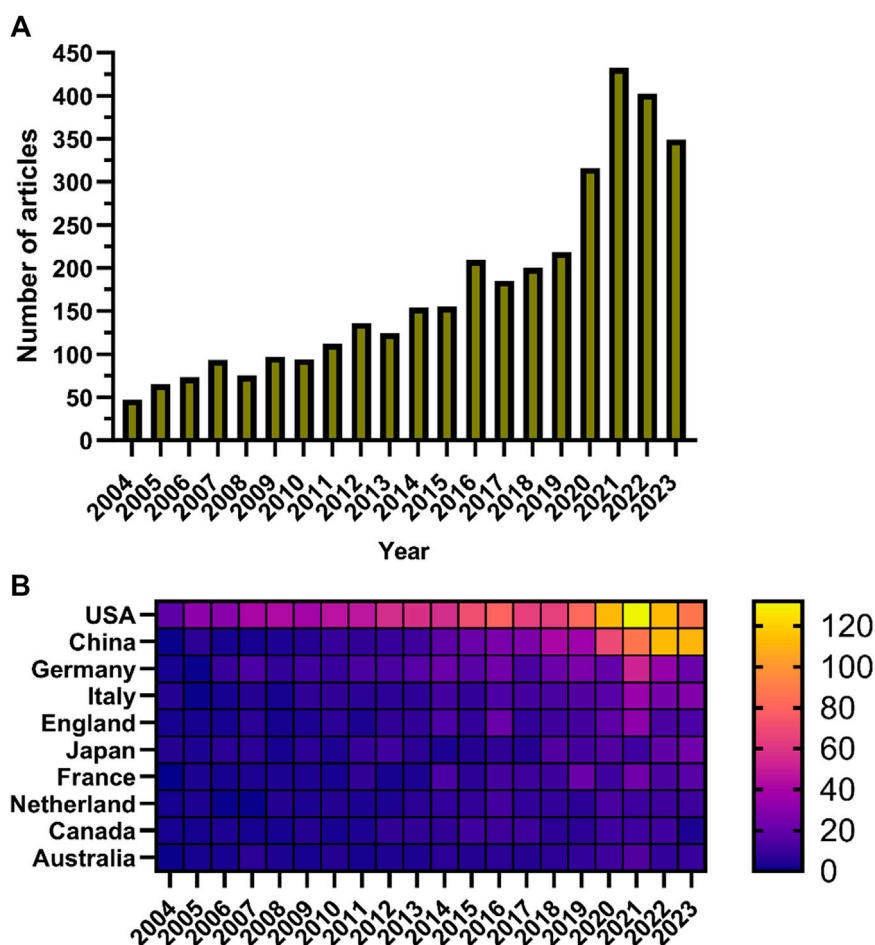
FIGURE 2
(Continued).

MED garnered the highest IF (158.5). All top co-cited journals were either Q1 or Q2.

The subject distribution of academic publications is depicted through dual maps (Figure 5), highlighting citation paths. Four colour citation paths were identified, showcasing research in medicine/medical/clinical fields primarily reported in molecular/biology/genetics and health/nursing/medicine reference research journals. The field of molecular/biology/immunology research was predominately reported in molecular/biology/genetics journals, with cross-referencing to health/nursing/medicine journals.

## 3.5 Analysis of authors and Co-cited authors

Table 5 and Figure 6A list the 10 authors who have published the most on immunisation associated with AKI. Together, these authors published 208 papers, constituting 5.88% of all papers in the field. Ronco, Claudio emerged as the most prolific author with 32 publications, followed by Okusa, Mark D. (30) and Anders, Hans-Joachim (27). Analysis reveals that five of the top 10 authors are affiliated with institutions in the United States, followed by Italy, Germany, the Netherlands, Brazil and China. Further examination

using CiteSpace visualises the network among authors, identifying Anders hans-joachim as the leading author in the field. Table 5 and Figure 6B delineate the top 10 co-cited and most cited authors, respectively. The 56 authors have been cited more than 50 times, indicating significant reputation and influence. Notably, most co-cited authors include LAMBIN P (367 citations), GILLIES RJ (328 citations) and LI H (210 citations).

## 3.6 Analysis of Co-cited references

In a 1-year time slice spanning 2004 to 2023, the co-citation reference network comprised 1,350 nodes and 5,443 links (Figure 7A). The top 10 most cited articles (Table 6) feature a paper from the Clinical Journal of the American Society of Nephrology (IF = 9.8) entitled 'The Incidence, Causes, and Risk Factors of Acute Kidney Injury in Patients Receiving Immune Checkpoint Inhibitors' as the most frequently cited reference. Authored by Seethapathy Harish, the paper discusses the escalating use of immune checkpoint inhibitors (ICIs) in oncology.

Co-cited reference clustering and temporal clustering analysis (Figures 7B, C) reveal various research hotspots over
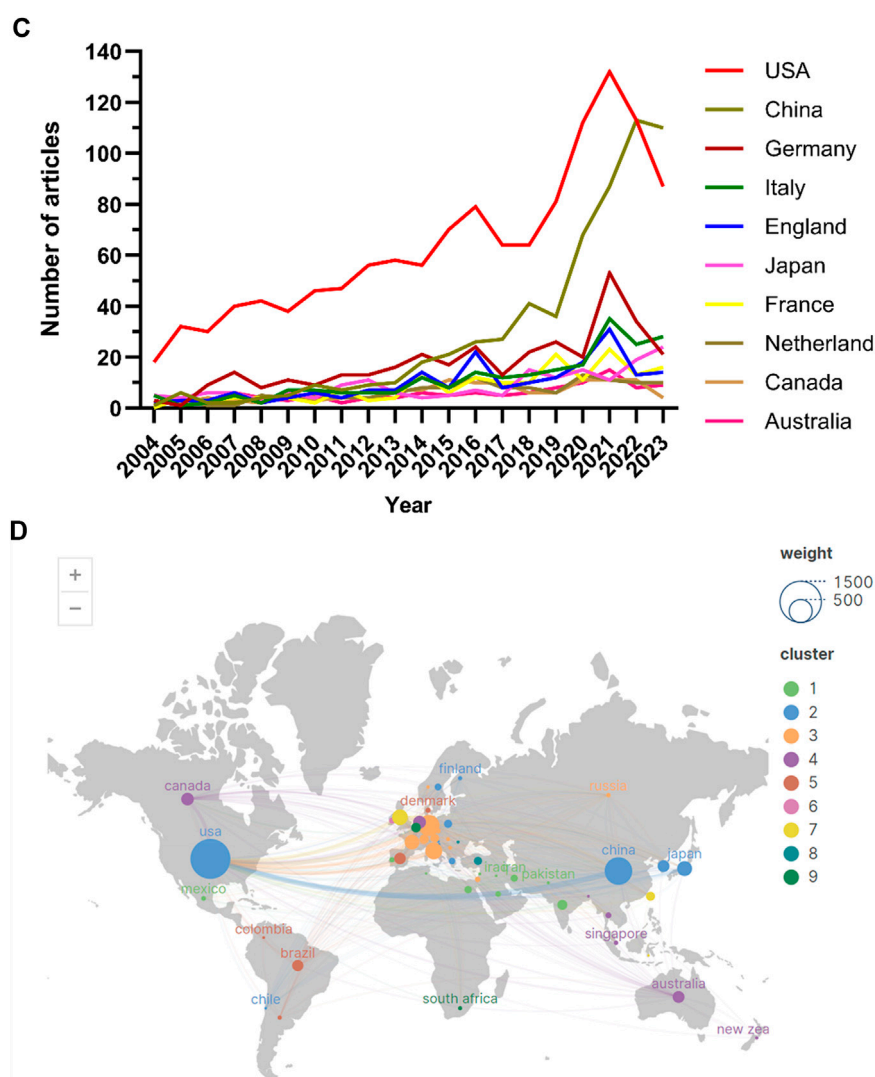
**FIGURE 2**
(Continued). **(A)** Line chart of the number of publications; **(B)** National publication calorimetric map; **(C)**; Line chart of the number of national publications; **(D)** Distribution map of articles published by different countries.

time, such as toll-like receptors (cluster 3), chronic allograft nephropathy (cluster 7) and ivig (cluster 8) in earlier periods, progressing to Netrin-1 (cluster 2), mesenchymal stem cell (cluster 9) and mesenchymal stromal cells (cluster 10), tlrs (cluster 11), screening (cluster 12), crossmath (cluster 13) as mid-term research hotspots. Currently, COVID-19 (cluster 0), immune checkpoint inhibitors (cluster 1), regulated necrosis (cluster 4), cirrhosis (cluster 5) and acute necrosis (kidney) injury (cluster 6) are the research trends in this field.

## 3.7 Keyword analysis

Keyword co-occurrence analysis in VOSwiever highlights inflammation (575) as the most popular keyword, followed by expression (330), ischaemia-reperfusion injury (283), disease (279) and sepsis (267) (Figures 8A,B; Table 7). Filtering out redundant keywords, a network of 176 keywords appearing at least 28 times reveals five distinct clusters. Group 1 (red) encompasses 56 keywords, including disease, glomerulonephritis, therapy, infection, failure, risk, safety, cancer, toxicity, antibody, kidney transplant, biopsy and vasculitis. Group 2 (green) comprises 53 keywords, including acute rejection, complement, tolerance, donor-specific antibody, survival, immunosuppression, recipients, T cell, TGF-β, toll-like receptors and dendritic cells. Group 3 (blue) contains 31 keywords, including sepsis, septic shock, acute lung injury, cytokines, dysfunction, model, neutrophil, rats, liver and necrosis factor-alpha. Group 4 comprises 30 keywords (yellow), including inflammation, activation, macrophages, fibrosis, renal injury, pathway, autophagy, cisplatin, protects, immunity, apoptosis and cell death. Group 5 (purple) contains six keywords, including ace2, coronavirus, covid-19, receptor, responses and sars-cov-2. Additionally, a volcano map generated using CiteSpace visualises the evolution of study hotspots over time (Figure 8C).

FIGURE 3
**(A)** Network of national cooperation; **(B)** Network of institutions' cooperation.
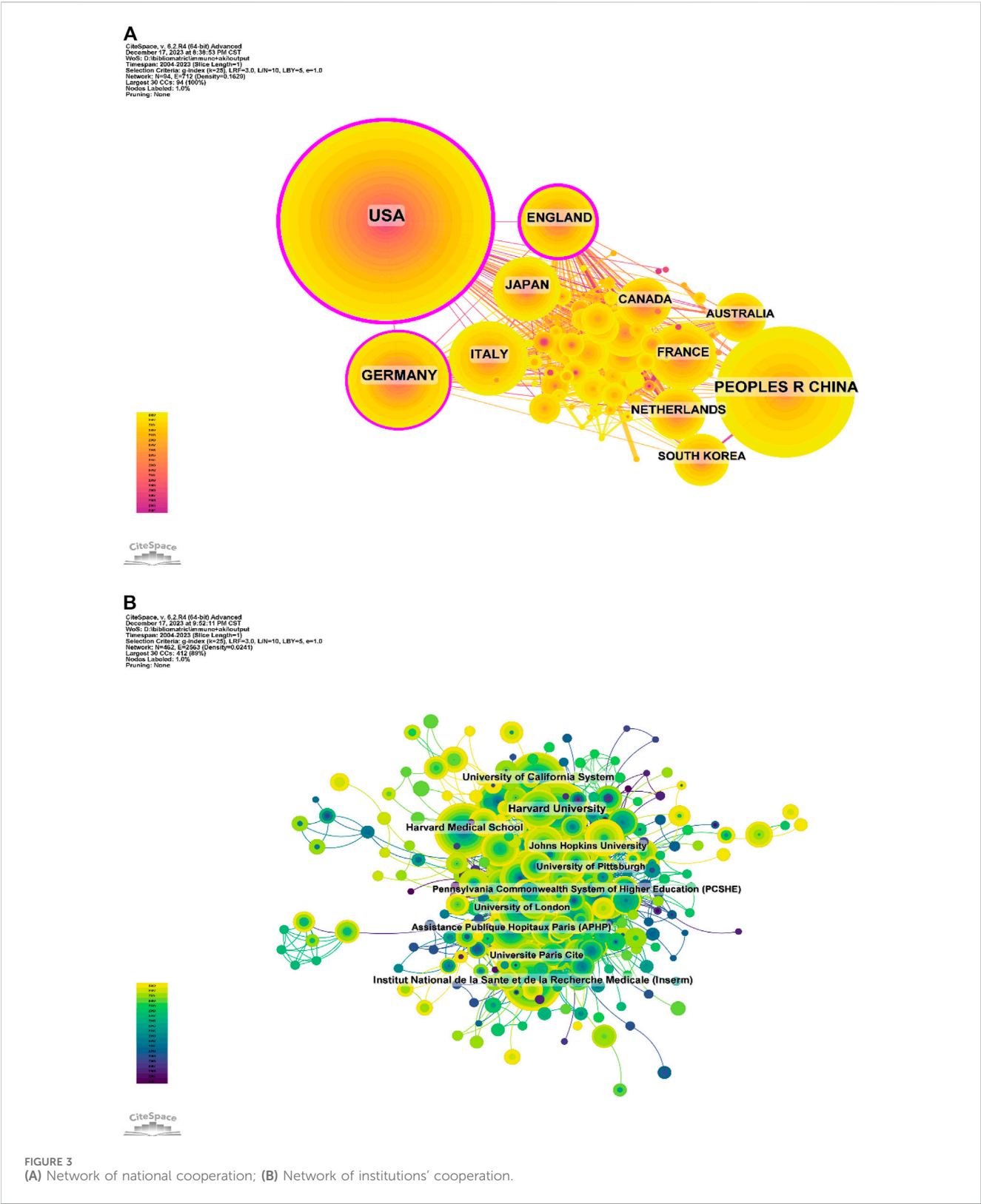
## 3.8 Highlighting Co-cited references and keywords

CiteSpace analysis, shown in Figure 9A, identified the 50 most reliable citation bursts, with the highest citation rate (21.56) attributed to "Clinicopathological features of acute kidney injury associated with immune checkpoint inhibitors" by Frank B. Cortazar. Notably, all 50 references were published between 2004 and 2023, indicating that these papers were frequently cited over nearly 2 decades. Importantly, 16 of these papers are currently

TABLE 1 National publication scale.

| Rank | Country/Region | Article counts | Centrality | Percentage (%) | Citation | Citation per publication |
|------|----------------|----------------|------------|----------------|----------|--------------------------|
| 1 | United States of America | 1,265 | 0.40 | 35.76 | 66,444 | 52.52 |
| 2 | China | 603 | 0.06 | 17.05 | 16,477 | 27.33 |
| 3 | Germany | 348 | 0.14 | 9.84 | 16,441 | 47.24 |
| 4 | Italy | 226 | 0.07 | 6.39 | 9,268 | 41.01 |
| 5 | England | 194 | 0.23 | 5.48 | 10,069 | 51.90 |
| 6 | Japan | 177 | 0.09 | 5.00 | 5,097 | 28.80 |
| 7 | France | 171 | 0.07 | 4.83 | 9,844 | 57.57 |
| 8 | Netherlands | 130 | 0.09 | 3.68 | 8,074 | 62.11 |
| 9 | Canada | 126 | 0.02 | 3.56 | 7,180 | 56.98 |
| 10 | Australia | 112 | 0.08 | 3.17 | 6,741 | 60.19 |

TABLE 2 Institutional publication scale.

| Rank | Institution | Country | Number of studies | Total citations | Average citation |
|------|-------------|---------|-------------------|-----------------|------------------|
| 1 | Harvard University | United States of America | 134 | 3,906 | 29.15 |
| 2 | Harvard Medical School | United States of America | 95 | 2,937 | 30.92 |
| 3 | Institut National de la Sante et de la Recherche Medical (Inserm) | France | 92 | 1,549 | 16.84 |
| 4 | University of California System | United States of America | 91 | 1,592 | 17.49 |
| 5 | Pennsylvania Commonwealth System of Higher Education (PCSHE) | United States of America | 86 | 1,246 | 14.49 |
| 6 | Assistance Publique Hopitaux Paris (APHP) | France | 76 | 1,218 | 16.03 |
| 7 | University of Pittsburgh | United States of America | 68 | 5,084 | 74.76 |
| 8 | Universite Paris Cite | France | 67 | 2,444 | 36.48 |
| 9 | University of London | England | 65 | 1,822 | 28.03 |
| 10 | Johns Hopkins University | United States of America | 65 | 4,045 | 62.23 |

experiencing their citation peak, underscoring ongoing interest in immune-related AKI research. Additionally, the analysis of the 257 strongest burst keywords (Figure 9B) highlights current research hotspots in the field and potential future research directions in the field.

## 4 Discussion

This study is the first bibliometric analysis aiming to elucidate the topic of immune researches related to AKI. Our objective was to provide a comprehensive overview of this field during the include peroid using bibliometric software. Through the visualisation of

quantitative data conducted, valuable insights into research hotspots and trends were obtained.

## 4.1 Bibliometric information

A search of the WoSCC database from 1st January 2004 to 10th December 2023, yielded 3,537 articles in the field of AKI and immunisation (Figure 1). The literature involved contributions from 94 countries and regions, 3,552 institutions and 18,243 authors. Publications rates showed a gradual increase since 2004 (Figure 2A); however, from 2004 to 2010, the growth declined. From 2011 to 2019, published papers gradually increased,

TABLE 3 Journal publication scale.

| Rank | Journal | Article counts | Percentage (3,537) | If | Quartile in category |
|------|---------|----------------|--------------------|----|----------------------|
| 1 | Frontiers In Immunology | 133 | 3.76 | 7.3 | Q1 |
| 2 | Kidney International | 83 | 2.35 | 19.6 | Q1 |
| 3 | Journal of the American Society of Nephrology | 78 | 2.21 | 13.6 | Q1 |
| 4 | International Journal of Molecular Sciences | 69 | 1.95 | 5.6 | Q1 |
| 5 | American Journal of Transplantation | 64 | 1.81 | 8.7 | Q1 |
| 6 | Plos One | 61 | 1.72 | 3.7 | Q2 |
| 7 | American Journal of Physiology-Renal Physiology | 56 | 1.58 | 4.2 | Q1 |
| 8 | Transplantation | 47 | 1.33 | 6.2 | Q2 |
| 9 | Paediatric Nephrology | 46 | 1.30 | 3.0 | Q2 |
| 10 | BMC nephrology | 45 | 1.27 | 2.3 | Q3 |

and post-2020, they increased rapidly, peaking in 2021. This suggests a growing interest in this area in recent years.

The top five countries contributing to annual publication volumes were the United States, China, Germany, Italy and the United Kingdom. The United States stood out with the highest citation count (66,444 citations) (Table 1), far surpassing other countries, and ranked fifth among all countries in the citations/publications ratio. China ranked second in published papers and citations but demonstrated a lower citation/publication ratio.

Among the top 10 publications, six were from the United States, three from France and one from the United Kingdom (Table 2; Figure 3B). Harvard University emerged as the leading contributor, followed by Harvard Medical School and Institut National de la Sante et de la Recherche Medicale (Inserm), respectively.

Table 3 and Figure 4A list the top 10 most produced and cited journals. Frontiers in Immunology was revealed as the most published journal in the field, followed by Kidney International, Journal of the American Society of Nephrology and International Journal of Molecular Sciences. Journal influence is determined by how often it is co-cited, which, in turn, indicates its impact on the scientific community. The journal with the most common citations was KIDNEY INT (2,205), followed by J AM SOC NEPHROL (2,017) and NEW ENGL J MED (1,781) (Table 4; Figure 4B). It as well demonstrated top journals on the topic included professional journals of nephrology and other fields like molecular sciences, indicating the multidisciplinary nature of this field.

The top 10 authors published 208 papers or 5.88% of all papers in the field (Table 5; Figure 6A), with Ronco, Claudio leading with the most publications (32), followed by Okusa, Mark D (30) and Anders, hans-joachim (27). Further analysis identified Anders hans-joachim, the third most published and cited author, as a leading figure in the field.

Among the top 10 most cited articles (Table 6), a paper from the Clinical Journal of the American Society of Nephrology (IF = 9.8) entitled 'The Incidence, Causes, and Risk Factors of Acute Kidney Injury in Patients Receiving Immune Checkpoint Inhibitors' is the most frequently cited reference. Seethapathy Harish, lead author of the paper, discusses the rapid increase in the use of ICIs in oncology. They intended to figure out the frequency, severity and causes of AKI in populations treated with ICIs. Treated with ICIs, AKI is

common in patients with varying causes. Nevertheless, the role of proton pump inhibitors (PPI) and other agents that induce nephritis in persistent AKI required further elucidation.

## 4.2 Hotspots and frontiers

The top 5 keywords were inflammation (575), followed by ischaemia-reperfusion injury (283), sepsis (267), covid-19 (174) and oxidative stress (171) (Figures 8A,B; Table 7). CiteSpace analysis, shown in Figure 9A, identified the 50 most reliable citations burst. Among them, the reference with the highest citation rate (21.56) was "Clinicopathological features of acute kidney injury associated with immune checkpoint inhibitors" by Frank B. Cortazar. This article reveals ICIs-induced AKI is a new entity that presents with clinical and histologic features similar to other causes of drug-induced acute tubulointerstitial nephritis, though with a longer latency period. Glucocorticoids appear to be a potentially effective treatment strategy. Hence, AKI due to ICIs may be caused by a unique mechanism of action linked to reprogramming of the immune system, leading to loss of tolerance. All 50 references were published between 2004 and 2023, with 16 currently peaking. These observations suggest that the application of immunity to AKI research will continue to be of interest in the future. Of the 257 strongest burst keywords in the field, we focus on the 50 keywords with the strongest mutations (Figure 9B), which represent current research hotspots and represent possible research directions. It is described and discussed from the following three aspects related mechanisms, associated immune cells and immune responses as well as underlying pathways of action.

### 4.2.1 Related mechanisms

The immune microenvironment and immune response are crucial to the occurrence and development of AKI, and might be a new therapeutic target research direction (Gumbert et al., 2020; Xu L. et al., 2024). Regulating inflammatory response and enhancing the regenerative potential of stem cells in the inflammatory microenvironment contribute to the regeneration of renal tubular epithelium. Studies have shown (Sprangers et al., 2022;
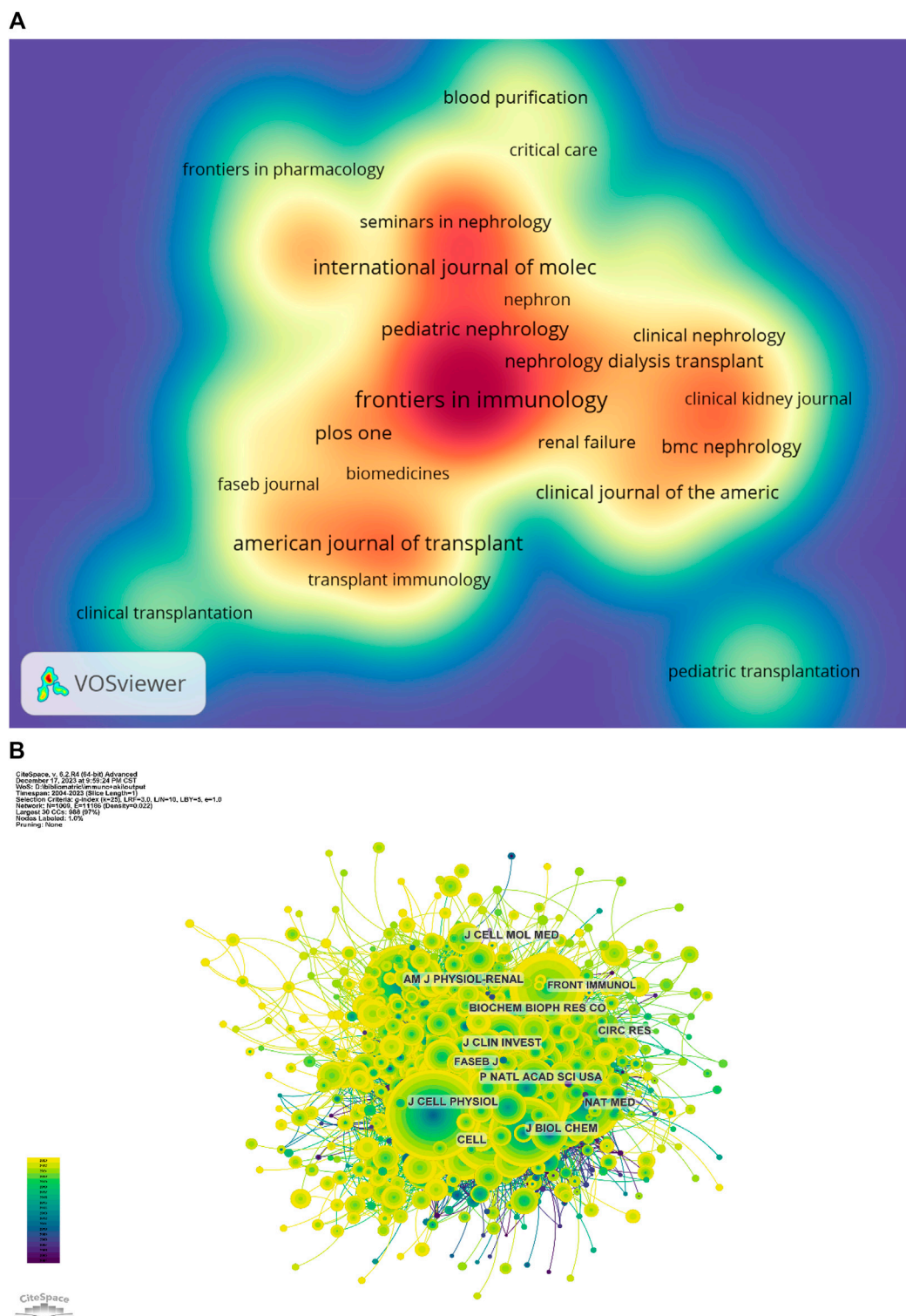
**FIGURE 4**
**(A)** Journal publication density chart; **(B)** Journal co-citation network diagram.

Deng et al., 2023) that the immune response induced by AKI is closely related to the formation of complex cytokine networks by T cell subsets (Th1, Th2, Th17, Th9, Th22, etc.) in renal tubular epithelial tissue, and targeted immunity can inhibit the progression of AKI. Therefore, the exploration of molecules or drugs that can control the inflammatory response, reverse the pro-inflammatory immune microenvironment, and improve the differentiation ability of stem cells to promote the regeneration of renal tubular epithelial tissue is currently a hot spot in the clinical treatment of AKI.

**TABLE 4 Journal's total citations.**

| Rank | Cited journal | Co-citation | If (2022) | Quartile in category |
|------|---------------|-------------|-----------|----------------------|
| 1 | Kidney International | 2,205 | 19.6 | Q1 |
| 2 | Journal of the American Society of Nephrology | 2017 | 13.6 | Q1 |
| 3 | New England Journal of Medicine | 1,781 | 158.5 | Q1 |
| 4 | The Journal of Clinical Investigation | 1,457 | 15.9 | Q1 |
| 5 | Journal of Immunology | 1,449 | 4.4 | Q2 |
| 6 | Nephrology Dialysis Transplantation | 1,433 | 6.1 | Q1 |
| 7 | Plos One | 1,351 | 3.7 | Q2 |
| 8 | Lancet | 1,338 | 168.9 | Q1 |
| 9 | Proceedings of the National Academy of Sciences of the United States of America | 1,260 | 11.5 | Q1 |
| 10 | American Journal of Kidney Diseases | 1,077 | 11.1 | Q1 |
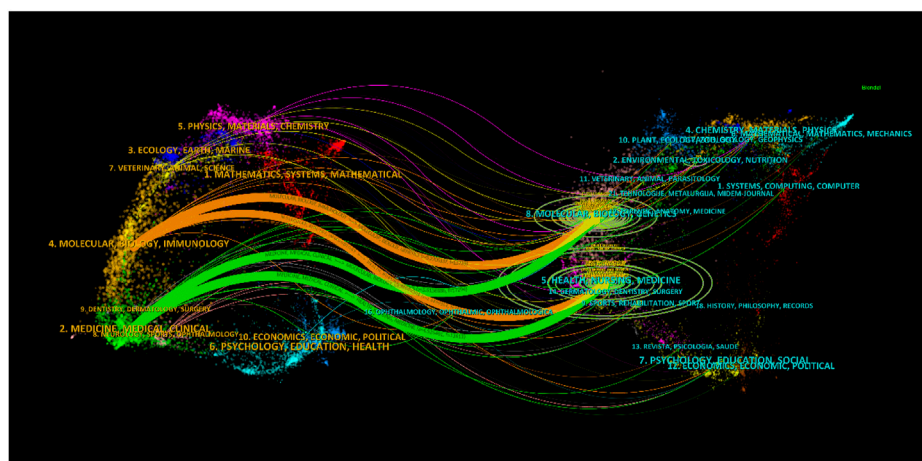


**FIGURE 5**
Periodical double overlay diagram.

**TABLE 5 Publications and co-citations of the top 10 authors.**

| Rank | Author | Count | Location | Rank | Co-cited author | Citation |
|------|--------|-------|----------|------|-----------------|----------|
| 1 | Ronco, claudio | 32 | Italy | 1 | BONVENTRE JV | 248 |
| 2 | Okusa, mark d | 30 | United States of America | 2 | LI L | 219 |
| 3 | Anders, hans-joachim | 27 | Germany | 3 | ANDERS HJ | 183 |
| 4 | Rabb, hamid | 26 | United States of America | 4 | JANG HR | 183 |
| 5 | Kellum, john a | 20 | United States of America | 5 | BELLOMO R | 176 |
| 6 | Perazella, mark a | 19 | United States of America | 6 | RABB H | 171 |
| 7 | Florquin, sandrine | 14 | Netherlands | 7 | RONCO C | 162 |
| 8 | Saraiva camara, niels olsen | 14 | Brazil | 8 | KINSEY GR | 160 |
| 9 | Huang, liping | 13 | China | 9 | CORTAZAR FB | 150 |
| 10 | Sarwal, minnie m | 13 | United States of America | 10 | WU HL | 139 |
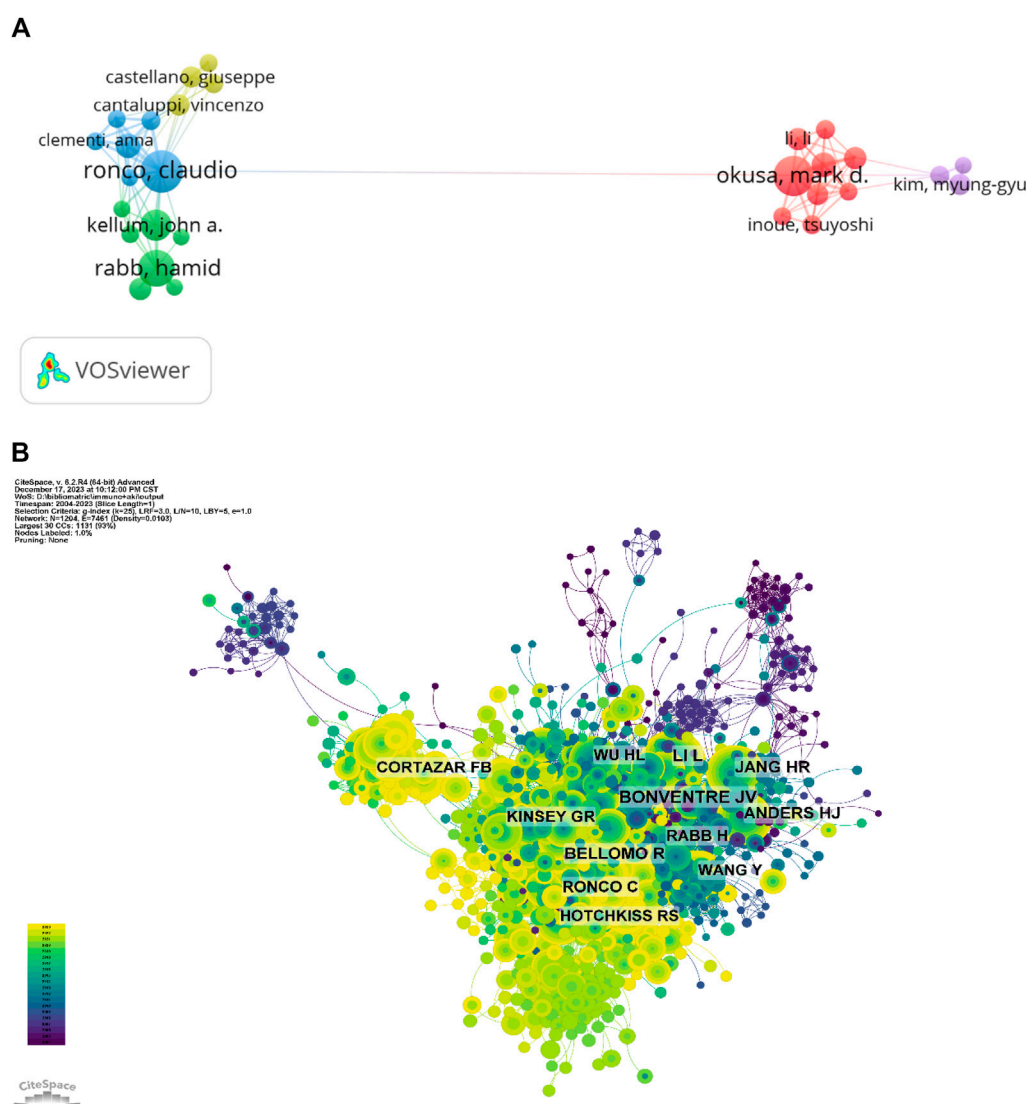
**FIGURE 6**
**(A)** Author collaboration network diagram; **(B)** Author co-citation network diagram.

Both inflammation and oxidative stress play a crucial role in the potential molecular mechanisms of acute kidney damage process (He et al., 2017; Choi et al., 2022; Fan et al., 2023). Addressing inflammatory reactions is a viable approach in the treatment of both CKD and AKI. Oxidative stress performs a fundamental function in the advancement of renal disorders and the progression of kidney-related problems. Inflammation and oxidative stress are inextricably related, jointly causing and exacerbating the effects of the other. Chuan Huang Fang (CHF) is a Chinese herbal formulation synthesized by Professor Xuezhong Gong in Shanghai Municipal Hospital of Traditional Chinese Medicine for the treatment of AKI on CKD (A on C) patients (Chen et al., 2022). Previous study (Gong et al., 2020) has demonstrated that after treatment with CHF, serum levels of oxidation-antioxidant related biomarkers malondialdehyde (MDA), superoxide dismutase (SOD) and heme oxygenase-1 (HO-1) in A on C patients showed significant changes compared with those before treatment, which showed levels of HO-1 and SOD in patients with A on C were higher than those before treatment, and MDA levels were lower.

Therefore, it is believed that CHF might have certain antioxidant effect on patients with A on C. As an inflammatory signal that has been paid much attention to in recent years, NOD-like receptor protein-3 (NLRP3) inflammasome plays an important role in the occurrence and development of AKI (Li Y. et al., 2024; Xue et al., 2024). Another study (Gong et al., 2021) have shown that CHF has a better inhibitory effect on NLRP3 inflammasome, which might be the effective treatment mechanisms of CHF. The antioxidant effects of CHF could also inhibit the increase of NLRP3 inflammatorome in patients with A on C to further exert the renal protection effects. Tetramethylpyrazine (TMP), an active component in both CHF and the medicinal herbs Ligusticum wallichii (Chuanxiong), has the potential to prevent AKI via a variety of processes, including ameliorating oxidative stress damage, suppressing inflammatory responses, deterring apoptotic cell death of intrinsic renal cells, and modulating autophagy (Li and Gong, 2022).

The pathogenesis of sepsis associated acute kidney injury (S-AKI) is complex. It is mainly related to renal hemodynamic changes, inflammation, oxidative stress injury, ischemia reperfusion

**FIGURE 7**
(Continued).
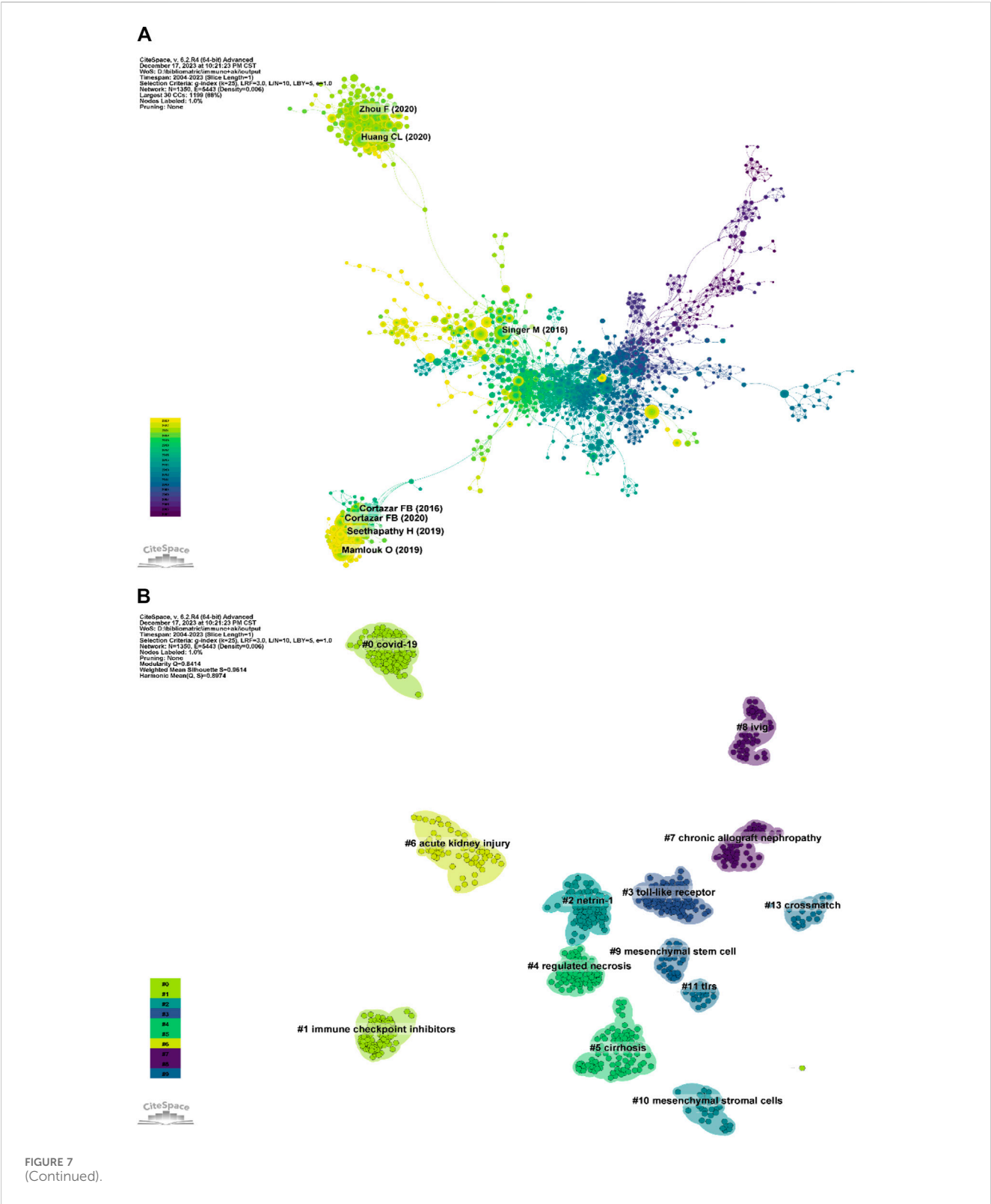
injury, apoptosis, coagulation dysfunction, adaptive mechanism of energy metabolism of renal tubular epithelial cells, gene differences and expression, etc (Kaushal and Shah, 2016; Yang et al., 2021; He et al., 2024). Emodin might play a renal protective role in S-AKI mice by enhancing the expression of Nrf2 and AUF1 proteins, regulating related oxidation-reduction enzyme, enhancing

antioxidant stress ability, inhibiting inflammatory response (Ding et al., 2023). Studies reveal that (Yancy et al., 2017) the mechanism of CRRT in the treatment of S-AKI is primarily through convection and adsorption of soluble inflammatory mediators and toxins, reducing immune suppression, inhibiting lymphocyte apoptosis, enhancing immune function, inhibiting inflammatory cascade

FIGURE 7
(Continued). **(A)** Network diagram of co-cited documents; **(B)** Clustering diagram of co-cited documents; **(C)** Volcano map of co-cited references.
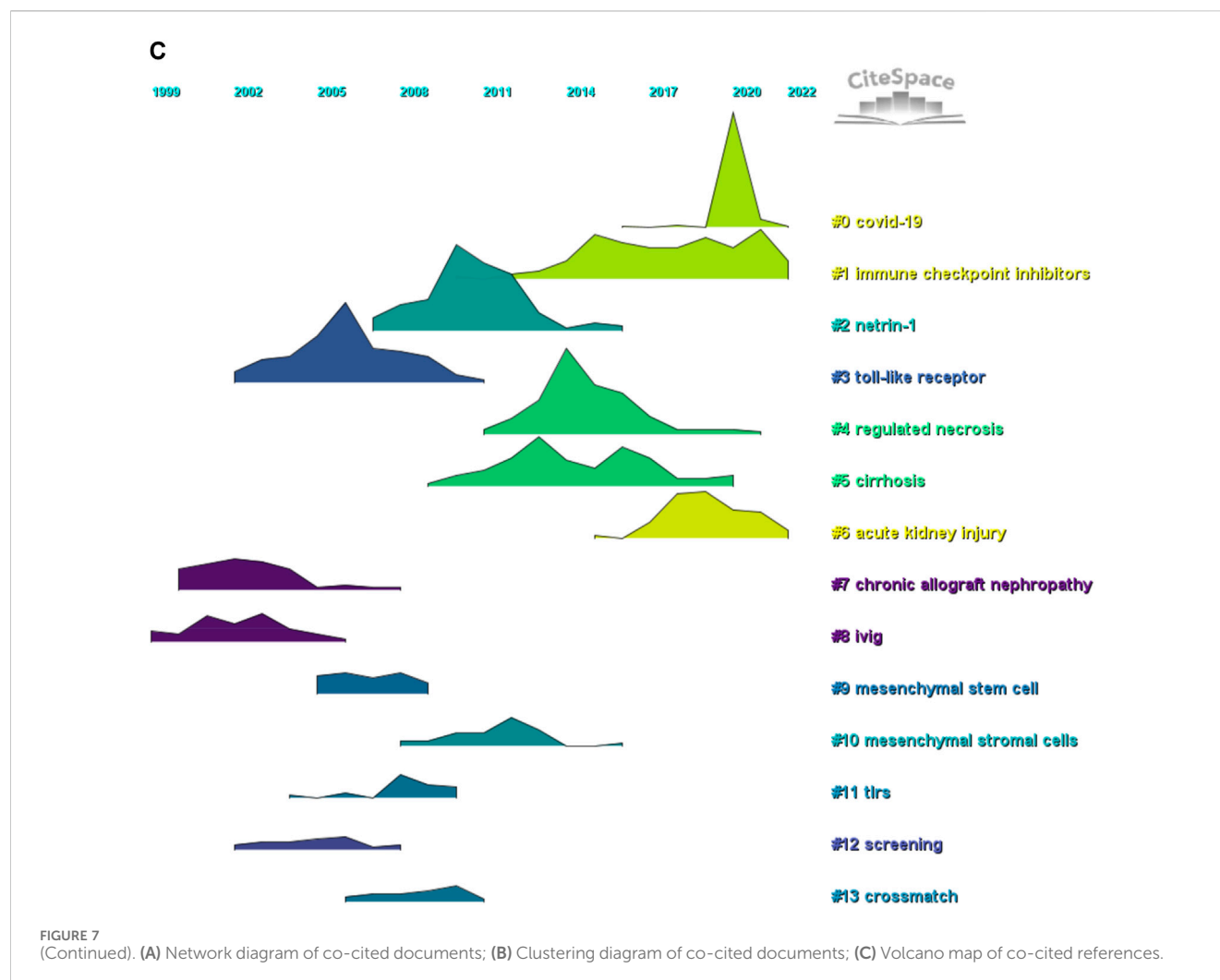
and improving renal function. A study revealed Changpu Yujin Decoction combined with CRRT is more effective than CRRT alone in the treatment of S-AKI, which could be attributed to the effective suppression of inflammation through reduced serum PCT levels, CRP and T cell subset regulations (Long et al., 2020).

The occurrence and development of renal ischemia-reperfusion injury (IRI) might mediate inflammatory response through inflammation-related signaling pathways, and blocking inflammatory response plays a very important role in improving the pathological status of AKI (Li et al., 2022; Creed et al., 2024). Relevant studies (Vande Walle and Lamkanfi, 2024; Xu K. et al., 2024) have shown that pyroptosis is a key mechanism of renal IRI. Pyroptosis is an inflammation-related programmed cell necrosis, following damage to NLRP3. The NLRP3 inflammasome is activated, which in turn promotes the release of inflammatory cytokines interleukin-1β (IL-1β) and IL-18 (Xue et al., 2024). Dl-3-N-butylphthalide (NBP) not only plays an anti-inflammatory role, but also participates in anti-oxidative stress, promoting angiogenesis, and protecting the function of the blood-brain barrier (Han et al., 2021). Studies (Dong et al., 2021; Zhu T. et al., 2024) have shown that NBP could reduce inflammation, prevent inflammatory damage caused by pyroptosis, improve microcirculation, etc. Besides, it has a good preventive effect on

IRI in heart, brain, and other tissues. Zhang et al. (2023) revealed NBP may downregulate the activity of NF-κB/NLRP3 signaling pathway and reduce the expression levels of cell pyroptosis-related proteins and inflammatory factors after renal IRI, thereby suppressing cell pyroptosis and alleviating renal IRI.

## 4.2.2 Associated immune cells and immune responses

The activation of immune cells and subsequent immune response are important factors that contribute to the further deterioration and persistence of renal function post-AKI. Therefore, the study of immune response in AKI is crucial for understanding its pathophysiology and developing novel preventive and therapeutic strategies. Various immune cells, such as neutrophils, dendritic cells (DC), macrophages, natural killer (NK) cells, NKT cells, CD4 + T cells and regulatory T cells (Tregs), are activated after AKI incidence and participate in kidney inflammation, with neutrophils, DC and Tregs playing important roles. Notably, the activation of immune cells and the resulting cascade reactions play an important role in AKI. Accordingly, interventions targeting these cells in animal studies have been demonstrated to reduce or worsen kidney damage. Targeting these cells may offer promising avenues for clinical intervention.

TABLE 6 Co-citation of top10 literature.

| Rank | Title | Journal if (2021) | Author(s) | Total citations |
|------|-------|-------------------|-----------|-----------------|
| 1 | The Incidence, Causes, and Risk Factors of Acute Kidney Injury in Patients Receiving Immune Checkpoint Inhibitors | Clinical Journal of the American Society of Nephrology (IF = 9.8) | Seethapathy H | 84 |
| 2 | Clinical Features and Outcomes of Immune Checkpoint Inhibitor-Associated AKI: A Multicenter Study | Journal of the American Society of Nephrology (IF = 13.6) | Cortazar FB | 80 |
| 3 | Clinicopathological features of acute kidney injury associated with immune checkpoint inhibitors | Kidney International (IF = 19.6) | Cortazar FB | 78 |
| 4 | Nephrotoxicity of immune checkpoint inhibitors beyond tubulointerstitial nephritis: single-centre experience | Journal for Immunotherapy of Cancer (IF = 10.9) | Mamlouk O | 74 |
| 5 | The Third International Consensus Definitions for Sepsis and Septic Shock (Sepsis-3) | Jama-Journal of the American Medical Association (IF = 120.7) | Singer M | 63 |
| 6 | Clinical features of patients infected with 2019 novel coronavirus in Wuhan, China | Lancet (IF = 168.9) | Huang CL | 62 |
| 7 | Clinical course and risk factors for mortality of adult inpatients with COVID-19 in Wuhan, China: a retrospective cohort study | Lancet (IF = 168.9) | Zhou F | 62 |
| 8 | Association of Acute Interstitial Nephritis With Programmed Cell Death 1 Inhibitor Therapy in Lung Cancer Patients | American Journal of Kidney Diseases (IF = 13.2) | Shirali AC | 60 |
| 9 | Renal histopathological analysis of 26 *postmortem* findings of patients with COVID-19 in China | Kidney International (IF = 19.6) | Su H | 59 |
| 10 | Immune-Related Adverse Events Associated with Immune Checkpoint Blockade | New England Journal of Medicine (IF = 158.5) | Postow MA | 55 |

T cells might have pathogenic and reparative effects resulting in AKI, but it is relatively unknown what is the certain mechanisms regulating T-cell responses. Noel et al. (2023) investigated the roles of the novel immune checkpoint molecule T cell immunoreceptor with Ig and immunoreceptor tyrosine-based inhibitory motif domains (TIGIT) in kidney T cells and AKI outcomes. TIGIT expression increased in mouse and kidney T cells, which would lead to worse AKI outcomes. Thus, it might be a potential therapeutic target for AKI. A experimental study (Packialakshmi et al., 2020) have demonstrated innate immune system is a leading cause to AKI (Uchida et al., 2023).

AKI is considered a common complication for patients receiving ICIs treatments, originating from either kidney injury or immune activation resulting in acute interstitial nephritis (AIN). Megan et al. (Baker et al., 2022) reported higher mortality in AKI patients unrelated to ICI than those with AIN as its underlying aetiology. It is reported tubulointerstitial nephritis as the most common renal lesion caused by ICIs (Mamlouk et al., 2019). ICIs are emerging immunotherapy that has revolutionised several kinds of malignancies (Cortazar et al., 2020). By targeting inhibitory receptors expressed on T lymphocytes, other immune cells and tumour cells, these monoclonal antibodies enhance tumour-directed immune responses, ensuring high efficacy in treating a broad spectrum of malignancies (Wei et al., 2018).

Immune-related AKI (irAKI) is the primary complication of all immune-related adverse events (Franzin et al., 2020). Correlations of irAKI incidence and causing factors have been studied, including impaired renal function at baseline, use of a PPI, ipilimumab, extrarenal irAEs, ICIs combined with chemotherapy or autoimmune disease history (Cortazar et al., 2020; Abdelrahim et al., 2021; Seethapathy et al., 2021). However, it is remain

unclear all the potential risk factors for irAKI. The outcomes of patients are greatly influenced by ICIs-induced irAKI. Therefore, when irAKI occurs, supportive treatments should be inniated instead of ICIs. There are still a lack of studiess on irAKI caused by ICIs. To our relief, the increasing number of clinical trials involving ICIs enable high-quality researches on irAKI (Liu F. et al., 2023).

The occurrence of AKI induced by ICIs may be related to the pharmacological action of the drugs themselves, leading to the release of immune brakes. Additionally, when ICIs inhibit CTLA-4/PD-1/PD-L1, the "immune brake" of the body is released, which not only strongly activates the immune ability of T cells to tumour cells, but also leads to the decrease in the tolerance of the kidney to endogenous antigens, thus triggering AKI (Izzedine et al., 2019). Furthermore, the occurrence of ICI-induced AKI could be attributed to the "multi-hit" of combined drugs on the kidney. ICIs not only affect the normal immune tolerance of the kidney to endogenous antigens but also reduce the immune tolerance of the body to other combined drugs (Wanchoo et al., 2017). The systemic immune-inflammatory index (SII), a novel inflammatory index based on neutrophils, lymphocytes and platelets, has shown promise in predicting the prognosis of various malignant tumours and inflammatory diseases (Tian et al., 2022; Chen et al., 2023). Recently, researchers have also found that SII could predict acute pancreatitis and contrast-induced AKI (Li and Liu, 2022), further highlighting its potential utility in AKI management.

AIN emerges as the most common biopsy-proven diagnosis in patients on ICI therapy experiencing AKI (Izzedine et al., 2019). The mechanism underlying this phenomenon remains elusive, but it is hypothesised that ICIs may provoke unregulated cell responses and proliferation in the tubulointerstitium. Additionally, it is plausible ICIs

FIGURE 8
(Continued).
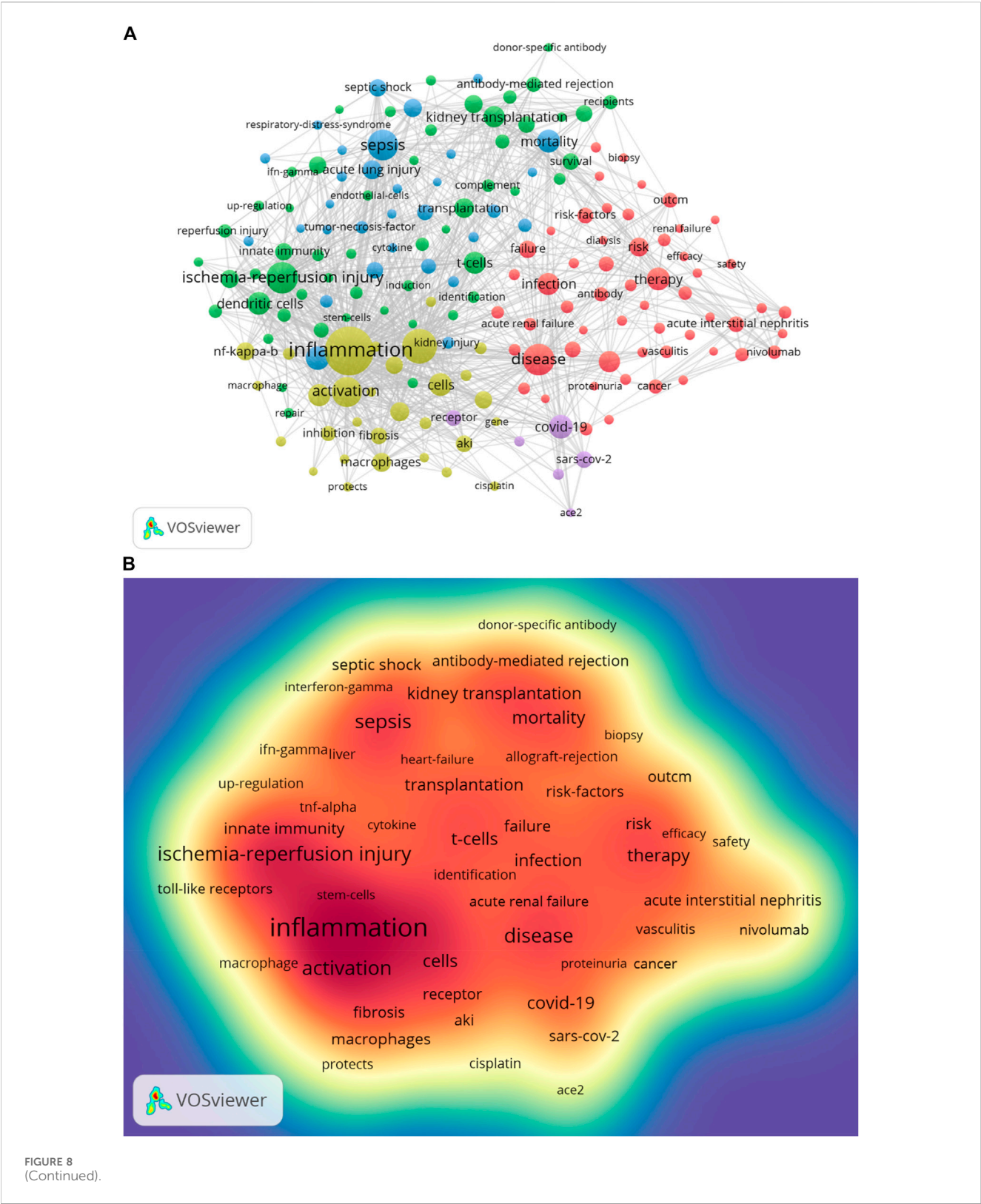
result in the loss of immune tolerance and activation of memory T cells previously primed by other haptens causing AIN (Sury et al., 2018). Studies have found a significant proportion of patients (14 of 19, 73%) on ICIs with biopsy-proven AIN had prior exposure to drugs resulting in AIN (Cortazar et al., 2016; Seethapathy et al., 2019).

Immunotherapy-related AIN could result from the loss of tolerance of drug specific effector T cells upon inhibition of PD-1 signalling. They could have experienced nephritogenic drug exposure. Another possible mechanism involves the procedure of autoimmunity to kidney self-antigens following the loss of self-

FIGURE 8
(Continued). **(A)** Keyword clustering network diagram; **(B)** Keyword density map; **(C)** Keyword volcano map.
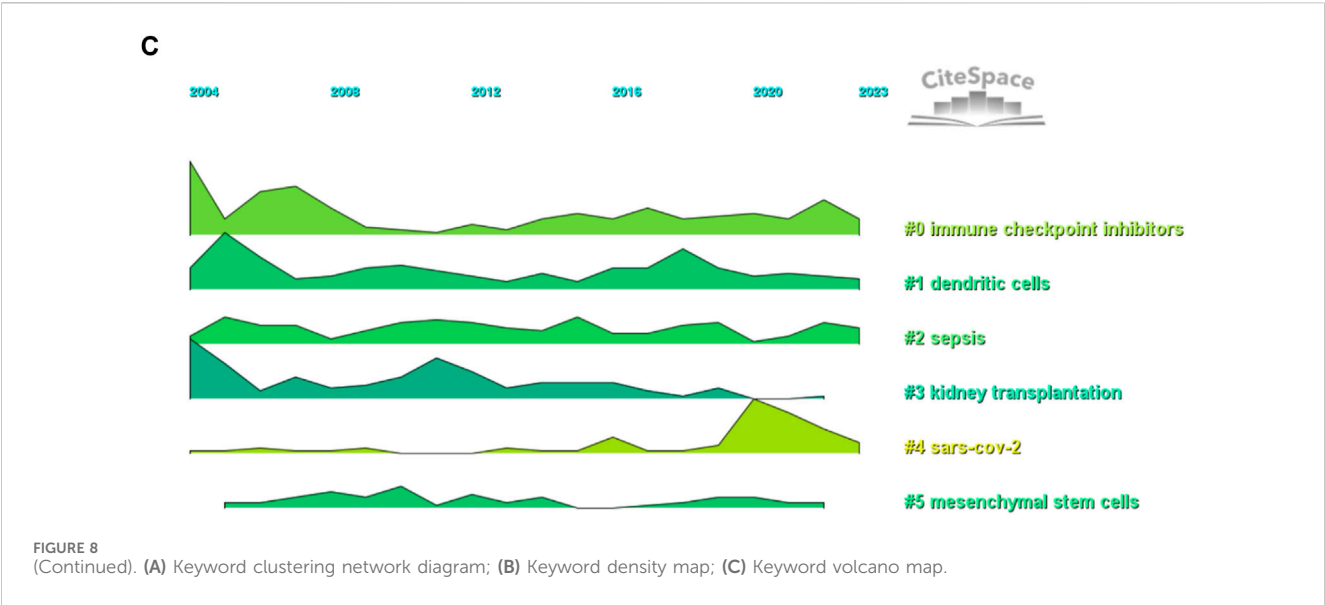
TABLE 7 High-frequency keywords.

| Rank | Keyword | Counts | Rank | Keyword | Counts |
|---|---|---|---|---|---|
| 1 | inflammation | 575 | 11 | dendritic cells | 164 |
| 2 | expression | 330 | 12 | mortality | 162 |
| 3 | ischaemia-reperfusion injury | 283 | 13 | t cells | 159 |
| 4 | disease | 279 | 14 | apoptosis | 156 |
| 5 | Sepsis | 267 | 15 | infection | 153 |
| 6 | activation | 256 | 16 | glomerulonephritis | 148 |
| 7 | covid-19 | 174 | 17 | kidney transplantation | 148 |
| 8 | oxidative stress | 171 | 18 | transplantation | 131 |
| 9 | Cells | 167 | 19 | acute lung injury | 123 |
| 10 | therapy | 165 | 20 | risk | 123 |

tolerance and potentiation of antigen recognition upon blocking the CTLA-4 or PD-1 pathway, which regulates immunity at peripheral and target organ levels, respectively (Mamlouk et al., 2019). Furthermore, individuals recovering from AKI have great possibility of developing CKD. The transition of underlying mechanisms might involve sustained activation of renal innate immunity, renal inflammation and fibrosis, et al. These existing factors offer a plausible explanation for increase in the transition rate from AKI to CKD (Albino et al., 2021).

### 4.2.3 Underlying pathways of action

It is gradually recognised mitochondrial dysfunction as a critical factor to AKI. Th of damaged mitochondria mediating AKI are multifactorial and complex. The cyclic GMP-AMP synthase (cGAS) stimulator of the interferon genes (STING) (cGAS-STING) pathway detects cytosolic DNA and induces innate immunity. Studies have shown that mitochondrial DNA (mtDNA) depletion and repletion might result in tubular inflammatory responses via the cGAS-STING signal activation by cytosolic mtDNA. Similarly, Hiroshi et al. (Maekawa et al., 2019) concluded mitochondrial dysfunction and subsequent mtDNA-cGAS-STING pathway activation as critical regulator of AKI. There have been showing great importance of circulating mtDNA and related pathways in the progression of AKI, and regulating the related proteins could serve as an potential strategy to alleviate AKI (Liu et al., 2021). Qi et al. (2023) observed the activation of cGAS-STING pathway in cisplatin induced AKI. After inhibiting this pathway, the activation of TNF-α, IL-6, IL-8, ICAM-1, MCP-1 and other inflammatory factors were inhibited, thus improving the renal tissue structure, and promoting the recovery of renal function. Luo et al. (2022) found in human kidney-2 (HK-2) cultured *in vitro* that the expressions of cGAS and STING were significantly increased after cisplatin intervention, while significantly decreased after β-hydroxybutyrate treatment, and the autophagy, inflammation and apoptosis of cells were also decreased.

## A

# Top 50 References with the Strongest Citation Bursts

| References | Year | Strength | Begin | End | 2004 - 2023 |
|---|---|---|---|---|---|
| Leemans JC, 2005, J CLIN INVEST, V115, P2894, DOI 10.1172/JCI22832, DOI | 2005 | 16.74 | 2007 | 2010 | |
| Bonventre JV, 2004, KIDNEY INT, V66, P480, DOI 10.1111/j.1523-1755.2004.761, 2.x, DOI | 2004 | 9.44 | 2007 | 2009 | |
| Wu HL, 2007, J CLIN INVEST, V117, P2847, DOI 10.1172/JCI31008, DOI | 2007 | 21.35 | 2008 | 2012 | |
| Shigeoka AA, 2007, J IMMUNOL, V178, P6252, DOI 10.4049/jimmunol.178.10.6252, DOI | 2007 | 15.85 | 2008 | 2012 | |
| Dong X, 2007, KIDNEY INT, V71, P619, DOI 10.1038/sj.ki.5002132, DOI | 2007 | 13.65 | 2008 | 2012 | |
| Day YJ, 2006, J IMMUNOL, V176, P3108, DOI 10.4049/jimmunol.176.5.3108, DOI | 2006 | 10.53 | 2008 | 2010 | |
| Li L, 2007, J IMMUNOL, V178, P5899, DOI 10.4049/jimmunol.178.9.5899, DOI | 2007 | 10.18 | 2009 | 2012 | |
| Jang HR, 2009, CLIN IMMUNOL, V130, P41, DOI 10.1016/j.clim.2008.08.016, DOI | 2009 | 14.44 | 2010 | 2014 | |
| Krüger B, 2009, P NATL ACAD SCI USA, V106, P3390, DOI 10.1073/pnas.0810169106, DOI | 2009 | 12.89 | 2010 | 2014 | |
| Li L, 2008, KIDNEY INT, V74, P1526, DOI 10.1038/ki.2008.500, DOI | 2008 | 12.79 | 2010 | 2013 | |
| Gandolfo MT, 2009, KIDNEY INT, V76, P717, DOI 10.1038/ki.2009.259, DOI | 2009 | 12.37 | 2010 | 2014 | |
| Kinsey GR, 2009, J AM SOC NEPHROL, V20, P1744, DOI 10.1681/ASN.2008111160, DOI | 2009 | 12.37 | 2010 | 2014 | |
| Pulskens WP, 2008, PLOS ONE, V3, P0, DOI 10.1371/journal.pone.0003596, DOI | 2008 | 10 | 2010 | 2013 | |
| Li L, 2010, SEMIN NEPHROL, V30, P268, DOI 10.1016/j.semnephrol.2010.03.005, DOI | 2010 | 11.33 | 2011 | 2015 | |
| Solez K, 2008, AM J TRANSPLANT, V8, P753, DOI 10.1111/j.1600-6143.2008.02159.x, DOI | 2008 | 10.59 | 2011 | 2013 | |
| Lee S, 2011, J AM SOC NEPHROL, V22, P317, DOI 10.1681/ASN.2009060615, DOI | 2011 | 13.6 | 2012 | 2016 | |
| Wu HL, 2010, J AM SOC NEPHROL, V21, P1878, DOI 10.1681/ASN.2009101048, DOI | 2010 | 12.24 | 2012 | 2014 | |
| Bonventre JV, 2011, J CLIN INVEST, V121, P4210, DOI 10.1172/JCI45161, DOI | 2011 | 19.55 | 2013 | 2016 | |
| Eltzschig HK, 2011, NAT MED, V17, P1391, DOI 10.1038/nm.2507, DOI | 2011 | 10.29 | 2013 | 2016 | |
| Lech M, 2014, J AM SOC NEPHROL, V25, P292, DOI 10.1681/ASN.2013020152, DOI | 2014 | 11.13 | 2014 | 2019 | |
| Eckardt KU, 2012, KIDNEY INT SUPPL, V2, P7, DOI 10.1038/kisup.2012.8, DOI | 2012 | 10.28 | 2014 | 2017 | |
| Moreau R, 2013, GASTROENTEROLOGY, V144, P1426, DOI 10.1053/j.gastro.2013.02.042, DOI | 2013 | 9.2 | 2014 | 2017 | |
| Kurts C, 2013, NAT REV IMMUNOL, V13, P738, DOI 10.1038/nri3523, DOI | 2013 | 13.45 | 2015 | 2018 | |
| Haas M, 2014, AM J TRANSPLANT, V14, P272, DOI 10.1111/ajt.12590, DOI | 2014 | 9.67 | 2015 | 2018 | |
| Jang HR, 2015, NAT REV NEPHROL, V11, P88, DOI 10.1038/nrneph.2014.180, DOI | 2015 | 18.62 | 2016 | 2020 | |
| Izzedine H, 2014, INVEST NEW DRUG, V32, P769, DOI 10.1007/s10637-014-0092-7, DOI | 2014 | 9.33 | 2016 | 2019 | |
| Cortazar FB, 2016, KIDNEY INT, V90, P638, DOI 10.1016/j.kint.2016.04.008, DOI | 2016 | 21.56 | 2017 | 2021 | |
| Singer M, 2016, JAMA-J AM MED ASSOC, V315, P801, DOI 10.1001/jama.2016.0287, DOI | 2016 | 17.37 | 2017 | 2021 | |
| Shirali AC, 2016, AM J KIDNEY DIS, V68, P287, DOI 10.1053/j.ajkd.2016.02.057, DOI | 2016 | 16.54 | 2017 | 2021 | |
| Rabb H, 2016, J AM SOC NEPHROL, V27, P371, DOI 10.1681/ASN.2015030261, DOI | 2016 | 10.44 | 2017 | 2021 | |
| Wanchoo R, 2017, AM J NEPHROL, V45, P160, DOI 10.1159/000455014, DOI | 2017 | 9.72 | 2018 | 2023 | |
| Mamlouk O, 2019, J IMMUNOTHER CANCER, V7, P0, DOI 10.1186/s40425-018-0478-8, DOI | 2019 | 10.02 | 2019 | 2023 | |
| Huang CL, 2020, LANCET, V395, P497, DOI 10.1016/S0140-6736(20)30183-5, DOI | 2020 | 16.83 | 2020 | 2021 | |
| Zhou F, 2020, LANCET, V395, P1054, DOI 10.1016/S0140-6736(20)30566-3, DOI | 2020 | 15.43 | 2020 | 2021 | |
| Hoffmann M, 2020, CELL, V181, P271, DOI 10.1016/j.cell.2020.02.052, DOI | 2020 | 14.26 | 2020 | 2023 | |
| Cheng YC, 2020, KIDNEY INT, V97, P829, DOI 10.1016/j.kint.2020.03.005, DOI | 2020 | 12.35 | 2020 | 2023 | |
| Su H, 2020, KIDNEY INT, V98, P219, DOI 10.1016/j.kint.2020.04.003, DOI | 2020 | 12.3 | 2020 | 2023 | |
| Varga Z, 2020, LANCET, V395, P1417, DOI 10.1016/S0140-6736(20)30937-5, DOI | 2020 | 11.04 | 2020 | 2023 | |
| Mehta P, 2020, LANCET, V395, P1033, DOI 10.1016/S0140-6736(20)30628-0, DOI | 2020 | 10.11 | 2020 | 2023 | |
| Guan W, 2020, NEW ENGL J MED, V382, P1708, DOI 10.1056/NEJMoa2002032, DOI | 2020 | 9.36 | 2020 | 2021 | |
| Manohar S, 2019, NEPHROL DIAL TRANSPL, V34, P108, DOI 10.1093/ndt/gfy105, DOI | 2019 | 9.19 | 2020 | 2023 | |
| Ronco C, 2019, LANCET, V394, P1949, DOI 10.1016/S0140-6736(19)32563-2, DOI | 2019 | 9.19 | 2020 | 2023 | |
| Cortazar FB, 2020, J AM SOC NEPHROL, V31, P435, DOI 10.1681/ASN.2019070676, DOI | 2020 | 18.75 | 2021 | 2023 | |
| Peerapornratana S, 2019, KIDNEY INT, V96, P1083, DOI 10.1016/j.kint.2019.05.026, DOI | 2019 | 10.23 | 2021 | 2023 | |
| Gupta S, 2021, J IMMUNOTHER CANCER, V9, P0, DOI 10.1136/jitc-2021-003467, DOI | 2021 | 20.14 | 2022 | 2023 | |
| Seethapathy H, 2019, CLIN J AM SOC NEPHRO, V14, P1692, DOI 10.2215/CJN.00990119, DOI | 2019 | 18.77 | 2022 | 2023 | |
| Meraz-Muñoz A, 2020, J IMMUNOTHER CANCER, V8, P0, DOI 10.1136/jitc-2019-000467, DOI | 2020 | 17.28 | 2022 | 2023 | |
| Espi M, 2021, EUR J CANCER, V147, P29, DOI 10.1016/j.ejca.2021.01.005, DOI | 2021 | 10.52 | 2022 | 2023 | |
| Hoste EAJ, 2018, NAT REV NEPHROL, V14, P607, DOI 10.1038/s41581-018-0052-0, DOI | 2018 | 10.04 | 2022 | 2023 | |
| Stein C, 2021, NEPHROL DIAL TRANSPL, V36, P1664, DOI 10.1093/ndt/gfaa137, DOI | 2021 | 9.56 | 2022 | 2023 | |

**FIGURE 9**
(Continued).

Studies (Tang et al., 2018; Pabla and Bajwa, 2022) have revealed that disruption of mitochondrial homeostasis related to mitochondrial biogenesis, mitochondrial autophagy and increased membrane permeability are all related to renal tubule injury and inflammation in AKI. Li et al. (2023) showed that phosphoglycerate mutase 5 (PGAM 5) mediated Bax dephosphorylation induced mtDNA release and cGAS-STING pathway activation are closely related to inflammation and kidney injury. In mice models with PGAM5 or cGAS knockout, renal injury and inflammation caused by IRI were alleviated to varying degrees. Besides, the same results were observed in the renal proximal tubule epithelial cells of mice treated with hypoxia/reoxygenation *in vitro*. Relevant study (Feng et al., 2022) has shown that receptor interacting protein 3 (RIP3) mediates the release of mtDNA through translocation to mitochondria, thereby activating cGAS-STING pathway and aggravating renal IRI. Therefore, the mtDNA-cGAS-STING pathway is a key regulator of tubular inflammation that contributes to AKI and is a potential therapeutic target for preventing the progression of tubular inflammation-mediated kidney injury.

**B**
## Top 50 Keywords with the Strongest Citation Bursts

| Keywords | Year | Strength | Begin | End | 2004 - 2023 |
|---|---|---|---|---|---|
| acute renal failure | 2004 | 49.99 | 2004 | 2012 | |
| delayed graft function | 2005 | 9.21 | 2007 | 2014 | |
| reperfusion injury | 2006 | 8.06 | 2009 | 2016 | |
| acute myocardial infarction | 2006 | 7.33 | 2011 | 2016 | |
| antibody mediated rejection | 2011 | 6.2 | 2011 | 2017 | |
| mesenchymal stem cells | 2008 | 5.75 | 2013 | 2014 | |
| regulatory t cells | 2010 | 9.09 | 2014 | 2017 | |
| renal transplantation | 2004 | 5.38 | 2014 | 2016 | |
| graft survival | 2005 | 5.7 | 2015 | 2017 | |
| systemic lupus erythematosus | 2004 | 4.79 | 2015 | 2017 | |
| hepatorenal syndrome | 2015 | 4.69 | 2015 | 2016 | |
| mechanisms | 2009 | 5.4 | 2016 | 2019 | |
| transplant recipients | 2016 | 4.43 | 2016 | 2016 | |
| ischemia reperfusion injury | 2005 | 10.17 | 2017 | 2018 | |
| macrophages | 2011 | 7.92 | 2018 | 2020 | |
| pathophysiology | 2018 | 7.6 | 2018 | 2023 | |
| clinical research | 2018 | 6.7 | 2018 | 2020 | |
| immune modulation | 2014 | 5.89 | 2018 | 2020 | |
| molecular mechanisms | 2018 | 4.75 | 2018 | 2023 | |
| extracellular vesicles | 2019 | 5.67 | 2019 | 2023 | |
| pathway | 2019 | 5.53 | 2019 | 2023 | |
| animal models | 2019 | 5.37 | 2019 | 2021 | |
| responses | 2013 | 4.89 | 2019 | 2021 | |
| infection | 2006 | 11.63 | 2020 | 2021 | |
| coronavirus | 2020 | 9.42 | 2020 | 2023 | |
| cytokine storm | 2020 | 9.16 | 2020 | 2021 | |
| covid 19 | 2020 | 7.8 | 2020 | 2023 | |
| management | 2009 | 7.55 | 2020 | 2023 | |
| ace2 | 2020 | 7.26 | 2020 | 2023 | |
| immunotherapy | 2020 | 5.92 | 2020 | 2023 | |
| coronavirus disease 2019 | 2020 | 5.72 | 2020 | 2021 | |
| acute respiratory syndrome | 2020 | 5.25 | 2020 | 2021 | |
| sars coronavirus | 2020 | 5.25 | 2020 | 2021 | |
| aki | 2016 | 5.14 | 2020 | 2023 | |
| immune-related adverse events | 2020 | 5.11 | 2020 | 2023 | |
| mitochondrial dysfunction | 2018 | 4.81 | 2020 | 2023 | |
| receptor | 2004 | 4.66 | 2020 | 2021 | |
| immune checkpoint inhibitors | 2018 | 13.33 | 2021 | 2023 | |
| case report | 2017 | 7.32 | 2021 | 2023 | |
| autophagy | 2021 | 5.88 | 2021 | 2023 | |
| association | 2008 | 5.55 | 2021 | 2023 | |
| pembrolizumab | 2021 | 5.43 | 2021 | 2023 | |
| vasculitis | 2004 | 4.71 | 2021 | 2023 | |
| hospitalized patients | 2021 | 4.53 | 2021 | 2021 | |
| melanoma | 2022 | 5.83 | 2022 | 2023 | |
| systemic immune-inflammation index | 2022 | 4.86 | 2022 | 2023 | |
| features | 2022 | 4.86 | 2022 | 2023 | |
| adverse events | 2015 | 4.66 | 2022 | 2023 | |
| neutrophil | 2022 | 4.63 | 2022 | 2023 | |
| nivolumab | 2017 | 4.59 | 2022 | 2023 | |

FIGURE 9
(Continued). **(A)** Top 50 references with the strongest citation bursts; **(B)** Top 50 keywords with the strongest citation bursts.

Inflammatory response is an important activation in maintaining body homeostasis. Involved in systemic immune response and inflammatory response, toll-like receptors (TLRs) can mediate immune cells to recognize pathogenic microorganisms and trigger systemic immune response (Jin et al., 2018). Toll like receptor 4 (TLR4) is an important pathogen pattern recognition receptor (Schattner, 2019), and it can initiate pro-inflammatory effects through various pathways including nucleotide binding oligomerization domain-like receptor protein 3 (NLRP3), myeloid differentiation factor 88 (MyD88), etc. (Wu et al., 2020; Ciesielska

et al., 2021). When AKI occurs, the expression of TLR4 in kidney tissue is significantly increased, which triggers inflammatory response and leads to a series of pathological changes. TLR4 recognizes endotoxin and its downstream reaction play an critical role in the pathophysiology of AKI caused by lipopolysaccharide (LPS) (Mohamed et al., 2017). Studies have shown that the expression of TLR4 is significantly increased in animal models of LPS-induced AKI, and the increase of TLR4 level after LPS induction may be related to the increase of inflammatory cytokine mediated receptor expression. Epigallocatechin gallate (EGCG), the main catechin of green tea extract, is a powerful antioxidant and active oxygen scavenger (Eng et al., 2018). EGCG exhibits a protective effect against LPS-induced AKI by inhibiting the activation of TLR4/Myd88/NF-κB pathway.

The renal tissue of SAKI patients showed capillary endothelial injury, renal interstitial neutrophils and other inflammatory cell infiltration, and high expression of inflammatory factors, suggesting that inflammation plays an important regulatory role in the pathogenesis of SAKI (Zarbock et al., 2023). Lipoxin A4 (LXA4) has a significant negative regulatory effect on inflammation (Han et al., 2022), which can reduce sepsis-related inflammation and improve the survival rate of patients with sepsis (Hu et al., 2020). Activation of TLR4/Myd88/NF-κB pathway is one of the generally recognized mechanisms in inflammatory response. The activation of this pathway promotes the transcription of many pro-inflammatory cytokines and adhesion molecules such as IL-1B, IL-6, TNF-α, etc. These inflammatory mediators further activate the body's defense system, resulting in continuous excessive release of inflammatory mediators, and ultimately lead to systemic inflammatory response syndrome characterized by the destruction of cells themselves (Feng et al., 2018). It is speculated that TLR4/Myd88/NF-κB signaling pathway aggravates renal tissue injury by mediating the production and release of inflammatory factors including IL-1B, IL-6 and TNF-α. Regulation of TLR4/Myd88/NF-κB signaling is of great significance in alleviating the occurrence and development of S-AKI.

Ferroptosis is involved in the development of AKI through pathological processes such as inflammation, endoplasmic reticulum stress and autophagy (Qiao et al., 2023). Zhu Z. et al. (2024) revealed that Ferroptosis inhibition Fer-1 and DFO promoted cell viability and reduced intracellular reactive oxygen species (ROS) production in contrast-induced AKI (CI-AKI). Besides, TMP significantly inhibited renal dysfunction, reduced AKI biomarkers, prevented ROS production, inhibited renal $Fe^{2+}$ accumulation and increased glutathione peroxidase 4 (GPX4) expression. Regarding siRNA knockdown, plasmid overexpression of transferrin receptor (TFRC) and ferroptosis inhibitors, it indicates that TFRC-mediated ferroptosis plays a crucial role in CIN, whereas antioxidant TMP could exert an anti-ferroptosis effect to prevent such a pathological process by inhibiting TFRC and intracellular ROS production. Ferroptosis is also involved in various stages of IRI, and GPX4 and solute carrier family 7 members 11 (SLC7A11) are downregulated in renal tissue of IRI-induced AKI. Nuclear factor-E2-related factor 2 (NRF2), NADPH oxidase 1 (NOX1), and cyclooxygenase-2 (COX2) are upregulated, indicating the occurrence of Ferroptosis in IRI-AKI. Among them, non-coding microRNAs, miR-182-5p and miR-378a-3p target downregulate the expression of GPX4 and SLC7A11, which might induce the occurrence of Ferroptosis (Ding et al., 2020).

NRF2 plays a key role in regulating the occurrence and development of AKI by participating in ferroptosis (Hu et al.,

2022). Studies (Zhang et al., 2021; Qiongyue et al., 2022) have shown that constitutionally activated NRF2 is closely related to the high incidence of various kidney diseases, and targeting NRF2 is regarded as an effective strategy for AKI treatment. NRF2 is an intracellular transcription factor that could protect against oxidative stress damage, and SLC7A11 is a substrate specific subunit of glutamate reverse transporter Xc-, and GPX4 is a core enzyme regulating the endogenous antioxidant system glutathione system. Therefore, NRF2 is a key factor in the classical pathway of ferroptosis. By down-regulating the expression of SLC7A11/GPX4, ferroptosis is induced, which interferes with the immune microenvironment of various diseases and affects the progression of diseases (Li P. et al., 2024; Yang et al., 2024). NRF2, as an upstream factor of the classical pathway of ferroptosis, could mediate the activation of the NRF2/SLC7A11/GPX4 axis to inhibit ferroptosis, interfere with the immune microenvironment of various diseases, and affect disease progression. Further, it is predicted that regulating the NRF2/SLC7A11/GPX4 axis-mediated process of ferroptosis and regulating the immune microenvironment to inhibit AKI progression might be the focus and direction of future research.

# 5 Conclusion

The bibliometric analysis offers a comprehensive overview of research trends and hotspots in the domain of immunisation associated with AKI. This method facilitates the visualisation of current research status and future trends. This study delved into the publication landscape of AKI-related immunisation research. Notably, the volume of publications is steadily increasing, with significant contributions from the United States and China. Furthermore, national institutions are providing substantial support for such research endeavours. Scholars exhibit unique research directions and demonstrate distinct preferences for particular journals. Keyword clustering analysis sheds light on current research hotspots, while the examination of highly cited and co-cited literature offers valuable guidance for newcoming peer studies. However, attention should be paied to insufficient collaborations among countries, institutions and researchers, which are significant for the future development of researches.

# 6 Limitations

While bibliometric analysis provides valuable insights into research focus and trends, it is not without limitations. First, the data source were solely from the WoSCC database, potentially introducing selective bias. Incorporating other databases such as PubMed and Scopus could enhance literature coverage and study accuracy. Second, as only English publications were retrieved, important articles in other languages may have been overlooked. Third, self-citation could introduce inherent bias in bibliometric analysis. Additionally, tools for bibliometric analysis, including CiteSpace and VOSviewer, may possess inherent limitations and biases that could impact analytic results. Finally, our search deadline was 10th December 2023, and while the WoSCC database is updated daily, some significant studies may not have been included. Nonetheless, we believe this study has incorporated

comprehensive publications up to 2023 and conclusions drawn remain robust even with the emergence of new data.

## Data availability statement

The original contributions presented in the study are included in the article/Supplementary material, further inquiries can be directed to the corresponding authors.

## Author contributions

LC: Writing–review and editing, Writing–original draft, Visualization, Validation, Supervision, Software, Resources, Project administration, Methodology, Investigation, Funding acquisition, Formal Analysis, Data curation, Conceptualization. JH: Writing–review and editing, Writing–original draft, Visualization, Validation, Supervision, Software, Resources, Project administration, Methodology, Investigation, Funding acquisition, Formal Analysis, Data curation, Conceptualization. JL: Writing–review and editing, Writing–original draft, Visualization, Validation, Supervision, Software, Resources, Project administration, Methodology, Investigation, Funding acquisition, Formal Analysis, Data curation, Conceptualization. XG: Writing–review and editing, Writing–original draft, Visualization, Validation, Supervision, Software, Resources, Project administration, Methodology, Investigation, Funding acquisition, Formal Analysis, Data curation, Conceptualization.

## Conflict of interest

The authors declare that the research was conducted in the absence of any commercial or financial relationships that could be construed as a potential conflict of interest.

## Publisher's note

All claims expressed in this article are solely those of the authors and do not necessarily represent those of their affiliated organizations, or those of the publisher, the editors and the reviewers. Any product that may be evaluated in this article, or claim that may be made by its manufacturer, is not guaranteed or endorsed by the publisher.

## References

Abdelrahim, M., Mamlouk, O., Lin, H., Lin, J., Page, V., Abdel-Wahab, N., et al. (2021). Incidence, predictors, and survival impact of acute kidney injury in patients with melanoma treated with immune checkpoint inhibitors: a 10-year single-institution analysis. *Oncoimmunology* 10 (1), 1927313. doi:10.1080/2162402x.2021.1927313

Albino, A. H., Zambom, F. F. F., Foresto-Neto, O., Oliveira, K. C., Ávila, V. F., Arias, S. C. A., et al. (2021). Renal inflammation and innate immune activation underlie the transition from gentamicin-induced acute kidney injury to renal fibrosis. *Front. Physiol.* 12, 606392. doi:10.3389/fphys.2021.606392

Baker, M. L., Yamamoto, Y., Perazella, M. A., Dizman, N., Shirali, A. C., Hafez, N., et al. (2022). Mortality after acute kidney injury and acute interstitial nephritis in patients prescribed immune checkpoint inhibitor therapy. *J. Immunother. Cancer* 10 (3), e004421. doi:10.1136/jitc-2021-004421

Chen, L., Ye, Z., Wang, D., Liu, J., Wang, Q., Wang, C., et al. (2022). Chuan Huang Fang combining reduced glutathione in treating acute kidney injury (grades 1-2) on chronic kidney disease (stages 2-4): a multicenter randomized controlled clinical trial. *Front. Pharmacol.* 13, 969107. doi:10.3389/fphar.2022.969107

Chen, Y., Wang, H., Zuo, X. G., and Cao, Q. (2023). The predictive value of systemic immune inflammation index for early acute kidney injury in patients undergoing adult cardiac surgery with cardiopulmonary bypass. *J. Clin. Emerg.* 24 (11), 561–566. doi:10.13201/j.issn.1009-5918.2023.11.002

Choi, H. S., Mathew, A. P., Uthaman, S., Vasukutty, A., Kim, I. J., Suh, S. H., et al. (2022). Inflammation-sensing catalase-mimicking nanozymes alleviate acute kidney injury via reversing local oxidative stress. *J. Nanobiotechnology* 20 (1), 205. doi:10.1186/s12951-022-01410-z

Ciesielska, A., Matyjek, M., and Kwiatkowska, K. (2021). TLR4 and CD14 trafficking and its influence on LPS-induced pro-inflammatory signaling. *Cell. Mol. Life Sci.* 78 (4), 1233–1261. doi:10.1007/s00018-020-03656-y

Cortazar, F. B., Kibbelaar, Z. A., Glezerman, I. G., Abudayyeh, A., Mamlouk, O., Motwani, S. S., et al. (2020). Clinical features and outcomes of immune checkpoint inhibitor-associated AKI: a multicenter study. *J. Am. Soc. Nephrol.* 31 (2), 435–446. doi:10.1681/asn.2019070676

Cortazar, F. B., Marrone, K. A., Troxell, M. L., Ralto, K. M., Hoenig, M. P., Brahmer, J. R., et al. (2016). Clinicopathological features of acute kidney injury associated with

immune checkpoint inhibitors. *Kidney Int.* 90 (3), 638–647. doi:10.1016/j.kint.2016.04.008

Creed, H. A., Kannan, S., Tate, B. L., Godefroy, D., Banerjee, P., Mitchell, B. M., et al. (2024). Single-cell RNA sequencing identifies response of renal lymphatic endothelial cells to acute kidney injury. *J. Am. Soc. Nephrol.* 35 (5), 549–565. doi:10.1681/asn.0000000000000325

Deng, B., Wang, S., Zhou, P., and Ding, F. (2023). New insights into immune cell diversity in acute kidney injury. *Cell. Mol. Immunol.* 20 (6), 680–682. doi:10.1038/s41423-023-01003-2

Ding, C., Ding, X., Zheng, J., Wang, B., Li, Y., Xiang, H., et al. (2020). miR-182-5p and miR-378a-3p regulate ferroptosis in I/R-induced renal injury. *Cell. Death Dis.* 11 (10), 929. doi:10.1038/s41419-020-03135-z

Ding, X. X., Wang, J. G., Liu, X. Y., Li, Q. Q., Deng, M. Y., and Li, T. (2023). Approach to protective effect and mechanism of pretreatment with emodin on acute renal injury in rats with sepsis. *Shanxi J. Traditional Chin. Med.* 39 (11), 57–61. doi:10.20002/j.issn.1000-7156.2023.11.022

Dong, Y., Yin, J., Chen, T., Wen, J., Zhang, Q., Li, X., et al. (2021). Dl-3-n-butylphthalide pretreatment attenuates renal ischemia/reperfusion injury. *Biochem. Biophys. Res. Commun.* 557, 166–173. doi:10.1016/j.bbrc.2021.04.006

Eisenstein, M. (2023). What is acute kidney injury? A visual guide. *Nature* 615 (7954), S112–s113. doi:10.1038/d41586-023-00804-9

Eng, Q. Y., Thanikachalam, P. V., and Ramamurthy, S. (2018). Molecular understanding of Epigallocatechin gallate (EGCG) in cardiovascular and metabolic diseases. *J. Ethnopharmacol.* 210, 296–310. doi:10.1016/j.jep.2017.08.035

Fan, F., and Xu, P. (2023). Global biomarkers trends in acute kidney injury: a bibliometric analysis. *Ren. Fail* 45 (2), 2278300. doi:10.1080/0886022x.2023.2278300

Fan, Y., Yuan, Y., Xiong, M., Jin, M., Zhang, D., Yang, D., et al. (2023). Tet1 deficiency exacerbates oxidative stress in acute kidney injury by regulating superoxide dismutase. *Theranostics* 13 (15), 5348–5364. doi:10.7150/thno.87416

Feng, D., Wang, Y., Liu, Y., Wu, L., Li, X., Chen, Y., et al. (2018). DC-SIGN reacts with TLR-4 and regulates inflammatory cytokine expression via NF-κB activation in renal

tubular epithelial cells during acute renal injury. *Clin. Exp. Immunol.* 191 (1), 107–115. doi:10.1111/cei.13048

Feng, Y., Imam Aliagan, A., Tombo, N., Draeger, D., and Bopassa, J. C. (2022). RIP3 translocation into mitochondria promotes mitofilin degradation to increase inflammation and kidney injury after renal ischemia-reperfusion. *Cells* 11 (12), 1894. doi:10.3390/cells11121894

Fortrie, G., de Geus, H. R. H., and Betjes, M. G. H. (2019). The aftermath of acute kidney injury: a narrative review of long-term mortality and renal function. *Crit. Care* 23 (1), 24. doi:10.1186/s13054-019-2314-z

Franzin, R., Netti, G. S., Spadaccino, F., Porta, C., Gesualdo, L., Stallone, G., et al. (2020). The use of immune checkpoint inhibitors in oncology and the occurrence of AKI: where do we stand? *Front. Immunol.* 11, 574271. doi:10.3389/fimmu.2020.574271

Gong, X., Duan, Y., Wang, Y., Ye, Z., Zheng, J., Lu, W., et al. (2020). Effects of Chuanhuang Decoction on renal function and oxidative stress in patients of chronic kidney disease at stage 2-4 complicated with acute kidney injury. *J. Shanghai Univ. Trad. Chin. Med. Sci.* 34 (1), 11–16. doi:10.16306/j.1008-861x.2020.01.002

Gong, X., Ye, Z., Xu, X., Chen, L., Xu, Y., Yuan, D., et al. (2021). Effects of Chuanhuang Formula combined with prostaglandin E1 in treating patients of chronic kidney disease complicated with acute kidney injury and its influence on NLRP3. *J. Shanghai Univ. Trad. Chin. Med. Sci.* 35 (06), 12–16. doi:10.16306/j.1008-861x.2021.06.002

Gumbert, S. D., Kork, F., Jackson, M. L., Vanga, N., Ghebremichael, S. J., Wang, C. Y., et al. (2020). Perioperative acute kidney injury. *Anesthesiology* 132 (1), 180–204. doi:10.1097/aln.0000000000002968

Han, B., Xu, J., Shi, X., Zheng, Z., Shi, F., Jiang, F., et al. (2021). DL-3-n-Butylphthalide attenuates myocardial hypertrophy by targeting gasdermin D and inhibiting gasdermin D mediated inflammation. *Front. Pharmacol.* 12, 688140. doi:10.3389/fphar.2021.688140

Han, M., Lai, S., Ge, Y., Zhou, X., and Zhao, J. (2022). Changes of lipoxin A4 and the anti-inflammatory role during parturition. *Reprod. Sci.* 29 (4), 1332–1342. doi:10.1007/s43032-021-00800-2

He, J. L., Nie, F. F., Hu, L., and Xu, Y. L. (2024). Pathogenesis of sepsis-associated acute kidney injury. *J. Med. Inf.* 37 (05), 174–177+187. doi:10.3969/j.issn.1006-1959.2024.05.033

He, L., Wei, Q., Liu, J., Yi, M., Liu, Y., Liu, H., et al. (2017). AKI on CKD: heightened injury, suppressed repair, and the underlying mechanisms. *Kidney Int.* 92 (5), 1071–1083. doi:10.1016/j.kint.2017.06.030

Hu, J., Gu, W., Ma, N., Fan, X., and Ci, X. (2022). Leonurine alleviates ferroptosis in cisplatin-induced acute kidney injury by activating the Nrf2 signalling pathway. *Br. J. Pharmacol.* 179 (15), 3991–4009. doi:10.1111/bph.15834

Hu, X. H., Situ, H. L., Chen, J. P., and Yu, R. H. (2020). Lipoxin A4 alleviates lung injury in sepsis rats through p38/MAPK signaling pathway. *J. Biol. Regul. Homeost. Agents* 34 (3), 807–814. doi:10.23812/20-108-a-20

Inoue, T., Abe, C., Kohro, T., Tanaka, S., Huang, L., Yao, J., et al. (2019). Non-canonical cholinergic anti-inflammatory pathway-mediated activation of peritoneal macrophages induces Hes1 and blocks ischemia/reperfusion injury in the kidney. *Kidney Int.* 95 (3), 563–576. doi:10.1016/j.kint.2018.09.020

Izzedine, H., Mathian, A., Champiat, S., Picard, C., Mateus, C., Routier, E., et al. (2019). Renal toxicities associated with pembrolizumab. *Clin. Kidney J.* 12 (1), 81–88. doi:10.1093/ckj/sfy100

Jin, S., Wang, J., Chen, S., Jiang, A., Jiang, M., Su, Y., et al. (2018). A novel limonin derivate modulates inflammatory response by suppressing the TLR4/NF-κB signalling pathway. *Biomed. Pharmacother.* 100, 501–508. doi:10.1016/j.biopha.2018.02.046

Joannidis, M., Meersch-Dini, M., and Forni, L. G. (2023). Acute kidney injury. *Intensive Care Med.* 49 (6), 665–668. doi:10.1007/s00134-023-07061-4

Kashani, K. B., Awdishu, L., Bagshaw, S. M., Barreto, E. F., Claure-Del Granado, R., Evans, B. J., et al. (2023). Digital health and acute kidney injury: consensus report of the 27th Acute Disease Quality Initiative workgroup. *Nat. Rev. Nephrol.* 19 (12), 807–818. doi:10.1038/s41581-023-00744-7

Kaushal, G. P., and Shah, S. V. (2016). Autophagy in acute kidney injury. *Kidney Int.* 89 (4), 779–791. doi:10.1016/j.kint.2015.11.021

Kurata, Y., and Nangaku, M. (2023). Use of antibiotics as a therapeutic approach to prevent AKI-to-CKD progression. *Kidney Int.* 104 (3), 418–420. doi:10.1016/j.kint.2023.05.022

Li, F., and Liu, C. S. (2022). Early predictive value of systemic immune inflammation index in severeacute pancreatitis complicated with acute renal injury. *J. Clin. Emerg.* 23 (02), 100–105. doi:10.13201/j.issn.1009-5918.2022.02.005

Li, J., and Gong, X. (2022). Tetramethylpyrazine: an active ingredient of Chinese herbal medicine with therapeutic potential in acute kidney injury and renal fibrosis. *Front. Pharmacol.* 13, 820071. doi:10.3389/fphar.2022.820071

Li, J., and Gong, X. (2023). Bibliometric and visualization analysis of kidney repair associated with acute kidney injury from 2002 to 2022. *Front. Pharmacol.* 14, 1101036. doi:10.3389/fphar.2023.1101036

Li, J., Sun, X., Yang, N., Ni, J., Xie, H., Guo, H., et al. (2023). Phosphoglycerate mutase 5 initiates inflammation in acute kidney injury by triggering mitochondrial DNA release

by dephosphorylating the pro-apoptotic protein Bax. *Kidney Int.* 103 (1), 115–133. doi:10.1016/j.kint.2022.08.022

Li, P., Chen, J. M., Ge, S. H., Sun, M. L., Lu, J. D., Liu, F., et al. (2024a). Pentoxifylline protects against cerebral ischaemia-reperfusion injury through ferroptosis regulation via the Nrf2/SLC7A11/GPX4 signalling pathway. *Eur. J. Pharmacol.* 967, 176402. doi:10.1016/j.ejphar.2024.176402

Li, T., Sun, H., Li, Y., Su, L., Jiang, J., Liu, Y., et al. (2022). Downregulation of macrophage migration inhibitory factor attenuates NLRP3 inflammasome mediated pyroptosis in sepsis-induced AKI. *Cell. Death Discov.* 8 (1), 61. doi:10.1038/s41420-022-00859-z

Li, Y., Hu, C., Zhai, P., Zhang, J., Jiang, J., Suo, J., et al. (2024b). Fibroblastic reticular cell-derived exosomes are a promising therapeutic approach for septic acute kidney injury. *Kidney Int.* 105 (3), 508–523. doi:10.1016/j.kint.2023.12.007

Liu, C., Zhou, W., Mao, Z., Li, X., Meng, Q., Fan, R., et al. (2023a). Bibliometric analysis of ferroptosis in acute kidney injury from 2014 to 2022. *Int. Urol. Nephrol.* 55 (6), 1509–1521. doi:10.1007/s11255-022-03456-2

Liu, F., Wang, Z., Li, X., Zhang, Z., Yang, Y., Chen, J., et al. (2023b). Comparative risk of acute kidney injury among cancer patients treated with immune checkpoint inhibitors. *Cancer Commun. (Lond)* 43 (2), 214–224. doi:10.1002/cac2.12396

Liu, J., Jia, Z., and Gong, W. (2021). Circulating mitochondrial DNA stimulates innate immune signaling pathways to mediate acute kidney injury. *Front. Immunol.* 12, 680648. doi:10.3389/fimmu.2021.680648

Liu, W.-C., Li, M.-P., Huang, H.-Y., Min, J.-J., Liu, T., Li, M.-X., et al. (2023c). Research trends of machine learning in traditional medicine: a big-data based ten-year bibliometric analysis. *Traditional Med. Res.* 8, 37–42. doi:10.53388/TMR20221113001

Long, B. S., Wang, Z. X., Lin, L. X., Li, Z. J., and Lin, M. H. (2020). Effects of Changpu Yujin decoction combined with CRRT therapy on immune function and serum procalcitonin and C-reactive protein in patients with sepsis-induced acute kidney injury. *Jilin J. Chin. Med.* 40 (06), 762–765. doi:10.13463/j.cnki.jlzyy.2020.06.018

Luo, S., Yang, M., Han, Y., Zhao, H., Jiang, N., Li, L., et al. (2022). β-Hydroxybutyrate against Cisplatin-Induced acute kidney injury via inhibiting NLRP3 inflammasome and oxidative stress. *Int. Immunopharmacol.* 111, 109101. doi:10.1016/j.intimp.2022.109101

Maekawa, H., Inoue, T., Ouchi, H., Jao, T. M., Inoue, R., Nishi, H., et al. (2019). Mitochondrial damage causes inflammation via cGAS-STING signaling in acute kidney injury. *Cell. Rep.* 29 (5), 1261–1273. doi:10.1016/j.celrep.2019.09.050

Mamlouk, O., Selamet, U., Machado, S., Abdelrahim, M., Glass, W. F., Tchakarov, A., et al. (2019). Nephrotoxicity of immune checkpoint inhibitors beyond tubulointerstitial nephritis: single-center experience. *J. Immunother. Cancer* 7 (1), 2. doi:10.1186/s40425-018-0478-8

Messerer, D. A. C., Halbgebauer, R., Nilsson, B., Pavenstädt, H., Radermacher, P., and Huber-Lang, M. (2021). Immunopathophysiology of trauma-related acute kidney injury. *Nat. Rev. Nephrol.* 17 (2), 91–111. doi:10.1038/s41581-020-00344-9

Mohamed, A. F., Safar, M. M., Zaki, H. F., and Sayed, H. M. (2017). Telluric acid ameliorates endotoxemic kidney injury in mice: involvement of TLR4, Nrf2, and PI3K/akt signaling pathways. *Inflammation* 40 (5), 1742–1752. doi:10.1007/s10753-017-0617-2

Noel, S., Lee, K., Gharaie, S., Kurzhagen, J. T., Pierorazio, P. M., Arend, L. J., et al. (2023). Immune checkpoint molecule TIGIT regulates kidney T cell functions and contributes to AKI. *J. Am. Soc. Nephrol.* 34 (5), 755–771. doi:10.1681/asn.0000000000000063

Okusa, M. D., Rosin, D. L., and Tracey, K. J. (2017). Targeting neural reflex circuits in immunity to treat kidney disease. *Nat. Rev. Nephrol.* 13 (11), 669–680. doi:10.1038/nrneph.2017.132

Pabla, N., and Bajwa, A. (2022). Role of mitochondrial therapy for ischemic-reperfusion injury and acute kidney injury. *Nephron* 146 (3), 253–258. doi:10.1159/000520698

Packialakshmi, B., Stewart, I. J., Burmeister, D. M., Chung, K. K., and Zhou, X. (2020). Large animal models for translational research in acute kidney injury. *Ren. Fail* 42 (1), 1042–1058. doi:10.1080/0886022x.2020.1830108

Qi, J., Luo, Q., Zhang, Q., Wu, M., Zhang, L., Qin, L., et al. (2023). Yi-Shen-Xie-Zhuo formula alleviates cisplatin-induced AKI by regulating inflammation and apoptosis via the cGAS/STING pathway. *J. Ethnopharmacol.* 309, 116327. doi:10.1016/j.jep.2023.116327

Qiao, O., Wang, X., Wang, Y., Li, N., and Gong, Y. (2023). Ferroptosis in acute kidney injury following crush syndrome: a novel target for treatment. *J. Adv. Res.* 54, 211–222. doi:10.1016/j.jare.2023.01.016

Qiongyue, Z., Xin, Y., Meng, P., Sulin, M., Yanlin, W., Xinyi, L., et al. (2022). Post-treatment with irisin attenuates acute kidney injury in sepsis mice through anti-ferroptosis via the SIRT1/nrf2 pathway. *Front. Pharmacol.* 13, 857067. doi:10.3389/fphar.2022.857067

Sanz, A. B., Sanchez-Niño, M. D., Ramos, A. M., and Ortiz, A. (2023). Regulated cell death pathways in kidney disease. *Nat. Rev. Nephrol.* 19 (5), 281–299. doi:10.1038/s41581-023-00694-0

Schattner, M. (2019). Platelet TLR4 at the crossroads of thrombosis and the innate immune response. *J. Leukoc. Biol.* 105 (5), 873–880. doi:10.1002/jlb.Mr0618-213r

Seethapathy, H., Street, S., Strohbehn, I., Lee, M., Zhao, S. H., Rusibamayila, N., et al. (2021). Immune-related adverse events and kidney function decline in patients with

genitourinary cancers treated with immune checkpoint inhibitors. *Eur. J. Cancer* 157, 50–58. doi:10.1016/j.ejca.2021.07.031

Seethapathy, H., Zhao, S., Chute, D. F., Zubiri, L., Oppong, Y., Strohbehn, I., et al. (2019). The incidence, causes, and risk factors of acute kidney injury in patients receiving immune checkpoint inhibitors. *Clin. J. Am. Soc. Nephrol.* 14 (12), 1692–1700. doi:10.2215/cjn.00990119

Sprangers, B., Leaf, D. E., Porta, C., Soler, M. J., and Perazella, M. A. (2022). Diagnosis and management of immune checkpoint inhibitor-associated acute kidney injury. *Nat. Rev. Nephrol.* 18 (12), 794–805. doi:10.1038/s41581-022-00630-8

Sury, K., Perazella, M. A., and Shirali, A. C. (2018). Cardiorenal complications of immune checkpoint inhibitors. *Nat. Rev. Nephrol.* 14 (9), 571–588. doi:10.1038/s41581-018-0035-1

Synnestvedt, M. B., Chen, C., and Holmes, J. H. (2005). CiteSpace II: visualization and knowledge discovery in bibliographic databases. *AMIA Annu. Symp. Proc.* 2005, 724–728.

Tang, C., Han, H., Yan, M., Zhu, S., Liu, J., Liu, Z., et al. (2018). PINK1-PRKN/PARK2 pathway of mitophagy is activated to protect against renal ischemia-reperfusion injury. *Autophagy* 14 (5), 880–897. doi:10.1080/15548627.2017.1405880

Tao, P., Huo, J., and Chen, L. (2024). Bibliometric analysis of the relationship between gut microbiota and chronic kidney disease from 2001–2022. *Integr. Med. Nephrol. Androl.* 11 (1), e00017. doi:10.1097/imna-d-23-00017

Tian, B. W., Yang, Y. F., Yang, C. C., Yan, L. J., Ding, Z. N., Liu, H., et al. (2022). Systemic immune-inflammation index predicts prognosis of cancer immunotherapy: systemic review and meta-analysis. *Immunotherapy* 14 (18), 1481–1496. doi:10.2217/imt-2022-0133

Uchida, T., Yamada, M., Inoue, D., Kojima, T., Yoshikawa, N., Suda, S., et al. (2023). Involvement of innate immune system in the pathogenesis of sepsis-associated acute kidney injury. *Int. J. Mol. Sci.* 24 (15), 12465. doi:10.3390/ijms241512465

Vande Walle, L., and Lamkanfi, M. (2024). Drugging the NLRP3 inflammasome: from signalling mechanisms to therapeutic targets. *Nat. Rev. Drug Discov.* 23 (1), 43–66. doi:10.1038/s41573-023-00822-2

van Eck, N. J., and Waltman, L. (2010). Software survey: VOSviewer, a computer program for bibliometric mapping. *Scientometrics* 84 (2), 523–538. doi:10.1007/s11192-009-0146-3

Wanchoo, R., Karam, S., Uppal, N. N., Barta, V. S., Deray, G., Devoe, C., et al. (2017). Adverse renal effects of immune checkpoint inhibitors: a narrative review. *Am. J. Nephrol.* 45 (2), 160–169. doi:10.1159/000455014

Wang, H., Gao, T., Zhang, R., Hu, J., Wang, Y., Wei, J., et al. (2023). The intellectual base and global trends in contrast-induced acute kidney injury: a bibliometric analysis. *Ren. Fail* 45 (1), 2188967. doi:10.1080/0886022x.2023.2188967

Wei, S. C., Duffy, C. R., and Allison, J. P. (2018). Fundamental mechanisms of immune checkpoint blockade therapy. *Cancer Discov.* 8 (9), 1069–1086. doi:10.1158/2159-8290.Cd-18-0367

Wu, H., Wang, Y., Zhang, Y., Xu, F., Chen, J., Duan, L., et al. (2020). Breaking the vicious loop between inflammation, oxidative stress and coagulation, a novel anti-thrombus insight of nattokinase by inhibiting LPS-induced inflammation and oxidative stress. *Redox Biol.* 32, 101500. doi:10.1016/j.redox.2020.101500

Xu, K., Yang, H., Fang, J., Qiu, K., Shen, H., Huang, G., et al. (2024a). Self-adaptive pyroptosis-responsive nanoliposomes block pyroptosis in autoimmune inflammatory diseases. *Bioact. Mater* 36, 272–286. doi:10.1016/j.bioactmat.2024.02.022

Xu, L., Xing, Z., Yuan, J., Han, Y., Jiang, Z., Han, M., et al. (2024b). Ultrasmall nanoparticles regulate immune microenvironment by activating IL-33/ST2 to alleviate renal ischemia-reperfusion injury. *Adv. Healthc. Mater* 13, e2303276. doi:10.1002/adhm.202303276

Xu, L., Zhu, Q.-H., Zhao, Y., Xiong, M., He, S., Xu, Y.-N., et al. (2023). Worldwide research trends on chloroquine: a bibliometric analysis from 2012 to 2021. *Traditional Med. Res.* 8, 71–72. doi:10.53388/TMR20230515001

Xue, R., Yiu, W. H., Chan, K. W., Lok, S. W. Y., Zou, Y., Ma, J., et al. (2024). Long non-coding RNA Neat1, NLRP3 inflammasome, and acute kidney injury. *J. Am. Soc. Nephrol.* doi:10.1681/asn.0000000000000362

Yancy, C. W., Jessup, M., Bozkurt, B., Butler, J., Casey, D. E., Jr., Colvin, M. M., et al. (2017). 2017 ACC/AHA/HFSA focused update of the 2013 ACCF/AHA guideline for the management of heart failure: a report of the American college of cardiology/American heart association task force on clinical practice guidelines and the heart failure society of America. *J. Am. Coll. Cardiol.* 70 (6), 776–803. doi:10.1016/j.jacc.2017.04.025

Yang, C. C., Sung, P. H., Chen, C. H., Chiang, J. Y., Shao, P. L., Wu, S. C., et al. (2021). Additional benefit of induced pluripotent stem cell-derived mesenchymal stem cell therapy on sepsis syndrome-associated acute kidney injury in rat treated with antibiotic. *Stem Cell. Res. Ther.* 12 (1), 526. doi:10.1186/s13287-021-02582-5

Yang, J., Liu, J., Kuang, W., Lin, Y., Zhong, S., Kraithong, S., et al. (2024). Structural characterization and ferroptosis-related immunomodulatory of a novel exopolysaccharide isolated from marine fungus Aspergillus medius. *Int. J. Biol. Macromol.* 265, 130703. doi:10.1016/j.ijbiomac.2024.130703

Zarbock, A., Nadim, M. K., Pickkers, P., Gomez, H., Bell, S., Joannidis, M., et al. (2023). Sepsis-associated acute kidney injury: consensus report of the 28th Acute Disease Quality Initiative workgroup. *Nat. Rev. Nephrol.* 19 (6), 401–417. doi:10.1038/s41581-023-00683-3

Zhang, B., Zeng, M., Li, B., Kan, Y., Wang, S., Cao, B., et al. (2021). Arbutin attenuates LPS-induced acute kidney injury by inhibiting inflammation and apoptosis via the PI3K/Akt/Nrf2 pathway. *Phytomedicine* 82, 153466. doi:10.1016/j.phymed.2021.153466

Zhang, R. B., Shen, K. W., Wang, Q., Yuan, Q., and Shen, J. (2023). Dl-3-N-butylphthalide alleviates renal ischemia-reperfusion injury by down-regulating NF-κB signaling pathway and inhibiting cell pyroptosis in rat models. *Organ Transplant.* 14 (04), 539–546. doi:10.3969/j.issn.1674-7445.2023.04.010

Zhao, Z. B., Marschner, J. A., Iwakura, T., Li, C., Motrapu, M., Kuang, M., et al. (2023). Tubular epithelial cell HMGB1 promotes AKI-CKD transition by sensitizing cycling tubular cells to oxidative stress: a rationale for targeting HMGB1 during AKI recovery. *J. Am. Soc. Nephrol.* 34 (3), 394–411. doi:10.1681/asn.0000000000000024

Zhong, K., Zhang, H.-Q., Fang, Y.-X., Lan, Q.-M., Zhou, Z.-J., Zhao, Y.-R., et al. (2023). Acute kidney injury: microRNAs and new therapeutic opportunities for natural products. *Traditional Med. Res.* 8, 61–66. doi:10.53388/TMR20230616001

Zhu, T., Dong, S., Qin, N., Liu, R., Shi, L., and Wan, Q. (2024a). Dl-3-n-butylphthalide attenuates cerebral ischemia/reperfusion injury in mice through AMPK-mediated mitochondrial fusion. *Front. Pharmacol.* 15, 1357953. doi:10.3389/fphar.2024.1357953

Zhu, Z., Li, J., Song, Z., Li, T., Li, Z., and Gong, X. (2024b). Tetramethylpyrazine attenuates renal tubular epithelial cell ferroptosis in contrast-induced nephropathy by inhibiting transferrin receptor and intracellular reactive oxygen species. *Clin. Sci. (Lond)* 138 (5), 235–249. doi:10.1042/cs20231184

Check for updates

# Association between PCSK9 inhibitors and acute kidney injury: a pharmacovigilance study

Hailing Liu*

Hunan Provincial People's Hospital, The First Affiliated Hospital of Hunan Normal University, Changsha, China

**Background:** PCSK9 inhibitors are a novel class of lipid-lowering medications, and numerous clinical studies have confirmed their significant role in improving the progression of chronic kidney disease. However, recent case reports have indicated new evidence regarding their association with acute kidney injury (AKI), with some patients experiencing acute tubular injury after PCSK9 inhibitors use.

**Objectives:** To clarify the relationship between PCSK9 inhibitors and AKI, we conducted a pharmacovigilance study.

**Methods:** Using the Food and Drug Administration Adverse Event Reporting System (FAERS) database from the third quarter of 2015 to the fourth quarter of 2022, a disproportionality analysis was employed to identify adverse events suggestive of AKI after PCSK9 inhibitors use. The drugs of interest included evolocumab and alirocumab.

**Results:** A total of 144,341 adverse event reports related to PCSK9 inhibitors were analyzed, among which 444 cases were suspected of AKI for evolocumab, and 172 cases for alirocumab. Evolocumab had a greater impact on AKI in males (ROR 1.4, 95% CI 1.54−1.69). The ROR and 95% CI for evolocumab and Alirocumab were 0.13 (0.12−0.14) and 0.26 (0.23−0.30) respectively. Further analysis of AKI associated with the concomitant use of PCSK9 inhibitors with cephalosporins, furosemide, torsemide, pantoprazole, omeprazole, and esomeprazole revealed ROR and 95% CI of 0.38 (0.23−0.62), 0.38 (0.31−0.48), 0.18 (0.08−0.38), 0.23 (0.17−0.29), 0.20 (0.16−0.26), and 0.14 (0.10−0.20) respectively.

**Conclusion:** Through the FAERS database, we analyzed the clinical characteristics of AKI associated with PCSK9 inhibitors, exploring its risks. Our findings suggest that PCSK9 inhibitors might have a potential protective effect against AKI and exhibit similar effects when co-administered with other nephrotoxic drugs.

## Highlights

- PCSK9 inhibitors may be potentially protective against AKI to some extent and show similar effects when combined with other nephrotoxic drugs.

# 1 Background

Proprotein Convertase Subtilisin/kexin Type 9 (PCSK9) is a serine protease synthesized by liver cells, which circulates in the bloodstream and forms complexes with Low-Density Lipoprotein Receptors (LDL-R). These complexes are eventually degraded in lysosomes within liver cells, leading to decreased surface LDL-R levels. LDL-R is a crucial factor for liver cell uptake and metabolism of LDL cholesterol (LDL-C). Consequently, PCSK9 elevates LDL-C levels in the body (Rosenson et al., 2018). Research indicates that elevated serum LDL-C levels are an independent risk factor for Atherosclerotic Cardiovascular Disease (ASCVD). Clinical trial data have demonstrated a correlation between lowering LDL-C levels and reducing cardiovascular risk (Silverman et al., 2016). Therefore, reducing LDL-C is a key strategy for primary and secondary prevention of ASCVD (Stone et al., 2014). PCSK9 inhibitors significantly reduce LDL-C levels in the human body through two main pathways: first, by inhibiting the binding of PCSK9 to LDL-C receptors and second, by intervening in the synthesis and processing of PCSK9 (Lagace, 2014). In a Phase I clinical trial, the anti-PCSK9 siRNA ALN-PCS reduced free PCSK9 levels by 70% and lowered LDL-C levels by 40% (Fitzgerald et al., 2014).

PCSK9 in circulation primarily originates from the liver. Additionally, it is expressed in the pancreas, kidneys, intestines, and central nervous system. While PCSK9 regulates cholesterol metabolism by modulating LDL receptor expression in the liver, *in vitro* and *in vivo* studies suggest that PCSK9 is involved in various other physiological processes (Stoekenbroek et al., 2018). Studies (Toth et al., 2018) have demonstrated the lipid-lowering effects of PCSK9 inhibitors in patients with chronic kidney disease (CKD), showing good safety and efficacy. At week 24, LDL-C reduction ranged from 46.1% to 62.2% in patients with or without renal impairment, respectively. The overall incidence of adverse reactions was similar between the treatment and control groups (82.1% vs. 82.8% in CKD patients; 78.4% vs. 78.2% in non-CKD patients). Furthermore, the more severe the CKD, the greater the absolute reduction in cardiovascular deaths, myocardial infarctions, or strokes associated with PCSK9 inhibitors use (Charytan et al., 2019). Patients with CKD stage 3 or higher, when treated with PCSK9 inhibitors for 30 months, experienced a significantly greater absolute risk reduction compared to patients with normal renal function, with reductions of −2.5% (95% confidence interval (CI) −4.7% to −0.4%) and −1.7% (95% CI: -2.8%–0.5%) respectively. Studies (Haas et al., 2016; Jatem et al., 2021) also revealed that knockout mice with nephrotic syndrome lacking liver Pcsk9 exhibited a 40%–50% reduction in plasma cholesterol and triglycerides. Patients with primary refractory nephrotic syndrome showed an average LDL-C reduction of 36.8% ± 4.9% mmol/L after 4 weeks of PCSK9 inhibitors therapy, which remained stable throughout the follow-up period. In contrast, total cholesterol or LDL-C levels showed no significant change in the statin-treated group, suggesting that PCSK9 inhibitors might be effective and safe alternatives for treating hypercholesterolemia associated with refractory nephrotic syndrome. Recent research (Skeby et al., 2023) has reported interactions between PCSK9 and Megalin in proximal tubular cells. By affecting megalin-driven protein reabsorption, PCSK9 influences urinary protein excretion. PCSK9 inhibitors increase renal megalin in mice with kidney disease, simultaneously reducing urinary albumin excretion. This discovery provides new strategies for treating CKD.

However, there are also case reports (Jhaveri et al., 2017; Pickett et al., 2020) suggesting that PCSK9 inhibitors can induce AKI. One case involved a 62-year-old female patient (Jhaveri et al., 2017) with comorbidities such as heart disease, hyperlipidemia, Stage 5 CKD, and hypertension. The patient denied using any non-steroidal anti-inflammatory drugs, antibiotics, or herbal supplements. After using alirocumab, her serum creatinine increased from a baseline of 2.3 mg/dL to 5.0 mg/dL. Kidney biopsy revealed acute tubular injury and necrosis. The authors speculated that this might be due to the overexpression of renal PCSK9 during the inhibition of the inflammatory process, which is actually a protective response to cellular damage. Another case involved a 72-year-old male patient (Pickett et al., 2020) with coronary artery disease, statin intolerance, and Stage 3 CKD. After using alirocumab, the patient also experienced acute tubular injury detected in kidney biopsy. Upon discontinuation of the medication, serum creatinine levels returned to baseline.

Currently, there are no specific research reports on the correlation between PCSK9 inhibitors and AKI. Whether they can reduce the risk of AKI remains unknown. AKI is characterized by a rapid decline in kidney function, accompanied by the accumulation of metabolic products such as creatinine and urea, constituting a clinical syndrome (Bellomo et al., 2012). It is typically transient and often overlooked. However, AKI is associated with increased risk of mortality. A prospective study (Kaddourah et al., 2017) involving 4,683 patients from multiple countries showed that by day 28, 543 patients developed severe AKI, leading to an increased risk of death (adjusted odds ratio 1.77; 95% CI, 1.17–2.68). The SEA-AKI study (Kulvichit et al., 2022) also reported an in-hospital mortality rate of up to 14.6% for AKI. Moreover, as the severity of AKI increases, the risk of death also rises (Hoste and Kellum, 2006; Hoste et al., 2015). The adjusted odds ratios for in-hospital death in AKI stages 1, 2, and 3 were 1.679 (95% CI 0.890–3.169; $p = 0.109$), 2.945 (95% CI 1.382–6.276; $p = 0.005$), and 6.884 (95% CI 3.876–12.228; $p < 0.001$), respectively (Hoste et al., 2015).

To further elucidate the correlation between PCSK9 inhibitors and AKI, we conducted a pharmacovigilance study using FAERS database. This spontaneously reported adverse reaction database is freely accessible and includes a diverse population and various medications. It is useful for capturing adverse events occurring shortly after drug exposure and can detect adverse events not found in clinical trials, especially for rare events with low background rates.

# 2 Methods

## 2.1 Data source

The data for this study were obtained from FAERS database, a large, publicly accessible database consisting of adverse reaction cases reported by various populations, including healthcare professionals, consumers, and lawyers. AERSMine, a website developed based on the FAERS database, provides convenient and precise search services. It has become a mature tool for
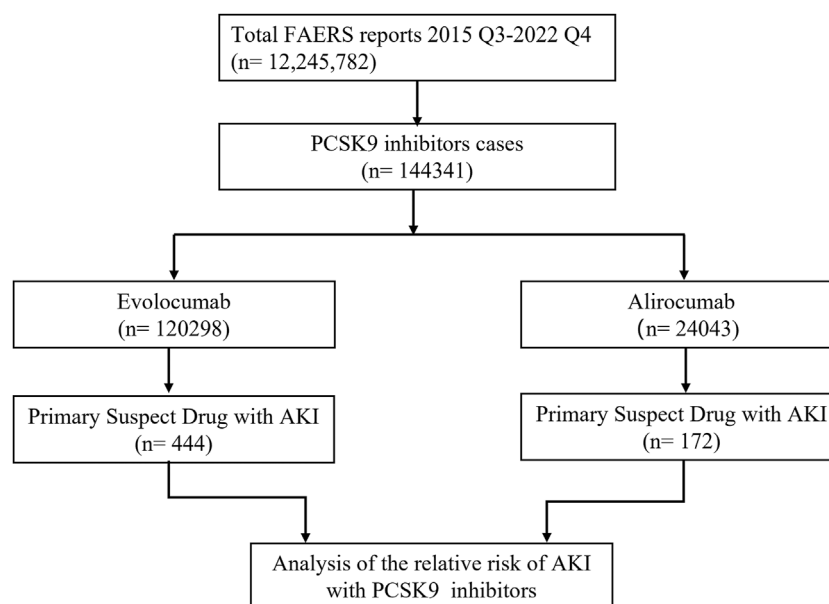
**FIGURE 1**
Flow chart of study design. In this study, 12, 245, 782 reports were retrieved from the FAERS database during the third quarter of 2015 to the fourth quarter of 2022. Among these reports, 144,341 cases were linked to adverse reactions related to PCSK9 inhibitors. To investigate the correlation between PCSK9 inhibitors and AKI, we selected the primary suspect drug for further analysis.

mining and analyzing drug adverse reactions (Sarangdhar et al., 2016; Xia et al., 2022; Xia et al., 2023). We conducted an observational, retrospective, cross-sectional pharmacovigilance study using post-marketing data from the FAERS database, spanning from the third quarter of 2015 to the fourth quarter of 2022. Ethical approval was not required for this study as it utilized de-identified data.

## 2.2 Drug selection and adverse reaction definition

The drugs of interest in this study were evolocumab and alirocumab, both approved by the FDA and EMA in 2015. We used the preferred terms (PTs) under the category of acute kidney failure based on the standard MedDRA query (SMQ) as keywords to identify target adverse reactions. Selected PTs are showed in Supplementary Material. For a better description of the characteristics and further analysis of PCSK9 inhibitors' association with AKI, we specified the drug role as "primary suspect."

## 2.3 Drug interaction analysis

In clinical practice, combination therapy is common. However, the impact of concomitant use of PCSK9 inhibitors with other medications on AKI is not well understood. Therefore, we analyzed commonly used nephrotoxic drugs to explore the effect of their co-administration with PCSK9 inhibitors on AKI. A nationwide cross-sectional survey (Liu et al., 2021) involving 23 academic hospitals in

17 provinces of China revealed that the top three categories of drugs causing drug-induced AKI were antimicrobial drugs, diuretics, and proton pump inhibitors (PPIs). Within these categories, the most common drugs were cephalosporins, glycopeptides, and carbapenems for antimicrobial drugs; furosemide, mannitol, and torsemide for diuretics; and pantoprazole, omeprazole, and esomeprazole for PPIs. We analyzed the occurrence of AKI when PCSK9 inhibitors were co-administered with these nine drugs.

## 2.4 Data mining and statistical methods

In this study, we employed the Reporting Odds Ratio (ROR) method, a disproportionality analysis, for risk analysis and mining. This method is also the most commonly used approach in current pharmacovigilance studies (Anand et al., 2019; Zhou et al., 2023). ROR with positive signal detection criteria was defined as having a report count ≥3 and a lower limit of the 95% CI of ROR >1. The method for calculating the ROR is provided in the Supplementary Material. Additionally, based on existing literature reports, we analyzed the risk of AKI when PCSK9 inhibitors were co-administered with common nephrotoxic drugs. Subgroup analyses were performed in different gender, age groups and underlying diseases to enhance the reliability and stability of the research results. Pearson's chi-squared test or Fisher's exact test was used to compare the reporting of PCSK9 inhibitors-related AKI, with statistical significance determined by a 95% CI, and $p < 0.05$ was considered significant. Statistical analysis was performed using SPSS 25.0 and Microsoft Excel 2019.

TABLE 1 Characteristics of patients with PCSK9 inhibitors-associated AKI in FAERS database.

| | Evolocumab N. (%) | Alirocumab N. (%) | *p*-Value |
|---|---|---|---|
| all AEs | 120,298 | 24,043 | |
| primary suspect drug with AKI | 444 (0.37) | 172 (0.72) | <0.05 |
| gender | | | |
| males | 216 (48.6) | 49 (28.5) | <0.05 |
| females | 206 (46.4) | 84 (48.8) | 0.65 |
| not reported | 22 (5.0) | 39 (22.7) | <0.05 |
| age groups | | | |
| 0–14 | 0 (0.0) | 0 (0.0) | - |
| 15–24 | 2 (0.4) | 0 (0.0) | - |
| 25–65 | 117 (26.4) | 48 (27.9) | 0.77 |
| ≥65 | 223 (50.2) | 59 (34.3) | <0.05 |
| not reported | 102 (23.0) | 65 (37.8) | <0.05 |
| Reporter occupation | | | |
| healthcare professionals | 324 (73.0) | 68 (39.5) | <0.05 |
| others | 120 (27.0) | 104 (60.5) | <0.05 |
| Year | | | |
| 2015 | 2 (0.5) | 3 (1.7) | 0.27 |
| 2016 | 43 (9.7) | 17 (9.9) | 0.94 |
| 2017 | 84 (18.9) | 29 (16.9) | 0.63 |
| 2018 | 138 (31.1) | 34 (19.8) | <0.05 |
| 2019 | 59 (13.3) | 34 (19.8) | 0.06 |
| 2020 | 35 (7.9) | 24 (13.9) | <0.05 |
| 2021 | 49 (11.0) | 15 (8.7) | 0.49 |
| 2022 | 34 (7.6) | 16 (9.3) | 0.61 |

Abbreviations: AEs, Adverse Events.

# 3 Results

## 3.1 Basic characteristics

In this study, we ultimately included 444 cases of evolocumab and 172 cases of alirocumab, as shown in Figure 1. All of which were primary suspect cases associated with AKI, reported in the FAERS database from the third quarter of 2015 to the fourth quarter of 2022. Table 1 summarizes the clinical characteristics of these cases. The reporting proportions of evolocumab-related AKI were similar between males (48.6%) and females (46.4%), *p* = 0.55, while alirocumab-related AKI was notably higher in females, *p* < 0.05. Evolocumab-related AKI cases were primarily reported in individuals aged 65 and above, with the rest distributed mainly between 25–65 years and in age-unreported cases. In contrast, alirocumab-related AKI cases were relatively evenly distributed among individuals aged 25–65, 65 and above, and those with unknown ages, accounting

for 27.9%, 34.3%, and 37.8%, respectively. Notably, AKI related to both drugs almost did not occur in individuals below 24 years old, likely due to the specific demographic of users. Evolocumab-related cases were predominantly reported by healthcare professionals, while the pattern was reversed for alirocumab, *p* < 0.05. The number of reported AKI adverse reactions for both drugs gradually increased after market introduction, reaching a peak in 2018 and subsequently declining, as shown in Table 1 and Figure 2. Specifically, evolocumab-related AKI cases reached 138 in 2018, accounting for 31.1% of the total cases. The most frequently reported PTs for evolocumab and alirocumab-related AKI were "blood creatinine increased," "renal failure," "renal impairment," and "acute kidney injury," as listed in Table 2. The patient outcomes for AKI cases associated with evolocumab and alirocumab are presented in the Supplementary Material. Overall, the number of hospitalizations and other serious outcomes is higher, while instances of death, disability, and life-threatening conditions are relatively fewer.
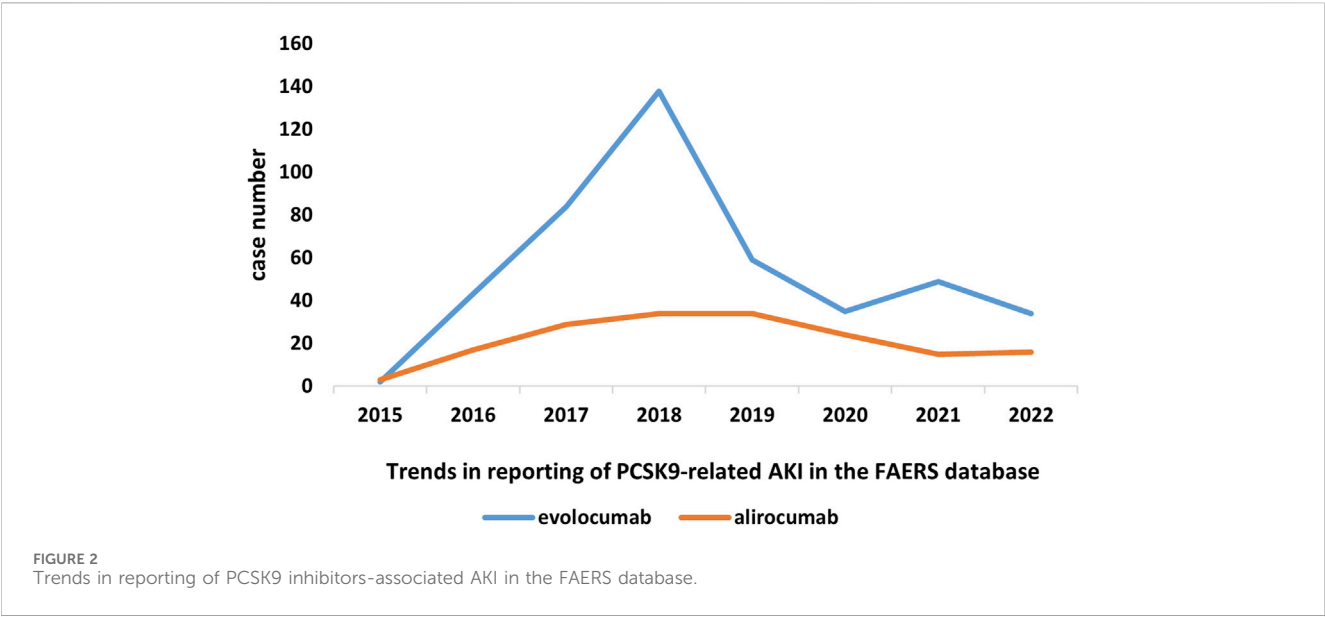
FIGURE 2
Trends in reporting of PCSK9 inhibitors-associated AKI in the FAERS database.

TABLE 2 Preferred terms reporting status for PCSK9 inhibitors-associated AKI.

| Evolocumab | | Alirocumab | |
|---|---|---|---|
| PTs | Case number | PTs | Case number |
| renal impairment | 114 | blood creatinine increased | 44 |
| renal failure | 97 | renal impairment | 37 |
| blood creatinine increased | 68 | renal failure | 36 |
| acute kidney injury | 48 | acute kidney injury | 23 |
| dialysis | 29 | blood urea increased | 11 |
| glomerular filtration rate decreased | 28 | glomerular filtration rate decreased | 8 |
| blood urea increased | 24 | proteinuria | 8 |
| renal function test abnormal | 20 | renal function test abnormal | 6 |
| protein urine present | 10 | renal tubular necrosis | 6 |
| urine output decreased | 8 | anuria | 5 |
| proteinuria | 7 | urine output decreased | 5 |
| renal transplant | 6 | dialysis | 5 |
| glomerular filtration rate abnormal | 5 | renal tubular injury | 3 |
| blood creatinine abnormal | 4 | renal transplant | 3 |
| peritoneal dialysis | 4 | oliguria | 3 |

Abbreviations: PTs, Preferred terms.

## 3.2 Disproportionality analysis

In this study, we used ROR algorithm in disproportionality analysis to detect the association between AKI and the use of evolocumab and alirocumab. The results are presented in Table 3. We found a negative correlation between the use of these two drugs and the reporting of AKI, indicating a potential protective effect against AKI. Furthermore, evolocumab demonstrated a stronger protective effect compared to alirocumab, with ROR and 95% CI for evolocumab-related and alirocumab-related AKI being 0.13 (0.12–0.14) and 0.26 (0.23–0.30), respectively.

## 3.3 Interaction analysis

In our analysis, we investigated the occurrence of AKI when PCSK9 inhibitors were combined with nine clinically common nephrotoxic drugs previously reported in studies (Liu et al., 2021).

| Drug | Primary suspect drug with AKI | ROR (95% CI) |
|------|-------------------------------|--------------|
| evolocumab | 444 | 0.13 (0.12–0.14) |
| alirocumab | 172 | 0.26 (0.23–0.30) |

Abbreviations: CI, confidence interval; ROR, reporting odds ratio.

The results demonstrated that PCSK9 inhibitors could mitigate the nephrotoxic effects of cephalosporins, furosemide, torsemide, pantoprazole, omeprazole, and esomeprazole, with significant differences observed (ROR and 95% CI: 0.38 [0.23–0.62], 0.38 [0.31–0.48], 0.18 [0.08–0.38], 0.23 [0.17–0.29], 0.20 [0.16–0.26], and 0.14 [0.10–0.20], respectively). The results are presented in Table 4. However, conclusive results could not be drawn for the other three drugs due to insufficient case numbers.

## 3.4 Subgroup analysis

Table 5 and Table 6 presents the results of subgroup analysis. In patients with underlying disease, PCSK9 inhibitors still showed potential AKI protection, see Table 5. Evolocumab-related AKI was more likely to occur in males (ROR = 1.40, 95% CI = 1.54–1.69). In comparison with the population aged 65 and above, individuals between the ages of 25–65 appeared to have a slightly lower risk of AKI after using evolocumab, although this difference was not statistically significant. On the other hand,

alirocumab showed a higher risk of AKI in patients aged 25–65, but again, this difference was not statistically significant. It is important to note that due to the limited number of reported cases in patients under 25 years old, a direct comparison for this age group could not be made. Additionally, the differences observed in this analysis require further investigation with larger sample sizes and more comprehensive prospective studies to draw definitive conclusions.

## 4 Discussion

Despite numerous clinical studies confirming the lipid-lowering effects of PCSK9 inhibitors in CKD patients and recent research indicating their potential to improve CKD, their protective role in AKI remains unclear. Most cases of AKI are transient and challenging to intervene in practical clinical trials. Additionally, case reports have suggested that PCSK9 inhibitors may cause acute renal tubular injury. Therefore, investigating the correlation between PCSK9 inhibitors and AKI in a large-scale pharmacovigilance database study is crucial.

This study, based on the FAERS database, analyzed the association between PCSK9 inhibitors evolocumab and alirocumab and AKI. The results revealed a protective effect of PCSK9 inhibitors against AKI. Moreover, the study identified the main characteristics of AKI cases related to PCSK9 inhibitors and explored the impact of PCSK9 inhibitors in combination with common nephrotoxic drugs on AKI. To our knowledge, this is the largest real-world study investigating the risk of AKI associated with PCSK9 inhibitors.

TABLE 4 Interactions between PCSK9 inhibitors and common nephrotoxic drugs.

| Drug A | Drug B | Patients total | NO. AKI | Proportion of AKI (%) | ROR (95% CI) | p-Value |
|--------|--------|----------------|---------|----------------------|--------------|---------|
| cephalosporins | with PCSK9 inhibitors | 371 | 17 | 4.58 | 0.38 (0.23–0.62) | <0.0001 |
|  | without PCSK9 inhibitors | 121,428 | 13,568 | 11.17 | 1 (reference) |  |
| glycopeptide | with PCSK9 inhibitors | 29 | 3 | 10.34 | 0.57 (0.17–1.87) | 0.46 |
|  | without PCSK9 inhibitors | 52,346 | 8,856 | 16.92 | 1 (reference) |  |
| carbopenems | with PCSK9 inhibitors | 4 | 1 | 25.00 | 2.93 (0.30–28.17) | 0.35 |
|  | without PCSK9 inhibitors | 35,381 | 3,615 | 10.22 | 1 (reference) |  |
| furosemide | with PCSK9 inhibitors | 1,512 | 78 | 5.16 | 0.38 (0.31–0.48) | <0.0001 |
|  | without PCSK9 inhibitors | 309,774 | 38,468 | 12.42 | 1 (reference) |  |
| mannitol | with PCSK9 inhibitors | 3 | 0 | 0.00 | - | - |
|  | without PCSK9 inhibitors | 4,769 | 563 | 11.81 |  |  |
| torsemide | with PCSK9 inhibitors | 223 | 7 | 3.14 | 0.18 (0.08–0.38) | <0.0001 |
|  | without PCSK9 inhibitors | 42,018 | 6,509 | 15.49 | 1 (reference) |  |
| pantoprazole | with PCSK9 inhibitors | 1,543 | 63 | 4.08 | 0.23 (0.17–0.29) | <0.0001 |
|  | without PCSK9 inhibitors | 309,700 | 49,232 | 15.90 | 1 (reference) |  |
| omeprazole | with PCSK9 inhibitors | 1933 | 68 | 3.52 | 0.20 (0.16–0.26) | <0.0001 |
|  | without PCSK9 inhibitors | 373,769 | 56,482 | 15.11 | 1 (reference) |  |
| esomeprazole | with PCSK9 inhibitors | 606 | 29 | 4.79 | 0.14 (0.10–0.20) | <0.0001 |
|  | without PCSK9 inhibitors | 188,105 | 49,652 | 26.40 | 1 (reference) |  |

TABLE 5 PCSK9 inhibitors-associated AKI in patients with several underlying diseases.

| Drug | Underlying diseases | NO. AKI | ROR (95% CI) |
|---|---|---|---|
| evolocumab | diabetes mellitus | 5 | 0.11 (0.05–0.27) |
| | hypertension | 11 | 0.15 (0.08–0.28) |
| | hyperlipidaemia | 55 | 0.05 (0.04–0.07) |
| | heart failures | 3 | 0.27 (0.09–0.85) |
| alirocumab | diabetes mellitus | 1 | 0.10 (0.01–0.71) |
| | hypertension | 6 | 0.13 (0.06–0.29) |
| | hyperlipidaemia | 28 | 0.09 (0.06–0.13) |
| | heart failures | 1 | 0.23 (0.03–1.72) |

The number of adverse events reported with alirocumab in patients with diabetes and heart failure was less than 3 cases of AKI, and therefore does not pose a risk.

TABLE 6 PCSK9 inhibitors-associated AKI compared across age groups and genders.

| Drug | | Patients total | NO. AKI | Proportion of AKI (%) | ROR (95% CI) | $p$-Value |
|---|---|---|---|---|---|---|
| evolocumab | males | 48,973 | 216 | 0.44 | 1.40 (1.54–1.69) | <0.001 |
| | females | 65,195 | 206 | 0.32 | 1 (reference) | |
| | 25–65 | 33,388 | 117 | 0.35 | 0.80 (0.64–1.00) | 0.05 |
| | ≥65 | 50,908 | 223 | 0.44 | 1 (reference) | |
| alirocumab | males | 8,436 | 49 | 0.58 | 0.84 (0.59–1.20) | 0.33 |
| | females | 12,154 | 84 | 0.69 | 1 (reference) | |
| | 25–65 | 5,369 | 48 | 0.89 | 1.42 (0.97–2.09) | 0.07 |
| | ≥65 | 9,365 | 59 | 0.63 | 1 (reference) | |

Because the number of cases between 0–25 years old was small, they were not included in the comparison. Abbreviations: CI, confidence interval; ROR, reporting odds ratio.

While some case reports have linked PCSK9 inhibitors to AKI, this retrospective large-scale pharmacovigilance analysis showed a reduced risk of AKI in patients using PCSK9 inhibitors compared to those who did not. Both target drugs, evolocumab and elirocumab, exhibited similar effects with ROR of 0.13 (95% CI 0.12–0.14) and 0.26 (95% CI 0.23–0.30), respectively. Subgroup analysis also reached consistent conclusions. Studies have indicated that PCSK9 inhibitors are associated with anti-inflammatory (Giunzioni et al., 2016; Liu and Frostegård, 2018), autophagic (Ding et al., 2018; Huang et al., 2022), and oxidative stress responses (Huang et al., 2022), which are independent of low-density lipoprotein reduction. Recent research has revealed that these effects are mediated by SIRT3 (D'Onofrio et al., 2023), a highly expressed mitochondrial deacetylase, which plays a vital role in preventing AKI by regulating energy metabolism, inhibiting oxidative stress, suppressing inflammation, improving apoptosis, inhibiting early fibrosis, and maintaining mitochondrial homeostasis (Yuan et al., 2023). Activation of TFEB-mediated autophagy can also alleviate mitochondrial dysfunction in cisplatin-induced AKI (Zhu et al., 2020).

A large multicenter cross-sectional study summarized common nephrotoxic drugs in medical institutions (Liu et al., 2021). We conducted a disproportionate analysis of these drugs in combination with PCSK9 inhibitors and found that

PCSK9 inhibitors can reduce the occurrence of AKI caused by common nephrotoxic drugs such as furosemide, pantoprazole, omeprazole, and esomeprazole. Therefore, considering PCSK9 inhibitors in patients with a high risk of AKI or those using nephrotoxic drugs seems wise. Additionally, existing real-world data studies have also shown the protective effect of PCSK9 inhibitors on AKI caused by medications. For example, the relative risk (RR) between the use of evolocumab and the occurrence of contrast-induced acute kidney injury (CI-AKI) was 0.34 (95% CI 0.17–0.66, $p < 0.01$) (Ma et al., 2022). It is worth mentioning that the common nephrotoxic drugs we selected may not be applicable to all countries and regions, although these drugs were derived from a nationwide cross-sectional survey that included 23 academic hospitals in 17 provinces in China. For example, cephalosporins and carbopenems may be uncommon as common nephrotoxic drugs. However, a pharmacovigilance study of FAERS found AKI ROR of cephalosporins is 6.07 (5.23–7.05) (Patek et al., 2020). Other studies believe that ceftriaxone calcium crystals induce AKI by NLRP3-mediated inflammation and oxidative stress injury (Yifan et al., 2020). Further investigation is warranted to accurately determine the nephrotoxicity of carbapenems. Nevertheless, current evidence suggests that, when co-administered with vancomycin, carbapenems present a reduced risk of AKI compared to piperacillin-tazobactam (Rutter and Burgess, 2018; Chen et al., 2023). However, risk of AKI after

piperacillin-tazobactam is comparable to meropenem without concurrent use of vancomycin (Su et al., 2023).

We conducted a risk analysis of PCSK9 inhibitors-related AKI in different genders and age groups. We found that evolocumab is more likely to induce AKI in males (ROR = 1.40, 95% CI = 1.54–1.69), while alirocumab showed the opposite trend (ROR = 0.84, 95% CI = 0.59–1.20), although the latter did not reach statistical significance. Due to limited case numbers for patients under 25 years old, we only compared the reporting differences related to PCSK9 inhibitor-induced AKI between the age groups of 25–65 and over 65. We found a slightly lower risk of AKI in the 25–65 age group with evolocumab use compared to those over 65, and a higher risk with alirocumab use in patients aged 25–65, although these differences were not statistically significant. We observed that males might be a risk factor for evolocumab-related AKI, consistent with previous research results (Siew et al., 2016). However, in another study (Hilmi et al., 2015) on risk prediction models for AKI in liver transplant patients, females were identified as a risk factor (OR = 1.8, 95% CI 1.18–2.88). In fact, studies indicate that alirocumab exhibits a more pronounced effect in reducing LDL-C levels in males compared to females (Vallejo-Vaz et al., 2018; Paquette et al., 2023). Upon performing an analysis based on each 50% reduction in LDL-C levels, there was observed a 24% lower risk of major adverse cardiac events (MACE) in females ($p = 0.1094$), and a 29% lower risk in males ($p = 0.0125$), respectively (Vallejo-Vaz et al., 2018). Consequently, it can be hypothesized that males may derive greater benefit from alirocumab therapy. Further large-scale clinical trials are necessary to substantiate this speculation. Since this study is based on publicly available spontaneously reported drug surveillance databases, the reporting of patient gender is not mandatory and may lead to missing data, potentially introducing bias to the study results. Additionally, the sample size in this study was limited, and the characteristics of the study subjects were not entirely consistent; hence, caution is needed when extrapolating the conclusions.

Our research results showed an increasing trend in PCSK9 inhibitors-related AKI reports since the drug's market launch, reaching its peak in 2018, followed by a gradual decline, especially for evolocumab. Evolocumab-related AKI cases were more common in people over 65 years old. Unfortunately, adverse event reporting in the FAERS database is spontaneous and influenced by various factors, such as the duration of drug marketing, media attention, types of adverse reactions, drug categories, indications, and related regulatory policies. Moreover, we do not have access to all clinical information related to the reported AKI cases, including gender, age, underlying diseases, concomitant medications, surgical procedures, and other AKI risk factors, which may confound the results. Drug surveillance studies based on the FAERS database cannot establish a causal relationship or determine the incidence rate of PCSK9 inhibitor-related AKI. They can only provide preliminary evidence of the potential correlation between the drug and adverse events. Regarding the selection of target populations, our study included a broad population, which might introduce bias into the results.

## 5 Conclusion

This study, based on the FAERS database, identified signals related to AKI associated with two PCSK9 inhibitors, Evolocumab

and Alirocumab, revealing the protective effect of PCSK9 inhibitors against AKI. Furthermore, when used in combination with common nephrotoxic drugs, these inhibitors can reduce the risk of AKI caused by these medications. This provides clinicians with more comprehensive grounds and reasons for selecting PCSK9 inhibitors, especially for patients with a higher risk of AKI or those concurrently using nephrotoxic drugs due to hyperlipidemia. However, further large-scale randomized controlled trials are still necessary to validate these findings.

## Data availability statement

Publicly available datasets were analyzed in this study. This data can be found here: https://research.cchmc.org/aers/home.

## Ethics statement

Written informed consent was not obtained from the individual(s) for the publication of any potentially identifiable images or data included in this article because the data in the article uses de-identified data and does not involve patient privacy.

## Author contributions

## Funding

## Conflict of interest

The author declares that the research was conducted in the absence of any commercial or financial relationships that could be construed as a potential conflict of interest.

## Publisher's note

## Supplementary material

The Supplementary Material for this article can be found online at: https://www.frontiersin.org/articles/10.3389/fphar.2024.1353848/full#supplementary-material

# References

Anand, K., Ensor, J., Trachtenberg, B., and Bernicker, E. H. (2019). Osimertinib-induced cardiotoxicity: a retrospective review of the FDA adverse events reporting System (FAERS). *JACC CardioOncol* 1, 172–178. doi:10.1016/j.jaccao.2019.10.006

Bellomo, R., Kellum, J. A., and Ronco, C. (2012). Acute kidney injury. *Lancet* 380, 756–766. doi:10.1016/S0140-6736(11)61454-2

Charytan, D. M., Sabatine, M. S., Pedersen, T. R., Im, K., Park, J. G., Pineda, A. L., et al. (2019). Efficacy and safety of evolocumab in chronic kidney disease in the FOURIER trial. *J. Am. Coll. Cardiol.* 73, 2961–2970. doi:10.1016/j.jacc.2019.03.513

Chen, A. Y., Deng, C. Y., Calvachi-Prieto, P., Armengol de la Hoz, M. Á., Khazi-Syed, A., Chen, C., et al. (2023). A large-scale multicenter retrospective study on nephrotoxicity associated with empiric broad-spectrum antibiotics in critically ill patients. *Chest* 164, 355–368. doi:10.1016/j.chest.2023.03.046

Ding, Z., Wang, X., Liu, S., Shahanawaz, J., Theus, S., Fan, Y., et al. (2018). PCSK9 expression in the ischaemic heart and its relationship to infarct size, cardiac function, and development of autophagy. *Cardiovasc Res.* 114, 1738–1751. doi:10.1093/cvr/cvy128

D'Onofrio, N., Prattichizzo, F., Marfella, R., Sardu, C., Martino, E., Scisciola, L., et al. (2023). SIRT3 mediates the effects of PCSK9 inhibitors on inflammation, autophagy, and oxidative stress in endothelial cells. *Theranostics* 13, 531–542. doi:10.7150/thno.80289

Fitzgerald, K., Frank-Kamenetsky, M., Shulga-Morskaya, S., Liebow, A., Bettencourt, B. R., Sutherland, J. E., et al. (2014). Effect of an RNA interference drug on the synthesis of proprotein convertase subtilisin/kexin type 9 (PCSK9) and the concentration of serum LDL cholesterol in healthy volunteers: a randomised, single-blind, placebo-controlled, phase 1 trial. *Lancet* 383, 60–68. doi:10.1016/S0140-6736(13)61914-5

Giunzioni, I., Tavori, H., Covarrubias, R., Major, A. S., Ding, L., Zhang, Y., et al. (2016). Local effects of human PCSK9 on the atherosclerotic lesion. *J. Pathol.* 238, 52–62. doi:10.1002/path.4630

Haas, M. E., Levenson, A. E., Sun, X., Liao, W. H., Rutkowski, J. M., de Ferranti, S. D., et al. (2016). The role of proprotein convertase subtilisin/kexin type 9 in nephrotic syndrome-associated hypercholesterolemia. *Circulation* 134, 61–72. doi:10.1161/CIRCULATIONAHA.115.020912

Hilmi, I. A., Damian, D., Al-Khafaji, A., Planinsic, R., Boucek, C., Sakai, T., et al. (2015). Acute kidney injury following orthotopic liver transplantation: incidence, risk factors, and effects on patient and graft outcomes. *Br. J. Anaesth.* 114, 919–926. doi:10.1093/bja/aeu556

Hoste, E. A., Bagshaw, S. M., Bellomo, R., Cely, C. M., Colman, R., Cruz, D. N., et al. (2015). Epidemiology of acute kidney injury in critically ill patients: the multinational AKI-EPI study. *Intensive Care Med.* 41, 1411–1423. doi:10.1007/s00134-015-3934-7

Hoste, E. A., and Kellum, J. A. (2006). RIFLE criteria provide robust assessment of kidney dysfunction and correlate with hospital mortality. *Crit. Care Med.* 34, 2016–2017. doi:10.1097/01.CCM.0000219374.43963.B5

Huang, G., Lu, X., Zhou, H., Li, R., Huang, Q., Xiong, X., et al. (2022). PCSK9 inhibition protects against myocardial ischemia-reperfusion injury via suppressing autophagy. *Microvasc. Res.* 142, 104371. doi:10.1016/j.mvr.2022.104371

Jatem, E., Lima, J., Montoro, B., Torres-Bondia, F., and Segarra, A. (2021). Efficacy and safety of PCSK9 inhibitors in hypercholesterolemia associated with refractory nephrotic syndrome. *Kidney Int. Rep.* 6, 101–109. doi:10.1016/j.ekir.2020.09.046

Jhaveri, K. D., Barta, V. S., and Pullman, J. (2017). Praluent (Alirocumab)-Induced renal injury. *J. Pharm. Pract.* 30, 7–8. doi:10.1177/0897190016683304

Kaddourah, A., Basu, R. K., Bagshaw, S. M., Goldstein, S. L., and Investigators, A. (2017). Epidemiology of acute kidney injury in critically ill children and young adults. *N. Engl. J. Med.* 376, 11–20. doi:10.1056/NEJMoa1611391

Kulvichit, W., Sarnvanichpitak, K., Peerapornratana, S., Tungsanga, S., Lumlertgul, N., Praditpornsilpa, K., et al. (2022). In-hospital mortality of critically Ill patients with interactions of acute kidney injury and acute respiratory failure in the resource-limited settings: results from SEA-AKI study. *J. Crit. Care* 71, 154103. doi:10.1016/j.jcrc.2022.154103

Lagace, T. A. (2014). PCSK9 and LDLR degradation: regulatory mechanisms in circulation and in cells. *Curr. Opin. Lipidol.* 25, 387–393. doi:10.1097/MOL.0000000000000114

Lameire, N. H., Bagga, A., Cruz, D., De Maeseneer, J., Endre, Z., Kellum, J. A., et al. (2013). Acute kidney injury: an increasing global concern. *Lancet* 382, 170–179. doi:10.1016/S0140-6736(13)60647-9

Liu, A., and Frostegård, J. (2018). PCSK9 plays a novel immunological role in oxidized LDL-induced dendritic cell maturation and activation of T cells from human blood and atherosclerotic plaque. *J. Intern Med.* 284, 193–210. doi:10.1111/joim.12758

Liu, C., Yan, S., Wang, Y., Wang, J., Fu, X., Song, H., et al. (2021). Drug-induced hospital-acquired acute kidney injury in China: a multicenter cross-sectional survey. *Kidney Dis. (Basel)* 7, 143–155. doi:10.1159/000510455

Ma, Y., Zha, L., Zhang, Q., Cao, L., Zhao, R., Ma, J., et al. (2022). Effect of PCSK9 inhibitor on contrast-induced acute kidney injury in patients with acute myocardial infarction undergoing intervention therapy. *Cardiol. Res. Pract.* 2022, 1638209. doi:10.1155/2022/1638209

Paquette, M., Faubert, S., Saint-Pierre, N., Baass, A., and Bernard, S. (2023). Sex differences in LDL-C response to PCSK9 inhibitors: a real world experience. *J. Clin. Lipidol.* 17, 142–149. doi:10.1016/j.jacl.2022.12.002

Patek, T. M., Teng, C., Kennedy, K. E., Alvarez, C. A., and Frei, C. R. (2020). Comparing acute kidney injury reports among antibiotics: a pharmacovigilance study of the FDA adverse event reporting System (FAERS). *Drug Saf.* 43, 17–22. doi:10.1007/s40264-019-00873-8

Pickett, J. K., Shah, M., Gillette, M., Jones, P., Virani, S., Ballantyne, C., et al. (2020). Acute tubular injury in a patient on a proprotein convertase subtilisin/kexin type 9 inhibitor. *JACC Case Rep.* 2, 1042–1045. doi:10.1016/j.jaccas.2020.04.039

Rosenson, R. S., Hegele, R. A., Fazio, S., and Cannon, C. P. (2018). The evolving future of PCSK9 inhibitors. *J. Am. Coll. Cardiol.* 72, 314–329. doi:10.1016/j.jacc.2018.04.054

Rutter, W. C., and Burgess, D. S. (2018). Incidence of acute kidney injury among patients treated with piperacillin-tazobactam or meropenem in combination with vancomycin. *Antimicrob. Agents Chemother.* 62, 002644–e318. doi:10.1128/AAC.00264-18

Sarangdhar, M., Tabar, S., Schmidt, C., Kushwaha, A., Shah, K., Dahlquist, J. E., et al. (2016). Data mining differential clinical outcomes associated with drug regimens using adverse event reporting data. *Nat. Biotechnol.* 34, 697–700. doi:10.1038/nbt.3623

Siew, E. D., Parr, S. K., Abdel-Kader, K., Eden, S. K., Peterson, J. F., Bansal, N., et al. (2016). Predictors of recurrent AKI. *J. Am. Soc. Nephrol.* 27, 1190–1200. doi:10.1681/ASN.2014121218

Silver, S. A., Long, J., Zheng, Y., and Chertow, G. M. (2017). Cost of acute kidney injury in hospitalized patients. *J. Hosp. Med.* 12, 70–76. doi:10.12788/jhm.2683

Silverman, M. G., Ference, B. A., Im, K., Wiviott, S. D., Giugliano, R. P., Grundy, S. M., et al. (2016). Association between lowering LDL-C and cardiovascular risk reduction among different therapeutic interventions: a systematic review and meta-analysis. *Jama* 316, 1289–1297. doi:10.1001/jama.2016.13985

Skeby, C. K., Hummelgaard, S., Gustafsen, C., Petrillo, F., Frederiksen, K. P., Olsen, D., et al. (2023). Proprotein convertase subtilisin/kexin type 9 targets megalin in the kidney proximal tubule and aggravates proteinuria in nephrotic syndrome. *Kidney Int.* 104, 754–768. doi:10.1016/j.kint.2023.06.024

Stoekenbroek, R. M., Lambert, G., Cariou, B., and Hovingh, G. K. (2018). Inhibiting PCSK9 - biology beyond LDL control. *Nat. Rev. Endocrinol.* 15, 52–62. doi:10.1038/s41574-018-0110-5

Stone, N. J., Robinson, J. G., Lichtenstein, A. H., Bairey Merz, C. N., Blum, C. B., Eckel, R. H., et al. (2014). 2013 ACC/AHA guideline on the treatment of blood cholesterol to reduce atherosclerotic cardiovascular risk in adults: a report of the American College of Cardiology/American Heart Association Task Force on Practice Guidelines. *J. Am. Coll. Cardiol.* 63, 2889–2934. doi:10.1016/j.jacc.2013.11.002

Su, G., Xiao, C., Cao, Y., Gao, P., Xie, D., Cai, Q., et al. (2023). Piperacillin/tazobactam and risk of acute kidney injury in adults hospitalized with infection without vancomycin: a multi-centre real-world data analysis. *Int. J. Antimicrob. Agents* 61, 106691. doi:10.1016/j.ijantimicag.2022.106691

Toth, P. P., Dwyer, J. P., Cannon, C. P., Colhoun, H. M., Rader, D. J., Upadhyay, A., et al. (2018). Efficacy and safety of lipid lowering by alirocumab in chronic kidney disease. *Kidney Int.* 93, 1397–1408. doi:10.1016/j.kint.2017.12.011

Uchino, S., Kellum, J. A., Bellomo, R., Doig, G. S., Morimatsu, H., Morgera, S., et al. (2005). Acute renal failure in critically ill patients: a multinational, multicenter study. *JAMA* 294, 813–818. doi:10.1001/jama.294.7.813

Vallejo-Vaz, A. J., Ginsberg, H. N., Davidson, M. H., Eckel, R. H., Cannon, C. P., Lee, L. V., et al. (2018). Lower on-treatment low-density lipoprotein cholesterol and major adverse cardiovascular events in women and men: pooled analysis of 10 ODYSSEY phase 3 alirocumab trials. *J. Am. Heart Assoc.* 7, e009221. doi:10.1161/JAHA.118.009221

Xia, S., Gong, H., Zhao, Y., Guo, L., Wang, Y., et al. (2023). Tumor lysis syndrome associated with monoclonal antibodies in patients with multiple myeloma: a pharmacovigilance study based on the FAERS database. *Clin. Pharmacol. Ther.* 114, 211–219. doi:10.1002/cpt.2920

Xia, S., Zhao, Y. C., Guo, L., Gong, H., Wang, Y. K., et al. (2022). Do antibody-drug conjugates increase the risk of sepsis in cancer patients? A pharmacovigilance study. *Front. Pharmacol.* 13, 967017. doi:10.3389/fphar.2022.967017

Yifan, Z., Benxiang, N., Zheng, X., Luwei, X., Liuhua, Z., Yuzheng, G., et al. (2020). Ceftriaxone calcium crystals induce acute kidney injury by NLRP3-mediated inflammation and oxidative stress injury. *Oxid. Med. Cell Longev.* 2020, 6428498. doi:10.1155/2020/6428498

Yuan, J., Zhao, J., Qin, Y., Zhang, Y., Wang, A., Ma, R., et al. (2023). The protective mechanism of SIRT3 and potential therapy in acute kidney injury. *Qjm* 117, 247–255. doi:10.1093/qjmed/hcad152

Zhou, C., Peng, S., Lin, A., Jiang, A., Peng, Y., Gu, T., et al. (2023). Psychiatric disorders associated with immune checkpoint inhibitors: a pharmacovigilance analysis of the FDA Adverse Event Reporting System (FAERS) database. *EClinicalMedicine* 59, 101967. doi:10.1016/j.eclinm.2023.101967

Zhu, L., Yuan, Y., Yuan, L., Li, L., Liu, F., Liu, J., et al. (2020). Activation of TFEB-mediated autophagy by trehalose attenuates mitochondrial dysfunction in cisplatin-induced acute kidney injury. *Theranostics* 10, 5829–5844. doi:10.7150/thno.44051

# Frontiers in
# Pharmacology

**Explores the interactions between chemicals and living beings**

The most cited journal in its field, which advances access to pharmacological discoveries to prevent and treat human disease.

## Discover the latest Research Topics

See more →

**Frontiers**

Avenue du Tribunal-Fédéral 34
1005 Lausanne, Switzerland
frontiersin.org

**Contact us**

+41 (0)21 510 17 00
frontiersin.org/about/contact

**frontiers** | Research Topics